

**Design, Synthesis and Biological Properties of Amphiphilic  
Aminoglycosides**

by

Xuan Yang

A Thesis submitted to the Faculty of Graduate Studies of

The University of Manitoba

in partial fulfillment of the requirements of the degree of

DOCTOR OF PHILOSOPHY

Department of Chemistry

University of Manitoba

Winnipeg, Manitoba, Canada

Copyright © 2019 by Xuan Yang

*For my cute little girl Lydia*

## Abstract

Antibiotic resistance is a serious threat to human health, as we are facing the emergence of pathogens resistant to all available antibiotics. Amphiphilic aminoglycosides (AAGs) are an emerging source of antibacterials to combat infections caused by antibiotic-resistant bacteria; however, we found that they can also play a role as antibiotic adjuvants in combination therapies. In this study, a new series of amphiphilic aminoglycoside-based (AG-based) adjuvants, tobramycin-based efflux pump inhibitor conjugates, tobramycin-based lysine peptoid conjugates, and nebramine-based conjugates, have been successfully developed. *In vitro* combination studies indicate the ability of these AG-based conjugates to potentiate multiple classes of legacy antibiotics particularly to tetracyclines, fluoroquinolones, and rifampicin against multidrug-resistant (MDR) Gram-negative bacilli. We also demonstrated *in vivo* that combinations of selected AG-based conjugates and certain legacy antibiotics (minocycline or rifampicin) protect *Galleria mellonella* larvae from the lethal effects of MDR *Pseudomonas aeruginosa*. Mode of action studies indicate that these AG-based conjugates appear to possess intrinsic physicochemical properties that induce multimodal effects including permeabilization of the bacterial outer membrane, depolarization of the inner membrane, and dissipation of the proton motive force (PMF), which energizes efflux pumps. In addition, we discovered AAGs can also boost the innate immune response that may be exploited therapeutically. The amphiphilic tobramycins are capable of inducing the production of the chemokine IL-8, which plays a critical role in the recruitment of immune cells such as neutrophils required for the resolution of infections. Moreover, AAGs can selectively control inflammatory responses induced in the presence of endotoxins. Thus, AAGs represent a promising avenue for the development of

multifunctional molecules or antibiotic adjuvants for the prevention or treatment of bacterial infections.

## Acknowledgements

I would like to gratefully acknowledge the guidance, support and inspiration of my supervisor Dr. Frank Schweizer. Your rigorous academic attitude and extraordinary human qualities would benefit me immeasurably in the long run.

Besides my supervisor, I would also like to thank the rest of my committee members, Dr. Neeloffer Mookherjee, Dr. Joe O'Neil, Dr. John Sorensen, and Dr. David L. Jakeman for your brilliant comments and valuable advice.

I would like to thank our collaborators Dr. George G. Zhanel, Dr. Ayush Kumar, and Dr. Gilbert Arthur who contributed to this research.

Similar, profound gratitude goes to members of the Schweizer Research Group, especially Dr. Ronald Domalaon, Dr. Temilolu Idowu, Dr. Yinfeng Lyu, Dr. Goutam Guchhait, Dr. Bala Kishan Gorityala, Dr. Sudeep Goswami, Camilo Fabra Prieto, Liting Bi, Pavan Badogoo, Dr. Yaozu Xu, Dr. Fan Zhang, Dr. Makanjoula Ogunsina, Dr. Brandon Findlay, and Ruochen (Tony) Mao. Thank you for providing a so pleasurable and friendly working atmosphere. I really enjoyed the time we spend together.

I would also like to thank all my friends and peers in China and Canada, especially Xiaobin Zhang, Dr. Wenhao Sun, Nan Zhang and my niece Nan Wang for your friendship and support.

A special thanks to my mother Zongying Xiong, my father Banggan Yang, and my husband Chuanyu Sun for all the sacrifices that you've made on my behalf. Many thanks to my cute little girl, Lydia Zhihan Sun, for all you have added to my life. The dissertation would not have been possible without the support of my family.

## Table of Contents

<b>Abstract.....</b>	<b>ii</b>
<b>Acknowledgements .....</b>	<b>iv</b>
<b>Table of Contents .....</b>	<b>v</b>
<b>List of Abbreviations.....</b>	<b>x</b>
<b>Chapter 1: Introduction and Background.....</b>	<b>1</b>
1.1 Introduction.....	1
1.2 Aminoglycosides.....	2
1.3 Amphiphilic Aminoglycosides.....	11
1.4 Physical Barriers to Drug Influx and Multiple Efflux Pumps as Main Challenges of Antibacterial Discovery .....	59
1.5 Efflux Pump Inhibitors – One Approach to Break the Permeability Barrier ..	68
1.6 References.....	75
<b>Chapter 2: Thesis Objectives .....</b>	<b>99</b>
2.1 Aim of the Thesis and Study Objectives.....	99
2.2 Organization of the Thesis .....	100
<b>Chapter 3: A tobramycin vector enhances synergy and efficacy of efflux pump inhibitors against multidrug-resistant Gram-negative bacteria .....</b>	<b>102</b>
3.1 Abstract .....	102
3.2 Introduction.....	103
3.3 Results.....	107
3.4 Discussion.....	128
3.5 Conclusions.....	130

3.6 Experimental Section .....	131
3.7 Acknowledgements .....	160
3.8 References.....	160

#### **Chapter 4: Tobramycin-Linked Efflux Pump Inhibitor Conjugates Synergize**

##### **Fluoroquinolones, Rifampicin and Fosfomycin against Multidrug-Resistant *Pseudomonas***

<b><i>aeruginosa</i> .....</b>	<b>169</b>
4.1 Abstract .....	169
4.2 Introduction.....	170
4.3 Results.....	172
4.4 Discussion.....	185
4.5 Conclusions.....	188
4.6 Experimental Section .....	189
4.7 Acknowledgements.....	191
4.8 References.....	191

#### **Chapter 5: Amphiphilic tobramycin-lysine conjugates sensitize multidrug resistant Gram-**

##### **negative bacteria to rifampicin and minocycline .....**

5.1 Abstract .....	196
5.2 Introduction.....	197
5.3 Results.....	201
5.4 Discussion.....	228
5.5 Conclusions.....	234
5.6 Experimental Section .....	235
5.7 Acknowledgments.....	255

5.8 References.....	255
<b>Chapter 6: Amphiphilic Nebramine-based Hybrids Rescue Legacy Antibiotics from Intrinsic Resistance in Multidrug-resistant Gram-negative Bacilli .....</b>	<b>265</b>
6.1 Abstract .....	265
6.2 Introduction.....	266
6.3 Results and Discussion .....	269
6.4 Conclusions.....	292
6.5 Experimental Section .....	293
6.6 Acknowledgments.....	305
6.7 References.....	305
<b>Chapter 7: Amphiphilic Tobramycins with Immunomodulatory Properties.....</b>	<b>312</b>
7.1 Abstract .....	312
7.2 Introduction.....	313
7.3 Results and Discussion .....	315
7.4 Conclusions.....	324
7.5 Acknowledgments.....	325
7.6 References.....	325
<b>Chapter 8: Conclusions and Future Work .....</b>	<b>332</b>
8.1 General Conclusions .....	332
8.2 Future Work .....	334
8.3 References.....	336
<b>Chapter 9: Supporting Information for Chapter 3.....</b>	<b>338</b>
9.1 Chemical Syntheses .....	338

9.2 HPLC analysis .....	354
9.4 References.....	358
9.5 Figures.....	358
9.6 Tables .....	368
9.7 NMR Spectra .....	374
9.8 HPLC Spectra .....	402
<b>Chapter 10: Supporting Information for Chapter 5.....</b>	<b>411</b>
10.1 Chemical Syntheses .....	411
10.2 Figures.....	415
10.3 Tables .....	419
10.4 NMR Spectra .....	421
10.5 HPLC Spectra .....	437
<b>Chapter 11: Supporting Information for Chapter 6.....</b>	<b>441</b>
11.1 Chemical Syntheses .....	441
11.2 HPLC Analysis.....	448
11.3 NMR Spectra.....	450
11.4 HPLC Spectra .....	469
11.5 Table .....	472
11.6. Cytotoxicity Studies.....	473
<b>Chapter 12: Supporting Information for Chapter 7.....</b>	<b>476</b>
12.1 Synthesis and Characterisation of Tobramycin Derivatives .....	476
12.2 Elemental Analysis.....	484
12.3 Biological Activity Assays .....	485

12.4 References .....	488
<b>Chapter 13: Copyrighted Works for which Permission was Obtained.....</b>	<b>490</b>
<b>List of Publications and Patents Related to Thesis Work .....</b>	<b>492</b>

## List of Abbreviations

ACN	acetonitrile
AcOH	acetic acid
ADJ	adjuvant
AMP	adenosine monophosphate
aq	aqueous
ATP	adenosine triphosphate
Bn	benzyl
Boc	<i>tert</i> -butyloxycarbonyl
(Boc) <sub>2</sub> O	di- <i>tert</i> -butyl dicarbonate
CAN	cerium ammonium nitrate
CAN-ICU	Canadian National Intensive Care Unit
CANWARD	Canadian Ward Surveillance
cat.	catalyst
Cbz	carboxybenzyl
CbzCl	benzyl chloroformate
CFU	colony-forming unit
CIP	ciprofloxacin
CLSI	Clinical and Laboratory Standards Institute
CSA	camphorsulfonic acid
CST	colistin

DBP	dibasic peptide
DCM	dichloromethane
DIPEA	<i>N,N</i> -diisopropylethylamine
DiSC <sub>3</sub> (5)	3,3'-dipropylthiadicarbocyanine iodide
DMAP	4-dimethylaminopyridine
DMF	dimethyl formamide
DMSO	dimethyl sulfoxide
EDTA	ethylenediaminetetraacetic acid
Et	ethyl
EtOH	ethanol
EUCAST	European Committee on Antimicrobial Susceptibility Testing
FBS	fetal bovine serum
FIC	fractional inhibitory concentration
FICI	fractional inhibitory concentration index
FOF	fosfomicin
HABA	2-hydroxy-4-aminobutyric amide
HDPs	host-defense peptides
HEPES	4-(2-hydroxyethyl)-1-piperazineethanesulfonic acid
Homophe	homophenylalanine
HSQC	heteronuclear single quantum coherence
HTS	high through put
Hyp	4 <i>R</i> -hydroxy-proline

ICUs	intensive care units
IL-1 $\beta$	interleukin-1 $\beta$
IL-8	interleukin-8
IL-1RA	interleukin-1 receptor antagonist
IM	inner membrane
<i>J</i>	coupling constant (in NMR)
KHMDS	potassium bis(trimethylsilyl)amide
LDH	lactate dehydrogenase
LPS	lipopolysaccharides
MATE	multidrug and toxic compound extrusion
MCP-1	monocyte chemotactic protein-1
<i>m</i> CPBA	<i>meta</i> -chloroperbenzoic acid
MD	molecular dynamic
MDR	multidrug-resistant
MeOH	methanol
MFS	major facilitator superfamily
MHB	Mueller-Hinton broth
MIC	minimum inhibitory concentration
MIN	minocycline
MOX	moxifloxacin
Ms	methanesulfonyl
MTS	3-(4,5-dimethylthiazol-2-yl)-5-(3-carboxymethoxyphenyl)-2-(4-sulfonyl)-2H-tetrazolium)

NEB	nebramine
NIS	<i>N</i> -iodosuccinimide
NMP	1-(1-naphthylmethyl)piperazine
NPN	1- <i>N</i> -phenylnaphthylamine
OD	optical density
OM	outer membrane
PAR	paroxetine
PCC	pyridinium chlorochromate
PDR	pandrug-resistant
ppm	parts per million
Pro	proline
RIF	rifampicin
RND	resistance-nodulation-division
rt	room temperature
Su	succinimidyl
TBAB	tetra- <i>n</i> -butylammonium bromide
TBAF	tetrabutylammonium fluoride
TBAHS	tetrabutylammonium hydrogen sulfate
TBAI	tetrabutylammonium iodide
TBDMS	<i>tert</i> -butyldimethylsilyl
TBDMSCl	<i>tert</i> -butyldimethylsilyl chloride
TBDPSCl	<i>tert</i> -butyl(chloro)diphenylsilane

TBSOTf	<i>tert</i> -butyldimethylsilyl trifluoromethanesulfonate
TBTU	2-(1H-benzotriazole-1-yl)-1,1,3,3-tetramethylamminium tetrafluoroborate
<i>t</i> Bu	<i>tert</i> -butyl
TC	tissue culture
TFA	trifluoroacetic acid
TfOH	trifluoromethanesulfonic acid
THF	tetrahydrofuran
TIBS	2,4,6-Triisopropylbenzenesulfonyl
TIBSCl	2,4,6-Triisopropylbenzenesulfonyl chloride
TIPS-Cl	triisopropylsilyl chloride
TNF- $\alpha$	tumor necrosis factor- $\alpha$
Trisyl	2,4,6-triisopropylbenzenesulfonyl
TOB	tobramycin
Troc	2,2,2-trichloroethoxycarbonyl
Ts	tosyl
XDR	extensively drug-resistant
$\delta$	chemical shift in parts per million

# Chapter 1: Introduction and Background

## 1.1 INTRODUCTION

Aminoglycosides (AGs) are a group of versatile antibiotics that exert broad-spectrum activity against both Gram-negative bacilli and Gram-positive cocci.<sup>1</sup> Even after almost seventy years in clinical use, they are still indispensable drugs that continue to be used for many serious infections caused by Gram-negative bacilli, often in combination with  $\beta$ -lactam antibiotics.<sup>2,3</sup> Decades of widespread use of aminoglycosides in clinical practice has led to evolutionarily driven bacterial resistance that strongly reduced their clinical efficacy.<sup>4</sup> Well-described aminoglycosides' adverse effects, including ototoxicity, nephrotoxicity, and susceptibility to enzymatic inactivation have also curtailed their clinical use.<sup>1,5</sup> Due to financial reasons and scientific hurdles, large pharmaceutical companies have been dismantling their antibiotic-discovery program even if incentivized.<sup>6</sup> As a result, the rate of discovery of novel antibacterial agents has been steadily decreasing. Only two novel antibiotic classes (lipopeptides and oxazolidinones) have been introduced to the clinic in the last four decades and neither of them possesses activity against Gram-negative bacilli.<sup>7</sup> There is an urgent need for new antibacterial agents, particularly active against Gram-negative bacilli, to combat the growing threat of antibiotic resistance.

The purpose of this thesis is to study the biological properties of novel amphiphilic aminoglycosides related to the aminoglycoside antibiotic tobramycin, with the goal to open up new opportunities to develop alternative therapies against Gram-negative pathogens. A background to the conventional aminoglycosides will be presented, including the history,

classification, mechanism of action, and resistance mechanism of aminoglycosides, along with the brief introduction of the next-generation aminoglycoside plazomicin. The development of amphiphilic aminoglycosides in the last decade will also be reviewed, with examples of novel antibacterial amphiphilic aminoglycosides and amphiphilic aminoglycoside adjuvants in combination therapies. An introduction to the main challenges of antibacterial discovery, the outer membrane permeability barriers and the efflux of agents from the cell with the help of multidrug efflux pumps that synergistically reduce the intracellular concentrations of antibiotics in the cell will be presented. Moreover, major classes of efflux pump inhibitors (EPIs) that block efflux activity and/or break the permeability barrier will be illustrated.

## 1.2 AMINOGLYCOSIDES

### 1.2.1 History of Aminoglycosides

Aminoglycosides (AGs) are natural products produced by *Actinomycete*, a group of Gram-positive bacteria, such as *Streptomyces* (AGs spelling end with -mycin) and *Micromonospora* (AGs spelling end with -micin) or their semisynthetic amino-modified sugars. The first member of AGs, streptomycin, was discovered through natural product screening and isolated from *Streptomyces griseus* by Schatz *et al.* in 1944.<sup>8</sup> Unlike many early discovered antibiotics such as penicillin only active against Gram-positive bacteria, streptomycin has broad spectrum activity against most Gram-negative bacteria and certain Gram-positive bacteria as well as *Mycobacterium tuberculosis*.<sup>9</sup> Ever since, a diverse panel of natural and semi-synthetic aminoglycosides were consequently discovered and introduced into clinical use including neomycin (isolated from *Streptomyces fradiae*), kanamycin (isolated from *Streptomyces*

*kanamyceticus*), paromomycin (isolated from *Streptomyces krestomuceticus*),<sup>10,11</sup> spectinomycin (isolated from *Streptomyces spectabilis*), gentamicin (isolated from *Micromonospora purpurea*), tobramycin (isolated from *Streptomyces tenebrarius*),<sup>12,13</sup> sisomicin (isolated from *Micromonospora inyoensis*),<sup>14,15</sup> netilmicin (derived from sisomicin),<sup>16</sup> dibekacin (derived from kanamycin B),<sup>17</sup> and amikacin (derived from kanamycin A).<sup>18</sup> AGs have become a standard weapon in our anti-infective armamentarium. Their broad-spectrum of activity has favored them over the past seventy years as a valuable class of antibiotics.

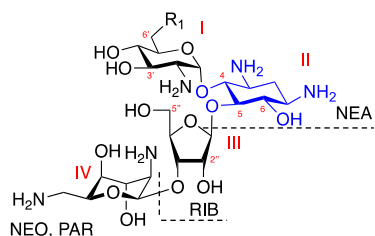
### 1.2.2 Classification of Aminoglycosides

Structurally, aminoglycosides can be classified into four subclasses: (1) 4,5-disubstituted-2-deoxystreptamine (2-DOS) ring; (2) 4,6-disubstituted-2-DOS ring; (3) mono-substituted-DOS ring; (4) aminoglycosides without DOS ring (Figure 1.2.2.1).<sup>19</sup>

The 4,5-2-DOS-linked family has DOS-hydroxyl groups substituted with other aminocyclitols at position 4 and 5 (e.g., neamine (NEA), neomycin B (NEO), paromomycin (PAR), and ribostamycin (RIB)) while the 4,6-2-DOS linked family has substitutions at position 4 and 6 (e.g., amikacin (AMK), arbekacin (ABK), dibekacin (DBK), kanamycin A (KANA), kanamycin B (KANB), tobramycin (TOB), gentamicin (GEN), geneticin (G418), sisomicin (SIS), and netilmicin (NET)).

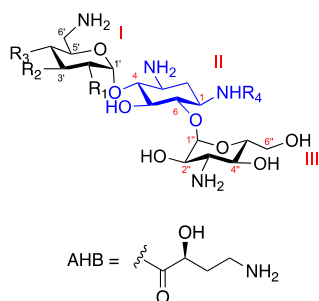
A few other aminoglycosides have a structural pattern that differs from a disubstituted 2-DOS motif such as apramycin (APR) which is made of a mono-substituted 2-DOS with an unusual fused bicyc amino-octodialdose. Similarly, hygromycin B (HYG) is a mono-substituted 2-DOS pseudotrisaccharide in which the 1,3-diaminocyclitol is *N*-methylated on only the position 3 amino group. As shown in Figure 1.2.2.1, spectinomycin (SPC) (with a 1,3-

diaminocyclitol embedded within a tricyclic ring system), fortimicin A (FTM-A) (with a 1,4-diaminocyclitol moiety) and streptomycin (STR) (a pseudotrisaccharide structure composed of a streptidine ring), AGs illustrate diverse structures that lack the 2-DOS ring.



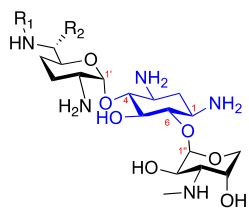
#### 4,5-Disubstituted 2-DOS AGs:

	R <sub>1</sub>
Neamine (NEA)	NH <sub>2</sub>
Neomycin (NEO)	NH <sub>2</sub>
Paromomycin (PAR)	OH
Ribostamycin (RIB)	NH <sub>2</sub>

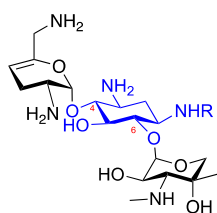


#### 4,6-Disubstituted 2-DOS AGs:

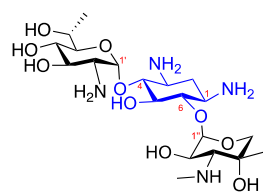
	R <sub>1</sub>	R <sub>2</sub>	R <sub>3</sub>	R <sub>4</sub>
Amikacin (AMK)	OH	OH	OH	AHB
Arbekacin (ABK)	NH <sub>2</sub>	H	H	AHB
Dibekacin (DBK)	NH <sub>2</sub>	H	H	H
Kanamycin A (KANA)	OH	OH	OH	H
Kanamycin B (KANB)	NH <sub>2</sub>	OH	OH	H
Tobramycin (TOB)	NH <sub>2</sub>	H	OH	H



	R <sub>1</sub>	R <sub>2</sub>
Gentamicin C <sub>1</sub> (GEN C <sub>1</sub> )	CH <sub>3</sub>	CH <sub>3</sub>
Gentamicin C <sub>2</sub> (GEN C <sub>2</sub> )	H	CH <sub>3</sub>
Gentamicin C <sub>1a</sub> (GEN C <sub>1a</sub> )	H	H

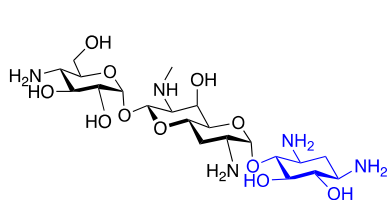


	R
Sisomicin (SIS)	H
Netilmicin (NET)	Et

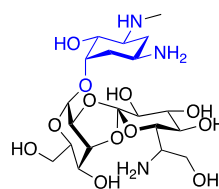


Geneticin (G418)

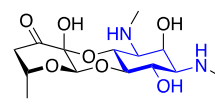
### Other AG scaffolds:



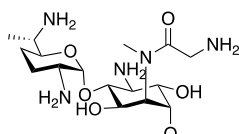
Apramycin (APR)



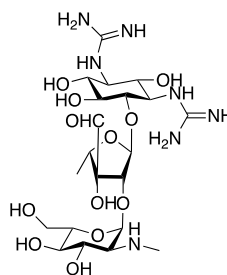
Hygromycin B (HYG)



Spectinomycin (SPC)



Fortimicin (FTM-A)



Streptomycin (STR)

**Figure 1.2.2.1.** Structures of representative aminoglycosides.

## 1.2.3 Mechanisms of Action

### 1.2.3.1 Bacterial Uptake of Aminoglycosides

Accumulation of aminoglycosides by intact bacterial cells is comprised of three consecutive phases: initial ionic binding, energy dependent phase I (EDP-I), and energy dependent phase II (EDP-II).<sup>20</sup>

The antibacterial action of aminoglycosides is facilitated by their polycationic nature. The overall positive charge ensures aminoglycosides bind electrostatically to negatively charged residues of the bacterial membrane, such as wall-associated teichoic acids in Gram-positive bacteria and lipopolysaccharide (LPS) in Gram-negative bacteria.<sup>21</sup> AGs transit the outer membrane of Gram-negative bacteria by displacing the divalent cations ( $Mg^{2+}$  or  $Ca^{2+}$ ) which cross-bridge adjacent polyanionic surface of LPS. This results in destabilization of the outer membrane that leads to a self-promoted uptake by which AGs are likely to enter into the periplasm through the lipid bilayer.<sup>21-24</sup>

After transit through the outer membrane, AGs transport across the cytoplasmic membrane is not precisely understood but involves two energy-dependent (EDP) but carrier-independent steps. EDP-I requires metabolic energy from active electron transport, in this case, the electrochemical gradient ( $\Delta\Psi$ ) of the proton motive force (PMF), in an oxygen-dependent process.<sup>20,21,25,26</sup> This then explains why aminoglycosides inherently lack activity against anaerobic bacteria.<sup>21,27,28</sup> Followed by the slow rate of uptake of EDP-I, the third phase of aminoglycoside uptake refers to EDP-II, which represents a rapid energy-dependent transport across the cytoplasmic membrane.<sup>29</sup>

### ***1.2.3.2 Inhibition of Bacterial Protein Synthesis***

Aminoglycoside bactericidal activity is due to inhibition of bacterial protein synthesis. In the cytosol, AGs bind to the A-site (aminoacyl site) on the 16S rRNA of the 30S ribosomal subunit through EDP-II.<sup>26,30,31</sup> As a result of this interaction, AGs interfere with the elongation process of the nascent chain by impairing the proofreading process that helps assure the accuracy of translation.<sup>25,33</sup> As a consequence of incorrect amino acids are assembled into polypeptides

that may be inserted into the cell membrane.<sup>21,25,26,32,33</sup> This then leads to altered permeability and further rapid uptake of additional aminoglycosides into the cytoplasm that ultimately result in disruption of the integrity of the bacterial cell membrane.<sup>19,32</sup>

Recently, some AGs, including neomycin, paromomycin and tobramycin, have been demonstrated to bind not only to the ribosomal decoding A-site on the 16S rRNA, but also have a secondary binding site at the major groove of helix 69 (H69) of the 23S rRNA within the 50S large subunit which is critical in the processes of mRNA/ tRNA translocation and ribosome recycling.<sup>34,35</sup>

### ***1.2.3.3 Disruption of the Outer Membrane of Gram-negative Bacteria***

In addition to the action of aminoglycosides on protein synthesis, disruption of the outer bacterial membrane is also observed. These two mechanisms of bacterial killing by aminoglycosides are concentration-dependent.<sup>36</sup> The studies on the aminoglycoside tobramycin eradication of *P. aeruginosa* showed the extracellular tobramycin concentration elicit immediate and rapid killing due to the disruption of the outer membrane at high tobramycin concentrations ( $\geq 8 \mu\text{g/mL}$ ), while the intracellular tobramycin concentrations cause a delayed bacterial killing that owing to the inhibition of bacterial protein synthesis at low-intermediate tobramycin concentration ( $< 4 \mu\text{g/mL}$ ).<sup>36</sup>

### **1.2.4 Resistance Mechanisms**

Three major mechanisms are responsible for AG-resistance: enzymatic drug modification, reduction of intracellular concentration of AGs by efflux transport systems, and alteration of the

molecular target by an enzyme or chromosomal mutation.<sup>1,19</sup> These mechanisms are not mutually exclusive and multiple mechanisms are often involved in the same bacterial strain.<sup>19</sup>

Enzymatic modification is the most prevalent AG-resistance mechanism and is achieved by covalent modification of the hydroxyl and amino groups of AGs with AG modifying enzymes (AMEs). There are three types of AMEs: (1) aminoglycoside acetyltransferases (AACs), which comprise the largest group of AMEs, that add an *N*-acetyl group to the amino functions of AGs in an acetyl-CoA-dependent reaction, (2) aminoglycoside phosphotransferases (APHs), which catalyze the ATP-dependent phosphorylation of hydroxyl groups, and (3) aminoglycoside nucleotidyltransferases (ANTs), which add adenosine monophosphate (AMP) from an adenosine triphosphate (ATP) donor to hydroxyl groups (Figure 1.2.4.1).<sup>1,19,21,37</sup> Enzymatic modification of AGs presumably disrupts the hydrogen features of the AGs, resulting in a large decrease in binding affinity to the therapeutic target (rRNA).

The regulation of intracellular concentration by overexpression of efflux pumps plays an important role as an AG resistance mechanism in a few pathogens including *Pseudomonas aeruginosa*, *Acinetobacter baumannii*, *Escherichia coli*, and *Burkholderia pseudomallei*.<sup>38</sup> Several members of the resistance–nodulation–division (RND) family of efflux systems were shown to be involved in intrinsic and/or acquired aminoglycoside resistance in these pathogens. For example, the MexXY-OprM multidrug efflux system of *P. aeruginosa*,<sup>39–41</sup> the AcrAD-TolC multidrug efflux system of *E. coli*,<sup>42</sup> the AmrAB-OprA and BpeAB-OprB multidrug efflux systems of *B. pseudomallei*.<sup>43,44</sup>

The resistance mechanism of target site modification is via the action of plasmid-encoded 16S rRNA methyltransferases which modify A-site rRNA residues that interferes with AGs

binding to their target, thereby lowering AG binding affinities.<sup>45–47</sup> Since 2003, 16S rRNA methyltransferases have conferred high-level resistance to nearly all AGs.<sup>48</sup>

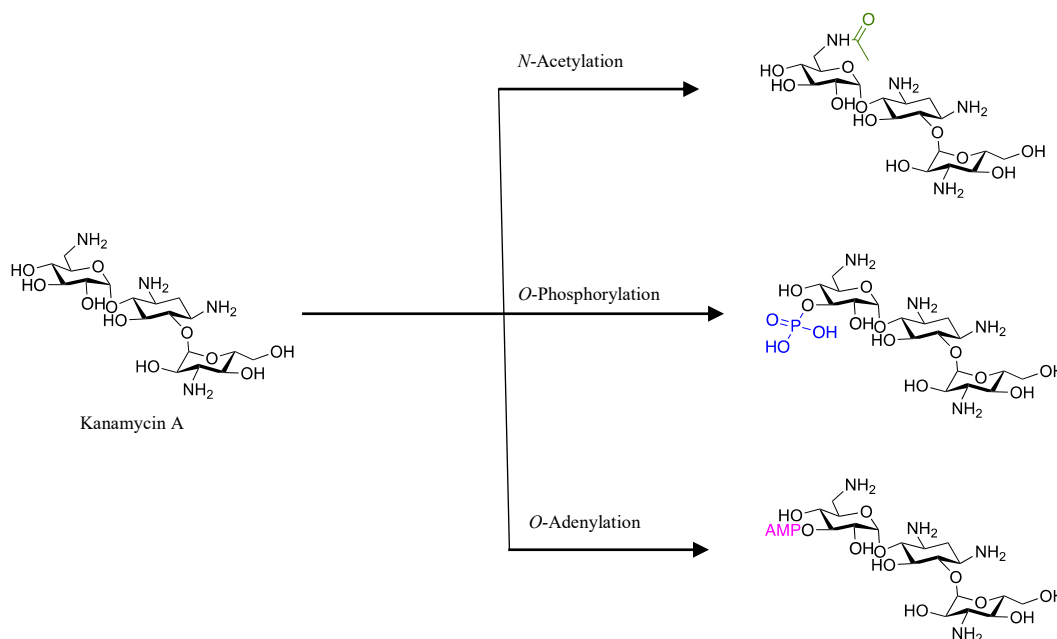


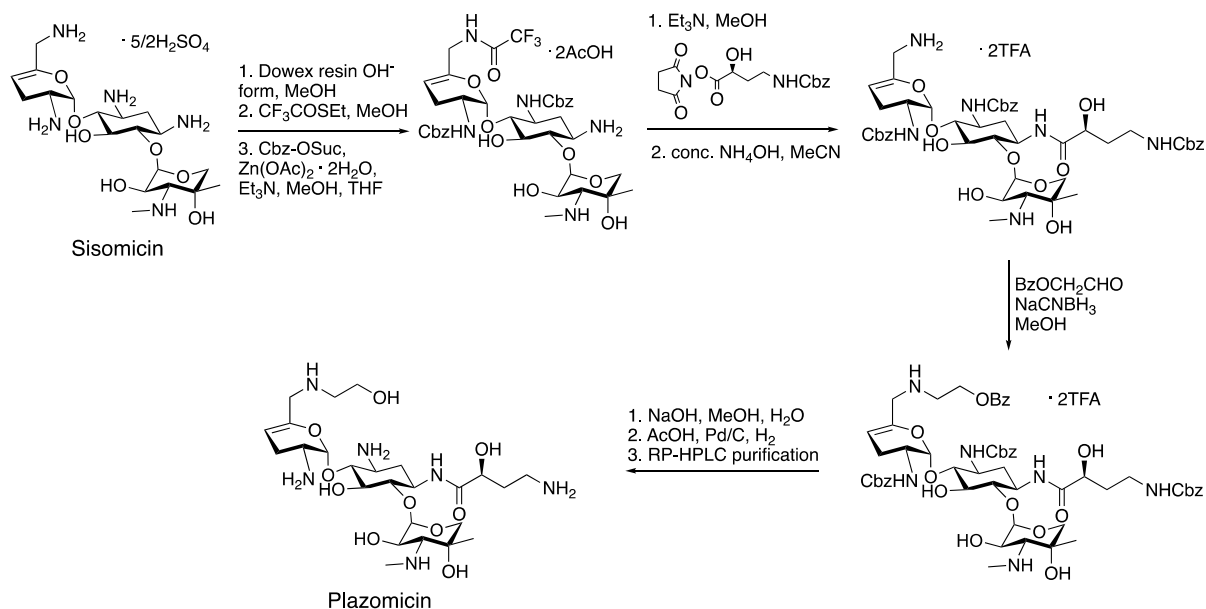
**Figure 1.2.4.1.** Inactivation of aminoglycosides by acetylation (green), phosphorylation (blue), and adenylation (pink).

### 1.2.5 The Next-Generation Aminoglycoside: Plazomicin (PLZ)

With an increasing understanding of AG-resistance mechanisms, extensive efforts have been devoted to structural modifications of AGs and AG resistance enzyme inhibitors with the goal of improving the antibacterial spectrum of natural AGs and overcoming the emergence of resistance. Thus, a semi-synthetic era has been opened with several semi-synthetic AGs such as amikacin, netilmicin, arbekacin and plazomicin have been introduced into the market.

Plazomicin (PLZ) (ZEMDRI™) which is considered as the next-generation of AG antibiotic, and is less susceptible to many AG resistance mechanisms, was approved by the FDA for the treatment of adults with complicated urinary tract infections (cUTI) in June 2018.<sup>49</sup> PLZ





**Scheme 1.2.5.1.** Synthesis of plazomicin (PLZ).<sup>50</sup>

### 1.3 AMPHIPHILIC AMINOGLYCOSIDES

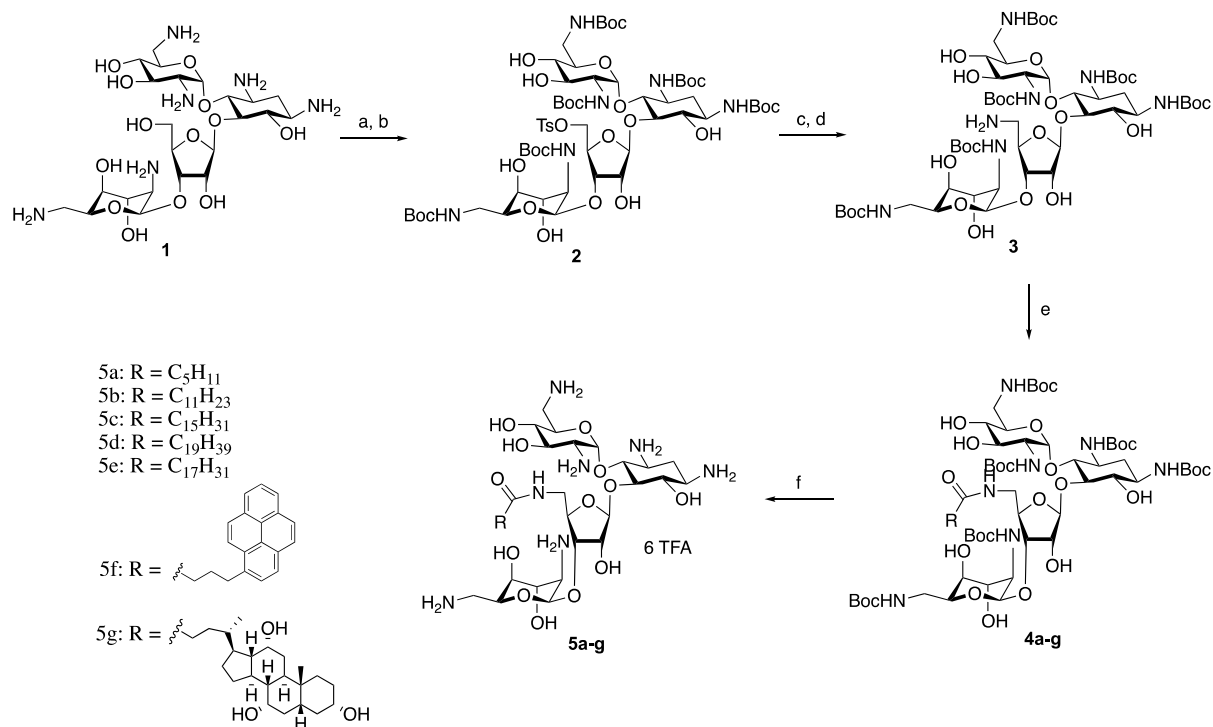
#### 1.3.1. An Overview of Antibacterial Amphiphilic Aminoglycosides in the Last Decade

Aminoglycosides are among the most potent antimicrobials in the treatment of *Pseudomonas aeruginosa* infections. However, the world-wide emergence of resistance and their toxicity issues have compromised their widespread use and clearly led to a shortage of treatment options, especially for immunocompromised patients with severe infections. In an effort to search new antibiotics to revive the antibacterial activity against aminoglycoside resistant bacteria, Hanessian and co-workers developed several paramomycin derivatives with lipophilic substituents attached at the 2'' position on ring III.<sup>53</sup> These 2''-O-substituted ether analogues showed potent inhibitory activity equal or better than paromomycin against *Staphylococcus aureus* (ATCC 13709) and *Escherichia coli* (ATCC 25922).<sup>53</sup> The works of Hanessian and co-

workers are the first reports on amphiphilic aminoglycosides (AAGs). Subsequently, the research on AAGs were expanded to the incorporation of hydrophobic moieties through modifications of the amino or hydroxyl groups of other AGs including neomycin,<sup>54–60</sup> tobramycin,<sup>61–65</sup> kanamycin,<sup>56,58,66</sup> and neamine.<sup>58,61,67–70</sup> Many AAGs significantly improved activity against AG-resistant bacteria and/or MDR bacteria in comparison to the parent AG drugs and other classes of antibiotics. The study of modes of action of antibacterial AAGs indicated that an increase in the AG lipophilicity results in a bacterial target shifting from the rRNA to cell surface membranes.<sup>71</sup> A strong binding to LPS of Gram-negative bacteria as well as membrane depolarization were observed and thus membrane perturbation became the primary antibacterial action of these AAGs.<sup>67,71</sup> The following part is an overview mostly limited to the main results obtained in the last decade in the field of antibacterial AAGs and focuses mainly on the chemical synthesis, biological evaluations, delineation of structure–activity relationships and understanding of their modes of action.

In 2008, our group reported a series of amphiphilic neomycin-lipid conjugates appending various hydrophobic spacers derived from lipophilic fatty acids, cholesterol, and pyrene.<sup>54</sup> The synthesis of this class of conjugates started with the protection of neomycin with (Boc)<sub>2</sub>O before selective tosylation of the reactive primary C5''-hydroxyl group in ribose. Subsequently, nucleophilic displacement of mono-tosylated derivative **2** to produce an azide intermediate, which was then subjected to catalytic hydrogenation to generate the C5''-amine **3** which was available for condensation with a variety of lipophilic acids (Scheme 1.3.1.1). The biological studies showed that Neomycin-C16 (**5c**) and neomycin-C20 (**5d**) conjugates are very active against Gram-positive bacteria particularly for MDR strains including MRSA and MRSE (Table

1.3.1.1).<sup>54</sup> SAR studies manifested that the antibacterial activity of neomycin-lipid conjugates depends on the length and nature of the lipid moiety.



**Scheme 1.3.1.1.** Synthesis of amphiphilic neomycin-lipid conjugates. Reagents and conditions:

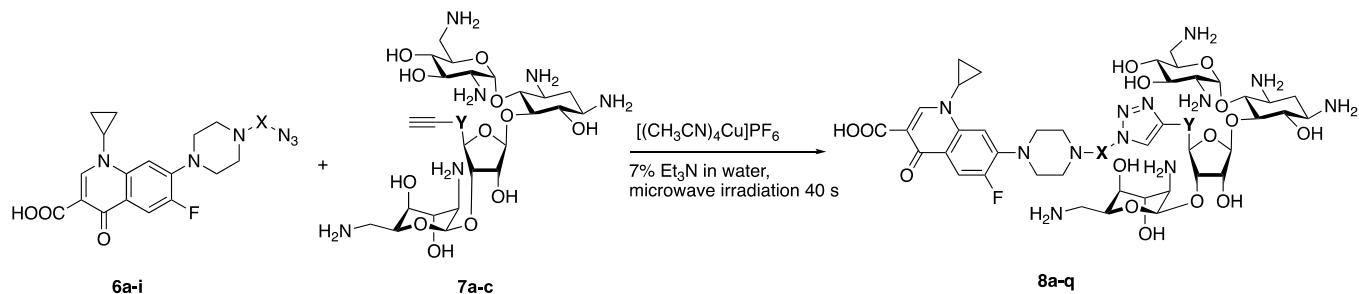
(a) (Boc)<sub>2</sub>O, Et<sub>3</sub>N, DMF/H<sub>2</sub>O, 80 °C, 6 h; (b) TsCl, Py, rt, 10 h; (c) NaN<sub>3</sub>, DMF, 60 °C, 8 h; (d) Pd(OH)<sub>2</sub>/C, H<sub>2</sub>, rt, 5 h; (e) TBTU, DMF, DIPEA, rt, 2 h, lipophilic acid, (RCOOH, R = hexanoic acid, dodecanoic acid, palmitic acid, arachidic acid, linoleic acid, pyrene butyric acid, cholic acid); (f) TFA, DCM, 0 °C, 3 min.<sup>54</sup>

**Table 1.3.1.1.** Minimal inhibitory concentrations (MIC) in  $\mu\text{g/mL}$  of gentamicin, neomycin B and amphiphilic neomycin-lipid conjugates.<sup>54</sup>

organism	gentamicin	neomycin B	5c	5d
<i>S. aureus</i> ATCC 29213	1	2	4	8
MRSA ATCC 33592	2	256	8	8
<i>S. epidermidis</i> ATCC 14990	0.25	1	2	4
MRSE ATCC 14990	32	0.5	2	4
<i>S. pneumoniae</i> ATCC 49619	4	64	64	64
<i>E. coli</i> ATCC 25922	1	8	32	128
<i>E. coli</i> ATCC 6174 (GEN-R)	128	4	64	128
<i>P. aeruginosa</i> ATCC 27853	4	512	128	64

In 2009, a hybrid strategy was pursued by the Baasov group by employing a combination of two different drugs, a fluoroquinolone (ciprofloxacin) and an aminoglycoside (neomycin B), in one molecule with a 1,2,3-triazole linkage.<sup>55</sup> Ciprofloxacin-azido derivatives and 5"-alkyne-neomycin derivatives were prepared separately which were further coupled via “click reaction” under microwave irradiation in the presence of organic base and the Cu(I) catalyst to ensure the production of ciprofloxacin-tiazole-linked neomycin B hybrids (Scheme 1.3.1.2). The lipophilic spacers X and Y were selected to vary both the length and chemical nature of the linkage between the ciprofloxacin and neomycin B pharmacophores. Most hybrids were more potent than the parent neomycin B but none of them showed superior antimicrobial activity than ciprofloxacin against MRSA and *E. coli* (kanamycin resistant or susceptible) strains. Importantly, emergence of bacterial resistance in both *E. coli* and *B. subtilis* was significantly delayed by the

hybrid in comparison to the treatment with ciprofloxacin, kanamycin B alone or a 1:1 ciprofloxacin/kanamycin B mixture.<sup>55</sup>



Compound	X	Y
<b>6a</b>	-(CH <sub>2</sub> ) <sub>2</sub> -	-C <sub>6</sub> H <sub>4</sub> -NHCO-
<b>6b</b>	-(CH <sub>2</sub> ) <sub>3</sub> -	-C <sub>6</sub> H <sub>4</sub> -NHCO-
<b>6c</b>	-(CH <sub>2</sub> ) <sub>4</sub> -	-C <sub>6</sub> H <sub>4</sub> -NHCO-
<b>6d</b>	-(CH <sub>2</sub> ) <sub>5</sub> -	-C <sub>6</sub> H <sub>4</sub> -NHCO-
<b>6e</b>	-(CH <sub>2</sub> ) <sub>6</sub> -	-C <sub>6</sub> H <sub>4</sub> -NHCO-
<b>6f</b>	-CH <sub>2</sub> CH(OH)CH <sub>2</sub> -	-C <sub>6</sub> H <sub>4</sub> -NHCO-
<b>6g</b>	-(CH <sub>2</sub> ) <sub>2</sub> -O-(CH <sub>2</sub> ) <sub>2</sub> -	-C <sub>6</sub> H <sub>4</sub> -NHCO-
<b>6h</b>	-CH <sub>2</sub> - <i>m</i> C <sub>6</sub> H <sub>4</sub> -CH <sub>2</sub> -	-C <sub>6</sub> H <sub>4</sub> -NHCO-
<b>6i</b>	-CH <sub>2</sub> - <i>p</i> C <sub>6</sub> H <sub>4</sub> -CH <sub>2</sub> -	-C <sub>6</sub> H <sub>4</sub> -NHCO-
<b>6j</b>	-(CH <sub>2</sub> ) <sub>2</sub> -	-CH <sub>2</sub> -NH-CO-
<b>6k</b>	-(CH <sub>2</sub> ) <sub>3</sub> -	-CH <sub>2</sub> -NH-CO-
<b>6l</b>	-(CH <sub>2</sub> ) <sub>5</sub> -	-CH <sub>2</sub> -NH-CO-
<b>6m</b>	-CH <sub>2</sub> CH(OH)CH <sub>2</sub> -	-CH <sub>2</sub> -NH-CO-
<b>6n</b>	-(CH <sub>2</sub> ) <sub>2</sub> -O-(CH <sub>2</sub> ) <sub>2</sub> -	-CH <sub>2</sub> -NH-CO-
<b>6o</b>	-CH <sub>2</sub> - <i>m</i> C <sub>6</sub> H <sub>4</sub> -CH <sub>2</sub> -	-CH <sub>2</sub> -NH-CO-
<b>6p</b>	-CH <sub>2</sub> - <i>p</i> C <sub>6</sub> H <sub>4</sub> -CH <sub>2</sub> -	-CH <sub>2</sub> -NH-CO-
<b>6q</b>	-(CH <sub>2</sub> ) <sub>2</sub> -	-CH <sub>2</sub> -O-CH <sub>2</sub> -

**Scheme 1.3.1.2.** Strategy for the assembly of amphiphilic Cipro-NeoB hybrids.<sup>55</sup>

In 2010, based on the previous study on amphiphilic neomycin-lipid conjugates, our group further explored the influence of guanidinylation of neomycin B and kanamycin A-derived lipid conjugates (Figure 1.3.1.1) on antibacterial potency.<sup>57</sup> A novel class of cationic guanidylated aminoglycoside-derived lipids were synthesized via guanidinylation of the amino groups of known aminoglycoside lipids using *N,N'*-di-Boc-*N''*-triflylguanidine, followed by deprotection of *tert*-butyloxycarbonyl (Boc) groups. Antibacterial evaluation indicated that this

series of conjugates restored the anti-MRSA activity of both parent aminoglycosides and the anti-MRSE activity of kanamycin A. Among these conjugates, the guanidinylated neomycin B-C16 lipid **10c** appears to be the most potent one which manifested potent anti-Gram-positive activity against MRSA, MRSE as well as Gram-negative activity against *E. coli* and *P. aeruginosa* (Table 1.3.1.2).

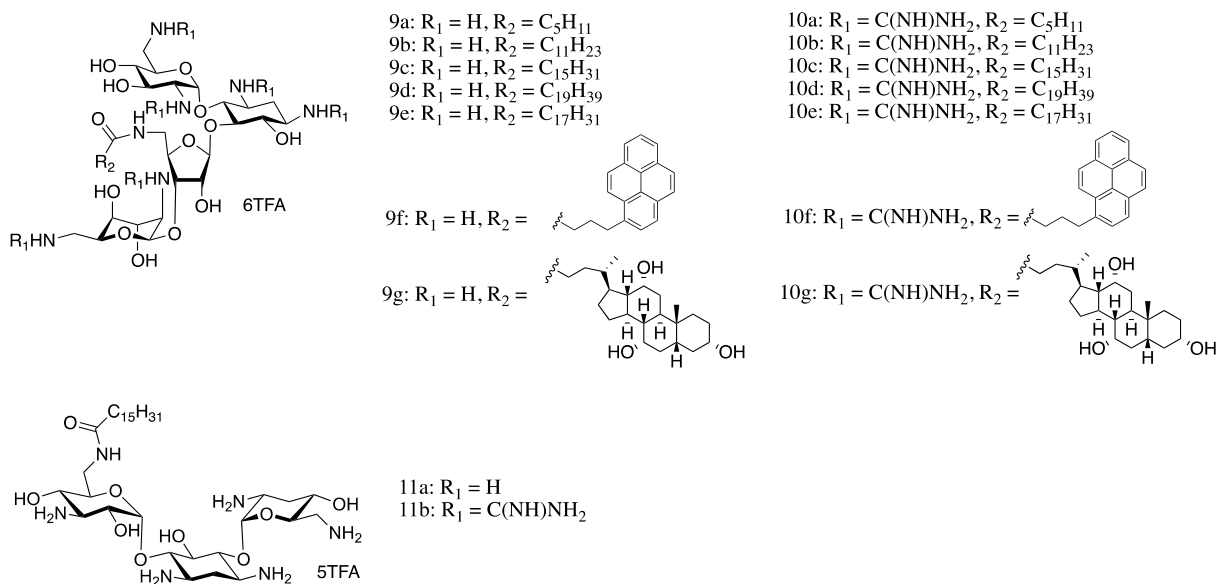


**Figure 1.3.1.1.** Structures of neomycin B-derived cationic lipids (**9a-g**) containing an amine-based polycationic headgroup, neomycin B-lipids (**10a-g**) containing a guanidinylated polycationic headgroup, and kanamycin A-derived cationic lipids (**11a** and **11b**) bearing a C16 tail.<sup>57</sup>

**Table 1.3.1.2.** Minimal inhibitory concentrations (MIC) in  $\mu\text{g/mL}$  of gentamicin, neomycin B and guanidinylated neomycin B-derived amphiphilic lipid conjugate.<sup>57</sup>

organism	gentamicin	neomycin B	<b>10c</b>
<i>S. aureus</i> ATCC 29213	1	1	4
MRSA ATCC 33592	2	256	4
<i>S. epidermidis</i> ATCC 14990	0.25	0.25	1
MRSE CAN-ICU 61589	32	0.5	4
<i>E. faecalis</i> ATCC 29212	N.D.	N.D.	4
<i>E. faecalis</i> ATCC 27270	N.D.	N.D.	0.5
<i>S. pneumoniae</i> ATCC 49619	4	32	32
<i>E. coli</i> ATCC 25922	1	4	32
<i>E. coli</i> CAN-ICU 61714 (GEN-R)	128	8	64
<i>E. coli</i> CAN-ICU 63074	8	N.D.	32
<i>P. aeruginosa</i> ATCC 27853	8	512	32
<i>P. aeruginosa</i> CAN-ICU 62308	128	512	8

In the same year, our group investigated the role of polyol lipophilic scaffolds (polycarbamates and polyethers) on neomycin B, kanamycin A, amikacin, and neamine (Figure 1.3.1.2).<sup>58</sup> Oligocationic polycarbamate analogues were synthesized via carbamoylation of hydroxyl groups with various hydrophobic isocyanates while oligocationic polyether analogues were synthesized via *O*-alkylation with corresponding alkyl bromides or methyl iodide. Antimicrobial evaluation showed that the neomycin B-based heptaphenyl carbamate (**12a**) was the most potent one with excellent Gram-positive activity against *S. aureus* (MIC = 1  $\mu\text{g/mL}$ ),

MRSA ((MIC = 1  $\mu\text{g}/\text{mL}$ , 256-fold enhanced antibacterial activity compared to neomycin B), *S. epidermidis* (MIC = 1  $\mu\text{g}/\text{mL}$ ), and MRSE (MIC = 0.5  $\mu\text{g}/\text{mL}$ ) (Table 1.3.1.3).

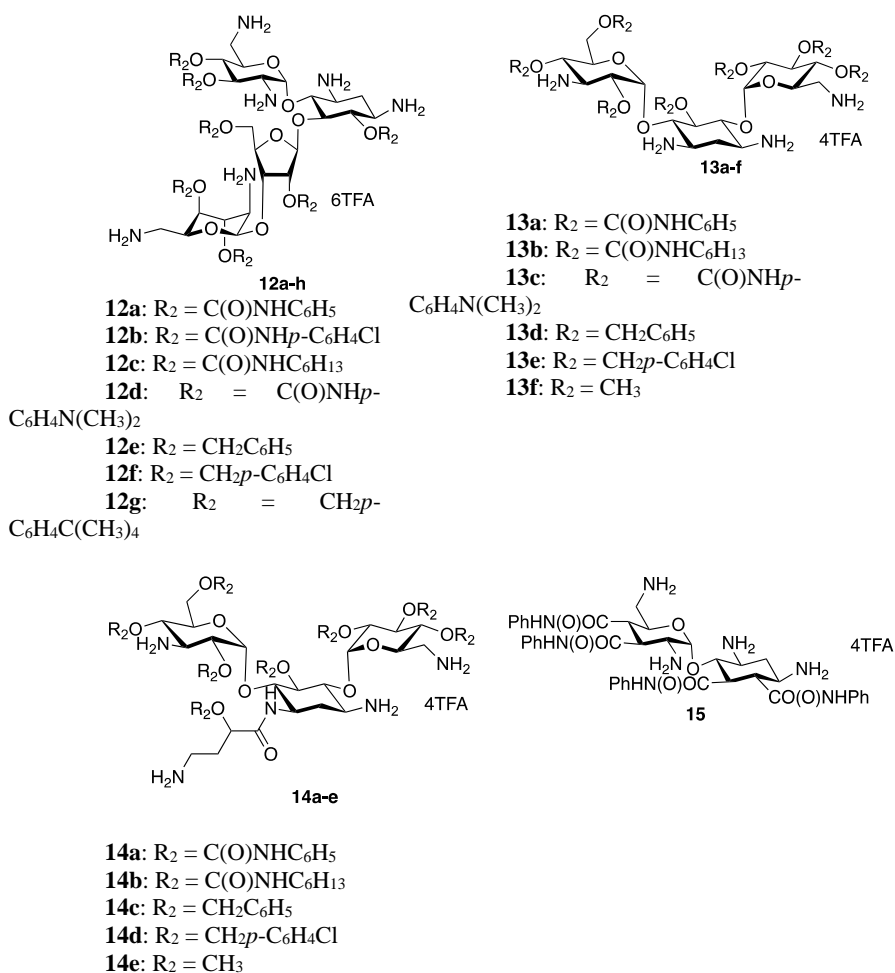


**Figure 1.3.1.2.** Polycarbamate modified amphiphilic aminoglycoside antibiotics (**12a-d**, **13a-c**, **14a**, **14b**, and **15**) and polyethers (**12e-g**, **13d-f**, **14c-e**).<sup>58</sup>

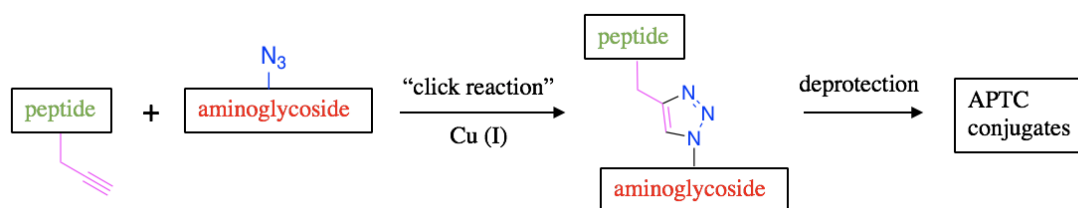
**Table 1.3.1.3.** Minimal inhibitory concentrations (MIC) in  $\mu\text{g/mL}$  of gentamicin, neomycin B and amphiphilic neomycin polycarbamate **12a**.<sup>58</sup>

organism	gentamicin	neomycin B	<b>12a</b>
<i>S. aureus</i> ATCC 29213	1	1	1
MRSA ATCC 33592	2	256	1
<i>S. epidermidis</i> ATCC 14990	0.25	1	0.5
MRSE ATCC 14990	32	0.5	0.5
<i>S. pneumoniae</i> ATCC 49619	4	32	16
<i>S. pneumoniae</i> ATCC 13883	4	512	128
<i>E. coli</i> ATCC 25922	1	4	32
<i>E. coli</i> ATCC 6174 (GEN-R)	128	8	16
<i>E. coli</i> CAN-ICU 63074	8	N.D.	16
<i>P. aeruginosa</i> ATCC 27853	4	512	256
<i>P. aeruginosa</i> CAN-ICU 62308	128	512	128
<i>S. maltophilia</i> CAN-ICU 62584	>512	>512	4
<i>A. baumannii</i> CAN-ICU 63169	128	64	32

In 2010, our group described the synthesis and the antibacterial evaluation of a novel class of amphiphilic aminoglycoside-peptide triazole conjugates (APTCS).<sup>56</sup> These cationic amphiphiles were prepared via “click reaction” between a neomycin B-C5"- or kanamycin A-C6"-derived azides and a hydrophobic and ultrashort peptide-based alkyne in solution and on the solid phase (Scheme 1.3.1.3). Antibacterial evaluation demonstrated that APTCS displayed enhanced antibacterial activity against resistant strains including neomycin B-, kanamycin A-

resistant MRSA, kanamycin A-resistant MRSE and gentamicin-resistant *P. aeruginosa*.

Activities of kanamycin A-dipeptide conjugate **16** and conjugate **17** which contain two neomycin A units were found to be relatively potent against Gram-positive and most Gram-negative strains (Table 1.3.1.4). The similar physicochemical properties of APTCs and AMPs suggest a membranolytic mode of action against bacterial strains.<sup>72</sup>



**Scheme 1.3.1.3.** Click-based glycoconjugation of neomycin B- and kanamycin A-based azides to hydrophobic alkyne-based peptides that form aminoglycoside-peptide triazole conjugates (APTCs).<sup>56</sup> Adapted with permission from *Bioorg. Med. Chem. Lett.* **2010**, *20* (10), 3031-3035.

Copyright (2010) Elsevier Ltd.

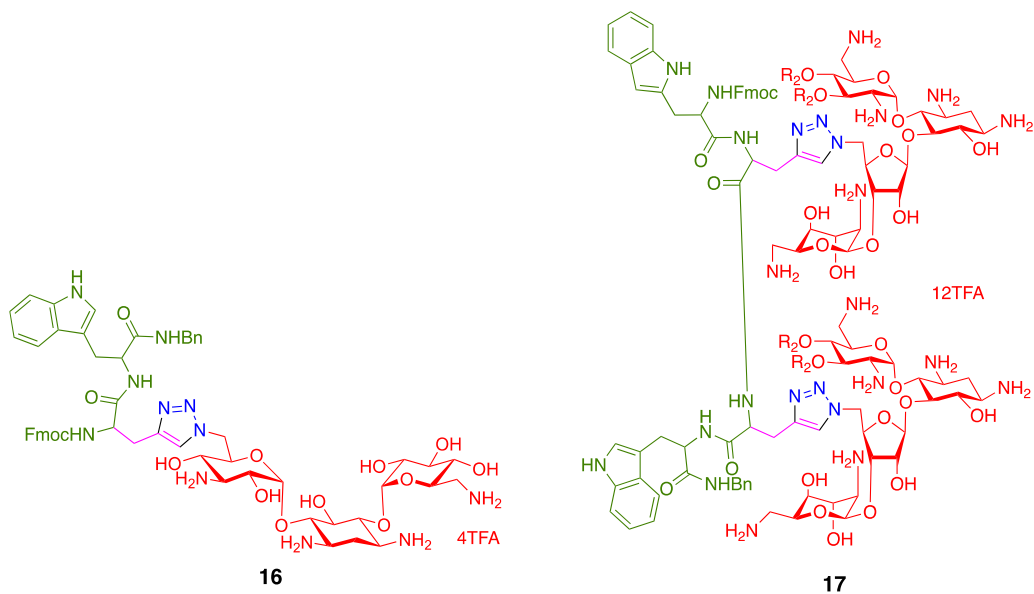


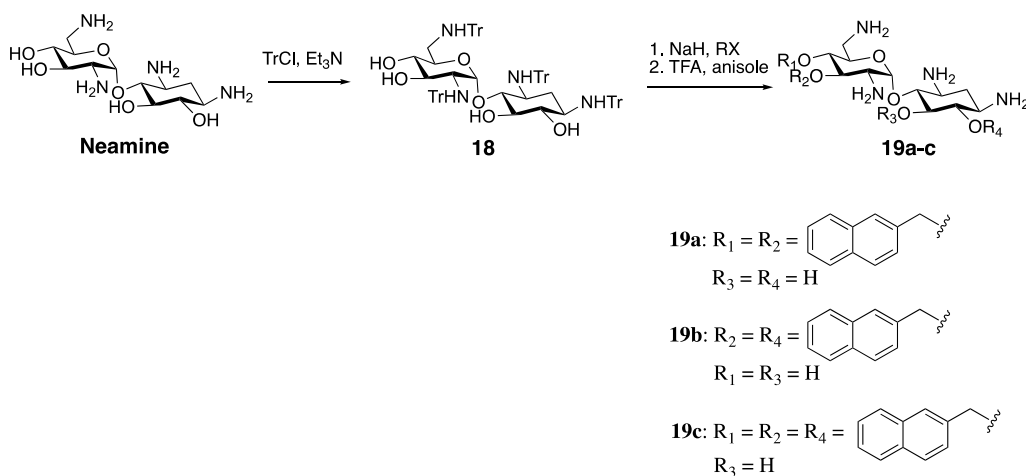
**Figure 1.3.1.3.** Structure of kanamycin A (red)-dipeptide (green) conjugate **16** and conjugate **17** which containing two neomycin A units (red).<sup>56</sup>

**Table 1.3.1.4.** Minimal inhibitory concentrations (MIC) in  $\mu\text{g/mL}$  of gentamicin, neomycin B, kanamycin A and aminoglycoside-peptide triazole conjugates (**16**, **17**).<sup>56</sup>

organism	gentamicin	neomycin B	kanamycin A	<b>16</b>	<b>17</b>
<i>S. aureus</i> ATCC 29213	1	1	4	16	8
MRSA ATCC 33592	2	256	>512	32	16
<i>S. epidermidis</i> ATCC 14990	0.25	0.25	2	8	2
MRSE CAN-ICU 61589	32	0.25	128	16	4
<i>S. pneumoniae</i> ATCC 49619	4	8	8	64	64
<i>E. coli</i> ATCC 25922	1	2	8	32	32
<i>E. coli</i> CAN-ICU 61714 (GEN-R)	128	4	16	32	64
<i>E. coli</i> CAN-ICU 63074 (AMK-R)	8	32	32	32	16
<i>P. aeruginosa</i> ATCC 27853	8	512	>512	128	128
<i>P. aeruginosa</i> CAN-ICU 62308	128	512	>512	16	32

In 2010, Décout and co-workers reported synthesis and antimicrobial evaluation of amphiphilic neamine derivatives.<sup>69</sup> The synthetic procedure was started with *O*-alkylation of hydroxyl groups of 1,3,2',6'-tetratrityl protected neamine derivative with hydrophobic phenyl, naphthyl, pyridyl or quinoyl rings followed by deprotection of trityl (Tr) and/or selective removal of the 2-naphthylmethylene (2NM) under acidic conditions to generate a series of mono-, di-, tri-, or tetra-alkyl neamine derivatives (Scheme 1.3.1.4). Among them, the 3',4'-di-2-naphthylmethylene (**19a**), 3',6-di-2-naphthylmethylene (**19b**) and 3',4',6-tri-naphthylmethylene (**19c**) derivatives showed good activity against sensitive and resistant *S. aureus* including MRSA and VRSA whereas the 3',4',6-tri-2-naphthylmethylene (**19c**) appeared to be remarkably active

against sensitive and resistant Gram-negative bacteria including *A. lwoffii*, *E. coli*, *K. pneumonia* and *P. aeruginosa* (Table 1.3.1.5). Moreover, it was proposed that bacterial membranes are the targets for explaining the antibacterial activity observed by 3',4'-di-2-naphthylmethylene (**19a**), 3',6-di-2-naphthylmethylene (**19b**) and 3',4',6-tri-2-naphthylmethylene (**19c**) derivatives. The following year it was demonstrated that amphiphilic neamine derivative 3',4',6-tri-2-naphthylmethylene bound to lipopolysaccharides and induced *P. aeruginosa* outer membrane depolarization.<sup>70</sup>



**Scheme 1.3.1.4.** Synthesis of 3',4'-di-2-naphthylmethylene (**19a**), 3',6-di-2-naphthylmethylene (**19b**) and 3',4',6-tri-naphthylmethylene (**19c**) derivatives.<sup>69</sup>

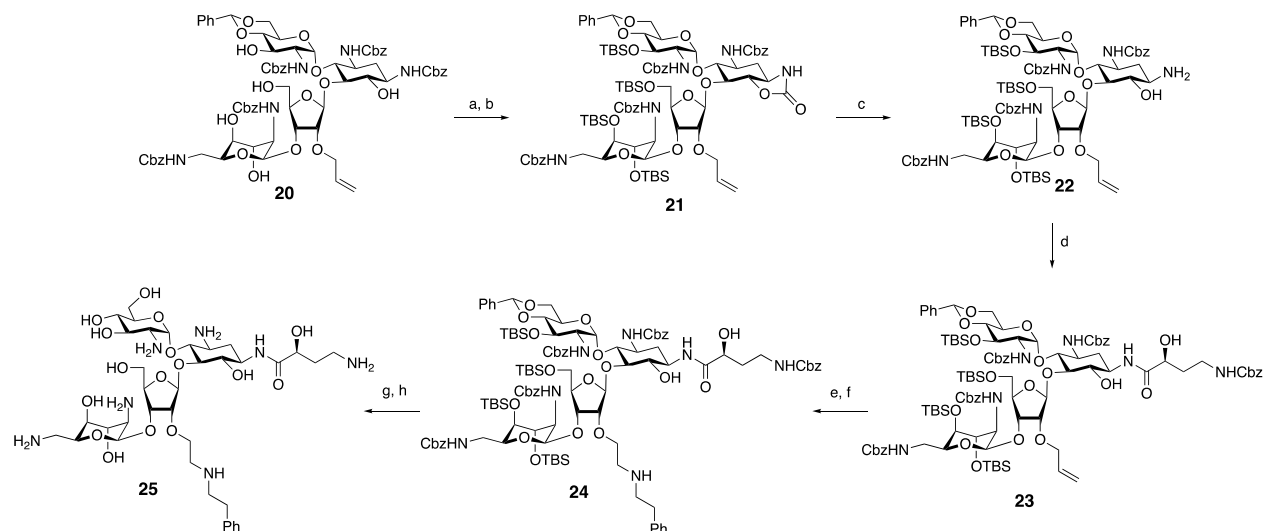
**Table 1.3.1.5.** Minimal inhibitory concentrations (MIC) in  $\mu\text{g/mL}$  of neomycin B, neamine, gentamicin, amikacin, tobramycin and neamine derivatives (**19a-c**).<sup>69</sup>

organism	neomycin B	neamine	gentamicin	amikacin	tobramycin	<b>19a</b>	<b>19b</b>	<b>19c</b>
<i>S. aureusa</i>	2	32	N.D.	N.D.	N.D.	4	8	4
<i>S. aureusb</i>	>128	>128	N.D.	N.D.	N.D.	8	16	2
<i>S. aureusc</i>	128	128	N.D.	N.D.	N.D.	4	16	4
<i>A. lwoffid</i>	0.5	2	0.5	0.5	0.5	8	64	4
<i>A. lwoffie</i>	>128	>128	4–8	>128	1	>128	>128	32
<i>P. aeruginosaf</i>	64	>128	1	2–4	0.5	32	128	8
<i>P. aeruginosag</i>	128	>128	>128	4	128	>128	128	8
<i>P. aeruginosah</i>	32	>128	4	8–16	1	>128	>128	4
<i>K. pneumoniaei</i>	16–32	32–64	8	0.5	4	>128	128–>128	16
<i>E. colij</i>	2	32	<0.5–1	4	0.5	32	64	16
<i>E. colik</i>	4	>128	1	32	32	16	64	4
<i>E. coli<sup>l</sup></i>	32	32	64–128	2	64	16	64	4

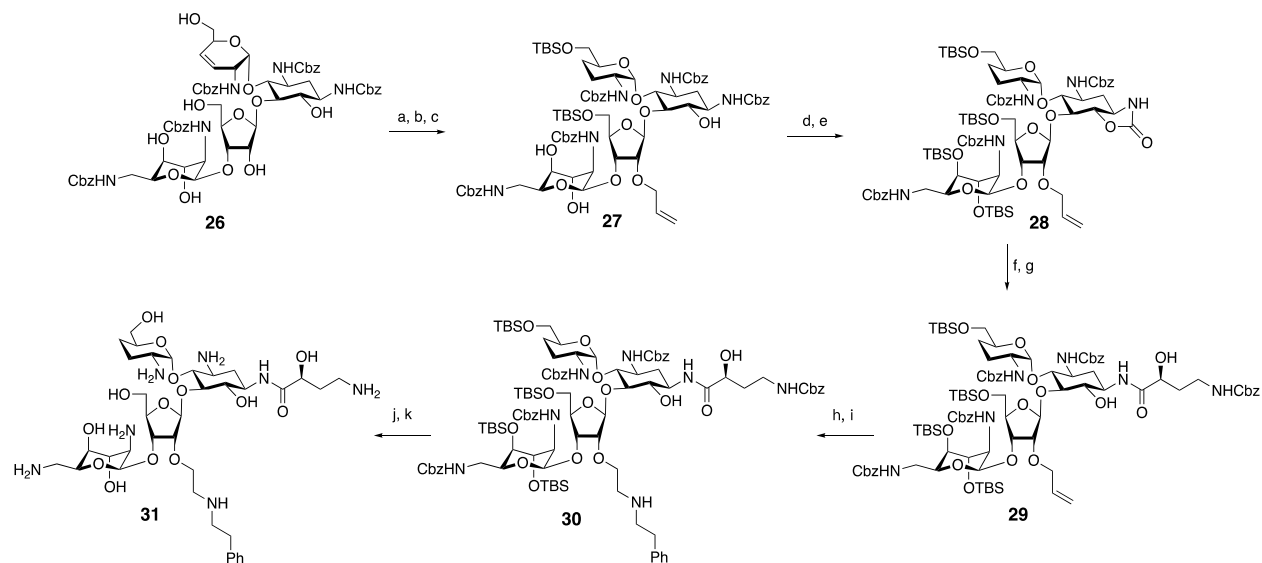
<sup>a</sup> *S. aureus* ATCC 25923; <sup>b</sup> *S. aureus* ATCC 33592 HA-MRSA; <sup>c</sup> *S. aureus* VRSA-VRS-2; <sup>d</sup> *A. lwoffii* ATCC 17925; <sup>e</sup> *A. lwoffii* AI.88-483 APH3'-Via; <sup>f</sup> *P. aeruginosa* ATCC 27853; <sup>g</sup> *P. aeruginosa* Psa.F03 AAC6'-IIa; <sup>h</sup> *P. aeruginosa* PA22 (PT629) surexp MexXY; <sup>i</sup> *K. pneumoniae* ATCC 700603; <sup>j</sup> *E. coli* ATCC 25922; <sup>k</sup> *E. coli* PAZ505H8101 AAC6'-IIb; <sup>l</sup> *E. coli* L58058.1 ANT2''-IIa.

In 2010, Hanessian and co-workers designed and synthesized novel analogs of paromomycin and dideoxyparomomycin harboring the hydrophobic ether group at the C2'' position and a N1-(2S)-2-hydroxy-4-aminobutyric amide (HABA) side chain.<sup>73</sup> The synthesis of

these analogs (**25** and **31**) is summarized in Scheme 1.3.1.5 and Scheme 1.3.1.6 and started with intermediates as previously described.<sup>53,74,75</sup> Antibacterial evaluation manifested that the combination of (phenethylamino)ethyl ether at C2'' and N1-HABA in 3',4'-dideoxyparomomycin (**31**) led to a remarkably improved activity against a panel of Gram-positive and Gram-negative resistant bacteria including vancomycin resistant (VRSA) and vancomycin intermediate (VISA) strains (Table 1.3.1.6).



**Scheme 1.3.1.5.** Synthesis of paromomycin derivative **25**. Reagents and conditions: (a) TBSOTf, 2,4,6-collidine, CH<sub>2</sub>Cl<sub>2</sub>; (b) NaH, DMF; (c) LiOH aq; (d) N-Cbz-Haba- OSu, Et<sub>3</sub>N, THF; (e) (i) O<sub>3</sub>, (ii) PPh<sub>3</sub>; (f) RNH<sub>2</sub>, NaBH<sub>3</sub>CN, MeOH, AcOH; (g) HF, pyridine; (h) AcOH/H<sub>2</sub>O (4:1), (ii) Pd(OH)<sub>2</sub>/C, H<sub>2</sub>.<sup>73</sup>



**Scheme 1.3.1.6.** Synthesis of 3',4'-dideoxyparomycin derivative **31**. Reagents and conditions:

(a) Wilkinson's cat., EtOH/THF; (b) TBSCl, imidazole, DCM; (c) allyl iodide, KHMDS, THF;

(d) TBSOTf, 2,4,6-collidine, DCM; (e) NaH, DMF; (f) LiOH aq; (g) N-Cbz-Haba-OSu, Et<sub>3</sub>N,

THF; (h) (1) O<sub>3</sub>, (2) Me<sub>2</sub>S; (i) phenethylamine, NaBH<sub>3</sub>CN, AcOH; (j) HF, pyridine; (k)

Pd(OH)<sub>2</sub>/C, H<sub>2</sub>, AcOH/H<sub>2</sub>O (4:1).<sup>73</sup>

**Table 1.3.1.6.** MIC range in  $\mu\text{g/mL}$  of gentamicin, amikacin, paromomycin derivative **25** and 3',4'-dideoxyparomomycin derivative **31**.<sup>73</sup>

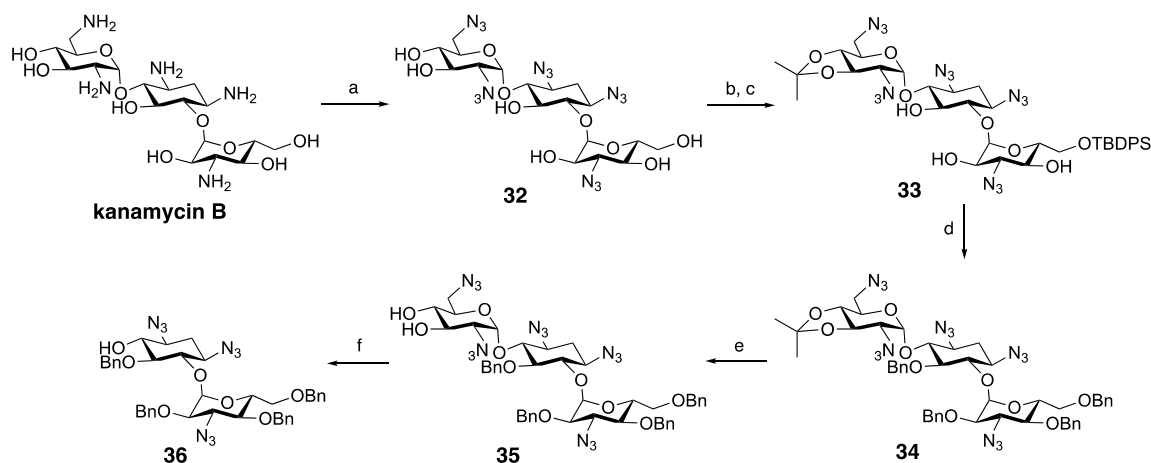
organism	MIC range			
	gentamicin	amikacin	<b>25</b>	<b>31</b>
<i>S. aureus</i> <sup>a</sup>	0.25–128	1–16	<0.12–>128	<0.12–1
<i>S. epidermidis</i> <sup>b</sup>	<0.12–64	0.8–8	<0.12–16	<0.12
<i>S. warneri</i> <sup>c</sup>	<0.12	<0.25	<0.12	<0.12
<i>S. capitis</i> <sup>d</sup>	0.12	0.5	<0.12	<0.12
<i>E. coli</i> <sup>e</sup>	0.5–>128	1–64	1–8	1–16

<sup>a</sup>  $n = 8$ ; *S. aureus* ATCC292213, *S. aureus* 1269615 (VRSA, gentamicin resistant (GEN-R)), *S. aureus* 1269616 (VISA, GEN-R), *S. aureus* 1269617 (VRSA, GEN-R), *S. aureus* 1269618 (VISA, GEN-R), *S. aureus* 9269619 (GEN-R), *S. aureus* 1269669, *S. aureus* 1269670; <sup>b</sup>  $n = 5$ ; *S. epidermidis* 1269663, *S. epidermidis* 1269675 (GEN-R), *S. epidermidis* 1269676 (GEN-R), *S. epidermidis* 1269677 (GEN-R), *S. epidermidis* 1269680 (GEN-R); <sup>c</sup>  $n = 1$ ; *S. warneri* 1269686; <sup>d</sup>  $n = 1$ ; *S. capitis* 1269682; <sup>e</sup>  $n = 7$ ; *E. coli* ATCC25922, *E. coli* 1269687, *E. coli* 1260640, *E. coli* 1269620 (VRSA, GEN-R), *E. coli* 1269621 (VRSA, GEN-R), *E. coli* 1269652 (VRSA, GEN-R), *E. coli* 1269653 (VRSA, GEN-R).

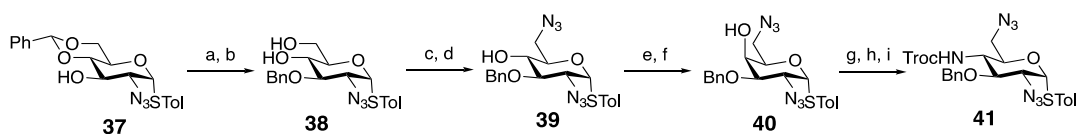
In 2011, Yan *et al.* reported a series of kanamycin B derivatives appending different functional groups at the C4' position on ring I.<sup>66</sup> Unlike direct modification using AGs as starting materials, diversification of ring I of kanamycin B via glycosylation was developed. Glycosyl acceptor (**36**) containing ring I and ring II was synthesized by disconnecting the ring I from kanamycin B according to the reported procedure<sup>76</sup> (Scheme 1.3.1.7). 4-Amino-protected thioglycoside donor (**41**) was prepared as shown in Scheme 1.3.1.8. Glycosylation of glycosyl acceptor (**36**) and donor (**41**) was accomplished in the presence of *N*-iodosuccinimide

(NIS)/TfOH to reconstruct kanamycin B framework (Scheme 1.3.1.9). Further modifications of the C4' position by attaching different functional groups and followed by deprotection of the protecting groups were conducted to generate the final novel kanamycin B derivatives.

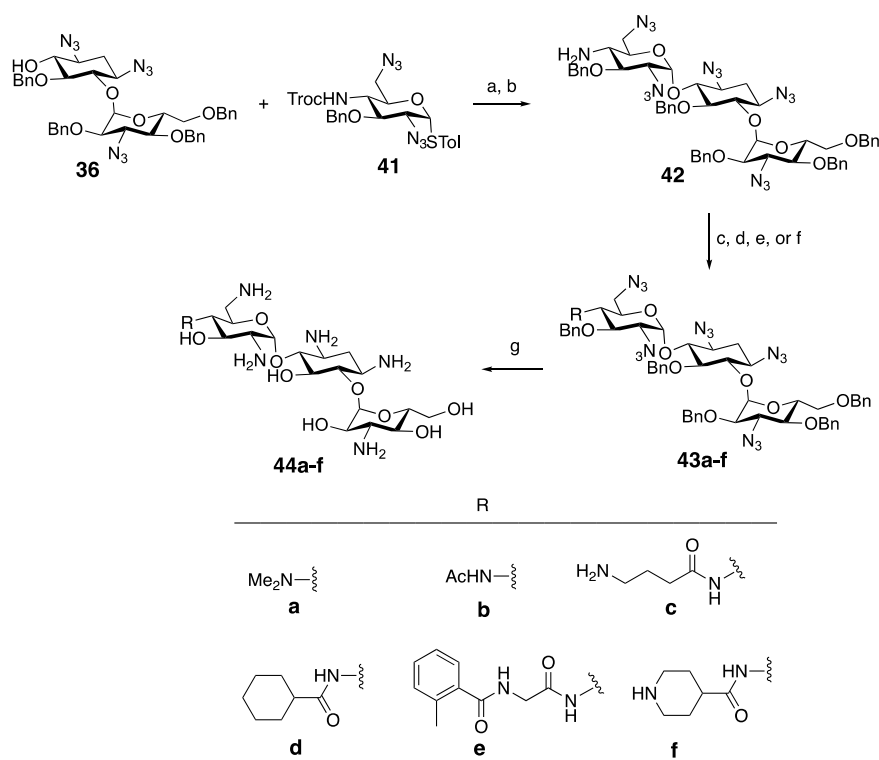
Antibacterial evaluation manifested that all these analogues have considerable antibacterial activities especially for compounds **44c** and **44f** both of which have a nitrogen atom at the end of each substituent and exhibited the most potent activity against drug-resistant bacteria (Table 1.3.1.7).



**Scheme 1.3.1.7.** Synthesis of glycosyl acceptor **36**. Reagents and conditions: (a) (i) TfN<sub>3</sub>, NEt<sub>3</sub>, Cu<sup>2+</sup>, CH<sub>3</sub>CN, H<sub>2</sub>O; (ii) acetic anhydride, pyridine; (iii) NaOMe, MeOH; (b) TBDPSCl, pyridine, DMAP; (c) 2,2-dimethoxypropane, CH<sub>2</sub>Cl<sub>2</sub>, CSA; (d) (i) TBAF, THF; (ii) NaH, BnBr, DMF; (e) AcOH, MeOH; (f) (i) NaIO<sub>4</sub>, MeOH; (ii) *n*-BuNH<sub>2</sub>, MeOH.<sup>66</sup>



**Scheme 1.3.1.8.** Synthesis of glycosyl donor **41**. Reagents and conditions: (a) NaH, BnBr, DMF; (b) CSA, MeOH; (c) TsCl, pyridine; (d) NaN<sub>3</sub>, DMF; (e) Dess–Martin’s periodinane, CH<sub>2</sub>Cl<sub>2</sub>; (f) NaBH<sub>4</sub>, MeOH; (g) Tf<sub>2</sub>O, pyridine, CH<sub>2</sub>Cl<sub>2</sub>; (h) NH<sub>3</sub>, MeOH; (i) TrocCl, NaHCO<sub>3</sub>, THF.<sup>66</sup>



**Scheme 1.3.1.9.** Synthesis of kanamycin B derivatives (**44a-f**). Reagents and conditions: (a) NIS, TfOH, 4 Å molecular sieves, DCM, -70 °C to rt,  $\alpha/\beta = 1.74/1$ ; (b) NaOH, H<sub>2</sub>O, 1,4-dioxane, reflux; (c) NaH, MeI, DMF; (d) Ac<sub>2</sub>O, pyridine; (e) (i) 4-chloro-butanoyl chloride, NaHCO<sub>3</sub>, THF; (ii) NaN<sub>3</sub>, DMF; (f) TBTU, carboxylic acids, DIPEA, DMF; (g) (i) H<sub>2</sub>S, pyridine, triethylamine, H<sub>2</sub>O; (ii) H<sub>2</sub>, Pd/C, MeOH, H<sub>2</sub>O, HCl.<sup>66</sup>

**Table 1.3.1.7.** MIC range in  $\mu\text{g/mL}$  of kanamycin A, kanamycin B, and kanamycin B derivatives (**44c** and **44f**).<sup>66</sup>

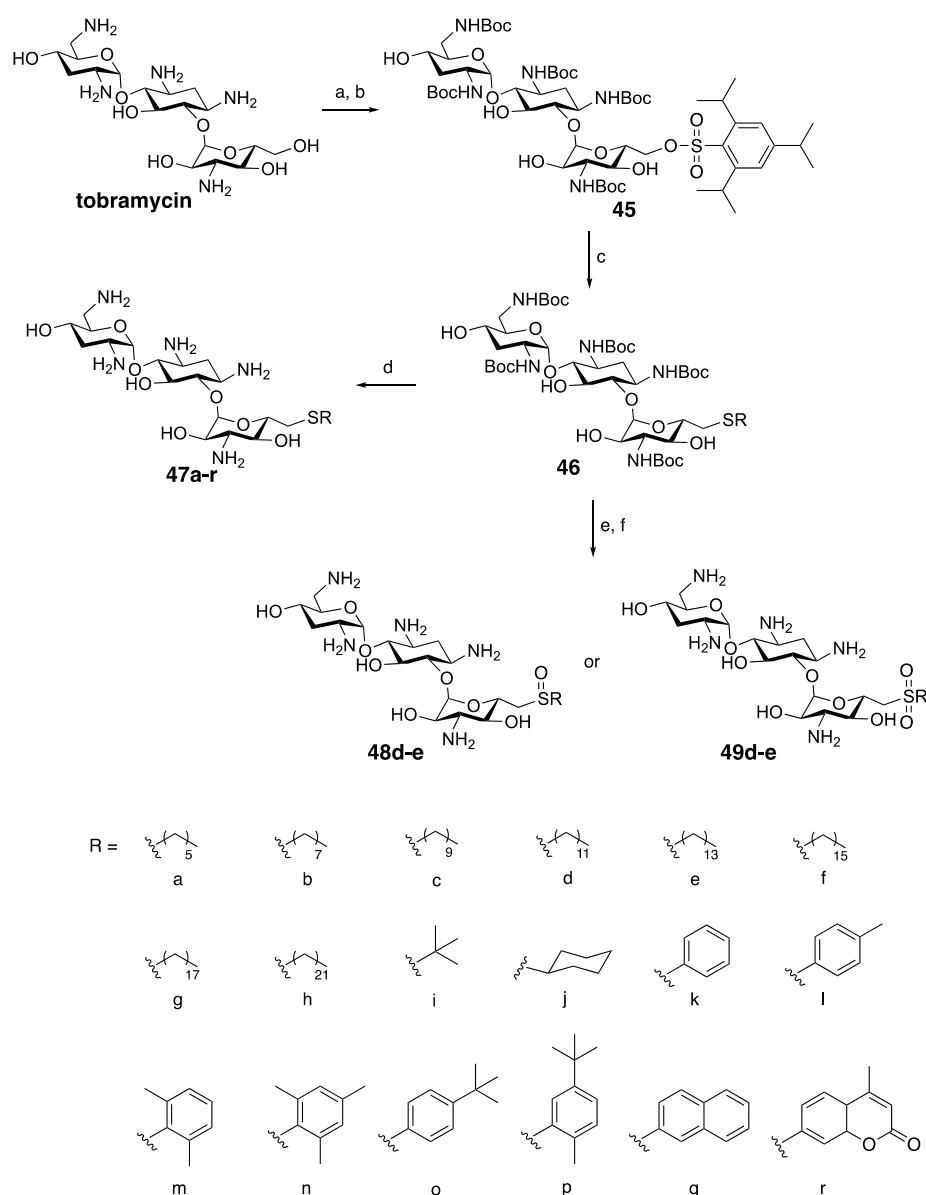
organism	kanamycin A	kanamycin B	<b>44c</b>	<b>44f</b>
<i>S. aureus</i> <sup>a</sup>	2	1	0.25	1
<i>S. aureus</i> <sup>b</sup>	128	>128	2	2
<i>S. epidermidis</i> <sup>c</sup>	1	0.25	<0.06	0.25
<i>S. epidermidis</i> <sup>d</sup>	8	32	0.25	0.25
<i>S. epidermidis</i> <sup>e</sup>	>128	>128	32	128
<i>E. faecalis</i> <sup>f</sup>	64	64	32	128
<i>E. coli</i> <sup>g</sup>	2	4	1	2
<i>E. coli</i> <sup>h</sup>	4	4	1	2
<i>K. pneumoniae</i> <sup>i</sup>	64	16	1	8
<i>P. aeruginosa</i> <sup>j</sup>	>128	64	0.5	2

<sup>a</sup> ATCC 29213; <sup>b</sup> ATCC 33591; <sup>c</sup> ATCC 12228; <sup>d</sup> methicillin-resistant clinical isolate; <sup>e</sup> clinical isolate expressing APH(3')-IIIa; <sup>f</sup> ATCC 29212; <sup>g</sup> ATCC 25922; <sup>h</sup> ATCC 35218; <sup>i</sup> ATCC 700603; <sup>j</sup> ATCC 27853.

In 2012, Herzog *et al.* described novel 6''-thioether tobramycin analogues and their corresponding S-oxidized compounds.<sup>65</sup> As shown in Scheme 1.3.1.10, the 6'' primary alcohol was selectively modified yielding analogs bearing hydrophobic alkyl chains, cyclic alkyls, and aryl rings to provide 6''-thioether tobramycin derivatives (**47a-r**). Further oxidations proceeded to generate 6''-sulfoxides **48d-e** and 6''-sulfones **49d-e** tobramycin derivatives. All these synthetic tobramycin amphiphiles were screened for their antibacterial activity against a panel of Gram-positive and Gram-negative bacterial strains including several tobramycin highly resistant strains

(Table 1.3.1.8). Compound **47e** with a C14 linear chain exhibited the greatest improvement in antibacterial activity with an MIC range between 0.3 to 18.8  $\mu\text{g/mL}$  against 19/21 strains.

Mechanistic studies indicated that the most potent amphiphile **47e** targets the bacterial membranes in contrast to the traditional AGs that target the ribosomal RNA.<sup>65</sup>



**Scheme 1.3.1.10.** Synthesis of 6''-thioether-, sulfoxide- and sulfone-based tobramycin

derivatives. Reagents and conditions: (a)  $(\text{Boc})_2\text{O}$ ,  $\text{Et}_3\text{N}$ ,  $\text{DMSO}/\text{H}_2\text{O}$ ; (b)  $\text{TrisylCl}$ , pyridine; (c)

RSH, Cs<sub>2</sub>CO<sub>3</sub>, DMF; (d) TFA; (e) *m*CPBA, CHCl<sub>3</sub>, (1.1 equiv. for **48** or 3 equiv. for **49**); (f) TFA.<sup>65</sup>

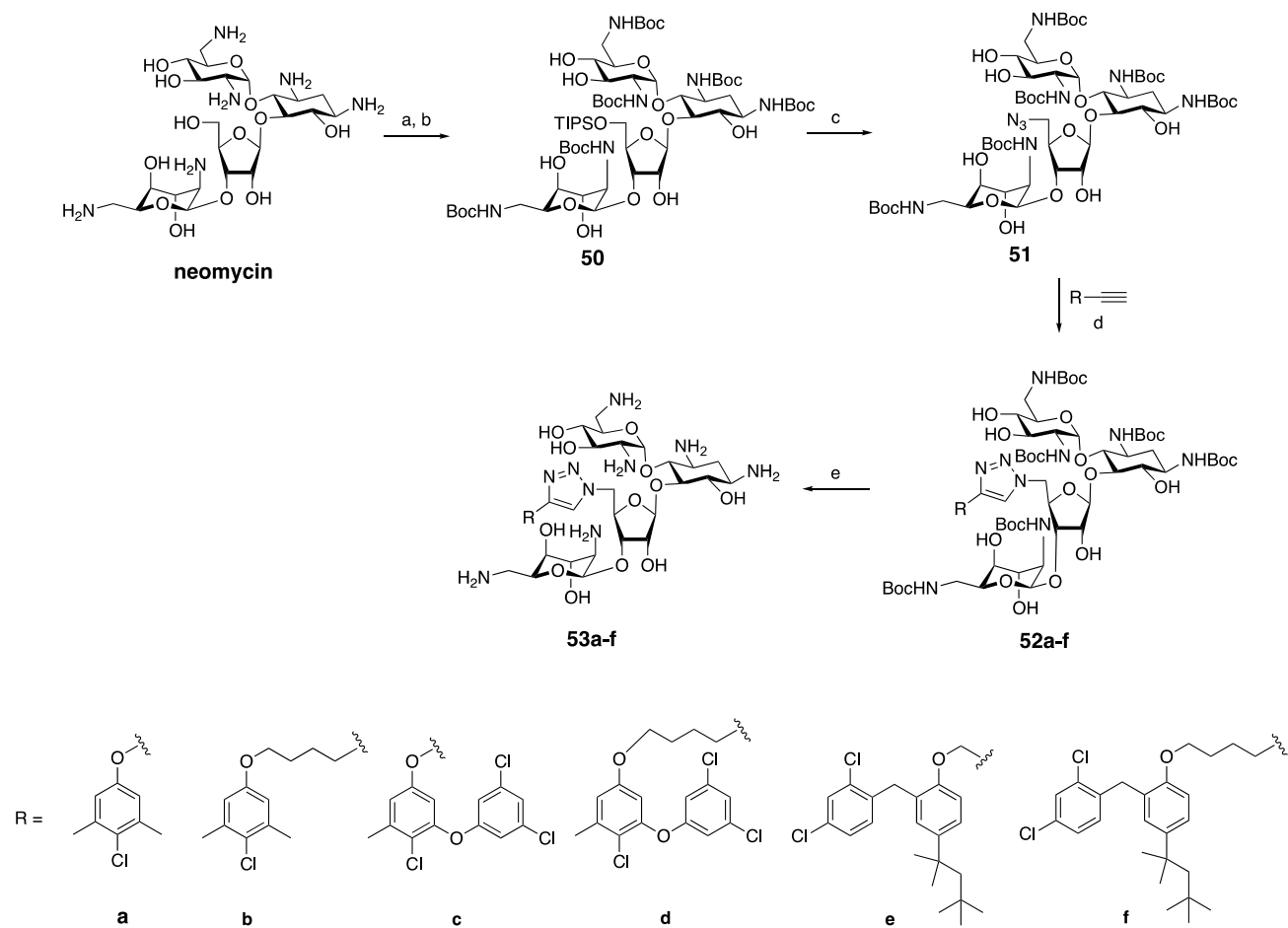
**Table 1.3.1.8.** MIC in µg/mL of tobramycin and 6"-thioether tobramycin analogue **47e**.<sup>65</sup>

organism	tobramycin	<b>47e</b>
<i>S. epidermidis</i> ATCC12228	0.3	1.2
<i>S. aureus</i> NorA	9.4	9.4
MRSA	>150	9.4
<i>S. pyogenes</i> serotype M12 (strain MGAS9429)	18.8	2.3
<i>S. mutans</i> UA159	75	2.3
<i>B. subtilis</i> 168	1.2	1.2
<i>B. subtilis</i> 168 with AAC(6'')/APH(2'')-pRB374	9.4	4.7
<i>B. cereus</i> ATCC11778	18.8	1.2
<i>B. anthracis</i> 34F2 Sterne strain	2.3	0.3
VRE	>150	18.8
<i>E. faecalis</i> ATCC29212	150	75
<i>L. monocytogenes</i> ATCC19115	4.7	9.4
<i>E. coli</i> BL21 (DE3)	4.7	4.7
<i>E. coli</i> BL21 (DE3) with pET22b	9.4	4.7
<i>E. coli</i> BL21 (DE3) with AAC(6'')/APH(2'')-pET22b	>150	4.7
<i>E. coli</i> BL21 (DE3) with AAC(3)-IV-Int-pET19b-pps	150	2.3
<i>E. coli</i> BL21 (DE3) with Eis	18.8	4.7

Table 1.3.1.8. *Cont.*

organism	tobramycin	<b>47e</b>
<i>E. coli</i> TolC	4.7	4.7
<i>E. coli</i> MC1061	9.4	4.7
<i>Shigella</i> clinical isolate 6831	18.8	18.8
<i>S. enterica</i> ATCC14028	150	37.5

In 2012, six novel neomycin-phenolic conjugates were designed and synthesized by our group.<sup>60</sup> “Click chemistry” was applied to create these amphiphilic conjugates from neomycin-C5"-derived azide and alkyne-modified phenolic disinfectants as the hydrophobic segment (Scheme 1.3.1.11). In general, these conjugates exhibited improved activity against neomycin resistant bacteria. When compared to parent neomycin antibiotic the most potent compounds appeared to be **53d** and **53e** which manifested significant activity against MDR strains such as MRSA (8  $\mu\text{g}/\text{mL}$ ) (Table 1.3.1.9). Moreover, these two conjugates were not appreciably hemolytic nor did they show strong binding to serum proteins commonly observed with other cationic antimicrobial peptides and detergents.<sup>77</sup>



**Scheme 1.3.1.11.** Synthesis of neomycin-phenolic conjugates (**53a-f**). Reagents and conditions:

(a)  $\text{Boc}_2\text{O}$ ,  $\text{Et}_3\text{N}/\text{MeOH}/\text{H}_2\text{O}$ ; (b) TIPS-Cl, pyridine; (c)  $\text{NaN}_3$ ,  $\text{DMF}/\text{H}_2\text{O}$ ; (d) alkyne-modified phenolic disinfectants, CuI, DIPEA, CAN; (e) TFA/ $\text{H}_2\text{O}$ .<sup>60</sup>

**Table 1.3.1.9.** MIC in  $\mu\text{g/mL}$  of neomycin and neomycin-phenolic conjugates.<sup>60</sup>

organism	neomycin <sup>a</sup>	53d	53e
<i>S. aureus</i> ATCC 29213	1	4	8
MRSA ATCC 33592	256	8	8
MSSE 81388 CANWARD 2008	0.5	4	4
MRSE CAN-ICU 61589	<0.25	2	1
<i>E. faecalis</i> ATCC 29212	16	16	8
<i>E. faecium</i> ATCC 27270	4	8	8
<i>S. pneumoniae</i> ATCC 49619	32	64	64
<i>E. coli</i> ATCC 25922	4	16	16
<i>E. coli</i> CAN-ICU 61714 (GEN-R)	1	16	64
<i>E. coli</i> CAN-ICU 63074 (AMK-R)	8	64	64
<i>P. aeruginosa</i> ATCC 27853	512	128	128
<i>P. aeruginosa</i> CAN-ICU 62308	256	64	64
<i>S. maltophilia</i> CAN-ICU 62584	>512	>512	512
<i>A. baumannii</i> CAN-ICU 63169	64	128	64
<i>K. pneumoniae</i> ATCC 13883	0.25	4	64

<sup>a</sup> Neomycin trisulfate hydrate

In the same year, our group prepared a series of tobramycin C6" modified-lipid and -peptide triazole conjugates (Figure 1.3.1.4) and studied their antibacterial activities against a panel of Gram-positive and Gram-negative bacterial strains, including MDR clinical isolates.<sup>64</sup>

Replacement of the hydrophobic tail in tobramycin C6" position by an aromatic tail, various

lengths of linear lipid tails, a partially fluorinated lipid or by a triazole-linked peptide revealed that the antibacterial activity of amphiphilic tobramycin is greatly affected by the nature of the hydrophobic lipid tail as tobramycin-C16-lipid **54d** displayed the most potent antibacterial activity among this series of analogues against most Gram-positive (MICs = 4 to 8  $\mu\text{g/mL}$ ) and some Gram-negative strains including *E. coli* and *P. aeruginosa* (Table 1.3.1.10). In contrast, the SAR studies of the aminoglycoside-derived lipid conjugates (**54d**, **55a** and **56a**) indicated that the polycationic aminoglycoside-based head group was less important for induction of antibacterial activity.

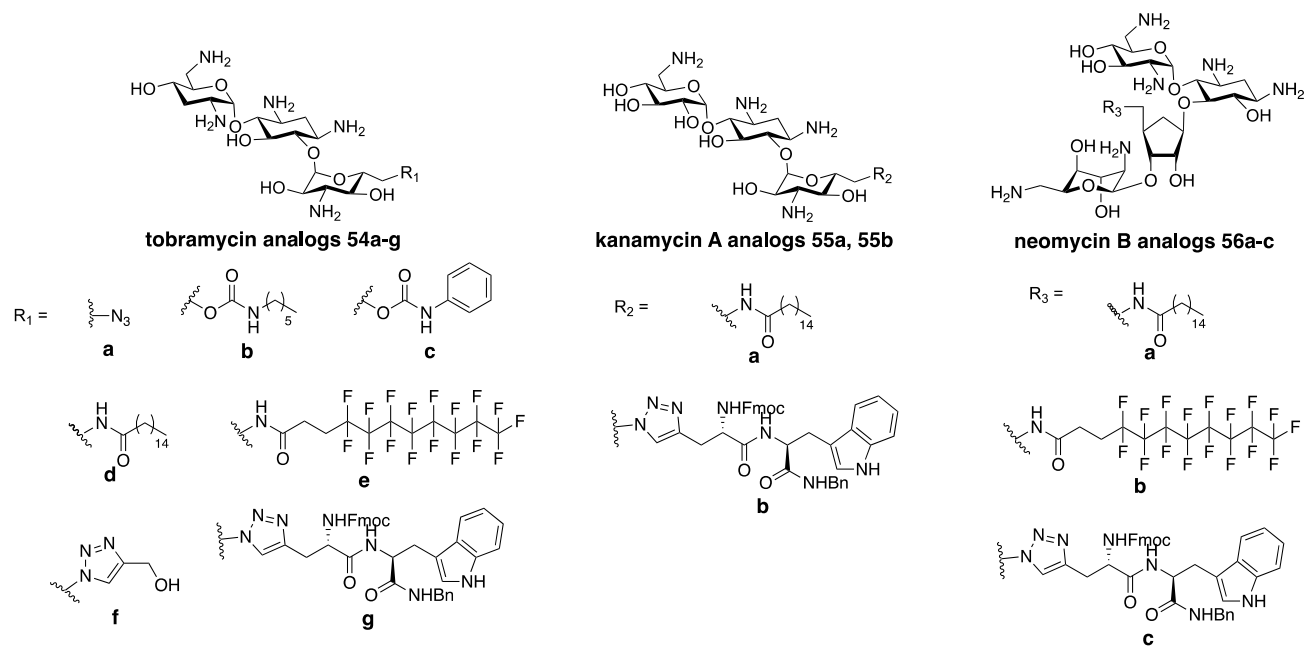


**Figure 1.3.1.4.** Structures of tobramycin, kanamycin A and neomycin B analogues.<sup>64</sup>

**Table 1.3.1.10.** MIC in  $\mu\text{g/mL}$  of tobramycin, kanamycin A, neomycin B and amphiphilic aminoglycosides conjugates.<sup>64</sup>

organism	tobramycin	<b>54d</b>	kanamycin	<b>55a</b>	neomycin	<b>56a</b>
<i>S. aureus</i> ATCC 29213	0.5	8	4	8	1	4
MRSA ATCC 33592	0.5	8	>512	16	256	8
<i>S. epidemidis</i> ATCC14990	$\leq 0.25$	4	2	2	0.25	2
MRSE CAN-ICU 61589	2	<0.25	128	2	0.5	2
<i>E. faecalis</i> ATCC 29212	8	8	N.D.	8	N.D.	N.D.
<i>E. faecium</i> ATCC 27270	16	4	N.D.	8	N.D.	N.D.
<i>S. pneumoniae</i> ATCC 49619	2	128	8	64	32	64
<i>E. coli</i> ATCC 25922	0.5	32	8	32	4	32
<i>E. coli</i> CAN-ICU 61714 (GEN-R)	8	32	16	32	8	64
<i>E. coli</i> CAN-ICU 63074 (AMK-R)	8	8	32	32	N.D.	N.D.
<i>P. aeruginosa</i> ATCC 27853	0.5	128	>512	64	512	128
<i>P. aeruginosa</i> CAN-ICU 62308	16	16	>512	64	512	128
<i>S. maltophilia</i> CAN-ICU 62584	>512	256	>512	<128	>512	N.D.
<i>A. baumannii</i> CAN-ICU 63169	16	256	16	<128	32	N.D.
<i>K. pneumoniae</i> ATCC 13883	>0.25	32	0.5	16	$\leq 0.25$	N.D.

In 2013, Décout and co-workers reported on the tuning of the antibacterial activities of amphiphilic neamine derivatives as an extension of previous work.<sup>68,69</sup> A series of di- or tri-alkylated neamine analogues and similar di- or tri-alkylated paromamine homologues (Figure 1.3.1.5) were synthesized as previously reported<sup>69</sup> in order to evaluate the antibacterial activities

and proceed to systematic SAR studies. It was discovered that the three neamine derivatives, 3',6-di-2-naphthylpropyl- (**58f**), 3',6-di-2-naphthylbutyl- (**58g**) and 3',6-dinonyl-derived neamine (**58k**), were active against susceptible and resistant Gram-positive and Gram-negative bacteria. Among them, 3',6-di-2-naphthylpropyl-derived neamine derivative (**58f**) appeared to be the most optimal compound with a broad spectrum of activity (Table 1.3.1.11) as well as the lowest toxicity in eukaryotic cells (at 10  $\mu$ M, 90% viability) which can be related to a higher selectivity for bacterial membranes. More importantly, quantitative SAR studies were conducted and, as an example, the 1/MIC (mL/ $\mu$ g) values of the 3',6-di-alkylated neamine derivatives as a function of the corresponding calculated logP for MRSA and susceptible *P. aeruginosa* was plotted (Figure 1.3.1.6). Critical windows of lipophilicity were discovered which are necessary for obtaining significant antibacterial effects (Figure 1.3.1.6). Further mode of action studies of the three potent amphiphilic neamine-based derivatives confirmed a strong binding to LPS of *P. aeruginosa* as well as membrane depolarization.<sup>78</sup>

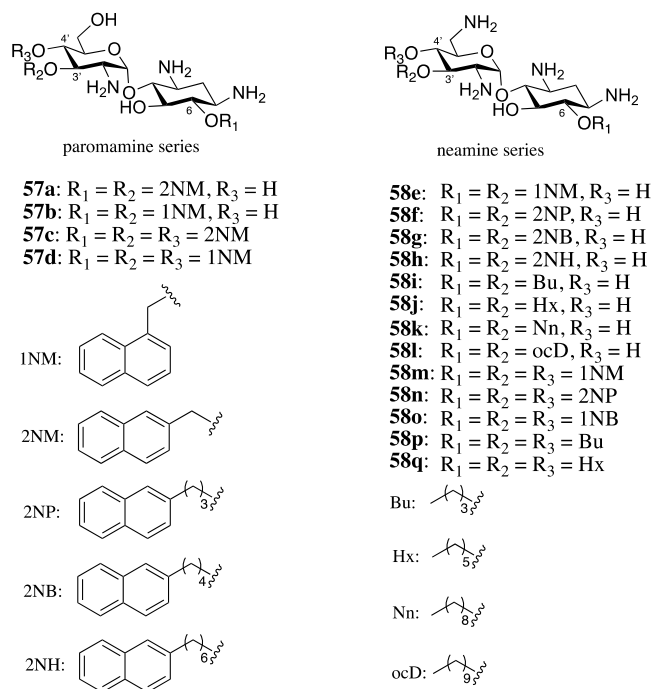


**Figure 1.3.1.5.** Structure of the synthesized di- or tri-alkylated paromamine and neamine derivatives.<sup>69</sup>

**Table 1.3.1.11.** Minimal inhibitory concentrations (MIC) in  $\mu\text{g/mL}$  of neomycin B, neamine, gentamicin, amikacin, tobramycin and neamine derivatives.<sup>69</sup>

organism	neomycin B	neamine	gentamicin	amikacin	tobramycin	58f	58g	58k
<i>S. aureus</i> <sup>a</sup>	2	32	N.D.	N.D.	N.D.	2	2	2
<i>S. aureus</i> <sup>b</sup>	>128	>128	N.D.	N.D.	N.D.	2	2	4
<i>S. aureus</i> <sup>c</sup>	128	128	N.D.	N.D.	N.D.	1	2	2
<i>A. lwoffii</i> <sup>d</sup>	0.5	2	0.5	0.5	0.5	N.D.	4	N.D.
<i>A. lwoffii</i> <sup>e</sup>	>128	>128	4–8	>128	1	N.D.	64	N.D.
<i>P. aeruginosa</i> <sup>f</sup>	64	>128	1	2–4	0.5	4	4	4
<i>P. aeruginosa</i> <sup>g</sup>	128	>128	>128	4	128	16	8	4
<i>P. aeruginosa</i> <sup>h</sup>	32	>128	4	8–16	1	16–32	8	4
<i>K. pneumoniae</i> <sup>i</sup>	16–32	32–64	8	0.5	4	N.D.	32	N.D.
<i>E. coli</i> <sup>j</sup>	2	32	<0.5–1	4	0.5	16	8	4–8
<i>E. coli</i> <sup>k</sup>	4	>128	1	64	32	8	4	2–4
<i>E. coli</i> <sup>l</sup>	32	32	64–128	2	64	16	8	4

<sup>a</sup> *S. aureus* ATCC 25923; <sup>b</sup> *S. aureus* ATCC 33592 HA-MRSA; <sup>c</sup> *S. aureus* VRSA-VRS-2; <sup>d</sup> *A. lwoffii* ATCC 17925; <sup>e</sup> *A. lwoffii* AI.88-483 APH3'-Via; <sup>f</sup> *P. aeruginosa* ATCC 27853; <sup>g</sup> *P. aeruginosa* Psa.F03 AAC6'-IIA; <sup>h</sup> *P. aeruginosa* PA22 (PT629) surexp MexXY; <sup>i</sup> *K. pneumoniae* ATCC 700603; <sup>j</sup> *E. coli* ATCC 25922; <sup>k</sup> *E. coli* PAZ505H8101 AAC6'-IB; <sup>l</sup> *E. coli* L58058.1 ANT2"-IA.

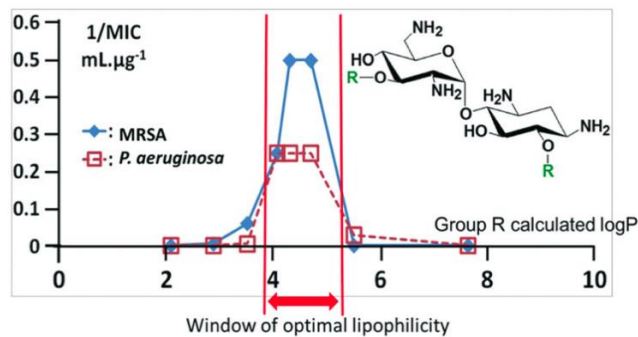
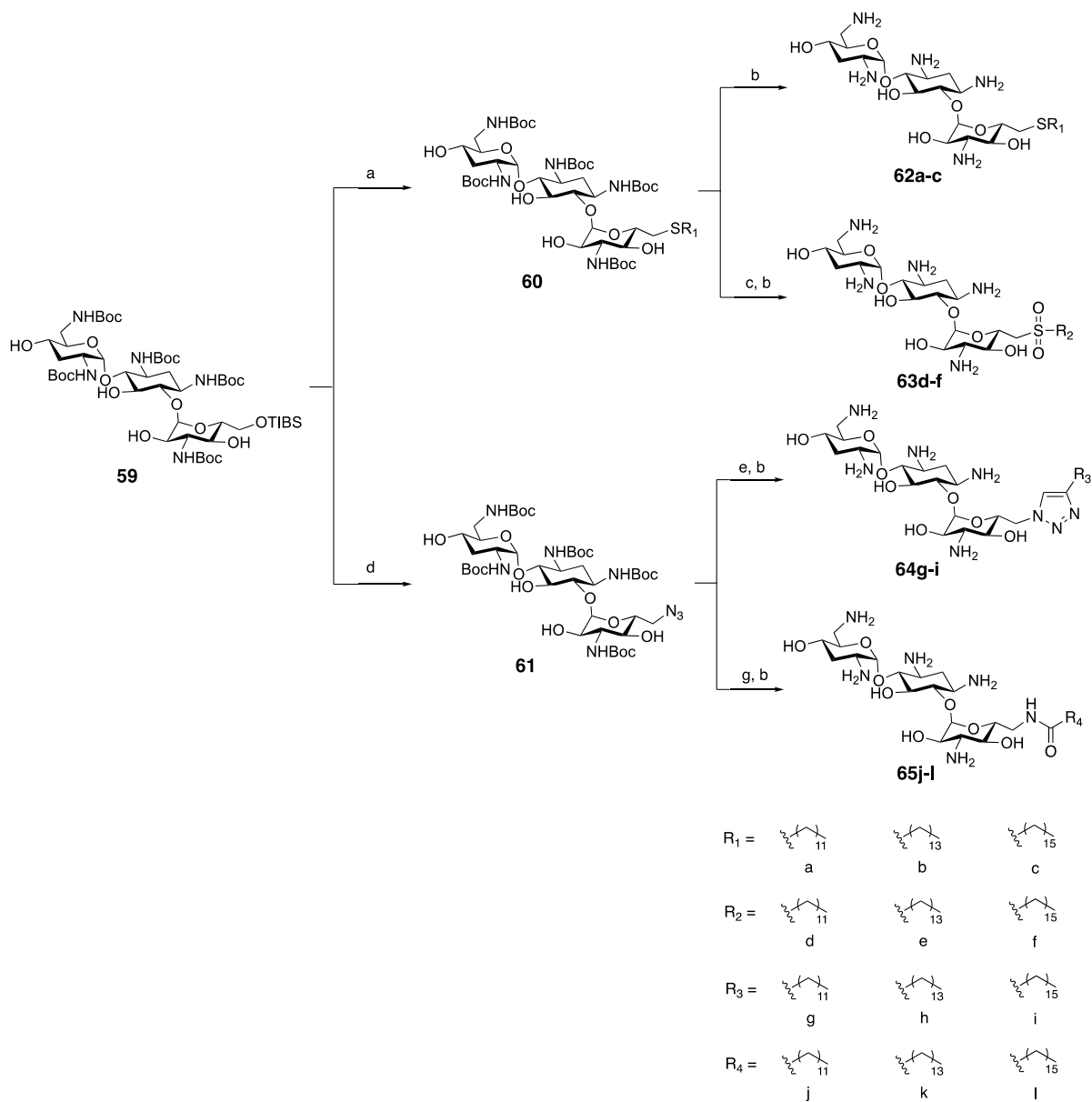


**Figure 1.3.1.6.** Values of 1/MIC ( $\text{mL}/\mu\text{g}$ ) against ATCC 33592 HA-MRSA and *P. aeruginosa* ATCC 27853 as a function of calculated logP of the lipophilic substituent carried by the synthesized 3',6-di-alkylated neamine derivatives (calculated logP of the corresponding alkanes).<sup>68</sup> Adapted with permission from *J. Med. Chem.* **2013**, *56* (19), 7691-7705. Copyright (2013) American Chemical Society.

In 2013, Herzog and Fridman *et al.* investigated the influence of different types of linkage between the AG and the hydrophobic chain on the specificity of these amphiphils towards bacterial membranes in terms of hemolytic activity.<sup>63</sup> A series of 6"-aliphatic chain-based tobramycin analogues altering the chemical linkage between the AG and the various lengths of hydrophobic linear chain segments were synthesized and biologically evaluated. The synthesis of thioether-linked, sulfone-linked, triazole ring-linked and amide bond-linked tobramycin analogues is summarized in Scheme 1.3.1.12 according to the previously reported procedure<sup>53</sup>. The MIC results showed that all the analogues with a C14 aliphatic chain (**62b**, **63e**, **64h**, and **65k**) manifested the most potent antibacterial activities compared to the parent drug indicating that the chemical links between the cationic hydrophilic AG and that hydrophobic aliphatic chain did not significantly affect the antibacterial performances except for the sulfone-linked analogues against the tested strains. Moreover, it was observed that the amide bond-linked

tobramycin analogue bearing a C12 aliphatic chain (**65j**) exhibited a dramatic reduction in red blood cells hemolysis, whereas the C12-analogues with triazole ring- (**64g**) and thioether-linkage (**62a**) caused extensive hemolysis at the same concentration.



**Scheme 1.3.1.12.** Synthesis of amphiphilic tobramycin analogues. Reagents and conditions: (a)  $R_1SH$ ,  $CS_2CO_3$ , DMF; (b) neat TFA, rt; (c) *m*CPBA (3 equiv.),  $CHCl_3$ , rt; (d)  $NaN_3$ , DMF; (e)  $R_3CCH$ ,  $CuSO_4 \cdot 5H_2O$  (0.1 equiv.), sodium ascorbate (0.2 equiv.), DMF, microwave irradiation;

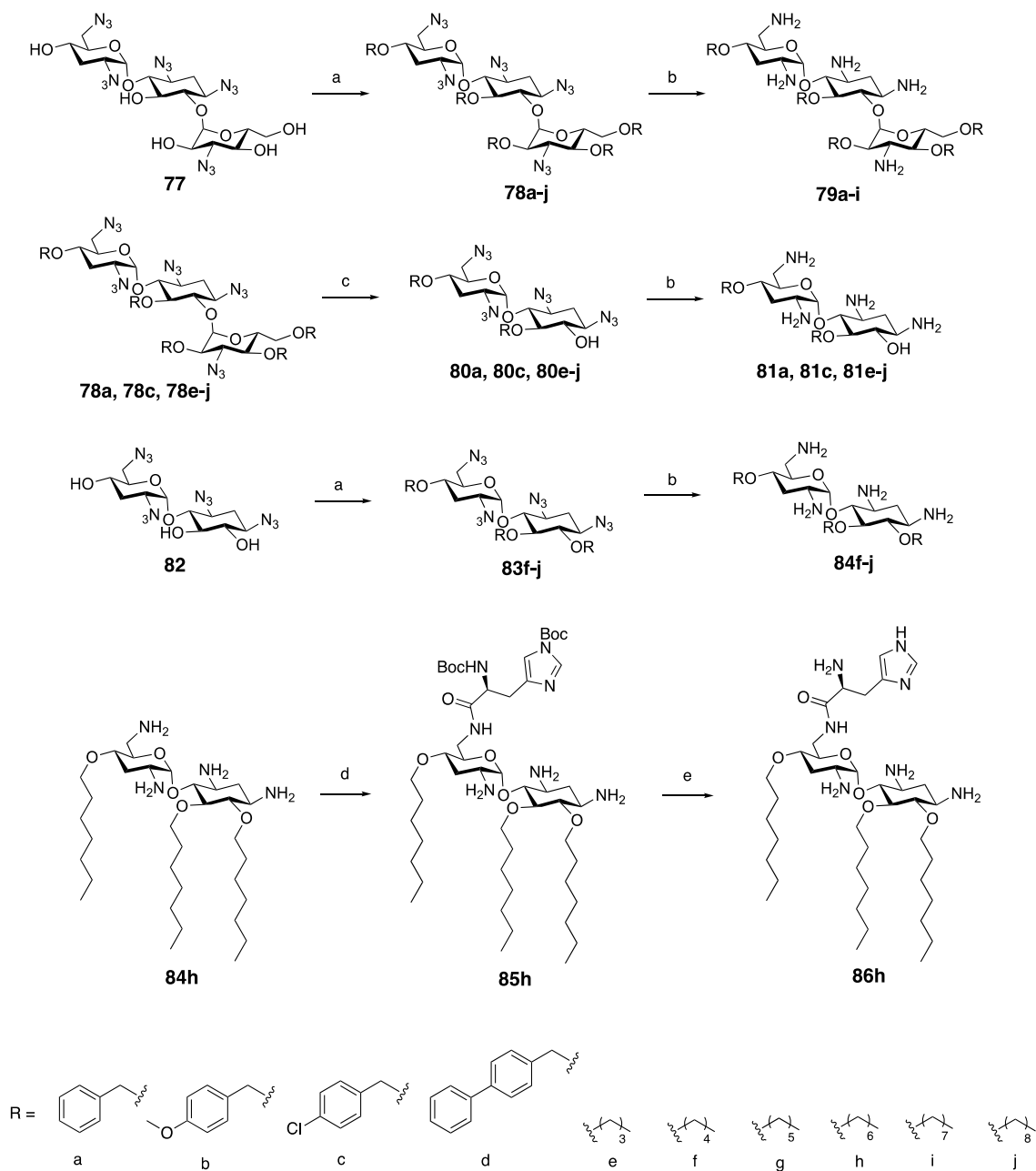
(f)  $\text{PMe}_3$  (1M in THF, 1.1 equiv.), 0.01 M aqueous NaOH/THF: 1/20; (g)  $\text{R}_4\text{COOH}$ , HBTU, DIEA, DMF.<sup>63</sup>

In the same year, Berkov-Zrihen and Fridman *et al.* developed a short site-selective strategy for the displacement of tobramycin hydroxyls for preparation of a series of hetero- and homo-dithioether tobramycin-based cationic amphiphiles.<sup>79</sup> It was found that the site-selective conversion of secondary alcohols of tobramycin into leaving groups is dependent on the amine protecting groups. Thus 4',6''-Di-*O*-TIBS tobramycin derivative (**67**) (34% isolated yield) was produced by penta-*NH*-Boc-tobramycin (**66**) reacting with an excess of 2,4,6-triisopropylbenzenesulfonyl chloride (TIBSCl) whereas 2'',6''-di-*O*-TIBS derivatives (**73**) (27% isolated yield) were synthesized by using penta-azido tobramycin (**72**) as the starting material in the same reaction (Scheme 1.3.1.13). Chemoselective thioetherification of *O*-TIBS groups of di-*O*-TIBS derivatives proceeded at different temperatures resulting in a set of 4',6''-homo-dithioether (**70a-c**), 4',6''-hetero-dithioether (**71a-c**) and 3'',6''-homo-dithioether (**76a-c**) tobramycin-based analogues. It is noteworthy to mention that the synthesis of 3'',6''-homo-dithioether tobramycin-based analogues (**76a-c**) from 2'',6''-di-*O*-TIBS intermediate (**74**) occurred via an intramolecular nucleophilic attack to form a Hough-Richardson type aziridine.<sup>80-</sup>  
<sup>82</sup> Next, nucleophilic opening of this ziridine occurred by attack at the C-3'' position to yield the products with  $\alpha$ -D-altro-configuration in accordance with the Fürst-Plattner rule<sup>83</sup> (Scheme 1.3.1.13). The antibacterial activity was tested on a panel of bacterial strains. 4',6''-dithioether analogues **70b**, **70c** and **71a** were potent against MRSA ( $\text{MICs} \leq 8 \mu\text{g/mL}$ ). Among the tested strains, compound **71a** demonstrated the most potent antibacterial activity and caused a low percentage of RBC hemolysis.



chloride (TIBSCl) (15 equiv), pyridine, rt, 18 h; (g) Pd/C, H<sub>2</sub>, MeOH; (h) Boc<sub>2</sub>O, dioxane; (i) R<sub>3</sub>SH (14 equiv), Cs<sub>2</sub>CO<sub>3</sub> (1 equiv), DMF, 75 °C, 15 h.<sup>79</sup>

Berkov-Zrihen and Fridman *et al.* investigated tobramycin and its pseudo-disaccharide nebramine as scaffolds for the development of antimicrobial cationic amphiphiles.<sup>61</sup> A set of tobramycin analogues **79a-i** were synthesized from penta-azido tobramycin followed by etherification of all five alcohol groups (Scheme 1.3.1.14). Reduction of the azido groups via the Staudinger reaction afforded the tobramycin-derived amphiphiles. Heating penta-azido tobramycin intermediates to reflux in acidic conditions resulted in selective cleavage of the protected 3-deoxy-3-amino-D-glucose ring (ring III) of the tobramycin pseudo-trisaccharide to generate the corresponding pseudo-disaccharide nebramine derivatives. Further synthetic steps were carried out as shown in Scheme 1.3.1.14 to generate a set of amphiphilic nebramine-based analogues. Several analogues (**79a**, **79c**, **79f**, **81j**, **84g-i**, and **86h**) manifested good antibacterial activity against tested Gram-positive bacteria compared to the parent AG tobramycin. Only **84h** exhibited marked activity against all the tested Gram-positive and Gram-negative bacterial strains (MICs  $\leq 8 \mu\text{g/mL}$ ). Mode of action studies indicated that the anti-Gram-negative activity of **84h** might be related to the interactions with LPS, a major component of the outer leaflet of the outer membrane. It was also confirmed that derivative **79a** selectively disrupted the bacterial membrane structure of Gram-positive bacteria, even though it did not cause significant RBC hemolysis at concentrations near the MIC values.



**Scheme 1.3.1.14.** Synthesis of amphiphilic nebramine analogues. Reagents and conditions: (a) alkyl bromide, alkyl chloride, or alkyl iodide; NaH; TBAI; DMF; (b) 1.0 M P(Me)<sub>3</sub> in THF, H<sub>2</sub>O/THF (1:9), 0.1M NaOH; (c) 1.5 M H<sub>2</sub>SO<sub>4</sub> in MeOH, reflux; (d) *N,N*-Bis-Boc-*L*-histidine *N*-hydroxysuccinimide ester, K<sub>2</sub>CO<sub>3</sub>, MeOH; (e) 95% TFA.<sup>61</sup>

**Table 1.3.1.12.** Minimal inhibitory concentrations (MIC) in  $\mu\text{g/mL}$  of polymyxin B, tobramycin and amphiphilic AG analogues.<sup>61</sup>

organism	polymyxin B	tobramycin	79a	79c	79f	81j	84g	84h	84i	86h
MRSA	64	>64	16	8	4	4	8	2	8	4
<i>S. aureus</i> <sup>a</sup>	64	4	8	8	16	4	4	2	4	4
<i>S. pyogenes</i> <sup>b</sup>	64	16	4	4	2	4	2	4	4	2
<i>S. pyogenes</i> <sup>c</sup>	64	4	4	8	2	4	2	1	4	4
<i>S. epidermidis</i> <sup>d</sup>	64	32	8	16	4	4	4	2	16	4
<i>E. coli</i> <sup>e</sup>	2	8	>64	>64	>64	>64	64	4	>64	32
<i>K. pneumoniae</i> <sup>f</sup>	16	2	>64	>64	>64	64	>64	8	>64	64
<i>K. pneumoniae</i> <sup>g</sup>	>64	4	>64	>64	>64	64	32	8	32	32
<i>P. aeruginosa</i> <sup>h</sup>	2	1	>64	>64	>64	32	32	4	32	>64
<i>P. aeruginosa</i> <sup>i</sup>	4	>64	>64	>64	>64	64	>64	8	>64	>64

<sup>a</sup> *S. aureus* Cowan ATCC 12598; <sup>b</sup> *S. pyogenes* glossy; <sup>c</sup> *S. pyogenes* JRS75; <sup>d</sup> *S. epidermidis* RP62A ATCC 35984; <sup>e</sup> *E. coli* ATCC 25922; <sup>f</sup> *K. pneumoniae* K36; <sup>g</sup> *K. pneumoniae* K21; <sup>h</sup> *P. aeruginosa* PAO1; <sup>i</sup> *P. aeruginosa* ATCC 33347.

In 2015, Benhamou and Fridman *et al.* reported the influence of di-*N*-methylation of the anti-Gram-positive aminoglycoside-derived bacterial membrane disruptors on antimicrobial activity.<sup>84</sup> Di-*N*-methylation of all the primary amines of nebramine-, tobramycin- and paromomycin-derived cationic amphiphiles via reductive amination reaction in the presence of formaldehyde and sodium cyanotrihydridoborate afforded a series of di-*N*-methylated analogues (Figure 1.3.1.7). All these modified analogues manifested either a broader antimicrobial

spectrum or improved antimicrobial activity, or both compared to their parent amphiphiles (Table 1.3.1.13). The possibility that this occurred by enhancing LPS affinity with this modification and, thereby facilitating the disruption of the outer membrane of Gram-negative bacteria was ruled out as it was shown that di-*N*-methylation of AG-based amphiphiles did not associate with improvement in LPS binding affinity. Further mechanism studies were carried out and indicated that the more hydrophobic di-*N*-methylated amphiphiles increased the van der Waals interactions with bacterial membrane lipids resulting in non-specific membrane disruption.

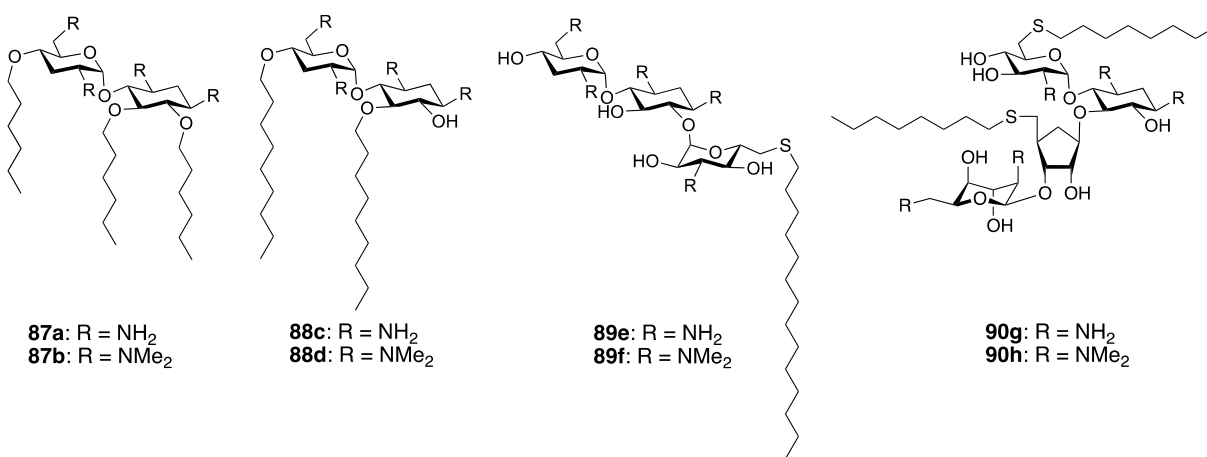


**Figure 1.3.1.7.** Structure of amphiphilic nebramine, tobramycin and paromomycin analogues.<sup>84</sup>

**Table 1.3.1.13.** Minimal inhibitory concentrations (MIC) in  $\mu\text{g/mL}$  of colistin, tobramycin and amphiphilic AG derivatives.<sup>84</sup>

organism	colistin	tobramycin	87a	87b	88c	88d	89e	89f	90g	90h
MRSA <sup>a</sup>	>64	>64	2	1	2	1	8	4	4	2
<i>S. pyogenes</i> <sup>b</sup>	>64	32	2	1	1	1	2	0.5	2	1
<i>S. aureus</i> <sup>c</sup>	>64	4	4	0.5	2	1	8	4	16	2
<i>L. monocytogenes</i> <sup>d</sup>	>64	4	4	2	2	2	4	2	4	2
<i>E. faecalis</i> <sup>e</sup>	>64	2	8	2	4	2	16	2	8	4
<i>E. coli</i> <sup>f</sup>	4	2	8	2	64	2	64	2	>64	8
<i>E. coli</i> <sup>g</sup>	2	4	16	2	32	2	64	4	64	8
<i>K. pneumoniae</i> <sup>h</sup>	16	2	16	8	64	8	64	4	>64	16
<i>K. pneumoniae</i> <sup>i</sup>	8	4	16	8	64	8	>64	8	>64	16
<i>K. pneumoniae</i> <sup>j</sup>	8	2	16	16	64	16	>64	8	>64	16
<i>S. sonnei</i> <sup>k</sup>	2	16	32	2	32	2	64	4	>64	4

<sup>a</sup> MRSA ATCC 33592; <sup>b</sup> *S. pyogenes* Rosenbach ATCC 14289; <sup>c</sup> *S. aureus* Cowan; <sup>d</sup> *L. monocytogenes* ATCC 19115; <sup>e</sup> *E. faecalis* ATCC 29212; <sup>f</sup> *E. coli* ATCC 25922; <sup>g</sup> *E. coli* ATCC 9637; <sup>h</sup> *K. pneumoniae* K21; <sup>i</sup> *K. pneumoniae* K36; <sup>j</sup> *K. pneumoniae* K55; <sup>k</sup> *S. sonnei* clinical isolate 6831.

Previous work in Décout's group had described amphiphilic 3',6-dialkyl neamine derivatives with a broad spectrum of activity and low toxicity in eukaryotic cells. It was demonstrated that the nature of the grafted hydrophobic moieties was critical for the molecule's ability to displace cations binding to LPS and altering the bacterial outer membrane.<sup>78</sup> In 2016, as a logical extension, Décout and coworkers delved into neamine by placing the same alkyl

hydrophobic scaffolds at C-3' and C-4' positions in ring II in comparison to their previously reported active 3',6-dialkyl neamine isomers (Figure 1.3.1.8).<sup>67</sup> Moreover, to investigate the role of ring I in neamine-based amphiphiles, further structure modifications were applied by replacing ring I with acyclic scaffold mimics generating amphiphilic 3,4-dialkyl derivatives of 6-amino-6-deoxyglucosamine named neosamine (Figure 1.3.1.8). The synthesis of neosamine derivative was from *N*-acetyl-D-glucosamine (Figure 1.3.1.8) to prepare the key intermediate  $\alpha$ -allyl neosamine. The reactive allyl group was chemically modified through epoxidation and ring-opening to introduce various side chains with hydroxyl and/or amine functions in order to mimic ring I of neamine and also to adjust the lipophilicity/hydrophilicity (Scheme 1.3.1.15).

Among the newly synthesized and the previously reported AAGs, the antibacterial evaluation manifested that the 3',6-dinonyl neamine derivative (3',6-diNn) (Figure 1.3.1.8) was the most active compound against all selected strains excepted the resistant *A. lwoffii* strain. The 3',4'-dinonyl isomer (3',4'-diNn) (**94**) showed similar good activities against *S. aureus* and *E. coli* and sensitive *A. lwoffii* strain but lower activities against *P. aeruginosa* and sensitive *K. pneumoniae*. The allyl neosamine derivatives **98**, **103**, and **104** showed only a good activity against *S. aureus* and sensitive *A. lwoffii* strains (MIC = 4–8  $\mu\text{g/mL}$ ). The more hydrophobic neosamine derivatives **116**, **117**, **108**, **109-121** exhibited similar good antibacterial activity against all selected sensitive and resistant strains (MIC = 1–16  $\mu\text{g/mL}$ ). A membrane permeabilization assay showed the 3',6-diNn neamine derivative (Figure 1.3.1.8) induced the highest dose-dependent effect among the most active dinonyl derivatives on permeabilization of the *P. aeruginosa* inner membrane.

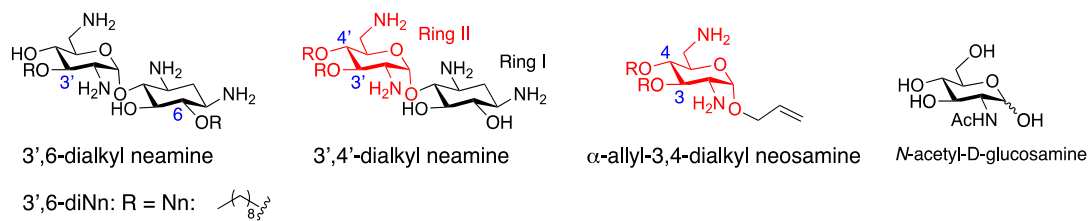
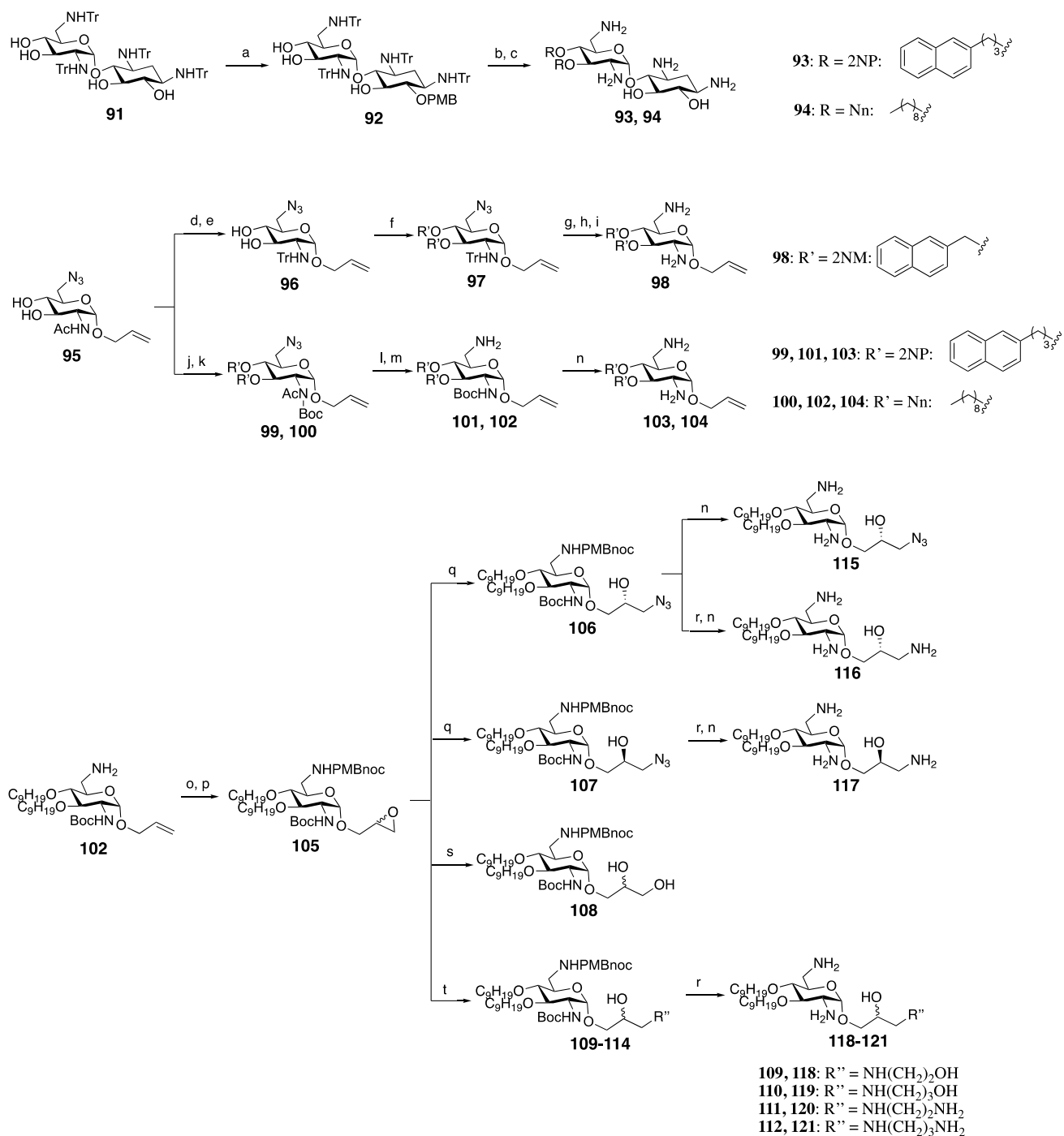


**Figure 1.3.1.8.** Structures of amphiphilic 3'6-dialkyl-neamine, 3'4'-dialkyl neamine derivatives, 1- $\alpha$ -allyl-3,4-dialkyl neosamine derivatives and *N*-acetyl-D-glucosamine.<sup>67</sup>



**Scheme 1.3.1.15.** Synthesis of amphiphilic neamine and neosamine derivatives. Reagents and conditions: (a) TBAF, 50% a.q. NaOH/toluene, PMBCl (2.5 equiv), rt, 1h; (b) R = 2NP: NaH/DMF, 3-(2'-naphthyl)propyl bromide, rt, 5 h; R = Nn: TBAF (2 equiv), 50% a.q. NaOH/toluene, 1-nonyl bromide, rt; (c) TFA, DCM, anisole, 0 °C; (d) KOH, EtOH, reflux; (e)

TrCl, DMF, Et<sub>3</sub>N, rt, 8 h; (f) 2NMBr, NaH, DMF, rt, 10 h; (g) Ph<sub>3</sub>P, THF/H<sub>2</sub>O (19/1), 80 °C, 6 h; (h) TFA/anisole (1/1), 0 °C, 3 h; (i) Dowex resin (Cl<sup>-</sup> ion exchange); (j) TBAF (2 equiv), 50% a.q. NaOH/toluene or NaH/DMF, C<sub>9</sub>H<sub>19</sub>Br (3 equiv), rt, 5 h; NaH, DMF, 2NPBr, 50 °C, 20 h; (k) Boc<sub>2</sub>O, DMAP, THF, 45 °C, 6 h; (l) (CH<sub>3</sub>O<sup>-</sup>,Na<sup>+</sup>)/CH<sub>3</sub>OH, rt, 6 h. (m) PPh<sub>3</sub>, THF/H<sub>2</sub>O, rt, 4 h; (n) TFA, DCM, rt, 4 h; (o) *p*-methoxybenzyl-S-(4,6-dimethylpyrimidin-2-yl) thiocarbonate, DCM, rt, 14 h; (p) *m*CPBA (2.5 equiv), DCM, rt, 14 h; (q) NaN<sub>3</sub> (excess), DMF, 70 °C, 14 h; (r) PPh<sub>3</sub>, THF/H<sub>2</sub>O, rt, 14 h; (s) TFA/H<sub>2</sub>O, rt, 14 h; (t) amine in excess, DCM, 35 °C, 6 h.<sup>67</sup>

### 1.3.2 Amphiphilic Aminoglycosides as Adjuvants in Combination Therapies

Resistance to available antibiotics in pathogenic bacteria is one of the greatest current threats to human health since there are growing numbers of reports of multi-drug resistant (MDR) and extremely drug-resistant (XDR) bacteria which have led to the reliance on older and more toxic antibiotics such as colistin in clinical practice.<sup>85,86</sup> Despite efforts aimed at the discovery of new antibiotics, especially those with truly novel chemical scaffolds and new modes of action, in the hope to replace those being abandoned for lack of significant activity against resistant isolates, this alone may not be enough to prevail in the battle against rapidly emerging bacterial resistance. There is a growing gap between the clinical need and a constant supply of new antibiotics. As a result, we must rethink and try to explore alternative approaches in order to prolong the lifespan of those lifesaving legacy antibiotics other than entirely relying on discovery and development of new antibiotics. One such approach is co-administration of antibiotic adjuvants,<sup>87-89</sup> which are compounds that have little or no antibiotic activity by themselves but potentiate the activity of current antibiotics by either blocking resistance or by boosting the host response to infection.<sup>90</sup> This approach has the potential to facilitate the re-introduction of

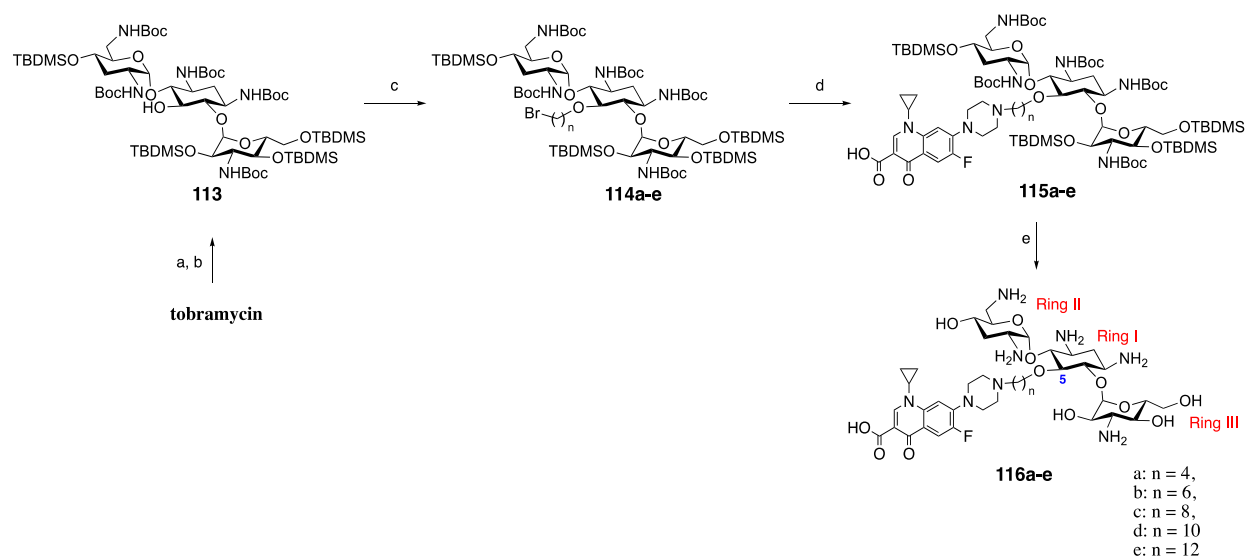
therapeutically ineffective antibiotics back into clinical use, and to broaden or narrow the spectrum of an antibiotic. One of the most successful type of adjuvants is  $\beta$ -lactamase inhibitor, such as clavulanic acid, which prevent degradation of  $\beta$ -lactam antibiotics. Administration of clavulanic acid in combination with the  $\beta$ -lactam antibiotic amoxicillin resulted in the drug Augmentin<sup>®</sup> that is currently widely used in clinical practice.<sup>89</sup> The other two major types of antibiotic adjuvants are outer membrane permeabilizers, that are capable of destabilizing the bacterial outer membrane, thereby enhancing uptake of antibiotics, and efflux pump inhibitors (EPIs), that block the function of efflux pumps, and hence increase intracellular drug accumulation. However, so far, neither of them has been approved for clinical use.

As previously stated, antibacterial amphiphilic aminoglycosides as stand-alone drugs possess impressive potent activity against sensitive and resistant Gram-positive and Gram-negative bacteria, but recent study reported by our group demonstrated that they can also play a role as adjuvants in adjunctive therapies with existing antibiotics.<sup>91-93</sup> These amphiphilic aminoglycoside-based adjuvants can resurrect legacy antibiotics and restore microbiological efficacy against MDR Gram-negative bacteria.<sup>91-93</sup>

In 2016, our group reported for the first time amphiphilic cationic tobramycin-ciprofloxacin hybrids that are capable of rescuing the activity of fluoroquinolone antibiotics against MDR and XDR drug-resistant *P. aeruginosa* isolates.<sup>93</sup> In this study, we covalently linked the C-5 position on ring I of tobramycin to the secondary amino group of the piperazine ring in ciprofloxacin through various lengths of linear alkyl chain to afford a series of tobramycin-ciprofloxacin hybrids (**116a-e**).

The synthetic strategy started with the global protection of the hydroxyl and amino groups of tobramycin with the exception of the C-5 alcohol because of the steric hindrance of

this alcohol which is adjacent to the C-4 and C-6 positions that were substituted by sugar rings I and III, respectively. Alkylation followed in the presence of KOH and the phase transfer catalyst TBAB (*tetra-n*-butylammonium bromide) to afford the bromoalkylated tobramycin intermediate (**114a-e**) which was then directly coupled with ciprofloxacin to generate the protected tobramycin-ciprofloxacin hybrid (**115a-e**). The deprotection step was carried out in acidic conditions to yield a series of fused tobramycin–ciprofloxacin hybrids (**116a-e**) (Scheme 1.3.2.1).<sup>93</sup>



**Scheme 1.3.2.1.** Synthesis of tobramycin-ciprofloxacin hybrids. Reagents and conditions: (a)  $(\text{Boc})_2\text{O}$ ,  $\text{Et}_3\text{N}$ ,  $\text{MeOH}/\text{H}_2\text{O}$ ; (b)  $\text{TBDMSCl}$ , 1-methylimidazole,  $\text{DMF}$ ; (c) 1,*n*-dibromoalkane ( $n = 4, 6, 8, 10, 12$ ),  $\text{KOH}$ , TBAB (*tetra-n*-butylammonium bromide), toluene; (d) ciprofloxacin,  $\text{K}_2\text{CO}_3$ ,  $\text{DMF}$ ; (e)  $\text{HCl}/\text{MeOH}$  (2:3, v/v).<sup>93</sup>

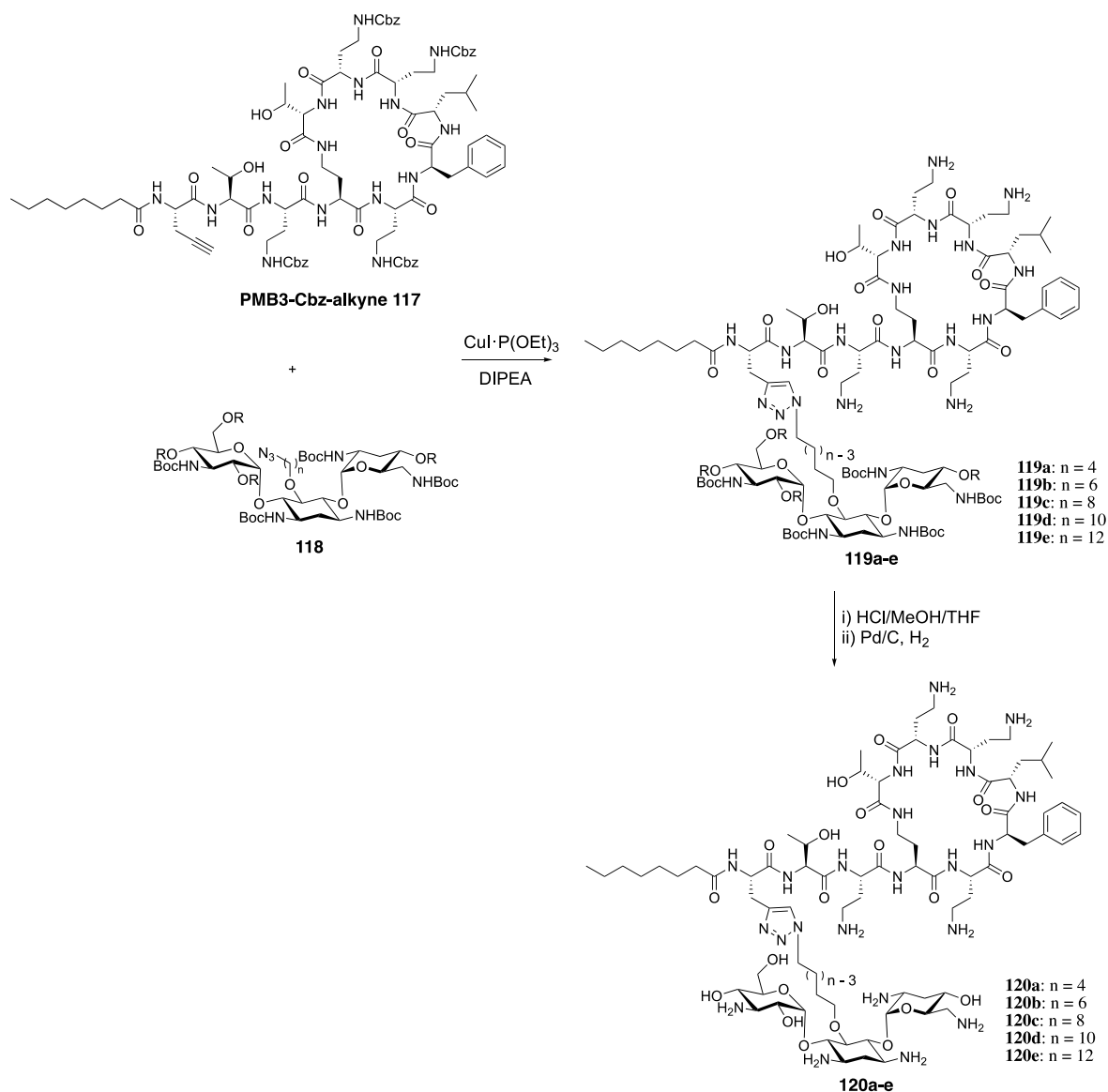
Regarding biological evaluations, most of these hybrids exerted only weak antibacterial activity when tested against a panel of Gram-positive and Gram-negative bacteria ( $\text{MIC} \geq 16 \mu\text{g/mL}$ ) but were found to restore ciprofloxacin and moxifloxacin potency in combination studies,

with emphasis on the hybrid with a C12 tether (**116e**), against six colistin-susceptible XDR *P. aeruginosa* clinical isolates (FIC indices of 0.03 – 0.28).<sup>93</sup> In this study, MIC breakpoints, also known as interpretive criteria, are used to define whether an organism is susceptible, intermediate, or resistant to antibacterials. For instance, if the MIC of an antibiotic against a particular organism is less than or equal to its susceptibility breakpoint, the bacterial strain is considered to be susceptible to the antibiotic. Whereas, if the MIC is greater than this value, this bacterial strain should be considered intermediate or resistant to the antibiotic. Clinical and Laboratory Standards Institute (CLSI, in the United States) and European Committee on Antimicrobial Susceptibility Testing (EUCAST, in Europe) update MIC breakpoint interpretations yearly on a basis of pharmacokinetic/pharmacodynamic data and clinical studies. This study has been shown that ciprofloxacin-susceptible (MIC  $\leq 1 \mu\text{g/mL}$ ) or intermediate (MIC =  $2 \mu\text{g/mL}$ ) CLSI breakpoints (susceptibility test interpretive criteria) were reached for most of the fluoroquinolone-resistant clinical isolates in the presence of  $\leq 8 \mu\text{g/mL}$  ( $6 \mu\text{M}$ ) of hybrid **116e**.<sup>93</sup> Moreover, this synergistic effect of hybrid **116e** on the growth inhibition of *P. aeruginosa* was well translated *in vivo* in a *Galleria mellonella* infection model. A single dose monotherapy of either the hybrid **116e** or moxifloxacin alone (50 mg/kg each) was ineffective and resulted in 100% killing of the larvae within 24 h, whereas the combination therapy with a single dose (37.5 mg/kg hybrid **116e** + 37.5 mg/kg moxifloxacin) resulted in 86% survival of the larvae after 24 h.<sup>93</sup>

Mechanistic studies demonstrated that hybrid **116e** permeabilizes the outer membrane of *P. aeruginosa* in a dose-dependent manner. An *in vitro* protein translation assay showed that the protein translation-inhibitory property of hybrid **116e** was significantly reduced (1290-fold reduction) in comparison to tobramycin. However, hybrid **116e** manifested better *in vitro*

inhibitory activities to DNA gyrase A and topoisomerase IV than that of ciprofloxacin. These results suggested that, in the tobramycin-ciprofloxacin hybrid **116e**, the original modes of action of the ciprofloxacin domain are retained while the role of the tobramycin domain is limited to the outer membrane perturbation, thus facilitating the accumulation of fluoroquinolone antibiotics.<sup>93</sup>

Encouraged by these results, in the following year, our group continuously developed a class of novel amphiphilic tobramycin-based polymyxin B<sub>3</sub> hybrids.<sup>91</sup> The alkyne-containing polymyxin B<sub>3</sub> (PMB3-Cbz-alkyne) and azide-containing tobramycin (Tobramycin-Boc-TBDMS-azide) intermediates were fused together through a copper-assisted azide alkyne cycloaddition to generate the tobramycin-polymyxin B<sub>3</sub> hybrids with a 1,2,3-triazole ring linkage and a variety of lengths of hydrocarbon linkers (Scheme 1.3.2.2). This series of compound exerted potent activity against carbapenem-resistant and MDR/XDR *P. aeruginosa* clinical isolates. Moreover, the most potent hybrid (**120d**), containing a ten carbon-long aliphatic hydrocarbon linker, was demonstrated to potentiate rifampicin, minocycline, and vancomycin antibiotics against MDR/XDR *P. aeruginosa* isolates in a fashion similar to the tobramycin-based ciprofloxacin hybrid as stated above.



**Scheme 1.3.2.2.** Synthesis of tobramycin-polymyxin B<sub>3</sub> hybrids.<sup>91</sup>

## 1.4 PHYSICAL BARRIERS TO DRUG INFLUX AND MULTIPLE EFFLUX PUMPS AS MAIN CHALLENGES OF ANTIBACTERIAL DISCOVERY

It is broadly acknowledged that antimicrobial drug resistance is a growing threat to human health. Multidrug resistance among the ‘ESKAPE’ organisms (*Enterococcus faecium*, *Staphylococcus aureus*, *Klebsiella pneumoniae*, *Acinetobacter baumannii*, *Pseudomonas*

*aeruginosa* and *Enterobacter* spp.) is of particular concern because they are responsible for many serious infections.<sup>93,94</sup> A number of classes of antibiotics including  $\beta$ -lactams, macrolides, aminoglycosides, tetracyclines, fluoroquinolones, oxazolidinones and daptomycin were discovered during the golden era of antibiotic drug discovery (1940s–1980s); however, little success was achieved during the last four decades, especially in the development of agents effective against MDR Gram-negative pathogens, such as *A. baumannii*, *P. aeruginosa* and members of the Enterobacteriaceae family.<sup>95–97</sup> Thus, there is an urgent need for novel antibacterial drugs and alternative therapies, particularly for those directed against multi-resistant Gram-negative bacilli. By the advent of genomics, numerous targets were generated that were tested in *in vitro* high-throughput biochemical screens in modern antibacterial drug discovery. A great deal of synthetic chemical libraries were screened, however this target-based approach was profoundly unsuccessful, especially for the development of anti-Gram-negative agents.<sup>86,94,96</sup> The main challenge we are currently facing is not the identification of new hits for the target enzyme or protein, but the process to convert these hits into whole-cell active compounds.<sup>94</sup> The difficulty ultimately stems from a lack of understanding of the rules governing entry of antibacterial agents into the cell and efflux systems.

#### **1.4.1 Physical Barriers to Drug Influx in Gram-negative Organisms**

Gram-negative bacteria are intrinsically resistant to many antibiotics due to the permeability barrier of their cell envelopes. This envelope comprises an outer membrane (OM) which is a sophisticated asymmetric lipid bilayer, and inner membrane (IM) that is a traditional phospholipid bilayer (Figure 1.4.1.1).<sup>98</sup> Between the two membranes lies a thin peptidoglycan (PG) matrix and a periplasmic space.<sup>98</sup> The OM that only exists in Gram-negative bacteria is a

permeability barrier itself because the influx and uptake of antibiotics are significantly slowed by it. The outer leaflet of the OM consists of glycolipids, principally lipopolysaccharide (LPS) while the phospholipids exclusively partition to the inner leaflet.<sup>99</sup>

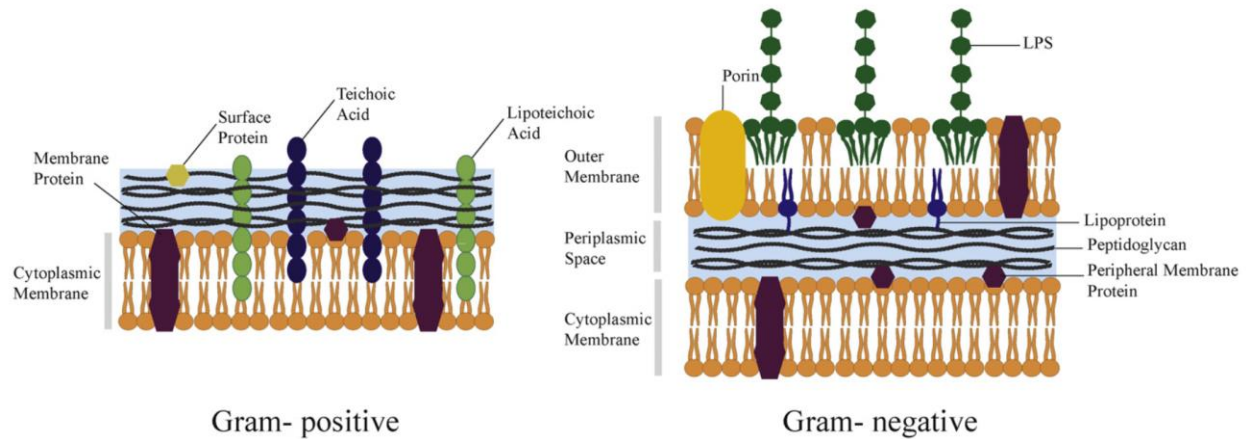


**Figure 1.4.1.1.** Schematic representation of Gram-positive (left) and Gram-negative (right) cell envelopes.<sup>100</sup> Adapted with permission from *Biochim. Biophys. Acta - Biomembr.* **2016**, 1858 (5), 980-987. Copyright (2015) Elsevier B.V.

The LPS layer of the OM serves as protection for Gram-negative bacteria against foreign substances that might be toxic in the extracellular environment.<sup>101–104</sup> In other words, the LPS layer plays a critical role in the barrier function of the OM. Starting from the outside and proceeding inward, the outmost domain of the LPS is a distal polysaccharide chain that is O-antigen, a short core oligosaccharide attached to it covalently, and a hydrophobic domain known as lipid A as the inner leaflet of LPS (Figure 1.4.1.2).<sup>105</sup> The O-antigen is an oligosaccharide consisting of repeating units which are fully hydrated that act as the hydrophilic coating of the Gram-negative bacterial OM; therefore, hydrophobic molecules are prevented from passing the OM on their way into the cell.<sup>106</sup> Lipid A is a phosphorylated glucosamine disaccharide bearing

six saturated fatty acid chains which anchor the LPS into the bacterial OM. Unlike typical phospholipid, the hydrocarbon regions of LPS is in a gel-like state of a very low fluidity due to the increased number of saturated fatty acyl substituents per molecule of lipid.<sup>104</sup> In addition, polyanionic LPS are cross-linked electrostatically via divalent cations ( $\text{Ca}^{2+}$  and  $\text{Mg}^{2+}$ ), which bind to the anionic phosphate substituents of lipid A and the inner core region, stabilizing the LPS molecules in the bilayers.<sup>107</sup> Hence, the strong lateral interactions between the LPS molecules and the low fluidity of the LPS hydrocarbon region are responsible for the slower permeation of lipophilic molecules through the LPS asymmetric bilayer than that of conventional phospholipid bilayer membranes.<sup>104,108</sup> All these characteristics make the LPS-containing asymmetric bilayer an effective permeability barrier to Gram-negative bacteria.

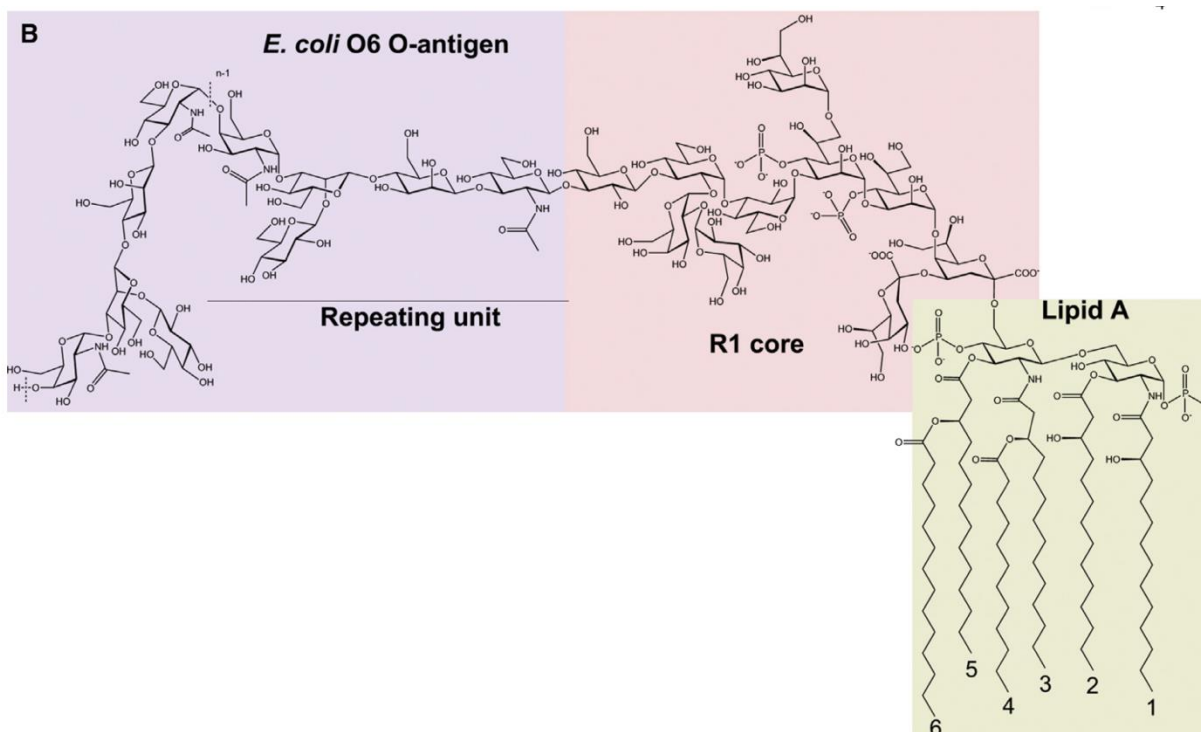


**Figure 1.4.1.2.** Chemical structure of *E. coli* R1 O6 LPS.<sup>106</sup> Adapted with permission from *Biophys. J.* **2013**, *105* (6), 1444-1455. Copyright (2013) Biophysical Society. Published by Elsevier Inc.

Generally, the majority of antibacterial drugs (e.g.  $\beta$ -lactams, fluoroquinolones, tetracyclines *et al.*) needs to transit through the OM or both the OM and IM in order to reach their requisite site of action to be effective.<sup>96</sup> As stated above, the Gram-negative OM is a permeability barrier itself, but molecules are permitted access through the OM by passive  $\beta$ -barrel transport proteins termed porins, which are water-filled protein channels, as well, a main entry for small (the cutoff M.W. for *E. coli*. is 600) and hydrophilic charged solutes.<sup>104</sup> The general *E. coli*-type trimeric porins, such as OmpF and OmpC, provide relatively rapid passive diffusion of small and hydrophilic drugs including  $\beta$ -lactams, fluoroquinolones, and tetracyclines.

However, the situation is very different for certain non-fermenting bacterial species, such as *P. aeruginosa* and *A. baumannii*. The  $\beta$ -lactams penetrate the *P. aeruginosa* OM at rates about 2 orders of magnitude lower than that for the *E. coli* OM.<sup>109,110</sup> The reason for such low permeability is due to the existence of “slow porins” rather than the high-permeability trimeric porins of *E. coli*.<sup>111,112</sup> OprF is the major nonspecific porin of *P. aeruginosa* which is a monomeric OM protein.<sup>112</sup> A majority of OprF (96% of the population) fold into closed-channel conformer that does not have porin activity whereas the minority conformer (only 4% of the population) fold into an open-channel with high porin activity.<sup>111,112</sup> The small number of open channels might explain the very slow rates of permeation of various solutes in *P. aeruginosa* and *Acinetobacter species*. Thus, these organisms are intrinsically resistant to a variety of clinically used common antibiotics. Aside from the nonspecific slow porins, *P. aeruginosa* and *A. baumannii* have a large number of substrate-specific channels dedicated to the uptake of amino acids, sugars and phosphate. For example, OprD of *P. aeruginosa* is specific for the diffusion of basic amino acids, peptides containing basic residues and zwitterionic carbapenems such as imipenem, and meropenem.<sup>113,114</sup> The reduced expression or changes of sequence in OprD or loss of it confer resistance to clinically important carbapenem antibiotics.<sup>115–117</sup> As porins are the main factors regulating drug permeability and resistance, a full understanding of small molecule passage through the OM via porins may help medicinal chemists efficiently design effective compounds with improved permeation across this barrier.

Upon passage through the Gram-negative bacterial OM, drugs are distributed to different compartments such as the periplasm, the IM and the cytoplasm in order to gain access to their targets. A number of clinically used drugs with cytosolic targets need to penetrate both the OM and IM of the Gram-negative cell envelope. The IM of Gram-negative bacteria is a traditional

phospholipid bilayer showing a preference for permeation of uncharged, lipophilic molecules by simple passive diffusion.<sup>97,118</sup> Some lipophilic agents with multiple functional groups that may become charged by protonation or deprotonation at physiological pH (e.g. tetracyclines and fluoroquinolones), cross the IM by passive diffusion with the aid of the proton motive force (PMF).<sup>119–122</sup> For example, tetracycline accumulation is driven by a transmembrane proton gradient ( $\Delta\text{pH}$ ) of PMF.<sup>119</sup> Very polar and strongly charged molecules, such as fosfomycin and cycloserine, may rely on solute-specific energy-dependent carriers for their passage through the IM.<sup>123,124</sup>

#### **1.4.2 Multiple Efflux Pumps Can Further Reduce Drug Permeation**

Aside from these physical barriers for influx, also of importance are multidrug resistance pumps that expel a variety of structurally diverse drugs and toxic compounds which play an important role in the reduction of net permeability of antibacterials into the cytoplasm and periplasm.<sup>125–128</sup> The overexpression of these pumps causes multidrug resistance that became a major concern in modern chemotherapy.

Based on sequence similarity, multidrug efflux pumps commonly belong to the ABC (ATP-binding cassette superfamily), RND (resistance-nodulation-cell division), MFS (major facilitator superfamily), MATE (multidrug and toxic compound extrusion), SMR (small multidrug resistance) and PACE (proteobacterial antimicrobial compound extrusion) superfamilies and families (Figure 1.4.2.1).<sup>129</sup> ABC transporters utilize ATP hydrolysis as the energy source to transport drugs across the membrane, but all others are  $\text{H}^+$  (or  $\text{Na}^+$ ) drug antiporters that depend on energy derived from the electrochemical gradient of the proton motive force (PMF).<sup>130</sup>

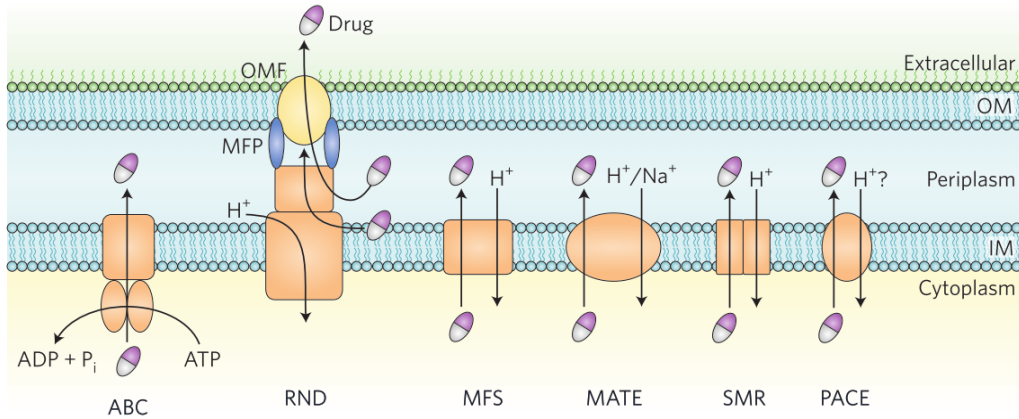


**Figure 1.4.2.1.** Schematic representation of the six common classes of MDR efflux pump in bacteria.<sup>129</sup> Adapted with permission from *Nat. Microbiol.* **2017**, 2 (3), 17001. Copyright (2017) Springer Nature.

Efflux transporters are also characterized by their subcellular organization. In Gram-negative organisms, efflux pumps exist as either single-component pumps or multi-component pumps. The single-component efflux transporters are embedded in the bacterial inner membrane that excrete drug molecules from the cytoplasm or inner leaflet of the IM only into the periplasm; however, drugs can re-enter the cytosol across the IM spontaneously via diffusion.<sup>130</sup> The multi-component pumps that is a tripartite complex are composed by three elements: an IM efflux transporter (RND, ABC or MFS) that binds the substrates, an outer membrane channel, and a membrane fusion protein (MFP), also known as the periplasmic adaptor protein, that is located in the periplasm bridging between the IM efflux transporter and the OM channel (Figure 1.4.2.2).<sup>129</sup> Gram-negative bacteria deploy the tripartite system to effectively pump out the drugs into the external medium after capture from the periplasm and the IM.<sup>129</sup>

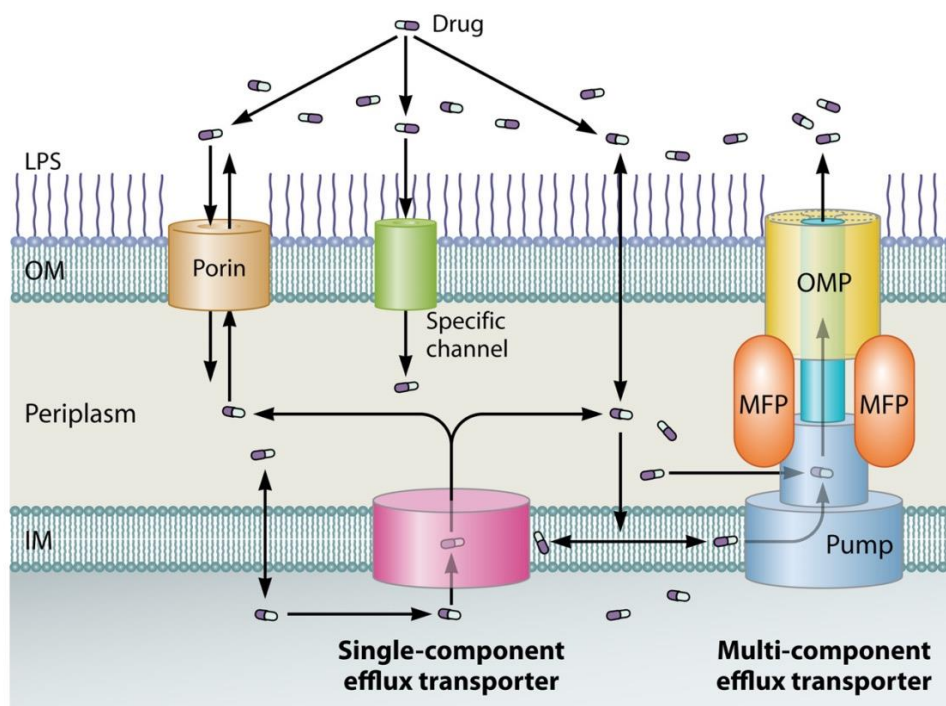


**Figure 1.4.2.2.** Efflux pumps and pathways of drug influx and efflux across the OM and IM in Gram-negative bacteria.<sup>130</sup> Adapted with permission from *Clin. Microbiol. Rev.* **2015**, *28* (2), 337-418. Copyright (2015) American Society for Microbiology.

RND-type exporters are the major multidrug efflux transporters in Gram-negative bacteria.<sup>131</sup> Among them, AcrAB-TolC of *E. coli* and MexAB-OprM of *P. aeruginosa* have been studied most intensively. One of the most intriguing features of RND-containing pumps is their exceptionally wide substrate specificity,<sup>132</sup> including antibiotics, detergents, dyes, bile, hormones, and even simple organic solvents.<sup>130</sup> Crystallographic analysis revealed two substrates binding sites in the periplasmic domains of AcrB from *E. coli*, the rather large access (proximal) pocket that is the binding site for larger substrates like macrolides, rifampin and a dimer of doxorubicin, and the deep (distal) binding pocket where low-molecular-weight drugs such as minocycline, rhodamine and a monomer of doxorubicin bind.<sup>133–136</sup> Analysis from AstraZeneca (AZ) high

throughput (HTS) screening illustrated that the compounds least susceptible to efflux were those which were highly polar and small in molecular weight or very large and typically zwitterionic.<sup>137</sup> However, physicochemical properties in terms of net charge, hydrophobicity and molecular weight of compounds that would distinguish substrates from nonsubstrates still remain elusive.

Gram-negative bacteria not only have outer membranes to restrict penetration but also have promiscuous efflux pumps which serve to expel potentially toxic foreign substances. Efflux pumps act synergistically with the OM barrier that can further reduce drug permeation.<sup>127</sup> If the drugs flow into the periplasm across the OM is slow, for example, with the relatively large and/or hydrophobic drugs that cross the OM slowly or the hydrophilic drugs that penetrate the “slow porins” of *P. aeruginosa* or *A. baumannii*, then efflux pumps can outpace entry, thus being able to confer detectable resistance to antibiotics.<sup>130</sup> This explains the intrinsic resistance of *P. aeruginosa* and *A. baumannii* to many antibacterial drugs. In contrast, if the drugs permeate through the OM rapidly enough to counteract the rate of efflux, efflux pumps cannot create a detectable decrease in susceptibility.

## **1.5 EFFLUX PUMP INHIBITORS – ONE APPROACH TO BREAK THE PERMEABILITY BARRIER**

Active efflux plays a major role in intrinsic resistance in both Gram-positive and Gram-negative bacteria. The overproduction of efflux pumps in pathogens became one of the permeability barriers of clinically useful antibiotics and thus limited their utility.<sup>130</sup> Hence, discovery and development of therapeutic agents that are able to interfere with efflux pump expression and function may provide a promising approach to restoring the activity of antibiotics

that are ineffective due to efflux. Co-administration of efflux pump inhibitors with existing antibiotics could be used as an alternative therapy to combat efflux-mediated resistance. This section will briefly provide the biological activities of the major classes of EPIs together with their mechanistic action studies.

**Table 1.5.1.** Most active efflux pump inhibitors, with substrates and bacterial species in which their activity has been demonstrated.

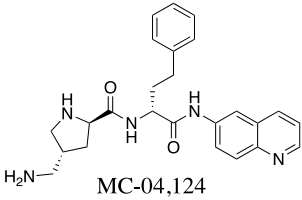
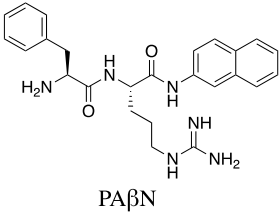
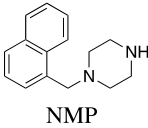
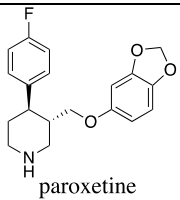
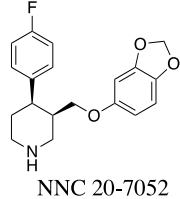
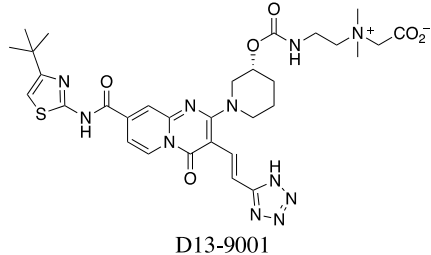
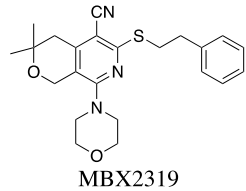
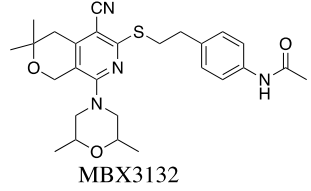
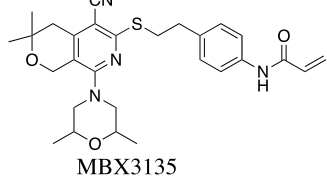
Type of inhibitor	Molecular structure	Bacterial species	Substrates	References
Peptidomimetic	 <p>MC-04,124</p>  <p>PAβN</p>	<i>P. aeruginosa</i> , <i>E. coli</i> , <i>E. aerogenes</i> , <i>K. pneumoniae</i> , <i>S. enterica</i>	Fluoroquinolones, Macrolides, Chloramphenicol	138–142
Arylpiperazine	 <p>NMP</p>	<i>E. coli</i> , <i>A. baumannii</i> , <i>E. aerogenes</i> , <i>K. pneumoniae</i> , <i>C. freundii</i>	Linezolid, Levofloxacin, Clarithromycin, Oxacillin, Rifampicin, Chloramphenicol, Tetracycline	143–147

Table 1.5.1. Cont.

Type of inhibitor	Molecular structure	Bacterial species	Substrates	References
Phenylpiperidine-selective serotonin reuptake inhibitors	 <p>paroxetine</p>	<i>S. aureus</i> , <i>E. coli</i>	Norfloxacin, Tetracycline, Ethidium bromide	148
	 <p>NNC 20-7052</p>			
Pyridopyrimidine	 <p>D13-9001</p>	<i>P. aeruginosa</i>	Levofloxacin, Aztreonam	149
Pyranopyridine	 <p>MBX2319</p>	<i>E. coli</i> , <i>Shigella flexneri</i> , <i>Salmonella enterica</i> , <i>E. aerogenes</i> , <i>E. cloacae</i> , <i>K. pneumoniae</i>	Ciprofloxacin, Levofloxacin, Piperacillin, Chloramphenicol, Erythromycin, Linezolid Minocycline	150–152
	 <p>MBX3132</p>			
	 <p>MBX3135</p>			

### 1.5.1 Peptidomimetics

In 1999, scientists at Microcide Pharmaceuticals and Daiichi Pharmaceutical Co. characterized a series of peptidomimetic compounds which were the first known class of broad-spectrum efflux pump inhibitors in *P. aeruginosa*.<sup>138</sup> Among this group of peptidomimetics, the lead compound phenylalanyl arginyl  $\beta$ -naphthylamide (PA $\beta$ N, also called MC-207,110), a low molecular weight dipeptide amide, has been found to restore activity of a broad class of antibiotics including fluoroquinolones, macrolides and chloramphenicol by inhibiting efflux pumps belonging to a wide range of clinical pathogens (Table 1.5.1). This compound is active against three multidrug resistance RND pumps (MexAB-OprM, MexCD-OprJ, and MexEF-OprN) in *P. aeruginosa* for the efflux of fluoroquinolones and *E. coli* AcrAB-TolC pump. The addition of PA $\beta$ N decreases the intrinsic resistance of *P. aeruginosa* to fluoroquinolones (8-fold for levofloxacin), while it also reverses acquired resistance due to the overexpression of efflux pumps (up to 64-fold reduction in the MIC of levofloxacin).

Due to the instability of PA $\beta$ N in murine and human serum, optimizations have been described, and one analogue of PA $\beta$ N, MC-04,124 (Table 1.5.1), has been reported with similar potency, reduced acute toxicity and significantly improved stability in serum than PA $\beta$ N, enabling an *in vivo* efficacy study.<sup>140,141</sup> In this series of compounds, the presence of two basic cationic moieties were shown to be essential for activity; however, they were also found to be associated with prolonged accumulation in tissues, particularly the kidney causing renal toxicity, and therefore, the development of this lead series was abandoned.<sup>141,142</sup>

PA $\beta$ N is used as a research agent to study the mechanism of action for this class of EPIs. It was demonstrated that PA $\beta$ N itself is a substrate for RND pumps, suggesting that it is likely to act as a competitive inhibitor in the transport process;<sup>139</sup> that is while the pump preferentially

pumps out PA $\beta$ N, the antibiotic remains in the cell increasing its concentration until the point where it meets the requirement of its activity on target.<sup>153</sup> Molecular dynamics simulation experiments predicted that binding of PA $\beta$ N to the lower part of the *E. coli* inner membrane component of the AcrB efflux pocket causes a conformational change that shrinks the substrate extrusion channel and thus interferes with the substrate movement.<sup>130,154,155</sup> A docking study also suggested that PA $\beta$ N appears to distort the structure of the distal pocket of AcrB, impairing the proper binding of substrates such as minocycline.<sup>156</sup> Beyond that, altering the permeability of the outer membrane was demonstrated as an additional mode of action of PA $\beta$ N due to its dicationic character.<sup>139,157</sup> The effect on bacteria membrane integrity is expected to increase the influx of antibiotics into the periplasm that would result in the increased susceptibility to an antibiotic. However, this activity was completely abolished by the addition of 1 mM Mg<sup>2+</sup>.<sup>139</sup>

### 1.5.2 Arylpiperazine Derivatives

Arylpiperazine derivatives have shown activity against *E. coli* strains overexpressing both *acrAB* and *acrEF*.<sup>147</sup> Among these compounds, 1-(1-Naphthylmethyl)-piperazine (NMP) (Table 1.5.1), one of the most potent derivatives, was reported to be an EPI capable of reversing the MDR phenotype of *E. coli* clinical isolates and could partially restore fluoroquinolone susceptibility.<sup>146,147</sup> It also reverses antibiotic resistance in several bacterial species including *A. baumannii*, and different Enterobacteriaceae, e.g., *Enterobacter aerogenes*, *Citrobacter freundii*, and *K. pneumoniae*, but not in *P. aeruginosa*.<sup>143–145</sup> However, due to the serotonin agonist properties of NMP, it is too toxic to become a clinically useful drug.<sup>158</sup>

NMP is usually used as a research tool. MD simulations suggested that it does not bind tightly to the binding sites in the periplasmic domain of the AcrB efflux transporter from *E. coli*;

it behaves as a substrate that can be pumped out.<sup>130,147,155</sup> Similar to PA $\beta$ N, NMP bound to the bottom of the AcrB efflux pocket that is rich in hydrophobic residues but moved out of the pocket owing to interactions with the G-loop, which was predicted by MD simulations.<sup>130,159</sup> This suggests the NMP inhibits the AcrB efflux pump by interfering with the movement of the G-loop that plays a critical role in the extrusion of certain substrates.<sup>160,161</sup>

### 1.5.3 Phenylpiperidine-Selective Serotonin Reuptake Inhibitors (PSSRIs)

Structural variants of certain phenylpiperidine selective serotonin reuptake inhibitors (PSSRIs) are capable of inhibiting the function of both NorA (MFS family)- and MepA (MATE family)-efflux pumps.<sup>148,162,163</sup> Among them, paroxetine, a well-known antidepressant used therapeutically, and its isomer NNC 20-7052 (Table 1.5.1) are demonstrated to be relatively weak EPIs but potentiate fluoroquinolones and tetracyclines against *S. aureus* and *E. coli* excluding *P. aeruginosa*.<sup>148</sup> Further SAR studies investigated whether the potency of efflux inhibition is maintained or enhanced by a deletion of 4-phenyl substituent on the piperidine ring or a replacement of the aryloxymethyl (ether-linked 3-aryl) substituent at position 3 of PSSRI-based inhibitors with arylalkene (alkene-linked 3-aryl) and arylthioether (thioether-linked 3-aryl) moieties.<sup>163</sup>

### 1.5.4 Pyridopyrimidine Derivatives

A high-throughput screen was applied by Daiichi Pharmaceuticals and Essential Therapeutics, Inc. to successfully explore the first example of a MexAB-OprM-specific efflux pump inhibitor which is used for the potentiation of  $\beta$ -lactams and quinolones against *P. aeruginosa*.<sup>164</sup> Systematic optimization of a hit compound resulted in the identification of a

potent pyridopyrimidine derivative (D13-9001) (Table 1.5.1) that exhibits conserved activity, with improved pharmacokinetic properties and reduced serum protein binding.<sup>149,164–169</sup>

Nakashima *et al.* (2013) described the three-dimensional structure of the zwitterionic EPI D13-9001 bound to AcrB and MexB trimers.<sup>170</sup> The crystal structure revealed that the hydrophobic part of the inhibitor binds tightly to the bottom of the distal binding pocket, called a “hydrophobic trap”, a narrow phenylalanine-lined groove, and thus interferes with the conformational changes that are needed for drug efflux through the pump.<sup>170</sup> In contrast, the hydrophilic portions of the inhibitor are bound to the upper part of the binding pocket and thereby prevent the binding of the other substrates to it.<sup>170</sup> This study elucidated the first example of the x-ray crystal structures of the RND-type pumps AcrB and MexB bound to inhibitor and well explained the molecular basis of pump inhibition, facilitating a rapid evolution in understanding the molecular mechanism of the EPIs.

### 1.5.5 Pyranopyridine Derivatives

In 2014, scientists at Microbiotix discovered a potent pyranopyridine-based inhibitor, MBX2319 (Table 1.5.1), of the AcrB efflux pump through a high-throughput screening campaign.<sup>150</sup> It is structurally distinct and orders of magnitude more powerful than the earlier EPIs mentioned above.<sup>150</sup> It significantly potentiates a broad range of antibiotics including fluoroquinolones,  $\beta$ -lactams, chloramphenicol, erythromycin, linezolid and minocycline against *E. coli* and other Enterobacteriaceae, but does not show activity in *P. aeruginosa* because it cannot penetrate through the *P. aeruginosa* outer membrane.<sup>150,151,171</sup> SAR studies showed that modifications of MBX2319 phenyl ring and morpholinyl group resulted in new pyranopyridine derivatives, the acetamide- and acrylamide-containing compounds MBX3132 and MBX3135

(Table 1.5.1), with significantly increased activities, improved solubilities and stabilities as compared to MBX2319.<sup>151,172</sup>

Mechanism of action studies in *E. coli* suggested that MBX2319 tightly binds to the “hydrophobic trap” of the AcrB efflux pump, similar to the EPI D13-9001, where they form extensive hydrophobic interactions that lead to the inhibition of the conformational changes required for pump function.<sup>170,172</sup> In addition, it was demonstrated that the increased potency of MBX3132 and MBX3135 is due to the tighter binding to the hydrophobic trap of AcrB that correlates with the formation of the protein- and water-mediated hydrogen bond networks.<sup>172</sup> With this in mind, further optimization of the pyranopyridine series is currently in progress to develop more potent inhibitors with lower toxicity which are clinically effective.

## 1.6 REFERENCES

- (1) Dozzo, P.; Moser, H. E. New Aminoglycoside Antibiotics. *Expert Opin. Ther. Pat.* **2010**, *20* (10), 1321–1341.
- (2) Craig, W. A. Optimizing Aminoglycoside Use. *Crit. Care Clin.* **2011**, *27* (1), 107–121.
- (3) Avent, M. L.; Rogers, B. A.; Cheng, A. C.; Paterson, D. L. Current Use of Aminoglycosides: Indications, Pharmacokinetics and Monitoring for Toxicity. *Intern. Med. J.* **2011**, *41* (6), 441–449.
- (4) Wright, G. D.; Berghuis, A. M.; Mobashery, S. Aminoglycoside Antibiotics. Structures, Functions, and Resistance. *Adv. Exp. Med. Biol.* **1998**, *456*, 27–69.
- (5) Mathews, A.; Bailie, G. R. Clinical Pharmacokinetics, Toxicity and Cost Effectiveness Analysis of Aminoglycosides and Aminoglycoside Dosing Services. *J. Clin. Pharm. Ther.* **1987**, *12* (5), 273–291.

- (6) Martens, E.; Demain, A. L. The Antibiotic Resistance Crisis, with a Focus on the United States. *J. Antibiot. (Tokyo)*. **2017**, *70* (5), 520–526.
- (7) Norrby, S. R.; Nord, C. E.; Finch, R. Lack of Development of New Antimicrobial Drugs: A Potential Serious Threat to Public Health. *Lancet. Infect. Dis.* **2005**, *5* (2), 115–119.
- (8) Schatz, A.; Bugle, E.; Waksman, S. A. Streptomycin, a Substance Exhibiting Antibiotic Activity Against Gram-Positive and Gram-Negative Bacteria. *Exp. Biol. Med.* **1944**, *55* (1), 66–69.
- (9) Waksman, S. A. Streptomycin: Background, Isolation, Properties, and Utilization. *Science*. **1953**, *118* (3062), 259–266.
- (10) Chopra, I.; Roberts, M. Tetracycline Antibiotics : Mode of Action , Applications , Molecular Biology , and Epidemiology of Bacterial Resistance Tetracycline Antibiotics : Mode of Action , Applications , Molecular Biology , and Epidemiology of Bacterial Resistance. *Microbiol. Mol. Biol. Rev.* **2001**, *65* (2), 232–260.
- (11) Daikos, G. K.; Kourkoumeli, P.; Paradelis, A. Aminocyclitol, a New Oligosaccharide Antibiotic: Bacteriologic and Pharmacologic Observations. *Antibiot. Chemother.* **1962**, *12* (4), 243–248.
- (12) Higgins, C. E.; Kastner, R. E. Nebramycin, a New Broad-Spectrum Antibiotic Complex. II. Description of *Streptomyces Tenebrarius*. *Antimicrob. Agents Chemother.* **1967**, *7*, 324–331.
- (13) Stark, W. M.; Hoehn, M. M.; Knox, N. G. Nebramycin, a New Broad-Spectrum Antibiotic Complex. I. Detection and Biosynthesis. *Antimicrob. Agents Chemother.* **1967**, *7*, 314–323.
- (14) Weinstein, M.; Wagman, G.; Waitz, J. Discovery and Isolation of Sisomicin. *Infection*

- 1976**, 4 (S4), S285–S288.
- (15) Weinstein, M. J.; Marquez, J. A.; Testa, R. T.; Wagman, G. H.; Oden, E. M.; Waitz, J. A. Antibiotic 6640, a New Micromonospora-Produced Aminoglycoside Antibiotic. *J. Antibiot. (Tokyo)*. **1970**, 23 (11), 551–554.
- (16) Miller, G. H.; Arcieri, G.; Weinstein, M. J.; Waitz, J. A. Biological Activity of Netilmicin, a Broad-Spectrum Semisynthetic Aminoglycoside Antibiotic. *Antimicrob. Agents Chemother.* **1976**, 10 (5), 827–836.
- (17) Umezawa, H.; Umezawa, S.; Tsuchiya, T.; Okazaki, Y. 3',4'-Dideoxy-Kanamycin B Active against Kanamycin-Resistant Escherichia Coli and Pseudomonas Aeruginosa. *J. Antibiot. (Tokyo)*. **1971**, 24 (7), 485–487.
- (18) Kawaguchi, H.; Naito, T.; Nakagawa, S.; Fujisawa, K.-I. BB-K 8, a New Semisynthetic Aminoglycoside Antibiotic. *J. Antibiot. (Tokyo)*. **1972**, 25 (12), 695–708.
- (19) Krause, K. M.; Serio, A. W.; Kane, T. R.; Connolly, L. E. Aminoglycosides: An Overview. *Cold Spring Harb. Perspect. Med.* **2016**, 6 (6), a027029.
- (20) Taber, H. W.; Mueller, J. P.; Miller, P. F.; Arrow, A. S. Bacterial Uptake of Aminoglycoside Antibiotics. *Microbiol. Rev.* **1987**, 51 (4), 439–457.
- (21) Ramirez, M. S.; Tolmasky, M. E. Aminoglycoside Modifying Enzymes. *Drug Resist. Updat.* **2010**, 13 (6), 151–171.
- (22) Hancock, R. E. W. Alterations in Outer Membrane Permeability. *Annu. Rev. Microbiol.* **1984**, 38 (1), 237–264.
- (23) Hancock, R. E.; Raffle, V. J.; Nicas, T. I. Involvement of the Outer Membrane in Gentamicin and Streptomycin Uptake and Killing in Pseudomonas Aeruginosa. *Antimicrob. Agents Chemother.* **1981**, 19 (5), 777–785.

- (24) Hancock, R. E.; Farmer, S. W.; Li, Z. S.; Poole, K. Interaction of Aminoglycosides with the Outer Membranes and Purified Lipopolysaccharide and OmpF Porin of *Escherichia Coli*. *Antimicrob. Agents Chemother.* **1991**, *35* (7), 1309–1314.
- (25) Davis, B. D. Mechanism of Bactericidal Action of Aminoglycosides. *Microbiol. Rev.* **1987**, *51* (3), 341–350.
- (26) Jana, S.; Deb, J. K. Molecular Understanding of Aminoglycoside Action and Resistance. *Appl. Microbiol. Biotechnol.* **2006**, *70* (2), 140–150.
- (27) Martin, W. J.; Gardner, M.; Washington, J. A. In Vitro Antimicrobial Susceptibility of Anaerobic Bacteria Isolated from Clinical Specimens. *Antimicrob. Agents Chemother.* **1972**, *1* (2), 148–158.
- (28) Kislak, J. W. The Susceptibility of *Bacteroides Fragilis* to 24 Antibiotics. *J. Infect. Dis.* **1972**, *125* (3), 295–299.
- (29) Taber, H. W.; Mueller, J. P.; Miller, P. F.; Arrow, A. S. Bacterial Uptake of Aminoglycoside Antibiotics. *Microbiol. Rev.* **1987**, *51* (4), 439–457.
- (30) Bryan, L. E.; Kwan, S. Roles of Ribosomal Binding, Membrane Potential, and Electron Transport in Bacterial Uptake of Streptomycin and Gentamicin. *Antimicrob. Agents Chemother.* **1983**, *23* (6), 835–845.
- (31) Kotra, L. P.; Haddad, J.; Mobashery, S. Aminoglycosides: Perspectives on Mechanisms of Action and Resistance and Strategies to Counter Resistance. *Antimicrob. Agents Chemother.* **2000**, *44* (12), 3249–3256.
- (32) Davis, B. D.; Chen, L. L.; Tai, P. C. Misread Protein Creates Membrane Channels: An Essential Step in the Bactericidal Action of Aminoglycosides. *Proc. Natl. Acad. Sci. U. S. A.* **1986**, *83* (16), 6164–6168.

- (33) Wilson, D. N. Ribosome-Targeting Antibiotics and Mechanisms of Bacterial Resistance. *Nat. Rev. Microbiol.* **2013**, *12* (1), 35–48.
- (34) Wang, L.; Pulk, A.; Wasserman, M. R.; Feldman, M. B.; Altman, R. B.; Cate, J. H. D.; Blanchard, S. C. Allosteric Control of the Ribosome by Small-Molecule Antibiotics. *Nat Struct Mol Biol* **2012**, *19* (9), 957–963.
- (35) Scheunemann, A. E.; Graham, W. D.; Vendeix, F. A. P.; Agris, P. F.; P, I.; J, S.; P, M.; A, S.; P, R.; E, P. Binding of Aminoglycoside Antibiotics to Helix 69 of 23S rRNA. *Nucleic Acids Res.* **2010**, *38* (9), 3094–3105.
- (36) Bulitta, J. B.; Ly, N. S.; Landersdorfer, C. B.; Wanigaratne, N. A.; Velkov, T.; Yadav, R.; Oliver, A.; Martin, L.; Shin, B. S.; Forrest, A.; Tsuji, B. T. Two Mechanisms of Killing of *Pseudomonas Aeruginosa* by Tobramycin Assessed at Multiple Inocula via Mechanism-Based Modeling. *Antimicrob. Agents Chemother.* **2015**, *59* (4), 2315–2327.
- (37) Wright, G. D. Aminoglycoside-Modifying Enzymes. *Curr. Opin. Microbiol.* **1999**, *2* (5), 499–503.
- (38) Poole, K. Efflux-Mediated Antimicrobial Resistance. *J. Antimicrob. Chemother.* **2005**, *56* (1), 20–51.
- (39) Vogne, C.; Aires, J. R.; Bailly, C.; Hocquet, D.; Plésiat, P. Role of the Multidrug Efflux System MexXY in the Emergence of Moderate Resistance to Aminoglycosides among *Pseudomonas Aeruginosa* Isolates from Patients with Cystic Fibrosis. *Antimicrob. Agents Chemother.* **2004**, *48* (5), 1676–1680.
- (40) Sobel, M. L.; McKay, G. A.; Poole, K. Contribution of the MexXY Multidrug Transporter to Aminoglycoside Resistance in *Pseudomonas Aeruginosa* Clinical Isolates. *Antimicrob. Agents Chemother.* **2003**, *47* (10), 3202–3207.

- (41) Poole, K. Efflux-Mediated Multiresistance in Gram-Negative Bacteria. *Clin. Microbiol. Infect.* **2004**, *10* (1), 12–26.
- (42) Rosenberg, E. Y.; Ma, D.; Nikaido, H. AcrD of Escherichia Coli Is an Aminoglycoside Efflux Pump. *J. Bacteriol.* **2000**, *182* (6), 1754–1756.
- (43) Moore, R. A.; DeShazer, D.; Reckseidler, S.; Weissman, A.; Woods, D. E. Efflux-Mediated Aminoglycoside and Macrolide Resistance in Burkholderia Pseudomallei. *Antimicrob. Agents Chemother.* **1999**, *43* (3), 465–470.
- (44) Chan, Y. Y.; Tan, T. M. C.; Ong, Y. M.; Chua, K. L. BpeAB-OprB, a Multidrug Efflux Pump in Burkholderia Pseudomallei. *Antimicrob. Agents Chemother.* **2004**, *48* (4), 1128–1135.
- (45) Cundliffe, E. How Antibiotic-Producing Organisms Avoid Suicide. *Annu. Rev. Microbiol.* **1989**, *43*, 207–233.
- (46) Wachino, J.; Arakawa, Y. Exogenously Acquired 16S RRNA Methyltransferases Found in Aminoglycoside-Resistant Pathogenic Gram-Negative Bacteria: An Update. *Drug Resist. Updat.* **2012**, *15* (3), 133–148.
- (47) Beauclerk, A. A. D.; Cundliffe, E. Sites of Action of Two Ribosomal RNA Methylases Responsible for Resistance to Aminoglycosides. *J. Mol. Biol.* **1987**, *193* (4), 661–671.
- (48) Zhou, Y.; Yu, H.; Guo, Q.; Xu, X.; Ye, X.; Wu, S.; Guo, Y.; Wang, M. Distribution of 16S RRNA Methylases among Different Species of Gram-Negative Bacilli with High-Level Resistance to Aminoglycosides. *Eur. J. Clin. Microbiol. Infect. Dis.* **2010**, *29* (11), 1349–1353.
- (49) [https://www.accessdata.fda.gov/drugsatfda\\_docs/nda/2018/210303Orig1s000TOC.cfm](https://www.accessdata.fda.gov/drugsatfda_docs/nda/2018/210303Orig1s000TOC.cfm) (accessed on Oct. 12, 2018).

- (50) Aggen, J. B.; Armstrong, E. S.; Goldblum, A. A.; Dozzo, P.; Linsell, M. S.; Gliedt, M. J.; Hildebrandt, D. J.; Feeney, L. A.; Kubo, A.; Matias, R. D.; Lopez, S.; Gomez, M.; Wlasichuk, K. B.; Diokno, R.; Miller, G. H.; Moser, H. E. Synthesis and Spectrum of the Neoglycoside ACHN-490. *Antimicrob. Agents Chemother.* **2010**, *54* (11), 4636–4642.
- (51) Zhanel, G. G.; Lawson, C. D.; Zelenitsky, S.; Findlay, B.; Schweizer, F.; Adam, H.; Walkty, A.; Rubinstein, E.; Gin, A. S.; Hoban, D. J.; Lynch, J. P.; Karlowsky, J. A. Comparison of the Next-Generation Aminoglycoside Plazomicin to Gentamicin, Tobramycin and Amikacin. *Expert Rev. Anti. Infect. Ther.* **2012**, *10* (4), 459–473.
- (52) Karaiskos, I.; Souli, M.; Giamarellou, H. Plazomicin: An Investigational Therapy for the Treatment of Urinary Tract Infections. *Expert Opin. Investig. Drugs* **2015**, *24* (11), 1501–1511.
- (53) Hanessian, S.; Szychowski, J.; Adhikari, S. S.; Vasquez, G.; Kandasamy, P.; Swayze, E. E.; Migawa, M. T.; Ranken, R.; François, B.; Wirmer-Bartoschek, J.; Jiro Kondo, A.; Westhof, E. Structure-Based Design, Synthesis, and A-Site RRNA Cocrystal Complexes of Functionally Novel Aminoglycoside Antibiotics: C2'' Ether Analogues of Paromomycin. *J. Med. Chem.* **2007**, *50* (10), 2352–2369.
- (54) Bera, S.; Zhanel, G. G.; Schweizer, F. Design, Synthesis, and Antibacterial Activities of Neomycin–Lipid Conjugates: Polycationic Lipids with Potent Gram-Positive Activity. *J. Med. Chem.* **2008**, *51* (19), 6160–6164.
- (55) Pokrovskaya, V.; Belakhov, V.; Hainrichson, M.; Yaron, S.; Baasov, T. Design, Synthesis, and Evaluation of Novel Fluoroquinolone–Aminoglycoside Hybrid Antibiotics. *J. Med. Chem.* **2009**, *52* (8), 2243–2254.
- (56) Bera, S.; Zhanel, G. G.; Schweizer, F. Evaluation of Amphiphilic Aminoglycoside–

- Peptide Triazole Conjugates as Antibacterial Agents. *Bioorg. Med. Chem. Lett.* **2010**, *20* (10), 3031–3035.
- (57) Bera, S.; Zhanel, G. G.; Schweizer, F. Antibacterial Activity of Guanidinylated Neomycin B- and Kanamycin A-Derived Amphiphilic Lipid Conjugates. *J. Antimicrob. Chemother.* **2010**, *65* (6), 1224–1227.
- (58) Bera, S.; Zhanel, G. G.; Schweizer, F. Antibacterial Activities of Aminoglycoside Antibiotics-Derived Cationic Amphiphiles. Polyol-Modified Neomycin B-, Kanamycin A-, Amikacin-, and Neamine-Based Amphiphiles with Potent Broad Spectrum Antibacterial Activity. *J. Med. Chem.* **2010**, *53* (9), 3626–3631.
- (59) Bera, S.; Dhondikubeer, R.; Findlay, B.; Zhanel, G. G.; Schweizer, F. Synthesis and Antibacterial Activities of Amphiphilic Neomycin B-Based Bilipid Conjugates and Fluorinated Neomycin B-Based Lipids. *Molecules* **2012**, *17* (12), 9129–9141.
- (60) Findlay, B.; Zhanel, G. G.; Schweizer, F. Neomycin–Phenolic Conjugates: Polycationic Amphiphiles with Broad-Spectrum Antibacterial Activity, Low Hemolytic Activity and Weak Serum Protein Binding. *Bioorg. Med. Chem. Lett.* **2012**, *22* (4), 1499–1503.
- (61) Berkov-Zrihen, Y.; Herzog, I. M.; Benhamou, R. I.; Feldman, M.; Steinbuch, K. B.; Shaul, P.; Lerer, S.; Eldar, A.; Fridman, M. Tobramycin and Nebramine as Pseudo-Oligosaccharide Scaffolds for the Development of Antimicrobial Cationic Amphiphiles. *Chem. Eur. J.* **2015**, *21* (11), 4340–4349.
- (62) Berkov-Zrihen, Y.; Herzog, I. M.; Feldman, M.; Fridman, M. Site-Selective Displacement of Tobramycin Hydroxyls for Preparation of Antimicrobial Cationic Amphiphiles. *Org. Lett.* **2013**, *15* (24), 6144–6147.
- (63) Herzog, I. M.; Feldman, M.; Eldar-Boock, A.; Satchi-Fainaro, R.; Fridman, M.; Burrows,

- L. L.; Reeves, P. R.; Wang, L.; Garneau-Tsodikova, S.; Fridman, M.; Mingeot-Leclercq, M.-P.; Schutz, G. J. Design of Membrane Targeting Tobramycin-Based Cationic Amphiphiles with Reduced Hemolytic Activity. *Med. Chem. Commun.* **2013**, *4* (1), 120–124.
- (64) Dhondikubeer, R.; Bera, S.; Zhanel, G. G.; Schweizer, F. Antibacterial Activity of Amphiphilic Tobramycin. *J. Antibiot. (Tokyo)*. **2012**, *65* (10), 495–498.
- (65) Herzog, I. M.; Green, K. D.; Berkov-Zrihen, Y.; Feldman, M.; Vidavski, R. R.; Eldar-Boock, A.; Satchi-Fainaro, R.; Eldar, A.; Garneau-Tsodikova, S.; Fridman, M. 6''-Thioether Tobramycin Analogues: Towards Selective Targeting of Bacterial Membranes. *Angew. Chem., Int. Ed. Engl.* **2012**, *51* (23), 5652–5656.
- (66) Yan, R.-B.; Yuan, M.; Wu, Y.; You, X.; Ye, X.-S. Rational Design and Synthesis of Potent Aminoglycoside Antibiotics against Resistant Bacterial Strains. *Bioorg. Med. Chem.* **2011**, *19* (1), 30–40.
- (67) Zimmermann, L.; Das, I.; Désiré, J.; Sautrey, G.; Barros R. S., V.; El Khoury, M.; Mingeot-Leclercq, M.-P.; Décout, J.-L. New Broad-Spectrum Antibacterial Amphiphilic Aminoglycosides Active against Resistant Bacteria: From Neamine Derivatives to Smaller Neosamine Analogues. *J. Med. Chem.* **2016**, *59* (20), 9350–9369.
- (68) Zimmermann, L.; Bussière, A.; Ouberai, M.; Baussanne, I.; Jolival, C.; Mingeot-Leclercq, M.-P.; Décout, J.-L. Tuning the Antibacterial Activity of Amphiphilic Neamine Derivatives and Comparison to Paromamine Homologues. *J. Med. Chem.* **2013**, *56* (19), 7691–7705.
- (69) Baussanne, I.; Bussière, A.; Halder, S.; Ganem-Elbaz, C.; Ouberai, M.; Riou, M.; Paris, J.-M.; Ennifar, E.; Mingeot-Leclercq, M.-P.; Décout, J.-L. Synthesis and Antimicrobial

- Evaluation of Amphiphilic Neamine Derivatives. *J. Med. Chem.* **2010**, *53* (1), 119–127.
- (70) Ouberai, M.; El Garch, F.; Bussiere, A.; Riou, M.; Alsteens, D.; Lins, L.; Baussanne, I.; Dufrière, Y. F.; Brasseur, R.; Decout, J.-L.; Mingeot-Leclercq, M.-P. The Pseudomonas Aeruginosa Membranes: A Target for a New Amphiphilic Aminoglycoside Derivative? *Biochim. Biophys. Acta - Biomembr.* **2011**, *1808* (6), 1716–1727.
- (71) Mingeot-Leclercq, M.-P.; Décout, J.-L. Bacterial Lipid Membranes as Promising Targets to Fight Antimicrobial Resistance, Molecular Foundations and Illustration through the Renewal of Aminoglycoside Antibiotics and Emergence of Amphiphilic Aminoglycosides. *Med. Chem. Commun.* **2016**, *7* (4), 586–611.
- (72) Hancock, R. E. W.; Sahl, H.-G. Antimicrobial and Host-Defense Peptides as New Anti-Infective Therapeutic Strategies. *Nat. Biotechnol.* **2006**, *24* (12), 1551–1557.
- (73) Hanessian, S.; Pachamuthu, K.; Szychowski, J.; Giguère, A.; Swayze, E. E.; Migawa, M. T.; François, B.; Kondo, J.; Westhof, E. Structure-Based Design, Synthesis and A-Site RRNA Co-Crystal Complexes of Novel Amphiphilic Aminoglycoside Antibiotics with New Binding Modes: A Synergistic Hydrophobic Effect against Resistant Bacteria. *Bioorg. Med. Chem. Lett.* **2010**, *20* (23), 7097–7101.
- (74) Battistini, C.; Franceschi, G.; Zarini, F.; Cassinelli, G.; Arcamone, F.; Sanfilippo, A. Semisynthetic Aminoglycoside Antibiotics. IV. 3',4'-Dideoxyparomomycin and Analogues. *J. Antibiot. (Tokyo)*. **1982**, *35* (1), 98–101.
- (75) François, B.; Szychowski, J.; Adhikari, S. S.; Pachamuthu, K.; Swayze, E. E.; Griffey, R. H.; Migawa, M. T.; Westhof, E.; Hanessian, S. Antibacterial Aminoglycosides with a Modified Mode of Binding to the Ribosomal-RNA Decoding Site. *Angew. Chemie, Int. Ed.* **2004**, *43* (48), 6735–6738.

- (76) van den Broek, S. (Bas) A. M. W.; Gruijters, B. W. T.; Rutjes, F. P. J. T.; van Delft, F. L.; Blaauw, R. H. A Short and Scalable Route to Orthogonally O-Protected 2-Deoxystreptamine. *J. Org. Chem.* **2007**, *72* (9), 3577–3580.
- (77) Svenson, J.; Brandsdal, B.-O.; Stensen, W.; Svendsen, J. S. Albumin Binding of Short Cationic Antimicrobial Micropeptides and Its Influence on the in Vitro Bactericidal Effect. *J. Med. Chem.* **2007**, *50* (14), 3334–3339.
- (78) Sautrey, G.; Zimmermann, L.; Deleu, M.; Delbar, A.; Souza Machado, L.; Jeannot, K.; Van Bambeke, F.; Buyck, J. M.; Decout, J.-L.; Mingeot-Leclercq, M.-P. New Amphiphilic Neamine Derivatives Active against Resistant *Pseudomonas Aeruginosa* and Their Interactions with Lipopolysaccharides. *Antimicrob. Agents Chemother.* **2014**, *58* (8), 4420–4430.
- (79) Berkov-Zrihen, Y.; Herzog, I. M.; Feldman, M.; Fridman, M. Site-Selective Displacement of Tobramycin Hydroxyls for Preparation of Antimicrobial Cationic Amphiphiles. *Org. Lett.* **2013**, *15* (24), 6144–6147.
- (80) Gibbs, C. F.; Hough, L.; Richardson, A. C. A New Synthesis of a 2,3-Epimino- $\alpha$ -D-Allopyranoside. *Carbohydr. Res.* **1965**, *1* (4), 290–296.
- (81) Richardson, A. C. Nucleophilic Replacement Reactions of Sulphonates : Part VI. A Summary of Steric and Polar Factors. *Carbohydr. Res.* **1969**, *10* (3), 395–402.
- (82) Hale, K. J. Anthony Charles Richardson: (1935–2011). *Adv. Carbohydr. Chem. Biochem.* **2011**, *66*, 3–68.
- (83) Fürst, A.; Plattner, P. A. Über Steroide Und Sexualhormone. 160. Mitteilung. 2 $\alpha$ , 3 $\alpha$ - Und 2 $\beta$ , 3 $\beta$ -Oxido-Cholestane; Konfiguration Der 2-Oxy-Cholestane. *Helv. Chim. Acta* **1949**, *32* (1), 275–283.

- (84) Benhamou, R. I.; Shaul, P.; Herzog, I. M.; Fridman, M. Di-N-Methylation of Anti-Gram-Positive Aminoglycoside-Derived Membrane Disruptors Improves Antimicrobial Potency and Broadens Spectrum to Gram-Negative Bacteria. *Angew. Chemie, Int. Ed.* **2015**, *54* (46), 13617–13621.
- (85) Li, J.; Nation, R. L.; Turnidge, J. D.; Milne, R. W.; Coulthard, K.; Rayner, C. R.; Paterson, D. L. Colistin: The Re-Emerging Antibiotic for Multidrug-Resistant Gram-Negative Bacterial Infections. *Lancet. Infect. Dis.* **2006**, *6* (9), 589–601.
- (86) Payne, D. J.; Gwynn, M. N.; Holmes, D. J.; Pompliano, D. L. Drugs for Bad Bugs: Confronting the Challenges of Antibacterial Discovery. *Nat. Rev. Drug Discov.* **2007**, *6* (1), 29–40.
- (87) Brown, D. Antibiotic Resistance Breakers: Can Repurposed Drugs Fill the Antibiotic Discovery Void? *Nat. Rev. Drug Discov.* **2015**, *14* (12), 821–832.
- (88) Gill, E. E.; Franco, O. L.; Hancock, R. E. W. Antibiotic Adjuvants: Diverse Strategies for Controlling Drug-Resistant Pathogens. *Chem. Biol. Drug Des.* **2015**, *85* (1), 56–78.
- (89) Kalan, L.; Wright, G. D. Antibiotic Adjuvants: Multicomponent Anti-Infective Strategies. *Expert Rev. Mol. Med.* **2011**, *13*, e5.
- (90) Wright, G. D. Antibiotic Adjuvants: Rescuing Antibiotics from Resistance. *Trends Microbiol.* **2016**, *24* (11), 862–871.
- (91) Domalaon, R.; Yang, X.; Lyu, Y.; Zhanel, G. G.; Schweizer, F. Polymyxin B 3 – Tobramycin Hybrids with *Pseudomonas Aeruginosa* -Selective Antibacterial Activity and Strong Potentiation of Rifampicin, Minocycline, and Vancomycin. *ACS Infect. Dis.* **2017**, *3* (12), 941–954.
- (92) Domalaon, R.; Idowu, T.; Zhanel, G. G.; Schweizer, F. Antibiotic Hybrids: The Next

- Generation of Agents and Adjuvants against Gram-Negative Pathogens? *Clin. Microbiol. Rev.* **2018**, *31* (2), e00077-17.
- (93) Gorityala, B. K.; Guchhait, G.; Fernando, D. M.; Deo, S.; McKenna, S. A.; Zhanel, G. G.; Kumar, A.; Schweizer, F. Adjuvants Based on Hybrid Antibiotics Overcome Resistance in *Pseudomonas Aeruginosa* and Enhance Fluoroquinolone Efficacy. *Angew. Chemie Int. Ed.* **2016**, *55* (2), 555–559.
- (94) Tommasi, R.; Brown, D. G.; Walkup, G. K.; Manchester, J. I.; Miller, A. A. ESKAPEing the Labyrinth of Antibacterial Discovery. *Nat. Rev. Drug Discov.* **2015**, *14* (8), 529–542.
- (95) Page, M. G. P.; Bush, K. Discovery and Development of New Antibacterial Agents Targeting Gram-Negative Bacteria in the Era of Pandrug Resistance: Is the Future Promising? *Curr. Opin. Pharmacol.* **2014**, *18*, 91–97.
- (96) Silver, L. L. Challenges of Antibacterial Discovery. *Clin. Microbiol. Rev.* **2011**, *24* (1), 71–109.
- (97) Silver, L. L. A Gestalt Approach to Gram-Negative Entry. *Bioorg. Med. Chem.* **2016**, *24* (24), 6379–6389.
- (98) Silhavy, T. J.; Kahne, D.; Walker, S. The Bacterial Cell Envelope. *Cold Spring Harb. Perspect. Biol.* **2010**, *2* (5), a000414.
- (99) Kamio, Y.; Nikaido, H. Outer Membrane of *Salmonella Typhimurium*: Accessibility of Phospholipid Head Groups to Phospholipase C and Cyanogen Bromide Activated Dextran in the External Medium. *Biochemistry* **1976**, *15* (12), 2561–2570.
- (100) Epanand, R. M.; Walker, C.; Epanand, R. F.; Magarvey, N. A. Molecular Mechanisms of Membrane Targeting Antibiotics. *Biochim. Biophys. Acta - Biomembr.* **2016**, *1858* (5), 980–987.

- (101) Zgurskaya, H. I.; López, C. A.; Gnanakaran, S. Permeability Barrier of Gram-Negative Cell Envelopes and Approaches To Bypass It. *ACS Infect. Dis.* **2015**, *1* (11), 512–522.
- (102) Pagès, J.-M.; James, C. E.; Winterhalter, M. The Porin and the Permeating Antibiotic: A Selective Diffusion Barrier in Gram-Negative Bacteria. *Nat. Rev. Microbiol.* **2008**, *6* (12), 893–903.
- (103) Delcour, A. H. Outer Membrane Permeability and Antibiotic Resistance. *Biochim. Biophys. Acta - Proteins Proteomics* **2009**, *1794* (5), 808–816.
- (104) Nikaido, H. Molecular Basis of Bacterial Outer Membrane Permeability Revisited. *Microbiol. Mol. Biol. Rev.* **2003**, *67* (4), 593–656.
- (105) Raetz, C. R. H.; Whitfield, C. Lipopolysaccharide Endotoxins. *Annu. Rev. Biochem.* **2002**, *71* (1), 635–700.
- (106) Wu, E. L.; Engström, O.; Jo, S.; Stuhlsatz, D.; Yeom, M. S.; Klauda, J. B.; Widmalm, G.; Im, W. Molecular Dynamics and NMR Spectroscopy Studies of E. Coli Lipopolysaccharide Structure and Dynamics. *Biophys. J.* **2013**, *105* (6), 1444–1455.
- (107) Clifton, L. A.; Skoda, M. W. A.; Le Brun, A. P.; Ciesielski, F.; Kuzmenko, I.; Holt, S. A.; Lakey, J. H. Effect of Divalent Cation Removal on the Structure of Gram-Negative Bacterial Outer Membrane Models. *Langmuir* **2015**, *31* (1), 404–412.
- (108) Plésiat, P.; Nikaido, H. Outer Membranes of Gram-Negative Bacteria Are Permeable to Steroid Probes. *Mol. Microbiol.* **1992**, *6* (10), 1323–1333.
- (109) Yoshimura, F.; Nikaido, H. Permeability of Pseudomonas Aeruginosa Outer Membrane to Hydrophilic Solutes. *J. Bacteriol.* **1982**, *152* (2), 636–642.
- (110) Angus, B. L.; Carey, A. M.; Caron, D. A.; Kropinski, A. M.; Hancock, R. E. Outer Membrane Permeability in Pseudomonas Aeruginosa: Comparison of a Wild-Type with

- an Antibiotic-Supersusceptible Mutant. *Antimicrob. Agents Chemother.* **1982**, *21* (2), 299–309.
- (111) Sugawara, E.; Nagano, K.; Nikaido, H. Factors Affecting the Folding of *Pseudomonas Aeruginosa* OprF Porin into the One-Domain Open Conformer. *MBio* **2010**, *1* (4), e00228-10.
- (112) Sugawara, E.; Nestorovich, E. M.; Bezrukov, S. M.; Nikaido, H. *Pseudomonas Aeruginosa* Porin OprF Exists in Two Different Conformations. *J. Biol. Chem.* **2006**, *281* (24), 16220–16229.
- (113) Trias, J.; Nikaido, H. Protein D2 Channel of the *Pseudomonas Aeruginosa* Outer Membrane Has a Binding Site for Basic Amino Acids and Peptides. *J. Biol. Chem.* **1990**, *265* (26), 15680–15684.
- (114) Trias, J.; Nikaido, H. Outer Membrane Protein D2 Catalyzes Facilitated Diffusion of Carbapenems and Penems through the Outer Membrane of *Pseudomonas Aeruginosa*. *Antimicrob. Agents Chemother.* **1990**, *34* (1), 52–57.
- (115) Pirnay, J.-P.; Vos, D. De; Mossialos, D.; Vanderkelen, A.; Cornelis, P.; Zizi, M. Analysis of the *Pseudomonas Aeruginosa* OprD Gene from Clinical and Environmental Isolates. *Environ. Microbiol.* **2002**, *4* (12), 872–882.
- (116) Quale, J.; Bratu, S.; Gupta, J.; Landman, D. Interplay of Efflux System, AmpC, and OprD Expression in Carbapenem Resistance of *Pseudomonas Aeruginosa* Clinical Isolates. *Antimicrob. Agents Chemother.* **2006**, *50* (5), 1633–1641.
- (117) Quinn, J. P.; Dudek, E. J.; DiVincenzo, C. A.; Lucks, D. A.; Lerner, S. A. Emergence of Resistance to Imipenem during Therapy for *Pseudomonas Aeruginosa* Infections. *J. Infect. Dis.* **1986**, *154* (2), 289–294.

- (118) Ruiz, N.; Kahne, D.; Silhavy, T. J. Advances in Understanding Bacterial Outer-Membrane Biogenesis. *Nat. Rev. Microbiol.* **2006**, *4* (1), 57–66.
- (119) Yamaguchi, A.; Ohmori, H.; Kaneko-Ohdera, M.; Nomura, T.; Sawai, T. Delta PH-Dependent Accumulation of Tetracycline in Escherichia Coli. *Antimicrob. Agents Chemother.* **1991**, *35* (1), 53–56.
- (120) Nikaido, H.; Thanassi, D. G. Penetration of Lipophilic Agents with Multiple Protonation Sites into Bacterial Cells: Tetracyclines and Fluoroquinolones as Examples. *Antimicrob. Agents Chemother.* **1993**, *37* (7), 1393–1399.
- (121) Fresta, M.; Guccione, S.; Beccari, A. R.; Furneri, P. M.; Puglisi, G. Combining Molecular Modeling with Experimental Methodologies: Mechanism of Membrane Permeation and Accumulation of Ofloxacin. *Bioorg. Med. Chem.* **2002**, *10* (12), 3871–3889.
- (122) Cramariuc, O.; Rog, T.; Javanainen, M.; Monticelli, L.; Polishchuk, A. V.; Vattulainen, I. Mechanism for Translocation of Fluoroquinolones across Lipid Membranes. *Biochim. Biophys. Acta - Biomembr.* **2012**, *1818* (11), 2563–2571.
- (123) Silver, L. L. Are Natural Products Still the Best Source for Antibacterial Discovery? The Bacterial Entry Factor. *Expert Opin. Drug Discov.* **2008**, *3* (5), 487–500.
- (124) Santoro, A.; Cappello, A. R.; Madeo, M.; Martello, E.; Iacopetta, D.; Dolce, V. Interaction of Fosfomycin with the Glycerol 3-Phosphate Transporter of Escherichia Coli. *Biochim. Biophys. Acta - Biomembr.* **2011**, *1810* (12), 1323–1329.
- (125) Li, X.-Z.; Nikaido, H. Efflux-Mediated Drug Resistance in Bacteria: An Update. *Drugs* **2009**, *69* (12), 1555–1623.
- (126) Li, X.-Z.; Nikaido, H. Efflux-Mediated Drug Resistance in Bacteria. *Drugs* **2004**, *64* (2), 159–204.

- (127) Nikaido, H. Multidrug Efflux Pumps of Gram-Negative Bacteria. *J. Bacteriol.* **1996**, *178* (20), 5853–5859.
- (128) Zgurskaya, H. I.; Nikaido, H. Multidrug Resistance Mechanisms: Drug Efflux across Two Membranes. *Mol. Microbiol.* **2000**, *37* (2), 219–225.
- (129) Masi, M.; Réfregiers, M.; Pos, K. M.; Pagès, J.-M. Mechanisms of Envelope Permeability and Antibiotic Influx and Efflux in Gram-Negative Bacteria. *Nat. Microbiol.* **2017**, *2* (3), 17001.
- (130) Li, X.-Z.; Plésiat, P.; Nikaido, H. The Challenge of Efflux-Mediated Antibiotic Resistance in Gram-Negative Bacteria. *Clin. Microbiol. Rev.* **2015**, *28* (2), 337–418.
- (131) Misra, R.; Bavro, V. N. Assembly and Transport Mechanism of Tripartite Drug Efflux Systems. *Biochim. Biophys. Acta - Proteins Proteomics* **2009**, *1794* (5), 817–825.
- (132) Nikaido, H.; Pagès, J.-M. Broad-Specificity Efflux Pumps and Their Role in Multidrug Resistance of Gram-Negative Bacteria. *FEMS Microbiol. Rev.* **2012**, *36* (2), 340–363.
- (133) Nakashima, R.; Sakurai, K.; Yamasaki, S.; Nishino, K.; Yamaguchi, A. Structures of the Multidrug Exporter AcrB Reveal a Proximal Multisite Drug-Binding Pocket. *Nature* **2011**, *480* (7378), 565–569.
- (134) Eicher, T.; Cha, H.; Seeger, M. A.; Brandstatter, L.; El-Delik, J.; Bohnert, J. A.; Kern, W. V.; Verrey, F.; Grutter, M. G.; Diederichs, K.; Pos, K. M. Transport of Drugs by the Multidrug Transporter AcrB Involves an Access and a Deep Binding Pocket That Are Separated by a Switch-Loop. *Proc. Natl. Acad. Sci. U. S. A.* **2012**, *109* (15), 5687–5692.
- (135) Nakashima, R.; Sakurai, K.; Yamasaki, S.; Hayashi, K.; Nagata, C.; Hoshino, K.; Onodera, Y.; Nishino, K.; Yamaguchi, A. Structural Basis for the Inhibition of Bacterial Multidrug Exporters. *Nature* **2013**, *500* (7460), 102–106.

- (136) Eicher, T.; Seeger, M. A.; Anselmi, C.; Zhou, W.; Brandstatter, L.; Verrey, F.; Diederichs, K.; Faraldo-Gomez, J. D.; Pos, K. M. Coupling of Remote Alternating-Access Transport Mechanisms for Protons and Substrates in the Multidrug Efflux Pump AcrB. *Elife* **2014**, *3*, e03145.
- (137) Brown, D. G.; May-Dracka, T. L.; Gagnon, M. M.; Tommasi, R. Trends and Exceptions of Physical Properties on Antibacterial Activity for Gram-Positive and Gram-Negative Pathogens. *J. Med. Chem.* **2014**, *57* (23), 10144–10161.
- (138) Renau, T. E.; Le, R.; Flamme, E. M.; Sangalang, J.; She, M. W.; Yen, R.; Gannon, C. L.; Griffith, D.; Chamberland, S.; Lomovskaya, O.; Hecker, S. J.; Lee, V. J.; Ohta, T. Inhibitors of Efflux Pumps in *Pseudomonas Aeruginosa* Potentiate the Activity of the Fluoroquinolone Antibacterial Levofloxacin. *J. Med. Chem.* **1999**, *42* (24), 4928–4931.
- (139) Lomovskaya, O.; Warren, M. S.; Lee, A.; Galazzo, J.; Fronko, R.; Lee, M.; Blais, J.; Cho, D.; Chamberland, S.; Renau, T.; Leger, R.; Hecker, S.; Watkins, W.; Hoshino, K.; Ishida, H.; Lee, V. J. Identification and Characterization of Inhibitors of Multidrug Resistance Efflux Pumps in *Pseudomonas Aeruginosa*: Novel Agents for Combination Therapy. *Antimicrob. Agents Chemother.* **2001**, *45* (1), 105–116.
- (140) Renau, T. E.; Leger, R.; Flamme, E. M.; She, M. W.; Gannon, C. L.; Mathias, K. M.; Lomovskaya, O.; Chamberland, S.; Lee, V. J.; Ohta, T.; Nakayama, K.; Ishida, Y. Addressing the Stability of C-Capped Dipeptide Efflux Pump Inhibitors That Potentiate the Activity of Levofloxacin in *Pseudomonas Aeruginosa*. *Bioorg. Med. Chem. Lett.* **2001**, *11* (5), 663–667.
- (141) Watkins, W. J.; Landaverry, Y.; Léger, R.; Litman, R.; Renau, T. E.; Williams, N.; Yen, R.; Zhang, J. Z.; Chamberland, S.; Madsen, D.; Griffith, D.; Tembe, V.; Huie, K.; Dudley,

- M. N. The Relationship between Physicochemical Properties, in Vitro Activity and Pharmacokinetic Profiles of Analogues of Diamine-Containing Efflux Pump Inhibitors. *Bioorganic Med. Chem. Lett.* **2003**, *13* (23), 4241–4244.
- (142) Lomovskaya, O.; Bostian, K. A. Practical Applications and Feasibility of Efflux Pump Inhibitors in the Clinic - A Vision for Applied Use. *Biochem. Pharmacol.* **2006**, *71* (7), 910–918.
- (143) Schumacher, A.; Trittler, R.; Bohnert, J. A.; Kümmerer, K.; Pagès, J.-M.; Kern, W. V. Intracellular Accumulation of Linezolid in *Escherichia Coli*, *Citrobacter Freundii* and *Enterobacter Aerogenes*: Role of Enhanced Efflux Pump Activity and Inactivation. *J. Antimicrob. Chemother.* **2007**, *59* (6), 1261–1264.
- (144) Pannek, S.; Higgins, P. G.; Steinke, P.; Jonas, D.; Akova, M.; Bohnert, J. A.; Seifert, H.; Kern, W. V. Multidrug Efflux Inhibition in *Acinetobacter Baumannii*: Comparison between 1-(1-Naphthylmethyl)-Piperazine and Phenyl-Arginine- $\beta$ -Naphthylamide. *J. Antimicrob. Chemother.* **2006**, *57* (5), 970–974.
- (145) Schumacher, A.; Steinke, P.; Bohnert, J. A.; Akova, M.; Jonas, D.; Kern, W. V. Effect of 1-(1-Naphthylmethyl)-Piperazine, a Novel Putative Efflux Pump Inhibitor, on Antimicrobial Drug Susceptibility in Clinical Isolates of Enterobacteriaceae Other than *Escherichia Coli*. *J. Antimicrob. Chemother.* **2006**, *57* (2), 344–348.
- (146) Kern, W. V.; Steinke, P.; Schumacher, A.; Schuster, S.; von Baum, H.; Bohnert, J. A. Effect of 1-(1-Naphthylmethyl)-Piperazine, a Novel Putative Efflux Pump Inhibitor, on Antimicrobial Drug Susceptibility in Clinical Isolates of *Escherichia Coli*. *J. Antimicrob. Chemother.* **2006**, *57* (2), 339–343.
- (147) Bohnert, J. A.; Kern, W. V. Selected Arylpiperazines Are Capable of Reversing Multidrug

- Resistance in Escherichia Coli Overexpressing RND Efflux Pumps Selected Arylpiperazines Are Capable of Reversing Multidrug Resistance in Escherichia Coli Overexpressing RND Efflux Pumps. *Antimicrob. Agents Chemother.* **2005**, 49 (2), 849–852.
- (148) Kaatz, G. W.; Moudgal, V. V.; Seo, S. M.; Hansen, J. B.; Kristiansen, J. E. Phenylpiperidine Selective Serotonin Reuptake Inhibitors Interfere with Multidrug Efflux Pump Activity in Staphylococcus Aureus. *Int. J. Antimicrob. Agents* **2003**, 22 (3), 254–261.
- (149) Yoshida, K.-I.; Nakayama, K.; Ohtsuka, M.; Kuru, N.; Yokomizo, Y.; Sakamoto, A.; Takemura, M.; Hoshino, K.; Kanda, H.; Nitantai, H.; Namba, K.; Yoshida, K.; Imamura, Y.; Zhang, J. Z.; Lee, V. J.; Watkins, W. J. MexAB-OprM Specific Efflux Pump Inhibitors in Pseudomonas Aeruginosa. Part 7: Highly Soluble and in Vivo Active Quaternary Ammonium Analogue D13-9001, a Potential Preclinical Candidate. *Bioorg. Med. Chem.* **2007**, 15 (22), 7087–7097.
- (150) Opperman, T. J.; Kwasny, S. M.; Kim, H. S.; Nguyen, S. T.; Houseweart, C.; D'Souza, S.; Walker, G. C.; Peet, N. P.; Nikaido, H.; Bowlin, T. L. Characterization of a Novel Pyranopyridine Inhibitor of the AcrAB Efflux Pump of Escherichia Coli. *Antimicrob. Agents Chemother.* **2014**, 58 (2), 722–733.
- (151) Nguyen, S. T.; Kwasny, S. M.; Ding, X.; Cardinale, S. C.; McCarthy, C. T.; Kim, H. S.; Nikaido, H.; Peet, N. P.; Williams, J. D.; Bowlin, T. L.; Opperman, T. J. Structure-Activity Relationships of a Novel Pyranopyridine Series of Gram-Negative Bacterial Efflux Pump Inhibitors. *Bioorganic Med. Chem.* **2015**, 23 (9), 2024–2034.
- (152) Aron, Z.; Opperman, T. J. Optimization of a Novel Series of Pyranopyridine RND Efflux

- Pump Inhibitors. *Curr. Opin. Microbiol.* **2016**, *33*, 1–6.
- (153) Bolla, J.-M.; Alibert-Franco, S.; Handzlik, J.; Chevalier, J.; Mahamoud, A.; Boyer, G.; Kieć-Kononowicz, K.; Pagès, J.-M. Strategies for Bypassing the Membrane Barrier in Multidrug Resistant Gram-Negative Bacteria. *FEBS Lett.* **2011**, *585* (11), 1682–1690.
- (154) Opperman, T. J.; Nguyen, S. T. Recent Advances toward a Molecular Mechanism of Efflux Pump Inhibition. *Front. Microbiol.* **2015**, *6*, 421.
- (155) Vargiu, A. V; Nikaido, H. Multidrug Binding Properties of the AcrB Efflux Pump Characterized by Molecular Dynamics Simulations. *Proc. Natl. Acad. Sci. U. S. A.* **2012**, *109* (50), 20637–20642.
- (156) Vargiu, A. V; Ruggerone, P.; Opperman, T. J.; Nguyen, S. T.; Nikaido, H. Molecular Mechanism of MBX2319 Inhibition of Escherichia Coli AcrB Multidrug Efflux Pump and Comparison with Other Inhibitors. *Antimicrob. Agents Chemother.* **2014**, *58* (10), 6224–6234.
- (157) Lamers, R. P.; Cavallari, J. F.; Burrows, L. L. The Efflux Inhibitor Phenylalanine-Arginine Beta-Naphthylamide (PAβN) Permeabilizes the Outer Membrane of Gram-Negative Bacteria. *PLoS One* **2013**, *8* (3), e60666.
- (158) Zechini, B.; Versace, I. Inhibitors of Multidrug Resistant Efflux Systems in Bacteria. *Recent Pat. Antiinfect. Drug Discov.* **2009**, *4* (1), 37–50.
- (159) Opperman, T.; Nguyen, S. Recent Advances toward a Molecular Mechanism of Efflux Pump Inhibition. *Frontiers in Microbiology*. 2015, p 421.
- (160) Cha, H. J.; Müller, R. T.; Pos, K. M. Switch-Loop Flexibility Affects Transport of Large Drugs by the Promiscuous AcrB Multidrug Efflux Transporter. *Antimicrob. Agents Chemother.* **2014**, *58* (8), 4767–4772.

- (161) Eicher, T.; Cha, H. -j.; Seeger, M. A.; Brandstatter, L.; El-Delik, J.; Bohnert, J. A.; Kern, W. V.; Verrey, F.; Grutter, M. G.; Diederichs, K.; Pos, K. M. Transport of Drugs by the Multidrug Transporter AcrB Involves an Access and a Deep Binding Pocket That Are Separated by a Switch-Loop. *Proc. Natl. Acad. Sci.* **2012**, *109* (15), 5687–5692.
- (162) Handzlik, J.; Matys, A.; Kieć-Kononowicz, K. Recent Advances in Multi-Drug Resistance (MDR) Efflux Pump Inhibitors of Gram-Positive Bacteria *S. Aureus*. *Antibiot. (Basel, Switzerland)* **2013**, *2* (1), 28–45.
- (163) German, N.; Kaatz, G. W.; Kerns, R. J. Synthesis and Evaluation of PSSRI-Based Inhibitors of Staphylococcus Aureus Multidrug Efflux Pumps. *Bioorg. Med. Chem. Lett.* **2008**, *18* (4), 1368–1373.
- (164) Nakayama, K.; Ishida, Y.; Ohtsuka, M.; Kawato, H.; Yoshida, K. ichi; Yokomizo, Y.; Hosono, S.; Ohta, T.; Hoshino, K.; Ishida, H.; Yoshida, K.; Renau, T. E.; Leger, R.; Zhang, J. Z.; Lee, V. J.; Watkins, W. J. MexAB-OprM-Specific Efflux Pump Inhibitors in *Pseudomonas Aeruginosa*. Part 1: Discovery and Early Strategies for Lead Optimization. *Bioorg. Med. Chem. Lett.* **2003**, *13* (23), 4201–4204.
- (165) Nakayama, K.; Ishida, Y.; Ohtsuka, M.; Kawato, H.; Yoshida, K.; Yokomizo, Y.; Ohta, T.; Hoshino, K.; Otani, T.; Kurosaka, Y.; Yoshida, K.; Ishida, H.; Lee, V. J.; Renau, T. E.; Watkins, W. J. MexAB-OprM Specific Efflux Pump Inhibitors in *Pseudomonas Aeruginosa*. Part 2: Achieving Activity in Vivo through the Use of Alternative Scaffolds. *Bioorg. Med. Chem. Lett.* **2003**, *13* (23), 4205–4208.
- (166) Nakayama, K.; Kawato, H.; Watanabe, J.; Ohtsuka, M.; Yoshida, K.; Yokomizo, Y.; Sakamoto, A.; Kuru, N.; Ohta, T.; Hoshino, K.; Yoshida, K.; Ishida, H.; Cho, A.; Palme, M. H.; Zhang, J. Z.; Lee, V. J.; Watkins, W. J. MexAB-OprM Specific Efflux Pump

- Inhibitors in *Pseudomonas Aeruginosa*. Part 3: Optimization of Potency in the Pyridopyrimidine Series through the Application of a Pharmacophore Model. *Bioorg. Med. Chem. Lett.* **2004**, *14* (2), 475–479.
- (167) Nakayama, K.; Kuru, N.; Ohtsuka, M.; Yokomizo, Y.; Sakamoto, A.; Kawato, H.; Yoshida, K.; Ohta, T.; Hoshino, K.; Akimoto, K.; Itoh, J.; Ishida, H.; Cho, A.; Palme, M. H.; Zhang, J. Z.; Lee, V. J.; Watkins, W. J. MexAB-OprM Specific Efflux Pump Inhibitors in *Pseudomonas Aeruginosa*. Part 4: Addressing the Problem of Poor Stability Due to Photoisomerization of an Acrylic Acid Moiety. *Bioorg. Med. Chem. Lett.* **2004**, *14* (10), 2493–2497.
- (168) Yoshida, K.; Nakayama, K.; Kuru, N.; Kobayashi, S.; Ohtsuka, M.; Takemura, M.; Hoshino, K.; Kanda, H.; Zhang, J. Z.; Lee, V. J.; Watkins, W. J. MexAB-OprM Specific Efflux Pump Inhibitors in *Pseudomonas Aeruginosa*. Part 5: Carbon-Substituted Analogues at the C-2 Position. *Bioorg. Med. Chem.* **2006**, *14* (6), 1993–2004.
- (169) Yoshida, K.; Nakayama, K.; Yokomizo, Y.; Ohtsuka, M.; Takemura, M.; Hoshino, K.; Kanda, H.; Namba, K.; Nitani, H.; Zhang, J. Z.; Lee, V. J.; Watkins, W. J. MexAB-OprM Specific Efflux Pump Inhibitors in *Pseudomonas Aeruginosa*. Part 6: Exploration of Aromatic Substituents. *Bioorg. Med. Chem.* **2006**, *14* (24), 8506–8518.
- (170) Nakashima, R.; Sakurai, K.; Yamasaki, S.; Hayashi, K.; Nagata, C.; Hoshino, K.; Onodera, Y.; Nishino, K.; Yamaguchi, A. Structural Basis for the Inhibition of Bacterial Multidrug Exporters. *Nature* **2013**, *500* (7460), 102–106.
- (171) Aron, Z.; Opperman, T. J. The Hydrophobic Trap-the Achilles Heel of RND Efflux Pumps. *Res. Microbiol.* **2017**, 1–8.
- (172) Sjutts, H.; Vargiu, A. V.; Kwasny, S. M.; Nguyen, S. T.; Kim, H.-S.; Ding, X.; Ornik, A. R.;

Ruggerone, P.; Bowlin, T. L.; Nikaido, H.; Pos, K. M.; Opperman, T. J. Molecular Basis for Inhibition of AcrB Multidrug Efflux Pump by Novel and Powerful Pyranopyridine Derivatives. *Proc. Natl. Acad. Sci. U. S. A.* **2016**, *113* (13), 3509–3514.

## Chapter 2: Thesis Objectives

### 2.1 AIM OF THE THESIS AND STUDY OBJECTIVES

The compilation of this thesis is based on the “Sandwich Thesis” format. The first aim of the work described in this thesis was to open up new opportunities to develop alternative therapies against Gram-negative pathogens. The study objectives include:

- 1) To design and synthesize amphiphilic aminoglycoside-based hybrid adjuvants;
- 2) To assess the adjuvant functions of the newly-synthesized compounds by using the fractional inhibitory concentration (FIC) index as a measure of the interaction between two agents;
- 3) To perform the *in vivo* antimicrobial efficacy studies in the *Galleria mellonella* larvae *in vivo* infection model;
- 4) To carry out mechanistic studies to determine the modes of action of the novel hybrid adjuvants that display strong synergies;
- 5) To explore the structure-activity relationships by replacing one domain of the aminoglycoside-based hybrids with other pharmacophoric fragments and then reevaluate the adjuvant properties of the optimized compounds.

In addition, we were also interested in developing new amphiphilic aminoglycosides that are capable of influencing host immune responses since immunomodulatory compounds are becoming increasingly important in anti-infective therapy. Thus, we set out to:

- 1) Design and synthesize amphiphilic tobramycin-based analogues;

- 2) Evaluate the antimicrobial activities against a panel of Gram-positive and Gram-negative bacteria;
- 3) Explore the immunomodulatory properties of the most potent amphiphilic tobramycin analogues that includes monitoring the production of the pro-inflammatory cytokines TNF- $\alpha$  and IL-1 $\beta$ , the anti-inflammatory cytokine IL-1RA as well as the chemokines Gro- $\alpha$  and IL-8 in THP-1 macrophages by ELISA.

## 2.2 ORGANIZATION OF THE THESIS

Chapter 1 provides a comprehensive review of the aminoglycoside antibiotics and a general introduction of the main challenges of antibacterial discovery.

Chapter 3 demonstrates that conjugation of a tobramycin (TOB) vector to efflux pump inhibitors (EPIs) enhances the synergy and efficacy of EPIs in combination with tetracycline antibiotics against multidrug-resistant (MDR) Gram-negative bacteria.

Chapter 4 examines the *in vitro* effect of TOB-EPI conjugates in combinations with fluoroquinolones, rifampicin and fosfomycin on the growth of MDR and extremely-drug resistant (XDR) *Pseudomonas aeruginosa*.

Chapter 5 reports on a novel class of tobramycin-lysine conjugates that sensitize Gram-negative bacteria to rifampicin and minocycline against MDR and XDR *P. aeruginosa* isolates.

Chapter 6 describes structural optimization studies that involve the modification of TOB-based hybrid adjuvants by replacing TOB by the pseudo-disaccharide nebramine (NEB).

In Chapter 7, we turn to studies of the immunomodulatory properties of amphiphilic tobramycin-based analogues.

Summary of the outcome of this work, perspectives, and future outlook are provided in Chapter 8.

Chapters 9, 10, 11, and 12 are supporting information for Chapters 3, 5, 6, and 7, respectively.

## **Chapter 3: A tobramycin vector enhances synergy and efficacy of efflux pump inhibitors against multidrug-resistant Gram-negative bacteria**

*By Xuan Yang, Sudeep Goswami, Bala Kishan Gorityala, Ronald Domalaon, Yinfeng Lyu, Ayush Kumar, George G. Zhanel, and Frank Schweizer. First published in Journal of Medicinal Chemistry, 60 (9), 2017, 3913-3932. Reproduced with permission.*

*Contributions of Authors: Xuan Yang was responsible for designing, synthesizing and characterizing the conjugates on the advice of Frank Schweizer. Xuan Yang, Sudeep Goswami, and Yinfeng Lyu performed the biochemical assays under the guidance of Frank Schweizer, Ayush Kumar, and George G. Zhanel. Bala Kishan Gorityala and Yinfeng Lyu performed in vivo studies. Xuan Yang and Frank Schweizer wrote the main manuscript with contributions from all authors.*

### **3.1 ABSTRACT**

Drug efflux mechanisms interact synergistically with the outer membrane permeability barrier of Gram-negative bacteria leading to intrinsic resistance that presents a major challenge for antibiotic drug development. Efflux pump inhibitors (EPIs), which block the efflux of antibiotics synergize antibiotics, but the clinical development of EPI/antibiotic combination therapy to treat multidrug-resistant (MDR) Gram-negative infections has been challenging. This is in part caused by the inefficiency of current EPIs to penetrate the outer membrane and resist

efflux. We demonstrate that conjugation of a tobramycin (TOB) vector to EPIs like NMP, paroxetine or DBP enhances synergy and efficacy of EPIs in combination with tetracycline antibiotics against MDR Gram-negative bacteria including *Pseudomonas aeruginosa*. Besides potentiating tetracycline antibiotics TOB-EPI conjugates can also suppress resistance development to the tetracycline antibiotic minocycline thereby providing a strategy to develop more effective adjuvants to rescue tetracycline antibiotics from resistance in MDR Gram-negative bacteria.

### 3.2 INTRODUCTION

Multidrug-resistant (MDR) Gram-negative bacterial infections pose a global threat to human health as our arsenal to treat infections is quickly drying up with no novel drug classes against Gram-negative pathogens in clinical development.<sup>1,2</sup> Among Gram-negative bacteria, infections caused by *Pseudomonas aeruginosa* are especially challenging as this organism is intrinsically resistant to many classes of antibiotics.<sup>3</sup> The Infectious Disease Society of America includes *P. aeruginosa* in its list of “ESKAPE” pathogens that pose the greatest threat to human health.<sup>4</sup> The molecular basis of intrinsic resistance in *P. aeruginosa* is the presence of a highly impermeable outer membrane with expression of multiple efflux pumps that effectively reduce the intracellular concentration of the given drug.<sup>5</sup> The inability to discover new antibacterials with novel modes of action against Gram-negative bacteria in general and *P. aeruginosa* in particular over the past 5 decades demands strategies capable of restoring meaningful activity in antibiotics against resistant pathogens. One such approach is the use of small molecule-based adjuvants capable of overcoming resistance in Gram-negative bacteria.<sup>6-8</sup> Examples of adjuvants include  $\beta$ -lactamase inhibitors which prevent inactivation of  $\beta$ -lactam antibiotics, membrane

permeabilizers which destabilize the outer membrane in bacteria, and efflux pump inhibitors (EPIs). So far only  $\beta$ -lactamase inhibitors have been approved as adjuvants for clinical use.<sup>1</sup>

EPIs block the function of efflux pumps in Gram-negative bacteria by competing with the antibiotic binding site or by perturbation of the outer membrane channel or assembly of the tripartite protein complex of resistance-nodulation-division (RND) pumps.<sup>9</sup> Alternatively, perturbation or disruption of the proton motive force (PMF) which energizes efflux pumps can also be used to block the function of RND pumps.<sup>9,10</sup> Several EPIs have been described<sup>11</sup> including 1-(1-naphthylmethyl)-piperazine (NMP),<sup>12</sup> paroxetine (PAR),<sup>11,13</sup> and dibasic peptides like DBP<sup>14</sup> (Figure 3.2.1). However, demonstration of the efficacy of EPI/antibiotic combinations has only rarely been documented in animal models of infection.<sup>15,16</sup> NMP is a broad spectrum EPI that synergizes with multiple classes of antibiotics including tetracyclines, fluoroquinolones, macrolides, penicillins, and rifampicin against certain clinically relevant Gram-negative pathogens like *E. coli*, *A. baumannii* and *K. pneumoniae* but not *P. aeruginosa*.<sup>12,17-19</sup> PAR is a weak EPI but potentiates tetracyclines and fluoroquinolones in Gram-positive and Gram-negative bacteria excluding *P. aeruginosa*.<sup>13</sup> PAR is a selective serotonin uptake inhibitor and clinically used to treat depression and multiple types of mental disorders.<sup>20</sup> DBP is an analogue of the dibasic dipeptide D-Ala-D-hPhe-aminoquinoline (MC-04,124<sup>14</sup>) a former drug candidate that strongly synergizes fluoroquinolone antibiotics in *P. aeruginosa*<sup>14,15</sup> and displays combined EPI- and membrane-destabilizing effects.<sup>14,15,21</sup> Mechanistic studies with NMP and DBP analogs using the *E. coli* AcrB efflux pump indicated that both EPIs bind to their respective binding sites resulting in a distortion of the binding pocket that prevents effective binding of the antibiotic.<sup>22</sup> Although EPIs such as DBP, NMP and PAR inhibit efflux of tetracycline and fluoroquinolone antibiotics in certain Gram-negative bacteria,

they are still subject to intrinsic resistance in organisms like *P. aeruginosa*. As a result, strategies that enhance outer membrane penetration and reduce efflux of EPIs or the combination of EPI/antibiotic are expected to provide more effective adjuvants. To reduce intrinsic resistance, we decided on a strategy that utilizes a tobramycin (TOB) vector to deliver the EPI through the outer membrane of *P. aeruginosa*. It was anticipated that joining a TOB-based vector to an EPI would facilitate penetration through the outer membrane of *P. aeruginosa* by the self-promoted uptake of aminoglycosides<sup>23</sup> and amphiphilic aminoglycosides.<sup>24-28</sup> In addition, the resultant amphiphilic TOB-EPI conjugate was expected to reduce efflux as aminoglycosides are considered to be poor substrates for most efflux pumps in *P. aeruginosa*<sup>11</sup> except the MexXY-OprM pump.<sup>29</sup> Moreover, we anticipated that the amphiphilic nature of the TOB-EPI conjugate may perturb the proton motive force of Gram-negative bacteria, resulting in reduced susceptibility to efflux as recently reported for tobramycin-fluorquinolone conjugates.<sup>23,24</sup>

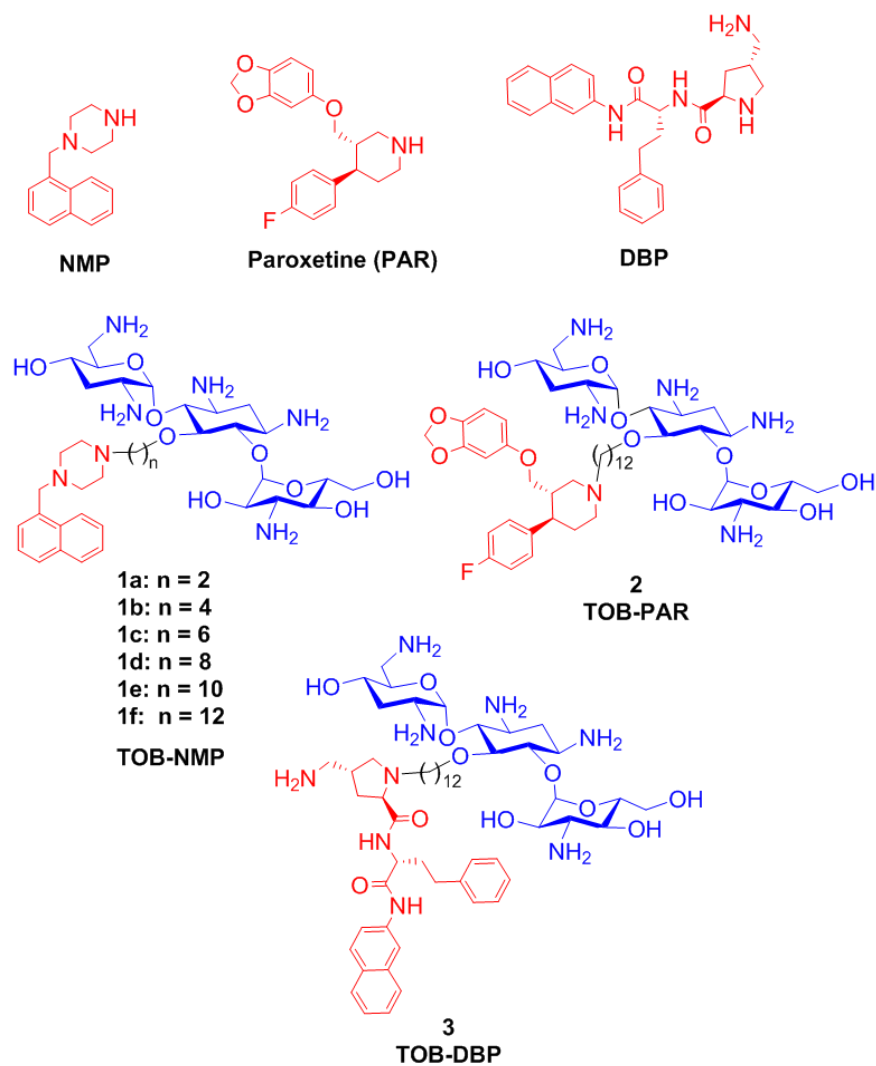
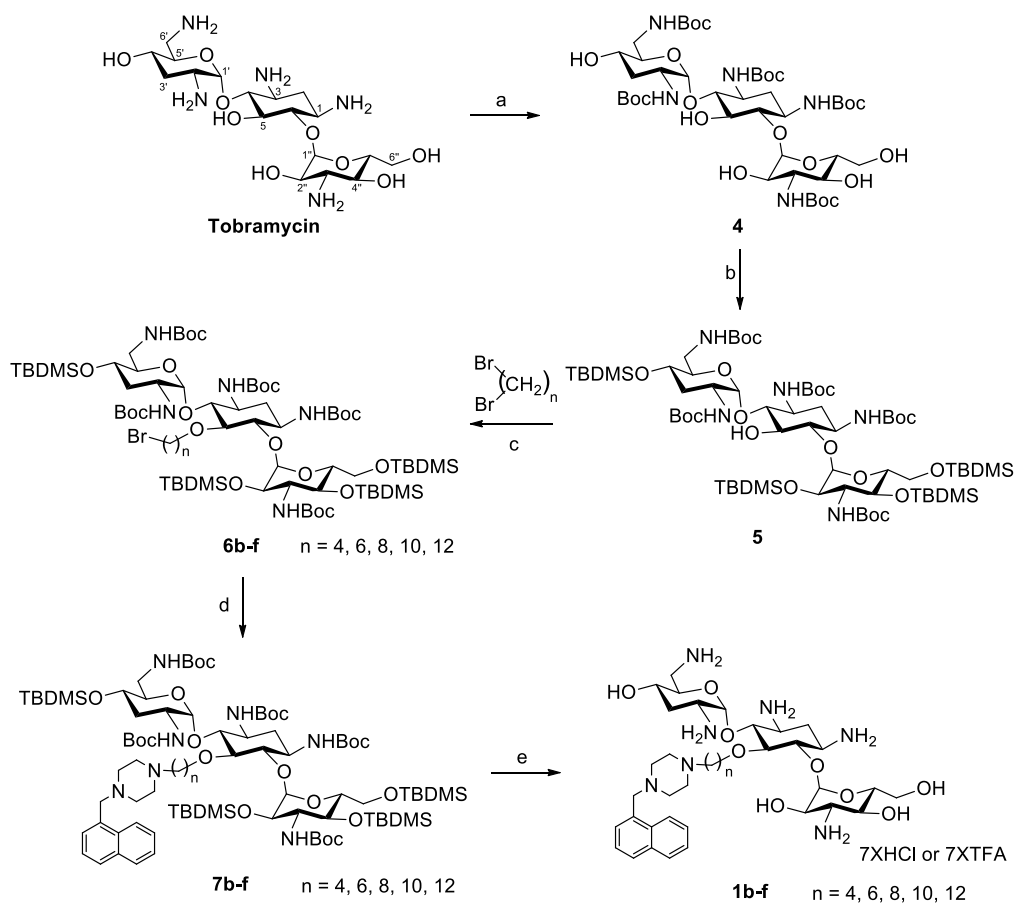


**Figure 3.2.1.** Structures of the efflux pump inhibitors (EPIs) NMP, PAR and DBP and tobramycin (TOB)-linked EPI conjugates TOB-NMP, TOB-PAR and TOB-DBP.

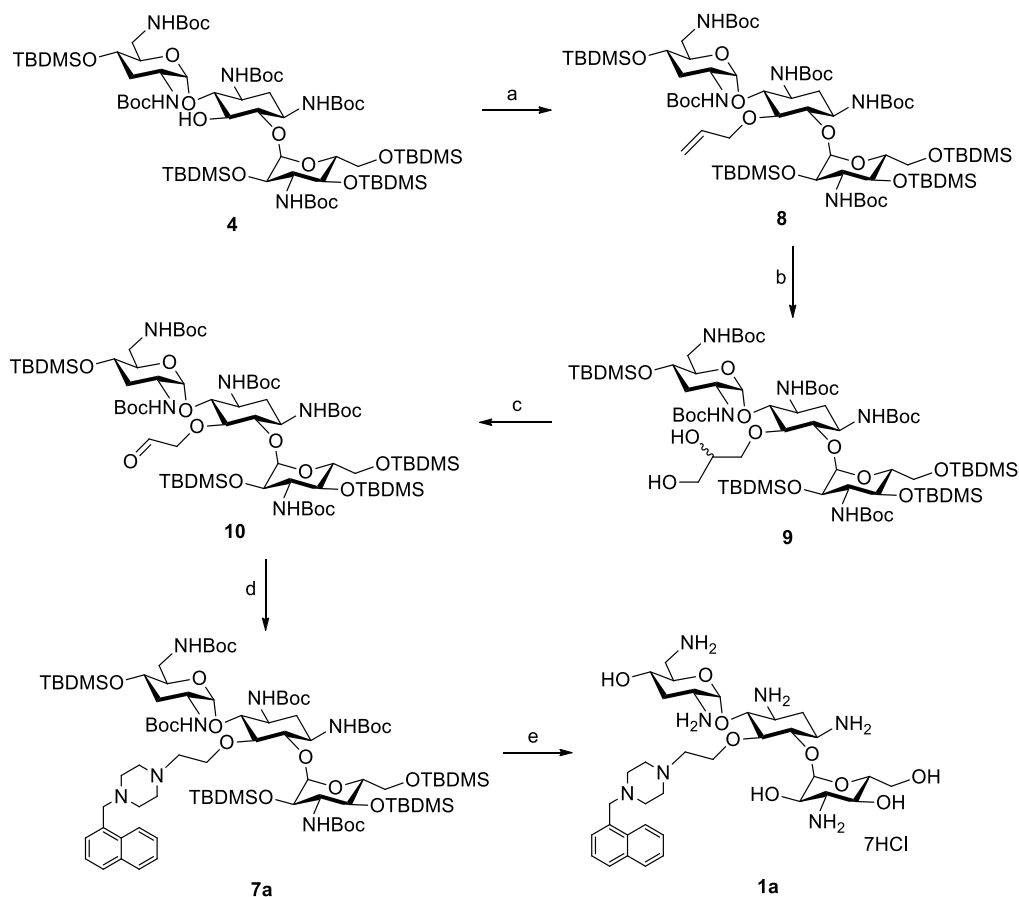
### 3.3 RESULTS

#### 3.3.1 Synthesis and Antibacterial Properties of Tobramycin-NMP Conjugates **1a–f**, Tobramycin-paroxetine Conjugate **2** and Tobramycin-DBP Conjugate **3**

With this in mind, we prepared a series of TOB-NMP conjugates **1a–f** differing in the length of the tether conjoining TOB and NMP (Figure 3.2.1). NMP was selected, as it does not potentiate efflux-prone antibiotics against *P. aeruginosa* but instead inhibits efflux pumps in *E. coli* and *A. baumannii*.<sup>11</sup> The absence of EPI function in *P. aeruginosa* by NMP is likely the result of intrinsic resistance. The secondary amino function of the piperazine ring in NMP was linked to the C5 position in tobramycin, as this position was expected to promote outer membrane penetration in TOB-NMP conjugates **1a–f**.<sup>24</sup>



**Scheme 3.3.1.1.** Synthesis of compounds **1b-f**. Reagents and conditions: (a)  $(\text{Boc})_2\text{O}$ ,  $\text{Et}_3\text{N}$ ,  $\text{MeOH}/\text{H}_2\text{O}$  (2:1), rt to 55 °C, overnight, 97%. (b)  $\text{TBDMSCl}$ , 1-methylimidazole,  $\text{DMF}$ ,  $\text{N}_2$ , rt, 4 days, 90%. (c) Dibromoalkane,  $\text{KOH}$ ,  $\text{TBAHS}$ , toluene, rt, overnight, 69%–81%. (d) 1-(1-Naphthylmethyl)-piperazine (NMP),  $\text{K}_2\text{CO}_3$ ,  $\text{DMF}$ , 75 °C, 8 h, 26–60%. (e) 40%  $\text{HCl}/\text{MeOH}$  (2:3, v/v), rt, 3 h, 63–70% (for compounds **1b-d**, **1f**); or (i)  $\text{TBAF}$ ,  $\text{THF}$ , rt; (ii)  $\text{TFA}$ ,  $\text{H}_2\text{O}$ , rt, 1 h, 74% (for compound **1e**).



**Scheme 3.3.1.2.** Synthesis of compound **1a**. Reagents and conditions: (a) allyl bromide, KOH, TBAHS, toluene, rt, 8 h, 79%. (b) OsO<sub>4</sub> (2.5 wt. % solution in tert-butanol), 2,6-lutidine, 1,4-dioxane, 60 °C, overnight. (c) NaIO<sub>4</sub>, 1,4-dioxane/H<sub>2</sub>O (3:1), 55 °C, overnight, 26% (two steps). (d) NaBH(OAc)<sub>3</sub>, NMP, AcOH, DCM, 0 °C to rt, overnight, 75%. (e) 40% HCl/MeOH (2:3, v/v), rt, 3 h, 55%.

The synthesis of TOB-NMP conjugates **1b-f** (Scheme 3.3.1.1) were performed as follows. Tobramycin was treated with di-*tert*-butyl dicarbonate and triethylamine to yield the Boc-protected tobramycin intermediate **4**. Silyl protection of the hydroxyl groups, all except at position C5, was achieved by treating **4** with TBDMSCl and 1-methylimidazole in DMF, to

provide intermediate **5** in excellent yield.<sup>24,26</sup> Reaction of compound **5** with 1,*n*-dibromoalkanes gave the bromoalkylated tobramycin derivatives **6b–f**, which were further coupled to NMP in the presence of potassium carbonate to produce protected conjugates **7b–f**. After deprotection, the desired TOB-NMP conjugates **1b–f** bearing 4-carbon to 12-carbon tethers were obtained.

However, we were unable to prepare conjugate **1a** following this protocol. Conjugate **1a** bearing a C2 tether was prepared as outlined in Scheme 3.3.1.2. Protected tobramycin intermediate **4** was treated with allyl bromide to generate allyl-C5 linked-tobramycin intermediate **8**. Dihydroxylation of the double bond was performed to yield intermediate **9** followed by oxidative cleavage to generate aldehyde **10**. The protected conjugate **7a** was prepared via reductive amination of aldehyde **10** with NMP. Deblocking was achieved by exposure to methanolic HCl to afford desired, unprotected TOB-NMP conjugate **1a**.

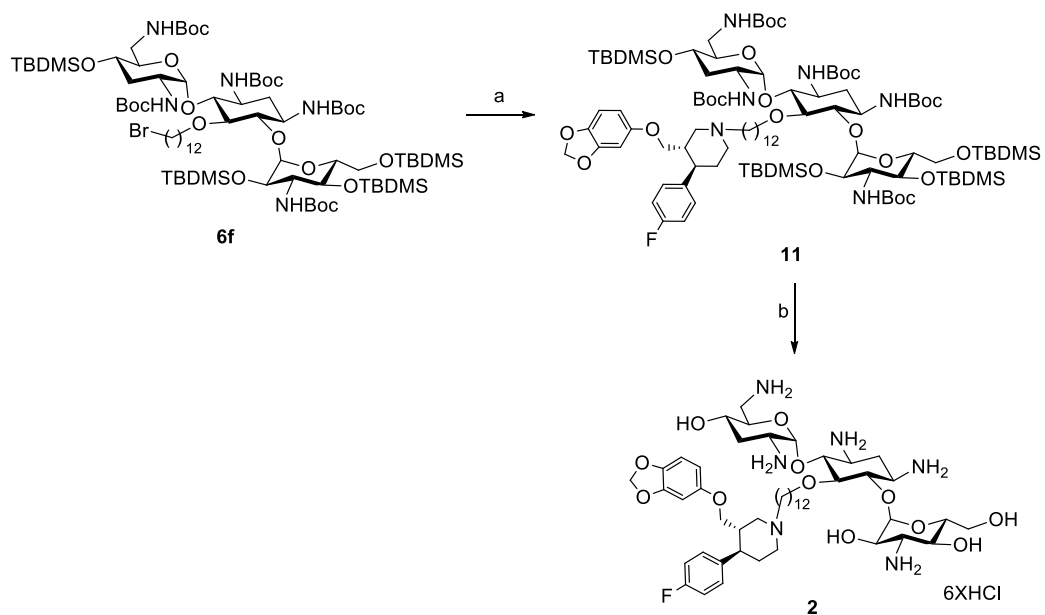
The antibacterial activity using the minimal inhibitory concentration (MIC) of TOB-NMP conjugates **1a–f** was evaluated against a panel of clinically relevant pathogens but none of the conjugates demonstrated potent anti-Gram-positive (MIC  $\geq 8 \mu\text{g/mL}$ ) and anti-Gram-negative (MIC  $\geq 32 \mu\text{g/mL}$ ) activity (Supplementary Table 9.6.1). We then assessed the adjuvant functions of **1a–f** by using the fractional inhibitory concentration (FIC) index<sup>30</sup> as a measure of the interaction between two agents. FIC indices of  $>0.5$  to  $<4$ ,  $\leq 0.5$ , and  $\geq 4$  indicate no interaction, synergy and antagonism, respectively.<sup>31</sup> We performed combination studies of **1a–f** with the tetracycline antibiotic minocycline which has been shown to be a substrate of *P. aeruginosa* RND efflux pumps.<sup>11</sup> Moreover, minocycline was selected as it inhibits preferentially the biosynthesis of envelope proteins<sup>32</sup> which may further compromise the intrinsic resistance barrier. We observed synergistic effects of conjugates **1b–f** with minocycline (FIC index 0.13–0.5) in *P. aeruginosa* PAO1 but no synergistic effects with **1a** (FIC index of  $>0.5$ ) or tobramycin (FIC

index of 1.06), indicating that a tether of >2 carbon atoms is required for synergy (Table 3.3.1). As expected, no synergy was observed with a combination of NMP and minocycline (FIC index of  $\geq 1.0$ ). These results indicate that TOB-NMP conjugates can overcome the intrinsic resistance of the pump inhibitor NMP in *P. aeruginosa* PAO1. Although TOB-NMP conjugates **1d-f** show comparable FIC indices, adjuvant **1f** bearing a C12 tether between TOB and EPI required the lowest concentration to achieve optimal synergy with minocycline (FIC index of 0.19). For instance, a fixed concentration of **1f** ( $8 \mu\text{g/mL}$  ( $7.2 \mu\text{M}$ )) achieved a 16-fold reduction of the MIC of minocycline (MIC =  $8 \mu\text{g/mL}$  reduced to  $0.5 \mu\text{g/mL}$ ) against *P. aeruginosa* PAO1 (Table 3.3.1).

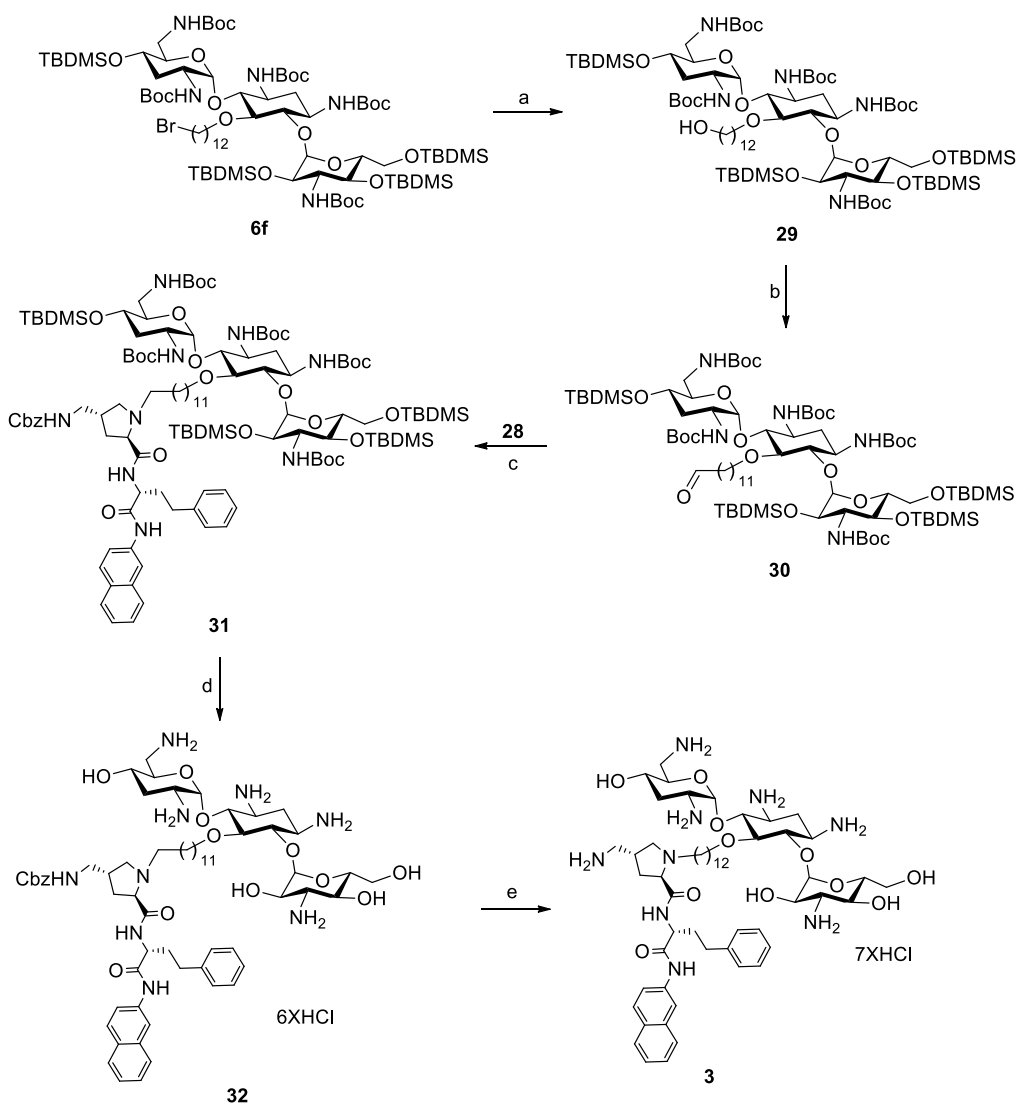
**Table 3.3.1.1.** Combination studies of TOB-EPIs (**1a–f**, **2**, or **3**), EPIs (NMP, PAR, or DBP) and tobramycin (TOB) with minocycline (MIN) against *P. aeruginosa* PAO1 strain.

Antibiotic	MIC <sub>antibiotic alone</sub> ( $\mu\text{g/mL}$ )	Adjuvant (ADJ)	MIC <sub>ADJ alone</sub> ( $\mu\text{g/mL}$ )	FIC index <sup>a</sup>	Absolute MIC <sup>b</sup> ( $\mu\text{g/mL}$ )
MIN	8	<b>1a</b>	128	0.53	4
MIN	8	<b>1b</b>	512	0.25–0.50	4
MIN	8	<b>1c</b>	>512	0.25–0.50	4
MIN	8	<b>1d</b>	>512	0.125–0.25	2
MIN	8	<b>1e</b>	>512	0.125–0.14	1
MIN	8	<b>1f</b>	64	0.19	0.5
MIN	8	NMP	512	1.02	8
MIN	8	<b>2</b>	32	0.19	0.25
MIN	8	PAR	512	1.02	8
MIN	8	<b>3</b>	32	0.09	0.12
MIN	8	DBP	256	0.13	1
MIN	8	TOB	0.25	1.06	N/A

<sup>a</sup>Fractional Inhibitory Concentration  $\text{FIC}_{\text{antibiotic}} = \text{MIC}_{\text{combo}} / \text{MIC}_{\text{antibiotic alone}}$ ,  $\text{FIC}_{\text{ADJ}} = \text{MIC}_{\text{combo}} / \text{MIC}_{\text{ADJ alone}}$ , where MIC combo is the lowest inhibitory concentration of drug in the presence of the co-drug.  $\text{FIC index} = \text{FIC}_{\text{antibiotic}} + \text{FIC}_{\text{ADJ}}$ . <sup>b</sup>Absolute MIC of minocycline in the presence of 8  $\mu\text{g/mL}$  of corresponding adjuvant. N/A: not applicable.



**Scheme 3.3.1.3.** Synthesis of compound **2**. Reagents and conditions: (a) paroxetine hydrochloride (PAR), K<sub>2</sub>CO<sub>3</sub>, DMF, 80 °C, 12 h, 84%. (b) 40% HCl/MeOH (2:3, v/v), rt, 3 h, 61%.



**Scheme 3.3.1.4.** Synthesis of compound **3**. Reagents and conditions: (a)  $K_2CO_3$ , DMF,  $H_2O$ ,  $80^\circ C$ , 24 h, 43%. (b) PCC, NaOAc, DCM, rt, 1 h, 93%. (c) Compound **14**,  $K_2CO_3$ ,  $NaBH(OAc)_3$ , AcOH, DCM,  $0^\circ C$  to rt, overnight, 72%. (d) 40% HCl/MeOH (2:3, v/v), rt, 3 h, 48% (e)  $H_2$ , Pd/C, AcOH, MeOH,  $H_2O$ , rt, overnight, 76%.

Intrigued by the potent adjuvant function of TOB-NMP **1f**, we also prepared TOB-PAR conjugate **2** and TOB-DBP conjugate **3** both bearing a C12 tether and explored their synergistic effects with minocycline. The synthesis of TOB-PAR conjugate **2** (Scheme 3.3.1.3) was

performed as follows. The bromoalkylated tobramycin intermediate **6f** was treated with commercially available paroxetine to yield TOB-PAR intermediate **11**. Deblocking of the Boc and TBDMS protecting groups was achieved by exposure to methanolic HCl to afford TOB-PAR conjugate **2**. The preparation of TOB-DBP conjugate **3** (Scheme 3.3.1.4) was performed as follows. The bromine substituent in intermediate **6f** was converted to alcohol **12**. Oxidation of primary alcohol **12** using PCC produced aldehyde **13** in good yield. Aldehyde **13** was coupled to dipeptide-based amine **14** via reductive amination (see supporting information (chapter 9) for detailed procedures of synthesis **14**) to afford the TOB-DBP intermediate **15**. Deprotection under acidic conditions followed by catalytic hydrogenation provided desired TOB-DBP conjugate **3**.

Similar to TOB-NMP **1f**, both TOB-PAR conjugate **2** (FIC index of 0.19) and TOB-DBP conjugate **3** (FIC index of 0.09) demonstrated strong synergism with minocycline against *P. aeruginosa* PAO1 (Table 3.3.1.1). As expected, no synergy was observed with paroxetine (FIC index of 1) while strong synergy was observed with the *P. aeruginosa*-active pump inhibitor DBP (FIC index of 0.13) as shown in Table 3.3.1.1. Comparing the adjuvant properties of DBP with TOB-DBP (**3**) to potentiate minocycline shows that TOB-DBP exhibits enhanced potency compared with DBP. For instance, using a fixed concentration (8  $\mu\text{g/mL}$ ) of DBP (12.1  $\mu\text{M}$ ) or TOB-DBP (5.8  $\mu\text{M}$ ) resulted in 8- or 64-fold reduction in MIC of minocycline in *P. aeruginosa* PAO1, respectively, indicating that the presence of a TOB vector in DBP enhances the adjuvant properties (Table 3.3.1.1). Besides potentiating minocycline, we also demonstrated that adjuvants **1f**, **2**, and **3** strongly synergized ( $0.13 \leq \text{FIC index} \leq 0.25$ ) with other members of the tetracycline class of antibiotics including doxycycline and tigecycline, leading to a 8- to 64-fold MIC reduction at a fixed concentration ( $\leq 8 \mu\text{g/mL}$ ) in *P. aeruginosa* PAO1 (Supplementary Table 9.6.2). It is noteworthy that synergistic potentiation of minocycline in *P. aeruginosa* PAO1

could not be achieved with detergent-like outer membrane permeabilizing agents such as benzethonium chloride (FIC index of >1) and cetrimonium bromide (FIC index of 0.75) and only marginal synergy was observed with outer membrane permeabilizing colistin (FIC index of 0.5) (Supplementary Table 9.6.3).

**Table 3.3.1.2.** Combination studies of TOB-EPIs (**1f**, **2**, or **3**) with minocycline (MIN) against MDR/XDR *P. aeruginosa* clinical isolates.

<i>P. aeruginosa</i>	Antibiotic	MIC <sub>antibiotic alone</sub> ( $\mu\text{g/mL}$ )	Adjuvant (ADJ)	MIC <sub>ADJ alone</sub> ( $\mu\text{g/mL}$ )	FIC index	Absolute MIC ( $\mu\text{g/mL}$ )
100036	MIN	64	<b>1f</b>	256	0.02	0.5 <sup>a</sup>
100036	MIN	64	<b>2</b>	64	0.05	$\leq 0.25^a$
100036	MIN	64	<b>3</b>	32	0.06	$\leq 0.25^a$
101885	MIN	32	<b>1f</b>	256	0.05	0.5 <sup>a</sup>
101885	MIN	32	<b>2</b>	32	0.13	1 <sup>a</sup>
101885	MIN	16	<b>3</b>	16	0.13	$\leq 0.125^a$
P259-96918	MIN	32	<b>1f</b>	>1024	0.02	$\leq 0.5^a$
P259-96918	MIN	32	<b>2</b>	>512	0.02	0.5 <sup>a</sup>
P259-96918	MIN	32	<b>3</b>	64	0.03	$\leq 0.5^a$
P260-97103	MIN	8	<b>1f</b>	2	0.25	0.5 <sup>b</sup>
P260-97103	MIN	16	<b>2</b>	8	0.19	$\leq 1^b$
P260-97103	MIN	8	<b>3</b>	4	0.31	0.5 <sup>b</sup>
P262-101856	MIN	128	<b>1f</b>	64	0.09	4 <sup>a</sup>
P262-101856	MIN	128	<b>2</b>	32	0.13	1 <sup>a</sup>
P262-101856	MIN	256	<b>3</b>	32	0.08	$\leq 1^a$

**Table 3.3.1.2. Cont.**

<i>P. aeruginosa</i>	Antibiotic	MIC <sub>antibiotic alone</sub> ( $\mu\text{g/mL}$ )	Adjuvant (ADJ)	MIC <sub>ADJ alone</sub> ( $\mu\text{g/mL}$ )	FIC index	Absolute MIC ( $\mu\text{g/mL}$ )
P264-104354	MIN	64	<b>1f</b>	128	0.03	$\leq 0.5^a$
P264-104354	MIN	64	<b>2</b>	64	0.06	$\leq 0.5^a$
P264-104354	MIN	64	<b>3</b>	8	0.25	$\leq 0.5^b$
91433 <sup>c</sup>	MIN	32	<b>1f</b>	32	0.13	0.25 <sup>a</sup>
91433 <sup>c</sup>	MIN	32	<b>2</b>	32	0.19	0.25 <sup>a</sup>
91433 <sup>c</sup>	MIN	32	<b>3</b>	8	0.16	0.25 <sup>b</sup>
101243 <sup>c</sup>	MIN	4	<b>1f</b>	64	0.28	1 <sup>a</sup>
101243 <sup>c</sup>	MIN	4	<b>2</b>	32	0.38	1 <sup>a</sup>
101243 <sup>c</sup>	MIN	4	<b>3</b>	16	0.19	0.5 <sup>a</sup>

<sup>a</sup> Absolute MIC of antibiotic in the presence of 8  $\mu\text{g/mL}$  of corresponding adjuvant. <sup>b</sup> Absolute MIC of antibiotic in the presence of  $\frac{1}{4} \times \text{MIC}$  of corresponding adjuvant. <sup>c</sup> Colistin-resistant *P. aeruginosa* isolate.

Next, we assessed the effect of the TOB-EPI conjugates **1f**, **2**, and **3** in combination with minocycline against a panel of eight clinical *P. aeruginosa* isolates including six MDR (nonsusceptible or resistant to  $\geq 3$  chemically unrelated antipseudomonal classes) and six extremely drug resistant (XDR) (nonsusceptible or resistant to  $\geq 5$  chemically unrelated antipseudomonal classes (Supplementary Table 9.6.4), obtained from different Canadian hospitals. The panel also included two colistin-nonsusceptible or resistant *P. aeruginosa* strains. The results indicate that all three TOB-EPI conjugates demonstrated strong synergistic effects ( $0.02 \leq \text{FIC index} \leq 0.38$ ) with minocycline against the selected panel of MDR and XDR *P. aeruginosa* isolates (Table 3.3.1.2). The following FIC index ranges for the TOB-EPI conjugates against the selected eight MDR or XDR *P. aeruginosa* isolates were observed: TOB-NMP

( $0.02 \leq \text{FIC index} \leq 0.28$ ), TOB-PAR ( $0.02 \leq \text{FIC index} \leq 0.38$ ), and TOB-DBP ( $0.03 \leq \text{FIC index} \leq 0.31$ ) as shown in Table 3.3.1.2. We also measured the absolute MIC of minocycline against the eight MDR/XDR *P. aeruginosa* isolates in the presence of conjugates **1f**, **2**, and **3** at a fixed concentration ( $\leq 8 \mu\text{g/mL}$ ,  $\leq 0.25 \times \text{MIC}$ ). These results show that all three conjugates lower the MIC of minocycline from 8- to 256-fold against the eight selected MDR or XDR *P. aeruginosa* isolates. Importantly, in 96 % of cases, conjugates **1f**, **2**, and **3** at a concentration of  $\leq 8 \mu\text{g/mL}$ ,  $\leq 0.25 \times \text{MIC}$  reached minocycline susceptibility ( $\text{MIC} \leq 1 \mu\text{g/mL}$ ) against the eight selected MDR or XDR *P. aeruginosa* isolates (Table 3.3.1.2).

To demonstrate that the adjuvant properties of the conjugates translate into a measurable *in vivo* effect, we selected the *Galleria mellonella* larvae infection model that is an established *in vivo* model to study the efficacy of antimicrobial therapy against *P. aeruginosa*.<sup>16,33</sup> In pilot studies, we determined that conjugates **1f** and **2** cause  $\leq 5\%$  hemolysis of ovine erythrocytes at  $1000 \mu\text{g/mL}$  (Supplementary Figure 9.5.1) and show low cytotoxicity ( $\text{CC}_{50} > 30 \mu\text{M}$ ) against cancer cell lines while increased toxicity was noted for conjugate **3** (Supplementary Figure 9.5.2). Tolerability studies in *G. mellonella* using a dosage of 200 mg/kg of **1f** or **2** or NMP or PAR showed no toxic effects up to 96 h, while a dose of 100 mg/kg of **3** or DBP resulted in 100% or 80% killing of the larvae after 24 h (Supplementary Figure 9.5.3). The toxicity of conjugate **3** or DBP in the larvae prevented further use of this compound in the insect model. Efficacy studies were performed by infecting the larvae with a lethal dose of  $1.0 \times 10^5 \text{ CFU/mL}$  of XDR *P. aeruginosa* strain P262-101856 followed by injection of the drug combination 2 h post infection. Monotherapy with a single dose (75 mg/kg) of minocycline or **1f** (75 mg/kg) or NMP (75 mg/kg) resulted in 100% killing of the larvae within 24 h indicating that monotherapy was not able to provide protection of the larvae. In contrast, combination therapy (37.5 mg/kg **1f** + 37.5 mg/kg

minocycline or 75 mg/kg **1f** + 75 mg/kg minocycline) resulted in 10% or 77% survival of the larvae, respectively, after 24 h (Figure 3.3.1.4(a)). Similarly, efficacy was seen for conjugate **2**. For instance, single dose combination therapy (75 mg of **2** + 75 mg of minocycline) resulted in 56% survival of the larvae while single dose monotherapy with minocycline (75 mg/kg) or conjugate **2** (75 mg/kg) resulted in 100% killing after 24 h (Figure 3.3.1.4(b)). Moreover, combination studies of NMP or PAR (75 mg/kg) with minocycline (75 mg/kg) resulted in 100 % deaths of the larvae after 24 h (Figure 3.3.1.4(a) and Figure 3.3.1.4(b)). These results suggest that combinations of minocycline/**1f** and minocycline/**2** possess therapeutic potential.

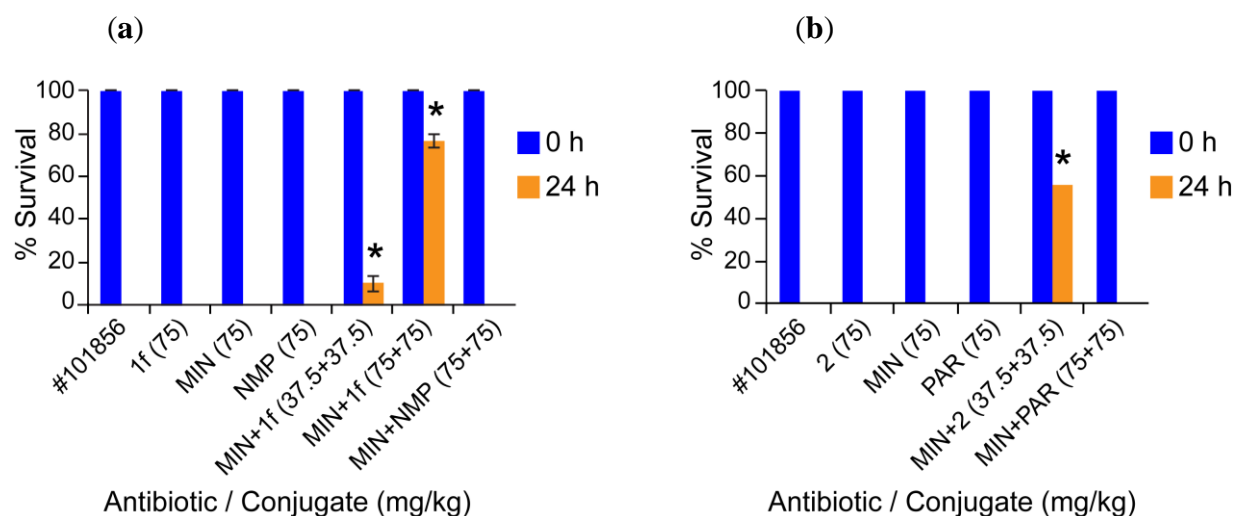


**Figure 3.3.1.4.** (a) Enhanced dose-dependent efficacy of a combination of conjugate **1f** and minocycline in XDR *P. aeruginosa* P262-101856 over a period of 24 h was demonstrated in a *Galleria mellonella* *in vivo* infection model. Combination therapy of (37.5 mg/kg **1f** + 37.5 mg/kg minocycline), (75 mg/kg **1f** + 75 mg/kg minocycline) and (75 mg/kg NMP + 75 mg/kg minocycline) resulted in 10%, 77%, and 0% survival of the larvae, respectively, after 24 h. In contrast, monotherapy using a single dosage of **1f** (75 mg/kg), minocycline (75 mg/kg), NMP (75 mg/kg) or no treatment resulted in 100% killing of the larvae at  $\leq 24$  h. Each experiment involved

usage of 15 larvae from different batches; in total two experiments were performed per one dosage of antibiotic/conjugate ( $n = 30$ ). Significant difference between 0 and 24 h indicated by \* ( $P \leq 0.05$ ). (b) Enhanced dose-dependent efficacies of minocycline in combination with conjugate **2** was demonstrated in *G. mellonella* model of XDR *P. aeruginosa* P262-101856 infection over a period of 24 h. Combination therapy of (75 mg/kg conjugate **2** + 75 mg/kg minocycline) resulted in 56% survival of the larvae after 24 h, whereas combination of (75 mg/kg PAR + 75 mg/kg minocycline) resulted in 100% killing of the larvae at  $\leq 24$  h. Monotherapy with a single dosage of conjugate **2** (75 mg/kg), minocycline (75 mg/kg), or PAR (75 mg/kg) resulted in 100% killing of the larvae within 24 h. Each experiment involved 15 larvae from different batches. Two *in vivo* experiments were performed per conjugate / antibiotic dosage ( $n = 30$ ). Significant difference between 0 and 24 h indicated by \* ( $P \leq 0.05$ ).

Besides *P. aeruginosa*, we also studied the effect of the conjugates **1f**, **2**, and **3** to synergize minocycline in other clinically relevant MDR Gram-negative pathogens such as *Klebsiella pneumoniae* and *Enterobacter cloacae* (Supplementary Table 9.6.5). Our results show that all three conjugates were able to synergize minocycline in these pathogens leading to a 4- to 256-fold reduction in MIC of minocycline at a fixed concentration ( $\leq 8 \mu\text{g/mL}$ ) of the conjugates (Table 3.3.1.3). In both pathogens the potency of the adjuvants **1f**, **2**, and **3** was superior when compared to NMP, PAR, or DBP. These results indicate that the adjuvant function of the conjugates is not limited to *P. aeruginosa* and can be extended to other clinically relevant Gram-negative pathogens. However, the properties of the adjuvants appear to be optimal for *P. aeruginosa*.

**Table 3.3.1.3.** Combination studies of TOB-EPIs (**1f**, **2**, or **3**) with minocycline (MIN) against MDR *Klebsiella pneumoniae* and *Enterobacter cloacae* isolates.

Stock no.	Organism	Antibiotic	MIC <sub>antibiotic alone</sub> ( $\mu\text{g/mL}$ )	Adjuvant (ADJ)	MIC <sub>ADJ alone</sub> ( $\mu\text{g/mL}$ )	FIC index	Absolute MIC <sup>a</sup> ( $\mu\text{g/mL}$ )
116381	<i>K. pneumoniae</i>	MIN	128	<b>1f</b>	> 32	0.13–0.38	16
116381	<i>K. pneumoniae</i>	MIN	128	<b>NMP</b>	> 512	0.25–0.38	128
116381	<i>K. pneumoniae</i>	MIN	128	<b>2</b>	> 32	0.25–0.38	32
116381	<i>K. pneumoniae</i>	MIN	128	<b>PAR</b>	128	0.63	128
116381	<i>K. pneumoniae</i>	MIN	128	<b>3</b>	> 32	0.03–0.16	4
116381	<i>K. pneumoniae</i>	MIN	128	<b>DBP</b>	256	0.06	4
117029	<i>E. cloacae</i>	MIN	256	<b>1f</b>	> 32	0.03–0.16	8
117029	<i>E. cloacae</i>	MIN	128	<b>NMP</b>	> 512	>0.5	128
117029	<i>E. cloacae</i>	MIN	256	<b>2</b>	> 32	0.02–0.14	4
117029	<i>E. cloacae</i>	MIN	128	<b>PAR</b>	64	0.5	64
117029	<i>E. cloacae</i>	MIN	256	<b>3</b>	32	0.13	1
117029	<i>E. cloacae</i>	MIN	128	<b>DBP</b>	64	0.13	8

<sup>a</sup> Absolute MIC of minocycline in the presence of 8  $\mu\text{g/mL}$  of corresponding adjuvant.

### 3.3.2 Mechanistic Studies

To gain insight into the protective function of the conjugates, we performed a series of mechanistic studies with *P. aeruginosa* PAO1. At first, we demonstrated that combinations of bacteriostatic minocycline ( $0.5 \times \text{MIC}$ ) and **1f** ( $0.5 \times \text{MIC}$ ) become bactericidal and result in complete eradication of the pathogen within 24 h (Supplementary Figure 9.5.4). Similar killing rates were observed for minocycline/**2**, while a combination of minocycline/**3** resulted in

complete killing of the organism after 9 h. We demonstrated that conjugate **1f** permeabilizes the outer membrane of PAO1 in a dose-dependent manner using the well-established outer membrane permeability NPN (1-*N*-phenyl-naphthylamine) assay<sup>15</sup> (Figure 3.3.2.1). Similar dose-dependent permeability was seen for conjugates **2** and **3** (Supplementary Figure 9.5.5). Next, we assessed whether the combination of conjugates **1f**, **2** or **3** with outer membrane impermeable antibiotics are synergistic in *P. aeruginosa* PAO1. For all three conjugates we observed strong synergy: with rifampicin (FIC index of <0.05), novobiocin (FIC index of <0.1), vancomycin (FIC index of  $\leq$ 0.15), and erythromycin (FIC index of  $\leq$ 0.2), indicating that the conjugates enhance cellular uptake of these antibiotics into *P. aeruginosa* PAO1 (Figure 3.3.2.2). As rifampicin is not a substrate for *P. aeruginosa* RND efflux pumps, these results must reflect enhanced membrane penetration (Supporting Table 9.6.6).

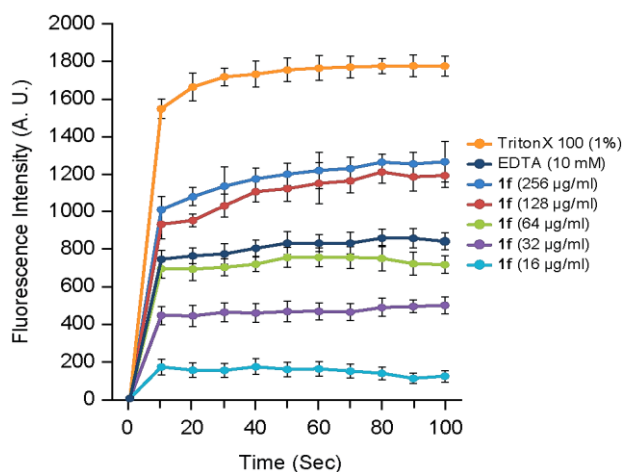


**Figure 3.3.2.1.** Permeabilization of outer membrane by conjugate **1f** was measured by accumulation of 1-*N*-phenyl-naphthylamine (NPN) in PAO1 cells. Permeabilization caused by **1f** is a concentration-dependent effect. Triton X-100 (1%) and EDTA (10 mM) were used as positive controls.

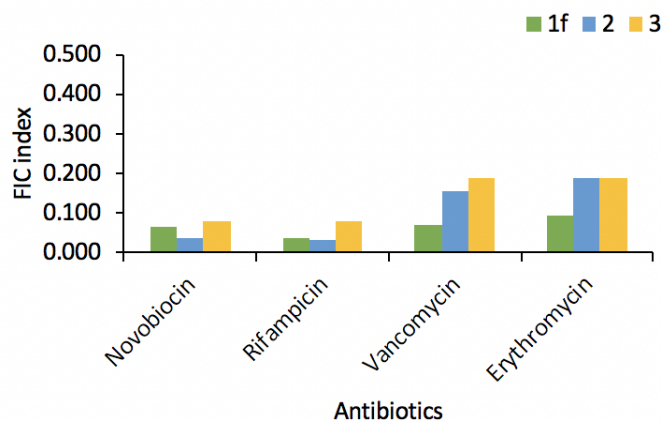


**Figure 3.3.2.2.** Synergistic effects of conjugates **1f** (TOB-NMP), **2** (TOB-PAR), and **3** (TOB-DBP) in combination with outer membrane impermeable antibiotics (novobiocin, rifampicin, vancomycin, and erythromycin) in *P. aeruginosa* PAO1.

We also assessed the ability of conjugates **1f**, **2**, and **3** to depolarize the cytoplasmic membrane in *P. aeruginosa* PAO1 using the membrane potential-sensitive dye 3,3'-dipropylthiadicarbocyanine iodide (DiSC<sub>3</sub>(5)).<sup>28</sup> The results demonstrate that the three conjugates induce dose-dependent depolarization of the cytoplasmic membrane in a comparable manner to colistin (Figure 3.3.2.3 and Supplementary Figure 9.5.6). Significant depolarization of the cytoplasmic membrane was seen for conjugates **1f**, **2**, and **3** at a concentration  $\geq 8 \mu\text{g/mL}$ . Moreover, we also assessed the effect of the conjugates **1f**, **2**, or **3** on the flagellum-dependent swimming motility of *P. aeruginosa* PAO1 and observed a strong and concentration-dependent reduction in motility at sub-MIC concentration. For instance, greatly reduced motility was observed for all three conjugates at  $1/64 \times \text{MIC}$  (Figure 3.3.2.4 and Supplementary Figure 9.5.7). Reduction in motility was further enhanced by addition of minocycline which has no effect on motility by itself (Supplementary Figure 9.5.8). As flagellar function requires an intact proton

motive force (PMF),<sup>34</sup> our results suggest that conjugates **1f**, **2**, or **3** dissipate the PMF at sub-MIC concentration that perhaps also results in a reduction in efflux pump activity leading to an increase in intracellular concentration of minocycline. We would also like to point out that the synergy of minocycline activity by conjugates **1f**, **2**, and **3** was maximal when RND efflux pumps are present and that there is a decrease in synergy in strains lacking RND efflux pumps. This observation is based on testing **1f**, **2**, or **3** in *P. aeruginosa* PAO200 (PAO1:ΔmexAB-oprM) as well as *P. aeruginosa* PAO750 (ΔmexAB-oprM, ΔmexCD-oprJ, ΔmexEF-oprN, ΔmexXY, ΔmexJK, ΔopmH) (Supplementary Table 9.6.6).<sup>35</sup> The decrease in synergy in absence of RND efflux pumps suggests that, in addition to dissipating the PMF, conjugates **1f**, **2**, or **3** perhaps also inhibit the activity of RND pumps, particularly that of the minocycline-relevant MexAB-OprM, in a more specific fashion. The effect of conjugates **1f**, **2**, or **3** on the uptake of tetracycline was also investigated in *P. aeruginosa* PAO1 using an uptake assay for Gram-negative bacteria.<sup>36</sup> This assay relies on monitoring the enhancement of tetracycline as it enters the cell (Figure 3.3.2.5). Our results indicate that conjugates **1f**, **2**, and **3** enhance the uptake of tetracycline in a concentration-dependent fashion. Comparable enhancements in tetracycline uptake were also observed with colistin, while CCCP an uncoupler of oxidative phosphorylation which disrupts the proton gradient of the bacterial membranes results in decreased uptake of tetracycline antibiotics.<sup>37</sup> In contrast, NMP and PAR were unable to enhance the uptake of tetracycline in PAO1. However, DBP showed a slight increase in tetracycline uptake at the highest concentration tested consistent with the dual efflux-inhibitory/membrane destabilizing effect of this compound.

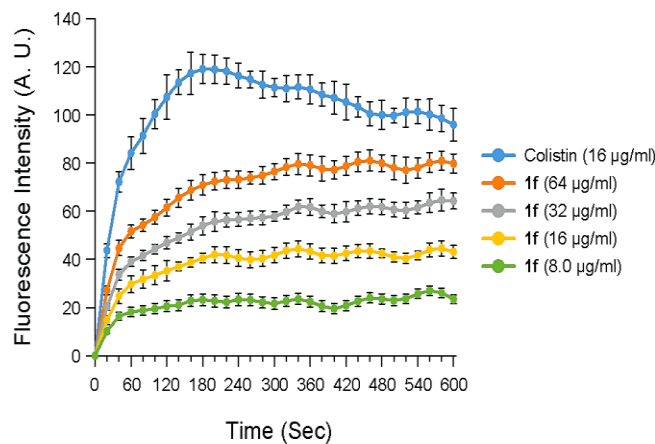


**Figure 3.3.2.3.** Dose-dependent cytoplasmic membrane depolarization assay ascertained by DiSC<sub>3</sub>(5) fluorescence in *P. aeruginosa* PAO1. Colistin was used as a positive control.

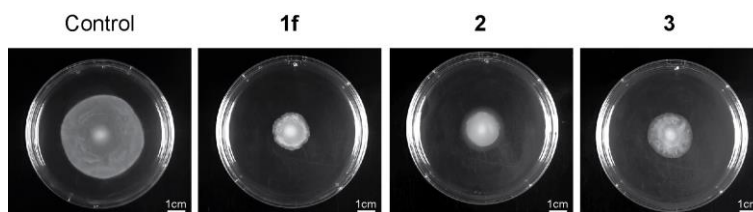


**Figure 3.3.2.4.** Motility of *P. aeruginosa* PAO1 is greatly reduced in presence of sub-MIC concentration of conjugates **1f** ( $1/64 \times \text{MIC} = 1 \mu\text{g/mL}$ ), **2** ( $1/64 \times \text{MIC} = 0.5 \mu\text{g/mL}$ ), and **3** ( $1/64 \times \text{MIC} = 0.5 \mu\text{g/mL}$ ). Swimming plates without conjugate serve as a control.

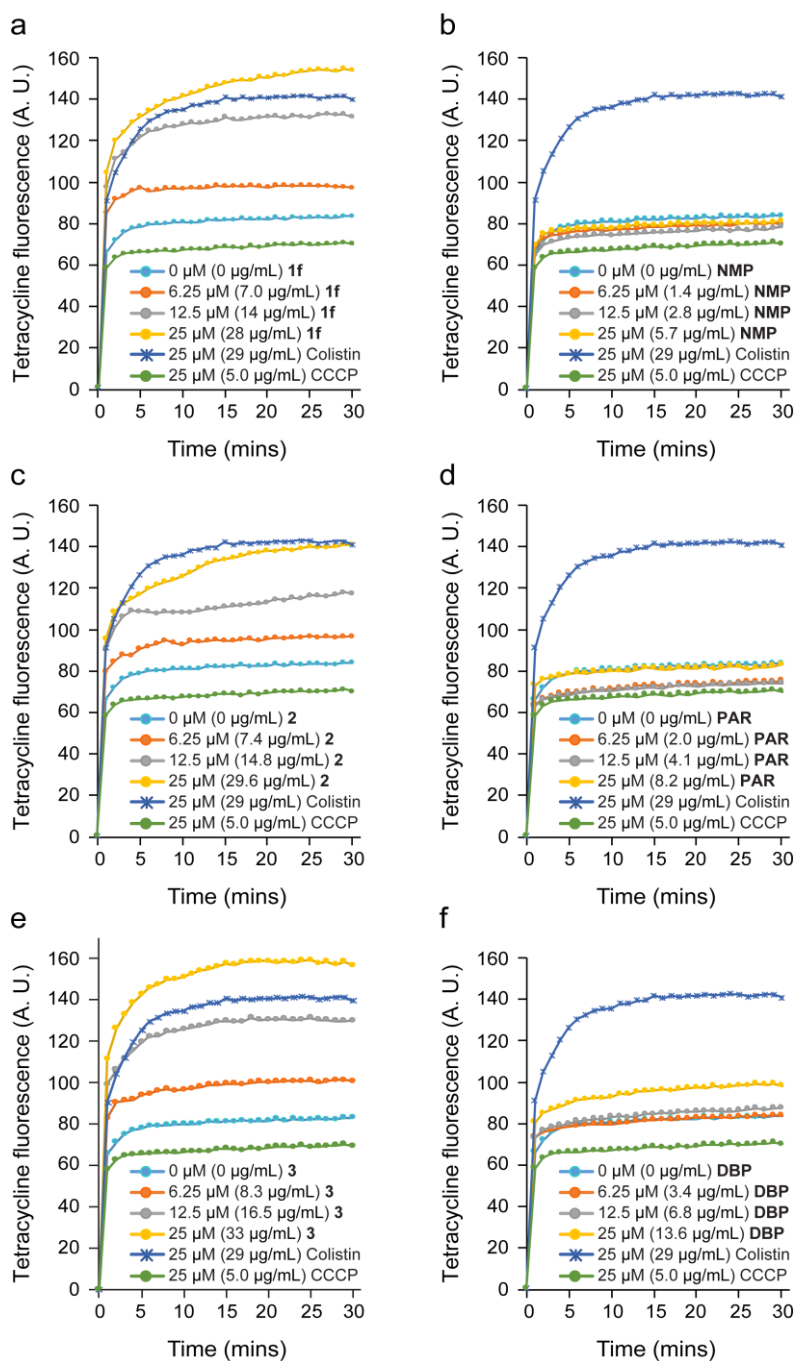


**Figure 3.3.2.5.** Tetracycline uptake in *P. aeruginosa* PAO1 in the presence of increasing concentrations of conjugate **1f** (a), NMP (b), conjugate **2** (c), PAR (d), conjugate **3** (e), and DBP (f). Tetracycline fluorescence gives an estimation of tetracycline uptake in the bacterial cells.

We also assessed the potential of adjuvants **1f**, **2**, and **3** to delay the occurrence of resistance in *P. aeruginosa* after 25 serial passages in the presence of subinhibitory concentrations (MIC/2) of adjuvant/minocycline mixture (1:1 mass ratio). Our results indicate that all three adjuvants reduce the potential of resistance development when co-administered with minocycline. After 25 days of exposure, the most effective adjuvants **2** and **3** led to a 2-fold increase in the relative MIC of adjuvant/minocycline mixture compared to MIC obtained for the first-time exposure while monotherapy with minocycline, tobramycin, or colistin resulted in 16-fold, 256-fold, and >1024-fold increase of their MIC, respectively. In comparison, the combination of DBP + minocycline also delayed resistance development but required a 4-fold higher mass ratio of both components (8-fold higher stoichiometric quantity of **3**) to select for a 2-fold increase in the relative MIC (Figure 3.3.2.6).

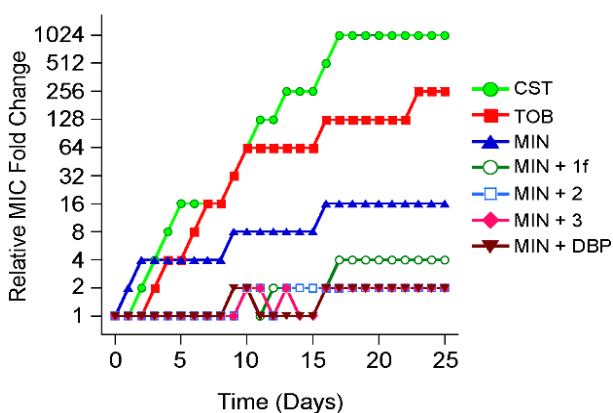


**Figure 3.3.2.6.** Comparative study on the emergence of resistance in *P. aeruginosa* PAO1 after 25 serial passages in the presence of colistin (CST), tobramycin (TOB), minocycline (MIN) as well as individual combinations of conjugates **1f**, **2**, **3**, and DBP with minocycline.

### 3.4 DISCUSSION

Infections caused by *P. aeruginosa* are difficult to treat. Our current armamentarium to combat *P. aeruginosa* infections is limited to select penicillins (e.g., piperacillin/tazobactam), cephalosporins (e.g., ceftolozane/tazobactam), carbapenems (e.g., imipenem), fluoroquinolones (e.g., ciprofloxacin), aminoglycosides (e.g., tobramycin), but resistance to these agents is steadily increasing with no new novel antipseudomonal agents in clinical development.<sup>1,2</sup> Our inability to develop antipseudomonal agents with novel modes of action demands exploration of alternative strategies. One such strategy is the search for small molecule-based adjuvants which when used in combination with legacy antibiotics rescue the antibiotic from resistance. Several principal modes of action by which an adjuvant rescues an antibiotic from resistance are possible:<sup>38</sup> (1) an adjuvant prevents the degradation or modification of an antibiotic; (2) an adjuvant allows the accumulation of an antibiotic by enhancing uptake; (3) an adjuvant allows the retention of an antibiotic by inhibiting the efflux pumps; (4) an adjuvant inhibits the intrinsic repair pathway or tolerance mechanism of cells to the antibiotic; and (5) an adjuvant affects the physiological state of bacteria, for instance by preventing the formation of biofilm. Clinical use of adjuvants is currently limited to combinations of  $\beta$ -lactam antibiotics/ $\beta$ -lactamase inhibitors which prevent degradation of  $\beta$ -lactam antibiotics. Adjuvants that inhibit efflux pumps and/or enhance cell penetration in Gram-negative bacteria are known and have recently been reviewed,<sup>39,40</sup> but their clinical efficacy/safety has not been demonstrated. Contemporary examples of adjuvants which enhance outer membrane permeability include polymyxin analogs such polymyxin B nonapeptide,<sup>41</sup> octanoyl-Thr-Abu-cyclo[Dab-Dab-DPhe-Leu-Dab-Dab-Thr] (SPR7061<sup>39</sup>) and acetyl-Thr-DSer-cyclo[Dab-Dab-DPhe-Leu-Dab-Dab-Thr] (SPR741<sup>39</sup>), cationic steroid antibiotics,<sup>42</sup> and oligo-acyl-lysyls<sup>43</sup> but also dicationic EPIs such as NMP, DBP, and the recently

optimized 4-oxo-4*H*-pyrido[1,2-*a*]pyrimidine analog<sup>44</sup> and pyranopyridine analogs.<sup>45,46</sup> Most of these adjuvants have in common a polycationic ( $\geq +2$  charge). A potential drawback of polycationic adjuvants is the risk of inducing nephrotoxicity and of concentration in acidic vesicles as seen for certain DBPs.<sup>47</sup> However, a number of polycationic molecules are devoid of nephrotoxicity in clinical settings. These include among others the antibiotic plazomicin<sup>48</sup> and the dibasic macrolides suggesting that nephrotoxicity may not be an inherent property of polycationic molecules.

In this project, we proposed that the adjuvant properties of known EPIs such as NMP, paroxetine, and DBP could be enhanced by linking them to a tobramycin vector. We hypothesized that tobramycin-EPI conjugates should (a) facilitate outer membrane uptake of the EPI via the self-promoted uptake mechanism of aminoglycosides, (b) reduce efflux as aminoglycosides are poor substrates for most RND pumps, and (c) depolarize the cytoplasmic membrane because of the cationic amphiphilic nature of the conjugates. Our results demonstrate that the adjuvant properties of three EPIs are greatly improved by linking them via a 12-carbon tether to a tobramycin vector. The resultant TOB-EPI conjugates **1f**, **2**, and **3** strongly synergize with outer membrane impermeable agents including novobiocin, rifampicin, vancomycin, and erythromycin against wild-type *P. aeruginosa* PAO1 and enhance outer membrane penetration in the NPN assay. Some of these outer membrane impermeable agents including rifampicin which shows the highest synergy are not substrates of RND efflux pumps, suggesting that the TOB-EPI conjugates destabilize the outer membrane in *P. aeruginosa*. This result is consistent with related amphiphilic tobramycin analogs described by us and other research groups.<sup>23,24,26,27,58</sup>

However, the membrane effects of adjuvants **1f**, **2**, and **3** are not limited to the outer membrane but also involve the cytoplasmic membrane as observed in the inner membrane

depolarization, motility assays, and tetracycline uptake assays. These assays indicate that adjuvants **1f**, **2**, and **3** decrease the electrical component ( $\Delta\psi$ ) of the proton motive force (PMF) in *P. aeruginosa* PAO1. In order to counter this effect and maintain ATP synthesis levels, bacteria increase the pH gradient across the inner membrane that results in enhanced uptake of tetracycline antibiotics in Gram-negative bacteria as previously observed for the antidiarrheal drug loperamide.<sup>36</sup> This interpretation is consistent with (i) the additive (non-synergistic) effect of the conjugates **1f**, **2**, and **3** with the aminoglycosides tobramycin and gentamicin (2.5 > FIC index >1.5) (data not shown) which require the electrical component ( $\Delta\psi$ ) of the proton motive force (PMF) for uptake<sup>49</sup> and (ii) the decrease in tetracycline uptake by CCCP which reduces the pH component ( $\Delta\text{pH}$ ) of the PMF.<sup>37</sup> The inhibitory effect of the conjugates on the efflux pumps is less clear, but it is possible that the observed effects of the adjuvants on the PMF may also compromise the function of efflux pumps leading to reduced efflux of antibiotics which are substrates of RND efflux pumps including tetracycline antibiotics.

### 3.5 CONCLUSIONS

The discovery that linking a tobramycin vector to the efflux pump inhibitors NMP, PAR, or DBP generates adjuvants capable of rescuing tetracycline antibiotics against MDR and XDR Gram-negative pathogens including *P. aeruginosa* isolates opens up opportunities to develop novel and optimized adjuvants. The aminoglycoside vector strategy is attractive because it induces multimodal effects in the adjuvant involving both outer and inner membranes, affecting the proton motive force (PMF) and possibly the function of the efflux pumps. The overall multimodal effects of the adjuvant/antibiotic combination on the bacterial membrane are expected to reduce the likelihood of resistance development as observed for other membrane

active or multitargeting antibiotics.<sup>50,51</sup> As such, the outlined development of adjuvant/tetracycline combination therapy may preserve the tetracycline class of antibiotics against MDR Gram-negative pathogens, which has the potential to fill the current antibiotic discovery void.<sup>7</sup>

## 3.6 EXPERIMENTAL SECTION

### 3.6.1 Synthetic Chemistry

#### 3.6.1.1 General Comments

Synthesis of compounds were not performed under anoxic or anhydrous conditions unless specifically noted. Reagents and solvents were purchased from commercially available sources and used without purification, unless otherwise noted. Normal- or reverse-phase flash chromatography was used. Reactions were monitored by thin-layer chromatography (TLC) on silica gel 60 F254 (0.25 mm, Merck), to which the compounds were visualized using ultraviolet light and/or stain with ninhydrin solution (ninhydrin and acetic acid in ethanol). 1D and 2D (<sup>1</sup>H, <sup>13</sup>C, DEPT, COSY, HSQC, HMBC) NMR characterization experiments were performed on either Bruker AMX-500 or Bruker AMX-300 spectrometer in the noted deuterated solvents. Chemical shifts ( $\delta$ ) are reported in parts per million with CHCl<sub>3</sub> (7.26 ppm), DHO (4.79 ppm) and CD<sub>2</sub>HOH (3.31 ppm) used as internal standards. Electrospray ionization (ESI) mass spectrometry (MS) experiments were carried out on a Varian 500 MS ion trap mass spectrometer. Matrix-assisted laser desorption ionization (MALDI) MS experiments were performed on a Bruker Daltonics Ultraflex MALDI TOF/TOF mass spectrometer. Analytical high-performance

liquid chromatography (HPLC) was carried out on Breeze HPLC Waters with 2998 PDA detector (1.2 nm resolution) connected to a Kinetex 5  $\mu\text{m}$  reverse-phase C18 100 Å LC column (150  $\times$  4.6 mm, Phenomenex) or a Synergi 4  $\mu\text{m}$  Polar-RP 80 Å LC column (50  $\times$  4.6 mm, Phenomenex). Yields are given following purification, unless otherwise stated. All of the biologically tested compounds are at least 95% pure as estimated by HPLC.

### 3.6.1.2 Synthetic Procedures

Detailed experimental procedures of compounds **4**, **5**, **6b–f**, **14** and DBP are described in the supporting information (chapter 9).

*General Synthetic Procedure A: Final Deprotection of Compounds 1a–d, 1f, 2, and 16.* Boc and TBDMS protected compounds were treated with 40% HCl in MeOH (2:3, v/v) and stirred at room temperature for 3 h. Methanolic HCl was removed under reduced pressure and purified by reverse-phase flash chromatography on a C18-silica (elution with 100% deionized water or from 100% deionized water to deionized water/MeOH = 1:1, v/v) to give analytically pure products.<sup>24–26</sup>

*General Synthetic Procedure B: Synthesis of Boc and TBDMS Protected TOB-NMP Derivatives (7b–f).* 1-(1-naphthylmethyl)-piperazine (NMP) (1.5 equiv) and  $\text{K}_2\text{CO}_3$  (3.0 equiv) were subsequently added to stirred solutions of **6b–f** (1.0 equiv) in anhydrous DMF under  $\text{N}_2$  gas. The reaction mixture was heated to 75 °C and stirred for 8 h. The solvent was removed *in vacuo* followed by purification using flash chromatography (elution with hexanes/ethyl acetate = 8:1 to 1:2, v/v) to afford the desired compounds.

*5-O-((2-(4-(naphthalen-1-ylmethyl)piperazin-1-yl)ethyl)-tobramycin 7 $\times$ HCl (1a).*

Synthesized following general procedure A from **7a** (50 mg, 0.03 mmol), 40% HCl (1 mL) and

MeOH (1.5 mL). The crude product was purified by reverse-phase flash chromatography on a C18-silica (elution with 100% deionized water). The product was isolated as a white solid. Yield: 16 mg (55%).  $^1\text{H}$  NMR (500 MHz, deuterium oxide)  $\delta$  8.26 (d,  $J$  = 8.5 Hz, 1H), 8.14 – 8.06 (m, 2H), 7.79 – 7.58 (m, 4H), 5.45 (d,  $J$  = 2.9 Hz, 1H, anomeric CH of H-1'), 5.23 (d,  $J$  = 3.4 Hz, 1H, anomeric CH of H-1''), 4.64 (s, 2H,  $\text{CH}_2$  of naphthylmethyl), 4.23 – 4.10 (m, 3H, CH of H-5', CH of H-4, CH of H-6), 4.10 – 3.31 (m, 21H, CH of H-2'', CH of H-4',  $\text{CH}_2$  of H-6'', CH of H-3'', CH of H-5'', CH of H-4'',  $\text{OCH}_2$  of linker, CH of H-5, CH of H-2',  $4\times\text{CH}_2$  of piperazine, CH of H-1, CH of H-3), 3.31 – 3.25 (m, 2H,  $\text{CH}_2$  of H-6'), 3.08 – 2.98 (m, 2H, piperazine- $\text{CH}_2$  of linker), 2.52 – 2.42 (m, 1H, CHH of H-2), 2.28 – 2.20 (m, 1H, CHH of H-3'), 2.17 – 2.08 (m, 1H, CHH of H-3'), 1.96 – 1.86 (m, 1H, CHH of H-2).  $^{13}\text{C}$  NMR (126 MHz, deuterium oxide)  $\delta$  133.74, 132.07, 130.93, 130.32, 129.09, 128.99, 127.29, 126.59, 125.57, 123.56, 100.71 (anomeric C-1''), 92.60 (anomeric C-1'), 82.45, 81.59, 76.84, 73.66, 68.62, 65.73, 63.68, 60.37, 57.03, 56.49, 54.53, 50.41, 49.75, 48.39, 47.46, 39.01, 28.61. MALDI-TOF-MS  $m/e$  calcd for  $\text{C}_{35}\text{H}_{58}\text{N}_7\text{O}_9$   $[\text{M}+\text{H}]^+$ : 720.430, found: 720.441.

*5-O-((4-(4-(Naphthalen-1-ylmethyl)piperazin-1-yl)butyl)-tobramycin 7×HCl (1b)).*

Synthesized following general procedure A from **7b** (27 mg, 0.016 mmol), 40% HCl (1 mL) and MeOH (1.5 mL). The crude product was purified by reverse-phase flash chromatography on C18-silica (elution with 100% deionized water). The product was isolated as a white solid. Yield: 10 mg (63%).  $^1\text{H}$  NMR (500 MHz, deuterium oxide)  $\delta$  8.23 (d,  $J$  = 8.5 Hz, 1H), 8.14 (d,  $J$  = 8.3 Hz, 1H), 8.09 (dd,  $J$  = 8.2, 1.3 Hz, 1H), 7.80 – 7.72 (m, 2H), 7.72 – 7.62 (m, 2H), 5.41 (d,  $J$  = 2.7 Hz, 1H, anomeric CH of H-1'), 5.25 (d,  $J$  = 3.5 Hz, 1H, anomeric CH of H-1''), 4.91 (s, 2H,  $\text{CH}_2$  of naphthylmethyl), 4.32 – 4.27 (m, 1H, CH of H-5'), 4.27 – 4.22 (m, 1H, CH of H-4), 4.04 – 3.51 (m, 22H, CH of H-6, CH of H-2'', CH of H-4',  $\text{CH}_2$  of H-6'', CH of H-3'', CH of H-5'', CH of

H-4", OCH<sub>2</sub> of linker, CH of H-5, CH of H-2', 4×CH<sub>2</sub> of piperazine, CH of H-1, CH of H-3), 3.48 (dd, *J* = 14.0, 9.1 Hz, 1H, CHH of H-6'), 3.38 – 3.27 (m, 3H, CHH of H-6', piperazine-CH<sub>2</sub> of linker), 2.60 – 2.52 (m, 1H, CHH of H-2), 2.38 – 2.30 (m, 1H, CHH of H-3'), 2.28 – 2.20 (m, 1H, CHH of H-3'), 2.08 – 1.98 (m, 1H, CHH of H-2), 1.93 – 1.79 (m, 2H, N-CH<sub>2</sub>-CH<sub>2</sub> of linker), 1.78 – 1.70 (m, 2H, O-CH<sub>2</sub>-CH<sub>2</sub> of linker). <sup>13</sup>C NMR (126 MHz, deuterium oxide) δ 133.76, 131.68, 131.42, 131.21, 129.20, 127.63, 126.78, 125.59, 124.95, 123.02, 100.91 (anomeric C-1"), 92.74 (anomeric C-1'), 82.19, 81.48, 76.87, 75.78, 73.13, 72.10, 68.55, 64.84, 63.17, 59.36, 57.49, 56.74, 54.81, 49.54, 49.11, 48.91, 48.39, 47.30, 38.53, 28.03, 27.69, 26.44, 20.09.

MALDI-TOF-MS *m/e* calcd for C<sub>37</sub>H<sub>62</sub>N<sub>7</sub>O<sub>9</sub> [M+H]<sup>+</sup>: 748.461, found: 748.472.

*5-O-((6-(4-(Naphthalen-1-ylmethyl)piperazin-1-yl)hexyl)-tobramycin 7×HCl (1c).*

Synthesized following general procedure A from **7c** (52 mg, 0.03 mmol), 40% HCl (1 mL) and MeOH (1.5 mL). The crude product was purified by reverse-phase flash chromatography on C18-silica (elution with 100% deionized water). The product was isolated as a white solid. Yield: 20 mg (65%). <sup>1</sup>H NMR (500 MHz, deuterium oxide) δ 8.22 (d, *J* = 8.5 Hz, 1H), 8.16 (d, *J* = 8.3 Hz, 1H), 8.10 (dd, *J* = 8.2, 1.3 Hz, 1H), 7.83 – 7.75 (m, 2H), 7.73 – 7.63 (m, 2H), 5.41 (d, *J* = 2.7 Hz, 1H, anomeric CH of H-1'), 5.22 (d, *J* = 3.5 Hz, 1H, anomeric CH of H-1"), 5.03 (s, 2H, CH<sub>2</sub> of naphthylmethyl), 4.33 – 4.28 (m, 1H, CH of H-5'), 4.28 – 4.22 (m, 1H, CH of H-4), 4.02 – 3.59 (m, 22H, CH of H-6, CH of H-2", CH of H-4', CH<sub>2</sub> of H-6", CH of H-3", CH of H-5", CH of H-4", OCH<sub>2</sub> of linker, CH of H-5, CH of H-2', 4×CH<sub>2</sub> of piperazine, CH of H-1, CH of H-3), 3.46 (dd, *J* = 14.0, 9.2 Hz, 1H, CHH of H-6'), 3.37 – 3.28 (m, 3H, CHH of H-6', piperazine-CH<sub>2</sub> of linker), 2.60 – 2.54 (m, 1H, CHH of H-2), 2.37 – 2.30 (m, 1H, CHH of H-3'), 2.29 – 2.22 (m, 1H, CHH of H-3'), 2.12 – 2.02 (m, 1H, CHH of H-2), 1.80 (p, *J* = 7.5 Hz, 2H, N-CH<sub>2</sub>-CH<sub>2</sub> of linker), 1.74 – 1.63 (m, 2H, O-CH<sub>2</sub>-CH<sub>2</sub> of linker), 1.47 – 1.36 (m, 4H, 2×CH<sub>2</sub> of linker). <sup>13</sup>C

NMR (126 MHz, deuterium oxide)  $\delta$  133.76, 131.94, 131.70, 131.64, 129.28, 127.84, 126.88, 125.61, 123.56, 122.84, 101.19 (anomeric C-1''), 92.66 (anomeric C-1'), 81.95, 81.66, 76.52, 75.57, 73.28, 73.08, 68.57, 64.81, 63.32, 59.27, 57.29, 56.95, 54.79, 49.72, 48.67, 48.51, 48.47, 47.36, 38.61, 29.24, 28.15, 27.68, 25.87, 24.64, 23.38. MALDI-TOF-MS *m/e* calcd for C<sub>39</sub>H<sub>66</sub>N<sub>7</sub>O<sub>9</sub> [M+H]<sup>+</sup>: 776.492, found: 776.507.

*5-O-((8-(4-(Naphthalen-1-ylmethyl)piperazin-1-yl)octyl)-tobramycin 7×HCl (1d).*

Synthesized following general procedure A from **7d** (31 mg, 0.018 mmol), 40% HCl (1 mL) and MeOH (1.5 mL). The crude product was purified by reverse-phase flash chromatography on C18-silica (elution with 100% deionized water). The product was isolated as a white solid. Yield: 13 mg (70%). <sup>1</sup>H NMR (500 MHz, deuterium oxide)  $\delta$  8.23 (d, *J* = 8.5 Hz, 1H), 8.15 (d, *J* = 8.3 Hz, 1H), 8.12 – 8.08 (m, 1H), 7.80 – 7.73 (m, 2H), 7.72 – 7.63 (m, 2H), 5.40 (d, *J* = 2.6 Hz, 1H, anomeric CH of H-1'), 5.20 (d, *J* = 3.5 Hz, 1H, anomeric CH of H-1''), 4.93 (s, 2H, CH<sub>2</sub> of naphthylmethyl), 4.33 – 4.28 (m, 1H, CH of H-5'), 4.25 – 4.19 (m, 1H, CH of H-4), 4.00 – 3.56 (m, 22H, CH of H-6, CH of H-2'', CH of H-4', CH<sub>2</sub> of H-6'', CH of H-3'', CH of H-5'', CH of H-4'', OCH<sub>2</sub> of linker, CH of H-5, CH of H-2', 4×CH<sub>2</sub> of piperazine, CH of H-1, CH of H-3), 3.44 (dd, *J* = 14.0, 9.0 Hz, 1H, CHH of H-6'), 3.34 (dd, *J* = 14.0, 3.8 Hz, 1H, CHH of H-6'), 3.29 – 3.24 (m, 2H, piperazine-CH<sub>2</sub> of linker), 2.60 – 2.53 (m, 1H, CHH of H-2), 2.33 – 2.22 (m, 2H, CH<sub>2</sub> of H-3'), 2.06 – 1.98 (m, 1H, CHH of H-2), 1.80 – 1.72 (m, 2H, N-CH<sub>2</sub>-CH<sub>2</sub> of linker), 1.72 – 1.61 (m, 2H, O-CH<sub>2</sub>-CH<sub>2</sub> of linker), 1.42 – 1.30 (m, 8H, 4×CH<sub>2</sub> of linker). <sup>13</sup>C NMR (126 MHz, deuterium oxide)  $\delta$  133.76, 131.66, 131.54, 131.34, 129.22, 127.68, 126.80, 125.59, 124.60, 122.94, 101.32 (anomeric C-1''), 92.72 (anomeric C-1'), 81.84, 81.79, 76.67, 75.75, 73.73, 73.12, 68.53, 64.76, 63.19, 59.23, 57.44, 57.03, 54.76, 49.74, 48.83, 48.43, 47.30, 38.52,

29.46, 28.80, 28.26, 28.07, 27.70, 25.66, 25.15, 23.37. MALDI-TOF-MS  $m/e$  calcd for  $C_{41}H_{70}N_7O_9$   $[M+H]^+$ : 804.524, found: 804.537.

*5-O-((10-(4-(Naphthalen-1-ylmethyl)piperazin-1-yl)docyl)-tobramycin 7×TFA (1e).*

TBAF solution (1M in THF, 0.67 mL) was added to a stirred solution of **7e** (120 mg, 0.067 mmol) in THF (2mL). The reaction mixture was stirred at room temperature for 2 h. It was then concentrated *in vacuo*. The residue was purified by flash chromatography (elution with DCM/MeOH = 20:1 to 5:1) to afford a white solid (77 mg) which was further treated with TFA (90% TFA of H<sub>2</sub>O, 5 mL) and stirred at room temperature for 1 h. The above solution was concentrated under reduced pressure and purified by reverse-phase flash chromatography on C18-silica (elution with 100% deionized water) to give the desired product **1e** as a white solid. Yield: 81 mg (74%, two steps). <sup>1</sup>H NMR (500 MHz, deuterium oxide)  $\delta$  8.20 (d,  $J = 8.4$  Hz, 1H), 8.13 – 8.05 (m, 2H), 7.79 – 7.57 (m, 4H), 5.38 (d,  $J = 2.6$  Hz, 1H, anomeric CH of H-1'), 5.16 (d,  $J = 3.5$  Hz, 1H, anomeric CH of H-1"), 4.75 (s, 2H, CH<sub>2</sub> of naphthylmethyl), 4.28 (m, 1H, CH of H-5'), 4.17 – 4.09 (m, 1H, CH of H-4), 3.99 – 3.69 (m, 12H, CH of H-6, CH of H-2", CH of H-4', CH<sub>2</sub> of H-6", CH of H-3", CH of H-5", CH of H-4", OCH<sub>2</sub> of linker, CH of H-5, CH of H-2'), 3.68 – 3.43 (m, 10H, 4×CH<sub>2</sub> of piperazine, CH of H-1, CH of H-3), 3.42 – 3.37 (m, 1H, CHH of H-6'), 3.31 (dd,  $J = 14.0, 3.9$  Hz, 1H, CHH of H-6'), 3.24 – 3.15 (m, 2H, piperazine-CH<sub>2</sub> of linker), 2.59 – 2.51 (m, 1H, CHH of H-2), 2.31 – 2.22 (m, 2H, CH<sub>2</sub> of H-3'), 1.99 – 1.88 (m, 1H, CHH of H-2), 1.76 – 1.68 (m, 2H, N-CH<sub>2</sub>-CH<sub>2</sub> of linker), 1.68 – 1.57 (m, 2H, O-CH<sub>2</sub>-CH<sub>2</sub> of linker), 1.43 – 1.23 (m, 12H, 6×CH<sub>2</sub> of linker). <sup>13</sup>C NMR (126 MHz, deuterium oxide)  $\delta$  133.74, 131.68, 131.02, 130.87, 129.12, 127.45, 126.68, 125.82, 125.54, 123.05, 101.38 (anomeric C-1"), 92.74 (anomeric C-1'), 81.91, 81.84, 76.89, 75.92, 73.82, 73.15, 68.51, 64.71, 63.07, 59.17, 57.60, 56.98, 54.77, 49.70, 49.25, 48.95, 48.34, 47.24, 38.35, 29.46, 29.00, 28.78, 28.58, 28.22,

28.01, 27.68, 25.65, 25.30, 23.36. MALDI-TOF-MS  $m/e$  calcd for  $C_{43}H_{73}N_7O_9Na$   $[M+Na]^+$ : 854.537, found: 854.531.

*5-O-((12-(4-(Naphthalen-1-ylmethyl)piperazin-1-yl)dodecyl)-tobramycin 7×HCl (1f).*

Synthesized following general procedure A from **7f** (38 mg, 0.021 mmol), 40% HCl (1 mL) and MeOH (1.5 mL). The crude product was purified by reverse-phase flash chromatography on C18-silica (elution with 100% deionized water). The product was isolated as a white solid. Yield: 16 mg (69%).  $^1H$  NMR (500 MHz, deuterium oxide)  $\delta$  8.21 (d,  $J = 8.5$  Hz, 1H), 8.16 (d,  $J = 8.3$  Hz, 1H), 8.12 – 8.07 (m, 1H), 7.84 – 7.73 (m, 2H), 7.72 – 7.62 (m, 2H), 5.40 (d,  $J = 2.3$  Hz, 1H, anomeric CH of H-1'), 5.21 – 5.17 (m, 1H, anomeric CH of H-1''), 5.03 (s, 2H,  $CH_2$  of naphthylmethyl), 4.33 – 4.28 (m, 1H, CH of H-5'), 4.25 – 4.19 (m, 1H, CH of H-4), 4.00 – 3.70 (m, 16H, CH of H-6, CH of H-2'', CH of H-4',  $CH_2$  of H-6'', CH of H-3'',  $OCH_2$  of linker, CH of H-5'', CH of H-4'', CH of H-5, CH of H-2',  $2\times CH_2$  of piperazine), 3.70 – 3.44 (m, 6H,  $2\times CH_2$  of piperazine, CH of H-1, CH of H-3), 3.43 – 3.39 (m, 1H, CHH of H-6'), 3.36 – 3.26 (m, 3H, CHH of H-6', piperazine- $CH_2$  of linker), 2.65 – 2.50 (m, 1H, CHH of H-2), 2.35 – 2.20 (m, 2H,  $CH_2$  of H-3'), 2.10 – 1.95 (m, 1H, CHH of H-2), 1.82 – 1.71 (m, 2H, N- $CH_2-CH_2$  of linker), 1.70 – 1.58 (m, 2H, O- $CH_2-CH_2$  of linker), 1.41 – 1.25 (m, 16H,  $8\times CH_2$  of linker).  $^{13}C$  NMR (126 MHz, deuterium oxide)  $\delta$  133.77, 131.91, 131.70, 131.62, 129.28, 127.82, 126.88, 125.59, 123.56, 122.78, 101.35 (anomeric C-1''), 92.71 (anomeric C-1'), 81.84, 81.80, 76.71, 75.83, 73.85, 73.14, 68.52, 64.77, 63.18, 59.22, 57.30, 57.11, 54.75, 49.76, 48.67, 48.44, 47.28, 38.49, 29.47, 29.04, 28.95, 28.86, 28.77, 28.62, 28.22, 28.05, 27.70, 25.61, 25.34, 23.34. MALDI-TOF-MS  $m/e$  calcd for  $C_{45}H_{78}N_7O_9$   $[M+H]^+$ : 860.5861, found: 860.5874.

*5-O-(dodecylparoxetine)-tobramycin 6×HCl (2).* Synthesized following general procedure A from **11** (97 mg, 0.05 mmol), 40% HCl (2 mL), and MeOH (3 mL). The crude

product was purified by reverse-phase flash chromatography on C18-silica (elution with 100% deionized water). The product was isolated as a white solid. Yield: 36 mg (61%).  $^1\text{H}$  NMR (500 MHz, deuterium oxide)  $\delta$  7.33 – 7.23 (m, 2H), 7.11 – 7.04 (m, 2H), 6.73 – 6.66 (m, 1H), 6.43 – 6.36 (m, 1H), 6.25 – 6.16 (m, 1H), 5.89 (s, 2H, O-CH<sub>2</sub>-O of paroxetine.), 5.42 (d,  $J$  = 2.5 Hz, 1H, anomeric CH of H-1'), 5.21 (d,  $J$  = 3.4 Hz, 1H, anomeric CH of H-1''), 4.36 – 4.30 (m, 1H, CH of H-5'), 4.28 – 4.17 (m, 1H, CH of H-4), 4.01 – 3.55 (m, 18H, CH of H-6, CH of H-2'', CH of H-4', CH<sub>2</sub> of H-6'', CH of H-3'', CH of H-5'', CH of H-4'', OCH<sub>2</sub> of linker, O-CH<sub>2</sub>-CH of paroxetine, CH of H-5, CH of H-2', N-CHH-CH<sub>2</sub> of piperidine, N-CHH-CH of piperidine, CH of H-1, CH of H-3), 3.44 (dd,  $J$  = 14.0, 9.2 Hz, 1H, CHH of H-6'), 3.35 (dd,  $J$  = 14.0, 3.9 Hz, 1H, CHH of H-6''), 3.26 – 3.15 (m, 2H, N-CH<sub>2</sub> of linker), 3.15 – 3.06 (m, 2H, N-CHH-CH<sub>2</sub> of piperidine, N-CHH-CH of piperidine), 2.98 – 2.90 (m, 1H, N-CH<sub>2</sub>-CH<sub>2</sub>-CH of piperidine), 2.61 – 2.54 (m, 1H, CHH of H-2), 2.54 – 2.45 (m, 1H, N-CH<sub>2</sub>-CH of piperidine), 2.33 – 2.24 (m, 2H, CH<sub>2</sub> of H-3'), 2.17 – 1.99 (m, 3H, N-CH<sub>2</sub>-CH<sub>2</sub>, CHH of H-2), 1.84 – 1.72 (m, 2H, N-CH<sub>2</sub>-CH<sub>2</sub> of linker), 1.71 – 1.61 (m, 2H, O-CH<sub>2</sub>-CH<sub>2</sub> of linker), 1.42 – 1.24 (m, 16H, 8×CH<sub>2</sub> of linker).  $^{13}\text{C}$  NMR (126 MHz, deuterium oxide)  $\delta$  161.65 (d,  $J$  = 242.9 Hz, CF), 153.51, 147.76, 141.58, 137.37, 137.35, 129.23, 129.16, 115.68, 115.51, 108.24, 106.42, 101.38 (anomeric C-1''), 101.35, 98.22, 92.70 (anomeric C-1'), 81.87, 81.83, 76.70, 75.84, 73.89, 73.18, 68.55, 68.20, 64.82, 63.25, 59.29, 57.58, 54.77, 54.66, 52.92, 49.78, 48.47, 47.32, 40.93, 39.82, 38.55, 30.78, 29.50, 29.06, 28.98, 28.90, 28.82, 28.67, 28.34, 28.09, 27.72, 25.91, 25.36, 23.52. MALDI-TOF-MS  $m/e$  calcd for C<sub>49</sub>H<sub>80</sub>FN<sub>6</sub>O<sub>12</sub> [M+H]<sup>+</sup>: 963.5818, found: 963.5819.

*TOB-DBP Conjugate (3)*. AcOH (5 mL) and 10% Pd/C were added to a stirred solution of compound **16** (86 mg, 0.07 mmol) in MeOH (4 mL) and H<sub>2</sub>O (1 mL). The reaction flask was subjected to catalytic hydrogenation via hydrogen balloon overnight at room temperature. The

reaction mixture was filtered through a bed of Celite<sup>®</sup> and washed with methanolic HCl. The solvents were removed under reduced pressure to afford a crude product which was purified by reverse-phase flash chromatography on C18-silica (elution with a gradient from 100% 0.1% TFA of deionized water to 20% MeOH and 80% 0.1% TFA of deionized water) to give the desired product as a white solid. Yield: 61 mg (77%). <sup>1</sup>H NMR (500 MHz, deuterium oxide)  $\delta$  8.03 – 7.86 (m, 4H, aromatic H), 7.65 – 7.54 (m, 2H, aromatic H), 7.50 (dd,  $J = 8.8, 2.2$  Hz, 1H, aromatic H), 7.42 – 7.37 (m, 2H, aromatic H), 7.36 – 7.28 (m, 3H, aromatic H), 5.39 (d,  $J = 2.6$  Hz, 1H, anomeric CH of H-1'), 5.19 (d,  $J = 3.4$  Hz, 1H, anomeric CH of H-1''), 4.60 – 4.49 (m, 2H, CH of Pro $_{\alpha}$ , CH of Homophe $_{\alpha}$ ), 4.33 – 4.29 (m, 1H, CH of H-5'), 4.24 – 4.18 (m, 1H, CH of H-4), 4.04 (dd,  $J = 11.4, 6.8$  Hz, 1H, CHH of Pro $_{\delta 1}$ ), 4.00 – 3.68 (m, 11H, CH of H-4', CH of H-2'', CH of H-6, CH<sub>2</sub> of H-6'', OCH<sub>2</sub> of linker, CH of H-4'', CH of H-5, CH of H-5'', CH of H-2'), 3.65 – 3.52 (m, 3H, CH of H-1, CH of H-3'', CH of H-3), 3.44 – 3.11 (m, 7H, , CH<sub>2</sub> of H-6', Pro $_{\gamma}$ -CH<sub>2</sub>-NH<sub>2</sub>, N-CH<sub>2</sub> of linker, CHH of Pro $_{\delta 2}$ ), 2.96 – 2.89 (m, 1H, CHH of Homophe $_{\gamma}$ ), 2.85 – 2.73 (m, 2H, CHH of Homophe $_{\gamma}$ , CH of Pro $_{\gamma}$ ), 2.59 – 2.54 (m, 1H, CHH of H-2), 2.54 – 2.42 (m, 2H, CH<sub>2</sub> of Pro $_{\beta}$ ), 2.36 – 2.24 (m, 4H, CH<sub>2</sub> of Homophe $_{\beta}$ , CH<sub>2</sub> of H-3'), 2.06 – 1.96 (m, 1H, CHH of H-2), 1.74 – 1.61 (m, 4H, N-CH<sub>2</sub>-CH<sub>2</sub> of linker, O-CH<sub>2</sub>-CH<sub>2</sub> of linker), 1.38 – 1.22 (m, 16H, 6 $\times$ CH<sub>2</sub> of linker). <sup>13</sup>C NMR (126 MHz, deuterium oxide)  $\delta$  171.84, 168.58, 140.52, 134.01, 133.22, 131.01, 129.03, 128.86, 128.69, 127.73, 127.64, 127.02, 126.57, 126.06, 121.29, 118.99, 101.39 (anomeric C-1''), 92.71 (anomeric C-1'), 81.88, 81.82, 76.76, 75.87, 73.92, 73.18, 68.52, 65.85, 64.75, 63.16, 59.23, 57.72, 55.87, 54.75, 54.40, 49.74, 48.42, 47.28, 40.32, 38.47, 34.90, 33.30, 32.51, 31.39, 29.49, 29.06, 28.99, 28.89, 28.84, 28.57, 28.36, 28.04, 27.72, 25.72, 25.36, 25.33. MALDI-TOF-MS  $m/e$  calcd for C<sub>56</sub>H<sub>89</sub>N<sub>9</sub>O<sub>11</sub>Na [M+Na]<sup>+</sup>: 1086.6579, found: 1086.6592.

*5-O-((2-(4-(naphthalen-1-ylmethyl)piperazin-1-yl)ethyl)-1,3,2',6',3''-penta-N-(tert-butoxycarbonyl)-4',2'',4'',6''-tetra-O-TBDMS-tobramycin (7a)*. Amount of 5 mL of DCM was added to a flask containing compound **10** (65 mg, 0.04 mmol) and 1-(1-naphthylmethyl)-piperazine (NMP) (12 mg, 0.05 mmol) under N<sub>2</sub> gas. Acetic acid (2 μL, 0.04 mmol) was then added to the solution at room temperature and stirred for 1 h. The reaction mixture was cooled down to 0 °C followed by the addition of NaBH(OAc)<sub>3</sub> (38 mg, 0.18 mmol). It was then stirred at room temperature for 18 h before being quenched with saturated NaHCO<sub>3</sub> solution at 0 °C. Water (3 mL) was added, and the resulting mixture was extracted with DCM (3 × 3 mL). The combined organic layers were washed with saturated brine and dried over anhydrous sodium sulfate. The solvent was removed *in vacuo* followed by purification using flash chromatography (elution with a gradient of hexanes/ethyl acetate = 10:1 to 1:1) to give product **7a** as a pale yellow oil. Yield: 50 mg (75%). <sup>1</sup>H NMR (500 MHz, chloroform-*d*) δ 8.33 – 8.25 (m, 1H), 7.84 (dd, *J* = 7.8, 1.6 Hz, 1H), 7.76 (d, *J* = 7.9 Hz, 1H), 7.59 – 7.34 (m, 4H), 5.34 – 5.14 (m, 2H, anomeric *CH* of H-1', anomeric *CH* of H-1''), 4.32 – 4.06 (m, 3H), 3.89 (s, 2H), 3.86 – 3.74 (m, 2H), 3.74 – 3.03 (m, 14H), 2.68 – 2.26 (m, 10H), 2.09 – 1.95 (m, 1H), 1.64 – 1.22 (m, 47H), 1.14 – 1.02 (m, 1H), 1.02 – 0.78 (m, 36H), 0.22 – -0.05 (m, 24H). <sup>13</sup>C NMR (126 MHz, chloroform-*d*) δ 155.91, 155.65, 155.18, 154.91, 154.78, 134.42, 133.94, 132.71, 128.46, 127.87, 127.32, 125.82, 125.67, 125.25, 124.89, 97.87 (anomeric C), 96.72 (anomeric C), 85.62, 79.98, 79.53, 79.42, 79.34, 79.16, 75.56, 72.94, 71.64, 70.67, 68.12, 67.31, 63.47, 61.24, 61.10, 59.07, 57.37, 54.23, 53.67, 53.51, 50.70, 49.51, 48.98, 41.81, 36.01, 35.46, 29.84, 28.80, 28.75, 28.67, 28.64, 28.58, 26.30, 26.18, 26.15, 25.95, 18.59, 18.47, 18.25, 18.07, -3.19, -3.55, -4.04, -4.67, -4.73, -4.85, -4.91, -4.93. MS (ESI) *m/e* calcd for C<sub>84</sub>H<sub>154</sub>N<sub>7</sub>O<sub>19</sub>Si<sub>4</sub> [M+H]<sup>+</sup>: 1678.5, found: 1677.8.

*5-O-((4-(4-(Naphthalen-1-ylmethyl)piperazin-1-yl)butyl)-1,3,2',6',3''-penta-N-(tert-butoxycarbonyl)-4',2'',4'',6''-tetra-O-TBDMS-tobramycin (7b)*. Synthesized following general procedure B from **6b** (48 mg, 0.03 mmol), NMP (11 mg, 0.05 mmol), and K<sub>2</sub>CO<sub>3</sub> (13 mg, 0.09 mmol). The product was isolated as a white solid. Yield: 27 mg (52%). <sup>1</sup>H NMR (500 MHz, chloroform-*d*) δ 8.29 (d, *J* = 8.2 Hz, 1H), 7.82 (dd, *J* = 7.9, 1.6 Hz, 1H), 7.75 (d, *J* = 8.0 Hz, 1H), 7.54 – 7.35 (m, 4H), 5.23 – 5.17 (m, 1H, anomeric H), 5.09 – 4.97 (m, 2H), 5.16 – 5.10 (m, 1H, anomeric), 4.31 – 4.03 (m, 3H), 3.89 (s, 2H), 3.85 – 3.73 (m, 2H), 3.73 – 3.64 (m, 2H), 3.64 – 3.05 (m, 11H), 2.69 – 2.35 (m, 8H), 2.34 – 2.18 (m, 2H), 2.04 – 1.93 (m, 1H), 1.58 – 1.35 (m, 50 H), 1.27 – 1.22 (m, 1H), 1.10 – 1.01 (m, 1H), 0.98 – 0.79 (m, 36H), 0.18 – -0.03 (m, 24H). <sup>13</sup>C NMR (75 MHz, chloroform-*d*) δ 155.89, 155.84, 155.61, 154.79, 154.67, 134.15, 133.88, 132.70, 128.29, 127.77, 127.36, 125.57, 125.53, 125.19, 124.87, 97.77 (anomeric C), 96.62 (anomeric C), 85.74, 79.58, 79.40, 79.36, 79.03, 75.39, 72.98, 72.93, 71.52, 67.91, 66.99, 67.85, 63.22, 61.09, 59.50, 58.74, 57.28, 53.38, 53.23, 50.48, 49.01, 48.34, 41.70, 35.71, 30.74, 30.12, 28.52, 27.67, 27.63, 26.92, 26.01, 26.00, 24.38, 18.53, 18.30, 18.19, 18.01, -3.42, -3.81, -4.12, -4.79, -4.88, -4.91, -5.06, -5.20. MS (ESI) *m/e* calcd for C<sub>84</sub>H<sub>158</sub>N<sub>7</sub>O<sub>19</sub>Si<sub>4</sub> [M+H]<sup>+</sup>: 1706.6, found: 1706.9.

*5-O-((6-(4-(Naphthalen-1-ylmethyl)piperazin-1-yl)hexyl)-1,3,2',6',3''-penta-N-(tert-butoxycarbonyl)-4',2'',4'',6''-tetra-O-TBDMS-tobramycin (7c)*. Synthesized following general procedure B from **6c** (183 mg, 0.12 mmol), NMP (39 mg, 0.17 mmol), and K<sub>2</sub>CO<sub>3</sub> (48 mg, 0.35 mmol). The product was isolated as a white solid. Yield: 52 mg (26%). <sup>1</sup>H NMR (500 MHz, chloroform-*d*) δ 8.29 (d, *J* = 8.0 Hz, 1H), 7.83 (dd, *J* = 7.7, 1.7 Hz, 1H), 7.75 (d, *J* = 8.0 Hz, 1H), 7.55 – 7.35 (m, 4H), 5.26 – 5.18 (m, 1H, anomeric H), 5.18 – 5.11 (m, 1H, anomeric H), 4.32 – 4.01 (m, 3H), 3.90 (s, 2H), 3.84 – 3.09 (m, 15H), 2.68 – 2.51 (m, 4H), 2.51 – 2.35 (m, 4H), 2.35 – 2.22 (m, 2H), 2.06 – 1.96 (m, 1H), 1.61 – 1.35 (m, 50H), 1.35 – 1.17 (m, 5H), 1.09 – 1.00 (m,

1H), 1.00 – 0.79 (m, 36H), 0.21 – -0.04 (m, 24H). <sup>13</sup>C NMR (75 MHz, chloroform-*d*) δ 155.99, 155.85, 155.67, 154.85, 154.71, 134.35, 133.94, 132.72, 128.45, 127.93, 127.42, 125.77, 125.64, 125.23, 124.93, 97.95 (anomeric C), 96.61 (anomeric C), 85.93, 80.07, 79.53, 79.36, 79.28, 79.12, 75.44, 73.37, 72.86, 71.68, 68.14, 67.02, 66.10, 63.29, 61.24, 59.00, 57.43, 53.48, 53.13, 50.82, 50.67, 49.06, 48.47, 41.83, 35.83, 31.04, 30.86, 28.79, 28.65, 28.57, 28.28, 27.11, 26.28, 26.17, 26.13, 25.93, 18.63, 18.47, 18.24, 18.06, -3.22, -3.63, -4.05, -4.73, -4.79, -4.90, -5.01, -5.06. MS (ESI) *m/e* calcd for C<sub>88</sub>H<sub>162</sub>N<sub>7</sub>O<sub>19</sub>Si<sub>4</sub> [M+H]<sup>+</sup>: 1734.6, found: 1734.6.

*5-O-((8-(4-(Naphthalen-1-ylmethyl)piperazin-1-yl)octyl)-1,3,2',6',3''-penta-N-(tert-butoxycarbonyl)-4',2'',4'',6''-tetra-O-TBDMS-tobramycin (7d)*. Synthesized following general procedure B from **6d** (61 mg, 0.04 mmol), NMP (13 mg, 0.06 mmol), and K<sub>2</sub>CO<sub>3</sub> (16 mg, 0.11 mmol). The product was isolated as a white solid. Yield: 31 mg (48%). <sup>1</sup>H NMR (500 MHz, chloroform-*d*) δ 8.28 (d, *J* = 8.1 Hz, 1H), 7.81 (dd, *J* = 7.7, 1.7 Hz, 1H), 7.74 (d, *J* = 8.2 Hz, 1H), 7.56 – 7.31 (m, 4H), 5.27 – 5.17 (m, 1H, anomeric H), 5.17 – 5.10 (m, 1H, anomeric H), 4.35 – 3.98 (m, 3H), 3.88 (s, 2H), 3.85 – 3.07 (m, 15H), 2.73 – 2.34 (m, 8H), 2.34 – 2.23 (m, 2H), 2.06 – 1.94 (m, 1H), 1.64 – 1.34 (m, 50H), 1.34 – 1.16 (m, 9H), 1.12 – 1.01 (m, 1H), 1.00 – 0.78 (m, 36H), 0.26 – -0.10 (m, 24H). <sup>13</sup>C NMR (126 MHz, chloroform-*d*) δ 155.75, 155.61, 155.61, 154.80, 154.64, 134.25, 133.88, 132.65, 128.39, 127.88, 127.35, 125.71, 125.58, 125.15, 124.87, 97.95 (anomeric C), 96.59 (anomeric C), 85.83, 79.97, 79.44, 79.28, 78.91, 75.38, 73.43, 72.77, 71.65, 68.11, 66.93, 65.56, 63.19, 61.31, 61.19, 61.12, 58.90, 57.34, 53.52, 53.42, 53.07, 50.61, 49.02, 48.45, 43.85, 41.76, 36.02, 35.75, 30.72, 30.10, 29.72, 28.73, 28.59, 28.49, 27.82, 27.02, 26.23, 26.11, 26.08, 25.88, 18.57, 18.55, 18.42, 18.18, 18.00, -3.32, -3.70, -4.10, -4.78, -4.85, -4.97, -5.07, -5.13. MS (ESI) *m/e* calcd for C<sub>90</sub>H<sub>166</sub>N<sub>7</sub>O<sub>19</sub>Si<sub>4</sub> [M+H]<sup>+</sup>: 1762.7, found: 1762.3.

*5-O-((10-(4-(Naphthalen-1-ylmethyl)piperazin-1-yl)docyl)-1,3,2',6',3''-penta-N-(tert-butoxycarbonyl)-4',2'',4'',6''-tetra-O-TBDMS-tobramycin (7e)*. Synthesized following general procedure B from **6e** (220 mg, 0.13 mmol), NMP (45 mg, 0.2 mmol), and K<sub>2</sub>CO<sub>3</sub> (55 mg, 0.40 mmol). The product was isolated as a white solid. Yield: 120 mg (50%). <sup>1</sup>H NMR (500 MHz, chloroform-*d*) δ 8.32 – 8.24 (m, 1H), 7.83 (dd, *J* = 7.7, 1.7 Hz, 1H), 7.75 (d, *J* = 8.0 Hz, 1H), 7.54 – 7.34 (m, 4H), 5.27 – 5.18 (m, 1H, anomeric H), 5.18 – 5.12 (m, 1H, anomeric H), 4.33 – 4.21 (m, 1H), 4.20 – 4.12 (m, 1H), 4.12 – 4.02 (m, 1H), 3.90 (s, 2H), 3.86 – 3.05 (m, 15H), 2.71 – 2.35 (m, 8H), 2.35 – 2.27 (m, 2H), 2.05 – 1.96 (m, 1H), 1.65 – 1.35 (m, 50H), 1.35 – 1.13 (m, 13H), 1.00 – 0.78 (m, 36H), 0.20 – -0.04 (m, 24H). <sup>13</sup>C NMR (126 MHz, chloroform-*d*) δ 155.72, 155.58, 155.52, 154.73, 154.55, 134.14, 133.79, 132.55, 128.30, 127.79, 127.28, 125.62, 125.50, 125.07, 124.76, 97.83 (anomeric C), 96.52 (anomeric C), 85.71, 79.89, 79.36, 79.20, 75.27, 73.37, 72.67, 71.53, 68.00, 66.82, 63.09, 61.21, 61.07, 60.34, 58.84, 57.27, 53.32, 53.29, 52.97, 50.52, 48.95, 48.36, 43.76, 41.66, 36.69, 35.90, 35.63, 30.63, 30.03, 29.69, 29.64, 29.62, 28.63, 28.50, 28.48, 28.40, 27.70, 26.91, 26.19, 26.13, 26.01, 25.98, 25.92, 25.78, 24.73, 22.62, 21.01, 18.48, 18.32, 18.09, 17.91, -3.43, -3.80, -4.20, -4.88, -4.95, -5.08, -5.18, -5.24. MS (ESI) *m/e* calcd for C<sub>92</sub>H<sub>170</sub>N<sub>7</sub>O<sub>19</sub>Si<sub>4</sub> [M+H]<sup>+</sup>: 1790.7, found: 1790.5.

*5-O-((12-(4-(Naphthalen-1-ylmethyl)piperazin-1-yl)dodecyl)-1,3,2',6',3''-penta-N-(tert-butoxycarbonyl)-4',2'',4'',6''-tetra-O-TBDMS-tobramycin (7f)*. Synthesized following general procedure B from **6f** (59 mg, 0.04 mmol), NMP (12 mg, 0.05 mmol), and K<sub>2</sub>CO<sub>3</sub> (15 mg, 0.11 mmol). The product was isolated as a white solid. Yield: 38 mg (60%). <sup>1</sup>H NMR (500 MHz, chloroform-*d*) δ 8.29 (d, *J* = 8.1 Hz, 1H), 7.83 (d, *J* = 7.9 Hz, 1H), 7.76 (d, *J* = 8.0 Hz, 1H), 7.58 – 7.33 (m, 4H), 5.27 – 5.18 (m, 1H, anomeric H), 5.18 – 5.12 (m, 1H, anomeric H), 4.35 – 4.22 (m, 1H), 4.22 – 4.13 (m, 1H), 4.13 – 4.02 (m, 1H), 3.90 (s, 2H), 3.86 – 3.07 (m, 15H), 2.72 –

2.36 (m, 8H), 2.35 – 2.26 (m, 2H), 2.07 – 1.95 (m, 1H), 1.61 – 1.35 (m, 50H), 1.35 – 1.16 (m, 17H), 1.12 – 1.00 (m, 1H), 1.01 – 0.77 (m, 36H), 0.22 – -0.04 (m, 24H).  $^{13}\text{C}$  NMR (126 MHz, chloroform-*d*)  $\delta$  155.59, 155.52, 154.73, 154.72, 154.55, 133.80, 132.54, 129.46, 128.33, 127.85, 127.32, 125.65, 125.52, 125.09, 124.76, 97.82 (anomeric C), 96.55 (anomeric C), 85.71, 79.90, 79.36, 79.20, 75.28, 73.40, 72.68, 71.53, 68.00, 67.75, 66.82, 63.10, 61.05, 58.79, 57.28, 53.28, 50.53, 48.96, 48.38, 41.65, 38.90, 35.94, 35.64, 32.80, 31.91, 30.63, 30.56, 30.05, 29.73, 29.71, 29.68, 29.65, 29.63, 28.97, 28.64, 28.51, 28.49, 28.40, 27.66, 26.87, 26.19, 26.14, 26.02, 25.99, 25.79, 23.98, 22.95, 22.67, 18.48, 18.33, 18.10, 17.92, -3.41, -3.80, -4.20, -4.87, -4.94, -5.07, -5.18, -5.23. MS (ESI) *m/e* calcd for  $\text{C}_{94}\text{H}_{174}\text{N}_7\text{O}_{19}\text{Si}_4$   $[\text{M}+\text{H}]^+$ : 1818.8, found: 1818.5.

*5-O-allyl-1,3,2',6',3''-penta-N-(tert-butoxycarbonyl)-4',2'',4'',6''-tetra-O-TBDMS-tobramycin* (**8**). Compound **4** (0.78 g, 0.55 mmol) was dissolved in anhydrous toluene (5 mL). Allyl bromide (95  $\mu\text{L}$ , 1.1 mmol) and a catalytic amount of tetrabutylammonium hydrogen sulfate (TBAHS) (19 mg, 0.06 mmol) were added into this solution subsequently, followed by KOH (84 mg, 1.5 mmol). This reaction mixture was stirred at room temperature under  $\text{N}_2$  gas for 8 h and then concentrated under reduced pressure. The residue was purified via flash chromatography (elution with a gradient of hexanes/ethyl acetate = 10:1 to 4:1) to give the desired product as a white solid. Yield: 0.64 g (79%).  $^1\text{H}$  NMR (500 MHz, chloroform-*d*)  $\delta$  5.95 – 5.80 (m, 1H,  $\text{CH}=\text{CH}_2$ ), 5.29 (d,  $J = 17.2$  Hz, 1H,  $\text{CH}=\text{CHH}$ ), 5.24 – 5.12 (m, 2H, anomeric H), 5.11 – 5.04 (m, 1H,  $\text{CH}=\text{CHH}$ ), 4.63 – 4.47 (m, 1H), 4.28 – 4.05 (m, 3H), 3.87 – 3.24 (m, 13H), 3.23 – 3.07 (m, 1H), 2.54 – 2.40 (m, 1H), 1.99 (m, 1H), 1.62 – 1.50 (m, 1H), 1.50 – 1.29 (m, 45H), 1.18 – 1.02 (m, 1H), 1.02 – 0.78 (m, 36H), 0.21 – -0.04 (m, 24H).  $^{13}\text{C}$  NMR (126 MHz, chloroform-*d*)  $\delta$  155.88, 155.69, 154.96, 154.89, 154.75, 134.48, 117.38, 97.99 (anomeric C), 96.85 (anomeric C), 85.14, 80.02, 79.53, 79.38, 79.21, 75.39, 73.79, 72.74, 71.62, 68.13, 67.25,

63.43, 57.42, 50.70, 49.22, 48.54, 41.78, 36.03, 35.70, 28.76, 28.63, 28.61, 28.54, 26.23, 26.14, 25.92, 18.61, 18.43, 18.23, 18.04, -3.35, -3.63, -4.07, -4.75, -4.78, -4.98, -5.01, -5.05. MS (ESI)  $m/e$  calcd for  $C_{70}H_{137}N_5O_{19}Si_4Na$   $[M+Na]^+$ : 1488.2, found: 1487.0.

*5-O-(2,3-dihydroxypropyl)-1,3,2',6',3''-penta-N-(tert-butoxycarbonyl)-4',2'',4'',6''-tetra-O-TBDMS-tobramycin (9)*. Compound **8** (250 mg, 0.17 mmol),  $OsO_4$  (69  $\mu$ L, 6.8  $\mu$ mol, 2.5 wt % solution in *tert*-butanol) and 2,6-lutidine (40  $\mu$ L, 0.34 mmol) were added to a stirred solution of 1,4-dioxane (6 mL) at room temperature. The reaction mixture was stirred at 60 °C overnight, quenched by saturated  $Na_2S_2O_3$  solution (2 mL), and extracted with ethyl acetate (5 mL  $\times$  3) subsequently. The organic layer extracts were combined, washed with saturated brine (8 mL), and dried over anhydrous  $Na_2SO_4$ . It was then concentrated *in vacuo* to afford 150 mg crude product as a yellow oil, which was used in the next step without further purification. MS (ESI)  $m/e$  calcd for  $C_{70}H_{139}N_5O_{21}Si_4Na$   $[M+Na]^+$ : 1522.2, found: 1521.2.

*5-O-acetaldehyde-1,3,2',6',3''-penta-N-(tert-butoxycarbonyl)-4',2'',4'',6''-tetra-O-TBDMS-tobramycin (10)*. Compound **9** (150 mg crude product from last step) was dissolved in 1,4-dioxane (15 mL) at room temperature.  $NaIO_4$  (107 mg, 0.5 mmol) solution in  $H_2O$  (5 mL) was added and stirred at 55 °C overnight. The reaction mixture was concentrated under reduced pressure and purified via flash chromatography (elution with a gradient of hexanes/ethyl acetate = 10:1 to 2:1) to give the desired product as a colorless oil. Yield: 65 mg (26% two steps).  $^1H$  NMR (500 MHz, chloroform-*d*)  $\delta$  9.53 (s, 1H, CHO), 5.18 – 5.10 (m, 1H, anomeric H), 5.10 – 5.04 (m, 1H, anomeric H), 4.80 (d,  $J = 17.5$  Hz, 1H), 4.37 – 4.23 (m, 1H), 4.23 – 3.98 (m, 2H), 3.86 – 3.24 (m, 13H), 3.24 – 3.02 (m, 1H), 2.55 – 2.36 (m, 1H), 2.01 – 1.87 (m, 1H), 1.61 – 1.32 (m, 46H), 1.13 – 1.02 (m, 1H) 1.00 – 0.73 (m, 36H), 0.21 – -0.05 (m, 24H).  $^{13}C$  NMR (126 MHz, chloroform-*d*)  $\delta$  197.58 (CHO), 155.88, 155.64, 154.90, 154.82, 154.75, 98.22 (anomeric C),

97.32 (anomeric C), 86.68, 80.21, 79.80, 79.66, 79.50, 79.23, 78.63, 77.41, 77.16, 76.91, 75.76, 72.76, 71.44, 67.82, 67.25, 63.42, 57.25, 50.56, 49.24, 48.56, 41.58, 36.79, 36.01, 35.44, 32.03, 29.80, 29.46, 28.73, 28.61, 28.59, 28.54, 28.48, 26.24, 26.18, 26.14, 25.94, 25.89, 24.82, 22.79, 18.62, 18.38, 18.28, 18.22, 18.15, 18.06, 18.01, 14.23, -3.41, -3.64, -4.08, -4.75, -4.78, -4.96, -5.02, -5.05. MS (ESI)  $m/e$  calcd for  $C_{69}H_{135}N_5O_{20}Si_4Na$   $[M+Na]^+$ : 1489.2, found: 1489.2.

*5-O-(dodecylparoxetine)-1,3,2',6',3''-penta-N-(tert-butoxycarbonyl)-4',2'',4'',6''-tetra-O-TBDMS-tobramycin (II)*. To a stirred solution of paroxetine hydrochloride (33 mg, 0.09 mmol) in MeOH (2 mL) and H<sub>2</sub>O (1 mL) was added K<sub>2</sub>CO<sub>3</sub> (41 mg, 0.3 mmol). The mixture was concentrated under reduced pressure to generate a white solid. A solution of compound **6f** (100 mg, 0.06 mmol) in DMF (3 mL) was added into the above white solid mixture and heated up to 80 °C. The reaction was stirred at this temperature for 12 h. DMF was removed under reduced pressure. Then, DCM (8 mL) and MeOH (2 mL) were added to the residue. It was then filtered to afford a clear solution which was concentrated *in vacuo*. The crude was purified by flash chromatography (elution with a gradient of hexanes/ethyl acetate = 10:1 to 1:1) to give a desired product as a white solid. Yield: 97 mg (84%). <sup>1</sup>H NMR (500 MHz, chloroform-*d*)  $\delta$  7.19 – 7.08 (m, 2H), 7.01 – 6.88 (m, 2H), 6.60 (d,  $J$  = 8.5 Hz, 1H), 6.33 (d,  $J$  = 2.5 Hz, 1H), 6.15 – 6.08 (m, 1H) 5.86 (s, 2H), 5.26 – 5.19 (m, 1H, anomeric H), 5.19 – 5.11 (m, 1H, anomeric H), 4.35 – 4.21 (m, 1H), 4.21 – 4.13 (m, 1H), 4.13 – 3.99 (m, 1H), 3.85 – 3.65 (m, 4H), 3.65 – 2.97 (m, 16H), 2.58 – 2.31 (m, 4H), 2.31 – 2.13 (m, 1H), 2.13 – 1.97 (m, 3H), 1.85 – 1.76 (m, 1H), 1.62 – 1.36 (m, 50H), 1.35 – 1.16 (m, 17H), 1.08 – 1.00 (m, 1H), 1.00 – 0.76 (m, 36H), 0.23 – -0.04 (m, 24H). <sup>13</sup>C NMR (126 MHz, chloroform-*d*)  $\delta$  161.44 (d,  $J$  = 244.2 Hz, CF), 155.51, 154.71, 154.54, 154.39, 148.08, 141.48, 139.82, 128.81, 128.75, 115.39, 115.23, 107.77, 105.55, 101.00, 97.96, 97.93, 96.53, 85.70, 79.88, 79.35, 79.18, 75.27, 73.40, 72.67, 71.52, 69.67, 68.00, 66.81,

63.08, 59.25, 57.75, 57.26, 54.13, 50.52, 48.95, 48.37, 44.22, 42.11, 41.66, 35.91, 35.63, 34.40, 30.62, 30.05, 29.74, 29.71, 29.68, 29.66, 28.62, 28.50, 28.48, 28.39, 27.77, 27.09, 26.19, 26.12, 26.00, 25.98, 25.77, 18.47, 18.32, 18.09, 17.90, -3.43, -3.81, -4.21, -4.89, -4.96, -5.08, -5.19, -5.24. MS (ESI)  $m/e$  calcd for  $C_{98}H_{176}FN_6O_{22}Si_4$   $[M+H]^+$ : 1921.8, found: 1921.7.

*5-O-(12-hydroxydodecyl)-1,3,2',6',3''-penta-N-(tert-butoxycarbonyl)-4',2'',4'',6''-tetra-O-TBDMS-tobramycin (12)*. DMF (15 mL) and  $H_2O$  (3 mL) were added to a flask containing compound **6f** (628 mg, 0.38 mmol) and  $K_2CO_3$  (104 mg, 0.75 mmol). The reaction mixture was heated to 80 °C and stirred for 24 h. Water (15 mL) was added, and the resulting mixture was extracted with ethyl acetate ( $3 \times 10$  mL). The organic layer was washed with saturated brine and dried over anhydrous sodium sulfate. The solvent was removed *in vacuo* followed by purification using flash chromatography (elution with a gradient of hexanes/ethyl acetate = 20:1 to 2:1) to give product **12** as a white solid. Yield: 260 mg (43%).  $^1H$  NMR (500 MHz, chloroform-*d*)  $\delta$  5.25 – 5.19 (m, 1H, anomeric H), 5.12 (m, 1H, anomeric H), 4.32 – 4.21 (m, 1H), 4.21 – 4.12 (m, 1H), 4.13 – 4.02 (m, 1H), 3.82 – 3.13 (m, 16H), 2.47 (d,  $J = 12.6$  Hz, 1H), 2.06 – 1.95 (m, 1H), 1.62 – 1.52 (m, 3H), 1.52 – 1.38 (m, 48H), 1.38 – 1.17 (m, 17H), 0.98 – 1.13 (m, 1H), 1.00 – 0.78 (m, 36H), 0.21 – -0.02 (m, 24H).  $^{13}C$  NMR (126 MHz, chloroform-*d*)  $\delta$  155.70, 155.52, 154.75, 154.70, 154.57, 97.85 (anomeric C), 96.52 (anomeric C), 85.73, 79.90, 79.22, 77.20, 75.29, 73.37, 72.65, 71.55, 68.01, 66.82, 63.11, 63.01, 57.27, 50.52, 48.95, 48.37, 41.67, 35.89, 35.63, 32.81, 30.61, 29.95, 29.57, 29.52, 29.38, 18.48, 18.32, 18.09, 17.91, -3.42, -3.80, -4.20, -4.89, -4.95, -5.09, -5.19, -5.24. MS (ESI)  $m/e$  calcd for  $C_{79}H_{157}N_5O_{20}Si_4Na$   $[M+Na]^+$ : 1632.5, found: 1631.4.

*5-O-(12-dodecanal)-1,3,2',6',3''-penta-N-(tert-butoxycarbonyl)-4',2'',4'',6''-tetra-O-TBDMS-tobramycin (13)*. PCC (pyridinium chlorochromate, 388 mg, 1.8 mmol) and NaOAc (5

mg, 0.06 mmol) were added to a stirred solution of compound **12** (0.965 g, 0.6 mmol) in dry DCM (20 mL). The reaction mixture was stirred at room temperature under N<sub>2</sub> gas for 1 h. When a TLC analysis shows that most of the starting alcohol is consumed, the chromium species were removed by filtration through a pad of silica gel and washed with ethyl acetate. The collected organic phase was concentrated under reduced pressure to afford the crude which was then purified via flash chromatography (elution with a gradient of hexanes/ethyl acetate = 1:1 to 100% ethyl acetate) to give the desired product **13** as a white solid. Yield: 0.897 g (93%). <sup>1</sup>H NMR (500 MHz, chloroform-*d*)  $\delta$  9.74 (s, 1H, CHO), 5.24 – 5.15 (m, 1H, anomeric), 5.16 – 5.10 (m, 1H, anomeric), 4.33 – 4.19 (m, 1H), 4.19 – 4.10 (m, 1H), 4.09 – 3.99 (m, 1H), 3.84 – 3.28 (m, 12H), 3.28 – 3.03 (m, 3H), 2.52 – 2.42 (m, 1H), 2.42 – 2.35 (m, 2H), 2.02 – 1.94 (m, 1H), 1.63 – 1.57 (m, 2H), 1.55 – 1.33 (m, 48H), 1.33 – 1.14 (m, 15H), 1.09 – 0.99 (m, 1H), 0.99 – 0.75 (m, 36H), 0.21 – -0.07 (m, 24H). <sup>13</sup>C NMR (126 MHz, chloroform-*d*)  $\delta$  202.8 (CHO), 155.67, 155.49, 154.70, 154.68, 154.53, 97.82 (anomeric C), 96.48 (anomeric C), 85.70, 79.85, 79.33, 79.17, 78.77, 75.25, 73.33, 72.64, 71.52, 67.99, 66.81, 63.08, 57.24, 50.50, 48.91, 48.34, 43.87, 41.64, 35.89, 35.61, 30.59, 29.97, 29.63, 29.58, 29.56, 29.39, 29.31, 29.15, 28.80 – 28.17, 26.28 – 25.50, 22.06, 18.45, 18.30, 18.07, 17.88, -3.45, -3.82, -4.23, -4.92, -4.98, -5.11, -5.21, -5.27. MS (ESI) *m/e* calcd for C<sub>79</sub>H<sub>155</sub>N<sub>5</sub>O<sub>20</sub>Si<sub>4</sub>Na [M+Na]<sup>+</sup>: 1630.5, found: 1631.1.

*Compound 15.* K<sub>2</sub>CO<sub>3</sub> solution (25 mg, 0.18 mmol in 3 mL of H<sub>2</sub>O) was added to a flask containing compound **14** (TFA salt, 350 mg, 0.22 mmol) and stirred for 5 min at room temperature. The mixture was extracted with ethyl acetate (3 × 3 mL), dried over anhydrous sodium sulfate, and concentrated under reduced pressure to give a pale yellow solid. The resulting solid was mixed with aldehyde **13** (350 mg, 0.22 mmol), followed by the addition of dry DCM (10 mL) and AcOH (10  $\mu$ L, 0.018 mmol) under N<sub>2</sub> gas. The reaction mixture was

stirred at room temperature for 7 h before  $\text{NaBH}(\text{OAc})_3$  (153 mg, 0.72 mmol) was added at 0 °C. The solution was gradually warmed to room temperature while stirring overnight. The reaction mixture was cooled to 0 °C and quenched carefully by the dropwise addition of saturated  $\text{NaHCO}_3$  solution (10 mL). The solution was then extracted with DCM ( $3 \times 5$  mL). The organic layer was washed with brine, dried over anhydrous sodium sulfate, and concentrated *in vacuo*. The crude product was purified by flash chromatography (elution with a gradient of hexanes/ethyl acetate = 10:1 to 1:2) to afford the desired product **15** as a white solid. Yield: 0.28 g (72%).  $^1\text{H}$  NMR (500 MHz, methanol- $d_4$ )  $\delta$  8.24 (d,  $J = 2.2$  Hz, 1H), 7.80 – 7.71 (m, 3H), 7.56 (dd,  $J = 8.8, 2.1$  Hz, 1H), 7.46 – 7.40 (m, 1H), 7.40 – 7.35 (m, 1H), 7.34 – 7.27 (m, 4H), 7.27 – 7.21 (m, 3H), 7.20 – 7.10 (m, 3H), 5.47 – 5.34 (m, 2H, anomeric), 5.05 (s, 2H, ,  $\text{OCH}_2\text{Ph}$ ), 4.67 – 4.61 (m, 1H), 4.21 – 4.12 (m, 1H), 3.98– 3.20 (m, 17H), 3.19 – 3.02 (m, 3H), 2.75 – 2.64 (m, 2H), 2.63-2.51(m, 1H), 2.51-2.41(m, 1H), 2.41-2.29 (m, 1H), 2.29 – 2.14 (m, 1H), 2.14 – 2.01 (m, 3H), 1.98-1.82 (m, 2H), 1.68 – 1.52 (m, 4H), 1.52 – 1.36 (m, 47H), 1.36 – 1.06 (m, 18H), 0.99 – 0.81 (m, 36H), 0.17 – 0.01 (m, 24H).  $^{13}\text{C}$  NMR (126 MHz, methanol- $d_4$ )  $\delta$  177.18, 171.66, 158.88, 158.17, 157.99, 157.47, 157.03, 156.98, 142.28, 138.37, 137.02, 135.20, 132.13, 129.62, 129.57, 129.46, 129.42, 128.92, 128.88, 128.72, 128.64, 128.61, 127.51, 127.16, 126.07, 121.09, 117.90, 96.78 (anomeric C), 95.41 (anomeric C), 86.59, 86.36, 80.64, 80.56, 80.33, 80.16, 79.54, 78.28, 75.20, 74.86, 73.87, 73.54, 72.60, 71.89, 68.80, 68.68, 67.38, 65.06, 58.90, 57.65, 57.31, 54.44, 52.98, 49.89, 44.26, 42.15, 39.66, 36.68, 35.99, 35.62, 33.02, 31.92, 31.31, 30.90, 30.88, 30.84, 30.82, 30.78, 30.12, 29.30, 29.25, 29.12, 28.97, 28.92, 28.90, 28.63, 27.71, 27.00, 26.92, 26.73, 26.68, 26.65, 26.53, 19.50, 19.10, 18.96, 18.90, -3.24, -3.79, -3.93, -4.15, -4.20, -4.41, -4.63, -4.85. MALDI-TOF-MS  $m/e$  calcd for  $\text{C}_{113}\text{H}_{191}\text{N}_9\text{O}_{23}\text{Na}$   $[\text{M}+\text{Na}]^+$ : 2177.303, found: 2177.592.

*Compound 16.* Synthesized following general procedure A from **15** (0.28 g, 0.13 mmol), 40% HCl (4 mL), and MeOH (6 mL). The compound was purified by reverse-phase flash chromatography on C18-silica (elution with a gradient from 100% deionized water to deionized water/MeOH = 1:1, v/v) to give the desired product as a white solid. Yield: 86 mg (52%). <sup>1</sup>H NMR (500 MHz, methanol-*d*<sub>4</sub>) δ 8.20 (d, *J* = 2.1 Hz, 1H), 7.83 – 7.73 (m, 3H), 7.57 (d, *J* = 8.9 Hz, 1H), 7.47 – 7.22 (m, 11H), 7.420 – 7.13 (m, 1H), 5.46 (d, *J* = 3.0 Hz, 1H, anomeric), 5.18 (d, *J* = 3.4 Hz, 1H, anomeric), 5.06 (s, 2H, , OCH<sub>2</sub>Ph), 4.65 – 4.58 (m, 1H), 4.42 – 4.34 (m, 1H), 4.31 – 4.22 (m, 1H), 4.22 – 4.14 (m, 1H), 3.29 – 3.22 (m, 4H), 3.97 – 3.84 (m, 2H), 3.84 – 3.48 (m, 13H), 3.19 – 3.06 (m, 2H), 2.95 – 2.69 (m, 3H), 2.59 – 2.50 (m, 1H), 2.51 – 2.41 (m, 1H), 2.40 – 2.28 (m, 1H), 2.28 – 2.05 (m, 6H), 1.71 – 1.55 (m, 4H), 1.40 – 1.19 (m, 16H). <sup>13</sup>C NMR (75 MHz, methanol-*d*<sub>4</sub>) δ 171.86, 169.47, 159.12, 142.11, 138.24, 136.98, 135.19, 132.23, 129.63, 129.54, 129.07, 128.84, 128.63, 128.56, 127.57, 127.31, 126.18, 121.24, 118.09, 102.34 (anomeric C), 93.89 (anomeric C), 83.41, 82.74, 77.06, 76.33, 75.40, 73.99, 70.53, 67.95, 67.69, 66.87, 65.58, 61.39, 59.18, 56.86, 56.41, 51.06, 50.04, 49.90, 49.61, 49.33, 49.21, 49.05, 48.88, 48.76, 48.48, 48.20, 42.72, 40.51, 39.07, 35.21, 34.36, 33.33, 31.30, 31.08, 30.94, 30.84, 30.71, 30.56, 30.30, 28.98, 27.60, 27.14, 26.97. MS (ESI) *m/e* calcd for C<sub>64</sub>H<sub>96</sub>N<sub>9</sub>O<sub>13</sub> [M+H]<sup>+</sup>: 1199.5, found: 1199.2.

## 3.6.2 Microbiology

### 3.6.2.1 Clinical Isolates

Bacterial isolates were obtained as part of the Canadian National Intensive Care Unit (CAN-ICU) study<sup>52</sup> and Canadian Ward Surveillance (CANWARD) studies.<sup>53,54</sup> Nineteen

medical centers from all regions of Canada with active intensive care units (ICUs) participated on the CAN-ICU study. Each participating center collected a maximum of 300 consecutive bacterial isolates recovered from blood, urine, wound/tissue, and respiratory specimens (one pathogen per cultured site per patient) of ICU patients from September 2005 to June 2006, inclusive. The 4180 bacterial isolates obtained represented 2580 patients (or 1.62 isolates per patient). Note that each of the participating study sites were requested to only collect “clinically significant” specimens from patients with a presumed infectious disease. All isolates were transported to the reference laboratory (Health Sciences Centre, Winnipeg, Canada) on Amies charcoal swabs, subcultured onto an appropriate media, and stocked in skim milk at -80 °C until antimicrobial susceptibility testing was carried out.

### ***3.6.2.2 Antimicrobial Susceptibilities***

Following two subcultures from frozen stock, the *in vitro* antibacterial activities of agents were determined by microbroth dilution susceptibility test in accordance with the Clinical and Laboratory Standards Institute (CLSI) guidelines.<sup>55</sup> All pathogens obtained from the CAN-ICU and CANWARD studies have been obtained from these national Health Canada endorsed studies that have received Ethics approval from the University of Manitoba Ethics Committee. In addition, individual hospitals obtain ethics approval in order to submit isolates. The minimum inhibitory concentration (MIC) of the antimicrobial agents for the bacterial isolates were determined using 96-well plates containing doubling antimicrobial dilutions of cation adjusted Mueller-Hinton broth (MHB) and inoculated to achieve a final concentration of approximately  $5 \times 10^5$  CFU/mL. We used stock concentration of either 10.24 or 5.12 mg/mL in deionized water or DMSO depending on the solubility of the compounds. The plates were then incubated in

ambient air for 18–24 h prior to reading. Reference bacterial strains including *Staphylococcus aureus* ATCC 29213, methicillin-resistant *S. aureus* (MRSA) ATCC 33592, *Enterococcus faecalis* ATCC 29212, *Enterococcus faecium* ATCC 27270, *Streptococcus pneumoniae* ATCC 49619, *Escherichia coli* ATCC 25922, *Pseudomonas aeruginosa* ATCC 27853 and *Klebsiella pneumoniae* ATCC 13883 were acquired from the American Type Culture Collection (ATCC) and were used as a quality control strain. The clinical isolates methicillin-resistant *Staphylococcus epidermidis* (MRSE cefazolin MIC > 32 µg/mL) CAN-ICU 61589, gentamicin-resistant *E. coli* CAN-ICU 61714, amikacin-resistant (MIC = 32 µg/mL) *E. coli* CAN-ICU 63074, gentamicin-resistant *P. aeruginosa* CAN-ICU 62584, *Stenotrophomonas maltophilia* CAN-ICU 62584 and *Acinetobacter baumannii* CAN-ICU 63169 were obtained from hospitals across Canada as a part of the CAN-ICU study.<sup>52</sup> Methicillin-susceptible *S. epidermidis* (MSSE) CANWARD-2008 81388 was obtained from the 2008 CANWARD study<sup>53</sup> while gentamicin-resistant tobramycin-resistant ciprofloxacin-resistant [aminoglycoside modifying enzyme aac(3)-IIa present] *E. coli* CANWARD-2011 97615 and gentamicin-resistant tobramycin-resistant *P. aeruginosa* CANWARD-2011 96846 were obtained from the 2011 CANWARD study.<sup>54</sup>

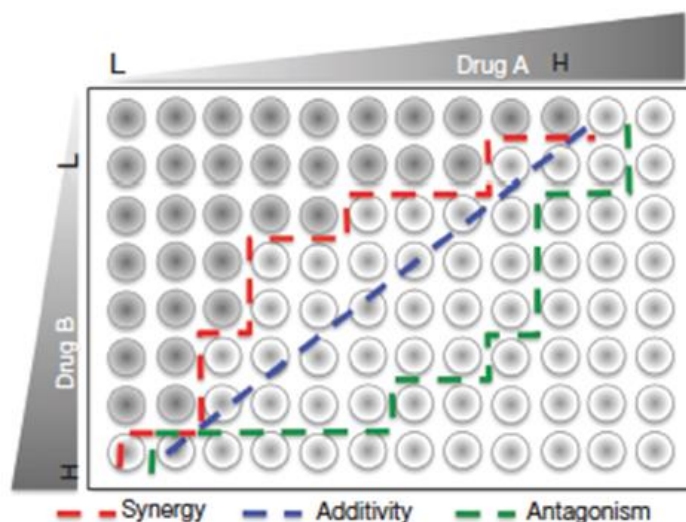
### **3.6.2.3 Antibacterial Combination Screening**

Checkerboard method.<sup>56</sup> The checkerboard consists of columns in which each well contains the same amount of the antibiotic being 2-fold diluted along the x axis of 96-well plate. Rows in which each well contains the same amount of the synthetic compound being 2-fold diluted on the y axis. The result is that each well in the checkerboard contains a unique combination of the two agents being tested. Overnight bacterial culture was standardized in

saline using the 0.5 McFarland turbidity standard and diluted 1:50 in MHB. A amount of 50  $\mu\text{L}$  of standardized culture was added to each of the wells and the plate was incubated at 37 °C for 18 h.

Fractional Inhibitory Concentration Index (FICI) Determination. FICs were determined by checkerboard method. The MIC for each drug was the lowest concentration showing no bacterial growth. The FIC values for the compounds and antibiotics were calculated as the [MIC of agents in combination] / [MIC of agent alone]. The FICI is the sum of the FIC of the compound and the antibiotic.<sup>6</sup> The combination is considered synergistic when the FICI is  $\leq 0.5$ , no interaction when the FICI is  $>0.5$  to  $<4.0$ , and antagonistic when the FICI is  $\geq 4.0$ .<sup>31</sup>

a



b

$$\text{FICI} = [\text{FIC}]_A + [\text{FIC}]_B = \text{MIC}_{\text{combo}} / \text{MIC}_{A \text{ alone}} + \text{MIC}_{\text{combo}} / \text{MIC}_{B \text{ alone}}$$

**Figure 3.6.2.3.1.** (a) Checkerboard assay to determine FIC. (b) The equation used to quantitatively assess combinations. Adapted with permission from *Expert Reviews in Molecular Medicine*, 2011, 13, e5. Copyright (2011) Cambridge University Press

#### **3.6.2.4 Hemolytic Assay**

The capability of the synthesized agents to lyse eukaryotic red blood cells was determined using ovine erythrocytes (obtained from a slaughter house) following institutional biosafety rules using a modified protocol.<sup>57</sup> First, the erythrocytes were washed in Tris-buffered saline (10 mM Tris, 150 mM NaCl, pH 7.4) three times and resuspended in the same solution. The original cell concentration was  $3.8 \times 10^8$  cells/mL. The cell suspension (350  $\mu$ L) and varying amounts of buffer and compound stock solution were mixed into Eppendorf tubes, resulting in 1500  $\mu$ L volume final suspension. The suspensions were then incubated for 30 min with gentle shaking. They were then cooled via ice-water and centrifuged at 2000g at 4 °C for 5 min. Then, 200  $\mu$ L of the supernatant was mixed with 1800  $\mu$ L of 0.5% NH<sub>4</sub>OH followed by optical density (OD<sub>540</sub>) determination at 540 nm. The blank and positive control (100% hemolysis) were determined using similarly treated supernatants, obtained after centrifugation of 350  $\mu$ L of erythrocyte stock suspension which was diluted and incubated in 1150  $\mu$ L of buffer or 1.0% NH<sub>4</sub>OH, respectively. The percent hemolysis shown are the mean  $\pm$  standard deviation obtained from three independent experiments.

#### **3.6.2.5 Cytotoxicity Assay**

The epithelial DU145 cell line was cultured from frozen stocks that were originally obtained from ATCC (Manassas, VA, USA), while the epithelial JIMT-1 cells were grown from frozen stocks obtained from DSMZ (Braunschweig, Germany). Both DU145 and JIMT-1 cells were grown in Dulbecco's Modified Eagle's Medium (DMEM). The cells were grown in media supplemented with 10% fetal bovine serum (FBS), penicillin (100 U/mL) and streptomycin (0.1 mg/mL) in a humidified 5% CO<sub>2</sub> atmospheric incubator at 37 °C. Cell viability was evaluated by

using CellTiter 96 AQueous One Solution cell proliferation assay / MTS Assay (Promega) as previously described.<sup>24</sup> MTS assay refers to a colorimetric assay that is based on the bioreduction of MTS tetrazolium salts (pale yellow) by viable cells to generate a formazan dye product [dark-blue (purple)] that is soluble in cell culture media.<sup>63</sup> This reduction process is carried out by NAD(P)H-dependent dehydrogenase enzymes of metabolically active cells.<sup>63</sup> The formazan dye product can be quantified by measuring the absorbance at OD=490-500 nm in terms of determining cell viability *in vitro*.<sup>63</sup> Briefly, equal numbers of the cancer cells (7500-9000) suspended in media (100  $\mu$ L) were dispersed into 96-well plates. Media without cells (100 mL) were placed in some wells as blanks and treated. After 24 h incubation, a solution of test compound in growth medium (100  $\mu$ L) at twice the desired concentration was added to each well. The treated cells were then incubated for 48 h, to which MTS reagent (20% v/v), containing [3-(4,5-dimethylthiazol-2-yl)-5-(carboxymethoxyphenyl)-2-(4-sulfophenyl)-2H-tetrazolium] salt and phenazine ethosulfate (PES), was added to each well. The plates were incubated for 1–4 h on a Nutating mixer in a 5% CO<sub>2</sub> incubator, and then the optical density (OD) was read at 490 nm by using a SpectraMax M2 plate reader (Molecular Devices Corp., Sunnyvale, CA, USA). The blank was subtracted from each spectral reading, and the viability of the treated cells relative to the controls with vehicle were calculated. The values shown on the plots are the mean standard deviation.

### **3.6.2.6 *Grallera mellonella* Model of *P. aeruginosa* Infection**

Batches of last instar *G. mellonella* waxworms were obtained from a commercial source and used within 7 days of delivery. Larvae on average were 250 mg and used to determine treatment dosage as previously described.<sup>58</sup> Single colonies of XDR *P. aeruginosa* P262-101856

were used to inoculate 3 mL of LB broth and grown overnight at 37 °C with 250 rpm shaking. Next day overnight culture was standardized in 2 mL PBS to  $1.0 \times 10^8$  CFU/mL using a 0.5 McFarland Standard (Remel, Lenexa, USA) and diluted to  $1.0 \times 10^5$  CFU/mL and 10  $\mu$ L injected into larvae. This CFU/mL concentration was optimized by previous infections of decreasing concentrations of *P. aeruginosa* P262-101856. Monotherapy experiment used 15 larvae, and these experiments were repeated two times using larvae from different batches ( $n = 30$ ). Monotherapies were assayed 2 h after bacterial infection, and tobramycin, minocycline, NMP, paroxetine (PAR), DBP, conjugates **1f**, **2**, and **3** were individually tested at 75 mg/kg. For combination therapy, equal dosages of minocycline and conjugates **1f**, **2**, **3** were used to give final dosages of 37.5 + 37.5 mg/kg and 75 + 75 mg/kg. The larvae were incubated at 37 °C in Petri dishes lined with filter paper and scored for survivability every 24 h. Larvae were considered dead if they do not respond to touch. Conjugate/antibiotic tolerability experiments were conducted on 10 larvae ( $n = 10$ ) for each of conjugate/antibiotic concentrations.

### **3.6.2.7 Outer Membrane Permeabilization Assay**

The ability of the synthesized agents to cause outer membrane permeabilization of *P. aeruginosa* PAO1 was evaluated by using the membrane-impermeable fluorescent probe 1-*N*-phenyl-naphthylamine (NPN). A compromised outer membrane as a result of the agent's action allows NPN to diffuse into the lipid bilayer. NPN weakly fluoresce in polar solvents. However, NPN strongly fluoresce in hydrophobic environment such as in lipid bilayer.<sup>59</sup> Briefly, *P. aeruginosa* PAO1 cells at mid-logarithmic phase ( $A_{600} = 0.4-0.5$ ) were harvested, washed, and resuspended in 5 mM HEPES buffer at pH 7.2. Subsequently, NPN (10  $\mu$ M final concentration) and sodium azide (10  $\mu$ M final concentration) were added to the cell suspension and incubated at

room temperature for 30 min in darkness. Varying concentrations of the agent (256, 128, 64, 32, and 16  $\mu\text{g}/\text{mL}$ ) were added onto the suspension to which the resulting NPN fluorescence change was recorded at a continuous interval on a FlexStation 3 (Molecular Devices, Sunnyvale, USA) microplate reader at the excitation wavelength of 350 nm and emission wavelength of 420 nm. 1% Triton X-100 (gold) and 10 mM EDTA is known to cause outer membrane permeability and therefore was used as a positive control. Conjugate-untreated cell suspension with NPN act as a negative control, and spectral reading was subtracted from experimental data to account for any background fluorescence.

#### **3.6.2.8 Membrane Depolarization Assay**

Depolarization of bacterial transmembrane potential due to the synthesized compound was probed using a membrane potential-sensitive dye 3,3'-dipropylthiadicarbocyanine iodide DiSC<sub>3</sub>(5).<sup>60</sup> Diffusion of the fluorescent DiSC<sub>3</sub>(5) probe into the cytoplasmic lipid bilayer, driven by intact transmembrane potential, quenches its fluorescence.<sup>61</sup> Following addition of a compound that disrupts transmembrane potential, the dye gets released into the medium and regains its fluorescence. Briefly, *P. aeruginosa* PAO1 cells were grown until mid-logarithmic phase ( $A_{600} = 0.4\text{--}0.5$ ) which were harvested by centrifugation. The cells were washed and resuspended in HEPES buffer containing 20 mM glucose at pH 7.2. The cell suspension was diluted using the previously used HEPES buffer solution along with 0.2 mM EDTA to achieve a desired concentration ( $A_{600}$  of 0.05). The cell suspensions were incubated with 0.4  $\mu\text{M}$  DiSC<sub>3</sub>(5) for 30 min at 37 °C with constant stirring. 0.1 M KCl was then added followed by further incubation for 15 min to ensure maximum dye uptake (stable fluorescence quenching was observed). The cell suspension was then treated with the desired concentration of the test

compounds (64, 32, 16, and 8  $\mu\text{g}/\text{mL}$ ). The fluorescence was monitored at an excitation wavelength of 622 nm and an emission wavelength of 670 nm on a FlexStation 3 (Molecular Devices, Sunnyvale, USA) microplate reader. A blank with dye-treated cells was used as background. Cells treated with colistin were used as positive control. Fluorescence measurements were recorded for three independent experiments.

### **3.6.2.9 Swimming Motility Assay**

The medium was composed of Trypticase Peptone (5 mg/mL), NaCl (2.5 mg/mL) and 0.3% (w/v) agar. The motility plates were prepared by mixing the molten media with the desired concentration of the agent which was allowed to dry for an hour. 2.5  $\mu\text{L}$  of an overnight grown culture of *P. aeruginosa* PAO1 was diluted in sterile PBS to an  $\text{OD}_{600}$  of 1.0. The culture was then point inoculated onto the motility plate and incubated for 20 h at 37 °C.<sup>36</sup>

### **3.6.2.10 Time-kill Curve**

The kinetics of bacterial killing was measured using *P. aeruginosa* PAO1 as previously described.<sup>36</sup> The synthesized compounds and minocycline were added alone, respectively (at  $1 \times \text{MIC}$ ) and in combination at desired concentrations ( $1 \times \text{MIC}$ ,  $0.5 \times \text{MIC}$  and  $0.25 \times \text{MIC}$ ) in freshly prepared MHB media containing grown *P. aeruginosa* PAO1 cells (approximately  $10^6$  CFU/mL). The resulting media was incubated at 37 °C and 250 rpm for 24 h. Untreated cells in media act as positive control. The kinetics of bacterial cell death were determined by calculating viable cell numbers ( $\log_{10}$  CFU/mL) at regular intervals of time (3 h, 6 h, 9 h, and 24 h) by serial dilution and plating.

### 3.6.2.11 Emergence of Resistance

The propensity of *in vitro* resistance development in *P. aeruginosa* PAO1 under the selection pressure of colistin, tobramycin, minocycline as well as individual combinations of conjugates **1f**, **2**, **3**, and DBP with minocycline in 1:1 mass ratio was determined in a multistep experiment following a standard method described earlier.<sup>62</sup> Primarily, MIC values of the tested compounds were ascertained by microtiter broth dilution method. Bacterial suspension from sub-MIC (MIC/2) of individual compound was used to prepare the inoculum for the next day MIC experiment by diluting it to a final concentration of approximately  $5 \times 10^5$  cells/mL in cation adjusted Mueller-Hinton broth (MHB). The process of determining MIC using the bacterial suspension from sub-MIC (at MIC/2) was repeated for the next 25 passages and the ratio of the MIC obtained during each passage relative to the MIC for first-time exposure (at 0 day) was determined. The results were expressed as relative fold increase in MIC with each passage or day.

### 3.6.2.12 Tetracycline Uptake Assay

Fluorescence-based tetracycline uptake assay in bacterial cells was performed following previously reported method.<sup>36</sup> It relies on monitoring the enhancement of tetracycline fluorescence as it enters the cell. Culture of *P. aeruginosa* PAO1 was grown to  $OD_{600} = 0.6$  followed by washing and resuspending it in 1/4 volume of 10 mM HEPES, pH 7.2. 100  $\mu$ L/well cell suspension was treated with varying concentrations (6.25  $\mu$ g/mL, 12.5  $\mu$ g/mL, and 25  $\mu$ g/mL) of test compounds in the presence of 128  $\mu$ g/mL tetracycline, and fluorescence was recorded at a continuous interval of 1 minute for 30 minutes at room temperature on a FlexStation 3 (Molecular Devices, Sunnyvale, USA) microplate reader at the excitation wavelength of 405 nm and emission wavelength of 535 nm. Experiments were performed in triplicates.

### 3.7 ACKNOWLEDGEMENTS

The work was supported by NSERC-DG (261311-2013), MHRC and CIHR (MOP-119335).

### 3.8 REFERENCES

- (1) Butler, M. S.; Blaskovich, M. A.; Cooper, M. A. Antibiotics in the Clinical Pipeline in 2013. *J. Antibiot. (Tokyo)*. **2013**, *66* (10), 571–591.
- (2) Butler, M. S.; Blaskovich, M. A.; Cooper, M. A. Antibiotics in the Clinical Pipeline at the End of 2015. *J. Antibiot. (Tokyo)*. **2017**, *70* (1), 3–24.
- (3) Breidenstein, E. B. M.; de la Fuente-Nunez, C.; Hancock, R. E. W. Pseudomonas Aeruginosa: All Roads Lead to Resistance. *Trends Microbiol.* **2011**, *19* (8), 419–426.
- (4) Boucher, H. W.; Talbot, G. H.; Bradley, J. S.; Edwards, J. E.; Gilbert, D.; Rice, L. B.; Scheld, M.; Spellberg, B.; Bartlett, J. Bad Bugs, No Drugs: No ESKAPE! An Update from the Infectious Diseases Society of America. *Clin. Infect. Dis.* **2009**, *48* (1), 1–12.
- (5) Nikaido, H. Prevention of Drug Access to Bacterial Targets: Permeability Barriers and Active Efflux. *Science* **1994**, *264* (5157), 382–388.
- (6) Kalan, L.; Wright, G. D. Antibiotic Adjuvants: Multicomponent Anti-Infective Strategies. *Expert Rev. Mol. Med.* **2011**, *13*, e5.
- (7) Brown, D. Antibiotic Resistance Breakers: Can Repurposed Drugs Fill the Antibiotic Discovery Void? *Nat. Rev. Drug Discov.* **2015**, *14* (12), 821–832.
- (8) Gill, E. E.; Franco, O. L.; Hancock, R. E. W. Antibiotic Adjuvants: Diverse Strategies for Controlling Drug-Resistant Pathogens. *Chem. Biol. Drug Des.* **2015**, *85* (1), 56–78.
- (9) Pagès, J. M.; Masi, M.; Barbe, J. Inhibitors of Efflux Pumps in Gram-Negative Bacteria.

- Trends Mol. Med.* **2005**, *11* (8), 382–389.
- (10) Feng, X.; Zhu, W.; Schurig-Briccio, L. A.; Lindert, S.; Shoen, C.; Hitchings, R.; Li, J.; Wang, Y.; Baig, N.; Zhou, T.; Kim, B. K.; Crick, D. C.; Cynamon, M.; McCammon, J. A.; Gennis, R. B.; Oldfield, E. Antiinfectives Targeting Enzymes and the Proton Motive Force. *Proc. Natl. Acad. Sci. U. S. A.* **2015**, *112* (51), E7073-82.
- (11) Van Bambeke, F.; Pages, J.-M.; Lee, V. J. Inhibitors of Bacterial Efflux Pumps as Adjuvants in Antibiotic Treatments and Diagnostic Tools for Detection of Resistance by Efflux. *Recent Pat. Antiinfect. Drug Discov.* **2006**, *1* (2), 157–175.
- (12) Bohnert, J. A.; Kern, W. V. Selected Arylpiperazines Are Capable of Reversing Multidrug Resistance in Escherichia Coli Overexpressing RND Efflux Pumps. *Antimicrob. Agents Chemother.* **2005**, *49* (2), 849–852.
- (13) Kaatz, G. W.; Moudgal, V. V.; Seo, S. M.; Hansen, J. B.; Kristiansen, J. E. Phenylpiperidine Selective Serotonin Reuptake Inhibitors Interfere with Multidrug Efflux Pump Activity in Staphylococcus Aureus. *Int. J. Antimicrob. Agents* **2003**, *22* (3), 254–261.
- (14) Kriengkauykiat, J.; Porter, E.; Lomovskaya, O.; Wong-Beringer, A. Use of an Efflux Pump Inhibitor to Determine the Prevalence of Efflux Pump-Mediated Fluoroquinolone Resistance and Multidrug Resistance in Pseudomonas Aeruginosa. *Antimicrob. Agents Chemother.* **2005**, *49* (2), 565–570.
- (15) Vila, J.; Martinez, J. L. Clinical Impact of the Over-Expression of Efflux Pump in Nonfermentative Gram-Negative Bacilli, Development of Efflux Pump Inhibitors. *Curr. Drug Targets* **2008**, *9* (9), 797–807.
- (16) Adamson, D. H.; Krikstopaityte, V.; Coote, P. J. Enhanced Efficacy of Putative Efflux

- Pump Inhibitor/Antibiotic Combination Treatments versus MDR Strains of *Pseudomonas Aeruginosa* in a *Galleria Mellonella* in Vivo Infection Model. *J. Antimicrob. Chemother.* **2015**, *70* (8), 2271–2278.
- (17) Kern, W. V.; Steinke, P.; Schumacher, A.; Schuster, S.; von Baum, H.; Bohnert, J. A. Effect of 1-(1-Naphthylmethyl)-Piperazine, a Novel Putative Efflux Pump Inhibitor, on Antimicrobial Drug Susceptibility in Clinical Isolates of *Escherichia Coli*. *J. Antimicrob. Chemother.* **2006**, *57* (2), 339–343.
- (18) Pannek, S.; Higgins, P. G.; Steinke, P.; Jonas, D.; Akova, M.; Bohnert, J. A.; Seifert, H.; Kern, W. V. Multidrug Efflux Inhibition in *Acinetobacter Baumannii*: Comparison between 1-(1-Naphthylmethyl)-Piperazine and Phenyl-Arginine-Beta-Naphthylamide. *J. Antimicrob. Chemother.* **2006**, *57* (5), 970–974.
- (19) Schumacher, A.; Steinke, P.; Bohnert, J. A.; Akova, M.; Jonas, D.; Kern, W. V. Effect of 1-(1-Naphthylmethyl)-Piperazine, a Novel Putative Efflux Pump Inhibitor, on Antimicrobial Drug Susceptibility in Clinical Isolates of Enterobacteriaceae Other than *Escherichia Coli*. *J. Antimicrob. Chemother.* **2006**, *57* (2), 344–348.
- (20) Munoz-Bellido, J. L.; Munoz-Criado, S.; Garcia-Rodriguez, J. A. Antimicrobial Activity of Psychotropic Drugs: Selective Serotonin Reuptake Inhibitors. *Int. J. Antimicrob. Agents* **2000**, *14* (3), 177–180.
- (21) Lomovskaya, O.; Warren, M. S.; Lee, A.; Galazzo, J.; Fronko, R.; Lee, M.; Blais, J.; Cho, D.; Chamberland, S.; Renau, T.; Leger, R.; Hecker, S.; Watkins, W.; Hoshino, K.; Ishida, H.; Lee, V. J. Identification and Characterization of Inhibitors of Multidrug Resistance Efflux Pumps in *Pseudomonas Aeruginosa*: Novel Agents for Combination Therapy. *Antimicrob. Agents Chemother.* **2001**, *45* (1), 105–116.

- (22) Li, X.-Z.; Plésiat, P.; Nikaido, H. The Challenge of Efflux-Mediated Antibiotic Resistance in Gram-Negative Bacteria. *Clin. Microbiol. Rev.* **2015**, *28* (2), 337–418.
- (23) Hancock, R. E. W.; Sahl, H.-G. Antimicrobial and Host-Defense Peptides as New Anti-Infective Therapeutic Strategies. *Nat. Biotechnol.* **2006**, *24* (12), 1551–1557.
- (24) Gorityala, B. K.; Guchhait, G.; Fernando, D. M.; Deo, S.; McKenna, S. A.; Zhanel, G. G.; Kumar, A.; Schweizer, F. Adjuvants Based on Hybrid Antibiotics Overcome Resistance in *Pseudomonas Aeruginosa* and Enhance Fluoroquinolone Efficacy. *Angew. Chemie Int. Ed.* **2016**, *55* (2), 555–559.
- (25) Gorityala, B. K.; Guchhait, G.; Goswami, S.; Fernando, D. M.; Kumar, A.; Zhanel, G. G.; Schweizer, F. Hybrid Antibiotic Overcomes Resistance in *P. Aeruginosa* by Enhancing Outer Membrane Penetration and Reducing Efflux. *J. Med. Chem.* **2016**, *59* (18), 8441–8455.
- (26) Guchhait, G.; Altieri, A.; Gorityala, B.; Yang, X.; Findlay, B.; Zhanel, G. G.; Mookherjee, N.; Schweizer, F. Amphiphilic Tobramycins with Immunomodulatory Properties. *Angew. Chem., Int. Ed. Engl.* **2015**, *54* (21), 6278–6282.
- (27) Herzog, I. M.; Green, K. D.; Berkov-Zrihen, Y.; Feldman, M.; Vidavski, R. R.; Eldar-Boock, A.; Satchi-Fainaro, R.; Eldar, A.; Garneau-Tsodikova, S.; Fridman, M. 6''-Thioether Tobramycin Analogues: Towards Selective Targeting of Bacterial Membranes. *Angew. Chem., Int. Ed. Engl.* **2012**, *51* (23), 5652–5656.
- (28) Ouberai, M.; El Garch, F.; Bussiere, A.; Riou, M.; Alsteens, D.; Lins, L.; Baussanne, I.; Dufrene, Y. F.; Brasseur, R.; Decout, J.-L.; Mingeot-Leclercq, M.-P. The *Pseudomonas Aeruginosa* Membranes: A Target for a New Amphiphilic Aminoglycoside Derivative? *Biochim. Biophys. Acta* **2011**, *1808* (6), 1716–1727.

- (29) Lau, C. H.-F.; Hughes, D.; Poole, K. MexY-Promoted Aminoglycoside Resistance in *Pseudomonas Aeruginosa*: Involvement of a Putative Proximal Binding Pocket in Aminoglycoside Recognition. *MBio* **2014**, *5* (2), e01068.
- (30) Pillai, S. K.; Moellering, R. C.; Eliopoulos, G. M. Antimicrobial Combinations. In *Antibiotics in Laboratory Medicine*; Lorian, V., Ed.; Philadelphia, PA : Lippincott Williams & Wilkins, 2005; pp 365–440.
- (31) Odds, F. C. Synergy, Antagonism, and What the Chequerboard Tells between Them. *J. Antimicrob. Chemother.* **2003**, *52* (1), 1.
- (32) Chopra, I.; Hacker, K. Effects of Tetracyclines on the Production of Extracellular Proteins by Members of the Propionibacteriaceae. *FEMS Microbiol. Lett.* **1989**, *60* (1), 21–24.
- (33) Krezdorn, J.; Adams, S.; Coote, P. J. A *Galleria Mellonella* Infection Model Reveals Double and Triple Antibiotic Combination Therapies with Enhanced Efficacy versus a Multidrug-Resistant Strain of *Pseudomonas Aeruginosa*. *J. Med. Microbiol.* **2014**, *63* (Pt 7), 945–955.
- (34) Paul, K.; Erhardt, M.; Hirano, T.; Blair, D. F.; Hughes, K. T. Energy Source of Flagellar Type III Secretion. *Nature* **2008**, *451* (7177), 489–492.
- (35) Kumar, A.; Chua, K.-L.; Schweizer, H. P. Method for Regulated Expression of Single-Copy Efflux Pump Genes in a Surrogate *Pseudomonas Aeruginosa* Strain: Identification of the BpeEF-OprC Chloramphenicol and Trimethoprim Efflux Pump of *Burkholderia Pseudomallei* 1026b. *Antimicrob. Agents Chemother.* **2006**, *50* (10), 3460–3463.
- (36) Ejim, L.; Farha, M. A.; Falconer, S. B.; Wildenhain, J.; Coombes, B. K.; Tyers, M.; Brown, E. D.; Wright, G. D. Combinations of Antibiotics and Nonantibiotic Drugs Enhance Antimicrobial Efficacy. *Nat. Chem. Biol.* **2011**, *7* (6), 348–350.

- (37) Mitchell, P. Chemiosmotic Coupling in Oxidative and Photosynthetic Phosphorylation. *Biochim. Biophys. Acta* **2011**, *1807* (12), 1507–1538.
- (38) Wright, G. D. Antibiotic Adjuvants: Rescuing Antibiotics from Resistance. *Trends Microbiol.* **2016**, *24* (11), 862–871.
- (39) Zabawa, T. P.; Pucci, M. J.; Parr, T. R.; Lister, T. Treatment of Gram-Negative Bacterial Infections by Potentiation of Antibiotics. *Curr. Opin. Microbiol.* **2016**, *33*, 7–12.
- (40) Aron, Z.; Opperman, T. J. Optimization of a Novel Series of Pyranopyridine RND Efflux Pump Inhibitors. *Curr. Opin. Microbiol.* **2016**, *33*, 1–6.
- (41) Vaara, M.; Vaara, T. Sensitization of Gram-Negative Bacteria to Antibiotics and Complement by a Nontoxic Oligopeptide. *Nature* **1983**, *303* (5917), 526–528.
- (42) Li, C.; Peters, A. S.; Meredith, E. L.; Allman, G. W.; Savage, P. B. Design and Synthesis of Potent Sensitizers of Gram-Negative Bacteria Based on a Cholic Acid Scaffolding. *J. Am. Chem. Soc.* **1998**, *120* (12), 2961–2962.
- (43) Radzishewsky, I. S.; Rotem, S.; Bourdetsky, D.; Navon-Venezia, S.; Carmeli, Y.; Mor, A. Improved Antimicrobial Peptides Based on Acyl-Lysine Oligomers. *Nat. Biotechnol.* **2007**, *25* (6), 657–659.
- (44) Yoshida, K.-I.; Nakayama, K.; Ohtsuka, M.; Kuru, N.; Yokomizo, Y.; Sakamoto, A.; Takemura, M.; Hoshino, K.; Kanda, H.; Nitani, H.; Namba, K.; Yoshida, K.; Imamura, Y.; Zhang, J. Z.; Lee, V. J.; Watkins, W. J. MexAB-OprM Specific Efflux Pump Inhibitors in *Pseudomonas Aeruginosa*. Part 7: Highly Soluble and in Vivo Active Quaternary Ammonium Analogue D13-9001, a Potential Preclinical Candidate. *Bioorg. Med. Chem.* **2007**, *15* (22), 7087–7097.
- (45) Opperman, T. J.; Kwasny, S. M.; Kim, H. S.; Nguyen, S. T.; Houseweart, C.; D'Souza, S.;

- Walker, G. C.; Peet, N. P.; Nikaido, H.; Bowlin, T. L. Characterization of a Novel Pyranopyridine Inhibitor of the AcrAB Efflux Pump of Escherichia Coli. *Antimicrob. Agents Chemother.* **2014**, *58* (2), 722–733.
- (46) Sjuts, H.; Vargiu, A. V.; Kwasny, S. M.; Nguyen, S. T.; Kim, H.-S.; Ding, X.; Ornik, A. R.; Ruggerone, P.; Bowlin, T. L.; Nikaido, H.; Pos, K. M.; Opperman, T. J. Molecular Basis for Inhibition of AcrB Multidrug Efflux Pump by Novel and Powerful Pyranopyridine Derivatives. *Proc. Natl. Acad. Sci. U. S. A.* **2016**, *113* (13), 3509–3514.
- (47) Watkins, W. J.; Landaverry, Y.; Leger, R.; Litman, R.; Renau, T. E.; Williams, N.; Yen, R.; Zhang, J. Z.; Chamberland, S.; Madsen, D.; Griffith, D.; Tembe, V.; Huie, K.; Dudley, M. N. The Relationship between Physicochemical Properties, in Vitro Activity and Pharmacokinetic Profiles of Analogues of Diamine-Containing Efflux Pump Inhibitors. *Bioorg. Med. Chem. Lett.* **2003**, *13* (23), 4241–4244.
- (48) Zhanel, G. G.; Lawson, C. D.; Zelenitsky, S.; Findlay, B.; Schweizer, F.; Adam, H.; Walkty, A.; Rubinstein, E.; Gin, A. S.; Hoban, D. J.; Lynch, J. P.; Karlowsky, J. A. Comparison of the Next-Generation Aminoglycoside Plazomicin to Gentamicin, Tobramycin and Amikacin. *Expert Rev. Anti.-Infect. Ther.* **2012**, *10* (4), 459–473.
- (49) Taber, H. W.; Mueller, J. P.; Miller, P. F.; Arrow, A. S. Bacterial Uptake of Aminoglycoside Antibiotics. *Microbiol. Rev.* **1987**, *51* (4), 439–457.
- (50) Kaneti, G.; Meir, O.; Mor, A. Controlling Bacterial Infections by Inhibiting Proton-Dependent Processes. *Biochim. Biophys. Acta* **2016**, *1858* (5), 995–1003.
- (51) Hurdle, J. G.; O'Neill, A. J.; Chopra, I.; Lee, R. E. Targeting Bacterial Membrane Function: An Underexploited Mechanism for Treating Persistent Infections. *Nat. Rev. Microbiol.* **2011**, *9* (1), 62–75.

- (52) Zhanel, G. G.; DeCorby, M.; Laing, N.; Weshnoweski, B.; Vashisht, R.; Taylor, F.; Nichol, K. A.; Wierzbowski, A.; Baudry, P. J.; Karlowsky, J. A.; Lagace-Wiens, P.; Walkty, A.; McCracken, M.; Mulvey, M. R.; Johnson, J.; Hoban, D. J. Antimicrobial-Resistant Pathogens in Intensive Care Units in Canada: Results of the Canadian National Intensive Care Unit (CAN-ICU) Study, 2005-2006. *Antimicrob. Agents Chemother.* **2008**, *52* (4), 1430–1437.
- (53) Zhanel, G. G.; DeCorby, M.; Adam, H.; Mulvey, M. R.; McCracken, M.; Lagace-Wiens, P.; Nichol, K. A.; Wierzbowski, A.; Baudry, P. J.; Taylor, F.; Karlowsky, J. A.; Walkty, A.; Schweizer, F.; Johnson, J.; Hoban, D. J. Prevalence of Antimicrobial-Resistant Pathogens in Canadian Hospitals: Results of the Canadian Ward Surveillance Study (CANWARD 2008). *Antimicrob. Agents Chemother.* **2010**, *54* (11), 4684–4693.
- (54) Zhanel, G. G.; Adam, H. J.; Baxter, M. R.; Fuller, J.; Nichol, K. A.; Denisuk, A. J.; Lagace-Wiens, P. R. S.; Walkty, A.; Karlowsky, J. A.; Schweizer, F.; Hoban, D. J. Antimicrobial Susceptibility of 22746 Pathogens from Canadian Hospitals: Results of the CANWARD 2007-11 Study. *J. Antimicrob. Chemother.* **2013**, *68 Suppl 1*, i7-22.
- (55) Clinical and Laboratory Standards Institute (CLSI). *Performance Standards for Antimicrobial Susceptibility Testing*, 26th ed.; Clinical and Laboratory Standards Institute: Wayne, Pennsylvania, USA, 2016.
- (56) Orhan, G.; Bayram, A.; Zer, Y.; Balci, I. Synergy Tests by E Test and Checkerboard Methods of Antimicrobial Combinations against *Brucella Melitensis*. *J. Clin. Microbiol.* **2005**, *43* (1), 140–143.
- (57) Domalaon, R.; Findlay, B.; Ogunsina, M.; Arthur, G.; Schweizer, F. Ultrashort Cationic Lipopeptides and Lipopeptoids: Evaluation and Mechanistic Insights against Epithelial

- Cancer Cells. *Peptides* **2016**, *84*, 58–67.
- (58) Krezdorn, J.; Adams, S.; Coote, P. J. A *Galleria Mellonella* Infection Model Reveals Double and Triple Antibiotic Combination Therapies with Enhanced Efficacy versus a Multidrug-Resistant Strain of *Pseudomonas Aeruginosa*. *J. Med. Microbiol.* **2014**, *63*, 945–955.
- (59) Wang, B.; Pachaiyappan, B.; Gruber, J. D.; Schmidt, M. G.; Zhang, Y.-M.; Woster, P. M. Antibacterial Diamines Targeting Bacterial Membranes. *J. Med. Chem.* **2016**, *59* (7), 3140–3151.
- (60) Ouberai, M.; El Garch, F.; Bussiere, A.; Riou, M.; Alsteens, D.; Lins, L.; Baussanne, I.; Dufrière, Y. F.; Brasseur, R.; Decout, J. L.; Mingeot-Leclercq, M. P. The *Pseudomonas Aeruginosa* Membranes: A Target for a New Amphiphilic Aminoglycoside Derivative? *Biochim. Biophys. Acta - Biomembr.* **2011**, *1808* (6), 1716–1727.
- (61) Zhang, L.; Dhillon, P.; Yan, H.; Farmer, S.; Hancock, R. E. Interactions of Bacterial Cationic Peptide Antibiotics with Outer and Cytoplasmic Membranes of *Pseudomonas Aeruginosa*. *Antimicrob. Agents Chemother.* **2000**, *44* (12), 3317–3321.
- (62) Ling, L. L.; Schneider, T.; Peoples, A. J.; Spoering, A. L.; Engels, I.; Conlon, B. P.; Mueller, A.; Schaberle, T. F.; Hughes, D. E.; Epstein, S.; Jones, M.; Lazarides, L.; Steadman, V. A.; Cohen, D. R.; Felix, C. R.; Fetterman, K. A.; Millett, W. P.; Nitti, A. G.; Zullo, A. M.; Chen, C.; Lewis, K. A New Antibiotic Kills Pathogens without Detectable Resistance. *Nature* **2015**, *517* (7535), 455–459.
- (63) Berridge, M. V.; Herst, P. M.; Tan, A. S. Tetrazolium dyes as tools in cell biology: new insights into their cellular reduction. *Biotechnol. Annu. Rev.* **2005**, *11*, 127–152.

## **Chapter 4: Tobramycin-Linked Efflux Pump Inhibitor Conjugates Synergize Fluoroquinolones, Rifampicin and Fosfomycin against Multidrug-Resistant *Pseudomonas aeruginosa***

*By Xuan Yang, Ronald Domalaon, Yinfeng Lyu, George G. Zhanel, and Frank Schweizer. First published in Journal of Clinical Medicine, 7 (7), 2018, 158. Reproduced with permission.*

Contributions of Authors: Xuan Yang was responsible for synthesizing the conjugates. Xuan Yang and Yinfeng Lyu performed the biochemical assays under the guidance of Frank Schweizer. Xuan Yang wrote the preliminary draft, annotated by Ronald Domalaon, George G. Zhanel, and Frank Schweizer.

### **4.1 ABSTRACT**

In this study, we examined the *in vitro* effect of tobramycin-efflux pump inhibitor (TOB-EPI) conjugates in combinations with fluoroquinolones, rifampicin and fosfomycin on the growth of multi-drug resistant (MDR) and extremely-drug resistant (XDR) *Pseudomonas aeruginosa*. The TOB-EPI conjugates include tobramycin covalently linked to 1-(1-naphthylmethyl)-piperazine (NMP) (**1**), paroxetine (PAR) (**2**) and a dibasic peptide analogue of MC-04,124 (DBP) (**3**). Potent synergism was found for combinations of TOB-NMP (**1**), TOB-PAR (**2**) or TOB-DBP (**3**) with either fluoroquinolones (moxifloxacin, ciprofloxacin), rifampicin or fosfomycin against a panel of multidrug-resistant/extensively drug-resistant (MDR/XDR) *P. aeruginosa* clinical isolates. In the presence of  $\leq 8 \mu\text{g/mL}$  ( $6.1\text{--}7.2 \mu\text{M}$ ) ( $\leq \frac{1}{4} \times \text{MIC}_{\text{adjuvant}}$ )

concentration of the three conjugates, the MIC<sub>80</sub> of moxifloxacin, ciprofloxacin, rifampicin and fosfomycin were dramatically reduced. Furthermore, the MIC<sub>80</sub> of rifampicin (0.25–0.5 µg/mL) and fosfomycin (8–16 µg/mL) were reduced below their interpretative susceptibility breakpoints. Our data confirm the ability of TOB-NMP (1), TOB-PAR (2) and TOB-DBP (3) conjugates to strongly synergize with moxifloxacin, ciprofloxacin, rifampicin and fosfomycin against MDR/XDR *P. aeruginosa*. These synergistic combinations warrant further studies as there is an urgent need to develop new strategies to treat drug-resistant *P. aeruginosa* infections

## 4.2 INTRODUCTION

The opportunistic *Pseudomonas aeruginosa* is the leading cause of nosocomial and chronic lung infections in immunocompromised (e.g. cystic fibrosis) patients.<sup>1,2</sup> The World Health Organization (WHO) has listed carbapenem-resistant *P. aeruginosa* as one of the most critical (priority 1) pathogen that pose serious threat to human health.<sup>3</sup> Among Gram-negative pathogens, infections caused by *P. aeruginosa* are particularly difficult to treat as the organism is both intrinsically resistant and capable of acquiring resistance (through mobile genetic elements) to most antibiotics.<sup>4</sup> The intrinsic resistance of *P. aeruginosa* is mostly due to its low outer membrane permeability, which is 12-100 times lower than that of *Escherichia coli*, presumably a result of their relatively selective porins.<sup>4</sup> Overexpressed multidrug efflux pumps that limit the intracellular concentration of antibiotics is another key contributor of intrinsic resistance. Several small molecules such as 1-(1-naphthylmethyl)-piperazine (NMP),<sup>5</sup> paroxetine (PAR)<sup>6,7</sup> and DBP,<sup>8</sup> the analogue of dibasic dipeptide D-Ala-D-hPhe-aminoquinoline (MC-04,124) (Figure 4.2.1) have been reported to inhibit efflux pumps in Gram-negative and/or Gram-positive bacteria, thereby restoring activity to legacy antibiotics.

In a previous study, we discovered that linking a tobramycin (TOB) vector to the efflux pump inhibitors (EPIs) NMP, PAR, and DBP generated TOB-EPI conjugates (Figure 4.2.1) capable of sensitizing multidrug-resistant/extensively drug-resistant (MDR/XDR) Gram-negative bacilli, especially *P. aeruginosa*, to tetracycline antibiotics.<sup>9</sup> Mechanistic studies revealed tobramycin with a twelve carbon aliphatic chain (C<sub>12</sub>) to be a core fragment needed for outer membrane perturbation that leads to a ‘self-promoted’ uptake mechanism.<sup>9-11</sup> We also found that TOB-EPI conjugates are able to depolarize the inner membrane of *P. aeruginosa*, disrupting the electrical component ( $\Delta\psi$ ) of bacterial proton motive force (PMF) that results in a compensatory transmembrane chemical component ( $\Delta\text{pH}$ ).<sup>9</sup> An increase in  $\Delta\text{pH}$  would consequently facilitate the increased uptake of tetracyclines as the process of accumulation of tetracyclines is  $\Delta\text{pH}$ -dependent.<sup>12</sup> Moreover, a compromised PMF affects PMF-dependent efflux systems that effectively negates the active efflux of susceptible antibiotics.<sup>9,10</sup> Herein, we describe the synergistic interactions of TOB-NMP (**1**), TOB-PAR (**2**) and TOB-DBP (**3**) with either fluoroquinolones (moxifloxacin and ciprofloxacin), rifampicin or fosfomycin against MDR/XDR *P. aeruginosa* clinical isolates.

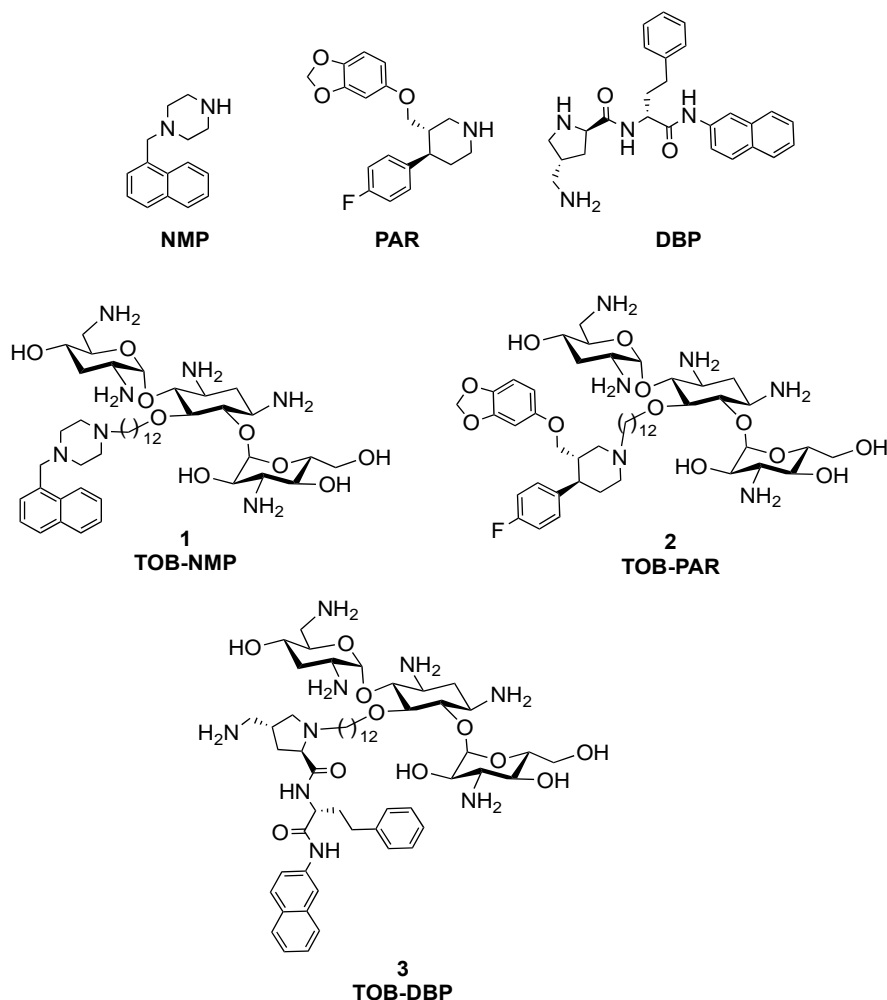


**Figure 4.2.1.** Structures of the efflux pump inhibitors (EPIs) 1-(1-naphthylmethyl)-piperazine (NMP), paroxetine (PAR), and a dibasic peptide analog of MC-04,124 (DBP) along with tobramycin-linked EPI conjugates **1**, **2** and **3**.

### 4.3 RESULTS

We recently reported the preparation and biological evaluation of three TOB-EPI conjugates (Figure 4.2.1), namely TOB-NMP (**1**), TOB-PAR (**2**) and TOB-DBP (**3**).<sup>9</sup> We found that the three conjugates were mostly inactive (MIC = 2–>1024  $\mu\text{g/mL}$ ) alone but significantly potentiated minocycline, in combination, against MDR/XDR *P. aeruginosa* clinical isolates.<sup>9</sup>

Preliminary results indicated that the adjuvant properties of **1-3** against *P. aeruginosa* are not limited to tetracycline antibiotics and can also be extended to other antimicrobial classes.<sup>9</sup> Herein, we further expand our understanding on the adjuvant properties of the three TOB-EPI conjugates to other antibacterial classes including rifampicin, fluoroquinolones (ciprofloxacin and moxifloxacin) and fosfomycin.

Aligned with our previous results with minocycline,<sup>9</sup> the *P. aeruginosa* inactive efflux pump inhibitors NMP and PAR displayed additive interaction (FICI = 0.63, 1.02) with rifampicin (Table 4.3.1). On the other hand, the *P. aeruginosa* active efflux pump inhibitor DBP was synergistic (FICI = 0.09) with rifampicin (Table 4.3.1) against wild-type *P. aeruginosa* PAO1. The absolute MIC of rifampicin (MIC = 32  $\mu\text{g}/\text{mL}$ ) in combination with 8  $\mu\text{g}/\text{mL}$  (6.1–7.2  $\mu\text{M}$ ) of either **1**, **2**, **3** or DBP was found to be  $\leq 0.25$ ,  $\leq 0.25$ ,  $\leq 0.25$  and 4  $\mu\text{g}/\text{mL}$ , respectively. Indeed, a  $\geq 128$ -fold potentiation of rifampicin was observed for the three conjugates relative to a meager 8-fold potentiation induced by DBP. However, we did not observe synergy of rifampicin with tobramycin (FICI = 1.0) in wild-type *P. aeruginosa* PAO1.

**Table 4.3.1** Combination studies of TOB-EPIs (**1**, **2**, or **3**) or EPIs (NMP, PAR or DBP) with moxifloxacin (MOX), rifampicin (RIF) or fosfomycin (FOF) against wild-type *P. aeruginosa* PAO1 strain.

antibiotic	MIC <sub>antibiotic alone</sub> ( $\mu\text{g/mL}$ )	Adjuvant (ADJ)	MIC <sub>ADJ alone</sub> ( $\mu\text{g/mL}$ )	FICI	absolute MIC <sup>a</sup> ( $\mu\text{g/mL}$ )	potentiation (fold) <sup>b</sup>
MOX	1	<b>1</b>	128	0.16	0.125	8
MOX	1	NMP	512	2.00	1	1
MOX	2	<b>2</b>	32	0.19	0.063	32
MOX	1	PAR	256	2.00	1	1
MOX	1	<b>3</b>	32	0.31	0.063	32
MOX	1	DBP	128	0.19	0.25	4
RIF	32	<b>1</b>	128	0.04	$\leq 0.25$	$\geq 128$
RIF	32	NMP	512	1.02	32	1
RIF	32	<b>2</b>	64	0.03	$\leq 0.25$	$\geq 128$
RIF	32	PAR	512	0.63	32	1
RIF	32	<b>3</b>	16	0.08	$\leq 0.25$	$\geq 128$
RIF	32	DBP	256	0.09	4	8
FOF <sup>c</sup>	32	<b>1</b>	64	0.09	1	32
FOF <sup>c</sup>	16	NMP	512	1.00	16	1
FOF <sup>c</sup>	16	<b>2</b>	32	0.25	2	8
FOF <sup>c</sup>	16	PAR	256	0.75	16	1
FOF <sup>c</sup>	32	<b>3</b>	32	0.13	1	32
FOF <sup>c</sup>	16	DBP	128	0.16	1	16

<sup>a</sup>Absolute MIC of antibiotic in the presence of 8  $\mu\text{g/mL}$  (6.1–7.2  $\mu\text{M}$ ) of corresponding potentiator. <sup>b</sup>Antibiotic activity potentiation at 8  $\mu\text{g/mL}$  (6.1–7.2  $\mu\text{M}$ ) of corresponding potentiator. FICI: fractional inhibitory concentration index.

Since fluoroquinolones are good substrates for *P. aeruginosa* RND efflux pumps,<sup>13,14</sup> we expanded our studies to combinations of TOB-EPI conjugates (**1**, **2** or **3**) or efflux pump inhibitors (NMP, PAR or DBP) with the fluoroquinolone antibiotic moxifloxacin against wild-type *P. aeruginosa* PAO1 (Table 4.3.1). Moxifloxacin was strongly potentiated by tobramycin-linked EPI conjugates **1** (FICI = 0.16), **2** (FICI = 0.19) and **3** (FICI = 0.31). However, as a control, the combination study of moxifloxacin with tobramycin against *P. aeruginosa* PAO1 strain was not synergistic (FICI = 1.1). No synergistic effect was observed for NMP (FICI = 2.00) nor PAR (FICI = 2.00), whereas synergy was found for DBP (FICI = 0.19). The absolute MICs of moxifloxacin (MIC = 2 µg/mL) in the presence of 8 µg/mL of conjugates **1**, **2** or **3** was found to be 0.125, 0.063 and 0.063 µg/mL, respectively (Table 4.3.1). Thus 8–16-fold potentiation of moxifloxacin was observed for the three conjugates. All three TOB-EPI conjugates (**1**, **2** or **3**) and DBP also displayed strong synergism with fosfomycin (FIC index of 0.09-0.25) (Table 4.3.1). At 8 µg/mL of TOB-EPI conjugates (**1**, **2** or **3**), the absolute MICs of fosfomycin (MIC = 32 µg/mL) were reduced to 1, 2 and 1 µg/mL, respectively (Table 4.3.1). Thus 8–32-fold potentiation of fosfomycin was observed for the three conjugates. As a control, a combination study of fosfomycin with tobramycin was performed and the result indicated no synergistic effect against wild-type *P. aeruginosa* PAO1 strain (FICI = 1.0).

Prompted by our findings in wild-type *P. aeruginosa* strain, we further assessed the synergism of the three TOB-EPI conjugates **1**, **2** and **3** in combination with either moxifloxacin, ciprofloxacin, rifampicin or fosfomycin against a panel of eight MDR/XDR *P. aeruginosa* clinical isolates. These *P. aeruginosa* isolates are resistant to many antibiotics as shown in chapter 9 Supplementary Table 9.6.4, to which all but one are ciprofloxacin-resistant. All the

three conjugates were found to be synergistic with the four tested antibiotics (Table 4.3.2). Both TOB-NMP (1) and TOB-PAR (2) strongly potentiated moxifloxacin (4-128 fold), ciprofloxacin (4-256 fold), rifampicin (32-128 fold), and fosfomycin (2-64 fold) against all tested MDR/XDR *P. aeruginosa* strains. Similar results were observed for the combinations of TOB-DBP (3) and moxifloxacin. TOB-DBP (3) also potentiated ciprofloxacin, rifampicin and fosfomycin against most of the strains tested. However, TOB-DBP (3) displayed no interactions with ciprofloxacin (FICI = 0.75) and rifampicin (FICI = 0.516) against *P. aeruginosa* PA260-97103 strain. Fosfomycin in combination with TOB-DBP (3) displayed no interaction (FICI = 0.75) against *P. aeruginosa* PA262-101856 strain.

We further assessed the potency of TOB-EPI conjugates as adjuvants by comparing the absolute MICs of the four antibiotics, in the presence of  $\leq 8 \mu\text{g/mL}$  ( $6.1-7.2 \mu\text{M}$ ) ( $\leq \frac{1}{4} \times \text{MIC}_{\text{adjuvant}}$ ) conjugates, to established susceptibility breakpoints (a chosen concentration ( $\mu\text{g/mL}$ ) of an antibiotic which defines whether a species of bacteria is susceptible or resistant to the antibiotic<sup>30</sup>). According to the Clinical and Laboratory Standards Institute (CLSI), the susceptibility breakpoint of ciprofloxacin for *Pseudomonas aeruginosa* is  $\leq 1 \mu\text{g/mL}$ . However, no established susceptibility breakpoint of moxifloxacin, rifampicin and fosfomycin exists for *Pseudomonas* spp., and therefore we used other breakpoints in other organisms for comparison. We interpreted susceptibility to moxifloxacin for *Pseudomonas aeruginosa* to be similar to the established one for ciprofloxacin, as both belong to the fluoroquinolone class of antibiotics. CLSI denotes susceptibility to rifampicin for *Enterococcus* spp. as  $\leq 1 \mu\text{g/mL}$ .<sup>15</sup> Conversely, susceptibility to fosfomycin was described to be  $\leq 64 \mu\text{g/mL}$  for Enterobacteriaceae.<sup>15</sup>

Next, we studied whether the absolute MIC of the four antibiotics in the presence of the three TOB-EPI conjugates at  $\leq 8 \mu\text{g/mL}$  ( $6.1-7.2 \mu\text{M}$ ) ( $\leq \frac{1}{4} \times \text{MIC}_{\text{adjuvant}}$ ) reaches the expected

susceptibility breakpoint of ciprofloxacin and moxifloxacin. Our results (Table 4.3.2) show that in 6/8 cases, the adjuvants cannot reach the expected susceptibility breakpoint of the two fluoroquinolone antibiotics. The two *P. aeruginosa* strains which reach the susceptibility breakpoint (91433 and 101243) do not contain DNA gyrase A mutation, indicating that fluoroquinolone resistance is mostly due to active efflux in these strains.<sup>11</sup> Out of the two fluoroquinolones, moxifloxacin seemed to be strongly potentiated by the conjugates relative to ciprofloxacin (Figure 4.3.1). In contrast, the MIC of rifampicin was reduced below the susceptibility breakpoint in all strains tested by conjugates **1** and **2** (Table 4.3.2). However, conjugate **3** was able to reduce the MIC of rifampicin below the susceptibility breakpoint to all strains except *P. aeruginosa* PA260-97103 (absolute MIC = 16  $\mu\text{g}/\text{mL}$ ). All the three conjugates lowered the absolute MIC of fosfomycin in all strains tested except *P. aeruginosa* 100036.

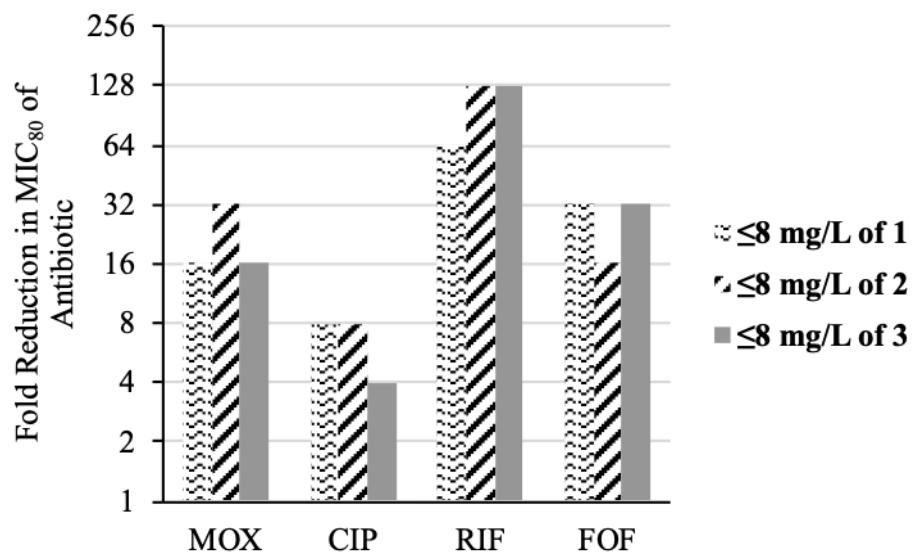


**Figure 4.3.1.** TOB-EPIs (**1**, **2** or **3**) potentiate the activity of moxifloxacin (MOX), ciprofloxacin (CIP), rifampicin (RIF) and fosfomycin (FOF) against a panel of MDR/XDR *P. aeruginosa* clinical isolates ( $n = 8$ ). The MIC<sub>80</sub> of MOX, CIP, RIF and FOF were significantly reduced in the

presence of  $\leq 8 \mu\text{g/mL}$  ( $6.1\text{--}7.2 \mu\text{M}$ ) ( $\leq 1/4 \times \text{MIC}_{\text{adjuvant}}$ ) of the corresponding potentiator (**1**, **2**, or **3**).

**Table 4.3.2** Combination studies of TOB-EPIs (**1**, **2**, or **3**) with moxifloxacin (MOX), ciprofloxacin (CIP), rifampicin (RIF) or fosfomycin (FOF) against MDR/XDR *P. aeruginosa* clinical isolates.

<i>P. aeruginosa</i>	antibiotic	MIC <sub>antibiotic alone</sub> ( $\mu\text{g/mL}$ )	Adjuvant (ADJ)	MIC <sub>ADJ alone</sub> ( $\mu\text{g/mL}$ )	FICI	absolute MIC ( $\mu\text{g/mL}$ )
PA262-101856	MOX	64	<b>1</b>	64	0.188	8 <sup>a</sup>
PA262-101856	MOX	128	<b>2</b>	32	0.125	2 <sup>a</sup>
PA262-101856	MOX	128	<b>3</b>	32	0.188	4 <sup>a</sup>
PA262-101856	CIP	32	<b>1</b>	64	0.188	4 <sup>a</sup>
PA262-101856	CIP	32	<b>2</b>	32	0.250	4 <sup>a</sup>
PA262-101856	CIP	32	<b>3</b>	64	0.250	4 <sup>a</sup>
PA262-101856	RIF	1024	<b>1</b>	128	0.047	4 <sup>a</sup>
PA262-101856	RIF	1024	<b>2</b>	32	0.070	$\leq 2^a$
PA262-101856	RIF	1024	<b>3</b>	64	0.078	$\leq 2^a$
PA262-101856	FOF	8	<b>1</b>	128	0.141	1 <sup>a</sup>
PA262-101856	FOF	8	<b>2</b>	32	0.375	2 <sup>a</sup>
PA262-101856	FOF	8	<b>3</b>	64	0.750	8 <sup>a</sup>
PA260-97103	MOX	64	<b>1</b>	2	0.250	2 <sup>b</sup>
PA260-97103	MOX	128	<b>2</b>	8	0.188	2 <sup>b</sup>
PA260-97103	MOX	64	<b>3</b>	4	0.500	16 <sup>b</sup>
PA260-97103	CIP	32	<b>1</b>	2	0.500	8 <sup>b</sup>

**Table 4.3.2 Cont.**

<i>P. aeruginosa</i>	antibiotic	MIC <sub>antibiotic alone</sub> ( $\mu\text{g/mL}$ )	Adjuvant (ADJ)	MIC <sub>ADJ alone</sub> ( $\mu\text{g/mL}$ )	FICI	absolute MIC ( $\mu\text{g/mL}$ )
PA260-97103	CIP	16	<b>2</b>	16	0.250	$\leq 0.125^a$
PA260-97103	CIP	32	<b>3</b>	4	0.750	$16^b$
PA260-97103	RIF	16	<b>1</b>	2	0.375	$0.5^a$
PA260-97103	RIF	16	<b>2</b>	16	0.070	$\leq 0.125^a$
PA260-97103	RIF	16	<b>3</b>	4	0.516	$16^b$
PA260-97103	FOF	8	<b>1</b>	4	0.188	$\leq 0.031^b$
PA260-97103	FOF	8	<b>2</b>	16	0.125	$\leq 0.031^a$
PA260-97103	FOF	4	<b>3</b>	4	0.375	$0.5^b$
100036	MOX	128	<b>1</b>	256	0.078	$8^a$
100036	MOX	128	<b>2</b>	64	0.094	$4^a$
100036	MOX	128	<b>3</b>	32	0.188	$2^a$
100036	CIP	64	<b>1</b>	256	0.156	$8^a$
100036	CIP	64	<b>2</b>	64	0.250	$8^a$
100036	CIP	64	<b>3</b>	32	0.313	$8^a$
100036	RIF	16	<b>1</b>	256	0.023	$\leq 0.125^a$
100036	RIF	16	<b>2</b>	128	0.047	$\leq 0.125^a$
100036	RIF	16	<b>3</b>	32	0.070	$\leq 0.125^a$
100036	FOF	>1024	<b>1</b>	256	$0.063 < x < 0.313$	$512^a$
100036	FOF	>1024	<b>2</b>	128	$0.125 < x < 0.625$	$> 512^a$
100036	FOF	>1024	<b>3</b>	32	$0.250 < x < 0.375$	$128^a$
101885	MOX	64	<b>1</b>	256	0.141	$8^a$

**Table 4.3.2 Cont.**

<i>P. aeruginosa</i>	antibiotic	MIC <sub>antibiotic alone</sub> ( $\mu\text{g/mL}$ )	Adjuvant (ADJ)	MIC <sub>ADJ alone</sub> ( $\mu\text{g/mL}$ )	FICI	absolute MIC ( $\mu\text{g/mL}$ )
101885	MOX	64	<b>2</b>	64	0.188	4 <sup>a</sup>
101885	MOX	64	<b>3</b>	8	0.375	8 <sup>b</sup>
101885	CIP	32	<b>1</b>	256	0.258	8 <sup>a</sup>
101885	CIP	32	<b>2</b>	32	0.375	4 <sup>a</sup>
101885	CIP	32	<b>3</b>	8	0.500	8 <sup>b</sup>
101885	RIF	16	<b>1</b>	256	0.031	$\leq 0.125^a$
101885	RIF	16	<b>2</b>	32	0.125	$\leq 0.125^a$
101885	RIF	16	<b>3</b>	16	0.094	$\leq 0.125^a$
101885	FOF	32	<b>1</b>	256	0.125	4 <sup>a</sup>
101885	FOF	32	<b>2</b>	32	0.188	4 <sup>a</sup>
101885	FOF	32	<b>3</b>	32	0.125	2 <sup>a</sup>
PA259-96918	MOX	512	<b>1</b>	>1024	0.031<x<0.033	16 <sup>a</sup>
PA259-96918	MOX	1024	<b>2</b>	>512	0.008<x<0.031	16 <sup>a</sup>
PA259-96918	MOX	512	<b>3</b>	64	0.047	4 <sup>a</sup>
PA259-96918	CIP	256	<b>1</b>	>1024	0.063<x<0.066	16 <sup>a</sup>
PA259-96918	CIP	512	<b>2</b>	>512	0.063<x<0.039	32 <sup>a</sup>
PA259-96918	CIP	256	<b>3</b>	64	0.125	16 <sup>a</sup>
PA259-96918	RIF	16	<b>1</b>	>1024	0.008<x<0.009	$\leq 0.125^a$
PA259-96918	RIF	16	<b>2</b>	>512	0.008<x<0.012	$\leq 0.125^a$
PA259-96918	RIF	16	<b>3</b>	32	0.039	$\leq 0.125^a$
PA259-96918	FOF	8	<b>1</b>	>1024	0.063	0.5 <sup>a</sup>

**Table 4.3.2 Cont.**

<i>P. aeruginosa</i>	antibiotic	MIC <sub>antibiotic alone</sub> ( $\mu\text{g/mL}$ )	Adjuvant (ADJ)	MIC <sub>ADJ alone</sub> ( $\mu\text{g/mL}$ )	FICI	absolute MIC ( $\mu\text{g/mL}$ )
PA259-96918	FOF	8	<b>2</b>	>512	0.063<x<0.094	1 <sup>a</sup>
PA259-96918	FOF	16	<b>3</b>	64	0.094	0.5 <sup>a</sup>
PA264-104354	MOX	128	<b>1</b>	128	0.078	8 <sup>a</sup>
PA264-104354	MOX	128	<b>2</b>	64	0.156	2 <sup>a</sup>
PA264-104354	MOX	128	<b>3</b>	16	0.125	1 <sup>a</sup>
PA264-104354	CIP	32	<b>1</b>	128	0.250	8 <sup>a</sup>
PA264-104354	CIP	32	<b>2</b>	64	0.313	8 <sup>a</sup>
PA264-104354	CIP	32	<b>3</b>	16	0.250	2 <sup>a</sup>
PA264-104354	RIF	32	<b>1</b>	128	0.020	$\leq 0.125^a$
PA264-104354	RIF	32	<b>2</b>	64	0.063	$\leq 0.125^a$
PA264-104354	RIF	32	<b>3</b>	8	0.129	$\leq 0.125^a$
PA264-104354	FOF	8	<b>1</b>	128	0.125	0.5 <sup>a</sup>
PA264-104354	FOF	16	<b>2</b>	64	0.125	0.5 <sup>a</sup>
PA264-104354	FOF	16	<b>3</b>	32	0.094	0.5 <sup>a</sup>
91433	MOX	8	<b>1</b>	32	0.156	0.25 <sup>a</sup>
91433	MOX	8	<b>2</b>	16	0.500	0.5 <sup>a</sup>
91433	MOX	8	<b>3</b>	8	0.281	0.25 <sup>b</sup>
91433	CIP	2	<b>1</b>	32	0.250	0.125 <sup>a</sup>
91433	CIP	2	<b>2</b>	16	0.500	0.125 <sup>a</sup>
91433	CIP	2	<b>3</b>	8	0.266	0.031 <sup>b</sup>
91433	RIF	16	<b>1</b>	16	0.375	0.25 <sup>a</sup>

**Table 4.3.2 Cont.**

<i>P. aeruginosa</i>	antibiotic	MIC <sub>antibiotic alone</sub> ( $\mu\text{g/mL}$ )	Adjuvant (ADJ)	MIC <sub>ADJ alone</sub> ( $\mu\text{g/mL}$ )	FICI	absolute MIC ( $\mu\text{g/mL}$ )
91433	RIF	16	<b>2</b>	32	0.188	0.25 <sup>a</sup>
91433	RIF	16	<b>3</b>	8	0.250	$\leq 0.125^b$
91433	FOF	4	<b>1</b>	16	0.188	0.25 <sup>a</sup>
91433	FOF	2	<b>2</b>	32	0.375	$\leq 0.25^a$
91433	FOF	2	<b>3</b>	8	0.375	0.25 <sup>b</sup>
101243	MOX	4	<b>1</b>	64	0.125	0.25 <sup>a</sup>
101243	MOX	4	<b>2</b>	32	0.250	0.125 <sup>a</sup>
101243	MOX	4	<b>3</b>	16	0.156	$\leq 0.0625^a$
101243	CIP	2	<b>1</b>	64	0.281	0.5 <sup>a</sup>
101243	CIP	2	<b>2</b>	32	0.375	0.5 <sup>a</sup>
101243	CIP	2	<b>3</b>	16	0.188	0.125 <sup>a</sup>
101243	RIF	8	<b>1</b>	64	0.063	$\leq 0.0625^a$
101243	RIF	8	<b>2</b>	32	0.125	$\leq 0.0625^a$
101243	RIF	16	<b>3</b>	16	0.094	$\leq 0.031^a$
101243	FOF	256	<b>1</b>	64	0.125	8 <sup>a</sup>
101243	FOF	256	<b>2</b>	32	0.188	16 <sup>a</sup>
101243	FOF	256	<b>3</b>	32	0.047	4 <sup>a</sup>

<sup>a</sup>Absolute MIC of antibiotic in the presence of 8  $\mu\text{g/mL}$  (6.1–7.2  $\mu\text{M}$ ) of corresponding adjuvant. <sup>b</sup>Absolute MIC of antibiotic in the presence of  $\frac{1}{4} \times \text{MIC}$  of corresponding adjuvant.

The MIC<sub>80</sub> of moxifloxacin, ciprofloxacin, rifampicin and fosfomycin in combination with  $\leq 8 \mu\text{g/mL}$  (6.1–7.2  $\mu\text{M}$ ) ( $\leq \frac{1}{4} \times \text{MIC}_{\text{adjuvant}}$ ) TOB-EPIs conjugates (**1**, **2**, or **3**) against the

tested *P. aeruginosa* panel were significantly lower than the MIC<sub>80</sub> of the antibiotic alone (Table 4.3.3 and Figure 4.3.1). More importantly, the absolute MIC<sub>80</sub> of rifampicin and fosfomycin were below their respective susceptibility breakpoints. In the presence of  $\leq 8 \mu\text{g/mL}$  ( $7.2 \mu\text{M}$ ) ( $\leq 1/4 \times \text{MIC}_{\text{adjutant}}$ ) TOB-NMP (**1**), the absolute MIC<sub>80</sub> of rifampicin was  $0.5 \mu\text{g/mL}$  while that of fosfomycin was  $8 \mu\text{g/mL}$ . The absolute MIC<sub>80</sub> of rifampicin and fosfomycin in the presence of  $\leq 8 \mu\text{g/mL}$  ( $6.9 \mu\text{M}$ ) ( $\leq 1/4 \times \text{MIC}_{\text{adjutant}}$ ) TOB-PAR (**2**) was found to be  $0.25 \mu\text{g/mL}$  and  $16 \mu\text{g/mL}$ . Similarly, the absolute MIC<sub>80</sub> of rifampicin and fosfomycin in the presence of  $\leq 8 \mu\text{g/mL}$  ( $6.1 \mu\text{M}$ ) ( $\leq 1/4 \times \text{MIC}_{\text{adjutant}}$ ) TOB-DBP (**3**) was  $0.25 \mu\text{g/mL}$  and  $8 \mu\text{g/mL}$ .

**Table 4.3.3** *In vitro* activity of moxifloxacin (MOX), ciprofloxacin (CIP), rifampicin (RIF) and fosfomycin (FOF) alone or in combination with fixed concentration ( $\leq 8 \mu\text{g/mL}$  ( $6.1\text{--}7.2 \mu\text{M}$ )) of TOB-EPIs (**1**, **2**, or **3**) against MDR/XDR *P. aeruginosa* clinical isolates ( $n = 8$ ).

antimicrobial	MIC <sub>50</sub> ( $\mu\text{g/mL}$ )	MIC <sub>80</sub> ( $\mu\text{g/mL}$ )	MIC Range ( $\mu\text{g/mL}$ )
MOX	64	128	4–512
CIP	32	64	2–512
RIF	16	32	8–1024
FOF	16	256	2–>256
<b>1</b>	64	256	2–>1024
<b>2</b>	32	128	8–>512
<b>3</b>	16	32	4–64
MOX + <b>1</b>	8	8	0.25–16
MOX + <b>2</b>	2	4	0.125–16
MOX + <b>3</b>	2	8	0.06–16

**Table 4.3.3** *Cont.*

antimicrobial	MIC <sub>50</sub> ( $\mu\text{g/mL}$ )	MIC <sub>80</sub> ( $\mu\text{g/mL}$ )	MIC Range ( $\mu\text{g/mL}$ )
CIP + <b>1</b>	8	8	0.125–8
CIP + <b>2</b>	4	8	0.125–32
CIP + <b>3</b>	4	16	0.03–16
RIF + <b>1</b>	0.125	0.5	0.06–4
RIF + <b>2</b>	0.125	0.25	0.06–2
RIF + <b>3</b>	0.125	0.25	0.03–2
FOF + <b>1</b>	0.5	8	0.03–512
FOF + <b>2</b>	1	16	0.03–>512
FOF + <b>3</b>	0.5	8	0.25–128

Considering the possible effect of tobramycin-efflux pump inhibitor conjugates to the active efflux of fluoroquinolones, we assessed the synergy of moxifloxacin and the three conjugates in efflux-deficient *P. aeruginosa* strains (Table 4.3.4). PAO200 is a MexAB–OprM deletion strain while PAO750 is an efflux-sensitive strain that lacks five different clinically relevant RND pumps (MexAB–OprM, MexCD–OprJ, MexEF–OprN, MexJK, and MexXY) and the OM protein OpmH.<sup>16</sup> These efflux pumps confer resistance on *P. aeruginosa* by expelling a wide variety of antibiotic substrates including quinolones, tetracyclines and others. As expected, a significant reduction in MIC of moxifloxacin was observed for PAO200 (MIC = 0.125  $\mu\text{g/mL}$ ) and PAO750 (MIC = 0.008  $\mu\text{g/mL}$ ) as active efflux contributes greatly to fluoroquinolone resistance. Interestingly, a 16-fold MIC reduction was observed for TOB-NMP (**1**) from wild-type *P. aeruginosa* PAO1 (MIC = 128  $\mu\text{g/mL}$ ) to PAO750 (MIC = 8  $\mu\text{g/mL}$ ) while only 2- to 4-fold difference was observed for the MIC of TOB-PAR (**2**) and TOB-DBP (**3**) against PAO1,

PAO200 and PAO750. The combination of conjugate **1** and moxifloxacin remained synergistic across the efflux-deficient strains, albeit weakly synergistic (FICI = 0.31) against *P. aeruginosa* PAO750. Both conjugates **2** (FICI = 0.19) and **3** (FICI = 0.25) were found to be synergistic with moxifloxacin against the MexAB-OprM-deficient PAO200 strain. However, no interaction was found between moxifloxacin and conjugates **2** (FICI = 0.63) or **3** (FICI = 0.63) against PAO750.

**Table 4.3.4** *In vitro* activity of moxifloxacin (MOX), TOB-EPIs (**1**, **2** and **3**) and combinations of thereof against wild-type *P. aeruginosa* PAO1 and efflux pump deficient PAO200 and PAO750 strains.

strain	MIC ( $\mu\text{g/mL}$ )				FICI		
	MOX	<b>1</b>	<b>2</b>	<b>3</b>	MOX + <b>1</b>	MOX + <b>2</b>	MOX + <b>3</b>
PAO1	1	128	32	32	0.16	0.19	0.31
PAO200	0.125	128	32	16	0.08	0.19	0.25
PAO750	0.008	8	8	8	0.31	0.63	0.63

PAO200 strain: PAO1,  $\Delta\text{mexAB-oprM}$ ; PAO750 strain: PAO1,  $\Delta\text{mexAB-oprM}$ ,  $\Delta\text{mexCD-oprJ}$ ,  $\Delta\text{mexEF-oprN}$ ,  $\Delta\text{mexXY}$ ,  $\Delta\text{mexJK}$ ,  $\Delta\text{oprM}$ .

#### 4.4 DISCUSSION

The low permeability of the outer membrane and overexpressed multidrug efflux pumps in Gram-negative bacteria, especially in *P. aeruginosa*, limits effective antibiotics for treatment.<sup>17</sup> The compounding effect of the restrictive lipid bilayer and active efflux prevents the intracellular accumulation of antibiotics to concentrations needed to achieve biological effect.

The problem is further exacerbated in drug-resistant organisms as they express genetically encoded resistance mechanism that may actively incapacitate antibiotics. Unfortunately, no new antibiotics with a novel mode of action for Gram-negative bacteria have been introduced in the clinic for more than five decades. There is a definite need to develop new strategies which are able to overcome resistance in Gram-negative pathogens, for which combination therapy of existing antibiotics with adjuvants is a promising option.<sup>18</sup>

We recently described the preparation of TOB-EPI conjugates (**1**, **2** or **3**) that synergize tetracycline antibiotics.<sup>9</sup> Moreover, we also demonstrated their ability to permeabilize the outer membrane of *P. aeruginosa* in a dose-dependent manner.<sup>9</sup> Herein, TOB-EPI conjugates (**1**, **2** or **3**) were found to significantly potentiate the outer membrane impermeable rifampicin (32–128 fold) against a panel of MDR/XDR *P. aeruginosa* clinical isolates. At  $\leq 8 \mu\text{g/mL}$  ( $6.1\text{--}7.2 \mu\text{M}$ ) ( $\leq \frac{1}{4} \times \text{MIC}_{\text{adjuvant}}$ ) concentration of either of the three conjugates, the absolute  $\text{MIC}_{80}$  of rifampicin was significantly reduced below susceptibility breakpoint. This suggests that conjugates **1**, **2** and **3** are good candidates for future adjuvant therapy development in combination with rifampicin. As rifampicin is a poor substrate for *P. aeruginosa* RND efflux pumps,<sup>9,10</sup> membrane permeabilization may be responsible for the observed synergism with TOB-EPI conjugates. The *P. aeruginosa* inactive efflux pump inhibitors NMP and PAR were found to exhibit additive interactions with rifampicin. In contrast, the *P. aeruginosa* active DBP was found to be synergistic with rifampicin against wild-type *P. aeruginosa* PAO1. A previous report of DBP analog PA $\beta$ N revealed its ability to permeabilize bacterial membranes in a concentration-dependent manner,<sup>19</sup> therefore this may have contributed to the observed rifampicin potentiation.

All three TOB-EPI conjugates strongly potentiated (fluoroquinolones (moxifloxacin 4–128 fold or ciprofloxacin 4–256 fold) against wild-type, fluoroquinolone-resistant and

MDR/XDR *P. aeruginosa*. Out of the two fluoroquinolones tested, combinations of the three TOB-EPI conjugates with moxifloxacin yielded stronger potentiation relative to ciprofloxacin (Figure 4.3.1). However, the conjugates were not able to bring down the absolute MIC<sub>80</sub> of both fluoroquinolones below their susceptibility breakpoints. It should be noted that the MIC of both fluoroquinolones were reduced below the susceptibility breakpoint in only two isolates (91433 and 101243 isolates which lack T<sup>83</sup> to I<sup>83</sup> mutation). This suggests that the conjugates enhance the intracellular concentration of fluoroquinolones. However, this effect cannot compensate acquired resistance caused by genetic mutations of the target enzyme.

Synergy of the conjugates with fluoroquinolones may not only be attributed to adjuvant-induced enhanced membrane permeability but may also be due to a compromised activity of PMF-dependent efflux pumps. We recently demonstrated that the TOB-EPI conjugates strongly reduce motility at sub-MIC concentration and disrupt the electrical component ( $\Delta\psi$ ) of the PMF.<sup>9</sup> This action in turn may affect efflux systems that are dependent on PMF, leading to reduced efflux of fluoroquinolones. Our data revealed that the three conjugates were poor substrates of the MexAB-OprM RND efflux pump (Table 4.3.4). However, TOB-NMP (**1**) may be a substrate of other efflux systems in *P. aeruginosa* since a 16-fold MIC reduction was observed from wild-type PAO1 to the multiple efflux pump-deficient PAO750. We found that the synergism between moxifloxacin and TOB-EPI conjugates was independent of the MexAB-OprM RND efflux pump. Yet, there was a clear effect on the tested combinations of moxifloxacin and TOB-EPI conjugates against PAO750. The potent synergistic interaction with moxifloxacin found against wild-type PAO1 were drastically reduced to either weakly synergistic (for conjugate **1**) or no interaction (for conjugates **2** and **3**) against PAO750. Therefore, we assume that either MexCD-OprJ, MexEF-OprN, MexXY, or MexJK efflux pumps

is affected by the TOB-EPI conjugates action on PMF. Certainly, moxifloxacin is a good substrate of many efflux pumps in *P. aeruginosa*.

Fosfomycin is a bactericidal antibiotic that inhibits cell wall biosynthesis.<sup>20</sup> Specifically, fosfomycin inactivates the enzyme UDP-*N*-acetylglucosamine enolpyruvyl transferase (MurA) that catalyzes the formation of peptidoglycan precursor UDP *N*-acetylmuramic acid (UDP-MurNAc).<sup>20,21</sup> The three TOB-EPI conjugates strongly potentiated the activity of fosfomycin (2–64 fold) against wild-type and MDR/XDR *P. aeruginosa* clinical isolates susceptible or resistant to fosfomycin. In the presence of  $\leq 8 \mu\text{g/mL}$  ( $6.1\text{--}7.2 \mu\text{M}$ ) ( $\leq 1/4 \times \text{MIC}_{\text{adjuvant}}$ ) concentration of the conjugates, the absolute MIC for 7/8 isolates was  $\leq 16 \mu\text{g/mL}$ , which is 4-fold lower than the expected susceptibility breakpoint of fosfomycin ( $\leq 64 \mu\text{g/mL}$ ). Fosfomycin is known to be a poor substrate of multidrug efflux system in *P. aeruginosa*<sup>22</sup> and it is understood that its cellular entry occurs through porins.<sup>23</sup> We hypothesize that the observed synergy of fosfomycin with TOB-EPI adjuvants reflects enhanced cellular permeation of fosfomycin via the self-promoted uptake of TOB-EPI adjuvants.

#### 4.5 CONCLUSIONS

In conclusion, we demonstrate promising synergistic combinations of TOB-EPI conjugates with either fluoroquinolones, rifampicin or fosfomycin against MDR/XDR *P. aeruginosa*. More importantly, the conjugates TOB-NMP (1), TOB-PAR (2) and TOB-DBP (3) significantly reduced the MIC<sub>80</sub> of rifampicin and fosfomycin below their respective susceptibility breakpoints. These findings show that the adjuvant potency of TOB-EPI conjugates is not limited to tetracyclines<sup>9</sup> but can be expanded to other legacy antibiotics.

## 4.6 EXPERIMENTAL SECTION

### 4.6.1 Bacterial strains

Clinically-relevant bacterial strains were collected from the Canadian National Intensive Care Unit (CAN-ICU) study<sup>24</sup> and Canadian Ward Surveillance (CANWARD) studies.<sup>25,26</sup> All isolates were transported to the reference laboratory (Health Sciences Centre, Winnipeg, Canada) on Amies charcoal swabs, subcultured onto an appropriate media, and stocked in skim milk with 10 % glycerol at -80°C until antimicrobial susceptibility testing was carried out. The efflux pump deficient strains, *P. aeruginosa* PAO200 and *P. aeruginosa* PAO750, were provided by Dr. Ayush Kumar from University of Manitoba, Canada. All pathogens obtained from CAN-ICU and CANWARD studies have received ethics approval from the University of Manitoba Ethics Committee. In addition, participating Canadian health centers have obtained appropriate ethics approval to submit clinical specimens.

### 4.6.2 Antimicrobial agents

Tobramycin sulfate, moxifloxacin hydrochloride, rifampicin, and ciprofloxacin hydrochloride were obtained from AK Scientific, Inc. (Union City, CA, USA). Fosfomycin sodium was obtained from Sigma-Aldrich (St. Louis, MO, USA). Glucose-6-phosphate (Sigma-Aldrich) was added to the medium at a final concentration of 25 µg/mL for all evaluations of fosfomycin.

### 4.6.3 Antimicrobial susceptibility testing

The antimicrobial activity of the compounds against a panel of bacteria was evaluated by broth microdilution assay in accordance with the Clinical and Laboratory Standards Institute (CLSI) guidelines.<sup>27</sup> The overnight bacterial culture was diluted in saline to 0.5 McFarland turbidity, and then 1:50 diluted in Mueller–Hinton broth (MHB) for inoculation. The minimum inhibitory concentrations (MICs) of the antimicrobial agents were determined using 96-well plates containing doubling antimicrobial dilutions with MHB and incubated with equal volumes of inoculum for 18 h at 37 °C. The lowest concentration that inhibited visible bacterial growth was taken as the MIC for each antimicrobial agent which was also confirmed using EMax Plus microplate reader (Molecular Devices, USA) at a wavelength of 590 nm. We used stock concentration of 10.24  $\mu\text{g/mL}$  in deionized water or DMSO depending on the solubility of the compounds.

### 4.6.4 Antimicrobial combination screening

Checkerboard method<sup>28</sup> was used to assess synergism in all tested combinations. The fractional inhibitory concentration index (FICI) of each combination was calculated as follows: FICI is the sum of fractional inhibitory concentration of antibiotic ( $\text{FIC}_{\text{antibiotic}}$ ) and fractional inhibitory concentration of adjuvant ( $\text{FIC}_{\text{ADJ}}$ );  $\text{FIC}_{\text{antibiotic}} = \text{MIC}_{\text{combo}} / \text{MIC}_{\text{antibiotic alone}}$ ;  $\text{FIC}_{\text{adjuvant}} = \text{MIC}_{\text{combo}} / \text{MIC}_{\text{adjuvant alone}}$ , where  $\text{MIC}_{\text{combo}}$  is the lowest inhibitory concentration of drug in the presence of the adjuvant; The combination is considered synergistic when the FICI is  $\leq 0.5$ , no interaction when the FICI is  $0.5 < \text{FICI} \leq 4.0$ , and antagonistic when the FICI is  $> 4.0$ .<sup>29</sup>

#### 4.7 ACKNOWLEDGEMENTS

This research was funded by a Discovery grant by the Natural Sciences and Engineering Research Council (NSERC) (DG-261311-2013) and Research Manitoba.

The authors thank Dr. Ayush Kumar for providing efflux pump deficient *P. aeruginosa* strains (PAO200 and PAO750).

#### 4.8 REFERENCES

- (1) Wisplinghoff, H.; Bischoff, T.; Tallent, S. M.; Seifert, H.; Wenzel, R. P.; Edmond, M. B. Nosocomial Bloodstream Infections in US Hospitals: Analysis of 24,179 Cases from a Prospective Nationwide Surveillance Study. *Clin. Infect. Dis.* **2004**, *39* (3), 309–317.
- (2) Sousa, A. M.; Pereira, M. O. Pseudomonas Aeruginosa Diversification during Infection Development in Cystic Fibrosis Lungs-a Review. *Pathog. (Basel, Switzerland)* **2014**, *3* (3), 680–703.
- (3) <http://www.who.int/mediacentre/news/releases/2017/bacteria-antibiotics-needed/en/> (accessed on Oct. 12, 2018).
- (4) Breidenstein, E. B. M.; de la Fuente-Nunez, C.; Hancock, R. E. W. Pseudomonas Aeruginosa: All Roads Lead to Resistance. *Trends Microbiol.* **2011**, *19* (8), 419–426.
- (5) Bohnert, J. A.; Kern, W. V. Selected Arylpiperazines Are Capable of Reversing Multidrug Resistance in Escherichia Coli Overexpressing RND Efflux Pumps. *Antimicrob. Agents Chemother.* **2005**, *49* (2), 849–852.
- (6) Van Bambeke, F.; Pages, J.-M.; Lee, V. J. Inhibitors of Bacterial Efflux Pumps as Adjuvants in Antibiotic Treatments and Diagnostic Tools for Detection of Resistance by Efflux. *Recent Pat. Anti-Infect. Drug Discov.* **2006**, *1* (2), 157–175.

- (7) Kaatz, G. W.; Moudgal, V. V.; Seo, S. M.; Hansen, J. B.; Kristiansen, J. E. Phenylpiperidine Selective Serotonin Reuptake Inhibitors Interfere with Multidrug Efflux Pump Activity in *Staphylococcus Aureus*. *Int. J. Antimicrob. Agents* **2003**, *22* (3), 254–261.
- (8) Kriengkauykiat, J.; Porter, E.; Lomovskaya, O.; Wong-Beringer, A. Use of an Efflux Pump Inhibitor to Determine the Prevalence of Efflux Pump-Mediated Fluoroquinolone Resistance and Multidrug Resistance in *Pseudomonas Aeruginosa*. *Antimicrob. Agents Chemother.* **2005**, *49* (2), 565–570.
- (9) Yang, X.; Goswami, S.; Gorityala, B. K.; Domalaon, R.; Lyu, Y.; Kumar, A.; Zhanel, G. G.; Schweizer, F. A Tobramycin Vector Enhances Synergy and Efficacy of Efflux Pump Inhibitors against Multidrug-Resistant Gram-Negative Bacteria. *J. Med. Chem.* **2017**, *60* (9), 3913–3932.
- (10) Lyu, Y.; Yang, X.; Goswami, S.; Gorityala, B. K.; Idowu, T.; Domalaon, R.; Zhanel, G. G.; Shan, A.; Schweizer, F. Amphiphilic Tobramycin–Lysine Conjugates Sensitize Multidrug Resistant Gram-Negative Bacteria to Rifampicin and Minocycline. *J. Med. Chem.* **2017**, *60* (9), 3684–3702.
- (11) Gorityala, B. K.; Guchhait, G.; Fernando, D. M.; Deo, S.; McKenna, S. A.; Zhanel, G. G.; Kumar, A.; Schweizer, F. Adjuvants Based on Hybrid Antibiotics Overcome Resistance in *Pseudomonas Aeruginosa* and Enhance Fluoroquinolone Efficacy. *Angew. Chemie Int. Ed.* **2016**, *55* (2), 555–559.
- (12) Yamaguchi, A.; Ohmori, H.; Kaneko-Ohdera, M.; Nomura, T.; Sawai, T. Delta PH-Dependent Accumulation of Tetracycline in *Escherichia Coli*. *Antimicrob. Agents Chemother.* **1991**, *35* (1), 53–56.

- (13) Li, X. Z.; Livermore, D. M.; Nikaido, H. Role of Efflux Pump(s) in Intrinsic Resistance of *Pseudomonas Aeruginosa*: Resistance to Tetracycline, Chloramphenicol, and Norfloxacin. *Antimicrob. Agents Chemother.* **1994**, *38* (8), 1732–1741.
- (14) Piddock, L. J. V. Clinically Relevant Chromosomally Encoded Multidrug Resistance Efflux Pumps in Bacteria. *Clin. Microbiol. Rev.* **2006**, *19* (2), 382–402.
- (15) Clinical and Laboratory Standards Institute (CLSI). *Performance Standards for Antimicrobial Susceptibility Testing*, 26th ed.; Clinical and Laboratory Standards Institute: Wayne, Pennsylvania, USA, 2016.
- (16) Kumar, A.; Chua, K.-L.; Schweizer, H. P. Method for Regulated Expression of Single-Copy Efflux Pump Genes in a Surrogate *Pseudomonas Aeruginosa* Strain: Identification of the BpeEF-OprC Chloramphenicol and Trimethoprim Efflux Pump of *Burkholderia Pseudomallei* 1026b. *Antimicrob. Agents Chemother.* **2006**, *50* (10), 3460–3463.
- (17) Tommasi, R.; Brown, D. G.; Walkup, G. K.; Manchester, J. I.; Miller, A. A. ESKAPEing the Labyrinth of Antibacterial Discovery. *Nat. Rev. Drug Discov.* **2015**, *14* (8), 529–542.
- (18) Wright, G. D. Antibiotic Adjuvants: Rescuing Antibiotics from Resistance. *Trends Microbiol.* **2016**, *24* (11), 862–871.
- (19) Lamers, R. P.; Cavallari, J. F.; Burrows, L. L. The Efflux Inhibitor Phenylalanine-Arginine Beta-Naphthylamide (PAβN) Permeabilizes the Outer Membrane of Gram-Negative Bacteria. *PLoS One* **2013**, *8* (3), e60666.
- (20) Kahan, F. M.; Kahan, J. S.; Cassidy, P. J.; Kropp, H. The Mechanism of Action of Fosfomycin (Phosphonomycin). *Ann. N. Y. Acad. Sci.* **1974**, *235* (1 Mode of Actio), 364–386.
- (21) Skarzynski, T.; Mistry, A.; Wonacott, A.; Hutchinson, S. E.; Kelly, V. A.; Duncan, K.

- Structure of UDP-N-Acetylglucosamine Enolpyruvyl Transferase, an Enzyme Essential for the Synthesis of Bacterial Peptidoglycan, Complexed with Substrate UDP-N-Acetylglucosamine and the Drug Fosfomycin. *Structure* **1996**, *4* (12), 1465–1474.
- (22) Mikuniya, T.; Hiraishi, T.; Maebashi, K.; Ida, T.; Takata, T.; Hikida, M.; Yamada, S.; Gotoh, N.; Nishino, T. Antimicrobial Activity of Fosfomycin under Various Conditions against Standard Strains, Beta-Lactam Resistant Strains, and Multidrug Efflux System Mutants. *Jpn. J. Antibiot.* **2005**, *58* (2), 105–122.
- (23) Borisova, M.; Gisin, J.; Mayer, C. Blocking Peptidoglycan Recycling in *Pseudomonas Aeruginosa* Attenuates Intrinsic Resistance to Fosfomycin. *Microb. Drug Resist.* **2014**, *20* (3), 231–237.
- (24) Zhanel, G. G.; DeCorby, M.; Laing, N.; Weshnoweski, B.; Vashisht, R.; Tailor, F.; Nichol, K. A.; Wierzbowski, A.; Baudry, P. J.; Karlowsky, J. A.; Lagace-Wiens, P.; Walkty, A.; McCracken, M.; Mulvey, M. R.; Johnson, J.; Hoban, D. J. Antimicrobial-Resistant Pathogens in Intensive Care Units in Canada: Results of the Canadian National Intensive Care Unit (CAN-ICU) Study, 2005-2006. *Antimicrob. Agents Chemother.* **2008**, *52* (4), 1430–1437.
- (25) Zhanel, G. G.; DeCorby, M.; Adam, H.; Mulvey, M. R.; McCracken, M.; Lagace-Wiens, P.; Nichol, K. A.; Wierzbowski, A.; Baudry, P. J.; Tailor, F.; Karlowsky, J. A.; Walkty, A.; Schweizer, F.; Johnson, J.; Hoban, D. J. Prevalence of Antimicrobial-Resistant Pathogens in Canadian Hospitals: Results of the Canadian Ward Surveillance Study (CANWARD 2008). *Antimicrob. Agents Chemother.* **2010**, *54* (11), 4684–4693.
- (26) Zhanel, G. G.; Adam, H. J.; Baxter, M. R.; Fuller, J.; Nichol, K. A.; Denisuk, A. J.; Lagace-Wiens, P. R. S.; Walkty, A.; Karlowsky, J. A.; Schweizer, F.; Hoban, D. J.

- Antimicrobial Susceptibility of 22746 Pathogens from Canadian Hospitals: Results of the CANWARD 2007-11 Study. *J. Antimicrob. Chemother.* **2013**, 68 Suppl 1, i7-22.
- (27) *Methods for Dilution Antimicrobial Susceptibility Tests for Bacteria That Grow Aerobically ; Approved Standard — Ninth Edition*; 2012; Vol. 32.
- (28) Orhan, G.; Bayram, A.; Zer, Y.; Balci, I. Synergy Tests by E Test and Checkerboard Methods of Antimicrobial Combinations against *Brucella Melitensis*. *J. Clin. Microbiol.* **2005**, 43 (1), 140–143.
- (29) Odds, F. C. Synergy, Antagonism, and What the Chequerboard Puts between Them. *J. Antimicrob. Chemother.* **2003**, 52 (1), 1.
- (30) <http://www.bsacsurv.org/science/mics/> (accessed on May. 18, 2019).

## **Chapter 5: Amphiphilic tobramycin-lysine conjugates sensitize multidrug resistant Gram-negative bacteria to rifampicin and minocycline**

*By Yinfeng Lyu, Xuan Yang, Sudeep Goswami, Bala Kishan Gorityala, Temilolu Idowu, Ronald Domalaon, George G. Zhanel, and Frank Schweizer. First published in Journal of Medicinal Chemistry, 60 (9), 2017, 3684-3702. Reproduced with permission.*

*Contributions of Authors: Yinfeng Lyu and Xuan Yang were responsible for designing, synthesizing and characterizing the conjugates on the advice of Frank Schweizer. Yinfeng Lyu and Sudeep Goswami performed the biochemical assays under the guidance of Frank Schweizer, Ayush Kumar, and George G. Zhanel. Yinfeng Lyu and Bala Kishan Gorityala performed the in vivo studies.*

### **5.1 ABSTRACT**

Chromosomally encoded low membrane permeability and highly efficient efflux systems are major mechanisms by which *Pseudomonas aeruginosa* evades antibiotic actions. Our previous reports have shown that amphiphilic tobramycin-fluoroquinolone hybrids can enhance efficacy of fluoroquinolone antibiotics against multidrug-resistant (MDR) *P. aeruginosa* isolates. Herein, we report on a novel class of tobramycin-lysine conjugates containing an optimized amphiphilic tobramycin-C12 tether that sensitize Gram-negative bacteria to legacy antibiotics. Combination studies indicate the ability of these conjugates to synergize rifampicin and

minocycline against MDR and extensively drug resistant (XDR) *P. aeruginosa* isolates and enhance efficacy of both antibiotics in the *Galleria mellonella* larvae *in vivo* infection model. Mode of action studies indicate that the amphiphilic tobramycin-lysine adjuvants enhance outer membrane cell penetration and affect the proton motive force, which energizes efflux pumps. Overall, this study provides a strategy for generating effective antibiotic adjuvants that overcome resistance of rifampicin and minocycline in MDR and XDR Gram-negative bacteria including *P. aeruginosa*.

## 5.2 INTRODUCTION

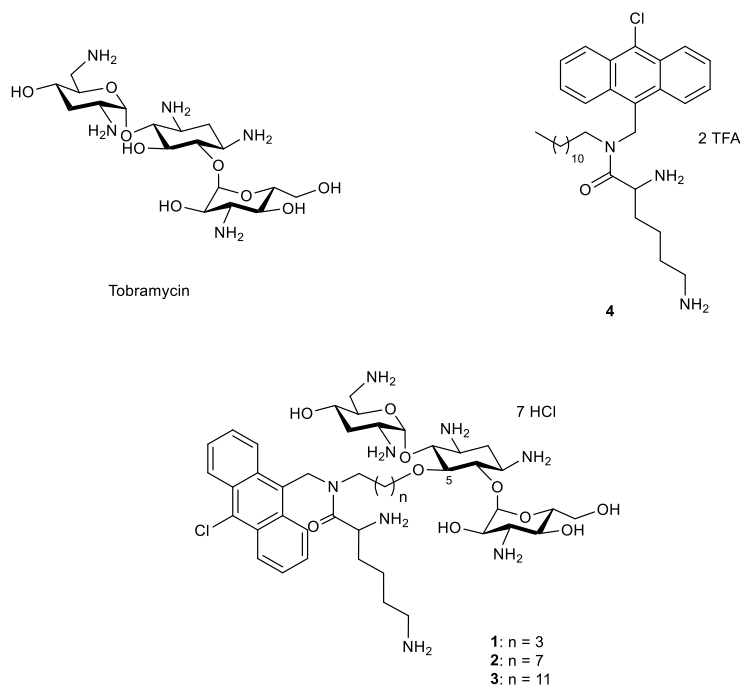
The global health crisis caused by the resurgence of multidrug resistant bacteria strains, once believed to have been defeated, has called for an urgent need to rethink the principle of antibacterial drug discovery and the judicious deployment of our current arsenal.<sup>1</sup> An FDA incentive of accelerated development and review process for breakthrough therapies<sup>2</sup> encourages the need to find alternative or better use of currently approved drugs instead of developing entirely new scaffolds. The Generating Antibiotics Incentives Now (GAIN) Acts of 2012 that seek to extend the exclusivity of new antibiotics<sup>3</sup> further stimulates the need to consolidate the valuable knowledge of existing antibacterial scaffolds as a way out of the current attrition of drug candidates. Among the most recalcitrant bacteria, typified by the ESKAPE pathogens,<sup>4</sup> *Pseudomonas aeruginosa*, an opportunistic pathogen that commonly affects immunocompromised patients, is particularly infamous for its highly sophisticated intrinsic and acquired resistance machineries.<sup>5,6</sup> Compared to other bacteria, *P. aeruginosa* displays low membrane permeability, which limits the penetration of most antibiotics into the cell, and a highly efficient membrane-associated efflux system of broad substrate specificity that

significantly reduces bioaccumulation of drugs within its cytosol.<sup>7, 8</sup> The reduced intracellular concentration further promotes the activation of secondary adaptive resistance mechanisms (such as overexpression of efflux pump proteins and a variety of sensor kinases) that renders it completely refractory to treatment.<sup>9</sup> In addition, resistance often emerges when antibiotics are administered as monotherapy;<sup>10,11</sup> thus combination therapy is the preferred choice in the treatment of complicated infections.<sup>12,13</sup> Although debatable, the argument for combination drug treatment is premised on the large-scale genetic interaction networks between targets.<sup>14</sup> The use of two or more antibiotics that impact multiple targets simultaneously or adjuvants that aid the action of legacy antibiotics can indeed extend the antimicrobial space as well as mitigate the development of antibiotic resistance.<sup>11</sup> Unfortunately, rational combination regimens and correlative synergistic mechanisms have remained largely unexplored, and clinical benefits are yet to be demonstrated. Since the outer membrane of *P. aeruginosa* remains a major impediment to the influx of antibiotics, we and others have been investigating the effects of adjuvants that perturb this “impermeable” layer and consequently synergize the activities of other antibiotics. For instance, Evotec AG and Spero Therapeutics are currently developing a polymyxin-based antimicrobial peptide, SPR-741, as a potentiator to overcome outer membrane impermeability of legacy antibiotics against Gram-negative pathogens in clinical trials.<sup>15</sup> Our group has recently shown that tobramycin-fluoroquinolone hybrids interact with both the outer- and inner-membranes of *P. aeruginosa* resulting in enhanced cell penetration and reduced efflux by dissipating the proton motive force (PMF) that drives efflux pumps in *P. aeruginosa*.<sup>16, 17</sup> Mode of action studies indicate that the function of the tobramycin moiety in these hybrids is limited to a membrane-destabilizing effect of the outer membrane that results in self-promoted uptake of the hybrid or the antibiotic. In contrast, the function of the fluoroquinolone moiety in the hybrid

is less clear, but the adjuvant and antibacterial properties appear to be correlated to the hydrophobic nature and membrane destabilizing effect of the fluoroquinolone group.<sup>16,17</sup> Amphiphilic aminoglycosides (AAGs) that combine aminoglycosides such as tobramycin with alkyl or other hydrophobic groups have also been previously reported to show improved activity and different modes of action in killing pathogens, compared to their constituent parent antibiotics.<sup>18</sup> For example, some amphiphilic tobramycin derivatives were demonstrated to primarily target the bacterial membrane,<sup>19-21</sup> as well as possess immunomodulatory properties that closely resemble that of the natural host defense peptides.<sup>22</sup> To put all these findings into context, we hypothesized that appending a lipophilic membrane-active component to a tobramycin vector will confer an adjuvant-like property that can revive the efficacies of clinical antibiotics against resistant pathogens in a similar fashion as previously reported for tobramycin-fluoroquinolone hybrid antibiotics.

To preserve the amphiphilic nature of the membrane-active tobramycin derivatives, it is imperative to carefully evaluate the hydrophobic nature of the moiety to be attached. Recently, Haldar and co-workers described a series of ultrashort antibacterial lysine-based peptoid mimics that contain facial segregation of positively charged L-lysine, hydrophobic aromatic core, and alkyl chain.<sup>23</sup> These molecules were reported to facilitate the attraction of compounds to bacterial surfaces and permeate cell membrane and displayed some promising antimicrobial properties.<sup>23</sup> We reasoned that the inherent amphipathic nature of these peptoids, combined with their antibacterial properties, could be amplified by linking to a tobramycin-based vector as previously reported for tobramycin-fluoroquinolone hybrid antibiotics.<sup>16,17</sup> In the current study, we designed a series of tobramycin analogs **1–3** by conjoining an amphiphilic peptoid mimic **4** to the C-5 position of tobramycin, with varied alkyl tether, to investigate the adjuvant property of the

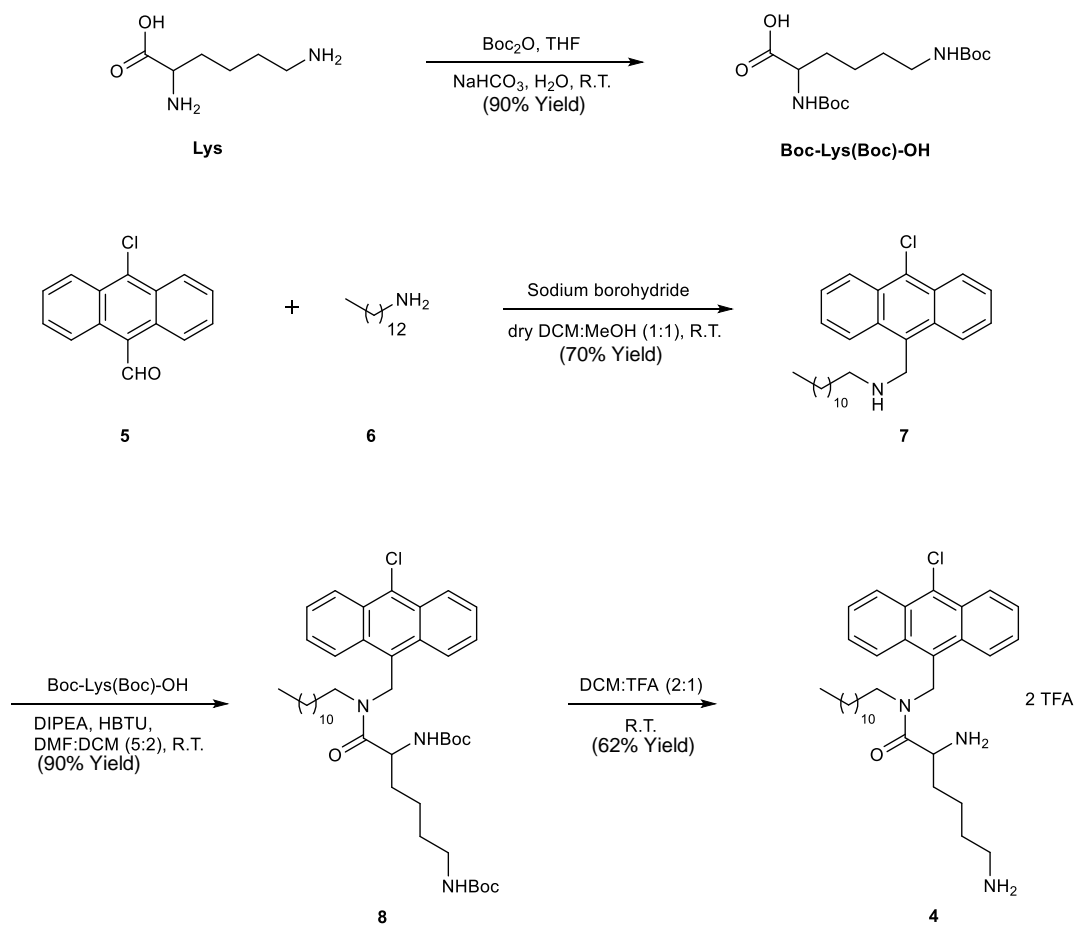
resultant conjugates in combination with commonly used antibiotics (Figure 5.2.1). The synergistic effects of the tobramycin-lysine conjugates in combination with various classes of antibiotics against *P. aeruginosa* (wild-type and clinical isolates) were determined using checkerboard study. The emergence of bacterial resistance was compared between single agent and combination therapy for 25 bacterial passages, and *Galleria mellonella* infection worm model was further used to assess *in vivo* synergistic benefits of the optimal drug combination that protects *P. aeruginosa*-challenged larvae. Hemolysis and cytotoxicity assays were carried out to ascertain toxicity against mammalian cells, and prokaryotic membrane-compound interactions were studied to gain mechanistic insights on possible modes of action.

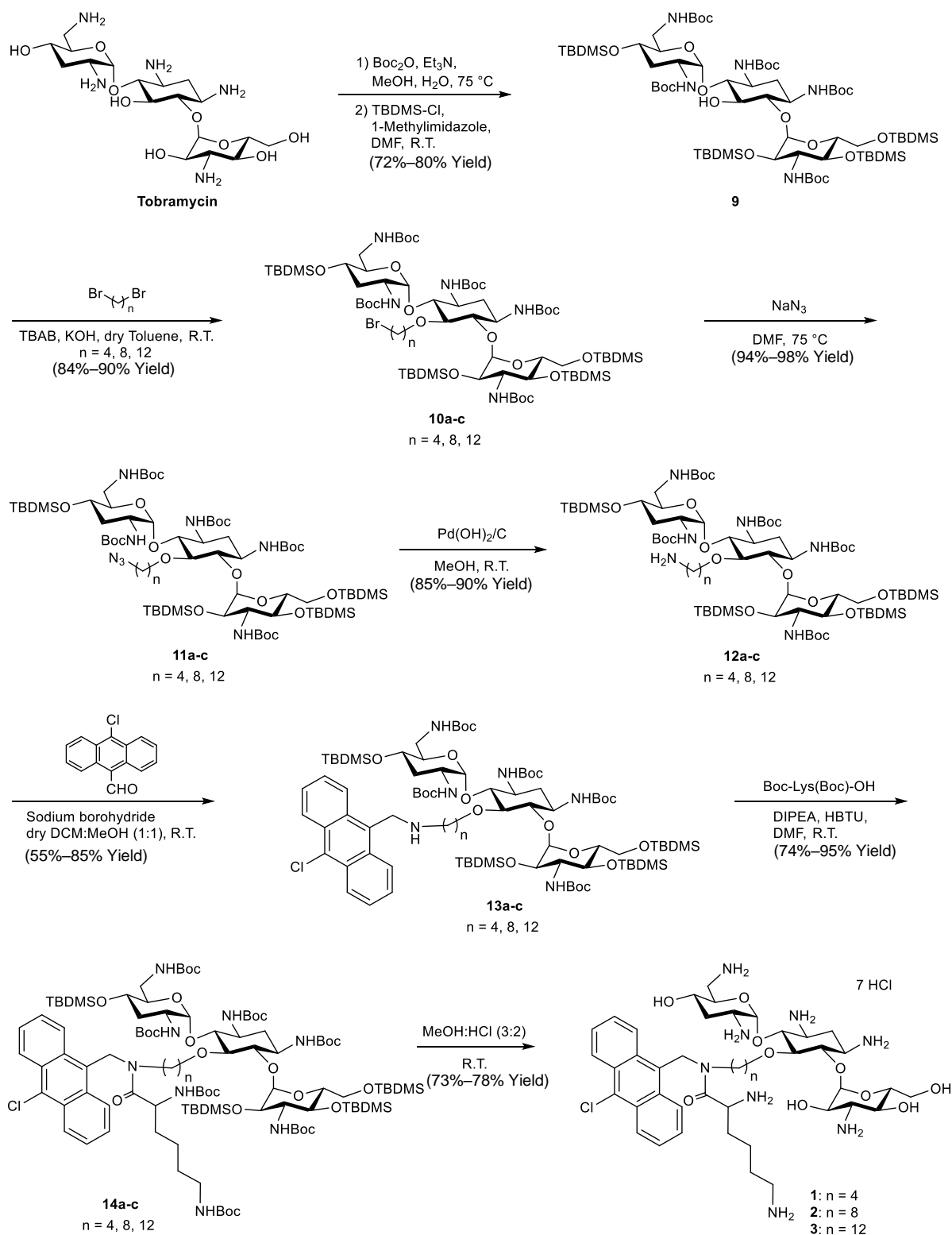


**Figure 5.2.1.** Structures of tobramycin, reference peptoid (4), and amphiphilic tobramycin-lysine conjugates with varied alkyl tether (1–3).

## 5.3 RESULTS

## 5.3.1 Chemical Synthesis

Scheme 5.3.1.1. Preparation of amphiphilic peptoid **4**.



**Scheme 5.3.1.2.** Preparation of amphiphilic tobramycin-lysine conjugates **1–3**.

The reference compound ultrashort peptoid mimic **4** was synthesized by reductive amination of aromatic aldehyde **5** with dodecylamine **6** generating secondary amine **7**, which after coupling to di-Boc-protected lysine produced protected lysine-based peptoid **8**. Deprotection of the Boc-protecting groups with TFA afforded ultrashort lysine peptoid **4** as previously described (Scheme 5.3.1.1).<sup>23</sup> The synthesis of tobramycin-lysine conjugates **1–3** was achieved by preparing amphiphilic tobramycin derivatives (5 steps), followed by a single-step reductive amination conjugating and a final deprotection (Scheme 5.3.1.2). Preparation of the tobramycin derivatives commenced by protecting the amines on commercially available tobramycin with (Boc)<sub>2</sub>O, followed by silylation of the hydroxyl groups with a bulky protecting group such as TBDMSCl to give **9**. This is to ensure the more hindered C-5 position of the Boc- and TBDMS-protected tobramycin intermediate, the desired point of alkylation, is unprotected. This is the preferred position because C-5-modified tobramycin derivatives retained antibacterial activity<sup>24</sup> and superior adjuvant properties against Gram-negative bacteria like *P. aeruginosa*.<sup>16</sup>

<sup>17</sup> The C-5 hydroxyl group of **9** was subsequently alkylated with 1,*n*-dibromoalkane (*n* = 4, 8, 12), under phase-transfer catalytic conditions, to afford alkylated tobramycin analogs **10a–c**. The terminal bromo-group of intermediate **10a–c** was then displaced by an azido nucleophile under anhydrous conditions to give **11a–c**, followed by reduction to free amine **12a–c** via catalytic hydrogenation. This free amine was successively reacted with commercially-available 10-chloro-9-anthracenaldehyde via reductive amination, to afford intermediate **13a–c** with secondary amine, which was then coupled to di-Boc-protected Lys to produce protected amphiphilic tobramycin amides **14a–c**. The final deprotection step involved the removal of Boc and TBDMS protecting groups using MeOH:HCl (3:2, v/v) to afford the desired target compounds **1–3**. The final

compounds were characterized by NMR, mass spectrometry, and reverse-phase HPLC, with >95% purity (Chapter 10).

### 5.3.2 Antimicrobial Activity

The antimicrobial activities of reference peptoid mimic (compound **4**) and tobramycin hybrids **1–3** against a panel of Gram-negative and Gram-positive bacteria are presented as the minimum inhibitory concentration (MIC) in Table 5.3.2.1. Reference peptoid mimic **4** with a C12 hydrophobe displayed weaker antimicrobial activity compared to the reported C10 peptoid,<sup>23</sup> with MIC  $\geq 8$   $\mu\text{g/mL}$  against all the strains tested in this study. For tobramycin-lysine conjugates, there was a positive correlation between antimicrobial activity and the length of the carbon chain tether. Compound **3** with C12 tether was the most potent analog of all the hybrids and displays moderate activity against Gram-positive bacteria (MIC of 2–32  $\mu\text{g/mL}$ ) but a relatively weak activity against Gram-negative bacteria (MIC  $\geq 16$   $\mu\text{g/mL}$ ). Further, the antipseudomonal activities of all compounds were evaluated against wild-type and seven clinical isolates of *P. aeruginosa*, including MDR, XDR, and colistin-resistant strains (Table 5.3.2.2). A similar trend of longer carbon chain displaying better activity was observed for drug-resistant *P. aeruginosa* as well, suggesting C12 as the optimal tether length of all analogues tested. In addition, we observed comparable activity of **3** against wild-type and drug-resistant strains (MIC ranging from 8 to 64  $\mu\text{g/mL}$ ) indicating that compound **3** is not greatly affected by resistance. Again, compound **4** did not show potent activity against any of the clinical isolates tested, with MIC  $\geq 64$   $\mu\text{g/mL}$ . The MIC of tobramycin increased from 0.25  $\mu\text{g/mL}$  in wild-type *P. aeruginosa* to  $>8$   $\mu\text{g/mL}$  in drug-resistant strains, particularly in P262 (MIC = 512  $\mu\text{g/mL}$ ). Similar results were also observed for other tested antibiotics, with the exception of colistin. It is however

interesting to note that compound **3** displayed better activity against P262 (MIC = 32  $\mu\text{g}/\text{mL}$ ) than tobramycin, moxifloxacin, minocycline, rifampicin, chloramphenicol, erythromycin, and trimethoprim (Table 5.3.2.2).

**Table 5.3.2.1.** MIC<sup>a</sup> of compounds against a panel of Gram-positive and Gram-negative bacteria

Organisms <sup>b</sup>	Tobramycin <sup>c</sup>	4	Tobramycin-lysine conjugates		
			1	2	3
Gram-positive bacteria					
<i>S. aureus</i> ATCC 29213	≤0.25	32	64	16	8
MRSA ATCC 33592	≤0.25	64	64	16	8
MSSE CANWARD-2008 81388	≤0.25	8	16	8	2
MRSE CAN-ICU 61589 (CAZ >32)	1	8	32	8	4
<i>E. faecalis</i> ATCC 29212	8	32	>128	64	16
<i>E. faecium</i> ATCC 27270	8	8	>128	16	8
<i>S. pneumoniae</i> ATCC 49619	2	32	>128	128	32
Gram-negative bacteria					
<i>E. coli</i> ATCC 25922	0.5	64	32	16	32
<i>E. coli</i> CAN-ICU 61714 (GEN-R)	8	128	64	32	32
<i>E. coli</i> CAN-ICU 63074 (AMK 32)	8	64	64	128	16
<i>E. coli</i> CANWARD-2011 97615 (GEN-R, TOB-R, CIP-R) aac(3) <sup>iiia</sup>	128	64	64	32	32
<i>P. aeruginosa</i> ATCC 27853	0.5	>128	>128	>128	32
<i>P. aeruginosa</i> CAN-ICU 62308 (GEN-R)	16	128	64	16	16
<i>P. aeruginosa</i> CANWARD-2011 96846 (GEN-R, TOB-R)	256	>128	>128	64	32
<i>S. maltophilia</i> CAN-ICU 62584	>512	>128	>128	>128	>128
<i>A. baumannii</i> CAN-ICU 63169	32	128	>128	>128	128
<i>K. pneumoniae</i> ATCC 13883	≤0.25	>128	128	>128	128

<sup>a</sup> Minimum inhibitory concentration (MIC) was determined as the lowest concentration of compound that inhibited bacteria growth. <sup>b</sup> MRSA: Methicillin-resistant *S. aureus*; MSSE: Methicillin-susceptible *S. epidermidis*; MRSE: Methicillin-resistant *S. epidermidis*; CANWARD: Canadian Ward surveillance; CAN-ICU: Canadian National Intensive Care Unit surveillance; CAZ: Ceftazidime; GEN-R: Gentamicin-resistant; AMK: Amikacin; TOB-R: Tobramycin-resistant; CIP-R: Ciprofloxacin-resistant. <sup>c</sup> MIC data of tobramycin as previously reported.<sup>16</sup>

**Table 5.3.2.2.** MIC ( $\mu\text{g/mL}$ ) of compounds **1–4** and antibiotics against wild-type and clinical isolate *P. aeruginosa*.

<i>P. aeruginosa</i> strains	TOB	<b>4</b>	Tobramycin-lysine conjugates				Antibiotics								
			<b>1</b>	<b>2</b>	<b>3</b>	MOX	CIP	MIN	RIF	CAZ	CAM	ERY	TMP	CST	
PAO1	0.25	256	>512	128	32	1	ND	8	16	2	64	256	256	1	
100036	64	256	>512	512	32	128	64	32	16	8	>512	256	256	2	
101885	0.25	128	256	64	16	64	32	32	16	8	512	256	>512	0.5	
P259-96918	128	64	>512	512	64	512	128	32	16	512	512	256	512	0.5	
P262-101856	512	128	>512	128	32	128	32	256	1024	16	1024	1024	>1024	2	
P264-104354	128	128	>512	256	32	128	32	64	16	64	1024	256	256	4	
91433	8	256	32	8	8	8	2	64	16	256	16	512	512	4	
101243	256	64	256	32	16	4	2	4	8	64	4	1024	1024	>1024	

TOB = Tobramycin; MOX = Moxifloxacin; CIP = Ciprofloxacin; MIN = Minocycline; RIF = Rifampicin; CAZ = Ceftazidime; CAM = Chloramphenicol; ERY = Erythromycin; TMP = Trimethoprim; CST = Colistin. ND = Not determined.

### 5.3.3 Combination Study of Hybrids with Antibiotics

To assess the adjuvant properties of the hybrids, checkerboard studies were performed to determine the synergistic effects of hybrids **1–3** with 14 different antibiotics (cutting across all classes) against wild type *P. aeruginosa* PAO1. The fractional inhibitory concentration (FIC) index, a numerical quantification of the interactions between antibiotics, was calculated as previously described.<sup>16</sup> FIC indices of  $\leq 0.5$ ,  $0.5–4$ , and  $\geq 4$  indicate synergy, no interaction, and antagonism respectively.<sup>25</sup> Compound **3** showed strong synergy with most antibiotics tested against PAO1 except ceftazidime, colistin, meropenem, and the aminoglycosides gentamicin, kanamycin A, and amikacin. The strongest potentiation was seen with novobiocin (FIC index = 0.071), minocycline, and rifampicin (FIC index = 0.094 for both) as shown in Table 5.3.3.1. Synergism with minocycline and rifampicin was also observed with **2**, but not with **1**, **4**, and tobramycin (Chapter 10, Table 10.3.1). As shown in Figure 5.3.3.1, the absolute MICs (the MIC of antibiotics in the presence of adjuvants at 4  $\mu\text{g}/\text{mL}$ ) of minocycline or rifampicin in combination therapy with hybrids was dramatically lower than monotherapy, in particular with compound **3** where MICs of minocycline and rifampicin were reduced from 8 and 16  $\mu\text{g}/\text{mL}$  in monotherapy to 0.25  $\mu\text{g}/\text{mL}$  (32-fold potentiation) and 0.0625  $\mu\text{g}/\text{mL}$  (256-fold potentiation), respectively. Thus, combinations of **3** with minocycline and rifampicin were selected for further synergy studies against a panel of *P. aeruginosa* clinical isolates (Table 5.3.3.2). Compound **3** demonstrated strong synergy with minocycline and rifampicin across the clinical isolates panel (FIC indices of 0.039 to 0.281), with the exception of rifampicin against *P. aeruginosa* 91433 (FIC index = 0.5). Since the breakpoints for minocycline and rifampicin against *P. aeruginosa* are not available (as they are not conventional drugs for treating *P. aeruginosa* infections), the susceptible or intermediate resistant breakpoints of minocycline against *Acinetobacter* spp. and

that of rifampicin against *Enterococcus* spp. reported by CLSI<sup>26</sup> were considered as interpretive MIC standards for this study. The susceptible breakpoints of minocycline (MIC  $\leq 4$   $\mu\text{g/mL}$ ) against *Acinetobacter* spp. were reached for all minocycline-resistant, MDR, or XDR *P. aeruginosa* isolates at 4  $\mu\text{g/mL}$  of 3. For rifampicin, susceptible (MIC  $\leq 1$   $\mu\text{g/mL}$ ) or intermediate resistant (MIC = 2  $\mu\text{g/mL}$ ) breakpoints against *Enterococcus* spp. were reached in 6/7 rifampicin-resistant, MDR, or XDR *P. aeruginosa* isolates, with the exception of strain P262.

**Table 5.3.3.1.** Combination study of compounds **1–3** with antibiotics against wild-type *P. aeruginosa* PAO1.

Antibiotics	MIC <sub>antibiotic alone</sub> <sup>a</sup>	Synergistic MIC <sup>a</sup>	FIC <sub>antibiotic</sub>	Hybrid	MIC <sub>hybrid alone</sub> <sup>a</sup>	Synergistic MIC <sup>a</sup>	FIC <sub>hybrid</sub>	FIC index
Moxifloxacin	1	0.25	0.25	<b>1</b>	>256	32	<0.125	<0.375
Moxifloxacin	1	0.125	0.125	<b>2</b>	128	8	0.063	0.188
Moxifloxacin	1	0.25	0.25	<b>3</b>	32	2	0.063	0.313
Novobiocin	1024	32	0.031	<b>1</b>	>256	16	<0.063	0.031<x<0.094
Novobiocin	1024	8	0.008	<b>2</b>	128	4	0.03125	0.039
Novobiocin	1024	8	0.008	<b>3</b>	32	2	0.063	0.071
Minocycline	8	4	0.5	<b>1</b>	>256	1	<0.004	0.5<x<0.504
Minocycline	8	0.5	0.063	<b>2</b>	128	1	0.008	0.071
Minocycline	8	0.5	0.063	<b>3</b>	32	1	0.031	0.094
Rifampicin	16	8	0.5	<b>1</b>	>256	1	<0.004	0.5<x<0.504
Rifampicin	16	1	0.063	<b>2</b>	128	1	0.008	0.071
Rifampicin	16	1	0.063	<b>3</b>	32	1	0.031	0.094
Ceftazidime	2	1	0.5	<b>1</b>	>256	2	<0.008	0.5<x<0.508
Ceftazidime	2	1	0.5	<b>2</b>	128	1	0.008	0.508
Ceftazidime	2	1	0.5	<b>3</b>	32	2	0.063	0.563

**Table 5.3.3.1. Cont.**

Antibiotics	MIC <sub>antibiotic alone</sub> <sup>a</sup>	Synergistic MIC <sup>a</sup>	FIC <sub>antibiotic</sub>	Hybrid	MIC <sub>hybrid alone</sub> <sup>a</sup>	Synergistic MIC <sup>a</sup>	FIC <sub>hybrid</sub>	FIC index
Chloramphenicol	64	8	0.125	<b>1</b>	>256	1	<0.004	0.125<x<0.129
Chloramphenicol	64	4	0.063	<b>2</b>	128	1	0.008	0.070
Chloramphenicol	64	2	0.031	<b>3</b>	32	4	0.125	0.156
Erythromycin	256	128	0.5	<b>1</b>	>256	1	<0.004	0.5<x<0.504
Erythromycin	256	32	0.125	<b>2</b>	128	1	0.008	0.125<x<0.133
Erythromycin	256	8	0.031	<b>3</b>	32	4	0.125	0.156
Trimethoprim	256	64	0.25	<b>1</b>	>256	1	<0.004	0.133
Trimethoprim	256	16	0.063	<b>2</b>	128	1	<0.008	0.063<x<0.254
Trimethoprim	256	16	0.063	<b>3</b>	32	2	0.063	0.125
Colistin	1	ND	ND	<b>1</b>	ND	ND	ND	ND
Colistin	1	ND	ND	<b>2</b>	ND	ND	ND	ND
Colistin	1	1	1	<b>3</b>	32	1	0.031	1.031
Gentamicin	1	2	2	<b>1</b>	>256	1	<0.004	2<x<2.004
Gentamicin	1	2	2	<b>2</b>	128	1	0.008	2.008
Gentamicin	1	1	1	<b>3</b>	32	4	0.125	1.125
Kanamycin A	64	ND	ND	<b>1</b>	ND	ND	ND	ND

**Table 5.3.3.1. Cont.**

Antibiotics	MIC <sub>antibiotic alone</sub> <sup>a</sup>	Synergistic MIC <sup>a</sup>	FIC <sub>antibiotic</sub>	Hybrid	MIC <sub>hybrid alone</sub> <sup>a</sup>	Synergistic MIC <sup>a</sup>	FIC <sub>hybrid</sub>	FIC index
Kanamycin A	64	ND	ND	<b>2</b>	ND	ND	ND	ND
Kanamycin A	64	64	1	<b>3</b>	32	0.5	0.016	1.016
Amikacin	1	ND	ND	<b>1</b>	ND	ND	ND	ND
Amikacin	1	ND	ND	<b>2</b>	ND	ND	ND	ND
Amikacin	1	1	1	<b>3</b>	32	2	0.063	1.063
Meropenem	0.5	1	2	<b>1</b>	>256	2	<0.008	2<x<2.008
Meropenem	0.5	2	4	<b>2</b>	128	1	0.008	4.008
Meropenem	0.5	1	2	<b>3</b>	32	1	0.031	2.031
Vancomycin	>1024	ND	ND	<b>1</b>	>256	ND	ND	ND
Vancomycin	>1024	256	<0.25	<b>2</b>	128	4	0.031	0.031<x<0.281
Vancomycin	>1024	128	<0.125	<b>3</b>	32	4	0.125	0.125<x< 0.25

<sup>a</sup>All MIC data presented in µg/mL. ND: not determined.

**Table 5.3.3.2.** Synergistic effects of compound **3** with minocycline or rifampicin against clinical MDR or XDR *P. aeruginosa* isolates.

<i>P. aeruginosa</i> strain	Antibiotics (MIC <sup>a</sup> )	FIC <sub>antibiotic</sub>	Hybrid (MIC <sup>a</sup> )	FIC <sub>hybrid</sub>	FIC index	Absolute MIC <sup>b</sup>	Potential <sup>c</sup>
100036	Minocycline (32)	0.063	<b>3</b> (32)	0.031	0.094	1	32-fold
100036	Rifampicin (16)	0.016	<b>3</b> (32)	0.063	0.079	0.125	128-fold
101885	Minocycline (32)	0.125	<b>3</b> (16)	0.031	0.156	2	16-fold
101885	Rifampicin (16)	0.063	<b>3</b> (16)	0.031	0.094	0.125	128-fold
P259-96918	Minocycline (32)	0.031	<b>3</b> (64)	0.016	0.047	0.5	64-fold
P259-96918	Rifampicin (16)	0.008	<b>3</b> (64)	0.031	0.039	0.063	256-fold
P262-101856	Minocycline (256)	0.008	<b>3</b> (32)	0.125	0.133	2	128-fold
P262-101856	Rifampicin (1024)	0.016	<b>3</b> (32)	0.125	0.141	16	64-fold
P264-104354	Minocycline (64)	0.016	<b>3</b> (32)	0.063	0.079	0.5	128-fold
P264-104354	Rifampicin (16)	0.031	<b>3</b> (32)	0.063	0.094	0.25	64-fold
91433	Minocycline (64)	0.016	<b>3</b> (8)	0.25	0.266	0.5	128-fold
91433	Rifampicin (16)	0.25	<b>3</b> (8)	0.25	0.5	2	8-fold
101243	Minocycline (4)	0.25	<b>3</b> (16)	0.031	0.281	1	4-fold
101243	Rifampicin (8)	0.063	<b>3</b> (16)	0.125	0.188	0.25	32-fold

<sup>a</sup> All MIC data presented in  $\mu\text{g/mL}$ . <sup>b</sup> Absolute MIC of antibiotic was determined in the presence of hybrid at 4  $\mu\text{g/mL}$ . <sup>c</sup> Antibiotic activity potentiation at 4  $\mu\text{g/mL}$  of hybrid.

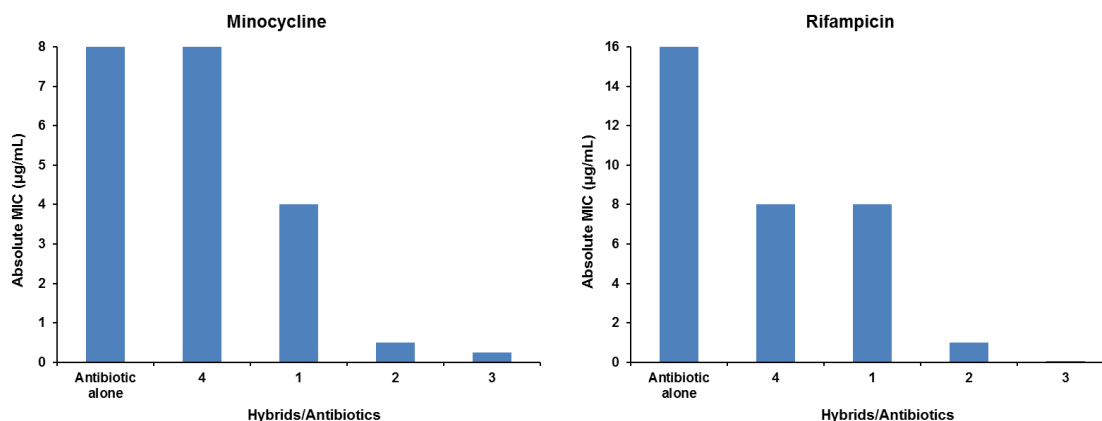


**Figure 5.3.3.1.** Absolute MIC of minocycline or rifampicin alone or in combination with 4  $\mu\text{g/mL}$  of compound 1–4 against *P. aeruginosa* PAO1.

To gain insights into the membrane effects and relevant synergistic mechanism of **3**, colistin, a membrane-active antibiotic, was tested in combination with five antibiotics against PAO1. Our results indicated that colistin was also able to potentiate the activity of rifampicin and novobiocin (Figure 5.3.3.2), but to a lesser extent than compound **3**. To investigate the relevance of efflux pumps on the observed adjuvant properties of **3**, combination studies of minocycline and rifampicin each with compound **3** were carried out in efflux pump-mutated strains, PAO200 and PAO750. PAO200 is a MexAB-OprM deletion strain while PAO750 is an efflux-sensitive strain that lacks five different clinically relevant RND pumps (MexAB-OprM, MexCD-OprJ, MexEF-OprN, MexJK, and MexXY) and the outer membrane protein OpmH. Some of these pumps are homologues of broad substrate specificities that expel different classes of antimicrobial agents and confer resistance on *P. aeruginosa*. For instance, the tripartite protein system MexAB-OprM, MexCD-OprJ, MexEF-OprN and MexXY-OprM allow the translocation of a wide variety of substrates such as quinolones, chloramphenicol, trimethoprim, imipenem,

and tetracyclines out of the cell.<sup>27</sup> As shown in Table 5.3.3.3, synergism was observed with rifampicin in both PAO200 (FIC index = 0.129) and PAO750 (FIC index = 0.156), but not with minocycline (FIC index >0.5). The ability to potentiate minocycline in PAO1 but not in efflux-deficient strains corroborates the hypothesis that tobramycin-lysine conjugate compromises the efficiency of efflux proteins. Rifampicin, which is not a substrate for these pumps, was however potentiated, suggesting a second mode of action consistent with membrane permeabilization.

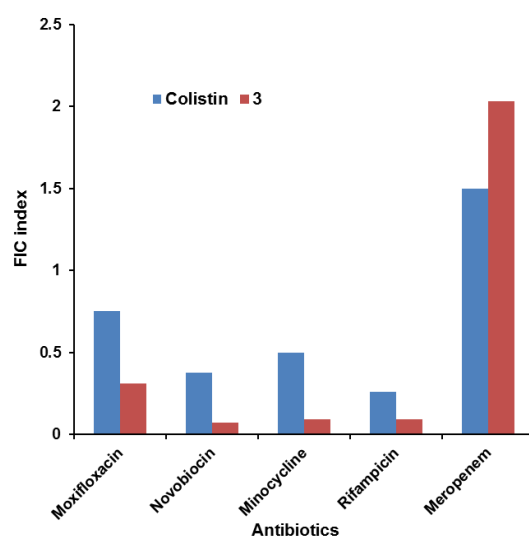


**Figure 5.3.3.2.** FIC index comparison of compound **3** and colistin in combination with antibiotics against *P. aeruginosa* PAO1.

**Table 5.3.3.3.** Synergistic effects of compound **3** with minocycline and with rifampicin against *P. aeruginosa* PAO1 and efflux pump deficient *P. aeruginosa* PAO200 and PAO750 strains.

<i>P. aeruginosa</i> strain	Antibiotic (MIC $\mu\text{g/mL}$ )	Adjuvant (MIC $\mu\text{g/mL}$ )	FIC index
PAO1	Minocycline (8)	<b>3</b> (32)	0.094
PAO1	Rifampicin (16)	<b>3</b> (32)	0.094
PAO200	Minocycline (1)	<b>3</b> (16)	0.531
PAO200	Rifampicin (8)	<b>3</b> (16)	0.129
PAO750	Minocycline (1)	<b>3</b> (8)	0.75
PAO750	Rifampicin (8)	<b>3</b> (8)	0.156

To study the spectrum of activity of **3** in combination with minocycline and with rifampicin, we examined *in vitro* potency against other clinical isolates of highly pathogenic Gram-negative bacteria, including *Acinetobacter baumannii*, *Enterobacter cloacae*, and *Klebsiella pneumoniae*. Table 5.3.3.4 summarizes these results and indicates strong synergy of **3** with minocycline in other Gram-negative species except AB031 and *K. pneumoniae* 110193 where the effect of **3** on minocycline is at best marginally additive. Surprisingly, combination of **3** with rifampicin displayed potent synergy in all tested isolates, with FIC indices  $<0.25$ . The synergistic MIC of rifampicin in combination with 4  $\mu\text{g/mL}$  of **3** against rifampicin-resistant *E. cloacae* 117029 was 0.063  $\mu\text{g/mL}$ , which is 16-fold lower than rifampicin-susceptible breakpoints of  $\leq 1 \mu\text{g/mL}$ .

**Table 5.3.3.4.** Combination study of compound **3** with minocycline or rifampicin against MDR *Acinetobacter baumannii*, *Enterobacter cloacae* and *Klebsiella pneumoniae*.

Organisms <sup>#</sup>	Antibiotics	MIC <sub>antibiotic alone</sub> ( $\mu\text{g/mL}$ )	Synergistic MIC ( $\mu\text{g/mL}$ )	FIC <sub>antibiotic</sub>	Hybrids	MIC <sub>hybrid alone</sub> ( $\mu\text{g/mL}$ )	Synergistic MIC ( $\mu\text{g/mL}$ )	FIC <sub>hybrid</sub>	FIC index
AB027	Minocycline	1	0.25	0.25	<b>3</b>	128	1	0.008	0.258
AB027	Rifampicin	2	0.031	0.016	<b>3</b>	128	8	0.063	0.079
AB030	Minocycline	4	0.5	0.125	<b>3</b>	64	16	0.25	0.375
AB030	Rifampicin	>256	32	<0.125	<b>3</b>	64	8	0.125	0.125<x<0.25
AB031	Minocycline	2	1	0.5	<b>3</b>	16	2	0.125	0.625
AB031	Rifampicin	2	0.125	0.06	<b>3</b>	32	1	0.03	0.09
110193	Minocycline	2	1	0.5	<b>3</b>	16	2	0.13	0.63
110193	Rifampicin	2	0.063	0.032	<b>3</b>	16	1	0.063	0.095
117029	Minocycline	128	4	0.031	<b>3</b>	256	8	0.031	0.062
117029	Rifampicin	16	0.063	0.004	<b>3</b>	256	4	0.016	0.02
116381	Minocycline	128	32	0.25	<b>3</b>	256	16	0.063	0.313
116381	Rifampicin	1024	32	0.031	<b>3</b>	256	4	0.016	0.047

#AB027, #AB030, #AB031, and #110193 = *Acinetobacter baumannii*; #117029 = *Enterobacter cloacae*; #116381 = *Klebsiella pneumoniae*.

### 5.3.4 Time-kill Curve

The kinetics of *P. aeruginosa* PAO1 killing as a function of time, using mono- and combination-therapy of minocycline, rifampicin, and compound **3**, are shown in Figure 5.3.4.1 and Figure 10.2.1 (Chapter 10). Minocycline alone was not bactericidal even at  $4 \times \text{MIC}$  after 6 h, while rifampicin as a monotherapy was bactericidal at  $4 \times \text{MIC}$  after 2 h of drug exposure (Chapter 10, Figure 10.2.1). Compound **3** showed bactericidal activity at  $1 \times \text{MIC}$  after 2 h, and more rapid killing was observed at  $2 \times \text{MIC}$  and  $4 \times \text{MIC}$  for only 30 and 10 mins antimicrobial exposure, respectively (Chapter 10, Figure 10.2.1). Minocycline, rifampicin, or **3** at subinhibitory concentrations were unable to suppress bacteria growth in monotherapy, even after 6 h exposure (Figure 5.3.4.1). However, upon combination with sub-MIC ( $[1/8 \text{ to } 1/2] \times \text{MIC}$ ) of **3**, *in vitro* bactericidal activities of minocycline and rifampicin were both enhanced, yielding synergistic killing at sub-MIC concentration ( $1/8 \times \text{MIC}$ ) after 90 mins of incubation (Figure 5.3.4.1).

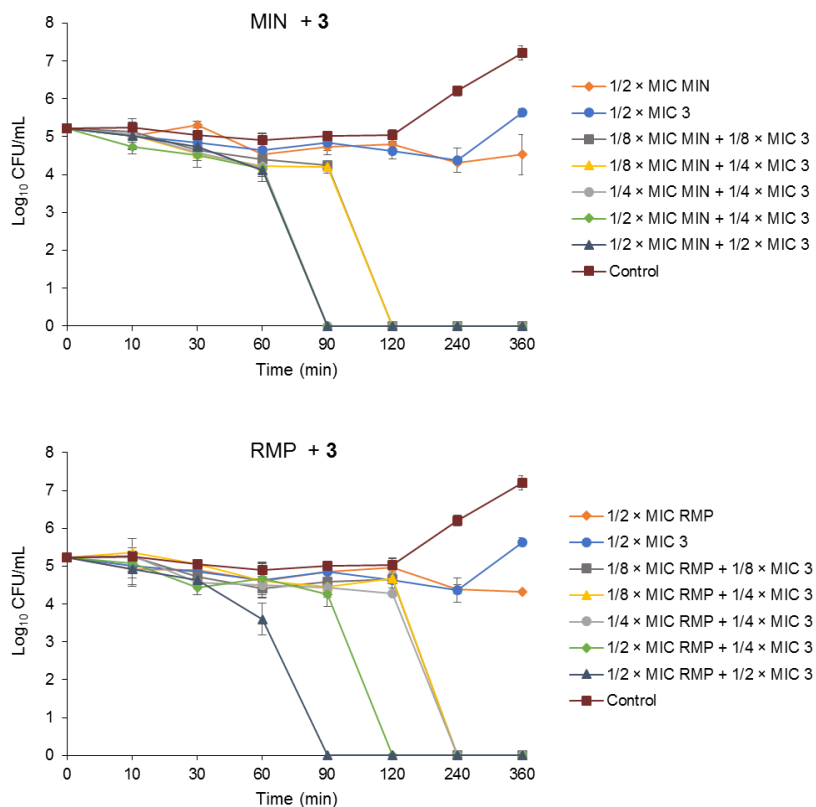


**Figure 5.3.4.1.** Time killing kinetics of minocycline (MIN) or rifampicin (RMP) alone at  $1/2 \times$  MIC ( $4 \mu\text{g/mL}$  for MIN and RMP for  $8 \mu\text{g/mL}$ ) or in combination with compound **3** against *P. aeruginosa* PAO1 at varied concentrations.

### 5.3.5 Resistance Study

The ability of drug combinations to suppress resistance development was determined using wild-type *P. aeruginosa* PAO1. This assay was validated by demonstrating that the MIC of colistin and tobramycin increased by 1024- and 256-fold, respectively, over 25 serial passages, while that of minocycline increased by 16-fold (Figure 5.3.5.1). Upon combination with compound **3**, the emergence of resistance in minocycline was suppressed by 4-fold while

rifampicin did not promote resistance either as monotherapy or in combination with **3** (Figure 5.3.5.1).

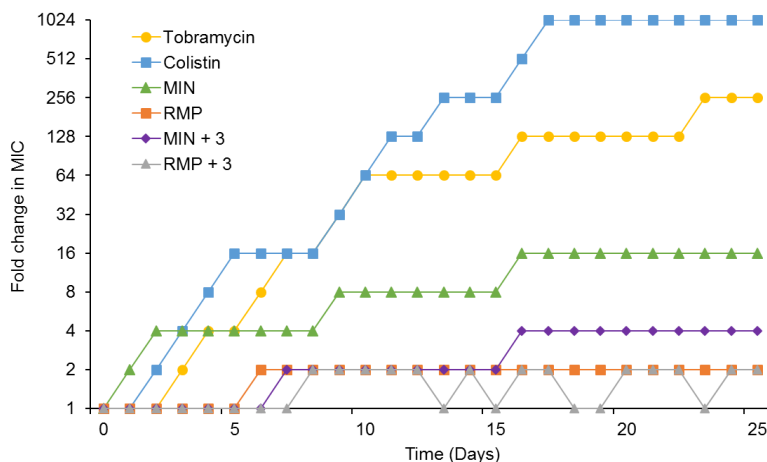


**Figure 5.3.5.1.** Emergence of bacterial resistance after treatment of *P. aeruginosa* PAO1 with antimicrobials for 25 passages at sub-MIC concentration was determined in monotherapy of tobramycin, colistin, minocycline (MIN), and rifampicin (RMP) or in combination therapy of MIN plus compound **3** or RMP plus compound **3**.

## 5.3.6 Mode of Action Studies

### 5.3.6.1 Outer Membrane Permeabilization

Since the negatively charged outer membrane of *P. aeruginosa* serves as the first barrier that prevents the uptake of antibiotics,<sup>7, 8</sup> the ability of the amphiphilic cationic compounds to perturb this lipid bilayer was investigated in PAO1 using carboxyfluorescein diacetate succinimidyl ester (CFDASE), a cell permeable dye.<sup>28</sup> We reasoned that the amphipathic nature of the hybrids might confer membrane effects similar to those of the host defense peptides on

them. The increased fluorescence induced by the compounds was calculated by subtracting the fluorescence of negative control that was treated similarly but in the absence of drug, while 1% Triton X-100, which exhibited the highest fluorescence compared to other treatments, served as the positive control (Figure 5.3.6.1.1). At the concentration tested ( $32 \mu\text{g/mL}$ ), the outer membrane permeabilization induced by **3** was slightly lower than that of colistin. In contrast, reference compound **4** displayed the weakest membrane permeabilizing ability with the lowest fluorescence increase.

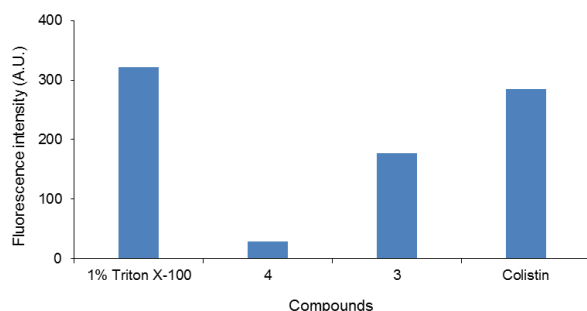


**Figure 5.3.6.1.1.** Outer membrane permeabilization of *P. aeruginosa* PAO1 by colistin, compound **3**, or **4** at  $32 \mu\text{g/mL}$  was determined using fluorescence dye CFDA at an excitation wavelength of 488 nm and an emission wavelength of 520 nm. 1% Triton X-100 was served as positive control.

### 5.3.6.2 Cytoplasmic Membrane Depolarization

Compounds that perturb the bacterial outer membrane can potentially be trapped within the periplasmic space where they could interfere with the respiratory chain on the cytoplasmic membrane to induce death. Indeed, this has been proposed as one of the mechanisms by which polymyxin exerts its antibacterial effects, among many others.<sup>29</sup> Depolarization of cytoplasmic

membrane can lead to loss of membrane potential, an important electrochemical gradient used by the bacteria to maintain an active and functional efflux system.<sup>30</sup> To investigate the effect of **3** on bacterial cytoplasmic membrane, DiSC<sub>3</sub>(5), a membrane potential-dependent probe, was used to study the differential in fluorescence caused by membrane depolarization.<sup>19</sup> A dose-dependent fluorescence increasing was observed for all the tested antimicrobials in PAO1 (Chapter 10, Figure 10.2.2). At 32  $\mu\text{g/mL}$ , colistin was observed to depolarize the cytoplasmic membrane faster than other compounds in the first 300 s, with an accompanying decrease in fluorescence thereafter (Figure 5.3.6.2.1). Although reference compound **4** displayed similar properties as colistin, the decline in fluorescence seems to be specific for colistin. Compound **3** however displayed the highest fluorescence up until 1200 s, while only weak membrane depolarization ability was observed for tobramycin at 32  $\mu\text{g/mL}$ , a 128-fold higher value than its MIC.

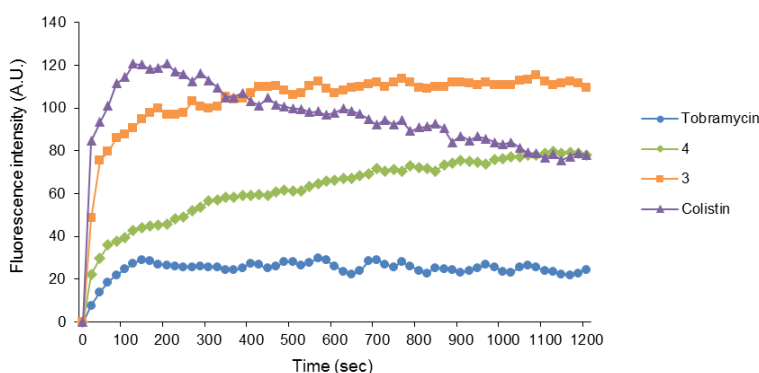


**Figure 5.3.6.2.1.** Cytoplasmic membrane depolarization of *P. aeruginosa* PAO1 treated with tobramycin, colistin, compound **3**, or **4** at 32  $\mu\text{g/mL}$  was measured using the membrane potential-sensitive dye DiSC<sub>3</sub>(5). The fluorescent intensity was monitored at an excitation wavelength of 622 nm and an emission wavelength of 670 nm over a 1200 seconds period.

### 5.3.6.3 Swimming Motility Assay

Swimming motility is a flagellum-dependent bacterial movement that is governed by the respiratory chain on the cytoplasmic membrane. When cytoplasmic membrane potential or proton motive force (PMF) is disrupted, the electron transfer across the respiratory chain is inhibited, resulting in a reduction of ATP synthesis, which is essential for flagellar function.<sup>31</sup> Previous studies have implicated that amphiphilic tobramycin-moxifloxacin hybrids can perturb the PMF resulting in reduced or inefficient efflux.<sup>17</sup> We therefore studied the effect of **3** and **4** on the swimming motility of PAO1 by monitoring its movement on low-viscosity swim plates (0.3% agar, w/v). Surprisingly, **3** and **4** were observed to significantly constrict the swimming bacteria diameter (at 4  $\mu\text{g}/\text{mL}$ ) relative to the untreated control (Figure 5.3.6.3.1). Meanwhile, these compounds repressed bacterial swimming motility in a dose-dependent manner, and the observed effects were superior to colistin at subinhibitory concentrations, while tobramycin was unable to inhibit bacterial motility with similar bacterial swimming diameters to untreated control (Chapter 10, Figure 10.2.3).

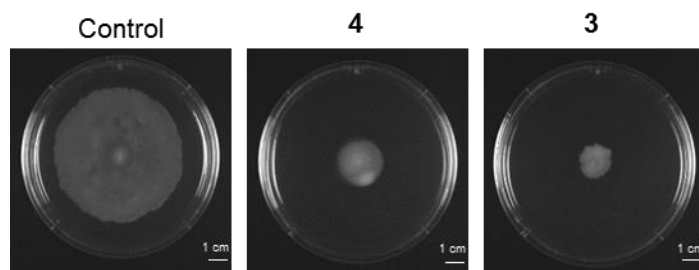


**Figure 5.3.6.3.1.** Swimming motility of *P. aeruginosa* PAO1 treated with compound **3** or **4** at 4  $\mu\text{g}/\text{mL}$ .

### 5.3.7 Hemolytic Activity and Cytotoxicity

A potential problem usually associated with membrane-active agents is their toxicity towards eukaryotic cells. The hemolytic properties of the hybrid molecules were first examined using freshly collected pig erythrocytes. All hybrids demonstrated lower hemolytic activities (<20%) relative to **4**, which is highly toxic with 87% hemolysis at the highest measured concentration of 512  $\mu\text{g/mL}$  (Figure 5.3.7.1A). As to the structure-activity relationships (SAR) between the hybrids, a slight increase in hemolytic activity with increase in carbon length was evident. Compound **3** was also tested against human epithelial prostate (DU145) and breast (JIMT-1) cancer cell lines, with greater than 50% viability at 20  $\mu\text{M}$  (25.2  $\mu\text{g/mL}$ ), a six times higher concentration than effective synergistic concentration (4  $\mu\text{g/mL}$ ) in combination therapy (Figure 5.3.7.1B).

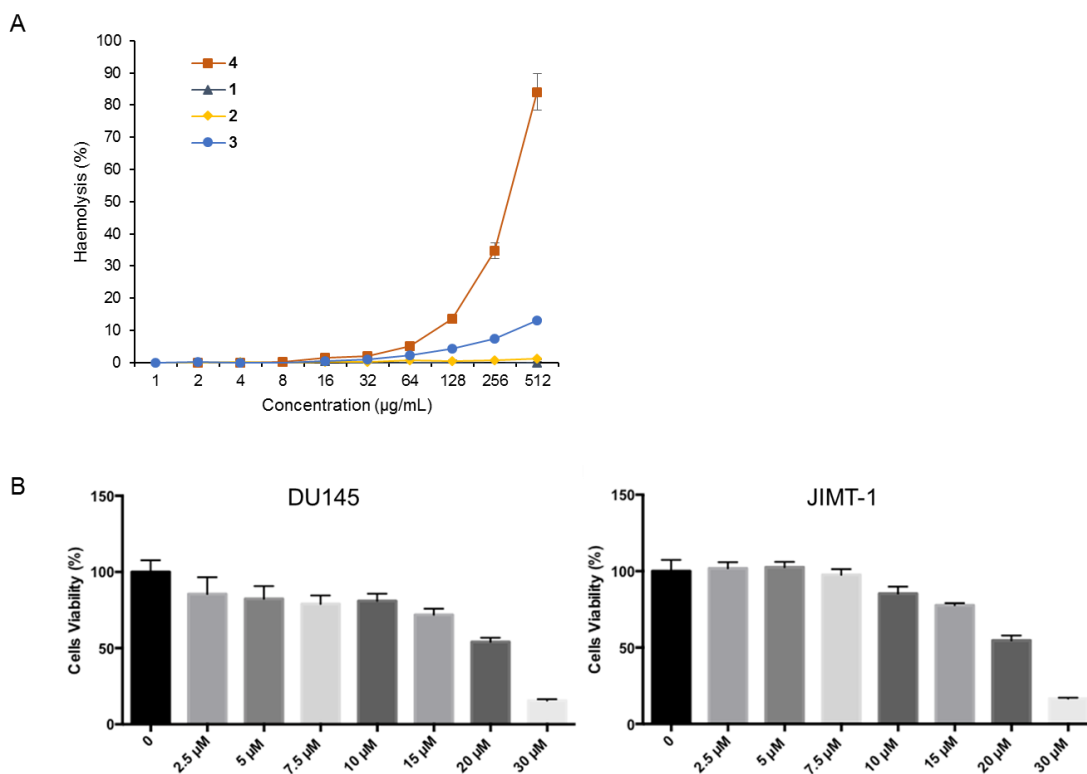


**Figure 5.3.7.1.** (A) Hemolytic activity of compounds **1–4** was evaluated against pig red blood cells. 0.1% Triton X-100 was employed as positive control to calculate the percentage of hemolysis. (B) Cytotoxicity of compound **3** was demonstrated against DU145 and JIMT-1 cell lines by MTS assay.

### 5.3.8 *In Vivo* Efficacy

To gain insights into the potential clinical benefits of compound **3**, an *in vivo* efficacy evaluation using *Galleria mellonella* infection model was initiated. The maximum tolerable dose was first determined by injecting drugs alone at high concentrations (100 or 200 mg/kg), and the survival rates scored for 4 days. As shown in Figure 10.2.4 (Chapter 10), 100% survival was observed after 4 days in the group that had been injected with 200 mg/kg of **3**, indicating the relative safety of the compound to the larvae at this dose. Next, the ability of the drug or drug combinations to protect larvae from XDR *P. aeruginosa* P262 infection was determined at single doses of 75 mg/kg in drug monotherapy or 12.5 + 12.5, 25 + 25, 37.5 + 37.5, or 75 + 75 mg/kg in drug combinations (Figure 5.3.8.1). Mortality of 100% was observed in the monotherapy of minocycline, rifampicin, and **3** at 75 mg/kg after 24 h, and in combination at lower doses. However, combinations of minocycline or rifampicin with **3** at a high dose of 75 + 75 mg/kg both resulted in 77% survival after 24 h, demonstrating the ability of this compound to offer protection against infection at very tolerable dose. Interestingly, it appears that combination therapy of rifampicin and **3** at low dosage appears to be superior when compared to combinations of minocycline and **3**. This is rather surprising as the *in vitro* studies suggest a lower MIC for minocycline when compared to rifampicin. This discrepancy may be related to

the different pharmacokinetics of minocycline and rifampicin in the larvae or the difference between bacteriostatic minocycline and bactericidal rifampicin (Chapter 10, Figure 10.2.1).

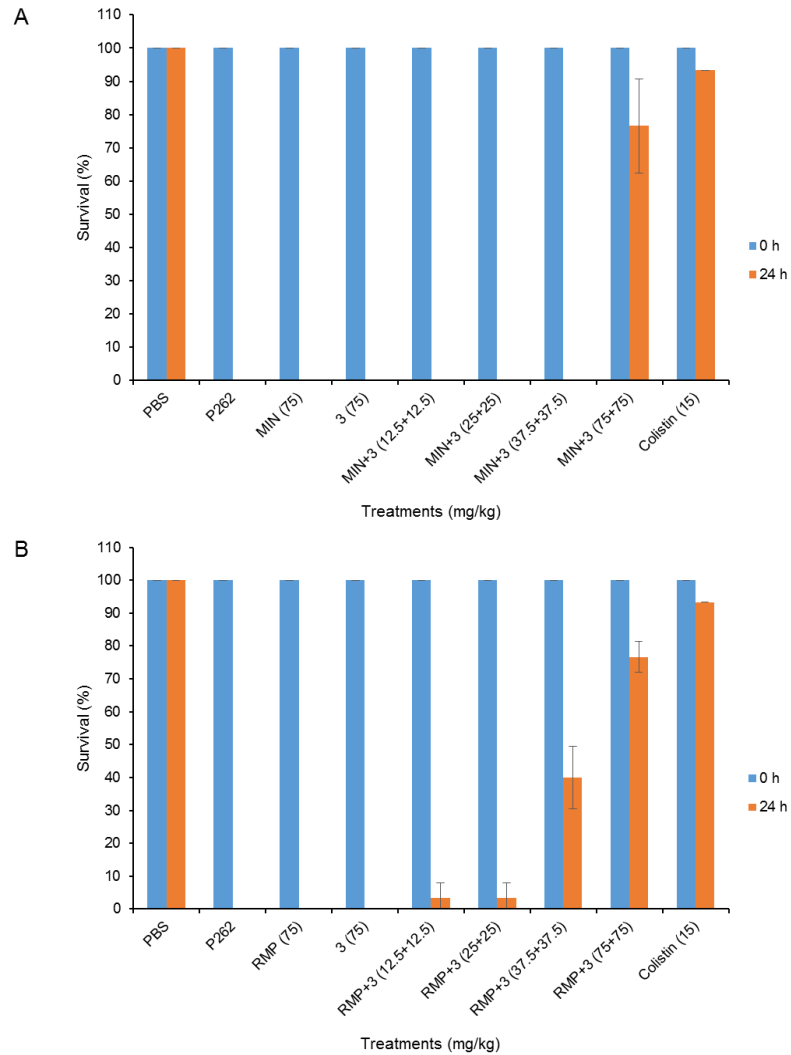


**Figure 5.3.8.1.** Evaluation of monotherapy and combination therapy in protecting *Galleria mellonella* larvae from XDR *P. aeruginosa* P262 infection. MIN = minocycline; RMP = rifampicin.

## 5.4 DISCUSSION

Bacterial resistance can frequently emerge in antibiotic monotherapy due to the selective pressure that naturally separates out the resistant phenotypes.<sup>10, 11</sup> Combination of two or more antimicrobials that can impact multiple targets simultaneously is believed to be capable of suppressing drug resistance, as well as broadening the spectrum of activity of a treatment course than single agents.<sup>32, 33</sup> In the last three years, the FDA has approved two new combination drugs Avycaz (ceftazidime + avibactam) and Zerbaxa (ceftolozane + tazobactam), to combat MDR Gram-negative infections. Ceftazidime/avibactam contains an older third generation cephalosporin ceftazidime, with avibactam, a synthetic non- $\beta$ -lactam,  $\beta$ -lactamase inhibitor that inhibits the activities of Ambler class A and C  $\beta$ -lactamases and some Ambler Class D enzymes.<sup>34</sup> Limited data suggest that the addition of avibactam does not improve the activity of ceftazidime versus *Pseudomonas aeruginosa*. Ceftolozane is a novel cephalosporin, with a chemical structure similar to that of ceftazidime, with the exception of a modified side-chain at the 3-position of the cephem nucleus, which confers potent antipseudomonal activity.<sup>35</sup> The addition of tazobactam extends the activity of ceftolozane to include most ESBL producers but not *P. aeruginosa*. Nevertheless, effective drug combinations often lead to inconclusive benefits of combination therapy over monotherapy during meta-analysis.<sup>36</sup> Recent reports about the potentials of amphiphilic tobramycin analogues to permeabilize cell membrane<sup>19,20</sup> and our previous studies that demonstrated the intrinsic ability of tobramycin-fluoroquinolone hybrids to potentiate the antimicrobial activity of several classes of antibiotics against clinical *P. aeruginosa* isolates<sup>16, 17</sup> encouraged a further optimization of this promising scaffold for use as adjuvants. In the current study, we prepared new amphiphilic tobramycin hybrids by taking advantage of the membrane-active peptoid **4** as a modulator. The antimicrobial properties of

these derivatives alone were assessed and demonstrated to be weaker compared to the parental tobramycin molecule (Table 5.3.2.1). Although tobramycin is believed to induce pleiotropic mechanisms of action,<sup>37</sup> the most acceptable hypothesis suggests tobramycin permeates the outer membrane via a self-promoted uptake mechanism<sup>38</sup> and acts by impairing bacterial protein synthesis through irreversible binding to the 30S ribosomal subunit.<sup>39</sup> The differing activity between tobramycin and the newly synthesized hybrid molecules suggests that the protein translation inhibitory effect is compromised by attachment of hydrophobic moieties to tobramycin as previously shown.<sup>16, 17</sup> Furthermore, activity trend between the hybrids revealed a correlation between antimicrobial potency and carbon chain length. The longer the carbon tether, the better the antimicrobial efficacy of the compound. This is however not surprising as studies have shown that high hydrophobicity facilitates penetration of membrane-active compounds across the bacterial membrane.<sup>40, 41</sup> The physicochemical properties necessary to navigate a complex membrane topology, especially as represented in *P. aeruginosa*, is perhaps the principal reason for the varied activity of the hybrid molecules. Although ultrashort and amphiphilic lysine-based peptoid mimics were previously reported to have promising activities against *P. aeruginosa* MTCC 424,<sup>23</sup> our evaluation of compound **4** (different alkyl chain) against a panel of organisms revealed otherwise (Table 5.3.2.1). This may be due to the slight change in the length of the alkyl chain (C10 to C12) and, perhaps, the different bacterial strains tested. The amphiphilic nature of **4**, the reported properties of tobramycin hybrids,<sup>16</sup> and the differential activity of the new molecules based on carbon chain length gave a clue to possible membrane effect of these compounds. Thus, we investigated antimicrobial activities of the amphiphilic conjugates in combination with other antibiotics, particularly against *P. aeruginosa*, the major nosocomial pathogen and leading cause of infection in cystic fibrosis patients. Although most of

the clinical isolates investigated in this study were resistant to tobramycin and other antibiotics (with the exception of colistin), the MIC values of the conjugates against these strains were similar to that of wild-type *P. aeruginosa* PAO1 (Table 5.3.2.2), suggesting that the target site or mechanism of action of the conjugates was different than that of tobramycin.

The ability of **3** to perturb the membrane was verified by its synergistic effect with vancomycin, a drug that cannot pass through the outer membrane of *P. aeruginosa* due to its large size (MW = 1449.2). Synergism was also observed for other antibiotics with different modes of action against *P. aeruginosa*, the most prominent being novobiocin, minocycline, and rifampicin. Importantly, combining **3** with minocycline or with rifampicin can revive the antimicrobial activities of these antibiotics against MDR and XDR *P. aeruginosa* isolates (Table 5.3.3.2). The uptake of tetracyclines, such as minocycline, is known to be driven by transmembrane chemical gradient ( $\Delta\text{pH}$ ) of PMF generated by the respiratory chain on the cytoplasmic membrane.<sup>42</sup> The other component of PMF is the electrical potential ( $\Delta\psi$ ), which is known to drive aminoglycosides uptake.<sup>43</sup> Bacteria control  $\Delta\psi$  and  $\Delta\text{pH}$  exquisitely to maintain a constant value of PMF, and disruption of either component is compensated for by a counteracting increase in the other.<sup>44</sup> When a compound disrupts  $\Delta\psi$ , an antagonism effect will be observed in combination with aminoglycosides, while synergism will show in combination with tetracyclines due to the compensatory increase of  $\Delta\text{pH}$ . Tetracyclines and aminoglycosides have therefore been used as two relevant antibiotics in combination studies with other drugs to identify compounds that affect membrane PMF and specifically dissipate either component of PMF.<sup>31</sup> In this study, compound **3** displayed different synergistic effects with minocycline (synergism) and aminoglycosides (no interaction), an observation that is consistent with dissipation of  $\Delta\psi$  component of the PMF by **3**. However, the expected antagonistic effect of **3**

with aminoglycosides was not observed, likely due to the membrane penetration induced by **3** that slightly affected aminoglycosides uptake into bacterial cells. The effect of **3** on  $\Delta\Psi$  was further corroborated by the increased DiSC<sub>3</sub>(5) fluorescence (Figure 5.3.6.2.1) and repression of swimming motility controlled by this parameter (Figure 5.3.6.3.1). Compounds that collapse the PMF are known to inhibit ATP synthesis and flagellar motility, preventing or reducing swimming activity.<sup>45</sup>

Membrane-associated efflux is another major mechanism that prevents bioaccumulation of drugs within the cytosol, thus preventing or reducing access of antibiotics to intracellular targets.<sup>46</sup> Efflux pump proteins localized in the cytoplasmic and outer membrane and linked by a periplasmic membrane fusion protein (MFP), play a major role in intrinsic and acquired resistance of *P. aeruginosa*.<sup>7-9</sup> The associated resistance is based on energy-dependent effluxes, which are usually driven by PMF.<sup>30</sup> We envisaged that the dissipation of  $\Delta\Psi$  in PMF will prevent electron transport across the respiratory chain, thus inhibiting ATP synthesis, and ultimately affect the efflux pump system. We therefore studied the effect of the conjugates on efflux pumps using *P. aeruginosa* efflux-deficient strains PAO200 and PAO750 and perhaps explain the observed synergistic mechanism more exquisitely. The efflux pump knockout decreased the MIC of minocycline by 8-fold (Table 5.3.3.3), confirming that minocycline is a substrate for these efflux pumps, which is consistent with previous study.<sup>47</sup> The synergism observed when **3** was combined with minocycline against wild-type PAO1 was not observed in PAO200 and PAO750, with FIC indices >0.5, indicating that the antimicrobial activity potentiation of minocycline by **3** is due to the inhibition of efflux pumps, particularly the RND pumps. To validate this hypothesis, the synergistic effects of **3** with other known *P. aeruginosa* efflux pump substrates were evaluated in PAO200 and PAO750, including chloramphenicol, erythromycin, trimethoprim, and

moxifloxacin.<sup>7, 48-50</sup> The results showed weak synergy or additive effects of **3** in these combinations (chapter 10, Table 10.3.2), corroborating the efflux pump inhibitory activity of **3**. We posited that the dissipation of the electrochemical gradient across the cytoplasmic membrane affected respiratory ATP production, thereby compromising efflux pump efficiency.

Surprisingly, rifampicin that is not a substrate of the five efflux pumps investigated in this study (MexAB-OprM, MexCD-OprJ, MexEF-OprN, MexJK, and MexXY), was similarly strongly synergized by **3** against PAO200 and PAO750 (Table 5.3.3.3). Rifampicin is known to kill bacteria by inhibiting RNA synthesis after binding to DNA-dependent RNA polymerase.<sup>51</sup> Both Gram-positive and Gram-negative bacteria are similarly sensitive to rifampicin, with higher MICs reported in Gram-negative bacteria due to its low penetration across the outer membrane.<sup>52</sup> A combination study of rifampicin with colistin (a well-known membrane permeabilizer) has demonstrated that perturbation of *P. aeruginosa* outer membrane can indeed potentate the antimicrobial activity of rifampicin,<sup>53</sup> thus confirming the results of this study with **3** (Figure 5.3.3.2). Outer membrane perturbation is perhaps the reason why **3** was able to synergize rifampicin against PAO200 and PAO750 despite not being a substrate for the pumps. It is however clear that minocycline is more sensitive to PMF dissipation caused by compound **3** than simply membrane penetration induced by colistin, as evident in the FIC indices >0.5 shown in Table 5.3.3.3. These results suggest that compound **3** is not just able to penetrate *P. aeruginosa* cell membrane like colistin but could also dissipate the cytoplasmic membrane and compromise the efficient functioning of the efflux systems. Although reference compound **4** similarly displayed cytoplasmic membrane depolarization activity and suppressed bacterial swimming motility, it was to a lesser extent than **3** at the same concentration (Figures 5.3.6.2.1 and 5.3.6.3.1), and did not display any synergistic effect in combination with minocycline and with

rifampicin (Chapter 10, Table 10.3.1). The inability of **4** to potentiate minocycline like **3** despite its ability to partially depolarize the cytoplasmic membrane as well may be due to its weak outer membrane perturbation that prevents uptake of other antimicrobial agents. The simultaneous occurrence of both phenomenon is indeed critical to the adjuvant properties of tobramycin-lysine conjugates.

In contrast to the bactericidal nature of rifampicin, minocycline is known to be only bacteriostatic, which was evident in the time-kill assay with constant bacterial cells number at all concentrations tested (Chapter 10, Figure 10.2.1), an observation that is consistent with previous studies.<sup>54,55</sup> However, the increased killing efficiency of minocycline when used in combination with **3** is likely attributable to the effect of **3** on the membrane. Attempts to select for resistance with combination of **3** and minocycline during 25 serial passages resulted in a 4-fold increase in MIC, as opposed to minocycline and tobramycin alone that had 16- and 256-folds increase, respectively (Figure 5.3.5.1). Indeed, it is more difficult for bacteria to develop resistance to simultaneously acting drug combination, especially when one of the drug acts on the membrane.<sup>56-58</sup>

A major concern about membrane-acting and PMF-collapsing agents is their toxicities towards eukaryotic cells.<sup>31</sup> To verify the safety of these compounds, the toxicities of the conjugates were evaluated against pig erythrocytes and mammalian cancer cell lines. It was surprising to see a dramatic reduction of the hemolytic activity of **4** when joined to tobramycin (Figure 5.3.7.1A). This is probably caused by changes to the molecular amphipathy as previously seen for antimicrobial peptides.<sup>59</sup> Moreover, combination therapy would allow for reduced doses to be used, minimizing cytotoxicity, and **3** displayed negligible toxicity at its effective synergistic concentration ( $\leq 4 \mu\text{g/mL}$ ). In the *in vivo* study, the high tolerance of *Galleria*

*mellonella* larvae to **3** (100% survival at 200 mg/kg after 96 h) further confirmed the safety of this compound. *Galleria mellonella* injection model has been commonly used in assessing the *in vivo* efficacy of antimicrobials against *P. aeruginosa* because it shares a high degree of structural and functional homology to the immune systems of vertebrates with both cellular and humoral defenses.<sup>60</sup> In contrast to monotherapy, single dose combination of **3** (75 mg/kg) plus minocycline (75 mg/kg) or **3** (75 mg/kg) plus rifampicin (75 mg/kg) effectively protected larvae from XDR *P. aeruginosa* P262 infection with more than 75% survival after 24 h, indicating the therapeutic potential of amphiphilic tobramycin as an adjuvant to treat infection caused by XDR *P. aeruginosa*.

## 5.5 CONCLUSIONS

In this study, we demonstrated that amphiphilic tobramycin-lysine conjugates preserve many of the known adjuvant properties of previously reported tobramycin-fluoroquinolone hybrids. From a medicinal chemistry point, linking a tobramycin C-12 vector to an amphiphilic lysine conjugate enhances the outer membrane destabilization effect of the amphiphilic lysine analog. As such, our study suggests that a tobramycin-C12 tether at C-5 position in tobramycin serves as an effective vector to promote delivery of compounds through the outer membrane barrier of Gram-negative bacteria with an optimized effect on *P. aeruginosa*. However, the effect of the tobramycin-C12 tether appears to be not limited to the outer membrane but also involves the cytoplasmic membrane. For instance, we provide evidence that conjugates containing a tobramycin-C12 tether reduces the  $\Delta\Psi$  component of the PMF located at the cytoplasmic membrane. This leads to decreased activity of the efflux associated pumps but at the same can lead to enhanced cytoplasmic uptake of agents that depend on the  $\Delta\text{pH}$  component of the PMF

like the tetracycline class of antibiotics. Overall, this study provides a promising strategy for generating effective antibiotic adjuvants that overcome drug resistance in MDR Gram-negative bacteria including *P. aeruginosa* by carefully designing amphiphilic tobramycin tethers. The discovery that compound **3** can potentiate several classes of antibiotics against resistant pathogens is set to expand the antimicrobial space and optimize our usage of antibiotics in our current armamentarium.

## 5.6 EXPERIMENTAL SECTION

### 5.6.1 Chemical Synthesis

#### 5.6.1.1 General Information

NMR spectra ( $^1\text{H}$ ,  $^{13}\text{C}$ , DEPT, COSY, HSQC and HMBC) were recorded on a Bruker Avance 500 spectrometer (500 MHz for  $^1\text{H}$  NMR, 126 MHz for  $^{13}\text{C}$ ). All reactions were monitored by analytical thin-layer chromatography (TLC) on pre-coated silica gel plates 60 F254 (0.25 mm, Merck, Ontario, Canada), and the spots were visualized by ultraviolet light and/or by staining with ninhydrin solution in *n*-butanol. Mass spectrometry was carried by ESI analyses on a Varian 500 MS Ion Trap Mass Spectrometer, and MALDI-TOF on a Bruker Daltonics Ultraflex MALDI TOF/TOF Mass Spectrometer. Chromatographic separations were performed on a silica gel column by flash chromatography (Kiesel gel 40, 0.040-0.063 mm; Merck, Ontario, Canada). Yields were calculated after purification. When reactions were carried out under anhydrous conditions, the mixtures were maintained under nitrogen atmosphere. Analytical HPLC was performed on Hitachi LC system equipped with autosampler, using Superspher 100

RP-18 column and a detection wavelength of 260 nm. The purity of final compounds determined by HPLC analysis were >95%. Detailed experimental procedures of the intermediates Boc-Lys(Boc)-OH, **11a–c** and **12a–c** were described in Chapter 10. Detailed experimental procedures of the compounds **10a–c** were described in chapter 9. The following data are for the intermediates after reductive amination and the final compounds tested in the biological studies.

### 5.6.1.2 Synthetic Procedures

**General Procedure A: Deprotection of Boc and TBDMS Groups for the Synthesis of Tobramycin-lysine Conjugates (1–3).** Compounds **14a–c** (1 equiv) were treated with 40% HCl in MeOH (~1.5 mL of solvent per 0.01 mmol of intermediates **14a–c**) at room temperature for 3 h. The reaction progress was monitored by TLC (MeOH/CH<sub>2</sub>Cl<sub>2</sub>/NH<sub>4</sub>OH, 6:4:3). At the end of the reaction, the mixture was concentrated under reduced pressure to get the solid tobramycin conjugate as HCl salt. The crude was further purified via C-18 reverse-phase flash column chromatography (eluted with deionized water) to afford analytically pure compounds as yellow solid.

**General Procedure B: Reductive Amination for the Synthesis of 5-O-(alkylated-10-aminomethyl-9-chloroanthracene)-1,3,2',6',3''-penta-N-(tert-butoxycarbonyl)-4',2'',4'',6''-tetra-OTBDMS-tobramycin (13a–c).** Compounds **12a–c** (1 equiv) and commercially available aromatic aldehyde **5** (1.2 equiv) were dissolved in dry CH<sub>2</sub>Cl<sub>2</sub>:MeOH (1:1, v/v) (~ 20.0 mL of solvent per mmol of intermediates **12a–c**) and stirred at room temperature overnight. The resulting clear solution was cooled to 0 °C, sodium borohydride (3 equiv) added and stirred at room temperature for 3 h. The solvents were then evaporated and the crude re-dispersed in diethyl ether followed by the addition of 2 N NaOH. The mixture was stirred at room

temperature for 15 mins and the organic layer separated from aqueous phase, washed with water and brine, and dried over anhydrous Na<sub>2</sub>SO<sub>4</sub>. The mixture was concentrated and purified by flash column chromatography (eluted with CH<sub>2</sub>Cl<sub>2</sub>/MeOH from 300:1 to 30:1, v/v) to give the desired product as yellow solid.

**General Procedure C: Secondary Amide Coupling for the Synthesis of Compounds 14a–c.**

Boc-Lys(Boc)-OH (1.5 equiv) dissolved in DMF (~30.0 mL of solvent per mmol of intermediates **13a–c**) was activated with DIPEA (3 equiv) and HBTU (1.5 equiv) at 0 °C for 15 mins and subsequently treated with **13a–c** (1 equiv). The mixture was stirred at 0 °C to room temperature overnight. The reaction progress was monitored by TLC (CH<sub>2</sub>Cl<sub>2</sub>/MeOH, 35:1), and at the end, the mixture was diluted with water and extracted with EtOAc. The organic layer was washed with water and brine, dried over anhydrous Na<sub>2</sub>SO<sub>4</sub>, and concentrated. The resulting residue was purified by flash column chromatography (eluted with CH<sub>2</sub>Cl<sub>2</sub>/MeOH from 300:1 to 30:1, v/v) to afford the desired compound as yellow solid.

**Compound 1.** Synthesized following general procedure A from **14a** (18.6 mg, 0.009 mmol). The crude material was purified by C-18 reverse-phase flash column chromatography using deionized water. The product was isolated as a yellow solid (6.3 mg, 78%). <sup>1</sup>H NMR (500 MHz, Deuterium Oxide) δ 8.74 – 8.60 (m, 2H, anthracene), 8.33 – 8.24 (m, 2H, anthracene), 7.86 – 7.73 (m, 4H, anthracene), 5.99 (d, *J* = 15.4 Hz, 1H, N-CH<sup>1</sup>H<sup>2</sup>-anthracene), 5.30 (d, *J* = 15.3 Hz, 1H, N-CH<sup>1</sup>H<sup>2</sup>-anthracene), 5.14 (d, *J* = 2.5 Hz, 1H, H-1'), 4.95 (d, *J* = 3.4 Hz, 1H, H-1''), 4.43 (t, *J* = 6.3 Hz, 1H, α-CH of Lys), 4.29 – 4.24 (m, 1H, H-5'), 4.03 – 3.94 (m, 2H, H-4, H-4'), 3.83 – 3.77 (m, 2H, H-6, H-2''), 3.65 – 3.46 (m, 5H, H-1, H-3, H-2', H-4'', H-5''), 3.39 – 3.30 (m, 2H, H-6'), 3.21 – 3.12 (m, 3H, H-5, H-3'', H-6''), 3.03 – 2.95 (m, 1H, N-CH<sup>1</sup>H<sup>2</sup>CH<sub>2</sub>), 2.90 – 2.64 (m, 5H, N-CH<sup>1</sup>H<sup>2</sup>CH<sub>2</sub>, ε-CH<sub>2</sub> of Lys, O-CH<sub>2</sub> of linker), 2.59 – 2.54 (m, 1H, H-2),

2.39 – 2.32 (m, 1H, H-6''), 2.24 – 2.12 (m, 2H, H-3'), 1.97 – 1.82 (m, 3H, H-2,  $\beta$ -CH<sub>2</sub> of Lys), 1.64 – 1.54 (m, 2H,  $\delta$ -CH<sub>2</sub> of Lys), 1.45 – 1.31 (m, 2H,  $\gamma$ -CH<sub>2</sub> of Lys), 1.27 – 1.10 (m, 3H, CH<sub>2</sub> of linker), 1.09 – 0.99 (m, 1H, CH<sub>2</sub> of linker). <sup>13</sup>C NMR (126 MHz, Deuterium Oxide)  $\delta$  169.34 (NCOCH), 131.18, 130.09, 128.13, 127.48, 127.40, 126.65, 125.62, 124.36, 100.79 (anomeric CH-1''), 93.15 (anomeric CH-1'), 82.41, 81.22, 77.20 (CH-4), 75.41 (CH-5'), 73.18, 72.80 (O-CH<sub>2</sub>-linker), 68.44, 64.30, 63.42 (CH-6), 58.41 (CH<sub>2</sub>-6''), 54.46, 50.61 ( $\alpha$ -CH of Lys), 49.36, 48.60, 47.65, 45.32 (N-CH<sub>2</sub>CH<sub>2</sub>), 40.74 (N-CH<sub>2</sub>-anthracene), 38.91 ( $\epsilon$ -CH<sub>2</sub> of Lys), 38.60 (CH-6'), 30.90 ( $\beta$ -CH<sub>2</sub> of Lys), 28.34 (CH<sub>2</sub>-3'), 28.18 (CH<sub>2</sub>-2), 26.55 ( $\delta$ -CH<sub>2</sub> of Lys), 25.36, 24.45, 21.16; MALDI-TOF-MS: *m/z* calc'd for C<sub>43</sub>H<sub>67</sub>ClN<sub>8</sub>O<sub>10</sub>Na: 913.457, found: 913.463 [M+Na]<sup>+</sup>.

*Compound 2.* Synthesized following general procedure A from **14b** (28 mg, 0.013 mmol).

The crude material was purified by C-18 reverse-phase flash column chromatography using deionized water. The product was isolated as a yellow solid (9.4 mg, 75%). <sup>1</sup>H NMR (500 MHz, Deuterium Oxide)  $\delta$  8.49 – 8.44 (m, 2H, anthracene), 8.15 – 8.11 (m, 2H, anthracene), 7.71 – 7.62 (m, 4H, anthracene), 5.70 (d, *J* = 15.4 Hz, 1H, N-CH<sup>1</sup>H<sup>2</sup>-anthracene), 5.35 – 5.28 (m, 2H, N-CH<sup>1</sup>H<sup>2</sup>-anthracene, H-1'), 5.16 (d, *J* = 3.5 Hz, 1H, H-1''), 4.37 (t, *J* = 6.3 Hz, 1H,  $\alpha$ -CH of Lys), 4.32 – 4.27 (m, 1H, H-5'), 4.15 (t, *J* = 9.8 Hz, 1H, H-4), 3.96 – 3.89 (m, 3H, H-6, H-4', H-2''), 3.83 – 3.76 (m, 4H, H-5, O-CH<sub>1</sub>H<sub>2</sub> of linker, H-4'', H-5''), 3.75 – 3.72 (m, 1H, H-6''), 3.67 – 3.55 (m, 5H, H-1, H-3, H-2', H-3'', O-CH<sub>1</sub>H<sub>2</sub> of linker), 3.53 – 3.49 (m, 1H, H-6''), 3.40 – 3.33 (m, 2H, H-6'), 2.98 – 2.90 (m, 1H, N-CH<sup>1</sup>H<sup>2</sup>CH<sub>2</sub>), 2.86 – 2.78 (m, 2H,  $\epsilon$ -CH<sub>2</sub> of Lys), 2.62 – 2.52 (m, 2H, H-2, N-CH<sup>1</sup>H<sup>2</sup>CH<sub>2</sub>), 2.25 – 2.20 (m, 2H, H-3'), 2.02 – 1.96 (m, 1H, H-2), 1.92 – 1.82 (m, 2H,  $\beta$ -CH<sub>2</sub> of Lys), 1.64 – 1.57 (m, 2H,  $\delta$ -CH<sub>2</sub> of Lys), 1.44 – 1.35 (m, 3H,  $\gamma$ -CH<sub>2</sub> of Lys, CH<sub>2</sub> of linker), 1.32 – 1.27 (m, 1H, CH<sub>2</sub> of linker), 1.11 – 1.04 (m, 1H, CH<sub>2</sub> of linker), 1.02 – 0.91 (m, 2H, CH<sub>2</sub> of linker), 0.83 – 0.63 (m, 4H, CH<sub>2</sub> of linker), 0.62 – 0.53 (m, 3H, CH<sub>2</sub> of

linker).  $^{13}\text{C}$  NMR (126 MHz, Deuterium Oxide)  $\delta$  169.14 (NCOCH), 131.04, 129.85, 127.86, 127.19, 127.09, 126.25, 125.25, 124.12, 101.39 (anomeric CH-1''), 92.71 (anomeric CH-1'), 82.04, 81.95, 76.97 (CH-4), 75.59 (CH-5'), 73.84 (O-CH<sub>2</sub>-linker), 73.18, 68.56, 64.70, 63.29, 59.12 (CH<sub>2</sub>-6''), 54.72, 50.72 ( $\alpha$ -CH of Lys), 49.76, 48.45, 47.37, 45.80 (N-CH<sub>2</sub>CH<sub>2</sub>), 40.80 (N-CH<sub>2</sub>-anthracene), 38.94 ( $\epsilon$ -CH<sub>2</sub> of Lys), 38.59 (CH-6'), 30.72 ( $\beta$ -CH<sub>2</sub> of Lys), 29.19, 28.20, 28.15, 28.08, 28.02, 27.25, 26.49 ( $\delta$ -CH<sub>2</sub> of Lys), 25.15, 24.86, 21.24; MALDI-TOF-MS  $m/z$  calc'd for C<sub>47</sub>H<sub>75</sub>ClN<sub>8</sub>O<sub>10</sub>Na: 969.519, found: 969.523 [M+Na]<sup>+</sup>.

*Compound 3.* Synthesized following general procedure A from **14c** (125 mg, 0.058 mmol). The crude material was purified by C-18 reverse-phase flash column chromatography using deionized water. The product was isolated as a yellow solid (42.3 mg, 73%).  $^1\text{H}$  NMR (500 MHz, Deuterium Oxide)  $\delta$  8.69 – 8.58 (m, 2H, anthracene), 8.30 – 8.24 (m, 2H, anthracene), 7.79 – 7.70 (m, 4H, anthracene), 5.87 (d,  $J = 15.4$  Hz, 1H, N-CH<sup>1</sup>H<sup>2</sup>-anthracene), 5.47 (d,  $J = 15.3$  Hz, 1H, N-CH<sup>1</sup>H<sup>2</sup>-anthracene), 5.43 (d,  $J = 2.6$  Hz, 1H, H-1'), 5.22 (d,  $J = 3.6$  Hz, 1H, H-1''), 4.40 (t,  $J = 6.3$  Hz, 1H,  $\alpha$ -CH of Lys), 4.32 – 4.28 (m, 1H, H-5'), 4.21 (t,  $J = 9.8$  Hz, 1H, H-4), 3.99 – 3.74 (m, 11H, H-5, H-6, H-2', H-4', H-2'', H-4'', H-5'', H-6'', O-CH<sub>2</sub> of linker), 3.67 – 3.57 (m, 3H, H-1, H-3, H-3''), 3.45 – 3.32 (m, 2H, H-6'), 3.03 – 2.96 (m, 1H, N-CH<sup>1</sup>H<sup>2</sup>CH<sub>2</sub>), 2.89 – 2.79 (m, 2H,  $\epsilon$ -CH<sub>2</sub> of Lys), 2.78 – 2.71 (m, 1H, N-CH<sup>1</sup>H<sup>2</sup>CH<sub>2</sub>), 2.58 – 2.54 (m, 1H, H-2), 2.32 – 2.23 (m, 2H, H-3'), 2.03 – 1.86 (m, 3H, H-2,  $\beta$ -CH<sub>2</sub> of Lys), 1.75 – 1.66 (m, 2H, CH<sub>2</sub> of linker), 1.65 – 1.59 (m, 2H,  $\delta$ -CH<sub>2</sub> of Lys), 1.45 – 1.29 (m, 6H,  $\gamma$ -CH<sub>2</sub> of Lys, CH<sub>2</sub> of linker), 1.25 – 1.18 (m, 2H, CH<sub>2</sub> of linker), 1.13 – 0.94 (m, 4H, CH<sub>2</sub> of linker), 0.91 – 0.83 (m, 2H, CH<sub>2</sub> of linker), 0.78 – 0.71 (m, 1H, CH<sub>2</sub> of linker), 0.68 – 0.59 (m, 3H, CH<sub>2</sub> of linker), 0.58 – 0.50 (m, 2H, CH<sub>2</sub> of linker).  $^{13}\text{C}$  NMR (126 MHz, Deuterium Oxide)  $\delta$  169.21 (NCOCH), 131.30, 130.11, 128.10, 127.30, 127.18, 126.53, 125.43, 124.24, 101.39 (anomeric CH-1''), 92.73 (anomeric CH-

1'), 81.93, 81.89, 76.82 (CH-4), 75.66 (CH-5'), 73.84 (O-CH<sub>2</sub>-linker), 73.22, 68.54, 64.77, 63.24, 59.27 (CH<sub>2</sub>-6''), 54.76, 50.73 ( $\alpha$ -CH of Lys), 49.79, 48.44, 47.34, 46.04 (N-CH<sub>2</sub>CH<sub>2</sub>), 41.03 (N-CH<sub>2</sub>-anthracene), 38.94 ( $\epsilon$ -CH<sub>2</sub> of Lys), 38.55 (CH-6'), 30.74 ( $\beta$ -CH<sub>2</sub> of Lys), 29.57 (CH<sub>2</sub> of linker), 29.13, 29.00, 28.70, 28.56, 28.19, 28.16 (CH<sub>2</sub>-3'), 27.98, 27.91 (CH<sub>2</sub>-2), 27.32, 26.50 ( $\delta$ -CH<sub>2</sub> of Lys), 25.40, 25.22, 21.28; MALDI-TOF-MS:  $m/z$  calc'd for C<sub>51</sub>H<sub>83</sub>ClN<sub>8</sub>O<sub>10</sub>Na: 1025.582, found: 1025.586 [M+Na]<sup>+</sup>.

*Lys-N-dodecyl-10-aminomethyl-9-chloroanthracene Trifluoroacetate (4)*. The Boc-Lys(Boc)-N-alkyl-aromatic compound **8** (22.8 mg, 0.031 mmol) was dissolved in CH<sub>2</sub>Cl<sub>2</sub>:TFA (2:1, v/v) (3 mL) and stirred at room temperature for 1 h. The reaction was monitored by TLC (CH<sub>2</sub>Cl<sub>2</sub>/NH<sub>4</sub>OH/MeOH, 5:1:1). At the end of the reaction, the mixture was evaporated to dryness, and purified by C-18 reverse-phase flash column chromatography (eluted with deionized water) to get analytically pure compound **4** as a yellow solid (10.3 mg, 62%). <sup>1</sup>H NMR (500 MHz, Methanol-*d*<sub>4</sub>)  $\delta$  8.61 – 8.57 (m, 2H, anthracene), 8.43 – 8.38 (m, 2H, anthracene), 7.69 – 7.61 (m, 4H, anthracene), 6.10 (d,  $J$  = 15.3 Hz, 1H, N-CH<sup>1</sup>H<sup>2</sup>-anthracene), 5.45 (d,  $J$  = 15.3 Hz, 1H, N-CH<sup>1</sup>H<sup>2</sup>-anthracene), 4.28 (t,  $J$  = 6.2 Hz, 1H,  $\alpha$ -CH of Lys), 3.02 – 2.96 (m, 1H, N-CH<sup>1</sup>H<sup>2</sup>CH<sub>2</sub>), 2.78 – 2.69 (m, 2H,  $\epsilon$ -CH<sub>2</sub> of Lys), 2.68 – 2.60 (m, 1H, N-CH<sup>1</sup>H<sup>2</sup>CH<sub>2</sub>), 1.86 – 1.76 (m, 2H,  $\beta$ -CH<sub>2</sub> of Lys), 1.59 – 1.52 (m, 2H,  $\delta$ -CH<sub>2</sub> of Lys), 1.48 – 1.39 (m, 2H,  $\gamma$ -CH<sub>2</sub> of Lys), 1.34 – 1.20 (m, 10H, N-CH<sub>2</sub>(CH<sub>2</sub>)<sub>10</sub>CH<sub>3</sub>), 1.17 – 1.11 (m, 2H, N-CH<sub>2</sub>(CH<sub>2</sub>)<sub>10</sub>CH<sub>3</sub>), 1.09 – 1.03 (m, 2H, N-CH<sub>2</sub>(CH<sub>2</sub>)<sub>10</sub>CH<sub>3</sub>), 0.97 – 0.77 (m, 9H, N-CH<sub>2</sub>(CH<sub>2</sub>)<sub>10</sub>CH<sub>3</sub>). <sup>13</sup>C NMR (126 MHz, Methanol-*d*<sub>4</sub>)  $\delta$  168.34 (NCOCH), 131.61, 130.03, 128.40, 127.33, 126.75, 126.61, 125.23, 124.19, 50.46 ( $\alpha$ -CH of Lys), 45.08 (N-CH<sub>2</sub>CH<sub>2</sub>), 39.48 (N-CH<sub>2</sub>-anthracene), 38.70 ( $\epsilon$ -CH<sub>2</sub> of Lys), 31.64, 30.92 ( $\beta$ -CH<sub>2</sub> of Lys), 29.27, 29.16, 29.06, 29.02, 28.82, 28.56, 28.37, 26.76 ( $\delta$ -CH<sub>2</sub>

of Lys), 25.95, 22.31, 21.25, 13.01 (CH<sub>2</sub>CH<sub>3</sub>); MALDI-TOF-MS:  $m/z$  calc'd for C<sub>33</sub>H<sub>49</sub>ClN<sub>3</sub>O: 538.356, found: 538.358 [M+H]<sup>+</sup>.

*N-dodecyl-10-aminomethyl-9-chloroanthracene Hydrochloride (7)*. Dodecylamine **6** (11.9 mg, 0.065 mmol) and aromatic aldehyde **5** (19 mg, 0.078 mmol) were dissolved in dry CH<sub>2</sub>Cl<sub>2</sub>:MeOH (1:1, v/v) (3 mL) and stirred at room temperature overnight. The mixture was cooled to 0 °C, and exposed to sodium borohydride (7 mg, 0.195 mmol) at room temperature overnight. The reaction mixture was subsequently concentrated, re-dispersed in diethyl ether, and treated with 2 N NaOH (3 mL) at room temperature for additional 15 mins. The organic layer was separated from the aqueous phase, washed with water and brine, dried over anhydrous Na<sub>2</sub>SO<sub>4</sub>, concentrated, and purified by flash column chromatography (eluted with CH<sub>2</sub>Cl<sub>2</sub>/MeOH from 300:1 to 30:1, v/v) to afford the desired compound as a yellow solid (19 mg, 70%). <sup>1</sup>H NMR (500 MHz, Chloroform-*d*) δ 8.60 – 8.55 (m, 2H, anthracene), 8.40 – 8.35 (m, 2H, anthracene), 7.64 – 7.54 (m, 4H, anthracene), 4.70 (s, 2H, NH-CH<sub>2</sub>-anthracene), 2.91 – 2.84 (m, 2H, NH-CH<sub>2</sub>CH<sub>2</sub>), 1.62 – 1.57 (m, 2H, NH-CH<sub>2</sub>CH<sub>2</sub>), 1.37 - 1.24 (m, 18H, NH-CH<sub>2</sub>CH<sub>2</sub>(CH<sub>2</sub>)<sub>9</sub>CH<sub>3</sub>), 0.89 (t,  $J = 6.8$  Hz, 3H, CH<sub>2</sub>CH<sub>3</sub>). <sup>13</sup>C NMR (126 MHz, Chloroform-*d*) δ 131.67, 130.70, 129.00, 128.66, 126.31, 126.21, 125.54, 124.53 (anthracene), 50.71 (NH-CH<sub>2</sub>CH<sub>2</sub>), 45.93 (NH-CH<sub>2</sub>-anthracene), 32.00, 30.17 (NH-CH<sub>2</sub>CH<sub>2</sub>), 29.75, 29.72, 29.70, 29.64, 29.44, 27.45, 22.77, 14.20 (CH<sub>2</sub>CH<sub>3</sub>); ESI-MS:  $m/z$  calc'd for C<sub>27</sub>H<sub>37</sub>ClN: 410.2, found: 410.1 [M+H]<sup>+</sup>.

*Boc-Lys(Boc)-N-dodecyl-10-aminomethyl-9-chloroanthracene (8)*. Boc-Lys(Boc)-OH (24 mg, 0.068 mmol) dissolved in DMF:CHCl<sub>3</sub> (5:2, v/v) (3.5 mL) was activated with DIPEA (18 mg, 0.135 mmol) and HBTU (26 mg, 0.068 mmol) at 0 °C for 15 mins, and treated with **7** (19 mg, 0.045 mmol). The mixture was stirred at 0 °C to room temperature overnight,

concentrated under reduced pressure, and the resulting solution diluted in ethyl acetate. The mixture was washed with 0.5 M KHSO<sub>4</sub>, water, and brine successively, and dried over anhydrous Na<sub>2</sub>SO<sub>4</sub>. The organic layer was concentrated and purified by flash column chromatography (eluted with CH<sub>2</sub>Cl<sub>2</sub>/MeOH from 300:1 to 100:1, v/v) to afford the desired compound as a yellow solid (30 mg, 90%). <sup>1</sup>H NMR (500 MHz, Chloroform-*d*) δ 8.64 – 8.54 (m, 2H, anthracene), 8.30 – 8.22 (m, 2H, anthracene), 7.64 – 7.51 (m, 4H, anthracene), 6.05 (d, *J* = 15.3 Hz, 1H, N-CH<sup>1</sup>H<sup>2</sup>-anthracene), 5.28 (d, *J* = 15.2 Hz, 1H, N-CH<sup>1</sup>H<sup>2</sup>-anthracene), 4.57 – 4.51 (m, 1H, α-CH of Lys), 3.12 – 2.95 (m, 2H, ε-CH<sub>2</sub> of Lys), 2.94 – 2.86 (m, 1H, N-CH<sup>1</sup>H<sup>2</sup>CH<sub>2</sub>), 2.77 – 2.66 (m, 1H, N-CH<sup>1</sup>H<sup>2</sup>CH<sub>2</sub>), 1.63 – 1.56 (m, 2H, β-CH<sub>2</sub> of Lys), 1.51 – 1.34 (m, 23H), 1.33 – 1.18 (m, 9H), 1.18 – 1.12 (m, 2H), 1.11 – 1.05 (m, 2H), 1.04 – 0.98 (m, 2H), 0.97 – 0.83 (m, 7H). <sup>13</sup>C NMR (126 MHz, Chloroform-*d*) δ 172.45 (NCOCH), 155.91, 155.49 (2 COOC), 131.66, 130.50, 128.51, 127.57, 126.74, 126.56, 125.78, 124.22, 50.28 (α-CH of Lys), 45.28 (N-CH<sub>2</sub>CH<sub>2</sub>), 40.29 (ε-CH<sub>2</sub> of Lys), 39.54 (N-CH<sub>2</sub>-anthracene), 33.77 (β-CH<sub>2</sub> of Lys), 31.90, 29.57, 29.51, 29.48, 29.39, 29.32, 29.25, 29.22, 28.84, 28.40 - 28.38 (CH<sub>3</sub>), 26.54, 22.67, 14.11 (CH<sub>2</sub>CH<sub>3</sub>); ESI-MS: *m/z* calc'd for C<sub>43</sub>H<sub>64</sub>ClN<sub>3</sub>O<sub>5</sub>Na: 760.443, found: 760.485 [M+Na]<sup>+</sup>.

*5-O-(4-butyl-10-Aminomethyl-9-chloroanthracene)-1,3,2',6',3''-penta-N-(tert-butoxycarbonyl)-4',2'',4'',6''-tetra-OTBDMS-tobramycin (13a)*. Synthesized following general procedure B from **12a** (33 mg, 0.022 mmol), aromatic aldehyde **5** (6 mg, 0.026 mmol) and sodium borohydride (2.5 mg, 0.066 mmol). The resulting residue was purified by flash column chromatography using CH<sub>2</sub>Cl<sub>2</sub>/MeOH (300:1 to 30:1, v/v) to afford the desired compound as a yellow solid (21 mg, 55%). <sup>1</sup>H NMR (500 MHz, Chloroform-*d*) δ 8.58 – 8.53 (m, 2H, anthracene), 8.41 – 8.36 (m, 2H, anthracene), 7.62 – 7.55 (m, 4H, anthracene), 5.29 – 5.13 (m, 2H, H-1', H-1''), 4.71 (s, 2H, NH-CH<sub>2</sub>-anthracene), 4.30 – 4.06 (m, 3H), 3.85 – 3.17 (m, 15H),

2.84 (t,  $J = 7.1$  Hz, 2H, NH-CH<sub>2</sub>CH<sub>2</sub>), 2.51 – 2.40 (m, 1H), 2.03 – 1.96 (m, 1H), 1.66 – 1.55 (m, 4H, CH<sub>2</sub> of linker), 1.55 – 1.51 (m, 1H), 1.48 – 1.29 (m, 45H), 1.10 – 1.01 (m, 1H), 0.94 – 0.81 (m, 36H, Si-CCH<sub>3</sub>), 0.14 – -0.05 (m, 24H, Si-CH<sub>3</sub>). <sup>13</sup>C NMR (126 MHz, Chloroform-*d*)  $\delta$  155.64, 155.47, 154.78, 154.56, 154.27 (5 COOC), 131.73, 130.81, 128.94, 128.65, 126.35, 126.28, 125.45, 124.69, 97.77 (anomeric CH-1''), 96.36 (anomeric CH-1'), 85.81, 79.91, 79.39, 79.27, 79.19, 78.71, 75.25, 73.17, 72.60, 71.49, 67.99, 66.93, 63.16, 57.26, 50.89 (NH-CH<sub>2</sub>CH<sub>2</sub>), 50.54, 48.89, 48.32, 45.81 (NH-CH<sub>2</sub>-anthracene), 41.62, 35.98, 35.73, 28.62 - 28.22 (O-CCH<sub>3</sub>), 26.72, 26.10 - 25.78 (Si-CCH<sub>3</sub>), 18.44, 18.29, 18.06, 17.91 (4 Si-CCH<sub>3</sub>), -3.45, -3.80, -4.22, -4.87, -4.92, -5.06, -5.19, -5.22 (8 Si-CH<sub>3</sub>); ESI-MS:  $m/z$  calc'd for C<sub>86</sub>H<sub>152</sub>ClN<sub>6</sub>O<sub>19</sub>Si<sub>4</sub>: 1721.9, found: 1721.6 [M+H]<sup>+</sup>.

*5-O-(8-octyl-10-aminomethyl-9-chloroanthracene)-1,3,2',6',3''-penta-N-(tert-butoxycarbonyl)-4',2'',4'',6''-tetra-OTBDMS-tobramycin (13b)*. Synthesized following general procedure B from **12b** (35 mg, 0.023 mmol), aromatic aldehyde **5** (7 mg, 0.028 mmol) and sodium borohydride (3 mg, 0.069 mmol). The resulting residue was purified by flash column chromatography using CH<sub>2</sub>Cl<sub>2</sub>/MeOH (300:1 to 30:1, v/v) to afford the desired compound as a yellow solid (28 mg, 70%). <sup>1</sup>H NMR (500 MHz, Chloroform-*d*)  $\delta$  8.62 – 8.52 (m, 2H, anthracene), 8.42 – 8.33 (m, 2H, anthracene), 7.67 – 7.50 (m, 4H, anthracene), 5.26 – 5.12 (m, 2H, H-1', H-1''), 4.71 (s, 2H, NH-CH<sub>2</sub>-anthracene), 4.31 – 4.21 (m, 1H), 4.21 – 4.13 (m, 1H), 4.12 – 4.04 (m, 1H), 3.83 – 3.18 (m, 15H), 2.87 (t,  $J = 7.4$  Hz, 2H, NH-CH<sub>2</sub>CH<sub>2</sub>), 2.51 – 2.44 (m, 1H), 2.03 – 1.98 (m, 1H), 1.61 – 1.56 (m, 2H, CH<sub>2</sub> of linker), 1.55 – 1.51 (m, 1H), 1.51 – 1.37 (m, 47H), 1.35 – 1.24 (m, 8H), 1.09 – 1.00 (m, 1H), 0.97 – 0.82 (m, 36H, Si-CCH<sub>3</sub>), 0.19 – -0.00 (m, 24H, Si-CH<sub>3</sub>). <sup>13</sup>C NMR (126 MHz, CDCl<sub>3</sub>)  $\delta$  155.69, 155.53, 154.73, 154.56, 154.18 (5 COOC), 131.19, 130.76, 129.16, 128.66, 126.37, 125.55, 124.51, 97.86 (anomeric CH-1''), 96.49

(anomeric CH-1'), 85.75, 79.91, 79.38, 79.22, 79.08, 78.88, 75.29, 73.33, 72.66, 71.55, 68.00, 66.86, 63.12, 57.25, 50.64 (NH-CH<sub>2</sub>CH<sub>2</sub>), 50.51, 48.91, 48.34, 45.79 (NH-CH<sub>2</sub>-anthracene), 41.67, 35.94, 35.67, 30.65, 30.04 (CH<sub>2</sub> of linker), 29.62, 28.63 - 28.40 (O-CCH<sub>3</sub>), 27.50, 26.18 - 25.78 (Si-CCH<sub>3</sub>), 18.48, 18.32, 18.09, 17.91 (4 Si-CCH<sub>3</sub>), -3.42, -3.79, -4.20, -4.88, -4.94, -5.07, -5.17, -5.22 (8 Si-CH<sub>3</sub>); ESI-MS: *m/z* calc'd for C<sub>90</sub>H<sub>160</sub>ClN<sub>6</sub>O<sub>19</sub>Si<sub>4</sub>: 1778.0, found: 1778.0 [M+H]<sup>+</sup>.

*5-O-(12-dodecyl-10-aminomethyl-9-chloroanthracene)-1,3,2',6',3''-penta-N-(tert-butoxycarbonyl)-4',2'',4'',6''-tetra-OTBDMS-tobramycin (13c)*. Synthesized following general procedure B from **12c** (116 mg, 0.072 mmol), aromatic aldehyde **5** (21 mg, 0.086 mmol) and sodium borohydride (8 mg, 0.216 mmol). The resulting residue was purified by flash column chromatography using CH<sub>2</sub>Cl<sub>2</sub>/MeOH (300:1 to 30:1, v/v) to afford the desired compound as a yellow solid (112 mg, 85%). <sup>1</sup>H NMR (500 MHz, Chloroform-*d*) δ 8.61 – 8.51 (m, 2H, anthracene), 8.41 – 8.32 (m, 2H, anthracene), 7.65 – 7.51 (m, 4H, anthracene), 5.25 – 5.12 (m, 2H, H-1', H-1''), 4.70 (s, 2H, NH-CH<sub>2</sub>-anthracene), 4.32 – 4.22 (m, 1H), 4.21 – 4.13 (m, 1H), 4.11 – 4.04 (m, 1H), 3.82 – 3.19 (m, 15H), 2.86 (t, *J* = 7.3 Hz, 2H, NH-CH<sub>2</sub>CH<sub>2</sub>), 2.51 – 2.43 (m, 1H), 2.04 – 1.98 (m, 1H), 1.61 – 1.55 (m, 2H, CH<sub>2</sub> of linker), 1.55-1.51 (m, 1H), 1.50 – 1.36 (m, 47H), 1.34 – 1.22 (m, 16H), 1.11 - 1.02 (m, 1H), 0.97 – 0.82 (m, 36H, Si-CCH<sub>3</sub>), 0.19 – -0.02 (m, 24H, Si-CH<sub>3</sub>). <sup>13</sup>C NMR (126 MHz, Chloroform-*d*) δ 155.67, 155.51, 154.72, 154.55, 154.19 (5 COOC), 131.59, 130.71, 129.00, 128.65, 126.32, 126.25, 125.53, 124.51, 97.79 (anomeric CH-1''), 96.54 (anomeric CH-1'), 85.71, 79.88, 79.35, 79.19, 79.04, 78.80, 75.28, 73.40, 72.68, 71.53, 68.01, 66.81, 63.09, 57.27, 50.67 (NH-CH<sub>2</sub>CH<sub>2</sub>), 50.52, 48.95, 48.38, 45.90 (NH-CH<sub>2</sub>-anthracene), 41.65, 35.90, 35.65, 30.63, 30.13, 30.05, 29.72, 29.70, 29.66, 29.61, 28.63 - 28.40 (O-CCH<sub>3</sub>), 27.42, 26.19 - 25.78 (Si-CCH<sub>3</sub>), 18.47, 18.33, 18.09, 17.90 (4 Si-CCH<sub>3</sub>), -3.42, -3.80,

-4.20, -4.88, -4.94, -5.07, -5.18, -5.23 (8 Si-CH<sub>3</sub>); ESI-MS:  $m/z$  calc'd for C<sub>94</sub>H<sub>168</sub>ClN<sub>6</sub>O<sub>19</sub>Si<sub>4</sub>: 1833.3, found: 1833.1 [M+H]<sup>+</sup>.

**Compound 14a.** Synthesized following general procedure C from **13a** (21 mg, 0.012 mmol), Boc-Lys(Boc)-OH (6 mg, 0.018 mmol), DIPEA (5 mg, 0.036 mmol) and HBTU (7 mg, 0.018 mmol). After column chromatography (eluted with CH<sub>2</sub>Cl<sub>2</sub>/MeOH from 300:1 to 30:1, v/v), the product was afforded as a yellow solid (18.6 mg, 74%). <sup>1</sup>H NMR (500 MHz, Chloroform-*d*)  $\delta$  8.66 – 8.55 (m, 2H, anthracene), 8.47 – 8.18 (m, 2H, anthracene), 7.71 – 7.54 (m, 4H, anthracene), 6.27 – 5.95 (m, 1H, N-CH<sup>1</sup>H<sup>2</sup>-anthracene), 5.36 – 5.23 (m, 1H, N-CH<sup>1</sup>H<sup>2</sup>-anthracene), 5.11 – 4.99 (m, 2H, H-1', H-1''), 4.52 – 4.39 (m, 1H,  $\alpha$ -CH of Lys), 4.26 – 3.95 (m, 2H), 3.83 – 3.73 (m, 1H), 3.70 – 3.10 (m, 15H), 3.08 – 2.95 (m, 2H,  $\epsilon$ -CH<sub>2</sub> of Lys), 2.95 – 2.68 (m, 2H, N-CH<sub>2</sub>CH<sub>2</sub>), 2.55 – 2.35 (m, 1H), 2.01 – 1.91 (m, 1H), 1.54 – 1.52 (m, 2H,  $\beta$ -CH<sub>2</sub> of Lys), 1.51 – 1.37 (m, 53H), 1.37 – 1.16 (m, 17H), 1.13 – 1.05 (m, 1H), 0.94 – 0.75 (m, 38H), 0.18 – -0.19 (m, 24H, Si-CH<sub>3</sub>). <sup>13</sup>C NMR (126 MHz, Chloroform-*d*)  $\delta$  172.15 (NCOCH), 155.88, 155.80, 155.65, 155.21, 154.82, 154.49, 154.35 (7 COOC), 131.89, 131.77, 130.49, 128.54, 127.87, 127.32, 126.92, 126.65, 125.94, 125.79, 125.65, 124.67, 124.38, 123.70, 98.24 (anomeric CH-1''), 96.55 (anomeric CH-1'), 86.13, 79.71, 79.38, 79.29, 79.24, 79.18, 78.92, 78.82, 75.56, 72.61, 72.30, 71.76, 67.59, 66.90, 63.15, 57.11, 50.53, 50.30 ( $\alpha$ -CH of Lys), 49.27, 48.44, 45.45 (N-CH<sub>2</sub>CH<sub>2</sub>), 41.47, 40.35 ( $\epsilon$ -CH<sub>2</sub> of Lys), 39.55 (N-CH<sub>2</sub>-anthracene), 35.77, 35.57, 33.2 ( $\beta$ -CH<sub>2</sub> of Lys), 29.67, 29.56, 28.72 - 28.30 (O-CCH<sub>3</sub>), 27.34, 26.12 - 25.78 (Si-CCH<sub>3</sub>), 22.45, 18.38, 18.31, 18.08, 17.92 (4 Si-CCH<sub>3</sub>), -3.35, -3.74, -4.25, -4.87, -5.03, -5.16, -5.22, -5.35 (8 Si-CH<sub>3</sub>); MALDI-TOF-MS:  $m/z$  calc'd for C<sub>102</sub>H<sub>179</sub>ClN<sub>8</sub>O<sub>24</sub>Si<sub>4</sub>Na: 2071.173, found: 2071.203 [M+Na]<sup>+</sup>

**Compound 14b.** Synthesized following general procedure C from **13b** (28 mg, 0.016 mmol), Boc-Lys(Boc)-OH (8 mg, 0.024 mmol), DIPEA (6 mg, 0.048 mmol) and HBTU (9 mg, 0.024 mmol). After column chromatography (eluted with CH<sub>2</sub>Cl<sub>2</sub>/MeOH from 300:1 to 30:1, v/v), the product was afforded as a yellow solid (28 mg, 85%). <sup>1</sup>H NMR (500 MHz, Chloroform-*d*) δ 8.66 – 8.56 (m, 2H, anthracene), 8.33 – 8.24 (m, 2H, anthracene), 7.71 – 7.50 (m, 4H, anthracene), 6.10 (d, *J* = 15.2 Hz, 1H, N-CH<sup>1</sup>H<sup>2</sup>-anthracene), 5.33 – 5.27 (m, 1H, N-CH<sup>1</sup>H<sup>2</sup>-anthracene), 5.25 – 5.19 (m, 1H, H-1'), 5.14 – 5.11 (m, 1H, H-1''), 4.56 – 4.51 (m, 1H, α-CH of Lys), 4.30 – 4.21 (m, 1H), 4.20 – 4.12 (m, 1H), 4.10 – 4.02 (m, 1H), 3.84 – 3.19 (m, 15H), 3.09 – 2.97 (m, 2H, ε-CH<sub>2</sub> of Lys), 2.96 – 2.86 (m, 1H, N-CH<sup>1</sup>H<sup>2</sup>CH<sub>2</sub>), 2.74 – 2.64 (m, 1H, N-CH<sup>1</sup>H<sup>2</sup>CH<sub>2</sub>), 2.54 – 2.42 (m, 1H), 2.04 – 1.97 (m, 1H), 1.58 – 1.55 (m, 2H, β-CH<sub>2</sub> of Lys), 1.54 – 1.52 (m, 1H), 1.51 - 1.38 (m, 65H), 1.38 – 1.31 (m, 4H, γ-CH<sub>2</sub> of Lys, δ-CH<sub>2</sub> of Lys), 1.31 – 1.21 (m, 2H, CH<sub>2</sub> of linker), 1.21 – 1.12 (m, 2H, CH<sub>2</sub> of linker), 1.12 – 1.00 (m, 5H), 1.00 – 0.79 (m, 38H), 0.22 – -0.09 (m, 24H, Si-CH<sub>3</sub>). <sup>13</sup>C NMR (126 MHz, Chloroform-*d*) δ 172.37 (NCOCH), 155.90, 155.74, 155.54, 155.42, 154.70, 154.56, 154.34 (7 COOC), 131.69, 130.49, 128.54, 127.70, 127.16, 126.76, 126.61, 125.79, 124.27, 123.92, 97.91 (anomeric CH-1''), 96.44 (anomeric CH-1'), 85.83, 79.91, 79.45, 79.38, 79.24, 79.18, 78.93, 78.78, 75.34, 73.23, 72.65, 71.57, 67.95, 66.87, 63.16, 57.24, 50.48, 50.31 (α-CH of Lys), 48.87, 48.32, 45.26 (N-CH<sub>2</sub>CH<sub>2</sub>), 41.69, 40.28 (ε-CH<sub>2</sub> of Lys), 39.36 (N-CH<sub>2</sub>-anthracene), 35.92, 35.69, 33.69 (β-CH<sub>2</sub> of Lys), 30.73, 30.03, 29.47, 29.28, 28.63 - 28.39 (O-CCH<sub>3</sub>), 26.95, 26.22 - 25.78 (Si-CCH<sub>3</sub>), 22.52, 18.47, 18.32, 18.10, 17.91 (4 Si-CCH<sub>3</sub>), -3.39, -3.77, -4.20, -4.87, -4.93, -5.08, -5.16, -5.20 (8 Si-CH<sub>3</sub>); MALDI-TOF-MS: *m/z* calc'd for C<sub>106</sub>H<sub>187</sub>ClN<sub>8</sub>O<sub>24</sub>Si<sub>4</sub>Na: 2127.206, found: 2127.219 [M+Na]<sup>+</sup>.

**Compound 14c.** Synthesized following general procedure C from **13c** (112 mg, 0.061 mmol), Boc-Lys(Boc)-OH (31.9 mg, 0.092 mmol), DIPEA (24 mg, 0.183 mmol) and HBTU (35 mg, 0.092 mmol). After column chromatography (eluted with CH<sub>2</sub>Cl<sub>2</sub>/MeOH from 300:1 to 30:1, v/v), the product was afforded as a yellow solid (125 mg, 95%). <sup>1</sup>H NMR (500 MHz, Chloroform-*d*) δ 8.63 – 8.55 (m, 2H, anthracene), 8.31 – 8.24 (m, 2H, anthracene), 7.64 – 7.53 (m, 4H, anthracene), 6.06 (d, *J* = 15.3 Hz, 1H, N-CH<sup>1</sup>H<sup>2</sup>-anthracene), 5.29 (d, *J* = 15.2 Hz, 1H, N-CH<sup>1</sup>H<sup>2</sup>-anthracene), 5.24 – 5.19 (m, 1H, H-1'), 5.17 – 5.12 (m, 1H, H-1''), 4.56 – 4.52 (m, 1H, α-CH of Lys), 4.31 – 4.21 (m, 1H), 4.20 – 4.12 (m, 1H), 4.11 – 4.03 (m, 1H), 3.82 – 3.15 (m, 15H), 3.08 – 2.96 (m, 2H, ε-CH<sub>2</sub> of Lys), 2.95 – 2.85 (m, 1H, N-CH<sup>1</sup>H<sup>2</sup>CH<sub>2</sub>), 2.76 – 2.67 (m, 1H, N-CH<sup>1</sup>H<sup>2</sup>CH<sub>2</sub>), 2.53 – 2.40 (m, 1H), 2.02 – 1.97 (m, 1H), 1.60 – 1.55 (m, 2H, β-CH<sub>2</sub> of Lys), 1.54 – 1.52 (m, 1H), 1.50 – 1.39 (m, 65H), 1.38 – 1.32 (m, 4H, γ-CH<sub>2</sub> of Lys, δ-CH<sub>2</sub> of Lys), 1.30 – 1.23 (m, 4H, CH<sub>2</sub> of linker), 1.22 – 1.11 (m, 6H, CH<sub>2</sub> of linker), 1.09 – 0.98 (m, 5H), 0.97 – 0.81 (m, 40H), 0.21 – -0.03 (m, 24H, Si-CH<sub>3</sub>). <sup>13</sup>C NMR (126 MHz, Chloroform-*d*) δ 172.42 (NCOCH), 155.89, 155.68, 155.66, 155.46, 154.72, 154.55, 154.43 (7 COOC), 131.67, 130.50, 128.52, 127.59, 127.14, 126.75, 126.57, 125.79, 124.23, 123.95, 97.82 (anomeric CH-1''), 96.51 (anomeric CH-1'), 85.74, 79.89, 79.76, 79.51, 79.36, 79.20, 78.94, 78.73, 75.29, 73.38, 72.68, 71.54, 68.03, 66.81, 63.09, 57.27, 50.51, 50.28 (α-CH of Lys), 48.94, 48.36, 45.28 (N-CH<sub>2</sub>CH<sub>2</sub>), 41.68, 40.27 (ε-CH<sub>2</sub> of Lys), 39.52 (N-CH<sub>2</sub>-anthracene), 35.93, 35.64, 33.75 (β-CH<sub>2</sub> of Lys), 30.68, 30.13, 29.75, 29.66, 29.53, 29.41, 29.26, 28.95, 28.62 - 28.37 (O-CCH<sub>3</sub>), 26.60, 26.25 - 25.77 (Si-CCH<sub>3</sub>), 22.55, 18.47, 18.32, 18.09, 17.90 (4 Si-CCH<sub>3</sub>), -3.42, -3.80, -4.21, -4.89, -4.95, -5.08, -5.19, -5.23 (8 Si-CH<sub>3</sub>); MALDI-TOF-MS: *m/z* calc'd for C<sub>110</sub>H<sub>195</sub>ClN<sub>8</sub>O<sub>24</sub>Si<sub>4</sub>Na: 2183.298, found: 2183.302 [M+Na]<sup>+</sup>.

## 5.6.2 Biological Activity Assays

### 5.6.2.1 Bacterial Isolates

Bacterial isolates were obtained as part of the Canadian National Intensive Care Unit (CAN-ICU) study<sup>61</sup> and Canadian Ward Surveillance (CANWARD) studies.<sup>62, 63</sup> The CAN-ICU study included 19 medical centres across Canada with active ICUs. From September 2005 to June 2006, 4180 isolates represented in 2580 ICU patients were recovered from clinical specimens including blood, urine, wound/tissue, and respiratory specimens (one pathogen per cultured site per patient). Only “clinically significant” specimens from patients with a presumed infectious disease were collected. The isolates obtained were shipped to the reference laboratory (Health Sciences Centre, Winnipeg, Canada) on Amies charcoal swabs. Then isolates were sub-cultured onto appropriate medium and stocked in skim milk at -80 °C until subsequent MIC testing was carried out. The quality control strains including *Staphylococcus aureus* ATCC 29213, methicillin-resistant *S. aureus* (MRSA) ATCC 33592, *Enterococcus faecalis* ATCC 29212, *Enterococcus faecium* ATCC 27270, *Streptococcus pneumoniae* ATCC 49619, *Escherichia coli* ATCC 25922, *Pseudomonas aeruginosa* ATCC 27853, and *Klebsiella pneumoniae* ATCC 13883 were acquired from the American Type Culture Collection (ATCC). The clinical strains, including methicillin-resistant *Staphylococcus epidermidis* (MRSE), CAN-ICU 61589 (cefazolin MIC >32 µg/mL), gentamicin resistant *E. coli* CAN-ICU 61714, Amikacin-resistant *E. coli* CAN-ICU 63074 (MIC = 32 µg/mL), gentamicin resistant *P. aeruginosa* CAN-ICU 62584, *Stenotrophomonas maltophilia* CAN-ICU 62584, and *Acinetobacter baumannii* CAN-ICU 63169 were obtained from hospitals across Canada as a part of the CAN-ICU study. Methicillin-susceptible *S. epidermidis* (MSSE) CANWARD-2008 81388

was obtained from the 2008 CANWARD study, while gentamicin-resistant tobramycin-resistant ciprofloxacin-resistant [aminoglycoside modifying enzyme *aac(3)-IIa* present] *E. coli* CANWARD-2011 97615, and gentamicin-resistant tobramycin-resistant *P. aeruginosa* CANWARD-2011 96846 were obtained from the 2011 CANWARD study. In addition, *P. aeruginosa* PAO1, *P. aeruginosa* P259-96918, *P. aeruginosa* P262-101856, *P. aeruginosa* P264-104354, colistin-resistant *P. aeruginosa* 91433, colistin-resistant *P. aeruginosa* 101243, *A. baumannii* AB027, *A. baumannii* AB030, *A. baumannii* AB031, *A. baumannii* 110193, *Enterobacter cloacae* 117029, and *Klebsiella pneumoniae* 116381 were kindly provided by Dr. George G. Zhanel. The efflux pump-mutated strains, *P. aeruginosa* PAO200 and *P. aeruginosa* PAO750, were provided by Dr. Ayush Kumar from University of Manitoba in Canada.

Multi-drug resistance in *P. aeruginosa* was defined as concomitant resistance to 3 or more chemically unrelated antimicrobial classes, while extensively drug resistant was defined as concomitant resistance to 5 or more chemically unrelated antimicrobial classes.

#### **5.6.2.2 Antimicrobial Activity Assay**

The antimicrobial activity of the compounds against a panel of bacteria was evaluated by microdilution method in accordance with the Clinical and Laboratory Standards Institute (CLSI) guidelines. The overnight bacterial culture was diluted in saline to 0.5 McFarland turbidity, and then 1:50 diluted in Mueller-Hinton broth (MHB) for inoculation. The antimicrobial agents were 2-fold serially diluted in MHB in 96-well plate and incubated with equal volumes of inoculum for 18 h at 37 °C. The lowest concentration that prevented visible bacterial growth was taken as the MIC for each antimicrobial agent. The broth with or without bacterial cells was employed as positive or negative controls, respectively.

### 5.6.2.3 Combination Studies with Different Antibiotics

FIC index was determined by setting up standard checkerboard assay in 96-well plate as previously described.<sup>64</sup> Each antibiotic to be tested was serially diluted along the abscissa in MHB, while adjuvant was diluted along the ordinate to create a  $10 \times 7$  matrix. The bacterial culture was prepared in MHB by 1:50 dilution from the 0.5 McFarland turbidity culture in saline. The inoculum was added to each well of the plate and incubated for 18 h at 37 °C. After the incubation, plates were read on EMax<sup>®</sup> Plus microplate reader (Molecular Devices, Sunnyvale, CA, USA). MIC was recorded as wells with the lowest concentration of drugs with no bacterial growth. The FIC for each antibiotic was calculated as the concentration of the antibiotic for a well showing no growth in the presence of adjuvant divided by the MIC for that antibiotic alone. The FIC for each adjuvant was calculated as the concentration of the adjuvant for a well showing no growth in the presence of antibiotic divided by the MIC for that adjuvant alone. The FIC index is the sum of the two FICs. Chemical-chemical interactions with a FIC index  $\leq 0.5$  was deemed synergistic; 0.5–4, no interaction; and  $\geq 4$ , antagonism.

### 5.6.2.4 Time-kill Curve Assay

The kinetics of bacterial killing was measured using *P. aeruginosa* PAO1, as previously described.<sup>59</sup> Overnight bacterial culture was diluted in saline to 0.5 McFarland turbidity and then 1:50 diluted in Luria-Bertani (LB) broth. The cell suspension was incubated with minocycline, rifampicin, or hybrid **3** diluted in PBS (pH 7.2) alone at desired concentrations ( $1/2 \times$ ,  $1 \times$ ,  $2 \times$ ,  $4 \times$  MIC). For synergistic time-kill, the combination of compound **3** with minocycline or rifampicin at various concentrations,  $1/8 + 1/8$ ,  $1/8 + 1/4$ ,  $1/4 + 1/4$ ,  $1/2 + 1/4$ , and  $1/2 + 1/2 \times$  MIC, were determined. Samples were incubated at 37 °C for 6 h. At specific intervals (0, 10, 30,

60, 90, 120, 240, and 360 mins), aliquots (50  $\mu$ L) were removed from the samples, serially diluted in PBS and plated on LB agar plates. Bacterial colonies were formed and counted after 20 h of incubation at 37 °C.

#### **5.6.2.5 Resistance Development Assay**

Wild-type *P. aeruginosa* PAO1 was used to study resistance development against antibiotics by sequential passaging method as previously described.<sup>65</sup> Briefly, MIC testing was first conducted for all drugs or drug combinations to be tested, as described above. After 18 h incubation, the bacterial cells growing in the well of half-MIC concentration were harvested and diluted to 0.5 McFarland in saline followed by 1:50 dilution in fresh MHB broth. The inoculum was subjected to next passage MIC testing, and the process repeated for 25 passages. The fold change in MIC was plotted against the number of passages.

#### **5.6.2.6 Outer Membrane Permeability Assay**

The CFDASE dye was used to determine the outer membrane permeability of drugs against *P. aeruginosa* PAO1, following established protocols.<sup>28</sup> Logarithmic phase *P. aeruginosa* was harvested by centrifugation and washed twice with PBS. The bacterial cells were resuspended in the same buffer to OD<sub>600</sub> of 0.5, followed by staining with CFDASE at 100  $\mu$ M for 30 mins at 37°C. The unbound dye was then removed by washing the cells with excess buffer, and the cells were again resuspended to the initial volume. The bacterial suspension was treated with drugs at 37 °C for 30 mins at desired concentration and the supernatant obtained by centrifugation was transferred to 96-well black plate for measuring the fluorescence at an

excitation wavelength of 488 nm and an emission wavelength of 520 nm using a microplate reader FlexStation 3 (Molecular Devices, Sunnyvale, CA, USA).

#### ***5.6.2.7 Cytoplasmic Membrane Depolarization Assay***

To assess the effect of the compounds on cytoplasmic membrane potential, diSC<sub>3</sub>-5, the membrane-potential-sensitive fluorescent dye was utilized to determine the membrane depolarization of *P. aeruginosa* PAO1 as previously described.<sup>19</sup> Overnight growth *P. aeruginosa* PAO1 was diluted in fresh LB broth and cultured to the mid-log phase. The bacterial cells were harvested and washed three times with 5 mM sodium HEPES buffer, pH 7.4, containing 20 mM glucose, and resuspended to OD<sub>600</sub> of 0.05 in the same buffer. The cell suspension was incubated with 0.2 mM EDTA and 0.4  $\mu$ M DiSC<sub>3</sub>(5) in the dark for 2 h at 37 °C under constant shaking (150 rpm). 100 mM KCl was then added to equilibrate the cytoplasmic and external K<sup>+</sup>, and incubated for additional 30 mins. The depolarization assay was carried out in 96-well black plate by adding the antimicrobial agents to 100  $\mu$ L of the above cell suspension to desired concentration. Fluorescence was monitored using a FlexStation 3 (Molecular Devices, Sunnyvale, CA, USA) microplate reader at an excitation wavelength of 622 nm and an emission wavelength of 670 nm.

#### ***5.6.2.8 Motility Assay***

Cell motility assay was performed on 0.3% (w/v) agar media supplemented with tryptone (5 g/L) and NaCl (2.5 g/L).<sup>66</sup> Antimicrobial agents were added to 25 mL medium to the desired concentration and poured on 100  $\times$  15 mm petri dishes followed by 2 h drying. Overnight *P. aeruginosa* PAO1 culture was diluted in 0.85% saline to 1.0 McFarland and point inoculated into

the center of the motility agar plates. Plates were incubated at 37 °C for 20 h. The images presented were taken using a FluroChem®Q (Cell biosciences).

#### ***5.6.2.9 Quantification of Hemolytic Activity***

The hemolytic activity of the compounds was determined as the amount of hemoglobin released by lysing pig erythrocytes.<sup>67</sup> Fresh pig blood (provided by Dr. Charles M. Nyachoti from University of Manitoba) drawn from pig antecubital were centrifuged at 1,000 × g for 5 mins at 4 °C, washed with PBS thrice, and resuspended in the same buffer. Compounds were 2-fold serially diluted in PBS in 96-well plate and mixed with equal volumes of erythrocyte solution. After 1 h incubation at 37 °C, intact erythrocytes were pelleted by centrifuging at 1,000 × g for 5 mins at 4 °C, and the supernatant was transferred to a new 96-well plate. The hemoglobin release was monitored at 570 nm using an EMax® Plus microplate reader (Molecular Devices, Sunnyvale, CA, USA). Blood cells in PBS and 0.1% Triton X-100 were employed as negative and positive controls respectively.

#### ***5.6.2.10 Cytotoxicity Assay***

DU145 (ATCC, Manassas, VA, USA) and JIMT-1 (DSMZ, Braunschweig, Germany) were cultured and maintained in Dulbecco's modified Eagle's References medium supplemented with 100 U/mL penicillin, 0.1 mg/mL streptomycin, and 10% (v/v) fetal bovine serum (FBS) at 37 °C under a humidified atmosphere of 5% CO<sub>2</sub> and 95% air. The MTS [3-(4,5-dimethylthiazol-2-yl)-5-(3-carboxymethoxyphenyl)-2-(4-sulfonyl)-2H-tetrazolium)] cell viability assay was employed to measure the cytotoxicity of compound **3** as previously described.<sup>16</sup> Briefly, the cells were seeded in 96-well plate with a final concentration of 7500-9000 cells per

well and incubated for 24 h. Then the cells were treated with test compound at final concentrations of 2.5 to 30  $\mu\text{M}$  and incubated for an additional 48 h at the same condition. MTS reagent (20%, v/v) was further added to each well and the plates were incubated for 4 h on a Nutating mixer in the incubator. The optical density was measured using a SpectraMax M2 plate reader (Molecular Devices, Sunnyvale, CA, USA) at 490 nm. Only medium without cells were served as blank and the blank values were subtracted from each sample value. The cell viability relative to the control with vehicle was calculated.

#### ***5.6.2.11 Galleria mellonella Model of P. aeruginosa Infection***

*Galleria mellonella* waxworms were obtained from The Worm Lady<sup>®</sup> Live Feeder Insects (<http://thewormlady.ca/>). Larvae (average weight at 250 mg) were used within 7 days of delivery to determine the survival rate after bacteria or antimicrobials injection using previously described methods.<sup>68</sup> The tolerability study was performed by only injecting antimicrobial agent into the worms at 100 and 200 mg/kg without bacteria. The larvae (ten larvae in each group) were incubated at 37 °C and monitored for 96 h for survival. For therapeutic study, overnight XDR *P. aeruginosa* P262 culture was diluted in PBS to a final concentration of  $1.0 \times 10^3$  CFU/mL. 15 larvae per group were infected with 10  $\mu\text{L}$  bacterial suspensions. After 2 h bacterial challenge, worms in monotherapy experimental groups received a 10  $\mu\text{L}$  injection of minocycline, rifampicin, or compound **3** individually at 75 mg/kg. For combination groups, **3** plus minocycline and **3** plus rifampicin were injected to give final dosages of 12.5 + 12.5, 25 + 25, 37.5 + 37.5, and 75 + 75 mg/kg respectively. Only vehicle (PBS) without antimicrobials was injected as control group. The larvae were monitored for 24 h at 37 °C in petri dishes lined with filter paper and scored for survivability. Larvae considered dead if they do not respond to touch.

## 5.7 ACKNOWLEDGMENTS

The work was supported by NSERC-DG (261311-2013), MHRC, and CIHR (MOP-119335).

## 5.8 REFERENCES

- (1) Brown, D. Antibiotic resistance breakers: can repurposed drugs fill the antibiotic discovery void? *Nat. Rev. Drug Discovery*. **2015**, *14*, 821-832.
- (2) Food and Drug Administration Safety and Innovation Act. Available at: <https://www.gpo.gov/fdsys/pkg/BILLS-112s3187enr/pdf/BILLS-112s3187enr.pdf>. Access date: February 13, 2012.
- (3) Spellberg, B.; Blaser, M.; Guidos, R. J.; Boucher, H. W.; Bradley, J. S.; Eisenstein, B. I.; Gerding, D.; Lynfield, R.; Reller, L. B.; Rex, J.; Schwartz, D.; Septimus, E.; Tenover, F. C.; Gilbert, D. N. Combating antimicrobial resistance: policy recommendations to save lives. *Clin. Infect. Dis.* **2011**, *52 Suppl 5*, S397-428.
- (4) Rice, L. B. Federal funding for the study of antimicrobial resistance in nosocomial pathogens: no ESKAPE. *J. Infect. Dis.* **2008**, *197*, 1079-1081.
- (5) Wagner, S.; Sommer, R.; Hinsberger, S.; Lu, C.; Hartmann, R. W.; Empting, M.; Titz, A. Novel strategies for the treatment of *Pseudomonas aeruginosa* infections. *J. Med. Chem.* **2016**, *59*, 5929-5969.
- (6) Oliver, A.; Mulet, X.; Lopez-Causape, C.; Juan, C. The increasing threat of *Pseudomonas aeruginosa* high-risk clones. *Drug Resist. Updates* **2015**, *21-22*, 41-59.
- (7) Nikaido, H. Prevention of drug access to bacterial targets: permeability barriers and active efflux. *Science* **1994**, *264*, 382-388.

- (8) Breidenstein, E. B.; de la Fuente-Nunez, C.; Hancock, R. E. *Pseudomonas aeruginosa*: all roads lead to resistance. *Trends Microbiol.* **2011**, *19*, 419-426.
- (9) Livermore, D. M. Multiple mechanisms of antimicrobial resistance in *Pseudomonas aeruginosa*: our worst nightmare? *Clin. Infect. Dis.* **2002**, *34*, 634-640.
- (10) Drusano, G. L.; Liu, W.; Fregeau, C.; Kulawy, R.; Louie, A. Differing effects of combination chemotherapy with meropenem and tobramycin on cell kill and suppression of resistance of wild-type *Pseudomonas aeruginosa* PAO1 and its isogenic MexAB efflux pump-overexpressed mutant. *Antimicrob. Agents Chemother.* **2009**, *53*, 2266-2273.
- (11) Paul, M.; Carmeli, Y.; Durante-Mangoni, E.; Mouton, J. W.; Tacconelli, E.; Theuretzbacher, U.; Mussini, C.; Leibovici, L. Combination therapy for carbapenem-resistant Gram-negative bacteria. *J. Antimicrob. Chemother.* **2014**, *69*, 2305-2309.
- (12) Louie, A.; Liu, W.; VanGuilder, M.; Neely, M. N.; Schumitzky, A.; Jelliffe, R.; Fikes, S.; Kurhanewicz, S.; Robbins, N.; Brown, D.; Baluya, D.; Drusano, G. L. Combination treatment with meropenem plus levofloxacin is synergistic against *Pseudomonas aeruginosa* infection in a murine model of pneumonia. *J. Infect. Dis.* **2015**, *211*, 1326-1333.
- (13) Rigatto, M. H.; Vieira, F. J.; Antochevis, L. C.; Behle, T. F.; Lopes, N. T.; Zavascki, A. P. Polymyxin B in combination with antimicrobials lacking *in vitro* activity versus polymyxin B in monotherapy in critically ill patients with *Acinetobacter baumannii* or *Pseudomonas aeruginosa* infections. *Antimicrob. Agents Chemother.* **2015**, *59*, 6575-6580.
- (14) Lehar, J.; Zimmermann, G. R.; Krueger, A. S.; Molnar, R. A.; Ledell, J. T.; Heilbut, A. M.; Short, G. F., 3rd; Giusti, L. C.; Nolan, G. P.; Magid, O. A.; Lee, M. S.; Borisy, A. A.; Stockwell, B. R.; Keith, C. T. Chemical combination effects predict connectivity in biological systems. *Mol. Syst. Biol.* **2007**, *3*, 80.

- (15) Zabawa, T. P.; Pucci, M. J.; Parr, T. R., Jr.; Lister, T. Treatment of Gram-negative bacterial infections by potentiation of antibiotics. *Curr. Opin. Microbiol.* **2016**, *33*, 7-12.
- (16) Gorityala, B. K.; Guchhait, G.; Fernando, D. M.; Deo, S.; McKenna, S. A.; Zhanel, G. G.; Kumar, A.; Schweizer, F. Adjuvants based on hybrid antibiotics overcome resistance in *Pseudomonas aeruginosa* and enhance fluoroquinolone efficacy. *Angew. Chem., Int. Ed. Engl.* **2016**, *55*, 555-559.
- (17) Gorityala, B. K.; Guchhait, G.; Goswami, S.; Fernando, D. M.; Kumar, A.; Zhanel, G. G.; Schweizer, F. Hybrid antibiotic overcomes resistance in *P. aeruginosa* by enhancing outer membrane penetration and reducing efflux. *J. Med. Chem.* **2016**, *59*, 8441-8455.
- (18) Chang, C. W.; Takemoto, J. Y. Antifungal amphiphilic aminoglycosides. *MedChemComm* **2014**, *5*, 1048-1057.
- (19) Ouberai, M.; El Garch, F.; Bussiere, A.; Riou, M.; Alsteens, D.; Lins, L.; Baussanne, I.; Dufrene, Y. F.; Brasseur, R.; Decout, J. L.; Mingeot-Leclercq, M. P. The *Pseudomonas aeruginosa* membranes: a target for a new amphiphilic aminoglycoside derivative? *Biochim. Biophys. Acta, Biomembr.* **2011**, *1808*, 1716-1727.
- (20) Shrestha, S. K.; Fosso, M. Y.; Green, K. D.; Garneau-Tsodikova, S. Amphiphilic tobramycin analogues as antibacterial and antifungal agents. *Antimicrob. Agents Chemother.* **2015**, *59*, 4861-4869.
- (21) Herzog, I. M.; Green, K. D.; Berkov-Zrihen, Y.; Feldman, M.; Vidavski, R. R.; Eldar-Boock, A.; Satchi-Fainaro, R.; Eldar, A.; Garneau-Tsodikova, S.; Fridman, M. 6"-Thioether tobramycin analogues: towards selective targeting of bacterial membranes. *Angew. Chem., Int. Ed. Engl.* **2012**, *51*, 5652-5656.

- (22) Guchhait, G.; Altieri, A.; Gorityala, B.; Yang, X.; Findlay, B.; Zhanel, G. G.; Mookherjee, N.; Schweizer, F. Amphiphilic tobramycins with immunomodulatory properties. *Angew. Chem., Int. Ed. Engl.* **2015**, *54*, 6278-6282.
- (23) Ghosh, C.; Manjunath, G. B.; Akkapeddi, P.; Yarlagadda, V.; Hoque, J.; Uppu, D. S.; Konai, M. M.; Haldar, J. Small molecular antibacterial peptoid mimics: the simpler the better! *J. Med. Chem.* **2014**, *57*, 1428-1436.
- (24) Hanessian, S.; Tremblay, M.; Swayze, E. E. Tobramycin analogues with C-5 aminoalkyl ether chains intended to mimic rings III and IV of paromomycin. *Tetrahedron* **2003**, *59*, 983-993.
- (25) Odds, F. C. Synergy, antagonism, and what the chequerboard puts between them. *J. Antimicrob. Chemother.* **2003**, *52*, 1.
- (26) Clinical and Laboratory Standards Institute (CLSI). Performance standards for antimicrobial susceptibility testing. 24th informational supplement. CLSI document M100-S24. Wayne, PA: CLSI, 2014.
- (27) Piddock, L. J. Clinically relevant chromosomally encoded multidrug resistance efflux pumps in bacteria. *Clin. Microbiol. Rev.* **2006**, *19*, 382-402.
- (28) Adhikari, M. D.; Das, G.; Ramesh, A. Retention of nisin activity at elevated pH in an organic acid complex and gold nanoparticle composite. *Chem. Commun. (Cambridge, U. K.)* **2012**, *48*, 8928-8930.
- (29) Sampson, T. R.; Liu, X.; Schroeder, M. R.; Kraft, C. S.; Burd, E. M.; Weiss, D. S. Rapid killing of *Acinetobacter baumannii* by polymyxins is mediated by a hydroxyl radical death pathway. *Antimicrob. Agents Chemother.* **2012**, *56*, 5642-5649.

- (30) Paulsen, I. T.; Brown, M. H.; Skurray, R. A. Proton-dependent multidrug efflux systems. *Microbiol. Rev.* **1996**, *60*, 575-608.
- (31) Farha, M. A.; Verschoor, C. P.; Bowdish, D.; Brown, E. D. Collapsing the proton motive force to identify synergistic combinations against *Staphylococcus aureus*. *Chem. Biol.* **2013**, *20*, 1168-1178.
- (32) Urban, C.; Mariano, N.; Rahal, J. J. *In vitro* double and triple bactericidal activities of doripenem, polymyxin B, and rifampin against multidrug-resistant *Acinetobacter baumannii*, *Pseudomonas aeruginosa*, *Klebsiella pneumoniae*, and *Escherichia coli*. *Antimicrob. Agents Chemother.* **2010**, *54*, 2732-2734.
- (33) Goldberg, K.; Sarig, H.; Zaknoon, F.; Eband, R. F.; Eband, R. M.; Mor, A. Sensitization of Gram-negative bacteria by targeting the membrane potential. *FASEB J.* **2013**, *27*, 3818-3826.
- (34) Zhanel, G. G.; Lawson, C. D.; Adam, H.; Schweizer, F.; Zelenitsky, S.; Lagace-Wiens, P. R.; Denisuik, A.; Rubinstein, E.; Gin, A. S.; Hoban, D. J.; Lynch, J. P., 3rd; Karlowsky, J. A. Ceftazidime-avibactam: a novel cephalosporin/beta-lactamase inhibitor combination. *Drugs* **2013**, *73*, 159-177.
- (35) Zhanel, G. G.; Chung, P.; Adam, H.; Zelenitsky, S.; Denisuik, A.; Schweizer, F.; Lagace-Wiens, P. R.; Rubinstein, E.; Gin, A. S.; Walkty, A.; Hoban, D. J.; Lynch, J. P., 3rd; Karlowsky, J. A. Ceftolozane/tazobactam: a novel cephalosporin/beta-lactamase inhibitor combination with activity against multidrug-resistant Gram-negative bacilli. *Drugs* **2014**, *74*, 31-51.

- (36) Heyland, D. K.; Dodek, P.; Muscedere, J.; Day, A.; Cook, D. Randomized trial of combination versus monotherapy for the empiric treatment of suspected ventilator-associated pneumonia. *Crit. Care Med.* **2008**, *36*, 737-744.
- (37) Bulitta, J. B.; Ly, N. S.; Landersdorfer, C. B.; Wanigaratne, N. A.; Velkov, T.; Yadav, R.; Oliver, A.; Martin, L.; Shin, B. S.; Forrest, A.; Tsuji, B. T. Two mechanisms of killing of *Pseudomonas aeruginosa* by tobramycin assessed at multiple inocula via mechanism-based modeling. *Antimicrob. Agents Chemother.* **2015**, *59*, 2315-2327.
- (38) Hancock, R. E.; Farmer, S. W.; Li, Z. S.; Poole, K. Interaction of aminoglycosides with the outer membranes and purified lipopolysaccharide and OmpF porin of *Escherichia coli*. *Antimicrob. Agents Chemother.* **1991**, *35*, 1309-1314.
- (39) Loh, B.; Grant, C.; Hancock, R. E. Use of the fluorescent probe 1-N-phenyl-naphthylamine to study the interactions of aminoglycoside antibiotics with the outer membrane of *Pseudomonas aeruginosa*. *Antimicrob. Agents Chemother.* **1984**, *26*, 546-551.
- (40) Chen, Y.; Guarnieri, M. T.; Vasil, A. I.; Vasil, M. L.; Mant, C. T.; Hodges, R. S. Role of peptide hydrophobicity in the mechanism of action of alpha-helical antimicrobial peptides. *Antimicrob. Agents Chemother.* **2007**, *51*, 1398-1406.
- (41) Domalaon, R.; Zhanel, G. G.; Schweizer, F. Short antimicrobial peptides and peptide scaffolds as promising antibacterial agents. *Curr. Top. Med. Chem.* **2016**, *16*, 1217-1230.
- (42) Yamaguchi, A.; Ohmori, H.; Kaneko-Ohdera, M.; Nomura, T.; Sawai, T. Delta pH-dependent accumulation of tetracycline in *Escherichia coli*. *Antimicrob. Agents Chemother.* **1991**, *35*, 53-56.
- (43) Taber, H. W.; Mueller, J. P.; Miller, P. F.; Arrow, A. S. Bacterial uptake of aminoglycoside antibiotics. *Microbiol. Rev.* **1987**, *51*, 439-457.

- (44) Bakker, E. P.; Mangerich, W. E. Interconversion of components of the bacterial proton motive force by electrogenic potassium transport. *J. Bacteriol.* **1981**, *147*, 820-826.
- (45) Paul, K.; Erhardt, M.; Hirano, T.; Blair, D. F.; Hughes, K. T. Energy source of flagellar type III secretion. *Nature* **2008**, *451*, 489-492.
- (46) Kaneti, G.; Meir, O.; Mor, A. Controlling bacterial infections by inhibiting proton-dependent processes. *Biochim. Biophys. Acta, Biomembr.* **2016**, *1858*, 995-1003.
- (47) Dean, C. R.; Visalli, M. A.; Projan, S. J.; Sum, P. E.; Bradford, P. A. Efflux-mediated resistance to tigecycline (GAR-936) in *Pseudomonas aeruginosa* PAO1. *Antimicrob. Agents Chemother.* **2003**, *47*, 972-978.
- (48) Sun, J.; Deng, Z.; Yan, A. Bacterial multidrug efflux pumps: mechanisms, physiology and pharmacological exploitations. *Biochem. Biophys. Res. Commun.* **2014**, *453*, 254-267.
- (49) Jeannot, K.; Sobel, M. L.; El Garch, F.; Poole, K.; Plesiat, P. Induction of the MexXY efflux pump in *Pseudomonas aeruginosa* is dependent on drug-ribosome interaction. *J. Bacteriol.* **2005**, *187*, 5341-5346.
- (50) Kohler, T.; Kok, M.; Michea-Hamzhepour, M.; Plesiat, P.; Gotoh, N.; Nishino, T.; Curty, L. K.; Pechere, J. C. Multidrug efflux in intrinsic resistance to trimethoprim and sulfamethoxazole in *Pseudomonas aeruginosa*. *Antimicrob. Agents Chemother.* **1996**, *40*, 2288-2290.
- (51) Schulz, W.; Zillig, W. Rifampicin inhibition of RNA synthesis by destabilisation of DNA-RNA polymerase-oligonucleotide-complexes. *Nucleic Acids Res.* **1981**, *9*, 6889-6906.
- (52) Jammal, J.; Zaknoon, F.; Kaneti, G.; Goldberg, K.; Mor, A. Sensitization of Gram-negative bacteria to rifampin and OAK combinations. *Sci. Rep.* **2015**, *5*, 9216.

- (53) Timurkaynak, F.; Can, F.; Azap, O. K.; Demirbilek, M.; Arslan, H.; Karaman, S. O. *In vitro* activities of non-traditional antimicrobials alone or in combination against multidrug-resistant strains of *Pseudomonas aeruginosa* and *Acinetobacter baumannii* isolated from intensive care units. *Int. J. Antimicrob. Agents* **2006**, *27*, 224-228.
- (54) Smilack, J. D. The tetracyclines. *Mayo Clin. Proc.* **1999**, *74*, 727-729.
- (55) Brenes-Salazar, J. A. Minocycline: a bacteriostatic antibiotic with pleiotropic cardioprotective effects. *Can. J. Physiol. Pharmacol.* **2015**, *93*, 863-866.
- (56) Tew, G. N.; Clements, D.; Tang, H.; Arnt, L.; Scott, R. W. Antimicrobial activity of an abiotic host defense peptide mimic. *Biochim. Biophys. Acta, Biomembr.* **2006**, *1758*, 1387-1392.
- (57) Koh, J. J.; Lin, S.; Aung, T. T.; Lim, F.; Zou, H.; Bai, Y.; Li, J.; Lin, H.; Pang, L. M.; Koh, W. L.; Salleh, S. M.; Lakshminarayanan, R.; Zhou, L.; Qiu, S.; Pervushin, K.; Verma, C.; Tan, D. T.; Cao, D.; Liu, S.; Beuerman, R. W. Amino acid modified xanthone derivatives: novel, highly promising membrane-active antimicrobials for multidrug-resistant Gram-positive bacterial infections. *J. Med. Chem.* **2015**, *58*, 739-752.
- (58) Bremner, J. B.; Keller, P. A.; Pyne, S. G.; Boyle, T. P.; Brkic, Z.; David, D. M.; Garas, A.; Morgan, J.; Robertson, M.; Somphol, K.; Miller, M. H.; Howe, A. S.; Ambrose, P.; Bhavnani, S.; Fritsche, T. R.; Biedenbach, D. J.; Jones, R. N.; Buckheit, R. W., Jr.; Watson, K. M.; Baylis, D.; Coates, J. A.; Deadman, J.; Jeevarajah, D.; McCracken, A.; Rhodes, D. I. Binaphthyl-based dicationic peptoids with therapeutic potential. *Angew. Chem., Int. Ed. Engl.* **2010**, *49*, 537-540.
- (59) Dong, N.; Zhu, X.; Chou, S.; Shan, A.; Li, W.; Jiang, J. Antimicrobial potency and selectivity of simplified symmetric-end peptides. *Biomaterials* **2014**, *35*, 8028-8039.

- (60) Cook, S. M.; McArthur, J. D. Developing *Galleria mellonella* as a model host for human pathogens. *Virulence* **2013**, *4*, 350-353.
- (61) Zhanel, G. G.; DeCorby, M.; Laing, N.; Weshnoweski, B.; Vashisht, R.; Taylor, F.; Nichol, K. A.; Wierzbowski, A.; Baudry, P. J.; Karlowsky, J. A.; Lagace-Wiens, P.; Walkty, A.; McCracken, M.; Mulvey, M. R.; Johnson, J.; Hoban, D. J. Antimicrobial-resistant pathogens in intensive care units in Canada: results of the Canadian National Intensive Care Unit (CAN-ICU) study, 2005-2006. *Antimicrob. Agents Chemother.* **2008**, *52*, 1430-1437.
- (62) Zhanel, G. G.; Adam, H. J.; Baxter, M. R.; Fuller, J.; Nichol, K. A.; Denisuik, A. J.; Lagace-Wiens, P. R.; Walkty, A.; Karlowsky, J. A.; Schweizer, F.; Hoban, D. J. Antimicrobial susceptibility of 22746 pathogens from Canadian hospitals: results of the CANWARD 2007-11 study. *J. Antimicrob. Chemother.* **2013**, *68 Suppl 1*, i7-22.
- (63) Zhanel, G. G.; DeCorby, M.; Adam, H.; Mulvey, M. R.; McCracken, M.; Lagace-Wiens, P.; Nichol, K. A.; Wierzbowski, A.; Baudry, P. J.; Taylor, F.; Karlowsky, J. A.; Walkty, A.; Schweizer, F.; Johnson, J.; Hoban, D. J. Prevalence of antimicrobial-resistant pathogens in Canadian hospitals: results of the Canadian Ward Surveillance Study (CANWARD 2008). *Antimicrob. Agents Chemother.* **2010**, *54*, 4684-4693.
- (64) Orhan, G.; Bayram, A.; Zer, Y.; Balci, I. Synergy tests by E test and checkerboard methods of antimicrobial combinations against *Brucella melitensis*. *J. Clin. Microbiol.* **2005**, *43*, 140-143.
- (65) Ling, L. L.; Schneider, T.; Peoples, A. J.; Spoering, A. L.; Engels, I.; Conlon, B. P.; Mueller, A.; Schaberle, T. F.; Hughes, D. E.; Epstein, S.; Jones, M.; Lazarides, L.; Steadman, V. A.; Cohen, D. R.; Felix, C. R.; Fetterman, K. A.; Millett, W. P.; Nitti, A. G.;

- Zullo, A. M.; Chen, C.; Lewis, K. A new antibiotic kills pathogens without detectable resistance. *Nature* **2015**, *517*, 455-459.
- (66) Ejim, L.; Farha, M. A.; Falconer, S. B.; Wildenhain, J.; Coombes, B. K.; Tyers, M.; Brown, E. D.; Wright, G. D. Combinations of antibiotics and nonantibiotic drugs enhance antimicrobial efficacy. *Nat. Chem. Biol.* **2011**, *7*, 348-350.
- (67) Stark, M.; Liu, L. P.; Deber, C. M. Cationic hydrophobic peptides with antimicrobial activity. *Antimicrob. Agents Chemother.* **2002**, *46*, 3585-3590.
- (68) Krezdorn, J.; Adams, S.; Coote, P. J. A *Galleria mellonella* infection model reveals double and triple antibiotic combination therapies with enhanced efficacy versus a multidrug-resistant strain of *Pseudomonas aeruginosa*. *J. Med. Microbiol.* **2014**, *63*, 945-955.

## **Chapter 6: Amphiphilic Nebramine-based Hybrids Rescue Legacy Antibiotics from Intrinsic Resistance in Multidrug-resistant Gram-negative Bacilli**

*By Xuan Yang, Derek Ammeter, Temilolu Idowu, Ronald Domalaon, Marc Brizuela, Oreofe Okunnu, Liting Bi, Yanelis Acebo Guerrero, George G. Zhanel, Ayush Kumar, and Frank Schweizer. First published in European Journal of Medicinal Chemistry, 175, 2019, 187-200. Reproduced with permission.*

Contributions of Authors: *Xuan Yang was responsible for designing the conjugates on the advice of Frank Schweizer. Xuan Yang conducted most of the synthetic work. Dereck Ammeter and Temilolu Idowu synthesized the NEB-CIP compound. Liting Bi was involved in the synthesis of a few intermediates. Xuan Yang, Marc Brizuela, Oreofe Okunnu, and Yanelis Acebo Guerrero performed the biological assays. Temilolu Idowu did the in vivo studies. Xuan Yang wrote the preliminary draft, that was annotated by Ronald Domalaon, Temilolu Idowu, George G. Zhane, Ayush Kuma and Frank Schweizer.*

### **6.1 ABSTRACT**

The inability to discover novel classes of antibacterial agents, especially against Gram-negative bacteria (GNB), compels us to consider a broader non-conventional approach to treat infections caused by multidrug-resistant (MDR) bacteria. One such approach is the use of adjuvants capable of revitalizing the activity of current existing antibiotics from resistant

pathogens. Recently, our group reported a series of tobramycin (TOB)-based hybrid adjuvants that were able to potentiate multiple classes of legacy antibiotics against various MDR GNB. Herein, we report the modification of TOB-based hybrid adjuvants by replacing the TOB domain by the pseudo-disaccharide nebramine (NEB) through selective cleavage of the  $\alpha$ -D-glucopyranosyl linkage of TOB. Potent synergism was found for combinations of NEB-based hybrid adjuvants with multiple classes of legacy antibiotics including fluoroquinolones (moxifloxacin and ciprofloxacin), tetracyclines (minocycline), or rifamycin (rifampicin) against both wild-type and MDR *P. aeruginosa* clinical isolates. We also demonstrated that a combination of the optimized NEB-CIP hybrid **1b** and rifampicin protects *Galleria mellonella* larvae from the lethal effects of extensively drug-resistant (XDR) *P. aeruginosa*. Mechanistic evaluation of NEB-based hybrid adjuvants revealed that the hybrids affect the outer- and inner membranes of wild-type *P. aeruginosa* PAO1. This study describes an approach to optimize aminoglycoside-based hybrids to yield lead adjuvant candidates that are able to resuscitate the activity of partner antibiotics against MDR GNB.

## 6.2 INTRODUCTION

Starting from Fleming's discovery of penicillin in 1929,<sup>1</sup> a large number of antibiotics have been discovered, developed, and marketed. Antibiotics have saved countless lives and played a key role in the advancement of medical science for the past 70 years.<sup>2,3</sup> However, rampant and indiscriminate use of antibiotics has escalated the prevalence of multidrug-resistant (MDR) bacterial infections, especially those that are caused by Gram-negative pathogens. Worse still, there is a steady decline in the discovery of novel drug classes able to eradicate MDR Gram-negative pathogens which is largely due to the lack of understanding of the

physicochemical properties necessary for antibacterial agents to efficiently traverse and accumulate inside Gram-negative bacterial cell.<sup>4,5</sup> There is an urgent need to find novel and perhaps unconventional approaches to address bacterial infection. Co-administration of helper molecules called adjuvants capable of enhancing the activity of currently used antibiotics and extend the life of legacy antibiotics is a viable strategy to overcome antimicrobial resistance.<sup>6,7</sup>

Our group recently has demonstrated that amphiphilic TOB-based conjugates were able to revive the antibacterial activity of multiple classes of antibiotics against MDR Gram-negative bacilli (GNB), especially against *P. aeruginosa*.<sup>7-14</sup> For example, we first reported TOB-ciprofloxacin hybrids with poor intrinsic antibacterial activity were able to restore the activity of fluoroquinolone antibiotics against ciprofloxacin-resistant MDR or XDR (extensively drug-resistant) *Pseudomonas aeruginosa* in combination therapy.<sup>8</sup> Structure-activity studies revealed that the presence of both TOB and ciprofloxacin pharmacophores tethered by a 12-carbon-long (C<sub>12</sub>) aliphatic linker is critical to the potentiation of fluoroquinolone antibiotics. Encouraged by these results, an unconventional structure-activity relationship study was pursued by replacing the ciprofloxacin fragment of TOB-ciprofloxacin hybrid by other pharmacophores. Since then, we have developed a series of TOB-moxifloxacin hybrids,<sup>9</sup> TOB-efflux pump inhibitors conjugates,<sup>11,14</sup> TOB-lysine peptoid conjugates,<sup>10,13</sup> as well as TOB-polymyxin B<sub>3</sub> hybrids.<sup>12</sup> Biological evaluations revealed that these TOB-based conjugates retained the adjuvant properties of TOB-ciprofloxacin hybrids to a variable extent. These results suggest that the TOB fragment linked to C<sub>12</sub> tether is the core scaffold that is responsible for the adjuvant properties. Mechanistic studies revealed that these TOB-based conjugates permeabilize the outer membrane and dissipate the proton motive force (PMF) located in the cytoplasmic membrane of *P. aeruginosa*.<sup>9-11</sup>

TOB is known to eradicate Gram-negative bacteria by disruption of the outer membrane at higher concentrations ( $\geq 8 \mu\text{g/mL}$ ).<sup>15</sup> However, at lower concentrations ( $< 4 \mu\text{g/mL}$ ), TOB, selectively interacts with the 16S rRNA, thereby causing inhibition of bacterial protein translation.<sup>15,16</sup> TOB's pseudo-disaccharide segment (ring I and ring II), namely NEB (NEB), is the essential pharmacophore responsible for most of the specificity of the interactions with the ribosome.<sup>17-21</sup> In addition, it was recently reported that an amphiphilic NEB derivative displayed potent activity against certain TOB-resistant Gram-negative bacteria suggesting that amphiphilic NEB analogs possess a different mode of action than TOB.<sup>22</sup> In addition, neamine-based and neosamine-based amphiphiles have been reported to possess potent antipseudomonal properties by interacting with the outer membrane of *P. aeruginosa*.<sup>23-25</sup>

To understand the effect of TOB on the overall adjuvant activity of previously reported TOB-based conjugates, we decided to replace TOB by NEB and evaluate its microbiological activity. We questioned whether the modified TOB domain would retain the adjuvant properties of our reported conjugates. To accomplish this aim, we selected TOB-moxifloxacin and TOB-ciprofloxacin as lead compounds and replaced TOB by NEB, while keeping the moxifloxacin (MOX) and ciprofloxacin (CIP) fragments and the  $C_{12}$  hydrocarbon tether as shown in hybrid NEB-MOX (**1a**) and NEB-CIP (**1b**) (Figure 6.2.1). In addition, we also prepared a NEB-NMP (1-(1-naphthylmethyl)-piperazine) hybrid **2** containing a slightly reduced  $C_{10}$  hydrocarbon tether to potentially reduce non-specific protein binding and investigated its adjuvant properties. NMP is a well-known efflux pump inhibitor (EPI) of various efflux pumps in Gram-negative bacteria except *P. aeruginosa*.<sup>26</sup>

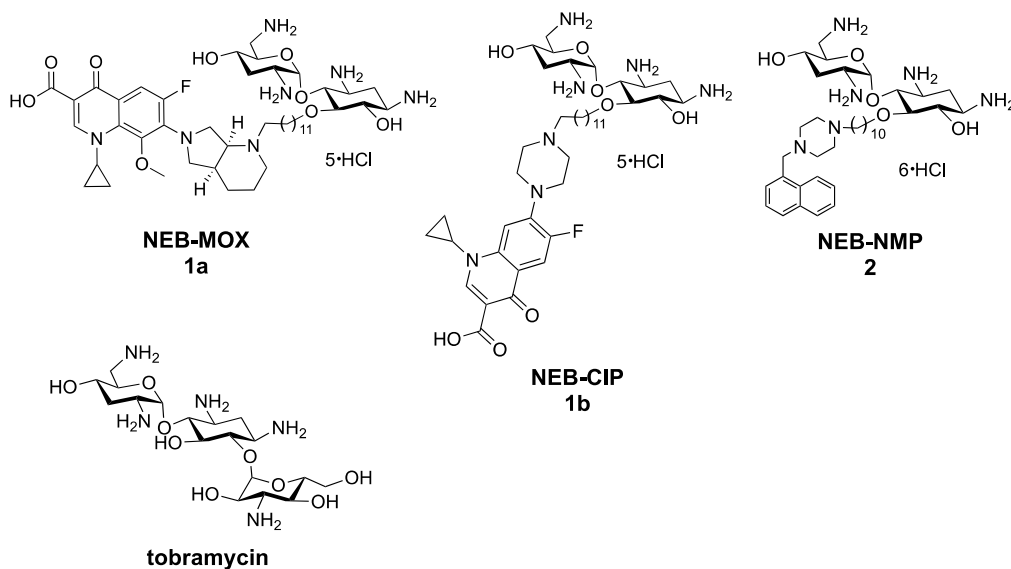


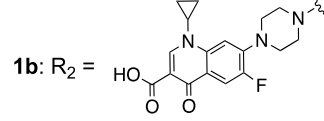
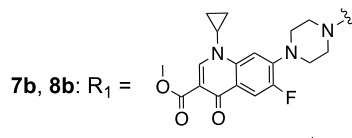
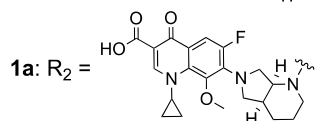
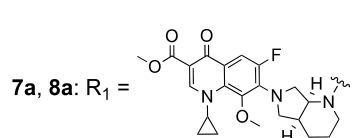
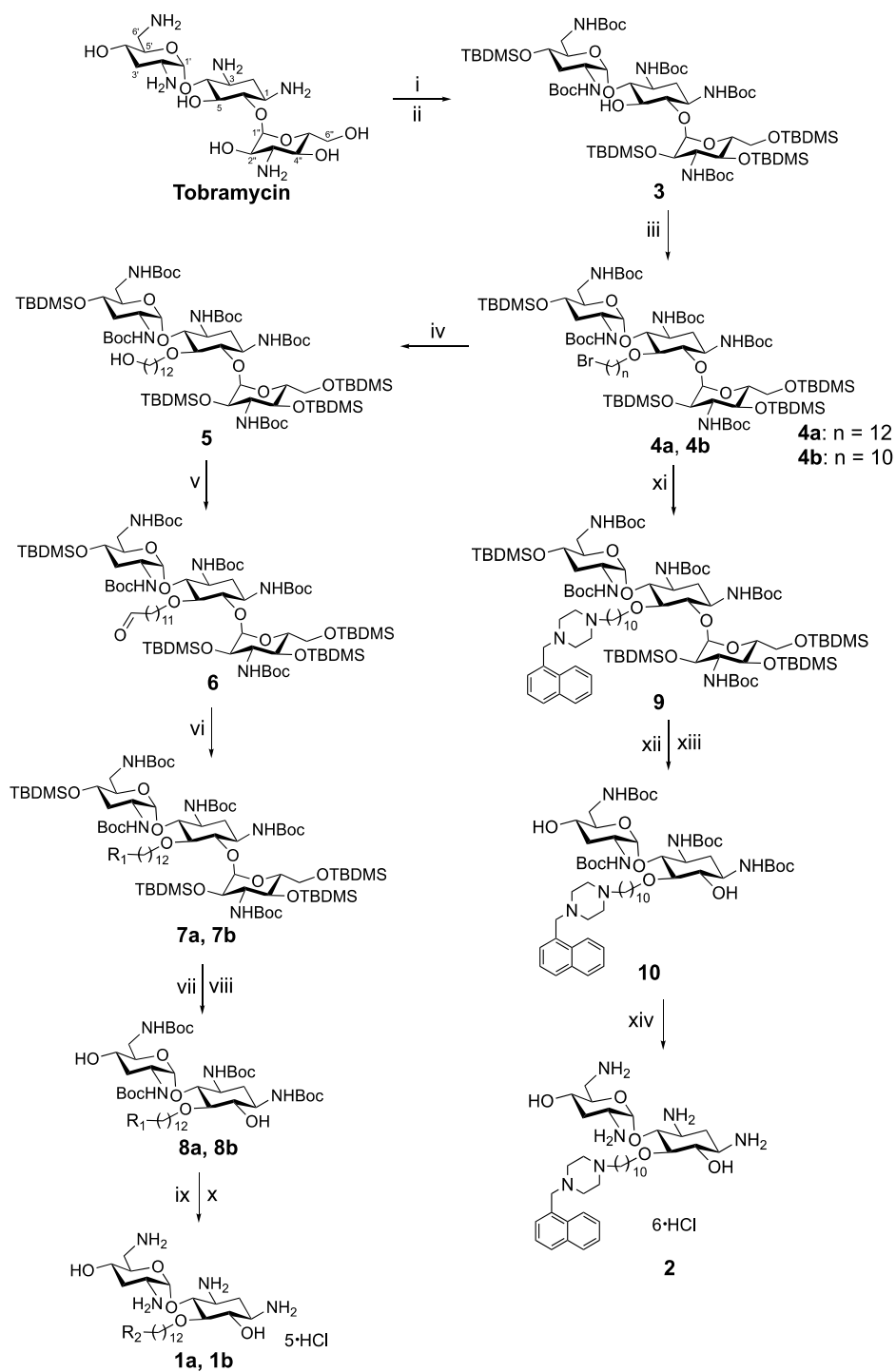
**Figure 6.2.1.** Structures of the nebramine-moxifloxacin (NEB-MOX) hybrid **1a**, nebramine-ciprofloxacin (NEB-CIP) hybrid **1b**, nebramine-NMP (NEB-NMP) hybrid **2**, and tobramycin.

## 6.3 RESULTS AND DISCUSSION

### 6.3.1 Chemistry

The preparation of NEB-based hybrids (**1a**, **1b**, and **2**) were done by selective degradation of TOB-based hybrids as outlined in Scheme 6.3.1.1. Commercially available tobramycin was transformed into the *N*-Boc-, and *O*-TBDMS-protected tobramycin **3** with the exception of the sterically hindered C-5 alcohol, following previously reported procedures (Scheme 6.3.1.1).<sup>9–11,27</sup> Alkylation of **3** with 1,12-dibromododecane or 1,10-dibromodecane in the presence of a phase transfer catalyst, tetrabutylammonium hydrogen sulfate (TBAHS), afforded bromoalkylated tobramycin (**4a** and **4b**). This bromide (**4a**) was then converted to primary alcohol **5** followed by an oxidation reaction using pyridinium chlorochromate (PCC) to generate aldehyde **6** in good yield. Protected hybrid **7a** and **7b** were synthesized via reductive

amination between moxifloxacin methyl ester or ciprofloxacin methyl ester and aldehyde **6**. Heating hybrids **7a** and **7b** in aqueous HCl solution resulted in regioselective hydrolysis of the  $\alpha$ -D-glucopyranosyl bond<sup>21,22</sup> along with the simultaneous removal of Boc and TBDMS protecting groups. To avoid a laborious separation and purification of the obtained pseudo-disaccharides, NEB-MOX and NEB-CIP hybrids, the four free amino groups of NEB were protected by (Boc)<sub>2</sub>O to afford the corresponding *N*-Boc-protected NEB-MOX hybrid **8a** and *N*-Boc-protected NEB-CIP hybrid **8b** that could easily be purified by flash chromatography. De-esterification and subsequent global deprotection of the amino groups finally resulted in the desired the NEB-MOX (**1a**) and NEB-CIP (**1b**) compounds (Scheme 6.3.1.1). A related strategy was used to synthesize NEB-NMP (**2**) (Scheme 6.3.1.1).



**Scheme 6.3.1.1.** Synthesis of NEB-MOX (**1a**), NEB-CIP (**1b**), and NEB-NMP (**2**). Reagents and conditions: (i) (Boc)<sub>2</sub>O, Et<sub>3</sub>N, MeOH/H<sub>2</sub>O (2:1), rt to 55 °C, overnight, 97%. (ii) TBDMS-Cl, 1-methylimidazole, DMF, N<sub>2</sub>, rt, 4 days, 90%. (iii) 1,12-dibromododecane or 1,10-dibromodecane, KOH, TBAHS, toluene, rt, overnight, 78–81%. (iv) Cs<sub>2</sub>CO<sub>3</sub>, H<sub>2</sub>O, DMF, 75 °C, 8 h, 67%. (v) PCC, NaOAc, DCM, rt, 2 h, 90%. (vi) moxifloxacin methyl ester, NaBH(OAc)<sub>3</sub>, AcOH, DCE, rt, 93% for **7a**, 69% for **7b**; (vii) 40% HCl, MeOH, 70 °C, 48 h. (viii) (Boc)<sub>2</sub>O, Et<sub>3</sub>N, MeOH, 55 °C, overnight, 65% for **8a**, 31% for **8b** (two steps). (ix) 2 N LiOH, MeOH, rt, 30 min. (x) TFA/H<sub>2</sub>O 2:1 (v/v), rt, 2 h, 52% for **1a**, 32% for **1b**. (xi) NMP (1-(1-naphthylmethyl)piperazine), K<sub>2</sub>CO<sub>3</sub>, DMF, 75 °C, 50%. (xii) 40% HCl, MeOH, 65 °C, 48 h. (xiii) (Boc)<sub>2</sub>O, Et<sub>3</sub>N, MeOH/H<sub>2</sub>O (2/1, v/v), rt to 55 °C, overnight, 53% (two steps). (xiv) TFA/H<sub>2</sub>O (2/1, v/v), rt, 30 min, 72%.

### 6.3.2 Combination Study of Hybrids with Antibiotics

To determine whether the NEB-MOX hybrid **1a** retained the adjuvant properties of previously reported TOB-moxifloxacin hybrids, checkerboard studies were performed. Initially, we assessed the combination of hybrid **1a** with three different classes of clinically-used antibiotics including the fluoroquinolone antibiotic moxifloxacin, the tetracycline antibiotic minocycline, and the rifamycin antibiotic rifampicin against wild-type *P. aeruginosa* PAO1 (Table 6.3.2.1) by using the fractional inhibitory concentration index (FICI) as a measure of the interaction between two agents. FICI of  $\leq 0.5$ ,  $>0.5$  to  $\leq 4$ , and  $>4$  indicate synergy, no interaction, and antagonism, respectively.<sup>28</sup> In accordance with previous findings against wild-type *P. aeruginosa* PAO1,<sup>8,10,11</sup> NEB-MOX hybrid **1a** displayed weak antibacterial activity (MIC = 32  $\mu\text{g/mL}$ ) as a stand-alone agent. However, it was found to be synergistic (FICI of 0.25) with the fluoroquinolone moxifloxacin (Table 6.3.2.1). Synergism was also observed with minocycline

(FICI of 0.38) as well as the outer membrane-impermeable antibiotic rifampicin (FICI of 0.07) (Table 6.3.2.1). The absolute MICs [the MIC of antibiotics in the presence of 8  $\mu\text{g/mL}$  (7.5  $\mu\text{M}$ ) hybrid **1a**] of three tested antibiotics, moxifloxacin, minocycline, or rifampicin, in combination therapy with hybrid **1a** were significantly reduced compared to monotherapy, especially for rifampicin ( $\geq 256$ -fold potentiation). It should be noted that the clinically-approved  $\beta$ -lactamase inhibitor avibactam is typically administered at 15  $\mu\text{M}$  concentration to potentiate the cephalosporin ceftazidime in *in vitro* studies.<sup>29,30</sup>

**Table 6.3.2.1.** Combination studies of NEB-MOX **1a** with moxifloxacin (MOX), minocycline (MIN) or rifampicin (RIF) against wild-type *P. aeruginosa* PAO1 strain.

Antibiotic (MIC <sup>a</sup> )	Hybrid (MIC <sup>a</sup> )	FICI	Absolute MIC <sup>b</sup>	Potentiation (fold) <sup>c</sup>
MOX (1)	<b>1a</b> (32)	0.25	0.13	8
MIN (8)	<b>1a</b> (32)	0.38	1	8
RIF (8)	<b>1a</b> (32)	0.07	$\leq 0.03$	$\geq 256$

<sup>a</sup> All MIC data presented in  $\mu\text{g/mL}$ . <sup>b</sup> Absolute MIC ( $\mu\text{g/mL}$ ) of antibiotic was determined in the presence of 8  $\mu\text{g/mL}$  (7.5  $\mu\text{M}$ ) of hybrid **1a**. <sup>c</sup> Antibiotic activity potentiation at 8  $\mu\text{g/mL}$  (7.5  $\mu\text{M}$ ) of hybrid **1a**.

To validate our findings in wild-type *P. aeruginosa* strain, we performed the same checkerboard study using a panel of eight MDR or XDR *P. aeruginosa* clinical isolates (Chapter 11, Table 11.5.1) as previously studied for TOB-based hybrids.<sup>8,10,11,14</sup> Notably, among this panel of clinical isolates, two strains (*P. aeruginosa* 91433 and 101243) are non-susceptible or resistant to colistin that is considered to be the antibiotic of last resort for the treatment of carbapenem-resistant Gram-negative bacterial infections.<sup>31</sup> We determined the FIC index of

hybrid **1a** in combination with moxifloxacin, ciprofloxacin, minocycline, or rifampicin across the eight clinical isolates panel. Strong potentiation was seen with moxifloxacin, ciprofloxacin, minocycline, or rifampicin (FIC indices of 0.004 to 0.28) against these pathogens, with the exception of ciprofloxacin against *P. aeruginosa* 100036 and 101885 strains (FICI >0.5) (Table 6.2.3.2, Table 6.2.3.3, Table 6.2.3.4).

**Table 6.3.2.2.** Combination studies of NEB-MOX **1a** with moxifloxacin (MOX) or ciprofloxacin (CIP) against MDR/XDR *P. aeruginosa* clinical isolates.

<i>P. aeruginosa</i>	Antibiotic (MIC <sup>a</sup> )	Hybrid (MIC <sup>a</sup> )	FICI	Absolute MIC <sup>b</sup>	Potential (fold) <sup>c</sup>
PA262-101856 <sup>d</sup>	MOX (64)	<b>1a</b> (>256)	0.13<x<0.16	8	8
PA262-101856 <sup>d</sup>	CIP (32)	<b>1a</b> (>256)	0.25<x<0.28	8	4
PA260-97103 <sup>d</sup>	MOX (64)	<b>1a</b> (32)	0.13	1	64
PA260-97103 <sup>d</sup>	CIP (32)	<b>1a</b> (32)	0.25	4	8
100036 <sup>d</sup>	MOX (128)	<b>1a</b> (128)	0.08	8	16
100036 <sup>d</sup>	CIP (32)	<b>1a</b> (128)	0.56	16	2
101885 <sup>d</sup>	MOX (64)	<b>1a</b> (128)	0.25	16	4
101885 <sup>d</sup>	CIP (16)	<b>1a</b> (128)	>1	NA	NA
PA259-96918 <sup>d</sup>	MOX (256)	<b>1a</b> (>256)	0.06<x<0.07	16	16
PA259-96918 <sup>d</sup>	CIP (128)	<b>1a</b> (>256)	0.25<x<0.27	32	4
PA264-104354 <sup>d</sup>	MOX (128)	<b>1a</b> (256)	0.09	8	16
PA264-104354 <sup>d</sup>	CIP (32)	<b>1a</b> (256)	0.16	4	8
91433 <sup>e</sup>	MOX (8)	<b>1a</b> (32)	0.31	0.5	16
91433 <sup>e</sup>	CIP (1)	<b>1a</b> (32)	0.25	0.06	16
101243 <sup>e</sup>	MOX (8)	<b>1a</b> (64)	0.16	0.25	32
101243 <sup>e</sup>	CIP (1)	<b>1a</b> (64)	0.25	0.13	8

<sup>a</sup> All MIC data presented in  $\mu\text{g/mL}$ . <sup>b</sup> Absolute MIC ( $\mu\text{g/mL}$ ) of antibiotic was determined in the presence of 8  $\mu\text{g/mL}$  (7.5  $\mu\text{M}$ ) of hybrid **1a**. <sup>c</sup> Antibiotic activity potentiation at 8  $\mu\text{g/mL}$  (7.5  $\mu\text{M}$ ) of hybrid **1a**. <sup>d</sup> with <sup>83</sup>Thr to <sup>83</sup>Ile mutation in gyr A. <sup>e</sup> without <sup>83</sup>Thr to <sup>83</sup>Ile mutation in gyr A. <sup>8</sup>

**Table 6.3.2.3.** Combination studies of NEB-MOX **1a** with minocycline (MIN) against MDR/XDR *P. aeruginosa* clinical isolates.

<i>P. aeruginosa</i>	Antibiotic (MIC <sup>a</sup> )	Hybrid (MIC <sup>a</sup> )	FICI	Absolute MIC <sup>b</sup>	Potential (fold) <sup>c</sup>
PA262-101856	MIN (64)	<b>1a</b> (>256)	0.03<x<0.05	2	32
PA260-97103	MIN (8)	<b>1a</b> (32)	0.09	0.25	32
100036	MIN (16)	<b>1a</b> (128)	0.06	0.5	32
101885	MIN (16)	<b>1a</b> (128)	0.07	1	16
PA259-96918	MIN (16)	<b>1a</b> (>256)	0.03<x<0.04	0.5	32
PA264-104354	MIN (32)	<b>1a</b> (256)	0.05	0.5	64
91433	MIN (16)	<b>1a</b> (32)	0.19	0.5	32
101243	MIN (4)	<b>1a</b> (64)	0.13	0.25	16

<sup>a</sup> All MIC data presented in  $\mu\text{g}/\text{mL}$ . <sup>b</sup> Absolute MIC ( $\mu\text{g}/\text{mL}$ ) of antibiotic was determined in the presence of 8  $\mu\text{g}/\text{mL}$  (7.5  $\mu\text{M}$ ) of hybrid **1a**. <sup>c</sup> Antibiotic activity potentiation at 8  $\mu\text{g}/\text{mL}$  (7.5  $\mu\text{M}$ ) of hybrid **1a**.

**Table 6.3.2.4.** Combination studies of NEB-MOX **1a** with rifampicin (RIF) against MDR/XDR *P. aeruginosa* clinical isolates.

<i>P. aeruginosa</i>	Antibiotic (MIC <sup>a</sup> )	Hybrid (MIC <sup>a</sup> )	FICI	Absolute MIC <sup>b</sup>	Potential (fold) <sup>c</sup>
PA262-101856	RIF (1024)	<b>1a</b> (>256)	0.008<x<0.02	4	512
PA260-97103	RIF (4)	<b>1a</b> (32)	0.06	≤0.03	≥128
100036	RIF (8)	<b>1a</b> (128)	0.01	0.03	256
101885	RIF (8)	<b>1a</b> (128)	0.05	0.06	128
PA259-96918	RIF (8)	<b>1a</b> (>256)	0.004<x<0.01	≤0.03	≥256
PA264-104354	RIF (16)	<b>1a</b> (256)	0.02	≤0.06	≥256
91433	RIF (16)	<b>1a</b> (32)	0.16	0.13	128
101243	RIF (4)	<b>1a</b> (64)	0.13	0.13	32

<sup>a</sup> All MIC data presented in  $\mu\text{g/mL}$ . <sup>b</sup> Absolute MIC ( $\mu\text{g/mL}$ ) of antibiotic was determined in the presence of 8  $\mu\text{g/mL}$  (7.5  $\mu\text{M}$ ) of hybrid **1a**. <sup>c</sup> Antibiotic activity potentiation at 8  $\mu\text{g/mL}$  (7.5  $\mu\text{M}$ ) of hybrid **1a**.

Next, we evaluated the adjuvant potencies of hybrid **1a** by comparing the absolute MICs [in the presence of 8  $\mu\text{g/mL}$  (7.5  $\mu\text{M}$ ) hybrid **1a**] of the four antibiotics to their established susceptibility breakpoints. According to the Clinical and Laboratory Standards Institute (CLSI), the susceptible breakpoint, a chosen concentration ( $\mu\text{g/mL}$ ) of an antibiotic which defines a strain of bacteria whether it is susceptible to this antibiotic, of ciprofloxacin for *P. aeruginosa* is 1  $\mu\text{g/mL}$ .<sup>32</sup> However, the established susceptibility breakpoints for the other three tested antibiotics against *P. aeruginosa* are not available since they are unconventional antibiotics for the treatment of *P. aeruginosa* infections. Therefore, the susceptibility breakpoints of minocycline for *Acinetobacter* spp. ( $\leq 4 \mu\text{g/mL}$ ) and rifampicin for *Enterococcus* spp. ( $\leq 1 \mu\text{g/mL}$ )

reported by CLSI were used as interpretative guidelines.<sup>32</sup> It is noteworthy that the French Society for Microbiology has established a rifampicin breakpoint for *Acinetobacter baumannii* based on MIC distributions (susceptible,  $\leq 4 \mu\text{g/mL}$ ; intermediate, 8–16  $\mu\text{g/mL}$ ; and resistant,  $\geq 16 \mu\text{g/mL}$ ).<sup>33</sup> In addition, we conservatively considered the susceptibility breakpoint of moxifloxacin for *P. aeruginosa* to be similar to that of ciprofloxacin, as both belong to the fluoroquinolone class of antibiotics.

For the two fluoroquinolones, combinations of NEB-MOX hybrid **1a** with moxifloxacin yielded stronger potentiation than ciprofloxacin against the panel of MDR/XDR *P. aeruginosa* clinical isolates (Table 6.3.2.2). The adjuvant potency of hybrid **1a** in combination with moxifloxacin is comparable to a previously reported TOB-ciprofloxacin hybrid.<sup>8</sup> In 37.5% of cases, both hybrid **1a** and TOB-ciprofloxacin hybrid **1b**, at concentrations of  $\leq 8 \mu\text{g/mL}$  (6.8 – 7.5  $\mu\text{M}$ ), were able to bring down the MIC of moxifloxacin below its interpretative susceptibility breakpoint ( $\leq 1 \mu\text{g/mL}$ ) against moxifloxacin-resistant MDR/XDR *P. aeruginosa* isolates (Table 6.3.2.2).<sup>8</sup> However, the same susceptibility breakpoint was not reached for ciprofloxacin in combination with hybrid **1a** at a concentration of 8  $\mu\text{g/mL}$  (7.5  $\mu\text{M}$ ) against all the tested ciprofloxacin-resistant MDR/XDR *P. aeruginosa* isolates (Table 6.3.2.2). In contrast, the MICs of minocycline (8/8 minocycline-resistant MDR/XDR *P. aeruginosa* isolates) and rifampicin (7/8 rifampicin-resistant MDR/XDR *P. aeruginosa* isolates) were strongly reduced below their susceptibility breakpoints in the presence of 8  $\mu\text{g/mL}$  (7.5  $\mu\text{M}$ ) hybrid **1a**, an effect that is consistent with previously reported TOB-efflux pump inhibitor conjugates and TOB-lysine peptoid conjugates (Table 6.3.2.3, Table 6.2.3.4).<sup>10,11</sup>

A summarized result of antibacterial activity of minocycline (MIN) and rifampicin (RIF) alone or in combination with a fixed concentration of 8  $\mu\text{g/mL}$  (7.5  $\mu\text{M}$ ) hybrid **1a** against the

panel of eight MDR/XDR *P. aeruginosa* clinical isolates is shown in Table 6.3.2.5. The MIC<sub>80</sub> of minocycline and rifampicin in combination with 8 µg/mL (7.5 µM) hybrid **1a** were significantly lower in comparison to the MIC<sub>80</sub> of the antibiotic alone. Moreover, the absolute MIC<sub>80</sub> of minocycline (1 µg/mL) and rifampicin (0.13 µg/mL) were found to be less than their respective CLSI susceptibility breakpoints. Similarly, we demonstrated strong synergy of NEB-CIP (**1b**) with minocycline or rifampicin against wild-type and MDR *P. aeruginosa* strains (Table 6.3.2.6). For instance, in presence of only 4 µg/mL (4.1 µM) of hybrid **1b**, minocycline showed a 32-fold potentiation while rifampicin resulted in a 128 – ≥256-fold potentiation in wild-type and MDR *P. aeruginosa* strains (Table 6.3.2.6).

**Table 6.3.2.5.** *In vitro* antibacterial activity of minocycline (MIN) and rifampicin (RIF) alone or in combination with a fixed concentration of 8 µg/mL (7.5 µM) NEB-MOX **1a** against MDR/XDR *P. aeruginosa* clinical isolates (*n* = 8).

Antimicrobial/Hybrid	MIC <sub>50</sub> <sup>a</sup> (µg/mL)	MIC <sub>80</sub> <sup>a</sup> (µg/mL)	MIC Range (µg/mL)
MIN	16 ⊥	32 ⊥	4–64
MIN+ <b>1</b>	0.5 †	1 †	0.25–2
RIF	8 ⊥	16 ⊥	4–1024
RIF+ <b>1</b>	0.06 †	0.13 †	≤0.03–4

†, susceptible; ⊥, resistant; <sup>a</sup>MIC<sub>50</sub> and MIC<sub>80</sub> are the MIC that inhibit the growth of 50% or 80% of all (*n* = 8) tested isolates.

**Table 6.3.2.6.** Combination studies of NEB-CIP **1b** with antibiotics against wild-type *P. aeruginosa* PAO1 and XDR *P. aeruginosa* strains.

<i>P. aeruginosa</i>	Antibiotic (MIC <sup>a</sup> )	Hybrid (MIC <sup>a</sup> )	FIC index	Absolute MIC <sup>b</sup>	Potential (fold)
PAO1	MIN (16)	<b>1b</b> (64)	0.047	0.5	32
PAO1	RIF (16)	<b>1b</b> (64)	0.047	≤0.06	≥256
PA259-96918	MIN (16)	<b>1b</b> (>128)	0.031<x<0.063	0.5	32
PA259-96918	RIF (16)	<b>1b</b> (>128)	0.008<x<0.016	≤0.06	≥256
PA264-104354	MIN (32)	<b>1b</b> (128)	0.039	1	32
PA264-104354	RIF (16)	<b>1b</b> (128)	0.039	0.13	128

<sup>a</sup> All MIC data presented in  $\mu\text{g/mL}$ . <sup>b</sup> Absolute MIC ( $\mu\text{g/mL}$ ) of antibiotic was determined in the presence of 4  $\mu\text{g/mL}$  (4.1  $\mu\text{M}$ ) of hybrid **1b**. <sup>c</sup> Antibiotic activity potentiation at 4  $\mu\text{g/mL}$  (4.1  $\mu\text{M}$ ) of hybrid **1b**.

The observed potentiation of rifampicin by hybrid **1a** and **1b** may be explained by our previous findings that demonstrated that amphiphilic TOB-based hybrid adjuvants perturb the outer membrane of *P. aeruginosa* in a dose-dependent manner, thus facilitating the entry of antibiotics that are unable to cross the outer membrane of Gram-negative bacteria, such as rifampicin.<sup>8-11</sup> NEB-based hybrids seem to have a similar membrane effect as that of TOB-based hybrids. Since rifampicin is a poor substrate for *P. aeruginosa* RND efflux pumps,<sup>10,11</sup> outer membrane perturbation is most likely to be the reason to explain the observed strong synergistic effects of hybrid **1a** and **1b** in combination with rifampicin against *P. aeruginosa*.

We also investigated the synergy of NEB-NMP hybrid **2** with various antibiotic classes including fluoroquinolones (moxifloxacin, ciprofloxacin), tetracyclines (minocycline), or rifamycin (rifampicin) against wild-type and MDR *P. aeruginosa* strains (Table 6.3.2.7). More

importantly, NEB-NMP (**2**) reduced the MIC of minocycline below its CLSI susceptibility breakpoint ( $\leq 4 \mu\text{g/mL}$ ) against all tested *P. aeruginosa* strains. The observed adjuvant property of NEB-NMP (**2**) is consistent with that of reported TOB-NMP conjugate.<sup>11</sup>

Besides *P. aeruginosa*, we also explored the synergistic effects of NEB-based hybrids (**1a** and **1b**) with minocycline or rifampicin against other MDR GNBs such as *Acinetobacter baumannii*, *Escherichia coli*, *Klebsiella pneumoniae*, and *Enterobacter cloacae* (Tables 6.3.2.8 and 6.3.2.9). Again, both NEB-MOX **1a** and NEB-CIP **1b** displayed poor antibacterial activity by themselves against these pathogens (MICs of  $\geq 8 \mu\text{g/mL}$ ). In the case of *A. baumannii*, minocycline was not potentiated against the four tested isolates while NEB-MOX **1a** was able to synergize rifampicin, leading to 32- to 64-fold reductions in MICs at a concentration of  $8 \mu\text{g/mL}$  ( $7.5 \mu\text{M}$ ) of the adjuvant. Similarly, against *A. baumannii*, we observed an additive relationship of NEB-CIP (**1b**) with minocycline while the combination of NEB-CIP (**1b**) with rifampicin remained synergistic (Table 6.3.2.9). With respect to *K. pneumoniae*, *E. cloacae*, or *E. coli*, NEB-MOX (**1a**) and NEB-CIP (**1b**) displayed strong synergism with rifampicin against all isolates tested while synergism of NEB-MOX (**1a**) and NEB-CIP (**1b**) with minocycline was only observed in few isolates (Tables 6.3.2.8 and 6.3.2.9).

**Table 6.3.2.7.** Combination studies of NEB-NMP **2** with antibiotics against wild-type *P. aeruginosa* PAO1 and MDR/XDR *P. aeruginosa* strains.

<i>P. aeruginosa</i>	Antibiotic (MIC <sup>a</sup> )	Hybrid (MIC <sup>a</sup> )	FICI	Absolute MIC <sup>b</sup>	Potential (fold) <sup>c</sup>
PAO1	MOX (1)	<b>2</b> (256)	0.05	0.03	32
PAO1	MIN (8)	<b>2</b> (256)	0.09	0.5	16

**Table 6.3.2.7. Cont.**

<i>P. aeruginosa</i>	Antibiotic (MIC <sup>a</sup> )	Hybrid (MIC <sup>a</sup> )	FICI	Absolute MIC <sup>b</sup>	Potential (fold) <sup>c</sup>
PAO1	RIF (16)	2 (256)	0.02	0.06	256
PA262-101856 <sup>d</sup>	MOX (64)	2 (512)	0.09	4	16
PA262-101856 <sup>d</sup>	CIP (32)	2 (512)	0.13	4	8
PA262-101856 <sup>d</sup>	MIN (128)	2 (512)	0.04	4	32
PA262-101856 <sup>d</sup>	RIF (1024)	2 (512)	0.02	4	256
PA260-97103 <sup>d</sup>	MOX (64)	2 (32)	0.08	0.5	128
PA260-97103 <sup>d</sup>	CIP (16)	2 (32)	0.38	2	8
PA260-97103 <sup>d</sup>	MIN (16)	2 (32)	0.09	0.25	64
PA260-97103 <sup>d</sup>	RIF (4)	2 (32)	0.05	0.06	64
100036 <sup>d</sup>	MOX (128)	2 (>512)	0.063<x<0.07	8	16
100036 <sup>d</sup>	CIP (64)	2 (>512)	0.125<x<0.133	8	8
100036 <sup>d</sup>	MIN (64)	2 (>512)	0.031<x<0.033	2	32
100036 <sup>d</sup>	RIF (16)	2 (>512)	0.004<x<0.012	0.06	256
101885 <sup>d</sup>	MOX (64)	2 (512)	0.07	4	16
101885 <sup>d</sup>	CIP (32)	2 (512)	0.13	4	8
101885 <sup>d</sup>	MIN (32)	2 (512)	0.04	0.5	64
101885 <sup>d</sup>	RIF (16)	2 (512)	0.02	0.13	128
PA259-96918 <sup>d</sup>	MOX (512)	2 (>512)	0.016<x<0.023	8	64
PA259-96918 <sup>d</sup>	CIP (256)	2 (>512)	0.063<x<0.078	16	16
PA259-96918 <sup>d</sup>	MIN (32)	2 (>512)	0.016<x<0.031	0.5	64
PA259-96918 <sup>d</sup>	RIF (16)	2 (>512)	0.004<x<0.006	≤0.06	≥256

**Table 6.3.2.7.** *Cont.*

<i>P. aeruginosa</i>	Antibiotic (MIC <sup>a</sup> )	Hybrid (MIC <sup>a</sup> )	FICI	Absolute MIC <sup>b</sup>	Potential (fold) <sup>c</sup>
91433 <sup>e</sup>	MOX (8)	<b>2</b> (32)	0.25	1	8
91433 <sup>e</sup>	CIP (2)	<b>2</b> (32)	0.38	0.25	8
91433 <sup>e</sup>	MIN (64)	<b>2</b> (32)	0.19	2	32
91433 <sup>e</sup>	RIF (16)	<b>2</b> (32)	0.50	4	4
101243 <sup>e</sup>	MOX (4)	<b>2</b> (512)	0.13	0.5	8
101243 <sup>e</sup>	CIP (2)	<b>2</b> (512)	0.16	0.5	4
101243 <sup>e</sup>	MIN (4)	<b>2</b> (512)	0.09	0.5	8
101243 <sup>e</sup>	RIF (8)	<b>2</b> (512)	0.05	0.25	32

<sup>a</sup> All MIC data presented in  $\mu\text{g/mL}$ . <sup>b</sup> Absolute MIC ( $\mu\text{g/mL}$ ) of antibiotic was determined in the presence of 8  $\mu\text{g/mL}$  (9.0  $\mu\text{M}$ ) of hybrid **2**. <sup>c</sup> Antibiotic activity potentiation at 8  $\mu\text{g/mL}$  (9.0  $\mu\text{M}$ ) of hybrid **2**. <sup>d</sup> with <sup>83</sup>Thr to <sup>83</sup>Ile mutation in *gyr A*.<sup>8</sup> <sup>e</sup> without <sup>83</sup>Thr to <sup>83</sup>Ile mutation in *gyr A*.<sup>8</sup>

**Table 6.3.2.8.** Combination studies of NEB-MOX **1** with minocycline (MIN) or rifampicin (RIF) against MDR *Acinetobacter baumannii*, *Klebsiella pneumoniae*, and *Enterobacter cloacae*.

Organisms	Antibiotic (MIC <sup>a</sup> )	Hybrid (MIC <sup>a</sup> )	FICI	Absolute MIC <sup>b</sup>	Potential (fold) <sup>c</sup>
<i>A. baumannii</i> AB027	MIN (1)	<b>1a</b> (>256)	>1	NA	NA
<i>A. baumannii</i> AB027	RIF (1)	<b>1a</b> (>256)	0.031<x<0.047	0.03	32
<i>A. baumannii</i> AB030	MIN (2)	<b>1a</b> (>16)	>1	NA	NA
<i>A. baumannii</i> AB030	RIF (1024)	<b>1a</b> (>16)	0.031<x<0.281	32	32
<i>A. baumannii</i> AB031	MIN (1)	<b>1a</b> (128)	>1	NA	NA

**Table 6.3.2.8. Cont.**

Organisms	Antibiotic (MIC <sup>a</sup> )	Hybrid (MIC <sup>a</sup> )	FICI	Absolute MIC <sup>b</sup>	Potential (fold) <sup>c</sup>
<i>A. baumannii</i> AB031	RIF (1)	<b>1a</b> (128)	0.04	0.02	64
<i>A. baumannii</i> 110193	MIN (1)	<b>1a</b> (>256)	>1	NA	NA
<i>A. baumannii</i> 110193	RIF (1)	<b>1a</b> (>256)	0.031<x<0.047	0.03	32
<i>K. pneumoniae</i> 116381	MIN (64)	<b>1a</b> (>256)	0.063<x<0.078	4	16
<i>K. pneumoniae</i> 116381	RIF (1024)	<b>1a</b> (>256)	0.002<x<0.006	≤1	≥1024
<i>E. cloacae</i> 117029	MIN (64)	<b>1a</b> (32)	0.19	4	16
<i>E. cloacae</i> 117029	RIF (4)	<b>1a</b> (32)	0.06	≤0.03	≥128

<sup>a</sup>All MIC data presented in  $\mu\text{g/mL}$ . <sup>b</sup>Absolute MIC ( $\mu\text{g/mL}$ ) of antibiotic was determined in the presence of 8  $\mu\text{g/mL}$  (7.5  $\mu\text{M}$ ) of hybrid **1a**. <sup>c</sup>Antibiotic activity potentiation at 8  $\mu\text{g/mL}$  (7.5  $\mu\text{M}$ ) of hybrid **1a**. NA, not available (no synergy was observed).

**Table 6.3.2.9.** Combination studies of NEB-CIP **1b** with minocycline (MIN) or rifampicin (RIF) against wild-type or MDR *Acinetobacter baumannii*, *Escherichia coli*, *Klebsiella pneumoniae*, and *Enterobacter cloacae*.

Organisms	Antibiotic (MIC <sup>a</sup> )	Hybrid (MIC <sup>a</sup> )	FICI	Absolute MIC	Potential (fold) <sup>d</sup>
<i>A. baumannii</i> ATCC 17978	MIN (0.25)	<b>1b</b> (128)	0.520	0.13 <sup>b</sup>	2
<i>A. baumannii</i> ATCC 17978	RIF (2)	<b>1b</b> (128)	0.016	0.008 <sup>b</sup>	256
<i>A. baumannii</i> AB92247	MIN (0.125)	<b>1b</b> (128)	0.531	0.06 <sup>b</sup>	2
<i>A. baumannii</i> AB92247	RIF (2)	<b>1b</b> (128)	0.039	0.02 <sup>b</sup>	128
<i>A. baumannii</i> AB110193	MIN (1)	<b>1b</b> (>128)	>1	NA	NA

**Table 6.3.2.9. Cont.**

Organisms	Antibiotic (MIC <sup>a</sup> )	Hybrid (MIC <sup>a</sup> )	FICI	Absolute MIC	Potentiatio (fold) <sup>d</sup>
<i>A. baumannii</i> AB110193	RIF (1)	<b>1b</b> (>128)	0.016<x<0.031	0.02 <sup>b</sup>	64
<i>E. coli</i> ATCC 25922	MIN (1)	<b>1b</b> (8)	0.504	NA	NA
<i>E. coli</i> ATCC 25922	RIF (4)	<b>1b</b> (8)	0.133	0.03 <sup>c</sup>	128
<i>E. coli</i> 94474	MIN (64)	<b>1b</b> (>128)	0.063<x<0.078	4 <sup>b</sup>	16
<i>E. coli</i> 94474	RIF (8)	<b>1b</b> (>128)	0.004<x<0.035	0.03 <sup>b</sup>	256
<i>E. coli</i> 107115	MIN (32)	<b>1b</b> (32)	0.133	2 <sup>b</sup>	16
<i>E. coli</i> 107115	RIF (32)	<b>1b</b> (32)	0.015<x≤0.020	≤0.13 <sup>b</sup>	≥256
<i>K. pneumoniae</i> 113250	MIN (2)	<b>1b</b> (128)	0.504	1 <sup>b</sup>	2
<i>K. pneumoniae</i> 113250	RIF (32)	<b>1b</b> (128)	0.039	0.25 <sup>b</sup>	128
<i>K. pneumoniae</i> 113254	MIN (2)	<b>1b</b> (128)	0.504	1 <sup>b</sup>	2
<i>K. pneumoniae</i> 113254	RIF (16)	<b>1b</b> (128)	0.047	0.25 <sup>b</sup>	64
<i>K. pneumoniae</i> 116381	MIN (64)	<b>1b</b> (>128)	0.063<x<0.070	4 <sup>b</sup>	16
<i>K. pneumoniae</i> 116381	RIF (>128)	<b>1b</b> (>128)	≤0.039	1 <sup>b</sup>	≥128
<i>E. cloacae</i> 117029	MIN (32)	<b>1b</b> (32)	0.125	2 <sup>b</sup>	16
<i>E. cloacae</i> 117029	RIF (8)	<b>1b</b> (32)	0.023	≤0.03 <sup>b</sup>	≥256

<sup>a</sup>All MIC data presented in  $\mu\text{g}/\text{mL}$ . <sup>b</sup>Absolute MIC ( $\mu\text{g}/\text{mL}$ ) of antibiotic was determined in the presence of 4  $\mu\text{g}/\text{mL}$  (4.1  $\mu\text{M}$ ) of hybrid **1b**. <sup>c</sup>Absolute MIC ( $\mu\text{g}/\text{mL}$ ) of antibiotic was determined in the presence of 2  $\mu\text{g}/\text{mL}$  (2.0  $\mu\text{M}$ ) of hybrid **1b**. <sup>d</sup>Antibiotic activity potentiation at 8  $\mu\text{g}/\text{mL}$  (4.1  $\mu\text{M}$ ) or 2  $\mu\text{g}/\text{mL}$  (2.0  $\mu\text{M}$ ) of hybrid **1b**. NA, not available (no synergy was observed).

### 6.3.3 Time-kill Curve

To confirm the synergistic activity between NEB-based hybrids and minocycline or rifampicin, time-kill assays were performed. We first studied the time killing kinetics of minocycline at  $4 \mu\text{g/mL}$  ( $\frac{1}{2} \times \text{MIC}$ ) in combination with NEB-MOX **1a** at sub-inhibitory concentration ( $\frac{1}{2} \times \text{MIC} = 16 \mu\text{g/mL}$  or  $\frac{1}{4} \times \text{MIC} = 8 \mu\text{g/mL}$ ) against *P. aeruginosa* wild-type PAO1 (Fig. 6.3.3.1A). We set a fixed concentration of  $4 \mu\text{g/mL}$  minocycline for the kinetic study since the CLSI susceptibility breakpoint of minocycline is  $\leq 4 \mu\text{g/mL}$ . It was demonstrated that combination of bacteriostatic minocycline ( $4 \mu\text{g/mL}$ ) with  $\frac{1}{2} \times \text{MIC}$  of hybrid **1a** became bactericidal and resulted in complete eradication of *P. aeruginosa* PAO1 over a 24 h time period. This enhanced killing efficiency of minocycline in combination with hybrid **1a** is consistent with our previous findings for TOB-based hybrids<sup>10,11</sup> and are likely the results of the membrane effects induced by hybrid **1a**. Furthermore, we also studied the killing kinetics of NEB-CIP **1b** in combination with rifampicin against XDR *P. aeruginosa* PA259. A combination of sub-MIC of **1b** ( $1 \mu\text{g/mL}$ , MIC of **1b** is  $>128 \mu\text{g/mL}$ ) and rifampicin ( $\frac{1}{16} \times \text{MIC} = 1 \mu\text{g/mL}$ ) yielded a 3-order magnitude decrease in viable bacterial counts over an 8 h time period (Fig. 6.3.3.1B). Complete eradications were observed at a higher concentration of **1b** ( $4 \mu\text{g/mL}$ ) in combination with rifampicin at  $1 \mu\text{g/mL}$  or  $4 \mu\text{g/mL}$  for only 4 h of antimicrobial exposure (Fig. 6.3.3.1B).

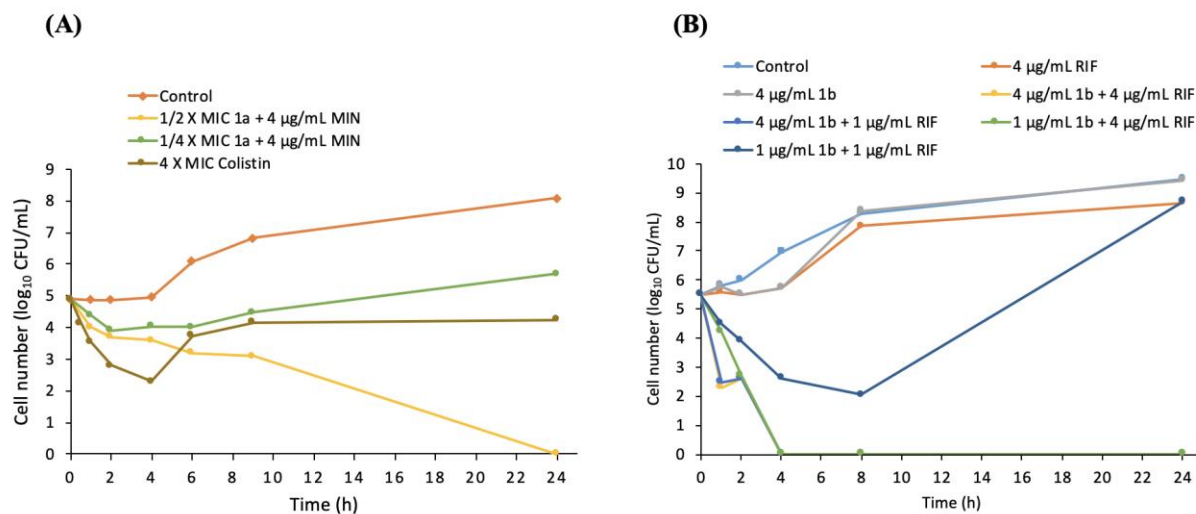


**Fig. 6.3.3.1.** (A) Time killing kinetics of minocycline (MIN) (4 µg/mL) in combination with NEB-MOX (**1a**) at  $\frac{1}{2} \times \text{MIC}$  (16 µg/mL) or  $\frac{1}{4} \times \text{MIC}$  (8 µg/mL) against *P. aeruginosa* PAO1. Untreated cells in media and cells treated with 4 × MIC (4 µg/mL) of colistin were used as negative and positive controls respectively. (B) Time killing kinetics of rifampicin in combination with NEB-CIP (**1b**) at various concentrations against XDR *P. aeruginosa* PA259. Untreated cells in media was used as a negative control. MIC of **1b** is >128 µg/mL and MIC of RIF is 16 µg/mL against *P. aeruginosa* PA259 strain. Mean values of duplicate CFU/mL measurements are plotted.

### 6.3.4 Hemolytic Activity and *In Vivo* Efficacy Study

To investigate whether the adjuvant properties of the NEB-based hybrids translates into a measurable *in vivo* effect, we selected the established *in vivo* *Galleria mellonella* larvae infection model to study the efficacy of hybrid **1b**-rifampicin combination therapies against *P. aeruginosa*.<sup>34,35</sup> Initially, we demonstrated that NEB-CIP **1b** was non-hemolytic to pig erythrocytes (<10% at 512 µg/mL) (Fig. 6.3.4.1). We also examined the tolerability of **1b** on *G.*

*mellonella* and found that the larvae survived beyond 96 h when administered with 100 mg/kg dosage of **1b** (Fig. 6.3.4.2). However, colistin resulted in 70% and 90% larvae deaths at the dosage of 75 mg/kg and 100 mg/kg, respectively, after 96 h, consistent with known toxicity of colistin to eukaryotic cells. We also established that 5 CFU of XDR *P. aeruginosa* PA264 alone resulted in 100% lethality of the larvae after 18 h. To assess the ability of combination therapy of **1b** and rifampicin to protect against XDR *P. aeruginosa* PA264-challenge larvae, single treatment doses of rifampicin + compound **1b** (25 + 25 mg/kg, 50 + 50 mg/kg, and 75+75 mg/kg) were administered 2 h post inoculation with 5 CFU XDR *P. aeruginosa* PA264 (bacterial isolate was only susceptible to colistin). The results showed that monotherapy with a single dose of rifampicin (75 mg/kg) or **1b** (100 mg/kg) resulted in 10% and 0% survival of the larvae after 18 h, respectively (Fig. 6.3.4.3). In contrast, combination of rifampicin and **1b** improved the survival of the wax moth larvae in a dose-dependent manner (Fig. 6.3.4.3). For instance, a single dose combination of rifampicin with **1b** (75 + 75 mg/kg) resulted in 87% and 53% survival after 18 h and 24 h respectively. A 50 + 50 mg/kg single dose combination of rifampicin and **1b** resulted in 60% and 33% survival after 18 h and 24 h, respectively, while a 25 + 25 mg/kg single dose combination of rifampicin and **1b** resulted in a 33% and 13% survival after 18 h and 24 h, respectively. This clearly demonstrates a dose-dependent survivability of the infected larvae when treated with a combination of rifampicin and compound **1b**. Overall, these results demonstrate the therapeutic potential of NEB-based hybrid **1b** + rifampicin to treat MDR/XDR infections *in vivo*. We also assessed the toxicity of adjuvants **1a** or **1b** against the HepG2 and HEK293 cell lines alone and in combination with rifampicin. These results confirmed that adjuvants **1a** and **1b** do not possess elevated toxicity at their synergistic concentration alone and in combination with rifampicin. (Chapter 11, Fig. 11.6.1).

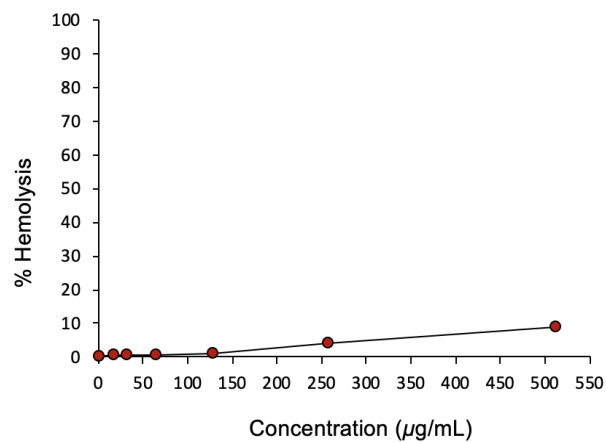


**Fig. 6.3.4.1.** Hemolytic activity of NEB-CIP (**1b**). Triton X-100 (0.1%) was employed as positive control to calculate the percentage of hemolysis.

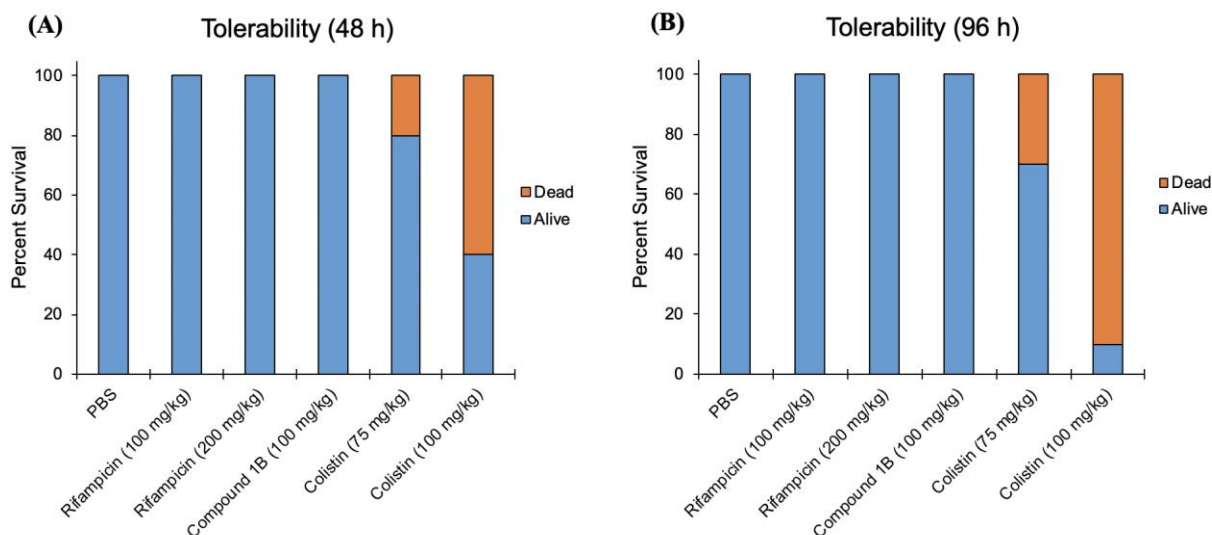


**Fig. 6.3.4.2.** Tolerability dosages of NEB-CIP (**1b**), rifampicin, and colistin on *G. mellonella* larvae ( $n = 10$ ). Larvae survived up to 96 h when administered with 100 mg/kg dosage of **1b**.

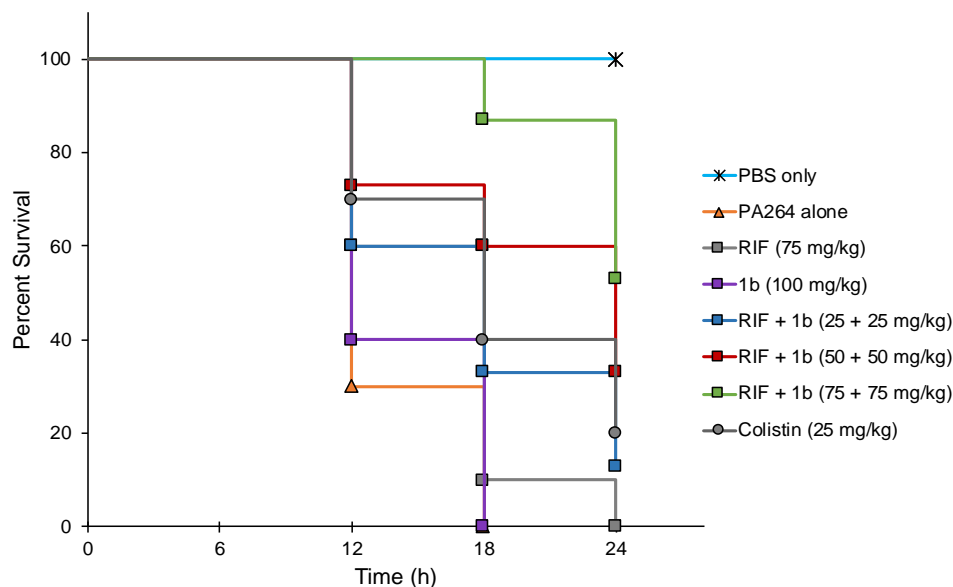


**Fig. 6.3.4.3.** Effect of treatment of *G. mellonella* larvae (inoculated with  $\sim 5$  CFU of XDR *P. aeruginosa* PA264,  $n = 30$  for each drug and dose combination) with rifampicin (75 mg/kg) and **1b** (100 mg/kg) alone, or rifampicin in combination with **1b** (25 + 25 mg/kg, 50 + 50 mg/kg, and 75+75 mg/kg) on survival. Single dose treatment administered at 0 h (2 h after inoculation).

### 6.3.5 Tetracycline Uptake Assay

To gain insight to the synergistic mechanism of NEB-MOX hybrid **1a** with minocycline, a fluorescence-based tetracycline uptake assay for Gram-negative bacteria<sup>36</sup> was performed to investigate the effect of hybrid **1a** on the uptake of tetracycline (Fig. 6.3.5.1). Our results indicate that, similar to TOB-based hybrids,<sup>11</sup> hybrid **1a** enhances the uptake of tetracycline in *P. aeruginosa* PAO1 in a concentration-dependent manner. Comparable enhancements in tetracycline uptake were also observed with membrane-targeting antibiotic colistin (Fig. 6.3.5.1). We previously reported that TOB-based hybrids not only permeabilize the Gram-negative bacterial outer membrane but also depolarize the cytoplasmic membrane.<sup>8-11</sup> TOB-based hybrids specifically dissipate the electrical component ( $\Delta\Psi$ ) of the proton motive force (PMF) resulting in a compensatory increase in the transmembrane chemical component ( $\Delta\text{pH}$ ) in order to counter this effect and maintain ATP synthesis. The effect of TOB-based hybrids on  $\Delta\Psi$  is likely retained in NEB-MOX hybrid **1** which is consistent with the observed synergy of hybrid **1a** with minocycline, as tetracycline uptake is  $\Delta\text{pH}$ -dependent.<sup>36</sup> Disruption of  $\Delta\Psi$  by hybrid **1a** is compensated by an increase in  $\Delta\text{pH}$  that in turn enhances the uptake of tetracycline antibiotics. This was further corroborated by the observation that CCCP (carbonyl cyanide *m*-chlorophenyl hydrazone) inhibits tetracycline accumulation (Fig. 6.3.5.1). CCCP is an uncoupler of oxidative phosphorylation that disrupts the proton gradient ( $\Delta\text{pH}$ ) of bacterial membranes.<sup>37</sup> Moreover, minocycline is known to inhibit preferentially the biosynthesis of envelope proteins<sup>38</sup> which, perhaps, elicits further compromise of the intrinsic resistance barrier (the Gram-negative bacterial outer membrane), thereby augmenting the effects of NEB-based hybrid **1a**.

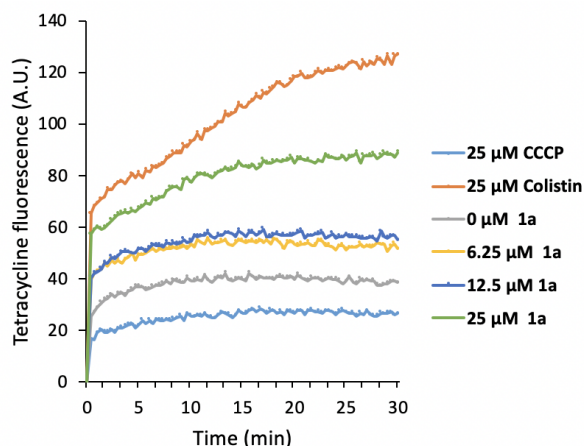


**Fig. 6.3.5.1.** Tetracycline uptake in *P. aeruginosa* PAO1 in the presence of increasing concentrations of NEB-MOX **1a**. Concentration of tetracycline was 128  $\mu\text{g}/\text{mL}$ . Averages of triplicate experiments are shown.

## 6.4 CONCLUSIONS

In this study, we demonstrated that NEB-based hybrids (**1a**, **1b**, and **2**) are capable of potentiating multiple classes of antibiotics including fluoroquinolones (moxifloxacin, ciprofloxacin), tetracycline (minocycline), and rifamycin (rifampicin) against wild-type and MDR/XDR GNBs including *P. aeruginosa*, *A. baumannii*, *K. pneumonia*, and *E. cloacae* strains *in vitro*. Moreover, NEB-CIP hybrid (**1b**) has been shown to break the intrinsic resistance of *P. aeruginosa* to rifampicin *in vivo*. The adjuvant potencies of NEB-based hybrids (**1a**, **1b**, and **2**) are comparable to that of TOB-based hybrids as studied before,<sup>7-14</sup> suggesting that cleavage of the 3-deoxy-3-amino  $\alpha$ -D-glucosidic linkage in TOB to yield NEB did not significantly alter the adjuvant properties of this scaffold. A mechanistic study of NEB-MOX **1a** confirmed that it also retains the membrane effects of TOB-based hybrid adjuvants including TOB-fluoroquinolone hybrids. Modification of the tobramycin domain of TOB-based hybrid suggests that the pseudo-

disaccharide NEB linked to the C<sub>12</sub> tether is the essential membrane active core responsible for the adjuvant properties. This study provides further insight into the structural optimization of previously investigated TOB-based hybrid adjuvants. Moreover, the reduced number of basic functions in NEB when compared to TOB may result in reduced aminoglycoside-induced cytotoxicity.

## 6.5 EXPERIMENTAL SECTION

### 6.5.1 Synthetic Chemistry

#### 6.5.1.1 General Comments

Reactions were monitored by thin-layer chromatography (TLC) on silica gel 60 F254 (0.25 mm, Merck) and the compounds were visualized using ultraviolet light and/or stain with ninhydrin solution (ninhydrin and acetic acid in ethanol). 1D and 2D (<sup>1</sup>H, <sup>13</sup>C, DEPT, COSY, HSQC, HMBC) nuclear magnetic resonance (NMR) characterization experiments were performed on either Bruker AMX-500 or Bruker AMX-300 spectrophotometer in the noted deuterated solvents. Chemical shifts ( $\delta$ ) are reported in parts per million with CHCl<sub>3</sub> (7.26 ppm), DHO (4.79 ppm), and CD<sub>2</sub>HOH (3.31 ppm) used as internal standards. Electrospray ionization (ESI) mass spectrometry (MS) experiments were carried out on a Varian 500 MS ion trap mass spectrometer. Matrix-assisted laser desorption ionization (MALDI) MS experiments were performed on a Bruker Daltonics Ultraflex MALDI TOF/TOF mass spectrometer. Analytical high-performance liquid chromatography (HPLC) was carried out on Breeze HPLC Waters with 2998 PDA detector (1.2 nm resolution) connected to a Synergi 4  $\mu$ m Polar-RP 80 Å LC column

(50 mm × 4.6 mm, Phenomenex). Yields are given following purification, unless otherwise stated. All of the tested compounds are at least 95% pure as estimated by HPLC.

### 6.5.1.2 Synthetic Procedures and Characterizations

Detailed experimental procedures of compounds **3**, **4a**, **4b**, **5**, **6**, **9**, moxifloxacin methyl ester and ciprofloxacin methyl ester were described in the supporting information.

*General synthetic procedure A: final deprotection of compounds 8a and 8b.* Compound **8a** or **8b** (0.014 mmol) was dissolved in MeOH (2 mL). 2 N lithium hydroxide solution (1 mL) was then added to the solution while stirring. The reaction mixture was stirred at room temperature for 30 min. In an ice bath, careful acidification of the solution to pH = 6 was done by slow addition of 1 N HCl (a.q.). The solvent was removed *in vacuo*. The residue was purified by flash chromatography (elution with a gradient of DCM/MeOH from 9:1 to 1:1, v/v) to afford a white solid which was dissolved in TFA (2 mL) and H<sub>2</sub>O (1 mL) solution and stirred for 2 h at room temperature. The solvent was removed under reduced pressure to give a yellow residue. 20 mL of methanol and ether solution (1:20, v/v) was added to this residue in several portions and then the solvent was decanted to get a yellow solid as nebramine-based hybrid TFA salt. Stoichiometric amount of HCl aqueous solution was added into it before lyophilizing the solution to afford a yellow solid as the final product as the HCl salt.

*General synthetic procedure B: synthesis of 7a and 7b via reductive amination.*

Moxifloxacin methyl ester (0.49 mmol) or ciprofloxacin methyl ester was mixed with aldehyde **6** (0.41 mmol), followed by the addition of dry DCE (25 mL) and AcOH (2.3 μL, 0.041 mmol) under N<sub>2</sub> gas. The reaction mixture was stirred at room temperature for 7 h before NaBH(OAc)<sub>3</sub> (1.64 mmol) was added at 0 °C. The solution was gradually warmed to room temperature while

stirring overnight. The reaction mixture was cooled to 0 °C and quenched carefully by the drop-wise addition of saturated NaHCO<sub>3</sub> solution (10 mL). The solution was then extracted with DCM (3 × 15 mL). The organic layer was washed with brine, dried over anhydrous sodium sulfate and concentrated in vacuo. The crude product was purified by flash chromatography (elution with a gradient of DCM/MeOH from 50:1 to 10:1, v/v) to afford the desired product as a white solid.

*General synthetic procedure C: synthesis of Boc-protected NEB-based hybrids 8a, 8b and 10.*<sup>21,22</sup> 40% HCl (3 mL) and MeOH (5 mL) were added to **7a**, **7b** or **9** (0.048 mmol) slowly. The reaction was heated to 70 °C and stirred 24 h. The solution was cooled down to room temperature and neutralized with solid sodium bicarbonate before concentrated to dryness. The residue was taken up in 30 mL of MeOH, filtered and concentrated to give a crude 5-*O*-(dodecyl-moxifloxacin methyl ester)-nebramine or 5-*O*-(dodecyl-ciprofloxacin methyl ester)-nebramine HCl salt. The above crude product was dissolved in MeOH (15 mL) at room temperature. Triethylamine (69 μL, 0.48 mmol) and (Boc)<sub>2</sub>O (0.38 mmol) were added into the solution and stirred overnight at 55 °C. Upon completion, the reaction mixture was concentrated *in vacuo*. Purification by flash column chromatography (elution with a gradient of DCM/MeOH from 30:1 to 10:1 for **8a** and **8b**, elution with a gradient of DCM/MeOH from 100:1 to 40:1 for compound **10**) to afford a white solid as desired product.

*5-O-(dodecyl-moxifloxacin)-nebramine 5·HCl (1a).* Synthesized following general procedure A. Yield: 8 mg (53%). <sup>1</sup>H NMR (500 MHz, deuterium oxide) δ 8.96 (s, 1H, N-CH of aromatic ring), 7.58 (d, *J* = 69.9 Hz, 1H, F-C-CH of aromatic ring), 5.67 – 5.53 (m, 1H, CH of H-1'), 4.39 – 4.02 (m, 5H, CH of cyclopropyl, 2×N-CHH of moxifloxacin, CH of H-5', CH of H-4), 4.02 – 3.56 (m, 13H, OCH<sub>2</sub> of linker, CH of H-4', CH of moxifloxacin, N-CHH of moxifloxacin, CH of H-2', N-CHH of linker, OCH<sub>3</sub> of moxifloxacin, CH of H-5, CH of H-6, CH

of H-1), 3.56 – 3.29 (m, 5H, 2×N-CHH of moxifloxacin, CH<sub>2</sub> of H-6', CH of H-3), 3.28 – 3.09 (m, 2H, N-CHH of moxifloxacin, N-CHH of linker), 3.09 – 2.95 (m, 1H, CH of moxifloxacin), 2.58 – 2.50 (m, 1H, CHH of H-2), 2.39 – 2.28 (m, 1H, CHH of H-3'), 2.23 – 2.14 (m, 1H, CHH of H-3'), 2.14 – 0.82 (m, 29H, CHH of H-2, 10×CH<sub>2</sub> of linker, 2×C-CH<sub>2</sub> of moxifloxacin, 2×CH<sub>2</sub> of cyclopropyl). <sup>13</sup>C NMR (125 MHz, deuterium oxide, some carbons are doubling due to fluorine atom) δ 176.37 (CO of quinoline), 169.71 (CO of carboxylic acid), 153.23 (CF of quinoline), 152.25 (CF of quinoline), 151.04 (CH, C-2 of quinoline), 141.77 (C-8 of quinoline), 135.02 (C-7 of quinoline), 134.85 (C-8a of quinoline), 117.57 (C-4a of quinoline), 106.84 (CH, C-5 of quinoline), 106.67 (C-3 of quinoline), 92.08 (C-1'), 82.73 (C-6), 75.07 (C-4), 73.48 (O-CH<sub>2</sub> of linker), 73.22 (C-5'), 72.69 (C-5), 63.83 (C-4'), 62.24 (O-CH<sub>3</sub>), 56.96 (N-CH<sub>2</sub> of linker), 54.21 (CH<sub>2</sub> of pyrrolidine), 52.41 (CH of pyrrolidine), 50.90 (CH<sub>2</sub> of pyrrolidine), 49.87 (C-1), 48.94 (C-3), 47.53 (C-2'), 41.36 (N-CH<sub>2</sub> of piperidine), 39.30 (C-6'), 36.00 (CH of cyclopropyl), 35.56 (CH of pyrrolidine), 29.64 (O-CH<sub>2</sub>-CH<sub>2</sub> of linker), 29.27 (CH<sub>2</sub> of linker), 29.12 (CH<sub>2</sub> of linker), 28.99 (C-3'), 28.82 (CH<sub>2</sub> of linker), 28.70 (CH<sub>2</sub> of linker), 28.21 (CH<sub>2</sub> of linker), 28.06 (C-2), 27.92 (CH<sub>2</sub> of linker), 26.04 (CH<sub>2</sub> of linker), 25.30 (CH<sub>2</sub> of linker), 20.15 (CH<sub>2</sub> of piperidine), 17.95 (CH<sub>2</sub> of piperidine), 9.90 (CH<sub>2</sub> of cyclopropyl), 8.17 (CH<sub>2</sub> of cyclopropyl). MALDI-TOF-MS *m/e* calcd for C<sub>45</sub>H<sub>72</sub>FN<sub>7</sub>O<sub>9</sub>Na [M+Na]<sup>+</sup>: 896.5273, found: 896.5290.

*5-O-(dodecyl-ciprofloxacin)-nebramine 5·HCl (Ib)*. Synthesized following general procedure A. Yield: 13.4 mg (32%). <sup>1</sup>H NMR (500 MHz, deuterium oxide) δ 8.67 (s, 1H, N-CH of aromatic ring), 7.62 – 7.44 (m, 2H, C-CH of aromatic ring), 5.58 (d, *J* = 3.2 Hz, 1H, anomeric H-1'), 4.14 – 4.06 (m, 2H, H of piperazine), 4.05 – 3.94 (m, 3H, NC-H of cyclopropyl, C-H of C-O of linker), 3.89 – 3.72 (m, 7H, H-6, H-2', H-4', 2C-H of C-O of linker, 2C-H of C-N of linker), 3.69 – 3.58 (m, 2H, H-1, H-5'), 3.48 – 3.26 (m, 9H, H-3, 2H of H-6', 4H of piperazine,

2C-H of linker), 2.53 (m, 1H, H-2), 2.32 (m, 1H, H-3'), 2.16 (m, 1H, H-3'), 1.96 (m, 1H, H-2), 1.88 – 1.78 (m, 2H, C-H of linker), 1.69 – 1.58 (m, 2H, C-H of linker), 1.50 – 1.28 (m, 18H, CH<sub>2</sub> of cyclopropyl and CH<sub>2</sub> of linker), 1.23 (m, 2H, CH<sub>2</sub> of cyclopropyl). <sup>13</sup>C NMR (125 MHz, deuterium oxide)  $\delta$  176.11 (CO of quinoline), 169.10 (CO of carboxylic acid), 154.48 (CF of quinoline), 152.48 (CF of quinoline), 148.48 (CH, C-2 of quinoline), 144.32 (C-7 of quinoline), 144.24 (C-7 of quinoline), 139.10 (C-8a of quinoline), 118.99 (C-4a of quinoline), 110.97 (C-5 of quinoline), 110.78 (C-5 of quinoline), 106.85 (C-8 of quinoline), 105.83 (C-3 of quinoline), 92.05 (C-1'), 82.69 (C-5), 74.99 (C-4), 73.59 (O-CH<sub>2</sub> of linker), 73.19 (C-5'), 72.68 (C-6), 63.86 (C-4'), 57.17 (N-CH<sub>2</sub> of linker), 51.46 (N-CH<sub>2</sub> of piperazine), 49.87 (C-1), 48.96 (C-3), 47.54 (C-2'), 46.61 (N-CH<sub>2</sub> of piperazine), 39.33 (C-6'), 36.28 (CH of cyclopropyl), 29.55 (O-CH<sub>2</sub>-CH<sub>2</sub> of linker), 28.93 (CH<sub>2</sub> of linker), 28.89 (CH<sub>2</sub> of linker), 28.82 (C-3'), 28.81 (CH<sub>2</sub> of linker), 28.68 (CH<sub>2</sub> of linker), 28.34 (CH<sub>2</sub> of linker), 27.90 (CH<sub>2</sub> of linker), 25.85 (CH<sub>2</sub> of linker), 25.33 (CH<sub>2</sub> of linker), 23.43 (CH<sub>2</sub> of linker), 7.60 (CH<sub>2</sub> of cyclopropyl). MALDI-TOF-MS *m/e* calcd for C<sub>41</sub>H<sub>66</sub>FN<sub>7</sub>O<sub>8</sub>Na [M+Na]<sup>+</sup>: 826.4851, found: 826.4820.

*5-O-((10-(4-(naphthalen-1-ylmethyl)piperazin-1-yl)docyl)-nebramine 6·HCl (2).*

Compound **10** (9 mg, 0.008 mmol) was dissolved in TFA (0.5 mL) and H<sub>2</sub>O (0.25 mL) solution and then stirred for 2 h at room temperature. The solvent was removed under reduced pressure to give a white residue. Amount of 5 mL of methanol and ether solution (1:20, v/v) was added to this residue in several portions and then the solvent was decanted to get the final product **2** as TFA salt. Stoichiometric amount of HCl aqueous solution was added into it before lyophilizing the solution to afford a white solid as the final product **2** as HCl salt. Yield: 5.4 mg (72%). <sup>1</sup>H NMR (500 MHz, deuterium oxide)  $\delta$  8.27 – 8.21 (m, 1H), 8.07 – 7.97 (m, 2H), 7.72 – 7.61 (m, 2H), 7.61 – 7.54 (m, 2H), 5.56 (d, *J* = 3.1 Hz, 1H, anomeric CH of H-1'), 4.22 (s, 2H, CH<sub>2</sub> of

naphthylmethyl), 4.08 – 3.93 (m, 3H), 3.88 – 3.48 (m, 8H), 3.43 – 3.29 (m, 4H), 3.28 – 2.78 (m, 7H), 2.56 – 2.45 (m, 1H, *CHH* of H-2), 2.34 – 2.27 (m, 1H, *CHH* of H-3'), 2.18 – 2.10 (m, 1H, *CHH* of H-3'), 1.92 – 1.82 (m, 1H, *CHH* of H-2), 1.74 – 1.66 (m, 2H, N-CH<sub>2</sub>-CH<sub>2</sub> of linker), 1.66 – 1.58 (m, 2H, O-CH<sub>2</sub>-CH<sub>2</sub> of linker), 1.41 – 1.24 (m, 12H, 6 × CH<sub>2</sub> of linker). <sup>13</sup>C NMR (125 MHz, deuterium oxide) δ 133.69 (C of naphthyl), 131.88 (C of naphthyl), 129.30 (CH of naphthyl), 129.13 (CH of naphthyl), 128.82 (CH of naphthyl), 126.77 (CH of naphthyl), 126.33 (CH of naphthyl), 125.53 (CH of naphthyl), 123.90 (CH of naphthyl), 92.10 (C-1'), 82.70 (C-6), 75.26 (C-4), 73.47 (O-CH<sub>2</sub> of linker), 73.11 (C-5'), 72.67 (C-5), 63.73 (C-4'), 58.24 (CH<sub>2</sub> of naphthylmethyl), 56.82 (4 × CH<sub>2</sub> of piperazine, N-CH<sub>2</sub> of linker), 49.82 (C-1), 48.85 (C-3), 47.47 (C-2'), 39.18 (C-6'), 29.48 (O-CH<sub>2</sub>-CH<sub>2</sub> of linker), 28.80 (C-3'), 28.70 (2 × CH<sub>2</sub> of linker), 28.55 (CH<sub>2</sub> of linker), 28.23 (CH<sub>2</sub> of linker), 28.03 (C-2), 25.77 (CH<sub>2</sub> of linker), 25.26 (CH<sub>2</sub> of linker), 23.46 (N-CH<sub>2</sub>-CH<sub>2</sub> of linker). MALDI-TOF-MS *m/e* calcd for C<sub>37</sub>H<sub>62</sub>N<sub>6</sub>O<sub>5</sub>Na [M+Na]<sup>+</sup>: 693.468, found: 693.469.

*5-O-(dodecyl-moxifloxacin methyl ester)-1,3,2',6',3''-penta-N-(tert-butoxycarbonyl)-4',2'',4'',6''-tetra-O-TBDMS-tobramycin (7a)*. Synthesized following general procedure B. Yield: 764 mg (93%). <sup>1</sup>H NMR (500 MHz, methanol-*d*<sub>4</sub>) δ 8.71 (s, 1H), 7.68 (d, *J* = 14.1 Hz, 1H), 5.51 – 5.39 (m, 2H, anomeric H), 4.26 – 4.17 (m, 1H), 4.16 – 4.08 (m, 1H), 4.07 – 3.89 (m, 3H), 3.87 (s, 3H), 3.82 – 3.52 (m, 16H), 3.53 – 3.35 (m, 5H), 3.31 – 3.25 (m, 1H), 2.87 – 2.78 (m, 1H), 2.66 – 2.55 (m, 1H), 2.52 – 2.35 (m, 3H), 2.15 – 2.00 (m, 1H), 1.99 – 1.90 (m, 1H), 1.90 – 1.81 (m, 1H), 1.80 – 1.72 (m, 1H), 1.72 – 1.16 (m, 72H), 1.03 – 0.90 (m, 37H), 0.26 – 0.06 (m, 24H). <sup>13</sup>C NMR (126 MHz, methanol-*d*<sub>4</sub>, some carbons are doubling due to fluorine atom) δ 174.88, 174.86, 166.74, 158.19, 158.03, 157.49, 157.44, 157.00, 155.93, 153.95, 152.25, 142.63, 142.57, 137.98, 137.89, 135.13, 121.96, 121.90, 109.81, 108.78, 108.59, 96.80 (2C, anomeric C), 86.59,

80.66, 80.57, 80.32, 80.16, 79.52, 78.28, 75.22, 74.83, 73.57, 72.62, 68.81, 65.12, 62.90, 61.65, 57.67, 56.98, 55.53, 55.48, 52.95, 52.08, 51.78, 50.17, 49.93, 42.14, 41.20, 38.54, 36.69, 31.90, 31.24, 30.84, 30.76, 30.73, 30.70, 29.29, 29.24, 29.12, 28.96, 28.91, 28.90, 28.71, 28.10, 27.69, 27.02, 26.93, 26.73, 26.68, 26.64, 26.54, 26.21, 25.18, 23.85, 19.52, 19.11, 18.97, 18.93, 10.00, 9.96, -3.26, -3.82, -3.93, -4.16, -4.21, -4.42, -4.62, -4.87. MALDI-TOF-MS  $m/e$  calcd for  $C_{101}H_{181}FN_8O_{23}Si_4Na$   $[M+Na]^+$ : 2028.2198, found: 2028.2174.

*5-O-(dodecyl-ciprofloxacin methyl ester)-1,3,2',6',3''-penta-N-(tert-butoxycarbonyl)-4',2'',4'',6''-tetra-O-TBDMS-tobramycin (7b)*. Synthesized following general procedure B. Yield: 724 mg (69%).  $^1H$  NMR (300 MHz,  $CDCl_3$ )  $\delta$  8.52 (s, 1H), 8.00 (d,  $J = 13.2$  Hz, 1H), 7.26 (d,  $J = 7.1$  Hz, 1H), 5.29 – 5.00 (m, 4H), 4.88 – 4.70 (m, 1H), 4.64 – 4.50 (m, 1H), 4.34 – 4.00 (m, 3H), 3.90 (s, 3H), 3.84 – 3.11 (m, 22H), 2.75 – 2.65 (m, 3H), 2.50 – 2.39 (m, 2H), 2.06 – 1.94 (m, 1H), 1.60 – 1.08 (m, 76H), 0.97 – 0.81 (m, 36H), 0.19 – -0.01 (m, 24H).  $^{13}C$  NMR (75 MHz,  $CDCl_3$ , some carbons are doubling due to fluorine atom)  $\delta$  173.11, 166.49, 155.08, 148.38, 144.56, 138.00, 123.02, 113.39, 113.08, 109.98, 104.79, 79.44, 79.25, 58.67, 52.89, 52.09, 49.83, 49.77, 48.33, 34.53, 30.08, 29.74, 29.67, 28.65, 28.52, 28.42, 27.59, 26.72, 26.16, 26.02, 25.80, 18.53, 18.36, 18.12, 17.93, 8.15, -3.77, -4.17, -4.87, -4.95, -5.05, -5.20. MALDI-TOF-MS  $m/e$  calcd for  $C_{97}H_{175}FN_8O_{22}Si_4Na$   $[M+Na]^+$ : 1958.178, found: 1958.125.

*5-O-(dodecyl-moxifloxacin methyl ester)-1,3,2',6'-tetra-N-(tert-butoxycarbonyl)-nebramine (8a)*. Synthesized following general procedure C. Yield: 40 mg (65%, two steps).  $^1H$  NMR (300 MHz, methanol- $d_4$ )  $\delta$  8.71 (s, 1H), 7.68 (d,  $J = 14.5$  Hz, 1H), 5.31 – 5.25 (m, 1H, anomeric H-1'), 4.16 – 4.06 (m, 1H), 3.99 – 3.88 (m, 1H), 3.87 (s, 3H), 3.76 – 3.51 (m, 12H), 3.50 – 3.36 (m, 4H), 3.31 – 3.23 (m, 3H), 2.92 – 2.81 (m, 1H), 2.68 – 2.58 (m, 1H), 2.50 – 2.37 (m, 3H), 2.07 – 1.90 (m, 2H), 1.89 – 1.40 (m, 46H), 1.39 – 1.14 (m, 19H), 0.99 (dd,  $J = 4.7, 2.4$

Hz, 1H).  $^{13}\text{C}$  NMR (75 MHz, methanol- $d_4$ , some carbons are doubling due to fluorine atom)  $\delta$  174.97, 166.77, 158.24, 157.95, 157.49, 156.56, 153.28, 152.30, 142.59, 142.49, 138.06, 137.91, 135.19, 121.93, 121.83, 109.81, 108.84, 108.52, 97.46 (anomeric C), 87.23, 80.81, 80.42, 80.25, 78.93, 77.23, 74.00, 73.26, 67.14, 63.05, 61.65, 56.74, 55.35, 52.29, 52.12, 49.00, 41.20, 38.59, 35.93, 34.84, 31.55, 30.80, 30.69, 30.51, 28.90, 28.88, 28.81, 28.76, 28.49, 27.85, 27.31, 24.98, 23.59, 21.01, 13.95, 10.01, 9.91. MS (ESI)  $m/e$  calcd for  $\text{C}_{66}\text{H}_{107}\text{FN}_7\text{O}_{17}$   $[\text{M}+\text{H}]^+$ : 1289.6, found: 1289.4.

*5-O-(dodecyl-ciprofloxacin methyl ester)-1,3,2',6'-tetra-N-(tert-butoxycarbonyl)-nebramine (8b)*. Synthesized following general procedure C. Yield: 52 mg (31%, two steps).  $^1\text{H}$  NMR (300 MHz,  $\text{CDCl}_3$ )  $\delta$  8.54 (s, 1H), 7.99 (d,  $J = 13.2$  Hz, 1H), 7.28 (d,  $J = 7.3$  Hz, 1H), 5.36 – 5.12 (m, 2H), 5.09 – 4.88 (m, 3H), 3.96 – 3.21 (m, 25H), 3.18 – 3.08 (m, 2H), 2.78 – 2.68 (m, 4H), 2.52 – 2.43 (m, 2H), 2.37 – 2.25 (m, 1H), 2.21 – 2.08 (m, 1H), 1.72 – 1.03 (m, 76H).  $^{13}\text{C}$  NMR (75 MHz,  $\text{CDCl}_3$ )  $\delta$  173.28, 166.28, 157.97, 155.12, 148.41, 144.56, 138.06, 122.91, 113.37, 113.07, 109.80, 104.90, 80.26, 79.40, 58.62, 52.85, 52.09, 49.65, 46.06, 34.66, 30.16, 29.60, 29.54, 29.50, 28.45, 28.42, 28.35, 28.33, 27.46, 26.52, 26.09, 8.18. MALDI-TOF-MS  $m/e$  calcd for  $\text{C}_{62}\text{H}_{100}\text{FN}_7\text{O}_{16}\text{Na}$   $[\text{M}+\text{Na}]^+$ : 1240.711, found: 1240.658.

*5-O-((10-(4-(naphthalen-1-ylmethyl)piperazin-1-yl)dodecyl)-1,3,2',6'-tetra-N-(tert-butoxycarbonyl)-nebramine (10)*. Synthesized following general procedure C. Yield: 27 mg (53%, two steps).  $^1\text{H}$  NMR (500 MHz, methanol- $d_4$ )  $\delta$  8.29 – 8.25 (m, 1H), 7.87 – 7.83 (m, 1H), 7.81 – 7.77 (m, 1H), 7.52 – 7.44 (m, 2H), 7.44 – 7.37 (m, 2H), 5.25 (d,  $J = 3.8$  Hz, 1H, anomeric CH of H-1'), 3.94 (s, 2H,  $\text{CH}_2$  of naphthylmethyl), 3.93 – 3.88 (m, 1H), 3.70 – 3.47 (m, 5H), 3.47 – 3.31 (m, 5H), 3.28 – 3.19 (m, 3H), 2.83 – 2.44 (m, 8H), 2.44 – 2.37 (m, 1H), 2.01 – 1.92 (m, 1H), 1.92 – 1.85 (m, 1H), 1.65 – 1.58 (m, 1H), 1.55 – 1.48 (m, 4H), 1.48 – 1.38 (m, 36H,  $4 \times$

*t*-Bu of Boc), 1.33 – 1.22 (m, 12H, 6 × CH<sub>2</sub> of linker). <sup>13</sup>C NMR (126 MHz, methanol-*d*<sub>4</sub>) δ 159.35, 158.27, 157.98, 157.49, 135.47, 134.63, 133.92, 129.42, 129.29, 128.92, 126.80, 126.70, 126.08, 125.78, 97.43, 87.27, 80.83, 80.43, 80.29, 78.92, 77.28, 74.04, 73.25, 67.14, 67.13, 61.63, 59.62, 54.06, 53.50, 52.85, 50.84, 50.29, 42.28, 35.95, 34.82, 31.54, 30.77, 30.61, 30.59, 30.56, 28.89, 28.86, 28.80, 28.75, 28.57, 27.30, 27.14. MALDI-TOF-MS *m/e* calcd for C<sub>57</sub>H<sub>95</sub>N<sub>6</sub>O<sub>13</sub> [M+H]<sup>+</sup>: 1071.696, found: 1071.716.

## 6.5.2 Microbiology

### 6.5.2.1 Clinical Isolates

Clinically-relevant bacterial strains were collected from the Canadian National Intensive Care Unit (CAN-ICU) study<sup>39</sup> and Canadian Ward Surveillance (CANWARD) studies.<sup>40,41</sup> All pathogens obtained from CAN-ICU and CANWARD studies have received ethics approval from the University of Manitoba Ethics Committee. In addition, participating Canadian health centers have obtained appropriate ethics approval to submit clinical specimens.

### 6.5.2.2 Antimicrobial Susceptibility Testing

The antimicrobial activity of the compounds against a panel of bacteria was evaluated by broth microdilution assay in accordance with the Clinical and Laboratory Standards Institute (CLSI) guidelines.<sup>32</sup> was performed to assess the *in vitro* antibacterial activity. Bacterial cultures grown overnight were diluted in saline to achieve a 0.5 McFarland turbidity, followed by 1:50 dilution in Mueller-Hinton broth (MHB) for inoculation to a final concentration of 5×10<sup>5</sup> CFU/mL. The minimum inhibitory concentrations (MICs) of the antimicrobial agents were

determined using 96-well plates containing 2-fold serial dilutions with MHB and incubated with equal volumes of inoculum for 18 h at 37 °C. MIC was determined as the lowest concentration to inhibit visible bacterial growth in the form of turbidity, which was confirmed using an EMax Plus microplate reader (Molecular Devices, San Jose, CA, USA) at a wavelength of 590 nm. The wells containing MHB broth with or without bacterial cells were used as positive or negative controls, respectively.

### 6.5.2.3 Checkerboard Assay

The checkerboard method<sup>42</sup> was used to assess synergism in all tested combinations. Fractional inhibitory concentrations (FICs) were calculated as follows:  $FIC_{\text{antibiotic}} = MIC_{\text{combo}}/MIC_{\text{antibiotic alone}}$ ;  $FIC_{\text{adjuvant}} = MIC_{\text{combo}}/MIC_{\text{adjuvant alone}}$ , where  $MIC_{\text{combo}}$  is the lowest inhibitory concentration of drug in the presence of the adjuvant. The FIC index was calculated by adding the FIC values. FIC indices (FICI) were interpreted as follows:  $\leq 0.5$ , synergy,  $0.5 < FICI \leq 4.0$ , no interaction, and  $\geq 4.0$ , antagonism.<sup>28</sup>

### 6.5.2.4 Time-kill Curve Assay

The kinetics of bacterial killing was measured using *P. aeruginosa* PAO1 and PA259 as previously described.<sup>10</sup> Overnight bacterial culture was diluted in saline to 0.5 McFarland turbidity and then 1:50 diluted in Luria-Bertani broth (LB). The cell suspension (*P. aeruginosa* PAO1) was incubated with the combination of  $\frac{1}{4} \times MIC$  (8  $\mu\text{g/mL}$ ) or  $\frac{1}{2} \times MIC$  (16  $\mu\text{g/mL}$ ) of hybrid **1a** with 4  $\mu\text{g/mL}$  of minocycline. Untreated cells in media and cells treated with  $4 \times MIC$  (4  $\mu\text{g/mL}$ ) of colistin were used as negative and positive controls respectively (Fig. 6.3.3.1A). Respect to the time-kill curve of **1b** (Fig. 6.3.3.1B), the cell suspension (*P. aeruginosa* PA259)

was incubated with rifampicin (4  $\mu\text{g}/\text{mL}$ ) and **1b** (4  $\mu\text{g}/\text{mL}$ ) alone or the combination of **1b** with rifampicin at various concentrations as shown in Fig 6.3.3.1B. Samples were incubated at 37 °C for 24 h. At specific intervals (Fig. 6.3.3.1), aliquots (100  $\mu\text{L}$ ) were removed from the samples, serially diluted in PBS, and plated on LB agar plates. Bacterial colonies were formed and counted after 20 h of incubation at 37 °C.

#### 6.5.2.5 Hemolytic Assay

The hemolytic activities of the newly synthesized compounds were determined and quantified as the amount of hemoglobin released by lysing porcine erythrocytes. Fresh blood drawn from the antecubital vein of a pig (Animal Care and Use Program, University of Manitoba) was centrifuged at 1000 g at 4 °C for 10 mins, washed with PBS thrice and resuspended in the same buffer. The final cell concentration used was  $3 \times 10^8$  cells/mL. Compounds were serially diluted with PBS and added to wells in a 96-well plate at twice the desired concentrations. Equal volumes of erythrocyte solution were then added to each well and incubated at 37 °C for 1 h. Intact erythrocytes were subsequently pelleted by centrifuging at 1000 g at 4 °C for 10 mins, and the supernatants were transferred to a new 96-well plate. Hemoglobin release was determined by measuring the absorbance on EMax<sup>®</sup> Plus microplate reader (Molecular Devices, Sunnyvale, CA, USA) at 570 nm. Blood cells in PBS (0% hemolysis) and 0.1 % Triton X-100 (100% hemolysis) were used as negative and positive controls, respectively. Percent hemolysis was calculated as [% hemolysis =  $(X - 0\%) / (100\% - 0\%)$ ], where X is the optical density values of the compounds at different concentrations.

### 6.5.2.6 *Galleria mellonella* Model of *P. aeruginosa* Infection

*In vivo* synergistic effects were determined using *Galleria mellonella* infection model, as previously described.<sup>8</sup> Briefly, worms were purchased from The Worm Lady® Live Feeder (ON, Canada), stored in their natural habitat at 16 °C, and used within 10 days of delivery. The worms (average weight of 250 mg) were used for tolerability and efficacy studies. Tolerability study was performed by injecting 10 µL of antimicrobial agents only at concentrations equivalent to 100 mg/kg or 200 mg/kg. The worms (ten in each group) were incubated at 37 °C and monitored for 96 h. For efficacy studies, the virulence and bacterial load required to kill 100 % of the worms within 12 – 18 h was first determined, which is approximately 5 CFU. Overnight grown culture of MDR *P. aeruginosa* PA264 isolate was standardized to 0.5 McFarland standard and diluted in PBS to a final concentration of  $5 \times 10^2$  CFU/mL. 10 µL of this solution (~ 5 CFU) was injected into each worm and incubated for 2 h at 37 °C. After the 2 h challenge, worms in monotherapy experimental groups (fifteen worms per group) were treated with 10 µL injection of rifampicin, compound **1b**, or PBS alone. The worms in combination therapy groups were treated with rifampicin + compound **1b** (25 + 25 mg/kg, 50 + 50 mg/kg, or 75 + 75 mg/kg). Worms treated with 10 µL PBS negative control. The worms were incubated at 37 °C in Petri dishes lined with filter paper and scored for survivability every 6 h for up to 24 h. This experiment was repeated to give a total of thirty worms ( $n = 30$ ) in each case. Survival data curves were plotted using Kaplan-Meier survival analysis. Worms were considered dead if they do not respond to touch.

### 6.5.2.7 Tetracycline Uptake Assay

Fluorescence-based tetracycline uptake assay in bacterial cells was performed following previously reported method.<sup>36</sup> Culture of *P. aeruginosa* PAO1 was grown to OD<sub>600</sub> = 0.6 followed by washing and re-suspending it in ¼ volume of 10 mM HEPES, pH 7.2, 100 µL/well cell suspension was treated with varying concentrations of test compounds in the presence of 128 µg/mL of tetracycline. Fluorescence was recorded at a continuous interval of 1 min for 30 min at room temperature on a FlexStation 3 (Molecular Devices, Sunnyvale, USA) microplate reader at the excitation wavelength of 405 nm and emission wavelength of 535 nm. Experiments were performed in triplicates. Averages of triplicate experiments are shown in Fig. 6.3.5.1.

## 6.6 ACKNOWLEDGMENTS

The work was supported by NSERC-DG 321252 and MHRC.

## 6.7 REFERENCES

- (1) American Chemical Society International Historic Chemical Landmarks. Discovery and Development of Penicillin.  
<http://www.acs.org/content/acs/en/education/whatischemistry/landmarks/flemingpenicillin.html> (accessed on October 11, 2018).
- (2) Coates, A.; Hu, Y.; Bax, R.; Page, C. The Future Challenges Facing the Development of New Antimicrobial Drugs. *Nat. Rev. Drug Discov.* **2002**, *1* (11), 895–910.
- (3) Powers, J. H. Antimicrobial Drug Development – the Past, the Present, and the Future. *Clin. Microbiol. Infect.* **2004**, *10*, 23–31.

- (4) Payne, D. J.; Gwynn, M. N.; Holmes, D. J.; Pompliano, D. L. Drugs for Bad Bugs: Confronting the Challenges of Antibacterial Discovery. *Nat. Rev. Drug Discov.* **2006**, *6*, 29.
- (5) Silver, L. L. Are Natural Products Still the Best Source for Antibacterial Discovery? The Bacterial Entry Factor. *Expert Opin. Drug Discov.* **2008**, *3* (5), 487–500.
- (6) Wright, G. D. Antibiotic Adjuvants: Rescuing Antibiotics from Resistance. *Trends Microbiol.* **2016**, *24* (11), 862–871.
- (7) Domalaon, R.; Idowu, T.; Zhanel, G. G.; Schweizer, F. Antibiotic Hybrids: The Next Generation of Agents and Adjuvants against Gram-Negative Pathogens? *Clin. Microbiol. Rev.* **2018**, *31* (2), e00077-17.
- (8) Gorityala, B. K.; Guchhait, G.; Fernando, D. M.; Deo, S.; McKenna, S. A.; Zhanel, G. G.; Kumar, A.; Schweizer, F. Adjuvants Based on Hybrid Antibiotics Overcome Resistance in *Pseudomonas Aeruginosa* and Enhance Fluoroquinolone Efficacy. *Angew. Chemie Int. Ed.* **2016**, *55* (2), 555–559.
- (9) Gorityala, B. K.; Guchhait, G.; Goswami, S.; Fernando, D. M.; Kumar, A.; Zhanel, G. G.; Schweizer, F. Hybrid Antibiotic Overcomes Resistance in *P. Aeruginosa* by Enhancing Outer Membrane Penetration and Reducing Efflux. *J. Med. Chem.* **2016**, *59* (18), 8441–8455.
- (10) Lyu, Y.; Yang, X.; Goswami, S.; Gorityala, B. K.; Idowu, T.; Domalaon, R.; Zhanel, G. G.; Shan, A.; Schweizer, F. Amphiphilic Tobramycin–Lysine Conjugates Sensitize Multidrug Resistant Gram-Negative Bacteria to Rifampicin and Minocycline. *J. Med. Chem.* **2017**, *60* (9), 3684–3702.
- (11) Yang, X.; Goswami, S.; Gorityala, B. K.; Domalaon, R.; Lyu, Y.; Kumar, A.; Zhanel, G.

- G.; Schweizer, F. A Tobramycin Vector Enhances Synergy and Efficacy of Efflux Pump Inhibitors against Multidrug-Resistant Gram-Negative Bacteria. *J. Med. Chem.* **2017**, *60* (9), 3913–3932.
- (12) Domalaon, R.; Yang, X.; Lyu, Y.; Zhanel, G. G.; Schweizer, F. Polymyxin B 3 – Tobramycin Hybrids with *Pseudomonas Aeruginosa* -Selective Antibacterial Activity and Strong Potentiation of Rifampicin, Minocycline, and Vancomycin. *ACS Infect. Dis.* **2017**, *3* (12), 941–954.
- (13) Lyu, Y.; Domalaon, R.; Yang, X.; Schweizer, F. Amphiphilic Lysine Conjugated to Tobramycin Synergizes Legacy Antibiotics against Wild-Type and Multidrug-Resistant *Pseudomonas Aeruginosa*. *Biopolymers* **2017**, e23091.
- (14) Yang, X.; Domalaon, R.; Lyu, Y.; Zhanel, G.; Schweizer, F. Tobramycin-Linked Efflux Pump Inhibitor Conjugates Synergize Fluoroquinolones, Rifampicin and Fosfomycin against Multidrug-Resistant *Pseudomonas Aeruginosa*. *J. Clin. Med.* **2018**, *7* (7), 158.
- (15) Bulitta, J. B.; Ly, N. S.; Landersdorfer, C. B.; Wanigaratne, N. A.; Velkov, T.; Yadav, R.; Oliver, A.; Martin, L.; Shin, B. S.; Forrest, A.; Tsuji, B. T. Two Mechanisms of Killing of *Pseudomonas Aeruginosa* by Tobramycin Assessed at Multiple Inocula via Mechanism-Based Modeling. *Antimicrob. Agents Chemother.* **2015**, *59* (4), 2315–2327.
- (16) Davies, J.; Davis, B. D. Misreading of Ribonucleic Acid Code Words Induced by Aminoglycoside Antibiotics. *J. Biol. Chem.* **1968**, *243* (12), 3312–3316.
- (17) Fourmy, D.; Recht, M. I.; Blanchard, S. C.; Puglisi, J. D. Structure of the A Site of *Escherichia Coli* 16S Ribosomal RNA Complexed with an Aminoglycoside Antibiotic. *Science* **1996**, *274* (5291), 1367–1371.
- (18) Fourmy, D.; Recht, M. I.; Puglisi, J. D. Binding of Neomycin-Class Aminoglycoside

- Antibiotics to the A-Site of 16 s RRNA. *J. Mol. Biol.* **1998**, *277* (2), 347–362.
- (19) Vicens, Q.; Westhof, E. Crystal Structure of a Complex between the Aminoglycoside Tobramycin and an Oligonucleotide Containing the Ribosomal Decoding A Site. *Chem. Biol.* **2002**, *9* (6), 747–755.
- (20) Lynch, S. R.; Gonzalez, R. L.; Puglisi, J. D. Comparison of X-Ray Crystal Structure of the 30S Subunit-Antibiotic Complex with NMR Structure of Decoding Site Oligonucleotide-Paromomycin Complex. *Structure* **2003**, *11* (1), 43–53.
- (21) Agnelli, F.; Sucheck, S. J.; Marby, K. A.; Rabuka, D.; Yao, S.-L.; Sears, P. S.; Liang, F.-S.; Wong, C.-H. Dimeric Aminoglycosides as Antibiotics. *Angew. Chem., Int. Ed. Engl.* **2004**, *43* (12), 1562–1566.
- (22) Berkov-Zrihen, Y.; Herzog, I. M.; Benhamou, R. I.; Feldman, M.; Steinbuch, K. B.; Shaul, P.; Lerer, S.; Eldar, A.; Fridman, M. Tobramycin and Nebramine as Pseudo-Oligosaccharide Scaffolds for the Development of Antimicrobial Cationic Amphiphiles. *Chem. Eur. J.* **2015**, *21* (11), 4340–4349.
- (23) Zimmermann, L.; Das, I.; Désiré, J.; Sautrey, G.; Barros R. S., V.; El Khoury, M.; Mingeot-Leclercq, M.-P.; Décout, J.-L. New Broad-Spectrum Antibacterial Amphiphilic Aminoglycosides Active against Resistant Bacteria: From Neamine Derivatives to Smaller Neosamine Analogues. *J. Med. Chem.* **2016**, *59* (20), 9350–9369.
- (24) Ouberai, M.; El Garch, F.; Bussiere, A.; Riou, M.; Alsteens, D.; Lins, L.; Baussanne, I.; Dufrière, Y. F.; Brasseur, R.; Decout, J.-L.; Mingeot-Leclercq, M.-P. The Pseudomonas Aeruginosa Membranes: A Target for a New Amphiphilic Aminoglycoside Derivative? *Biochim. Biophys. Acta - Biomembr.* **2011**, *1808* (6), 1716–1727.
- (25) Zimmermann, L.; Kempf, J.; Briée, F.; Swain, J.; Mingeot-Leclercq, M.-P.; Décout, J.-L.

- Broad-Spectrum Antibacterial Amphiphilic Aminoglycosides: A New Focus on the Structure of the Lipophilic Groups Extends the Series of Active Dialkyl Neamines. *Eur. J. Med. Chem.* **2018**, *157*, 1512–1525.
- (26) Bohnert, J. A.; Kern, W. V. Selected Arylpiperazines Are Capable of Reversing Multidrug Resistance in Escherichia Coli Overexpressing RND Efflux Pumps Selected Arylpiperazines Are Capable of Reversing Multidrug Resistance in Escherichia Coli Overexpressing RND Efflux Pumps. *Antimicrob. Agents Chemother.* **2005**, *49* (2), 849–852.
- (27) Guchhait, G.; Altieri, A.; Gorityala, B.; Yang, X.; Findlay, B.; Zhanel, G. G.; Mookherjee, N.; Schweizer, F. Amphiphilic Tobramycins with Immunomodulatory Properties. *Angew. Chem., Int. Ed. Engl.* **2015**, *54* (21), 6278–6282.
- (28) Odds, F. C. Synergy, Antagonism, and What the Checkerboard Tells between Them. *J. Antimicrob. Chemother.* **2003**, *52* (1), 1.
- (29) Berkhout, J.; Melchers, M. J.; Van Mil, A. C.; Nichols, W. W.; Mouton, J. W. In Vitro Activity of Ceftazidime-Avibactam Combination in in Vitro Checkerboard Assays. *Antimicrob. Agents Chemother.* **2015**, *59* (2), 1138–1144.
- (30) Sader, H. S.; Castanheira, M.; Mendes, R. E.; Flamm, R. K.; Farrell, D. J.; Jones, R. N. Ceftazidime-Avibactam Activity against Multidrug-Resistant Pseudomonas Aeruginosa Isolated in U.S. Medical Centers in 2012 and 2013. *Antimicrob. Agents Chemother.* **2015**, *59* (6), 3656–3659.
- (31) Kaye, K. S.; Pogue, J. M.; Tran, T. B.; Nation, R. L.; Li, J. Agents of Last Resort: Polymyxin Resistance. *Infect. Dis. Clin. North Am.* **2016**, *30* (2), 391–414.
- (32) Clinical and Laboratory Standards Institute (CLSI). *Performance Standards for*

- Antimicrobial Susceptibility Testing*, 26th ed.; Clinical and Laboratory Standards Institute: Wayne, Pennsylvania, USA, 2016.
- (33) Bonnet, R., Caron, F., Cavallo, J.D.; Chardon, H., Chidiac, C., Courvalin, P., Drugeon, H., Dubreuil, L., Jarlier, V.; Jehl, F., Lambert, T., Leclercq, R., Nicolas-Chanoine, M.H., Plesiat, P.; Ploy, M.C., Quentin, C., Soussy, C.J., Varon, E., Weber, P. Comité de L'Antibiogramme de La Société Française de Microbiologie-Recommandations 2012. January Edition. **2012**.
- (34) Adamson, D. H.; Krikstopaityte, V.; Coote, P. J. Enhanced Efficacy of Putative Efflux Pump Inhibitor/Antibiotic Combination Treatments versus MDR Strains of *Pseudomonas Aeruginosa* in a *Galleria Mellonella* in Vivo Infection Model. *J. Antimicrob. Chemother.* **2015**, *70* (8), 2271–2278.
- (35) Krezdorn, J.; Adams, S.; Coote, P. J. A *Galleria Mellonella* Infection Model Reveals Double and Triple Antibiotic Combination Therapies with Enhanced Efficacy versus a Multidrug-Resistant Strain of *Pseudomonas Aeruginosa*. *J. Med. Microbiol.* **2014**, *63* (Pt\_7), 945–955.
- (36) Ejim, L.; Farha, M. A.; Falconer, S. B.; Wildenhain, J.; Coombes, B. K.; Tyers, M.; Brown, E. D.; Wright, G. D. Combinations of Antibiotics and Nonantibiotic Drugs Enhance Antimicrobial Efficacy. *Nat. Chem. Biol.* **2011**, *7* (6), 348–350.
- (37) Mitchell, P. Chemiosmotic Coupling in Oxidative and Photosynthetic Phosphorylation. *Biochim. Biophys. Acta* **2011**, *1807* (12), 1507–1538.
- (38) Chopra, I.; Hacker, K. Effects of Tetracyclines on the Production of Extracellular Proteins by Members of the Propionibacteriaceae. *FEMS Microbiol. Lett.* **1989**, *60* (1), 21–24.
- (39) Zhanel, G. G.; DeCorby, M.; Laing, N.; Weshnoweski, B.; Vashisht, R.; Tailor, F.; Nichol,

- K. A.; Wierzbowski, A.; Baudry, P. J.; Karlowsky, J. A.; Lagace-Wiens, P.; Walkty, A.; McCracken, M.; Mulvey, M. R.; Johnson, J.; Hoban, D. J. Antimicrobial-Resistant Pathogens in Intensive Care Units in Canada: Results of the Canadian National Intensive Care Unit (CAN-ICU) Study, 2005-2006. *Antimicrob. Agents Chemother.* **2008**, *52* (4), 1430–1437.
- (40) Zhanel, G. G.; Adam, H. J.; Baxter, M. R.; Fuller, J.; Nichol, K. A.; Denisuk, A. J.; Lagace-Wiens, P. R. S.; Walkty, A.; Karlowsky, J. A.; Schweizer, F.; Hoban, D. J. Antimicrobial Susceptibility of 22746 Pathogens from Canadian Hospitals: Results of the CANWARD 2007-11 Study. *J. Antimicrob. Chemother.* **2013**, *68 Suppl 1*, i7-22.
- (41) Zhanel, G. G.; DeCorby, M.; Adam, H.; Mulvey, M. R.; McCracken, M.; Lagace-Wiens, P.; Nichol, K. A.; Wierzbowski, A.; Baudry, P. J.; Tabor, F.; Karlowsky, J. A.; Walkty, A.; Schweizer, F.; Johnson, J.; Hoban, D. J. Prevalence of Antimicrobial-Resistant Pathogens in Canadian Hospitals: Results of the Canadian Ward Surveillance Study (CANWARD 2008). *Antimicrob. Agents Chemother.* **2010**, *54* (11), 4684–4693.
- (42) Orhan, G.; Bayram, A.; Zer, Y.; Balci, I. Synergy Tests by E Test and Checkerboard Methods of Antimicrobial Combinations against *Brucella Melitensis*. *J. Clin. Microbiol.* **2005**, *43* (1), 140–143.

## Chapter 7: Amphiphilic Tobramycins with Immunomodulatory Properties

*By Goutam Guchhait, Antony Altieri, Balakishan Gorityala, Xuan Yang, Brandon Findlay, George G. Zhanel, Neeloffer Mookherjee, and Frank Schweizer. First published in Angewandte Chemie, International Edition, 54 (21), 2015, 6278-6282. Reproduced with permission.*

Contributions of Authors: *Goutam Guchhait conducted the synthetic work. Balakishan Gorityala and Brandon Findlay were involved in the development of the synthetic method. Antony Altieri and Xuan Yang performed the immunomodulatory assays under the guidance of Neeloffer Mookherjee.*

### 7.1 ABSTRACT

Amphiphilic aminoglycosides (AAGs) are an emerging source of antibacterials to combat infections caused by antibiotic-resistant bacteria. Mode-of-action studies indicate that AAGs predominately target bacterial membranes, thereby leading to depolarization and increased permeability. To assess whether AAGs also induce host-directed immunomodulatory responses, we determined the AAG-dependent induction of cytokines in macrophages in the absence or presence of lipopolysaccharide (LPS). Our results show for the first time that AAGs can boost the innate immune response, specifically the recruitment of immune cells such as neutrophils required for the resolution of infections. Moreover, AAGs can selectively control inflammatory responses induced in the presence of endotoxins to prevent septic shock. In conclusion, our study

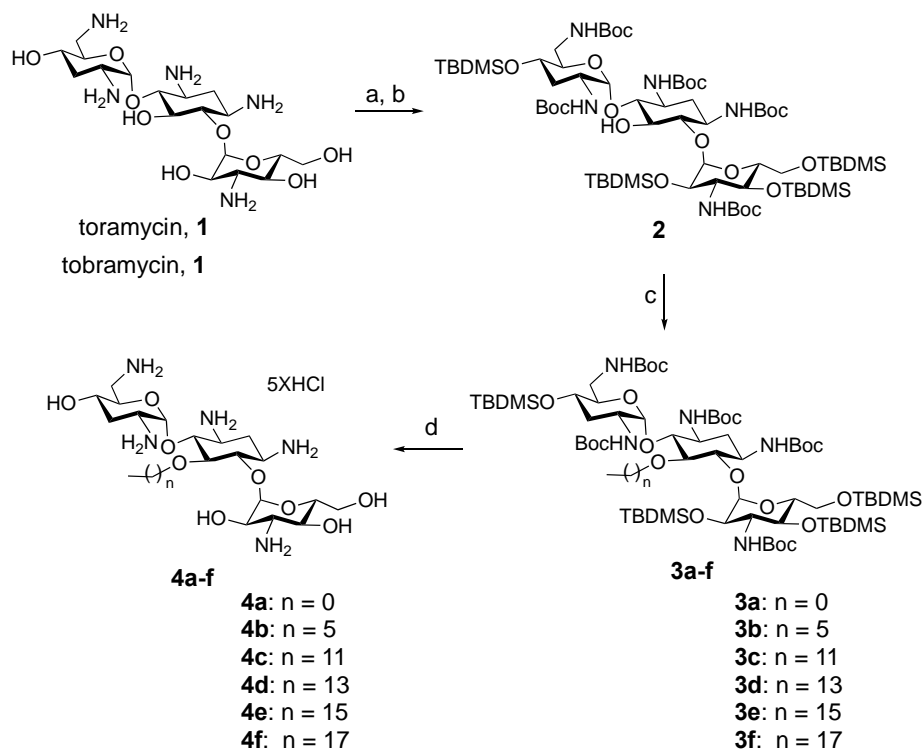
demonstrates that AAGs possess multifunctional properties that combine direct antibacterial activity with host-directed clearance effects reminiscent of those of host-defense peptides.

## 7.2 INTRODUCTION

The world is facing an enormous threat from the emergence and dissemination of bacteria that are resistant to almost all currently available antibiotics.<sup>1,2</sup> Two strategies, multiple-component antibiotic adjuvants<sup>3</sup> and single-component-based antibacterial polypharmacology<sup>4</sup> are currently under investigation to combat bacterial resistance. Both strategies seek to exploit multiple modes of action. Recently, amphiphilic aminoglycosides (AAGs) have emerged as a source of antibacterial agents to combat bacterial resistance.<sup>5-15</sup> Mode-of-action studies have shown that AAGs can show different modes of action<sup>5,8-10,12</sup> to AGs, which bind to the 30S ribosomal subunit, thereby leading to the disruption of protein synthesis.<sup>16-19</sup> For instance, it was shown that the antibacterial effect of a neamine-based AAG against *P. aeruginosa* was caused by changes in membrane depolarization and permeability and not by inhibition of protein synthesis.<sup>5,12</sup> Strong evidence for membrane-targeting interactions of AAGs were also reported for amphiphilic neomycin and tobramycin analogues.<sup>8-10</sup>

Encouraged by the multimodal activity of cationic amphiphilic host-defense peptides (HDPs) in the host-directed clearance of an infection,<sup>20-22</sup> we developed an interest in exploring whether AAGs can show HDP-like properties. AAGs that combine direct antibacterial effects with the induction of immunomodulatory responses in host immune cells may display superior efficacy against multiple-drug-resistant (MDR) bacteria. It is noteworthy that for cationic amphiphilic HDPs like LL-37, the direct antibacterial activity is antagonized by physiological concentrations of divalent cations and polyanions, and other host factors.<sup>21,22</sup> However, HDP-

mediated protection has been observed in several *in vivo* infection models, thus suggesting that the broad range of immunomodulatory activities exhibited by these peptides is the predominant function of HDPs for the resolution of microbial infections.<sup>21,23–25</sup> With this in mind, we set out to explore the potential immunomodulatory properties of AAGs. We were initially interested in developing multitargeting AAGs that combine the direct antibacterial effect of AGs with the membrane-targeting effects of AAGs. We selected tobramycin (**1**; Scheme 7.2.1) as the parent aminoglycoside since it is indispensable in intravenous or inhaled therapy to treat *P. aeruginosa* lung infections in cystic fibrosis patients.<sup>26</sup> Previous studies have shown that amphiphilic tobramycin analogues bearing a lipophilic group at C-6'' or C-5 retain potent antibacterial activity.<sup>9,10,27</sup> Furthermore, it was shown that C-6''-modified amphiphilic tobramycin targets bacterial membranes as its major mode of antibacterial action,<sup>9,10</sup> while C-5-modified tobramycin analogues containing positively charged small hydrophobic chains retain their capacity to interfere with protein synthesis.<sup>27</sup> Moreover, there is crystallographic evidence that the C-5 hydroxy group in tobramycin is not involved in direct contacts to model RNA, thus suggesting that structural modifications at this position may not interfere with RNA binding.<sup>28</sup>



**Scheme 7.2.1.** Synthesis of amphiphilic tobramycins (**4a–f**). Reagents and conditions: (a)  $(\text{Boc})_2\text{O}$ ,  $\text{Et}_3\text{N}$ ,  $\text{MeOH}/\text{H}_2\text{O}$  (2:1), rt to 55 °C, overnight. (b) TBDMSCl, 1-methylimidazole, DMF,  $\text{N}_2$ , rt, 24 h, 75% (two steps). (c) Alkyl iodide, KOH, TBAB (tetra-*n*-butylammonium bromide), toluene, rt, overnight, 75%–90%. (d)  $\text{MeOH}/40\% \text{HCl}$  (3:2), v/v, rt, 1–5 h, 80%–85%.

### 7.3 RESULTS AND DISCUSSION

We report herein our investigations into the antimicrobial properties of the C-5-substituted amphiphilic tobramycin analogues **4a–f** (Scheme 7.2.1), which were prepared from tobramycin (**1**) by using phase-transfer catalysis for the alkylation (Scheme 7.2.1). Compounds **4a–f** were tested for antibacterial activity by determining the minimal inhibitory concentrations (MIC) against a panel of bacterial strains, including tobramycin-resistant clinical isolates (Table S1 in the Supporting Information). Our results show that the amphiphilic tobramycin analogues

**4d–f**, which bear lipophilic tetradecyl, hexadecyl, and octadecyl ether appendages, respectively, show good activity against Gram-positive bacteria (GPBs; MIC = 2–16  $\mu\text{g/mL}$ ) and reduced activity against Gram-negative bacteria (GNBs; Table 7.3.1). The most active AAG **4f** contains an octadecyl ether chain and consistently displayed the highest activity against both GPBs (MIC = 2–4  $\mu\text{g/mL}$ ) and GNBs (MIC = 16–128  $\mu\text{g/mL}$ ). Notably, when compared to tobramycin (**1**), an 8-fold reduction in MIC was observed for **4f** against resistant GNB strains including a tobramycin-resistant *E. coli* strain and a tobramycin-resistant *P. aeruginosa* strain, while a 4-fold or higher reduction was observed against tobramycin-resistant *S. maltophilia*. By contrast, the poorly amphiphilic tobramycin analogue **4b**, which contains a weakly lipophilic hexyl ether chain, showed poor antibacterial activity (MIC = 128  $\mu\text{g/mL}$ ) against most bacterial strains tested (Table 7.3.1). Overall, the activity of the AAGs **4d–f** is comparable to the antibacterial activity often observed for antimicrobial peptides and HDPs like LL-37.

**Table 7.3.1.** MIC ( $\mu\text{g/mL}$ ) of compounds **4a–f** against a panel of Gram-positive and Gram-negative bacteria.

Organisms <sup>a</sup>	Tobramycin	<b>4a</b>	<b>4b</b>	<b>4c</b>	<b>4d</b>	<b>4e</b>	<b>4f</b>
Gram-positive bacteria							
<i>S. aureus</i> ATCC 29213	≤0.25	4	128	64	16	8	4
MRSA ATCC 33592	≤0.25	4	128	128	16	8	4
MSSE CANWARD-2008 81388	≤0.25	64	32	16	4	4	2
MRSE CAN-ICU 61589 (CAZ >32)	1	64	256	16	4	4	2
<i>E. faecalis</i> ATCC 29212	8	512	512	16	16	8	4
<i>E. faecium</i> ATCC 27270	8	32	>512	32	8	8	4
<i>S. pneumoniae</i> ATCC 49619	2	4	>128	128	32	32	16

Gram-negative bacteria							
<i>E. coli</i> ATCC 25922	0.5	32	128	128	16	32	32
<i>E. coli</i> CAN-ICU 61714 (GEN-R)	8	64	256	128	32	32	32
<i>E. coli</i> CAN-ICU 63074 (AMK 32)	8	64	512	128	64	32	16
<i>E. coli</i> CANWARD-2011 97615 (GEN-R, TOB-R, CIP-R) aac(3)iiiA	128	256	>512	128	32	32	16
<i>P. aeruginosa</i> ATCC 27853	0.5	16	512	512	128	128	32
<i>P. aeruginosa</i> CAN-ICU 62308 (GEN-R)	16	512	>512	256	64	64	32
<i>P. aeruginosa</i> CANWARD-2011 96846 (GEN-R, TOB-R)	256	>512	>512	512	128	128	32
<i>S. maltophilia</i> CAN-ICU 62584	>512	>512	>512	>512	512	256	128
<i>A. baumannii</i> CAN-ICU 63169	32	512	>512	>512	256	256	128
<i>K. pneumoniae</i> ATCC 13883	≤0.25	2	2	64	128	32	8

<sup>a</sup>MRSA: Methicillin-resistant *S. aureus*; MSSE: Methicillin-susceptible *S. epidermidis*; MRSE: Methicillin-resistant *S. epidermidis*; CANWARD: Canadian Ward surveillance; CAN-ICU: Canadian National Intensive Care Unit surveillance; CAZ: Ceftazidime; GEN-R: Gentamicin-resistant; AMK: Amikacin; TOB-R: Tobramycin-resistant; CIP-R: Ciprofloxacin-resistant.

Next, we explored the immunomodulatory properties of the most potent amphiphilic tobramycin ether analogues **4d–f**, while the nonamphiphilic tobramycin methyl ether **4a** served as a negative control. There is little data on the immunomodulatory effects of tobramycin, although it has been suggested that a tobramycin–copper complex may display anti-inflammatory properties.<sup>29</sup> We monitored the cytotoxic effects of amphiphilic tobramycin analogues in human monocytic THP-1 cells (ATCC TIB-202). The release of lactate dehydrogenase was monitored in the tissue culture (TC) supernatants after 24 h stimulation to assess cytotoxicity. The amphiphilic tobramycin ether analogues **4d–f** showed negligible or less than 10% cytotoxicity at 5–10  $\mu$ M, with a dose-dependent cytotoxicity response between 20 and 80  $\mu$ M. By contrast, the nonamphiphilic control analogue **4a** showed 20% cytotoxicity at all

concentrations tested (Figure 7.3.1). It should be noted that the immunomodulatory properties of the HDP cathelicidin LL-37 and its analogues are typically studied at concentrations of 2.5 to 10  $\mu\text{M}$ .<sup>30,31</sup> Therefore, we selected a dose of 10  $\mu\text{M}$  for further assessment of the immunomodulatory activity of these analogues. Plastic-adherent macrophage-like THP-1 cells were stimulated with **4a** and **4d–f** (10  $\mu\text{M}$ ), and the TC supernatants were monitored for production of the pro-inflammatory cytokines TNF- $\alpha$  and IL-1 $\beta$  as well as the chemokines Gro- $\alpha$  and IL-8 after 24 h, and production of the anti-inflammatory cytokine IL-1RA after 48 h of stimulation. None of the compounds induced the production of either TNF- $\alpha$ , IL-1 $\beta$ , or Gro- $\alpha$  (Figure 7.3.2). Likewise, no production of the IL-1-antagonist IL-1RA was observed (data not shown). By contrast, AAGs **4d–f**, but not **4a**, significantly induced the production of the chemokine IL-8 in macrophages (Figure 7.3.2). Previous studies have shown that HDPs such as LL-37 and indolicidin show similar activity: they do not induce the production of TNF- $\alpha$  but are potent inducers of the neutrophil chemokine IL-8.<sup>30,32</sup> However, LL-37 can also induce the production of other chemokines such as MCP-1 and Gro- $\alpha$ , which act as chemoattractants for other leukocytes such as macrophages.<sup>30,33</sup> The fact that **4d–f** selectively induced IL-8 but not Gro- $\alpha$  suggests that these analogues may be selectively chemoattractant to neutrophils. Since the chemokine IL-8 is a potent neutrophil chemotactic factor required for the resolution of infections,<sup>34,35</sup> our results suggest that the three AAGs **4d–f** may, in addition to their antibacterial activity, be able to mediate the recruitment of immune cells, in particular neutrophils, to the site of infection.

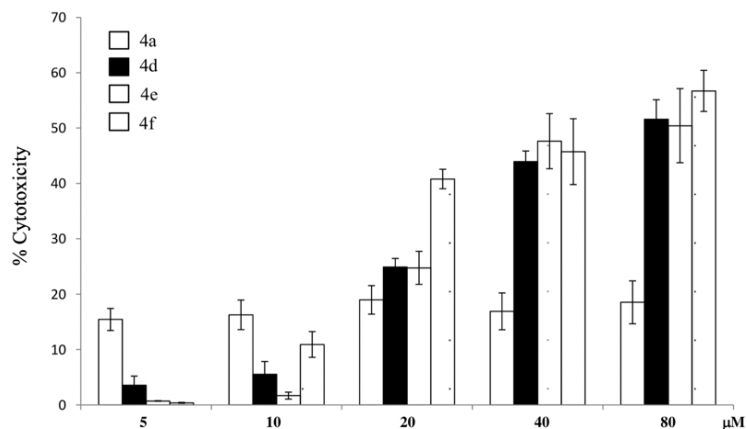


**Figure 7.3.1.** Cytotoxicity of **4a–f** in human monocytic THP-1 cells. Plastic adherent human macrophage-like THP-1 cells were stimulated with the tobramycin analogs (5–80  $\mu\text{M}$ ). Lactate dehydrogenase (LDH) was monitored in the tissue culture supernatants after 24 h by a colorimetric assay. Percent cytotoxicity was calculated relative to cells treated with triton as 100%. The y-axis shows percent cytotoxicity after background subtraction with unstimulated cells. Results shown are an average of at least three independent experiments  $\pm$  standard error.

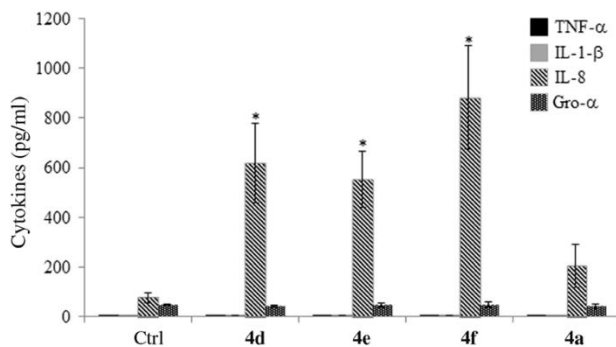


**Figure 7.3.2.** Plastic-adherent human macrophage-like THP-1 cells were stimulated with the tobramycin analogues (10  $\mu\text{M}$ ). TC supernatants were monitored after 24 h by ELISA for the production of the cytokines TNF- $\alpha$  and IL-1 $\beta$ , as well as the chemokines IL-8 and Gro- $\alpha$ . The

values shown are an average of at least three independent experiments  $\pm$  standard error (\*  $p < 0.05$ ).

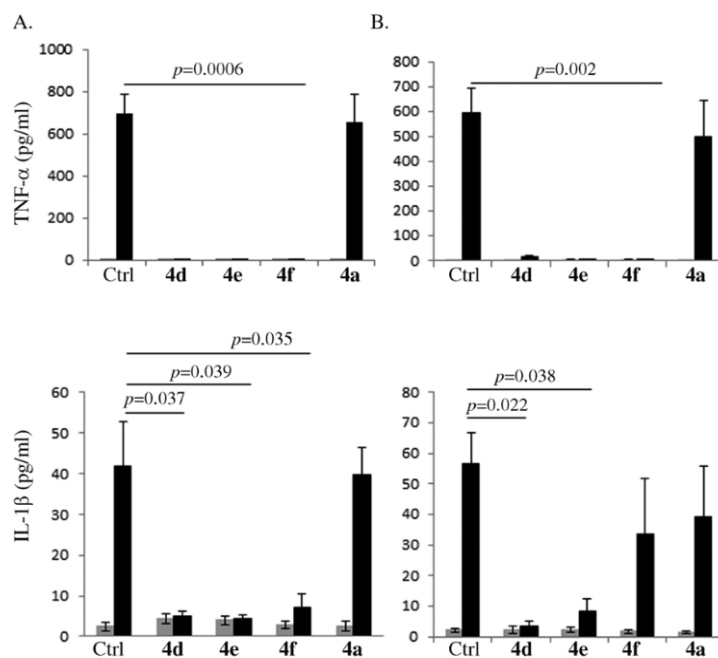


**Figure 7.3.3.** Plastic-adherent human macrophage-like THP-1 cells were stimulated with 10 ng/mL of bacterial LPS (gray = without LPS, black = with LPS), in the presence and absence of the tobramycin analogues (10  $\mu$ M). The tobramycin analogues were added either at the same time as LPS stimulation (A) or 30 min prior to LPS stimulation (B). TC supernatants were monitored after 24 h by ELISA for the production of the pro-inflammatory cytokines TNF- $\alpha$  and IL-1 $\beta$ . The values shown are an average of at least three independent experiments  $\pm$  standard error.

Previous studies have demonstrated that amphiphilic cationic HDPs, such as LL-37, can neutralize bacterial products such as lipopolysaccharide (LPS) and switch the signaling of Toll-like receptors to the NF- $\kappa$ B pathway induced by bacterial ligands to control bacterial infections

and pathogen-induced inflammation.<sup>30,36,37</sup> Since the primary target cell type involved in the immunomodulatory activity of HDPs and their analogues has been shown to be macrophages,<sup>38,39</sup> we monitored LPS-induced cytokine production in the presence and absence of **4d–f** and **4a** in THP-1 macrophages after 24 h stimulation as previously described.<sup>30,31</sup> The analogues **4d–f** abrogated the production of LPS-induced pro-inflammatory TNF- $\alpha$  when the compounds were added either at the same time as LPS stimulation (Figure 7.3.3A) or 30 min prior to LPS stimulation (Figure 7.3.3B). Furthermore, **4d** and **4e** significantly suppressed LPS-induced IL-1 $\beta$  production when added either at the same time or 30 min prior to LPS stimulation (Figure 7.3.3). The analogue **4f** significantly suppressed LPS-induced IL-1 $\beta$  production when added simultaneously with LPS stimulation (Figure 7.3.3A) but not when added 30 min prior to stimulation (Figure 7.3.3B). The analogues **4d–f** also significantly suppressed the LPS-induced production of chemokines IL-8 and Gro- $\alpha$  by between 50 and 70 % when added either simultaneously or 30 min prior to LPS stimulation, but they did not completely neutralize chemokine production (Figure 7.3.4). The nonamphiphilic analogue **4a** did not suppress the LPS-induced production of either pro-inflammatory cytokines or chemokines under any conditions (Figure 7.3.4 and Figure 7.3.5). Next, to determine whether the ability of the analogues to suppress LPS-induced cytokine production was due to binding to LPS, we tested the activity of the analogues in LPS-primed macrophages. The cells were stimulated for 30 min with LPS, followed by removal of the TC media and washing of the cells to ensure the removal of residual LPS in the TC media. Subsequently, the cells were stimulated with the tobramycin analogues 30 min after LPS stimulation. The analogues **4d** and **4e** significantly suppressed LPS-induced TNF- $\alpha$  production, even when added 30 min after LPS stimulation (Figure 7.3.5A), which suggests that the effect of **4d** and **4e** in controlling LPS-induced TNF- $\alpha$  may be due to the alteration of

intracellular signaling mechanisms rather than direct LPS binding. However, none of the compounds significantly altered the LPS- induced production of either IL-1 $\beta$ , IL-8, or Gro- $\alpha$  when added 30 min after LPS stimulation (Figure 7.3.5). This is consistent with previous studies demonstrating that HDPs such as cathelicidins LL-37 and BMAP-27 inhibit TNF- $\alpha$  production,<sup>40</sup> whereas defensin HNP-1 promotes IL-1 $\beta$  production<sup>41</sup> in LPS-primed macrophages. Previous studies have also demonstrated that HDPs, for example, LL-37 and BMAP-27, induce the expression of several chemokines and do not neutralize LPS-induced chemokines.<sup>30,33,42</sup> Taken together, these results suggest that that the selective modulation of endotoxin-induced inflammatory responses by certain HDPs, as with **4d** and **4e**, may be in part mediated through alteration of the intracellular signaling downstream of pattern-recognition receptors in macrophages.

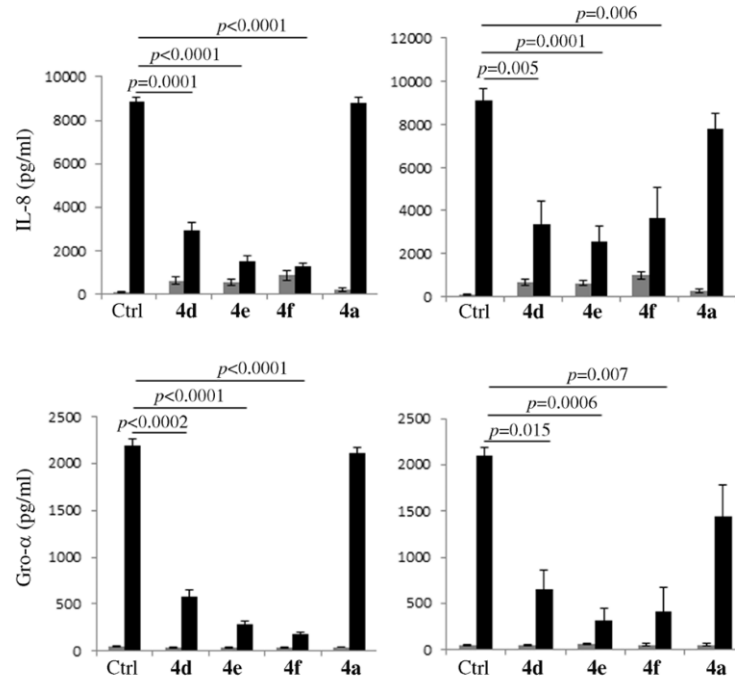


**Figure 7.3.4.** Plastic-adherent human macrophage-like THP-1 cells were stimulated with 10 ng/mL of bacterial LPS (gray = without LPS, black = with LPS) in the presence and absence of the tobramycin analogues (10  $\mu$ M). The tobramycin analogues were added either at the same time as LPS stimulation (A) or 30 min prior to LPS stimulation (B). TC supernatants were monitored after 24 h by ELISA for the production of the chemokines IL-8 and Gro- $\alpha$ . The values shown are an average of at least three independent experiments  $\pm$  standard error.

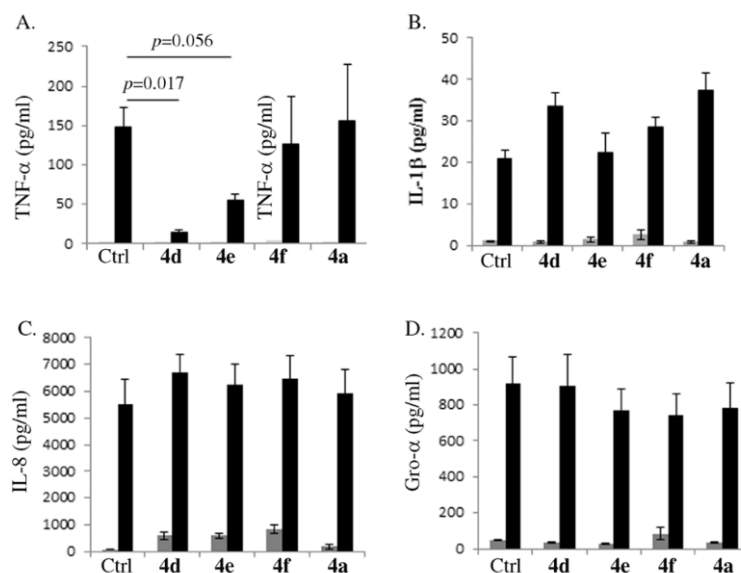


**Figure 7.3.5.** Plastic-adherent human macrophage-like THP-1 cells were stimulated with 10 ng/mL of bacterial LPS (gray = without LPS, black = with LPS) for 30 min, the TC medium was removed and the cells washed with fresh medium, followed by stimulation with tobramycin analogues (10  $\mu$ M) for 24 h. TC supernatants were monitored by ELISA for production of the pro-inflammatory cytokines TNF- $\alpha$  (A) and IL-1 $\beta$  (B), as well as the chemokines IL-8 (C) and Gro- $\alpha$  (D). The values shown are an average of at least three independent experiments  $\pm$  standard error.

## 7.4 CONCLUSIONS

In summary, our results demonstrate for the first time that AAGs, besides their direct antibacterial activity, can also induce immunomodulatory responses at concentrations that are nontoxic to host cells. The multimodal activity of AAGs, whereby direct antibacterial activity is combined with an immunomodulatory response, is encouraging since immunomodulatory compounds are becoming increasingly important in anti-infective therapy. Although AAGs were

originally designed to overcome bacterial resistance by targeting both ribosomal RNA and the bacterial membrane, our study shows that AAGs can also influence host immune responses. We have shown that AAGs are capable of inducing the production of the chemokine IL-8, which plays a critical role in the recruitment of immune cells such as neutrophils required for the resolution of infections. Furthermore, AAGs can selectively control inflammatory responses induced in the presence of endotoxin to prevent septic shock. As with certain amphiphilic HDPs, for example, LL-37, AAGs exhibit modest direct antibacterial activity and immunomodulatory properties for the control of both infection and pathogen-induced hyperinflammation. AAGs thus represent a promising avenue for the development of multifunctional molecules for the prevention or treatment of bacterial infections.

## 7.5 ACKNOWLEDGMENTS

The work was supported by CIHR (MOP 119335), Research Manitoba and NSERC.

## 7.6 REFERENCES

- (1) Boucher, H. W.; Talbot, G. H.; Bradley, J. S.; Edwards, J. E.; Gilbert, D.; Rice, L. B.; Scheld, M.; Spellberg, B.; Bartlett, J. Bad Bugs, No Drugs: No ESKAPE! An Update from the Infectious Diseases Society of America. *Clin. Infect. Dis.* **2009**, *48* (1), 1–12.
- (2) Butler, M. S.; Blaskovich, M. A.; Cooper, M. A. Antibiotics in the Clinical Pipeline in 2013. *J. Antibiot. (Tokyo)*. **2013**, *66* (10), 571–591.
- (3) Kalan, L.; Wright, G. D. Antibiotic Adjuvants: Multicomponent Anti-Infective Strategies. *Expert Rev. Mol. Med.* **2011**, *13*, e5.
- (4) Brotz-Oesterhelt, H.; Brunner, N. A. How Many Modes of Action Should an Antibiotic

- Have? *Curr. Opin. Pharmacol.* **2008**, *8* (5), 564–573.
- (5) Sautrey, G.; Zimmermann, L.; Deleu, M.; Delbar, A.; Souza Machado, L.; Jeannot, K.; Van Bambeke, F.; Buyck, J. M.; Decout, J.-L.; Mingeot-Leclercq, M.-P. New Amphiphilic Neamine Derivatives Active against Resistant *Pseudomonas aeruginosa* and Their Interactions with Lipopolysaccharides. *Antimicrob. Agents Chemother.* **2014**, *58* (8), 4420–4430.
- (6) Udumula, V.; Ham, Y. W.; Fosso, M. Y.; Chan, K. Y.; Rai, R.; Zhang, J.; Li, J.; Chang, C.-W. T. Investigation of Antibacterial Mode of Action for Traditional and Amphiphilic Aminoglycosides. *Bioorg. Med. Chem. Lett.* **2013**, *23* (6), 1671–1675.
- (7) Bera, S.; Zhanel, G. G.; Schweizer, F. Design, Synthesis, and Antibacterial Activities of Neomycin–Lipid Conjugates: Polycationic Lipids with Potent Gram-Positive Activity. *J. Med. Chem.* **2008**, *51* (19), 6160–6164.
- (8) Zhang, J.; Keller, K.; Takemoto, J. Y.; Bensaci, M.; Litke, A.; Czyryca, P. G.; Chang, C.-W. T. Synthesis and Combinational Antibacterial Study of 5''-Modified Neomycin. *J. Antibiot. (Tokyo)*. **2009**, *62* (10), 539–544.
- (9) Herzog, I. M.; Feldman, M.; Eldar-Boock, A.; Satchi-Fainaro, R.; Fridman, M. Design of Membrane Targeting Tobramycin-Based Cationic Amphiphiles with Reduced Hemolytic Activity. *Med. Chem. Commun.* **2013**, *4* (1), 120–124.
- (10) Herzog, I. M.; Green, K. D.; Berkov-Zrihen, Y.; Feldman, M.; Vidavski, R. R.; Eldar-Boock, A.; Satchi-Fainaro, R.; Eldar, A.; Garneau-Tsodikova, S.; Fridman, M. 6''-Thioether Tobramycin Analogues: Towards Selective Targeting of Bacterial Membranes. *Angew. Chemie Int. Ed.* **2012**, *51* (23), 5652–5656.
- (11) Zimmermann, L.; Bussière, A.; Ouberai, M.; Baussanne, I.; Jolival, C.; Mingeot-Leclercq,

- M.-P.; Décout, J.-L. Tuning the Antibacterial Activity of Amphiphilic Neamine Derivatives and Comparison to Paromamine Homologues. *J. Med. Chem.* **2013**, *56* (19), 7691–7705.
- (12) Ouberai, M.; El Garch, F.; Bussiere, A.; Riou, M.; Alsteens, D.; Lins, L.; Baussanne, I.; Dufrêne, Y. F.; Brasseur, R.; Decout, J.-L.; Mingeot-Leclercq, M.-P. The Pseudomonas Aeruginosa Membranes: A Target for a New Amphiphilic Aminoglycoside Derivative? *Biochim. Biophys. Acta - Biomembr.* **2011**, *1808* (6), 1716–1727.
- (13) Bera, S.; Zhanel, G. G.; Schweizer, F. Antibacterial Activities of Aminoglycoside Antibiotics-Derived Cationic Amphiphiles. Polyol-Modified Neomycin B-, Kanamycin A-, Amikacin-, and Neamine-Based Amphiphiles with Potent Broad Spectrum Antibacterial Activity. *J. Med. Chem.* **2010**, *53* (9), 3626–3631.
- (14) Baussanne, I.; Bussière, A.; Halder, S.; Ganem-Elbaz, C.; Ouberai, M.; Riou, M.; Paris, J.-M.; Ennifar, E.; Mingeot-Leclercq, M.-P.; Décout, J.-L. Synthesis and Antimicrobial Evaluation of Amphiphilic Neamine Derivatives. *J. Med. Chem.* **2010**, *53* (1), 119–127.
- (15) Zhang, J.; Chiang, F.-I.; Wu, L.; Czyryca, P. G.; Li, D.; Chang, C.-W. T. Surprising Alteration of Antibacterial Activity of 5''-Modified Neomycin against Resistant Bacteria. *J. Med. Chem.* **2008**, *51* (23), 7563–7573.
- (16) ERDŐS, T.; ULLMANN, A. Effect of Streptomycin on the Incorporation of Amino-Acids Labeled with Carbon-14 into Ribonucleic Acid and Protein in a Cell-Free System of a Mycobacterium. *Nature* **1959**, *183* (4661), 618–619.
- (17) Becker, B.; Cooper, M. A. Aminoglycoside Antibiotics in the 21st Century. *ACS Chem. Biol.* **2013**, *8* (1), 105–115.
- (18) Kaul, M.; Barbieri, C. M.; Pilch, D. S. Aminoglycoside-Induced Reduction in Nucleotide

- Mobility at the Ribosomal RNA A-Site as a Potentially Key Determinant of Antibacterial Activity. *J. Am. Chem. Soc.* **2006**, *128* (4), 1261–1271.
- (19) Feldman, M. B.; Terry, D. S.; Altman, R. B.; Blanchard, S. C. Aminoglycoside Activity Observed on Single Pre-Translocation Ribosome Complexes. *Nat. Chem. Biol.* **2010**, *6* (1), 54–62.
- (20) Thaker, H. D.; Som, A.; Ayaz, F.; Lui, D.; Pan, W.; Scott, R. W.; Anguita, J.; Tew, G. N. Synthetic Mimics of Antimicrobial Peptides with Immunomodulatory Responses. *J. Am. Chem. Soc.* **2012**, *134* (27), 11088–11091.
- (21) Hilchie, A. L.; Wuerth, K.; Hancock, R. E. W. Immune Modulation by Multifaceted Cationic Host Defense (Antimicrobial) Peptides. *Nat. Chem. Biol.* **2013**, *9* (12), 761–768.
- (22) Mansour, S. C.; Pena, O. M.; Hancock, R. E. W. Host Defense Peptides: Front-Line Immunomodulators. *Trends in Immunology*. Elsevier September 1, 2014, pp 443–450.
- (23) Pena, O. M.; Afacan, N.; Pistolic, J.; Chen, C.; Madera, L.; Falsafi, R.; Fjell, C. D.; Hancock, R. E. W. Synthetic Cationic Peptide IDR-1018 Modulates Human Macrophage Differentiation. *PLoS One* **2013**, *8* (1), 1–10.
- (24) Koczulla, R.; von Degenfeld, G.; Kupatt, C.; Krötz, F.; Zahler, S.; Gloe, T.; Issbrücker, K.; Unterberger, P.; Zaiou, M.; Lebherz, C.; Karl, A.; Raake, P.; Pfosser, A.; Boekstegers, P.; Welsch, U.; Hiemstra, P. S.; Vogelmeier, C.; Gallo, R. L.; Clauss, M.; Bals, R. An Angiogenic Role for the Human Peptide Antibiotic LL-37/HCAP-18. *J. Clin. Invest.* **2003**, *111* (11), 1665–1672.
- (25) Yang, D.; Chertov, O.; Bykovskaia, S. N.; Chen, Q.; Buffo, M. J.; Shogan, J.; Anderson, M.; Schroder, J. M.; Wang, J. M.; Howard, O. M.; Oppenheim, J. J.  $\beta$ -Defensins: Linking Innate and Adaptive Immunity through Dendritic and T Cell CCR6. *Science* **1999**, 286

- (5439), 525–528.
- (26) Bothra, M.; Lodha, R.; Kabra, S. K. Tobramycin for the Treatment of Bacterial Pneumonia in Children. *Expert Opin. Pharmacother.* **2012**, *13* (4), 565–571.
- (27) Hanessian, S.; Tremblay, M.; Swayze, E. E. Tobramycin Analogues with C-5 Aminoalkyl Ether Chains Intended to Mimic Rings III and IV of Paromomycin. *Tetrahedron* **2003**, *59* (7), 983–993.
- (28) Vicens, Q.; Westhof, E. Crystal Structure of a Complex between the Aminoglycoside Tobramycin and an Oligonucleotide Containing the Ribosomal Decoding a Site. *Chem. Biol.* **2002**, *9* (6), 747–755.
- (29) Gziut, M.; MacGregor, H.; Nevell, T.; Mason, T.; Laight, D.; Shute, J. K. Anti-Inflammatory Effects of Tobramycin and a Copper-Tobramycin Complex with Superoxide Dismutase-like Activity. *Br. J. Pharmacol.* **2013**, *168* (5), 1165–1181.
- (30) Choi, K. Y. G.; Napper, S.; Mookherjee, N. Human Cathelicidin LL-37 and Its Derivative IG-19 Regulate Interleukin-32-Induced Inflammation. *Immunology* **2014**, *143* (1), 68–80.
- (31) Mookherjee, N.; Brown, K. L.; Bowdish, D. M. E.; Doria, S.; Falsafi, R.; Hokamp, K.; Roche, F. M.; Mu, R.; Doho, G. H.; Pistolic, J.; Powers, J.-P.; Bryan, J.; Brinkman, F. S. L.; Hancock, R. E. W. Modulation of the TLR-Mediated Inflammatory Response by the Endogenous Human Host Defense Peptide LL-37. *J. Immunol.* **2006**, *176* (4), 2455–2464.
- (32) Bowdish, D. M. E.; Davidson, D. J.; Scott, M. G.; Hancock, R. E. W. Immunomodulatory Activities of Small Host Defense Peptides. *Antimicrob. Agents Chemother.* **2005**, *49* (5), 1727–1732.
- (33) Scott, M. G.; Davidson, D. J.; Gold, M. R.; Bowdish, D.; Hancock, R. E. W. The Human Antimicrobial Peptide LL-37 Is a Multifunctional Modulator of Innate Immune Responses.

- J. Immunol.* **2002**, *169* (7), 3883–3891.
- (34) Kunkel, S. L.; Lukacs, N. W.; Strieter, R. M. The Role of Interleukin-8 in the Infectious Process. *Ann. N. Y. Acad. Sci.* **1994**, *730* (1), 134–143.
- (35) Mukaida, N. Interleukin-8: An Expanding Universe beyond Neutrophil Chemotaxis and Activation. *Int. J. Hematol.* **2000**, *72* (4), 391–398.
- (36) Singh, D.; Qi, R.; Jordan, J. L.; Mateo, L. S.; Kao, C. C. The Human Antimicrobial Peptide LL-37, but Not the Mouse Ortholog, MCRAMP, Can Stimulate Signaling by Poly(I:C) through a FPRL1-Dependent Pathway. *J. Biol. Chem.* **2013**, *288* (12), 8258–8268.
- (37) Into, T.; Inomata, M.; Shibata, K.; Murakami, Y. Effect of the Antimicrobial Peptide LL-37 on Toll-like Receptors 2-, 3- and 4-Triggered Expression of IL-6, IL-8 and CXCL10 in Human Gingival Fibroblasts. *Cell. Immunol.* **2010**, *264* (1), 104–109.
- (38) Scott, M. G.; Dullaghan, E.; Mookherjee, N.; Glavas, N.; Waldbrook, M.; Thompson, A.; Wang, A.; Lee, K.; Doria, S.; Hamill, P.; Yu, J. J.; Li, Y.; Donini, O.; Guarna, M. M.; Finlay, B. B.; North, J. R.; Hancock, R. E. W. An Anti-Infective Peptide That Selectively Modulates the Innate Immune Response. *Nat. Biotechnol.* **2007**, *25* (4), 465–472.
- (39) Wan, M.; van der Does, A. M.; Tang, X.; Lindbom, L.; Agerberth, B.; Haeggstrom, J. Z. Antimicrobial Peptide LL-37 Promotes Bacterial Phagocytosis by Human Macrophages. *J. Leukoc. Biol.* **2014**, *95* (6), 971–981.
- (40) Mookherjee, N.; Hancock, R. E. W. Cationic Host Defence Peptides: Innate Immune Regulatory Peptides as a Novel Approach for Treating Infections. *Cell. Mol. Life Sci.* **2007**, *64* (7–8), 922–933.
- (41) Chen, Q.; Jin, Y.; Zhang, K.; Li, H.; Chen, W.; Meng, G.; Fang, X. Alarmin HNP-1

Promotes Pyroptosis and IL-1 $\beta$  Release through Different Roles of NLRP3 Inflammasome via P2X7 in LPS-Primed Macrophages. *Innate Immun.* **2014**, *20* (3), 290–300.

- (42) Mookherjee, N.; Wilson, H. L.; Doria, S.; Popowych, Y.; Falsafi, R.; Yu, J.; Li, Y.; Veatch, S.; Roche, F. M.; Brown, K. L.; Brinkman, F. S. L.; Hokamp, K.; Potter, A.; Babiuk, L. A.; Griebel, P. J.; Hancock, R. E. W. Bovine and Human Cathelicidin Cationic Host Defense Peptides Similarly Suppress Transcriptional Responses to Bacterial Lipopolysaccharide. *J. Leukoc. Biol.* **2006**, *80* (6), 1563–1574.

## Chapter 8: Conclusions and Future Work

### 8.1 GENERAL CONCLUSIONS

In this work, we have successfully developed amphiphilic tobramycin-based efflux pump inhibitor conjugates (TOB-NMP, TOB-PAR, and TOB-DBP) and tobramycin-based lysine peptoid conjugates that are capable of preserving multiple legacy antibiotics including the tetracycline antibiotic minocycline, the fluoroquinolone antibiotic moxifloxacin and ciprofloxacin, rifampicin, and fosfomycin against MDR and XDR Gram-negative pathogens. More importantly, TOB-NMP and TOB-lysine peptoid conjugates enhanced minocycline or rifampicin efficacy *in vivo* in XDR *P. aeruginosa*-challenged *G. mellonella* larvae.

Our study suggests that the TOB domain linked to the C<sub>12</sub> tether appears to be an effective vector to promote delivery of legacy antibiotics through the outer membrane of Gram-negative bacilli with optimized effect on *P. aeruginosa*. In addition, we also demonstrated that these TOB-based conjugates induce a dose-dependent depolarization of the cytoplasmic membrane. It was evidenced that TOB-based conjugates specifically reduce the electrical component ( $\Delta\psi$ ) of the proton motive force (PMF) resulting in a compensatory increase in transmembrane chemical component ( $\Delta\text{pH}$ ) in order to counter this effect and maintain a constant PMF. This leads to enhanced cytoplasmic uptake of agents that is  $\Delta\text{pH}$ -dependent like the tetracycline class of antibiotics.<sup>1</sup> Furthermore, the PMF-driven flagellum-dependent motility of *P. aeruginosa* PAO1 was greatly inhibited in the presence of TOB-based conjugates at sub-MIC values suggesting these conjugates dissipate the PMF that perhaps affects the function of the efflux pumps. The overall multimodal effects of the TOB-based conjugates/antibiotic

combination on the bacterial membrane result in the suppression of antibiotic resistance development that suggests a strategy for developing effective antibiotic adjuvants that rescue legacy antibiotics from resistance in MDR Gram-negative bacilli.

Based on the results described in this thesis and research papers by our group,<sup>2-6</sup> it is suggested that the tobramycin fragment linked to a C<sub>12</sub> tether is the core scaffold that is responsible for the adjuvant properties. Mechanistic studies on the TOB-based conjugates indicate that the conjugates possess different properties when compared to their constituent pharmacophoric fragments.

Enthused by the biological properties of the TOB-based conjugates, we further optimized TOB-based conjugates by replacing the TOB domain by the pseudo-disaccharide nebramine (NEB). Potent synergism was found for combinations of NEB-based hybrid adjuvants with multiple classes of legacy antibiotics including fluoroquinolones (moxifloxacin and ciprofloxacin), tetracyclines (minocycline), or rifamycin (rifampicin) against wild-type and MDR/XDR Gram-negative bacilli including *P. aeruginosa*, *A. baumannii*, *K. pneumonia*, and *E. cloacae* strains. *In vivo* efficacy studies demonstrated the ability of the NEB-CIP hybrid to offer protection when used in combination with rifampicin in XDR *P. aeruginosa*-challenged *G. mellonella* larvae. This optimization study suggests that the degradation of TOB-based hybrids to yield NEB-based hybrids does not significantly alter the adjuvant properties of this scaffold. Mechanistic evaluation of the NEB-based hybrids confirmed that the membrane effects of the TOB-based hybrid adjuvants are retained by replacing the larger TOB unit by a smaller NEB moiety suggesting that the NEB linked by a C<sub>12</sub> tether is the essential membrane active core responsible for the adjuvant properties. Furthermore, reduction in the number of basic functions in TOB-based hybrid adjuvants may result in reduced aminoglycoside-induced cytotoxicity.

Overall, this study provides an attractive aminoglycoside vector strategy for generating effective antibiotic adjuvants that induce multimodal effects involving both outer and inner membrane of Gram-negative bacilli, affecting the PMF and perhaps the function of the efflux pumps. As such, the outlined development of aminoglycoside-based adjuvant/antibiotic therapy is set to optimize the usage of legacy antibiotics and expand the antimicrobial space which has the potential to fill the current antibiotic discovery void.<sup>7</sup>

In a different project, C-5-substituted amphiphilic tobramycin analogues were synthesized. These amphiphilic aminoglycosides (AAGs) exhibited good activity against sensitive and tobramycin-resistant Gram-positive bacteria (MIC = 2–16  $\mu\text{g}/\text{mL}$ ) and reduced activity against Gram-negative bacteria (MIC = 16–256  $\mu\text{g}/\text{mL}$ ). In addition, our results show for the first time that AAGs can influence host immune responses. Specifically, in macrophage-like THP-1 cells, the AAG analogues greatly induced the production of the chemokine IL-8, which plays a critical role in the recruitment of immune cells such as neutrophils necessary for the resolution of infections. Moreover, the AAG analogues significantly suppressed the production of LPS-induced pro-inflammatory cytokines TNF- $\alpha$  and IL-1 $\beta$  in the absence or presence of LPS. Thus, our study demonstrates that AAGs possess multifunctional properties that control both infection and pathogen-induced hyperinflammation which represent a promising approach to prevent or treat infectious diseases.

## 8.2 FUTURE WORK

This thesis and research papers<sup>2–6</sup> by our group have demonstrated that amphiphilic tobramycin-based conjugates are able to revive the antibacterial activity of multiple classes of antibiotics against MDR Gram-negative bacteria. They also suggest that the tobramycin fragment

linked by a C<sub>12</sub> tether is the core structure responsible for the adjuvant properties. As described in Chapter 6, we have replaced tobramycin domain by nebramine and found that the adjuvant properties are retained. In the future it would be interesting to perform a structural optimization study by replacing the tobramycin moiety with a variety of aminoglycoside structures to gain additional insight into the aminoglycoside moiety's contribution to the adjuvant properties. Structurally, tobramycin is a member of the 4,6-disubstituted-2-deoxystreptamine (2-DOS) linked family so that we could explore other 4,6-disubstituted-2-DOS aminoglycoside structures such as kanamycin A, kanamycin B, or sisomicin in order to evaluate their potency and toxicity. In addition, the 4,5-disubstituted-2-DOS aminoglycoside neomycin B and its fragment neamine could also be selected to develop novel aminoglycoside (AG)-based conjugates.

Antibiotic resistance is a global challenge. Besides outer membrane impermeability, efflux, target mutation and antibiotic inactivation the efficacy of antibiotics is also compromised by biofilm formation. It has been suggested that the antibacterial activity of antibiotics against biofilms is 10-100-times reduced when compared to the planktonic form.<sup>8</sup> In this thesis, we have examined the bactericidal effect of legacy antibiotics (e.g. minocycline and rifampicin) in combination with AG-based conjugates against planktonic bacteria. Therefore, we could also investigate their effects on biofilm formation in future work.

In the Chapter 7, we have described amphiphilic tobramycin analogues capable of inducing the innate immune response in the host-directed clearance of an infection. These AAGs may also have the potential to act as adjuvants targeting host defense mechanisms to treat infectious diseases. In this regard, it would be worthwhile to study the synergistic effects of AAGs in combination with multiple legacy antibiotics in the host. Moreover, it would be interesting to combine the host-directed effects of amphiphilic aminoglycosides described in Chapter 7 with the pathogen-directed effects of adjuvants outlined in Chapters 3-6. This might

lead to a novel multimodal antibacterial therapeutic strategy that rivals the functions of naturally occurring antimicrobial peptides.

### 8.3 REFERENCES

- (1) Ejim, L.; Farha, M. A.; Falconer, S. B.; Wildenhain, J.; Coombes, B. K.; Tyers, M.; Brown, E. D.; Wright, G. D. Combinations of Antibiotics and Nonantibiotic Drugs Enhance Antimicrobial Efficacy. *Nat. Chem. Biol.* **2011**, *7* (6), 348–350.
- (2) Domalaon, R.; Idowu, T.; Zhanel, G. G.; Schweizer, F. Antibiotic Hybrids: The Next Generation of Agents and Adjuvants against Gram-Negative Pathogens? *Clin. Microbiol. Rev.* **2018**, *31* (2), e00077-17.
- (3) Domalaon, R.; Yang, X.; Lyu, Y.; Zhanel, G. G.; Schweizer, F. Polymyxin B 3 – Tobramycin Hybrids with *Pseudomonas Aeruginosa* -Selective Antibacterial Activity and Strong Potentiation of Rifampicin, Minocycline, and Vancomycin. *ACS Infect. Dis.* **2017**, *3* (12), 941–954.
- (4) Lyu, Y.; Domalaon, R.; Yang, X.; Schweizer, F. Amphiphilic Lysine Conjugated to Tobramycin Synergizes Legacy Antibiotics against Wild-Type and Multidrug-Resistant *Pseudomonas aeruginosa*. *Biopolymers* **2017**, e23091.
- (5) Gorityala, B. K.; Guchhait, G.; Goswami, S.; Fernando, D. M.; Kumar, A.; Zhanel, G. G.; Schweizer, F. Hybrid Antibiotic Overcomes Resistance in *P. Aeruginosa* by Enhancing Outer Membrane Penetration and Reducing Efflux. *J. Med. Chem.* **2016**, *59* (18), 8441–8455.
- (6) Gorityala, B. K.; Guchhait, G.; Fernando, D. M.; Deo, S.; McKenna, S. A.; Zhanel, G. G.; Kumar, A.; Schweizer, F. Adjuvants Based on Hybrid Antibiotics Overcome Resistance in

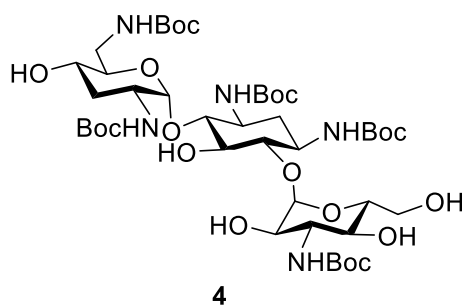
*Pseudomonas Aeruginosa* and Enhance Fluoroquinolone Efficacy. *Angew. Chem., Int. Ed. Engl.* **2016**, *55* (2), 555–559.

- (7) Brown, D. Antibiotic Resistance Breakers: Can Repurposed Drugs Fill the Antibiotic Discovery Void? *Nat. Rev. Drug Discov.* **2015**, *14* (12), 821–832.
- (8) Mah, T. F.; O’Toole, G. A. Mechanisms of Biofilm Resistance to Antimicrobial Agents. *Trends Microbiol.* **2001**, *9* (1), 34–39.

## Chapter 9: Supporting Information for Chapter 3

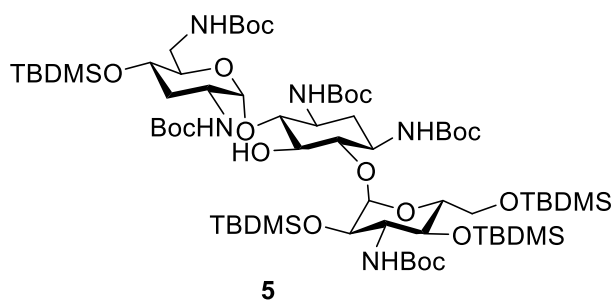
### 9.1 CHEMICAL SYNTHESSES

#### 9.1.1 Synthetic procedure and characterization of 1,3,2',6',3''-penta-*N*-(*tert*-butoxycarbonyl)-tobramycin (**4**) and 1,3,2',6',3''-penta-*N*-(*tert*-butoxycarbonyl)-tetra-*O*-TBDMS-tobramycin (**5**)



**1,3,2',6',3''-penta-*N*-(*tert*-butoxycarbonyl)-tobramycin (**4**).**<sup>1,2</sup> To a stirred solution of tobramycin (4.0 g, 8.6 mmol) in MeOH (80 mL) and H<sub>2</sub>O (40 mL), triethylamine (27.2 mL, 188.3 mmol) and di-*tert*-butyl dicarbonate ((Boc)<sub>2</sub>O) (18.7 g, 85.6 mmol) were added at

room temperature. The resultant reaction mixture was stirred at 55 °C overnight. It was then concentrated under reduced pressure to afford **4** as a white solid to which was used in the next step without further purification. Yield: 8.0 g (97%). MS (ESI) *m/e* calcd for C<sub>43</sub>H<sub>77</sub>N<sub>5</sub>O<sub>19</sub>K [M+K]<sup>+</sup>: 1007.2, found: 1007.2.



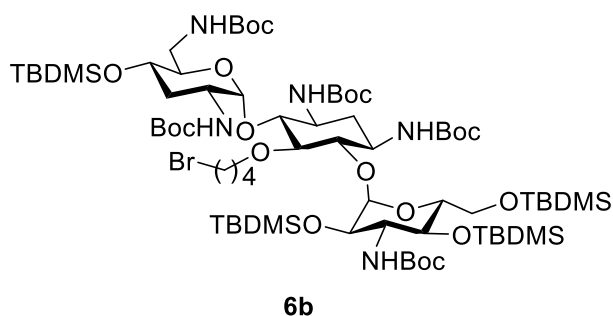
**1,3,2',6',3''-penta-*N*-(*tert*-butoxycarbonyl)-4',2'',4'',6''-tetra-*O*-TBDMS-tobramycin (**5**).**<sup>1,2</sup> To a stirred solution of **4** (8.0 g, 8.3 mmol) in anhydrous DMF (20 mL) under N<sub>2</sub> gas, TBDMSCl (12.0 g,

79.7 mmol) and 1-methylimidazole (6.6 mL, 83 mmol) were added subsequently. The reaction mixture was stirred at room temperature for 4 days. Water (30 mL) was added into the mixture

and extracted with ethyl acetate (3×30 mL). The combined organic extracts were washed with saturated brine, dried over anhydrous sodium sulfate and purified by flash chromatography (elution with a gradient of hexanes/ethyl acetate = 20:1 to 3:1) to give **5** as a white solid. Yield: 10.6 g (90%). <sup>1</sup>H NMR (500 MHz, chloroform-*d*) δ 5.04 – 4.81 (m, 2H, anomeric H), 3.95 – 3.79 (m, 3H), 3.79 – 2.98 (m, 13H), 2.78 – 2.66 (m, 1H), 2.03 – 1.94 (m, 1H), 1.70 – 1.32 (m, 47H), 0.96 – 0.79 (m, 36H), 0.17 – -0.02 (m, 24H). <sup>13</sup>C NMR (126 MHz, chloroform-*d*) δ 156.27, 155.87, 155.56, 155.09, 154.61, 99.35 (anomeric C), 98.97 (anomeric C), 84.03, 81.83, 79.84, 79.49, 79.42, 78.92, 78.67, 76.05, 75.33, 72.90, 71.10, 68.72, 67.53, 63.19, 56.69, 51.06, 50.37, 49.62, 41.50, 34.75, 33.64, 28.57, 28.47, 28.43, 28.41, 26.12, 26.04, 25.96, 25.76, 18.47, 18.19, 18.11, 17.85, -3.53, -3.75, -4.17, -4.67, -4.87, -4.91, -4.99, -5.15. MS (ESI) *m/e* calcd for C<sub>67</sub>H<sub>133</sub>N<sub>5</sub>O<sub>19</sub>Si<sub>4</sub>Na [M+Na]<sup>+</sup>: 1448.1, found: 1448.8.

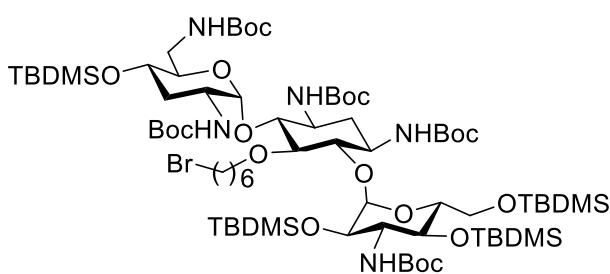
### 9.1.2 General procedure and characterization of 5-*O*-(4-bromoalkyl)-1,3,2',6',3''-penta-*N*-(*tert*-butoxycarbonyl)-4',2'',4'',6''-tetra-*O*-TBDMS-tobramycin derivatives (**6b–f**)

Compound **5** (0.5 mmol) was dissolved in anhydrous toluene (5 mL). Dibromoalkane (1.5 mmol) and a catalytic amount of tetrabutylammonium hydrogen sulfate (TBAHS) (0.05 mmol) were added into this solution subsequently, followed by KOH (1.5 mmol). This reaction mixture was stirred at room temperature under N<sub>2</sub> gas overnight and then concentrated under reduced pressure. The residue was purified by flash chromatography (elution with a gradient of hexanes/ethyl acetate = 10:1 to 4:1) to give the desired product as a white solid.<sup>1,2</sup>



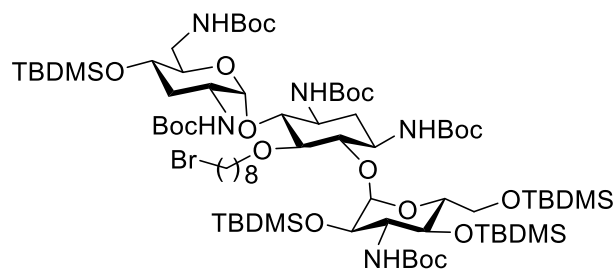
**5-*O*-(4-bromobutyl)-1,3,2',6',3''-penta-*N*-(*tert*-butoxycarbonyl)-4',2'',4'',6''-tetra-*O*-TBDMS-tobramycin (**6b**).** Yield:

78%.  $^1\text{H}$  NMR (500 MHz, chloroform-*d*)  $\delta$  5.22 – 5.07 (m, 2H, anomeric H), 4.33 – 4.03 (m, 3H), 3.86 – 3.16 (m, 17H), 2.45 (d,  $J = 7.7$  Hz, 1H), 2.03 – 1.97 (m, 1H), 1.94 – 1.84 (m, 2H), 1.65 – 1.57 (m, 2H), 1.56 – 1.50 (m, 1H), 1.48 – 1.29 (m, 45H), 1.08 – 0.98 (m, 1H), 0.96 – 0.82 (m, 36H), 0.22 – -0.06 (m, 24H).  $^{13}\text{C}$  NMR (126 MHz, chloroform-*d*)  $\delta$  155.69, 155.65, 155.47, 154.72, 154.59, 97.85 (anomeric C), 96.49 (anomeric C), 85.90, 79.95, 79.41, 79.27, 79.11, 78.78, 75.41, 72.67, 72.26, 71.57, 67.98, 67.05, 63.22, 57.14, 50.49, 48.82, 48.31, 41.61, 36.64, 36.03, 35.61, 34.62, 34.47, 33.72, 29.47, 29.22, 29.01, 28.60, 28.48, 28.41, 26.09, 25.97, 25.76, 25.24, 18.46, 18.28, 18.07, 17.89, -3.42, -3.76, -4.22, -4.91, -4.93, -5.06, -5.17, -5.20. MS (ESI)  $m/e$  calcd for  $\text{C}_{71}\text{H}_{140}\text{BrN}_5\text{O}_{19}\text{Si}_4\text{Na}$   $[\text{M}+\text{Na}]^+$ : 1583.2, found: 1583.5.

**6c**

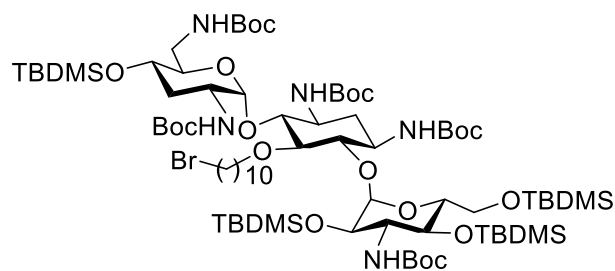
**5-*O*-(6-bromohexyl)-1,3,2',6',3''-penta-*N*-(*tert*-butoxycarbonyl)-4',2'',4'',6''-tetra-*O*-TBDMS-tobramycin (6c).** Yield: 69%.  $^1\text{H}$  NMR (500 MHz, chloroform-*d*)  $\delta$  5.22 – 5.06

(m, 2H, anomeric H), 4.27 – 3.98 (m, 3H), 3.81 – 3.09 (m, 17H), 2.48 – 2.37 (m, 1H), 1.99 – 1.91 (m, 1H), 1.89 – 1.74 (m, 2H), 1.53 (s, 1H), 1.51 – 1.22 (m, 51H), 1.06 – 0.95 (m, 1H), 0.93 – 0.77 (m, 36H), 0.16 – -0.03 (m, 24H).  $^{13}\text{C}$  NMR (126 MHz, chloroform-*d*)  $\delta$  155.76, 155.66, 155.46, 154.75, 154.58, 97.72 (anomeric C), 96.42 (anomeric C), 85.75, 79.89, 79.70, 79.37, 79.20, 78.78, 75.25, 73.17, 72.65, 71.56, 68.06, 67.00, 63.16, 57.25, 50.55, 48.90, 48.34, 41.68, 35.98, 35.72, 33.74, 33.52, 32.82, 32.59, 32.50, 30.42, 28.63, 28.50, 28.43, 27.27, 26.13, 26.00, 25.80, 25.33, 18.49, 18.32, 18.10, 17.92, -3.46, -3.77, -4.19, -4.87, -5.02, -5.15, -5.18, -5.28. MS (ESI)  $m/e$  calcd for  $\text{C}_{73}\text{H}_{144}\text{BrN}_5\text{O}_{19}\text{Si}_4\text{Na}$   $[\text{M}+\text{Na}]^+$ : 1611.2, found: 1611.6.

**6d****5-O-(8-bromooctyl)-1,3,2',6',3''-****penta-N-(tert-butoxycarbonyl)-4',2'',4'',6''-****tetra-O-TBDMS-tobramycin (6d).** Yield:72%. <sup>1</sup>H NMR (500 MHz, chloroform-*d*)  $\delta$ 

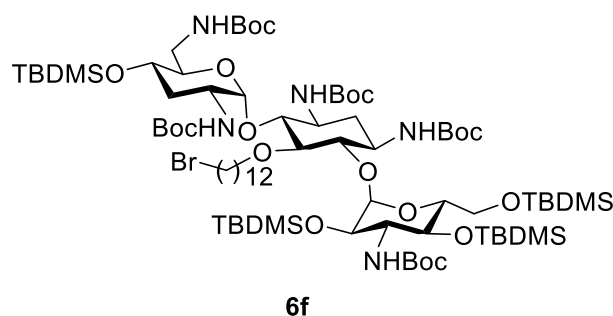
5.24 – 5.09 (m, 2H, anomeric H), 4.31 – 4.18

(m, 1H), 4.18 – 4.10 (m, 1H), 4.10 – 4.00 (m, 1H), 3.83 – 3.14 (m, 17H), 2.44 (d,  $J = 7.0$  Hz, 1H), 2.02 – 1.95 (m, 1H), 1.86 – 1.78 (m, 2H), 1.56 – 1.51 (m, 1H), 1.51 – 1.39 (m, 45H), 1.38 – 1.18 (m, 10H), 1.07 – 0.98 (m, 1H), 0.96 – 0.80 (m, 36H), 0.18 – -0.03 (m, 24H). <sup>13</sup>C NMR (126 MHz, chloroform-*d*)  $\delta$  155.69, 155.50, 154.72, 154.65, 154.55, 97.80 (anomeric C), 96.42 (anomeric C), 85.75, 79.90, 79.37, 79.21, 78.92, 78.84, 75.21, 73.26, 72.63, 71.55, 68.01, 66.88, 63.10, 57.25, 50.51, 48.88, 48.31, 41.65, 36.64, 35.91, 35.64, 33.88, 32.81, 30.56, 29.76, 28.72, 28.61, 28.48, 28.38, 28.14, 26.10, 26.03, 25.97, 25.76, 24.67, 23.46, 18.46, 18.30, 18.07, 17.89, -3.44, -3.81, -4.22, -4.90, -4.96, -5.09, -5.19, -5.24. MS (ESI)  $m/e$  calcd for C<sub>75</sub>H<sub>148</sub>BrN<sub>5</sub>O<sub>19</sub>Si<sub>4</sub>Na [M+Na]<sup>+</sup>: 1639.3, found: 1639.1.

**6e****5-O-(10-bromodecyl)-1,3,2',6',3''-****penta-N-(tert-butoxycarbonyl)-4',2'',4'',6''-****tetra-O-TBDMS-tobramycin (6e).** Yield:81%. <sup>1</sup>H NMR (300 MHz, chloroform-*d*)  $\delta$ 5.23 (d,  $J = 3.1$  Hz, 1H, anomeric H), 5.19 –

5.13 (m, 1H, anomeric H), 4.33 – 4.22 (m, 1H), 4.18 (d,  $J = 10.2$  Hz, 1H), 4.09 (d,  $J = 5.8$  Hz, 1H), 3.87 – 3.10 (m, 17H), 2.48 (d,  $J = 11.4$  Hz, 1H), 2.07 – 1.96 (m, 1H), 1.92 – 1.80 (m, 2H), 1.57 – 1.50 (m, 1H), 1.48 – 1.40 (m, 45H), 1.39 – 1.18 (m, 14H), 1.12 – 1.00 (m, 1H), 0.99 – 0.82 (m, 36H), 0.22 – -0.03 (m, 24H). <sup>13</sup>C NMR (75 MHz, chloroform-*d*)  $\delta$  155.63, 155.55,

154.85, 154.77, 154.59, 97.87 (anomeric C), 96.54 (anomeric C), 85.78, 79.95, 79.63, 79.39, 79.24, 79.11, 77.45, 75.31, 73.37, 72.69, 71.56, 68.07, 66.88, 63.16, 63.13, 57.32, 50.57, 48.97, 48.38, 41.73, 36.66, 35.97, 35.90, 35.68, 33.99, 33.80, 32.88, 30.66, 30.43, 29.98, 29.72, 29.70, 29.65, 29.56, 29.47, 29.38, 28.80, 28.66, 28.53, 28.42, 28.20, 26.15, 26.02, 26.01, 25.80, 24.70, 23.45, 18.51, 18.35, 18.12, 17.93, -3.39, -3.77, -4.18, -4.86, -4.92, -5.06, -5.14, -5.20. MS (ESI)  $m/e$  calcd for  $C_{77}H_{152}BrN_5O_{19}Si_4Na$   $[M+Na]^+$ : 1667.3, found: 1667.4.



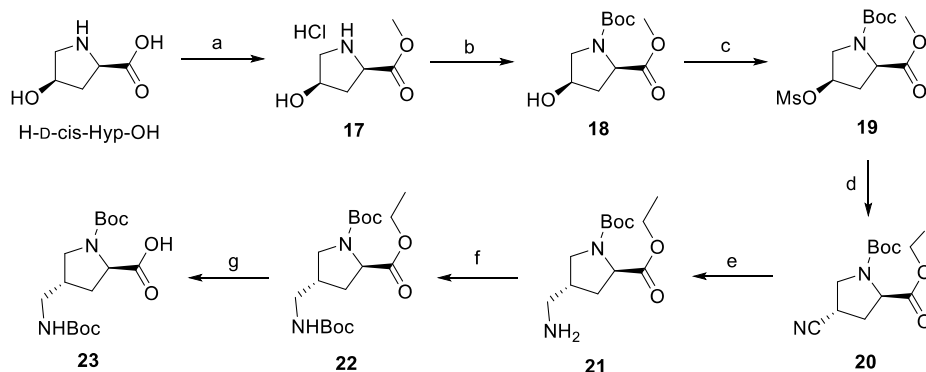
**5-*O*-(12-bromododecyl)-1,3,2',6',3''-penta-*N*-(*tert*-butoxycarbonyl)-4',2'',4'',6''-tetra-*O*-TBDMS-tobramycin (6f).** Yield:

80%.  $^1H$  NMR (500 MHz, chloroform-*d*)  $\delta$

5.26 – 5.12 (m, 2H, anomeric H), 4.33 – 4.21

(m, 1H), 4.16 (d,  $J = 9.9$  Hz, 1H), 4.12 – 4.02 (m, 1H), 3.82 – 3.17 (m, 17H), 2.46 (d,  $J = 7.7$  Hz, 1H), 2.04 – 1.96 (m, 1H), 1.87 – 1.82 (m, 2H), 1.59 – 1.53 (m, 1H), 1.47 – 1.39 (m, 45H), 1.34 – 1.20 (m, 18H), 1.10 – 1.00 (m, 1H), 0.97 – 0.81 (m, 36H), 0.23 – -0.04 (m, 24H).  $^{13}C$  NMR (126 MHz, chloroform-*d*)  $\delta$  155.89, 155.67, 154.93, 154.88, 154.71, 97.94 (anomeric C), 96.68 (anomeric C), 85.87, 80.04, 79.99, 79.51, 79.35, 79.24, 75.45, 73.55, 72.85, 71.68, 68.16, 66.98, 63.49, 63.45, 63.25, 57.44, 50.67, 49.09, 48.52, 41.79, 36.79, 36.05, 35.79, 34.13, 33.97, 33.07, 33.01, 32.96, 30.77, 30.46, 30.17, 29.79, 29.70, 29.64, 29.58, 29.55, 29.53, 29.41, 29.30, 29.11, 28.94, 28.90, 28.87, 28.78, 28.66, 28.55, 28.34, 28.31, 28.29, 28.22, 26.31, 26.28, 26.16, 26.14, 25.93, 25.81, 24.83, 24.02, 23.57, 18.63, 18.48, 18.25, 18.06, -3.26, -3.65, -4.05, -4.73, -4.80, -4.93, -5.03, -5.08. MS (ESI)  $m/e$  calcd for  $C_{79}H_{156}BrN_5O_{19}Si_4Na$   $[M+Na]^+$ : 1695.4, found: 1695.5.

## 9.1.3 Synthetic procedures and characterizations of compounds 17–23

**Scheme 9.1.3.1.** Synthesis of *trans*-1-(*tert*-butoxycarbonyl)-4-((*tert*-

*butoxycarbonyl)amino)methyl)-D-proline (23). Reagents and conditions: (a) SOCl<sub>2</sub>, EtOH, 0 °C, 1 h, then 85 °C, 3 h, 98%. (b) (Boc)<sub>2</sub>O, Et<sub>3</sub>N, DCM, 0 °C to rt, overnight, 91%. (c) MsCl, pyridine, DCM, 0 °C to rt, 18 h, 94%. (d) NaCN, DMSO, 55 °C 48 h. (e) H<sub>2</sub>, Raney Ni, MeOH, rt. (f) (Boc)<sub>2</sub>O, Et<sub>3</sub>N, DCM, rt, 10 h, 74% (two steps). (g) a.q. LiOH, MeOH, rt, 99%.*

***Cis*-4-hydroxy-D-proline ethyl ester hydrochloride (17).** To a stirred solution of H-D-*cis*-Hyp-OH (1.31 g, 10.0 mmol) in ethanol (20 mL), thionyl chloride (1.45 mL, 20.0 mmol) was added dropwise at 0 °C and stirred for 1 h. The mixture was then stirred at 85 °C for 3 h. The solvent was removed under reduced pressure to afford the desired compound as a white solid. Yield: 1.92 g (98%). <sup>1</sup>H NMR (300 MHz, methanol-*d*<sub>4</sub>) δ 4.62 – 4.50 (m, 2H, Pro<sub>α</sub>, Pro<sub>γ</sub>), 4.43 – 4.23 (m, 2H, OCH<sub>2</sub>CH<sub>3</sub>), 3.43 – 3.37 (m, 2H, Pro<sub>δ</sub>), 2.58 – 2.33 (m, 2H, Pro<sub>β</sub>), 1.35 (t, *J* = 7.1 Hz, 3H, OCH<sub>2</sub>CH<sub>3</sub>). <sup>13</sup>C NMR (75 MHz, methanol-*d*<sub>4</sub>) δ 170.36, 70.12, 64.05, 59.76, 54.99, 38.44, 14.34. MS (ESI) *m/e* calcd for C<sub>7</sub>H<sub>14</sub>NO<sub>3</sub> [M+H]<sup>+</sup>: 160.2, found: 160.2.

**Cis-1-(tert-butoxycarbonyl)-4-hydroxy-D-proline ethyl ester (18).** To a stirred solution of compound **17** (1.92 g, 9.8 mmol) in DCM (20 mL), triethylamine (3.5 mL, 24.5 mmol) and di-*tert*-butyl dicarbonate (2.78 g, 12.8 mmol) were added at 0 °C. The resultant reaction mixture was then stirred at room temperature overnight. Subsequently, the mixture was washed with 1N HCl (10 mL) solution and dried over anhydrous sodium sulfate. The solvent was removed *in vacuo* followed by purification using flash chromatography (elution with a gradient of hexanes/ethyl acetate = 6:1 to 1:2) to afford a pale yellow oil. Yield: 2.18 g (91%). <sup>1</sup>H NMR (500 MHz, chloroform-*d*, rotamers present)  $\delta$  4.38 – 4.14 (m, 4H, Pro <sub>$\alpha$</sub> , Pro <sub>$\gamma$</sub> , OCH<sub>2</sub>CH<sub>3</sub>), 3.72 – 3.32 (m, 3H, Pro <sub>$\delta$</sub> , OH), 2.38 – 2.24 (m, 1H, Pro <sub>$\beta$ 1</sub>), 2.12 – 2.00 (m, 1H, Pro <sub>$\beta$ 2</sub>), 1.52 – 1.34 (m, 9H, *t*Bu), 1.34 – 1.24 (m, 3H, OCH<sub>2</sub>CH<sub>3</sub>). <sup>13</sup>C NMR (75 MHz, chloroform-*d*, rotamers present)  $\delta$  175.18, 174.98, 154.43, 153.72, 71.31, 70.31, 61.83, 61.67, 58.05, 57.89, 56.01, 55.49, 38.62, 37.77, 28.36, 28.28, 14.14, 14.01. MS (ESI) *m/e* calcd for C<sub>12</sub>H<sub>21</sub>NO<sub>5</sub>Na [M+Na]<sup>+</sup>: 282.3, found: 282.3.

**Cis-1-(tert-butoxycarbonyl)-4-((methylsulfonyl)oxy)-D-proline ethyl ester (19).** A solution of methanesulfonyl chloride (1.57 mL, 20.3 mmol) in DCM (5 mL) was added dropwise to a solution of **18** (2.1 g, 8.1 mmol) and pyridine (3.28 mL, 40.5 mmol) in DCM (10 mL) at 0 °C. The solution was gradually warmed to room temperature while stirring for 18 h. The reaction mixture was cooled to 0 °C and quenched carefully by the drop-wise addition of water (10 mL). The organic layer was washed with saturated sodium bicarbonate solution, dried over anhydrous sodium sulfate and concentrated *in vacuo*. The crude was purified by flash chromatography (elution with a gradient of hexanes/ethyl acetate = 5:1 to 1:2) to give a pale yellow oil. Yield: 2.57 g (94%). <sup>1</sup>H NMR (300 MHz, chloroform-*d*, rotamers present)  $\delta$  5.33 – 5.18 (m, 1H, Pro <sub>$\gamma$</sub> ), 4.55 – 4.33 (m, 1H, Pro <sub>$\alpha$</sub> ), 4.30 – 4.08 (m, 2H, OCH<sub>2</sub>CH<sub>3</sub>), 3.85 – 3.70 (m, 2H, Pro <sub>$\delta$</sub> ), 3.02 (s, 3H,

OMs), 2.60 – 2.43 (m, 2H, Pro $\beta$ ), 1.55 – 1.36 (m, 9H, *t*Bu), 1.35 – 1.19 (m, 3H, OCH<sub>2</sub>CH<sub>3</sub>). <sup>13</sup>C NMR (75 MHz, chloroform-*d*, rotamers present)  $\delta$  171.42, 171.15, 153.76, 153.46, 78.34, 61.42, 57.53, 57.21, 52.49, 52.08, 38.92(CH<sub>3</sub> of mesylate), 37.19, 36.23, 28.36, 28.25, 14.24, 14.13.

***Trans*-1-(*tert*-butoxycarbonyl)-4-cyano-D-proline ethyl ester (20)**<sup>3</sup>. Compound **19** (1.03 g, 3.1 mmol) was dissolved in DMSO (15 mL) in room temperature followed by the addition of sodium cyanide (748 mg, 15.3 mmol) while stirring. This reaction mixture was heated to 55 °C and further stirred for 48 h. Water (20 mL) was added and the resulting mixture was extracted with ethyl acetate. The organic layer was washed with ample amount of water and dried over anhydrous sodium sulfate. The solvent was removed *in vacuo* followed by purification using flash chromatography (elution with a gradient of hexanes/ethyl acetate = 9:1 to 1:1) to give a colorless oil. Yield: 0.54 g (66%). <sup>1</sup>H NMR (300 MHz, chloroform-*d*, rotamers present)  $\delta$  4.34 – 4.15 (m, 1H, Pro $\alpha$ ), 4.12 – 3.92 (m, 2H, OCH<sub>2</sub>CH<sub>3</sub>), 3.81 – 3.66 (m, 1H, Pro $\delta_1$ ), 3.58 – 3.42 (m, 1H, Pro $\delta_2$ ), 3.21 – 3.05 (m, 1H, Pro $\gamma$ ), 2.48 – 2.28 (m, 1H, Pro $\beta_1$ ), 2.28 – 2.15 (m, 1H, Pro $\beta_2$ ), 1.44 – 1.20 (m, 9H, *t*Bu), 1.20 – 1.01 (m, 3H, OCH<sub>2</sub>CH<sub>3</sub>). <sup>13</sup>C NMR (75 MHz, chloroform-*d*, rotamers present)  $\delta$  171.64, 171.41, 153.28, 152.82, 119.12, 119.04, 80.67, 80.63, 61.31, 57.87, 57.77, 49.10, 49.00, 34.39, 33.43, 28.12, 28.01, 26.90, 26.28, 14.07, 13.96.

***Trans*-1-(*tert*-butoxycarbonyl)-4-aminomethyl-D-proline ethyl ester (21)**. A solution of **20** (0.54 g, 2.0 mmol) in isopropanol (13 mL) was degassed followed by the addition of 10% Raney nickel. The reaction flask was subjected to catalytic hydrogenation via hydrogen balloon for 10 h at room temperature. The solution was filtered through a bed of Celite<sup>®</sup> and washed with MeOH. Solvent was removed under reduced pressure to afford **21** as a white solid which was used in the next step without further purification. MS (ESI) *m/e* calcd for C<sub>8</sub>H<sub>17</sub>N<sub>2</sub>O<sub>2</sub> [M-Boc+H]<sup>+</sup>: 173.2, found: 173.2.

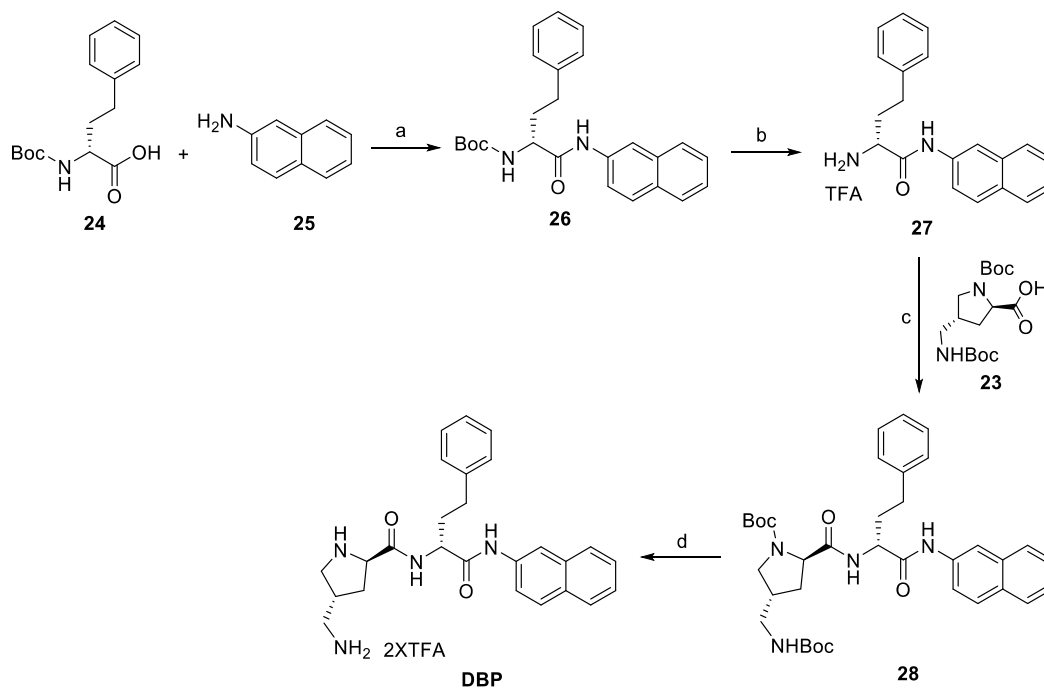
***Trans*-1-(*tert*-butoxycarbonyl)-4-((*tert*-butoxycarbonyl)amino)methyl)-D-proline ethyl ester (22).** Compound **21** (0.48 g, 1.8 mmol) was dissolved into DCM (12 mL).

Triethylamine (0.51 mL, 3.5 mmol) was added followed by di-*tert*-butyl dicarbonate (0.58 g, 2.6 mmol). The reaction was stirred at room temperature for 10 h. It was concentrated under reduced pressure to afford the crude product which was purified by flash chromatography (elution with a gradient of hexanes/ethyl acetate = 8:1 to 1:1) to give a white solid. Yield: 0.55 g (74% after two steps). <sup>1</sup>H NMR (300 MHz, chloroform-*d*, rotamers present)  $\delta$  4.36 – 4.19 (m, 1H, Pro $\alpha$ ), 4.19 – 4.04 (m, 2H, OCH<sub>2</sub>CH<sub>3</sub>), 3.72 – 3.57 (m, 1H, Pro $\delta_1$ ), 3.23 – 2.95 (m, 3H, Pro $\delta_2$ , CH<sub>2</sub>NHBoc), 2.55 – 2.32 (m, 1H, Pro $\gamma$ ), 2.12 – 1.82 (m, 2H, Pro $\beta$ ), 1.54 – 1.31 (m, 18H, *t*Bu), 1.31 – 1.15 (m, 3H, OCH<sub>2</sub>CH<sub>3</sub>). <sup>13</sup>C NMR (75 MHz, chloroform-*d*, rotamers present)  $\delta$  172.92, 172.64, 155.93, 154.24, 153.71, 79.96, 79.90, 79.41, 60.99, 60.95, 58.84, 58.65, 49.80, 49.47, 42.60, 37.29, 34.07, 28.38, 28.34, 28.26, 14.24, 14.11. MS (ESI) *m/e* calcd for C<sub>18</sub>H<sub>32</sub>N<sub>2</sub>O<sub>6</sub>K [M+K]<sup>+</sup>: 411.6, found: 411.5.

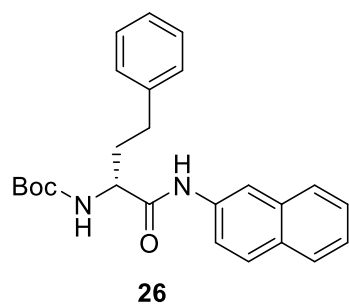
***Trans*-1-(*tert*-butoxycarbonyl)-4-((*tert*-butoxycarbonyl)amino)methyl)-D-proline (23).**

Compound **22** (70 mg, 0.19 mmol) was dissolved in MeOH (7 mL). 2 N lithium hydroxide solution (3 mL) was then added to the solution while stirring. The reaction mixture was stirred at room temperature for 5 h. TLC was used to monitor the completion of the reaction. In an ice bath, careful acidification of the solution to pH 6 was done by slow addition of 1 N HCl. The solvent was removed *in vacuo*. MeOH (5 mL) was added to the residue and filtered. The filtrate was concentrated under reduced pressure to afford a white solid as the desired compound which was used in the next step directly. Yield: 65 mg (99%).

## 9.1.4 Synthetic procedures and characterizations of compounds 26-28 and DBP



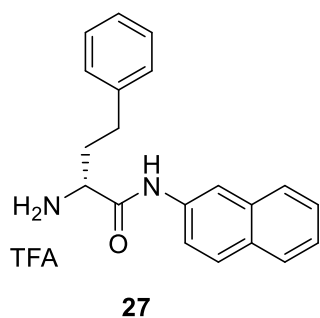
**Scheme 9.1.4.1.** Synthesis of DBP. Reagents and conditions: (a) TBTU, DIPEA, DMF, N<sub>2</sub>, rt, 18 h, 85%. (b) TFA, DCM, rt, 100%. (c) Compound **23**, TBTU, DIPEA, DMF, N<sub>2</sub>, rt, 18 h, 60%. (d) TFA, DCM, rt, 100%.



**(R)-tert-butyl (1-(naphthalen-2-ylamino)-1-oxo-4-phenylbutan-2-yl)carbamate (26).** DMF (6 mL) was added to a flask containing Boc-D-Homophe-OH (**24**) (390 mg, 1.4 mmol), TBTU (674 mg, 2.1 mmol) and DIPEA (0.78 mL, 4.2 mmol) under N<sub>2</sub> gas. The mixture was stirred for 15 min followed by the addition

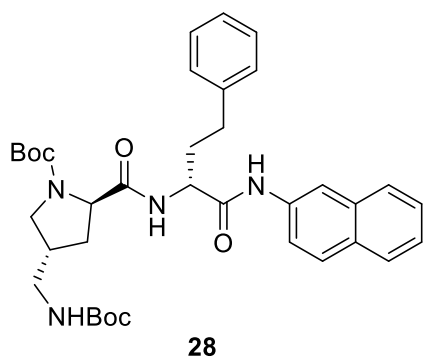
of 2-naphthylamine (**25**) (200 mg, 1.4 mmol). The reaction was stirred at room temperature for 18 h. Water (10 mL) was added and the resulting mixture was extracted with ethyl acetate. The

organic layer was washed with ample amount of water and dried over anhydrous sodium sulfate. The solvent was removed *in vacuo* followed by purification using flash chromatography (elution with a gradient of hexanes/ethyl acetate = 10:1 to 2:1) to give the desired product. Yield: 0.48 g (85%).  $^1\text{H}$  NMR (300 MHz, chloroform-*d*)  $\delta$  8.20 (s, 1H, aromatic), 7.77 – 7.48 (m, 3H, aromatic), 7.48 – 7.06 (m, 8H, aromatic), 5.78 – 5.69 (m, 1H, Homophe $_{\alpha}$ ), 2.98 – 2.66 (m, 2H, Homophe $_{\gamma}$ ), 2.40 – 2.22 (m, 1H, Homophe $_{\beta 1}$ ), 2.22 – 2.03 (m, 1H, Homophe $_{\beta 2}$ ), 1.49 (s, 9H, *t*Bu).  $^{13}\text{C}$  NMR (75 MHz, chloroform-*d*)  $\delta$  170.68, 156.36, 140.72, 135.16, 133.75, 130.65, 128.68, 128.58, 128.4, 127.66, 127.49, 126.39, 126.25, 124.96, 119.87, 116.78, 80.68, 55.02, 33.67, 32.06, 28.40. MS (ESI) *m/e* calcd for  $\text{C}_{25}\text{H}_{28}\text{N}_2\text{O}_3\text{Na}$  [ $\text{M}+\text{Na}$ ] $^+$ : 427.5, found: 427.4.



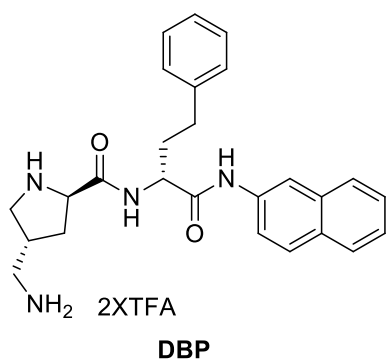
**(*R*)-2-amino-*N*-(naphthalen-2-yl)-4-phenylbutanamide trifluoroacetate (27).** Compound **26** was dissolved in DCM (10 mL). Trifluoroacetic acid (TFA) (3 mL) was added to this solution and stirred for 2 h in room temperature. The reaction mixture was concentrated *in vacuo* to give the desired compound which was used

in the next step without further purification. Yield: 0.50 g (100%).  $^1\text{H}$  NMR (300 MHz, methanol-*d*<sub>4</sub>)  $\delta$  8.28 (s, 1H, aromatic), 7.91 – 7.76 (m, 3H, aromatic), 7.61 (dd,  $J = 8.8, 2.1$  Hz, 1H, aromatic), 7.56 – 7.37 (m, 2H, aromatic), 7.38 – 7.20 (m, 4H, aromatic), 7.25 – 7.13 (m, 1H, aromatic), 4.19 (t,  $J = 6.4$  Hz, 1H, Homophe $_{\alpha}$ ), 2.83 2.83 (t,  $J = 8.5$  Hz, 2H, Homophe $_{\gamma}$ ), 2.44 – 2.17 (m, 2H, Homophe $_{\beta}$ ).  $^{13}\text{C}$  NMR (75 MHz, methanol-*d*<sub>4</sub>)  $\delta$  168.62, 141.33, 136.48, 135.15, 132.39, 129.84, 129.73, 129.34, 128.68, 128.66, 127.67, 127.53, 126.38, 121.10, 118.35, 55.22, 34.83, 32.21.



**(2*R*,4*R*)-tert-butyl 4-(((tert-butoxycarbonyl)amino)methyl)-2-(((*R*)-1-(naphthalen-2-**

**ylamino)-1-oxo-4-phenylbutan-2-yl)carbamoyl)pyrrolidine-1-carboxylate (28).** Compound **27** (79 mg, 0.19 mmol) was dissolved in DMF (6 mL). DIPEA (0.11 mL, 0.57 mmol) was added to this solution and stirred for 5 min. Compound **7** (65 mg, 0.19 mmol) and TBTU (93 mg, 0.29 mmol) were added to the reaction mixture and stirred for 18 h at room temperature under N<sub>2</sub> gas. DMF was removed *in vacuo* followed by purification using preparatory TLC (eluent: hexanes/ethyl acetate = 3:2) to give a white solid. Yield: 72 mg (60%). <sup>1</sup>H NMR (300 MHz, methanol-*d*<sub>4</sub>, rotamers present)  $\delta$  8.26 (s, 1H, aromatic), 7.94 – 7.73 (m, 3H, aromatic), 7.73 – 7.54 (m, 1H, aromatic), 7.54 – 7.35 (m, 2H, aromatic), 7.35 – 7.11 (m, 5H, aromatic), 4.74 – 4.52 (m, 1H, Homophe <sub>$\alpha$</sub> ), 4.51 – 4.31 (m, 1H, Pro <sub>$\alpha$</sub> ), 3.81 – 3.60 (m, 1H, Pro <sub>$\delta$ 1</sub>), 3.28 – 2.97 (m, 3H, Pro <sub>$\delta$ 2</sub>, Pro <sub>$\gamma$</sub> -CH<sub>2</sub>-NHBoc), 2.95 – 2.65 (m, 2H, Homophe <sub>$\gamma$</sub> ), 2.65 – 2.41 (m, 1H, Pro <sub>$\gamma$</sub> ), 2.41 – 1.89 (m, 4H, Homophe <sub>$\beta$</sub> , Pro <sub>$\beta$</sub> ), 1.64 – 1.34 (m, 18H, *t*Bu). <sup>13</sup>C NMR (75 MHz, methanol-*d*<sub>4</sub>, rotamers present)  $\delta$  175.14, 174.96, 172.25, 172.02, 158.19, 156.32, 155.57, 141.98, 136.65, 134.81, 131.82, 129.53 – 128.97, 128.26, 128.21, 127.14, 126.86, 126.78, 125.74, 121.13, 120.90, 117.91, 117.67, 81.27, 79.73, 60.96, 54.97, 54.76, 51.18, 50.86, 43.00, 39.32, 35.57, 35.08, 34.50, 34.36, 33.04, 32.85, 28.45, 28.41. MS (ESI) *m/e* calcd for C<sub>36</sub>H<sub>46</sub>N<sub>4</sub>O<sub>6</sub>Na [M+Na]<sup>+</sup>: 653.8, found: 653.6.



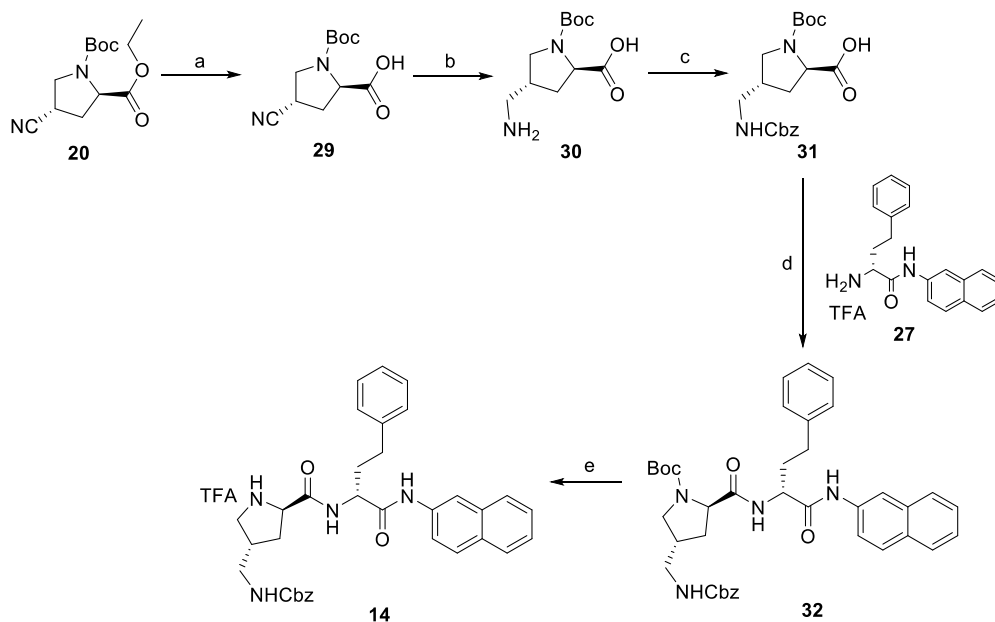
**(2R,4R)-4-(aminomethyl)-N-((R)-1-(naphthalen-2-ylamino)-1-oxo-4-phenylbutan-2-yl)pyrrolidine-2-**

**carboxamide trifluoroacetate (DBP).** Compound **28** (72 mg, 0.11 mmol) was dissolved in DCM (6 mL). TFA (2 mL) was added to the solution and stirred at room temperature for 1 h.

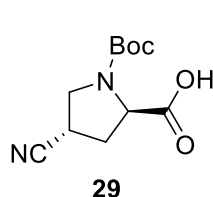
The solvent and TFA were removed under reduced pressure. The residue was then triturated three times with Et<sub>2</sub>O/MeOH (99/1), to produce the desired compound as TFA salt. Yield: 72 mg (100%). <sup>1</sup>H NMR (500 MHz, methanol-*d*<sub>4</sub>)  $\delta$  8.19 (s, 1H,

aromatic), 7.81 (dd,  $J = 8.9$  Hz, 2H, aromatic), 7.76 (d,  $J = 8.1$  Hz, 1H, aromatic), 7.56 (dd,  $J = 8.8, 2.0$  Hz, 1H, aromatic), 7.46 (dd,  $J = 7.5$  Hz, 1H, aromatic), 7.41 (dd,  $J = 7.4$  Hz, 1H, aromatic), 7.32 – 7.22 (m, 4H, aromatic), 7.22 – 7.13 (m, 1H, aromatic), 4.65 – 4.56 (m, 2H, Pro $_{\alpha}$ , Homophe $_{\alpha}$ ), 3.72 (dd,  $J = 11.6, 7.6$  Hz, 1H, Pro $_{\delta 1}$ ), 3.19 – 3.03 (m, 3H, Pro $_{\delta 2}$ , Pro $_{\gamma}$ -CH $_2$ -NH $_2$ ), 2.91 – 2.81 (m, 1H, Homophe $_{\gamma 1}$ ), 2.81 – 2.71 (m, 1H, Homophe $_{\gamma 2}$ ), 2.70 – 2.60 (m, 1H, Pro $_{\gamma}$ ), 2.59 – 2.50 (m, 1H, Pro $_{\beta 1}$ ), 2.33 – 2.19 (m, 2H, Pro $_{\beta 2}$ , Homophe $_{\beta 1}$ ), 2.19 – 2.08 (m, 1H, Homophe $_{\beta 2}$ ).  $^{13}\text{C}$  NMR (126 MHz, methanol- $d_4$ )  $\delta$  172.40, 169.62, 142.10, 136.88, 135.12, 132.20, 129.63, 129.58, 129.56, 129.48, 128.61, 128.58, 128.45, 127.56, 127.24, 126.18, 121.26, 118.14, 60.73, 55.97, 49.91, 41.84, 36.93, 35.25, 35.17, 33.28. MS (ESI)  $m/e$  calcd for C $_{26}$ H $_{31}$ N $_4$ O $_2$  [M + H] $^+$ : 431.6, found: 431.5.

### 9.1.5 Synthetic procedures and characterizations of compounds 29–32 and 14.



**Scheme 9.1.5.1.** Synthesis of compound **14**. Reagents and conditions: (a) a.q. LiOH, MeOH, rt, 1h. (b) H<sub>2</sub>, Raney Ni, MeOH, rt, 10 h. (c) CbzCl, aq Na<sub>2</sub>CO<sub>3</sub>, THF, 0 °C to rt, 65% in three steps. (d) Compound **27**, TBTU, DIPEA, DMF, N<sub>2</sub>, rt, 76%. (e) TFA, DCM, rt, 100%.

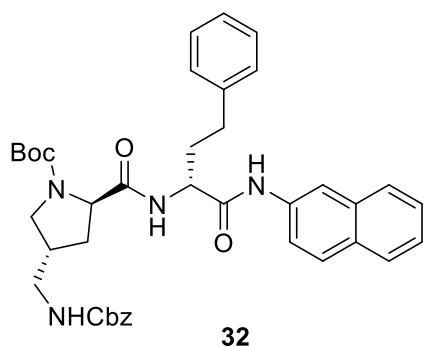


**(4S)-1-(tert-butoxycarbonyl)-4-cyano-D-proline (29).**<sup>3</sup> 2 N lithium hydroxide (3 mL) was added to a stirred solution of compound **20** (300 mg, 1.1 mmol) in MeOH (15 mL). The reaction mixture was stirred at room temperature for 1 h. TLC was used to monitor the completion of the reaction. In an ice bath, 1 N HCl was slowly added to neutralize the solution to pH 7~8. The solvent was removed *in vacuo* to give a crude product (**29**) as a white solid (283 mg) which was used in the next step directly.

**Trans-1-(tert-butoxycarbonyl)-4-aminomethyl-D-proline (30).** A solution of compound **29** (283 mg crude product from last step) in MeOH (15 mL) was degassed followed by the addition of 10% Raney nickel was added. The reaction flask was subjected to catalytic hydrogenation via hydrogen balloon for 10 h at room temperature. The reaction mixture was filtered through a bed of Celite<sup>®</sup> and washed with MeOH. Solvent was removed under reduced pressure to afford compound (**30**) as a white solid (251 mg), to which was used in the next step without further purification. MS (ESI) *m/e* calcd for C<sub>6</sub>H<sub>13</sub>N<sub>2</sub>O<sub>2</sub> [M-Boc+H]<sup>+</sup>: 145.2, found: 145.2.

**Trans-1-(tert-butoxycarbonyl)-4-(((benzyloxy)carbonyl)amino)methyl)-D-proline (31).** Benzyl chloroformate (CbzCl) (0.18 mL, 1.3 mmol) was added to a mixture of compound **30** (251 mg crude product from last step) and Na<sub>2</sub>CO<sub>3</sub> (175 mg, 1.7 mmol) dissolved in H<sub>2</sub>O (5 mL) and THF (2 mL) at 0 °C. The resulting solution was stirred overnight at room temperature. The mixture was then acidified with 10% (w/v) citric acid solution to pH 6 and subsequently

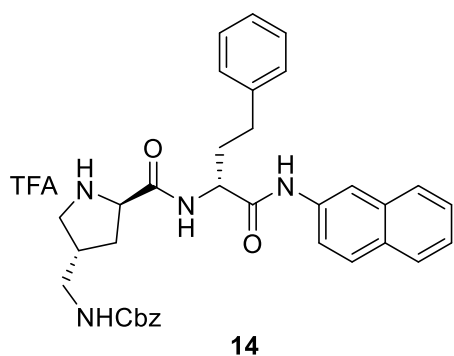
concentrated *in vacuo*. The crude was subjected to flash chromatography (elution with a gradient of DCM/MeOH = 10:1 to 1:1, 1% acidic acid) to afford compound **31** as a colorless oil. Yield: 0.27 g (65% in three steps).  $^1\text{H}$  NMR (300 MHz, methanol- $d_4$ , rotamers present)  $\delta$  7.42 – 7.25 (m, 5H, aromatic), 5.09 (s, 2H,  $\text{OCH}_2\text{Ph}$ ), 4.38 – 4.20 (m, 1H,  $\text{Pro}_\alpha$ ), 3.68 – 3.54 (m, 1H,  $\text{Pro}_{\delta 1}$ ), 3.24 – 3.04 (m, 3H,  $\text{Pro}_{\delta 2}$ ,  $\text{CH}_2\text{NHCbz}$ ), 2.60 – 2.40 (m, 1H,  $\text{Pro}_\gamma$ ), 2.15 – 1.89 (m, 2H,  $\text{Pro}_\beta$ ), 1.53 – 1.38 (m, 9H, *t*Bu).  $^{13}\text{C}$  NMR (75 MHz, methanol- $d_4$ , rotamers present)  $\delta$  176.47, 176.18, 159.01, 156.23, 155.88, 138.37, 129.56, 129.43, 129.07, 128.88, 128.07, 81.61, 81.43, 67.57, 60.29, 59.98, 51.09, 50.69, 43.82, 39.37, 38.57, 35.04, 34.41, 28.89, 28.72.



**(2*R*,4*R*)-tert-butyl 4-  
(((benzyloxy)carbonyl)amino)methyl)-2-(((*R*)-1-  
(naphthalen-2-ylamino)-1-oxo-4-phenylbutan-2-  
yl)carbamoyl)pyrrolidine-1-carboxylate (**32**).** DMF (6 mL)  
was added to a flask containing compound **31** (270 mg, 0.71

mmol), TBTU (342 mg, 1.1 mmol) and DIPEA (0.4 mL, 2.1 mmol) under  $\text{N}_2$  gas. The mixture was stirred for 15 min followed by the addition of compound **27** (299 mg, 0.71 mmol). The reaction was stirred at room temperature for 18 h. Water (10 mL) was added and the resulting mixture was extracted with ethyl acetate. The organic layer was washed with saturated brine and ample amount of water. It was then dried over anhydrous sodium sulfate. The solvent was removed *in vacuo* followed by purification using flash chromatography (elution with a gradient of hexanes/ethyl acetate = 8:1 to 1:1) to yield **32** as an amber oil. Yield: 0.36 g (76%).  $^1\text{H}$  NMR (500 MHz, methanol- $d_4$ , rotamers present)  $\delta$  8.21 (d,  $J = 2.0$  Hz, 1H, aromatic), 7.79 – 7.66 (m, 3H, aromatic), 7.56 (dd,  $J = 30.5, 8.6$  Hz, 1H, aromatic), 7.44 – 7.32 (m, 2H, aromatic), 7.32 – 7.07 (m, 10H, aromatic), 5.10 – 4.95 (m, 2H,  $\text{OCH}_2\text{Ph}$ ), 4.65 – 4.48 (m, 1H,  $\text{Homophe}_\alpha$ ), 4.44 –

4.29 (m, 1H, Pro $_{\alpha}$ ), 3.70 – 3.58 (m, 1H, Pro $_{\delta 1}$ ), 3.20 – 3.02 (m, 3H, Pro $_{\delta 2}$ ), 2.86 – 2.74 (m, 1H, Homophe $_{\gamma 1}$ ), 2.74 – 2.64 (m, 1H, Homophe $_{\gamma 2}$ ), 2.59 – 2.43 (m, 1H, Pro $_{\gamma}$ ), 2.31 – 1.86 (m, 4H, Pro $_{\beta}$ , Homophe $_{\beta}$ ), 1.50 – 1.34 (m, 9H, *t*Bu).  $^{13}\text{C}$  NMR (75 MHz, methanol-*d*<sub>4</sub>, rotamers present)  $\delta$  175.52, 175.34, 172.64, 172.41, 159.02, 156.69, 155.95, 142.39, 142.30, 138.36, 137.00, 135.19, 132.22, 129.68, 129.58, 129.54, 129.48, 128.97, 128.76, 128.62, 128.58, 127.51, 127.49, 127.22, 127.14, 126.11, 121.49, 121.26, 118.29, 118.05, 81.68, 67.48, 61.31, 55.35, 55.12, 51.53, 51.19, 49.90, 49.75, 49.62, 49.46, 49.34, 49.18, 49.05, 48.90, 48.77, 48.61, 48.49, 48.33, 48.20, 43.81, 39.62, 38.61, 35.90, 35.42, 34.86, 34.71, 33.40, 33.20, 28.80, 28.74. MS (ESI) *m/e* calcd for C<sub>39</sub>H<sub>44</sub>N<sub>4</sub>O<sub>6</sub>Na [M+Na]<sup>+</sup>: 687.8, found: 687.4.



**Benzyl (((3*S*,5*R*)-5-(((*R*)-1-(naphthalen-2-ylamino)-1-oxo-4-phenylbutan-2-yl)carbamoyl)pyrrolidin-3-yl)methyl)carbamate**

**trifluoroacetic acid (14).** TFA (2 mL) was added to a stirred solution of compound **32** (0.36 g, 0.54 mmol) in DCM (6 mL). The reaction mixture was stirred at room

temperature for 1 h and concentrated under reduced pressure to give product **14** as a yellow solid.

Yield: 0.36 g (100%).  $^1\text{H}$  NMR (300 MHz, methanol-*d*<sub>4</sub>)  $\delta$  8.22 (s, 1H, aromatic), 7.88 – 7.73 (m, 3H, aromatic), 7.62 – 7.35 (m, 3H, aromatic), 7.39 – 7.26 (m, 6H, aromatic), 7.31 – 7.15 (m, 5H, aromatic), 5.09 (s, 2H, OCH<sub>2</sub>Ph), 4.61 (dd, *J* = 8.9, 5.3 Hz, 1H, Homophe $_{\alpha}$ ), 4.49 (dd, *J* = 9.0, 5.0 Hz, 1H, Pro $_{\alpha}$ ), 3.57 (dd, *J* = 11.7, 7.3 Hz, 1H, Pro $_{\delta 1}$ ), 3.28 – 3.21 (m, 2H, Pro $_{\gamma}$ -CH<sub>2</sub>-NH), 3.15 – 2.96 (m, 1H, Pro $_{\delta 2}$ ), 2.92 – 2.68 (m, 2H, Homophe $_{\gamma}$ ), 2.66 – 2.49 (m, 1H, Pro $_{\gamma}$ ), 2.46 – 1.97 (m, 4H, Pro $_{\beta}$ , Homophe $_{\beta}$ ).  $^{13}\text{C}$  NMR (75 MHz, methanol-*d*<sub>4</sub>)  $\delta$  172.21, 169.85, 159.20, 142.14, 138.21, 136.96, 135.20, 132.23, 129.65, 129.59, 129.50, 129.46, 129.06, 128.82, 128.62, 128.55,

127.56, 127.27, 126.16, 121.22, 118.09, 67.68, 60.69, 55.89, 42.78, 39.59, 38.90, 35.21, 34.62, 33.28. MS (ESI)  $m/e$  calcd for  $C_{34}H_{37}N_4O_4$   $[M+H]^+$ : 565.7, found: 565.3.

## 9.2 HPLC ANALYSIS

### 9.2.1 HPLC Methodology

Method I: Kinetex 5  $\mu$ m reverse-phase C18 100 Å LC column (150  $\times$  4.6 mm, Phenomenex); flow: 1 mL/min; buffer A: 0.1% TFA in water; buffer B: 0.1% TFA in acetonitrile; see Table 9.2.1.1 for gradient used; run time: 20 min; UV detection at 283 nm.

Method II: Kinetex 5  $\mu$ m reverse-phase C18 100 Å LC column (150  $\times$  4.6 mm, Phenomenex); flow: 1 mL/min; buffer A: 0.1% TFA in water; buffer B: 0.1% TFA in acetonitrile; see Table 9.2.1.1 for gradient used; run time: 20 min; UV detection at 295 nm.

Method III: Kinetex 5  $\mu$ m reverse-phase C18 100 Å LC column (150  $\times$  4.6 mm, Phenomenex); flow: 1 mL/min; buffer A: 0.1% TFA in water; buffer B: 0.1% TFA in acetonitrile; see Table 9.2.1.1 for gradient used; run time: 20 min; UV detection at 271 nm.

Method IV Kinetex 5  $\mu$ m reverse-phase C18 100 Å LC column (150  $\times$  4.6 mm, Phenomenex); flow: 1 mL/min; buffer A: 0.1% TFA in water; buffer B: 0.1% TFA in acetonitrile; see Table 9.2.1.2 for gradient used; run time: 40 min; UV detection at 223 nm.

Method V: Kinetex 5  $\mu$ m reverse-phase C18 100 Å LC column (150  $\times$  4.6 mm, Phenomenex); flow: 1 mL/min; buffer A: 0.1% TFA in water; buffer B: 0.1% TFA in acetonitrile; see Table 9.2.1.2 for gradient used; run time: 40 min; UV detection at 343 nm.

Method VI: Kinetex 5  $\mu\text{m}$  reverse-phase C18 100 Å LC column (150  $\times$  4.6 mm, Phenomenex); flow: 1 mL/min; buffer A: 0.1% TFA in water; buffer B: 0.1% TFA in acetonitrile; see Table 9.2.1.2 for gradient used; run time: 40 min; UV detection at 244 nm.

Method VII: Synergi™ 4  $\mu\text{m}$  Plolar-RP 80 Å LC column (50  $\times$  4.6 mm, Phenomenex); flow: 0.7 mL/min; buffer A: 0.1% TFA in water; buffer B: 0.1% TFA in acetonitrile; see Table 9.2.1.3 for gradient used; run time: 30 min; UV detection at 223 nm.

Method VIII: Synergi™ 4  $\mu\text{m}$  Plolar-RP 80 Å LC column (50  $\times$  4.6 mm, Phenomenex); flow: 0.7 mL/min; buffer A: 0.1% TFA in water; buffer B: 0.1% TFA in acetonitrile; see Table 9.2.1.3 for gradient used; run time: 30 min; UV detection at 283 nm.

**Table 9.2.1.1.** HPLC methodology

Time duration (min)	% Buffer A	% Buffer B
0	85	15
3	85	15
4	80	20
6	80	20
7	70	30
9	70	30
10	60	40
13	60	40
14	50	50
15	50	50
18	85	15
20	85	15

**Table 9.2.1.2.** HPLC methodology

Time duration (min)	% Buffer A	% Buffer B
0	95	5
5	95	5
8	80	20
11	80	20
15	70	30
18	70	30
20	60	40
22	60	40
23	50	50
30	50	50
31	70	30
35	95	5
40	95	5

**Table 9.2.1.3.** HPLC methodology

Time duration (min)	% Buffer A	% Buffer B
0.01	95	5
5	95	5
8	80	20

10	80	20
12	70	30
15	70	30
17	60	40
<b>19</b>	60	40
<b>20</b>	50	50
<b>22</b>	50	50
<b>23</b>	70	30
<b>27</b>	95	5
<b>30</b>	95	5

### 9.1.3 Purity determination of final compounds using HPLC

**Table 9.1.3.1** Purity determination of final compounds

Compound	Method	Retention Time (min)	% Purity
1f	I	7.98	98.3
1e	II	11.04	98.3
1d	VII	12.25	95.4
1c	IV	10.34	99.8
1b	VIII	11.66	99.4
1a	V	13.53	100
2	II	10.34	97.4
DBP	VI	18.04	96.6

---

3	III	9.58	96.9
---	-----	------	------

---

## 9.4 REFERENCES

- (1) Guchhait, G.; Altieri, A.; Gorityala, B.; Yang, X.; Findlay, B.; Zhanel, G. G.; Mookherjee, N.; Schweizer, F. Amphiphilic Tobramycins with Immunomodulatory Properties. *Angew. Chem., Int. Ed. Engl.* **2015**, *54* (21), 6278–6282.
- (2) Gorityala, B. K.; Guchhait, G.; Fernando, D. M.; Deo, S.; McKenna, S. A.; Zhanel, G. G.; Kumar, A.; Schweizer, F. Adjuvants Based on Hybrid Antibiotics Overcome Resistance in *Pseudomonas Aeruginosa* and Enhance Fluoroquinolone Efficacy. *Angew. Chem., Int. Ed. Engl.* **2016**, *55* (2), 555–559.
- (3) Webb, T. R.; Eigenbrot, C. Conformationally Restricted Arginine Analogues. *J. Org. Chem.* **1991**, *56* (9), 3009–3016.

## 9.5 FIGURES

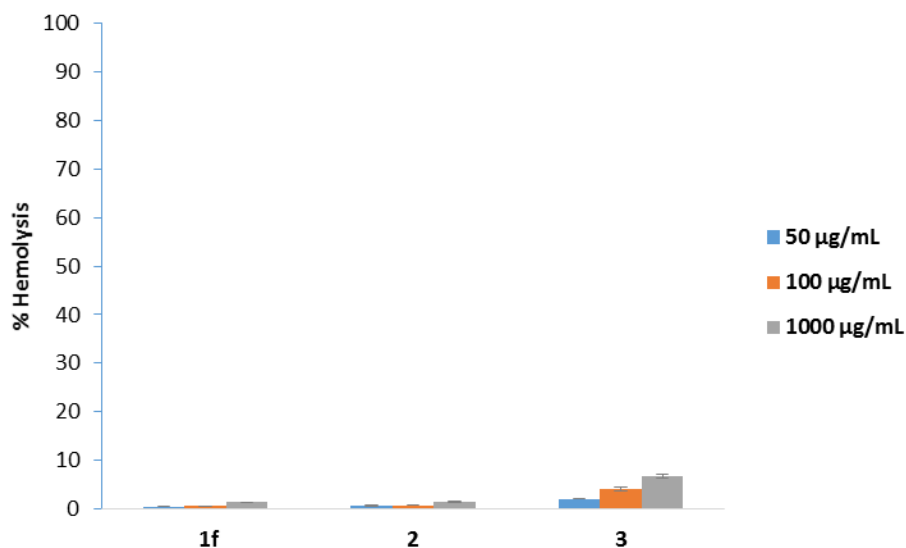


**Figure 9.5.1.** Percentages of hemolysis of conjugates **1f**, **2**, and **3**.

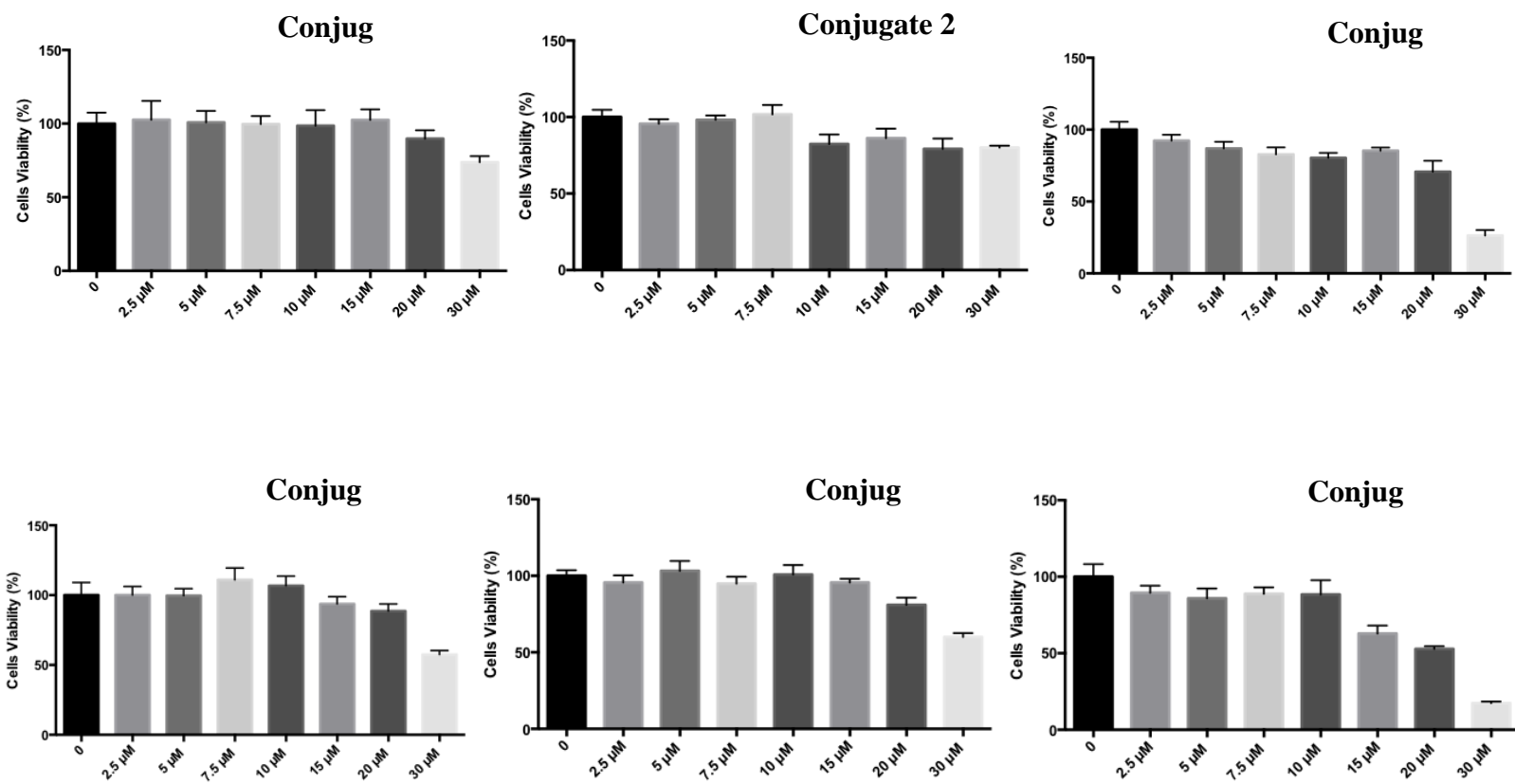


**Figure 9.5.2.** a: Cytotoxicity of conjugates **1f**, **2**, and **3** on prostate cancer (DU145) cell line; b: cytotoxicity of conjugates **1f**, **2**, and **3** on breast cancer (JIMT-1) cell line.

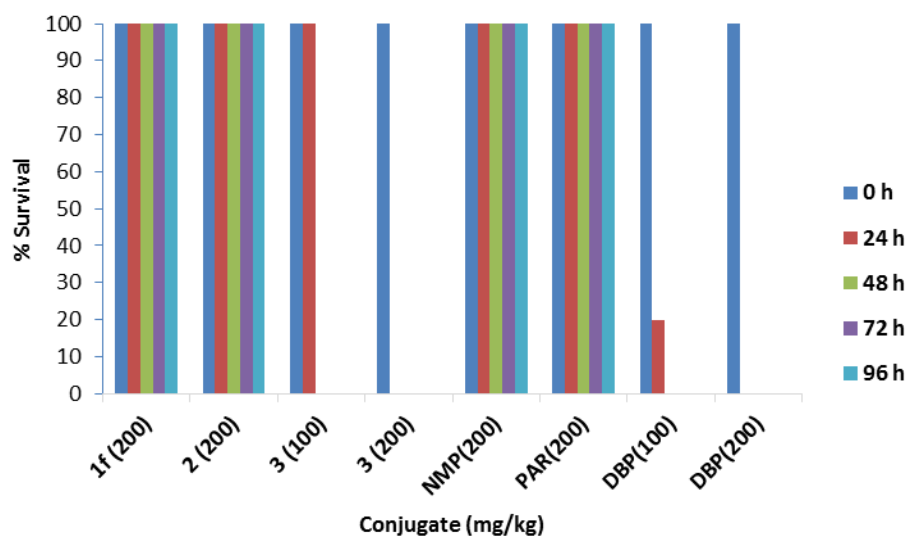


**Figure 9.5.3.** Tolerability dosages of **1f**, **2**, **3**, NMP, PAR, and DBP on *G. mellonella*. Larvae ( $n = 10$ ) survived up to 96 h when administered with 200 mg/kg dosage of conjugates **1f**, **2**, NMP, or PAR, whereas conjugate **3** or DBP (200 mg/kg) proved to be lethal as larvae ( $n = 10$ ) were found dead even after 24 h.

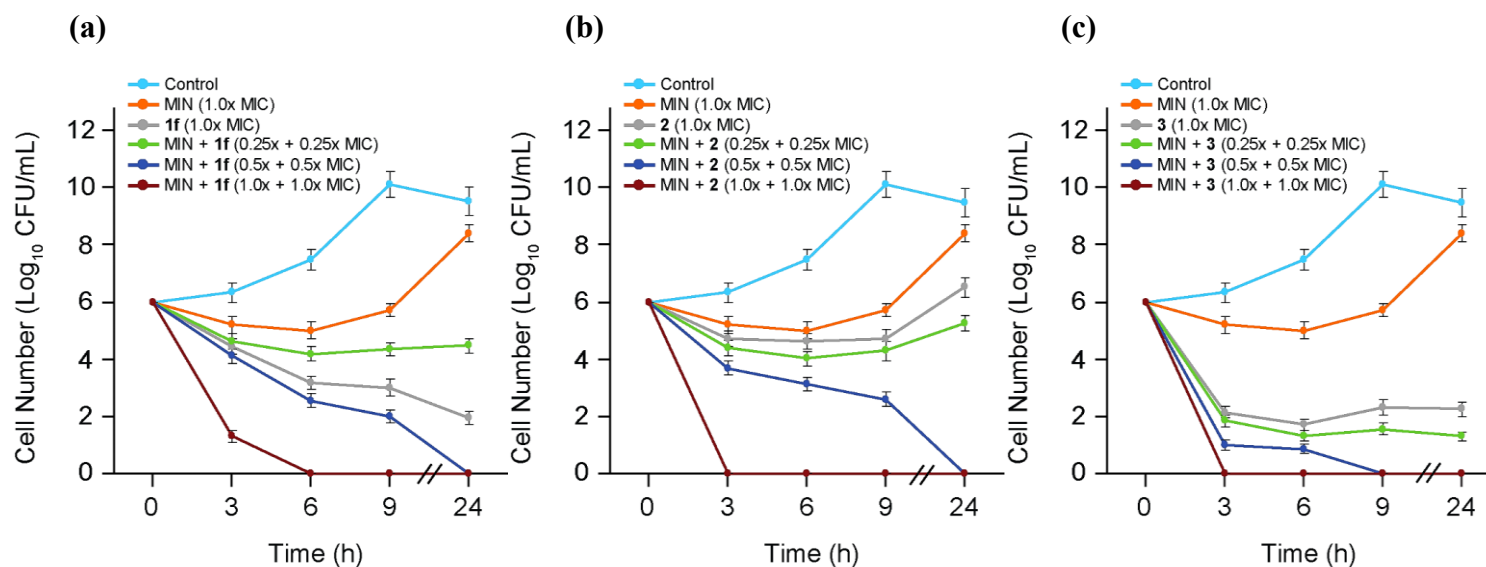


**Figure 9.5.4.** Time-kill curve of conjugates **1f**, **2**, and **3**. Enhanced dose-dependent bactericidal effect of conjugates **1f** (a), **2** (b) and **3** (c) in combination with minocycline on the viability of *P. aeruginosa* PAO1 cells grown in MHB. Results were determined by three independent time-kill experiments. No colony-forming units (CFU) were found when cells ( $10^6$  CFU/mL) treated with a combination of conjugate **1f** ( $1.0 \times$  MIC) and minocycline ( $1.0 \times$  MIC) (maroon) for 6 h (a). However, minocycline ( $1.0 \times$  MIC) combinations with either conjugates **2** ( $1.0 \times$  MIC) or **3** ( $1.0 \times$  MIC) resulted to complete cell eradication after 3 h incubation (b, c). Combinations of conjugate **1f** ( $0.5 \times$  MIC) or **2** ( $0.5 \times$  MIC) with minocycline ( $0.5 \times$  MIC) (blue) yielded zero cell viability post 24 h incubation (a, b). On the other hand, zero cell viability was observed post 9 h exposure to combination of conjugate **3** ( $0.5 \times$  MIC) and minocycline ( $0.5 \times$  MIC) (c). Growth inhibitory effect was also observed on cells treated with respective conjugates (**1f**, **2** or **3**) ( $0.25 \times$  MIC) and

minocycline ( $0.25 \times \text{MIC}$ ) (green) (a, b and c). In contrast, all three conjugates (**1f**, **2** or **3**) ( $1.0 \times \text{MIC}$ ) (grey) or minocycline ( $1.0 \times \text{MIC}$ ) (orange) alone have only bacteriostatic effect on the cells and cannot eradicate viable cell population even after 24 h of exposure. Each data point is the average of 3 determinations  $\pm$  SEM.

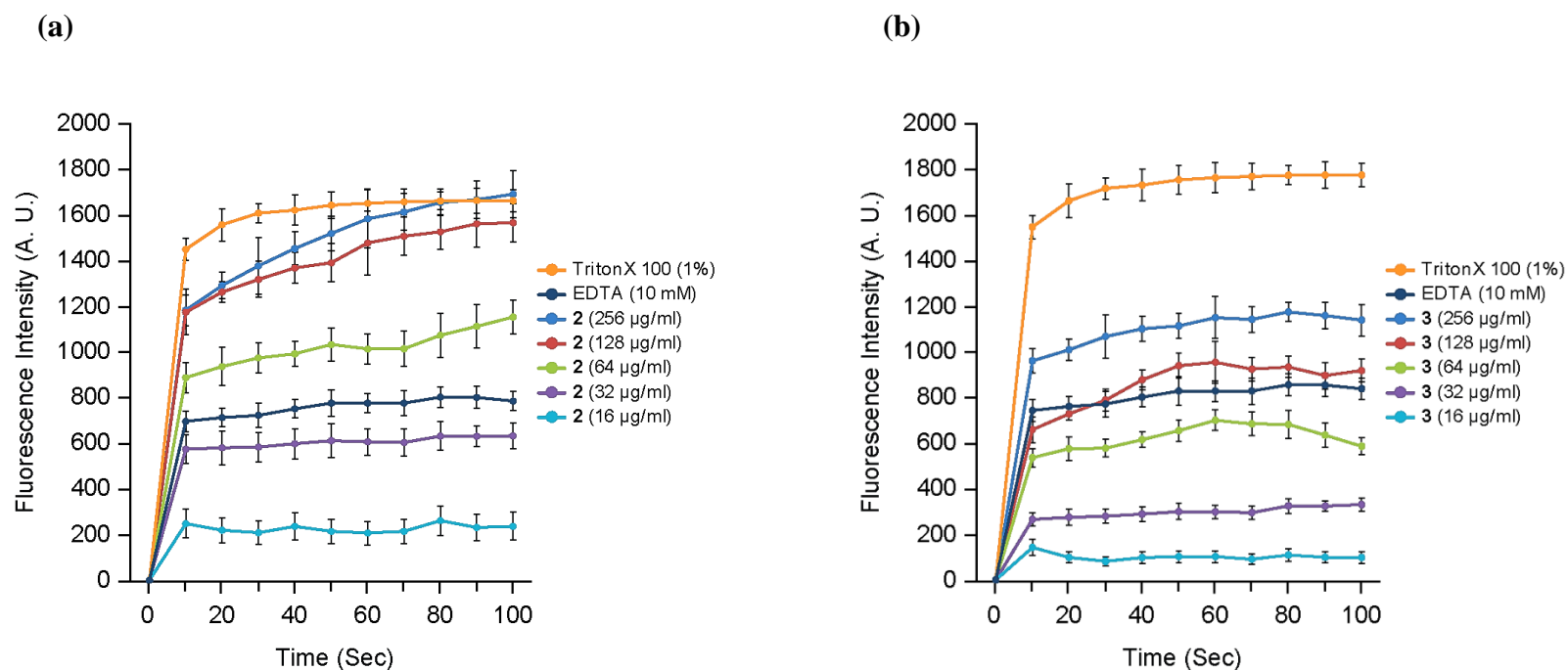


**Figure 9.5.5.** Effect of conjugates **2** and **3** on outer membrane permeabilization. Concentration-dependent permeabilization of the outer membrane by conjugates **2** and **3** are indicated by the uptake of NPN in *P. aeruginosa* PAO1. 256 µg/mL (blue), 128 µg/mL (red), 64 µg/mL (green), 32 µg/mL (purple) and 16 µg/mL (sky blue) of conjugates **2** and **3** were used, along with 1% Triton X-100 (orange) and 10 mM EDTA (dark blue) as positive controls. Any background NPN fluorescence from untreated cells were subtracted from the experimental data.

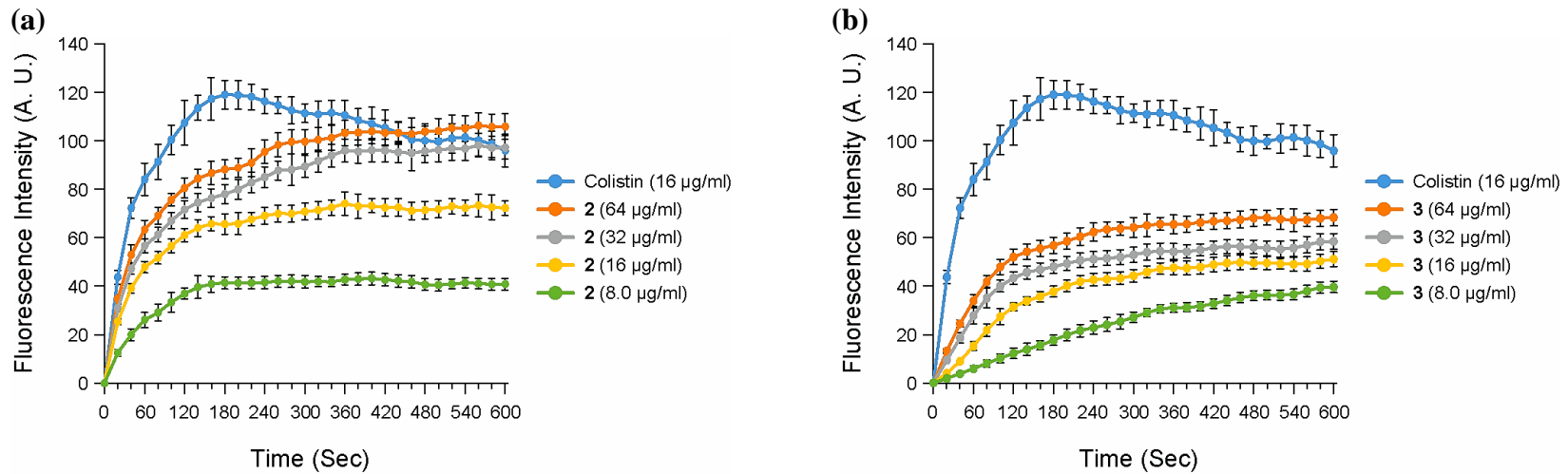


**Figure 9.5.6.** Effect of conjugates **2** and **3** on transmembrane potential. Concentration-dependent cytoplasmic membrane depolarization induced by conjugates **2** and **3** in *P. aeruginosa* PAO1 as determined through DiSC<sub>3</sub>(5) fluorescence. 64  $\mu\text{g/mL}$  (orange), 32  $\mu\text{g/mL}$  (grey), 16  $\mu\text{g/mL}$  (yellow) and 8  $\mu\text{g/mL}$  (green) are the conjugate concentrations used for the assay. Cells treated with 16  $\mu\text{g/mL}$  of colistin (blue) was used as positive control.

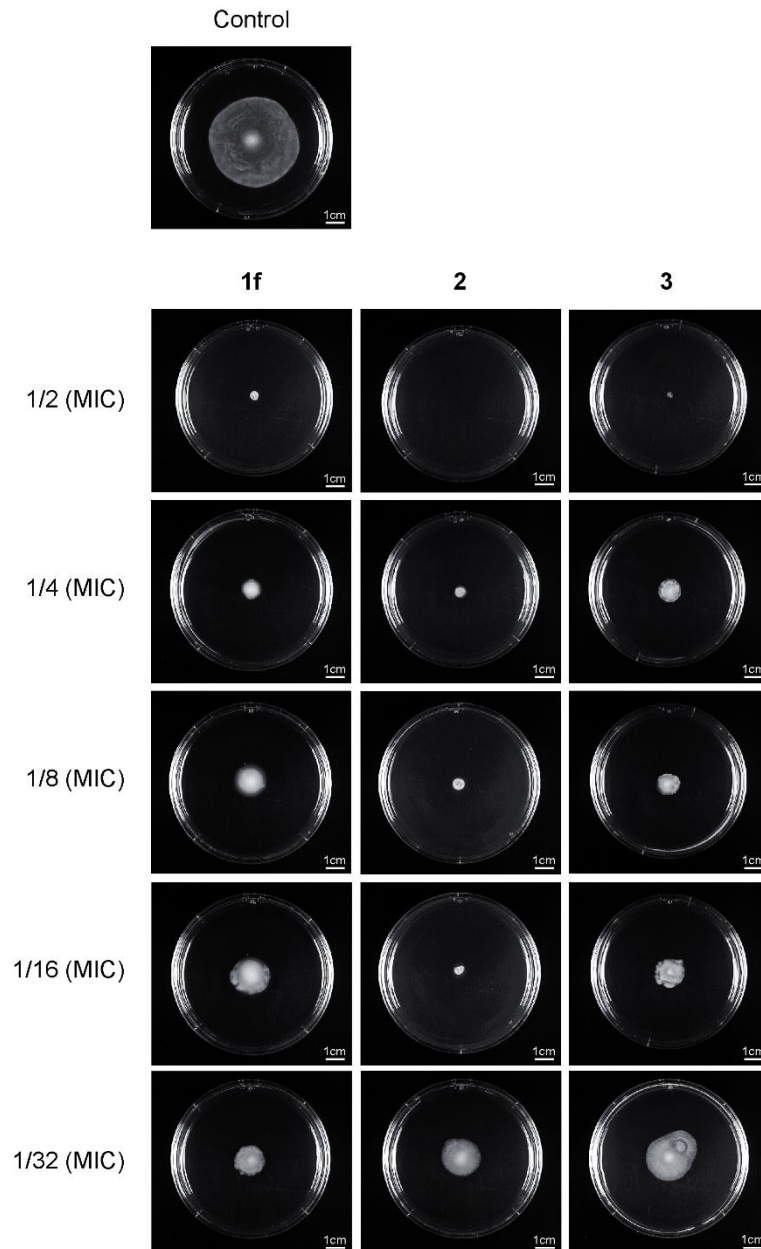


**Figure 9.5.7.** Impact of conjugates **1f**, **2** and **3** on swimming motility of *P. aeruginosa*

PAO1. Dose-dependent reduction in the swimming motility of *P. aeruginosa* (PAO1) on exposure to sub-MIC concentrations ( $1/2 \times \text{MIC}$ ,  $1/4 \times \text{MIC}$ ,  $1/8 \times \text{MIC}$ ,  $1/16 \times \text{MIC}$ ,  $1/32 \times \text{MIC}$ ) of the conjugates **1f** (MIC =  $64 \mu\text{g/mL}$ ), **2** (MIC =  $32 \mu\text{g/mL}$ ), and **3** (MIC =  $32 \mu\text{g/mL}$ ). Swimming plates without conjugate serve as control.

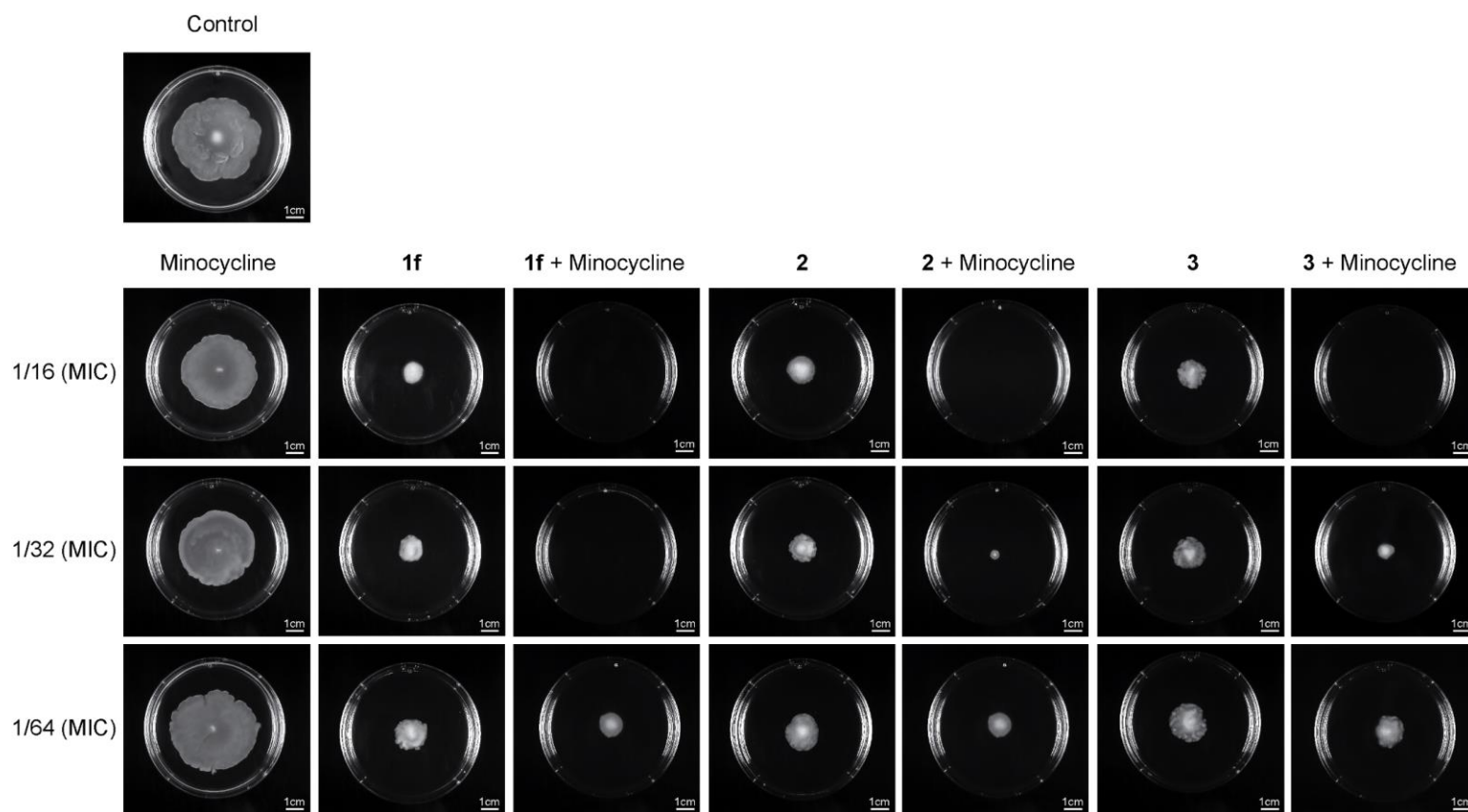


**Figure 9.5.8.** Combined effect of minocycline and conjugates **1f**, **2** and **3** on swimming motility of *P. aeruginosa* PAO1. Conjugates **1f** (MIC = 64  $\mu\text{g}/\text{mL}$ ), **2** (MIC = 32  $\mu\text{g}/\text{mL}$ ), and **3** (MIC = 32  $\mu\text{g}/\text{mL}$ ) exhibited enhanced dose-dependent reduction in the swimming motility of *P. aeruginosa* (PAO1) in the presence of minocycline at varying concentrations ( $1/16 \times \text{MIC}$ ,  $1/32 \times \text{MIC}$  and  $1/64 \times \text{MIC}$ ) in combination. For comparison motility assay was also conducted in plates containing different conjugates and minocycline alone at respective concentrations. Swimming plates without conjugate/antibiotic serve as a control.

## 9.6 TABLES

**Table 9.6.1.** Minimal inhibitory concentration (MIC) ( $\mu\text{g/mL}$ ) of compounds against a panel of Gram-positive and Gram-negative bacteria.

<b>Control Organism</b>	<b>1a</b>	<b>1b</b>	<b>1c</b>	<b>1d</b>	<b>1e</b>	<b>1f</b>	<b>2</b>	<b>3</b>	<b>NMP</b>	<b>PAR</b>	<b>DBP</b>	<b>TOB</b>
<i>S. aureus</i> ATCC 29213	16	128	128	128	32	32	8	8	512	128	128	$\leq 0.25$
MRSA ATCC 33592	16	128	>128	128	32	64	16	8	512	128	128	0.5
MSSE CANWARD-2008 81388	8	64	64	64	16	16	4	8	512	128	64	$\leq 0.25$
MRSE CAN-ICU 61589 (CAZ >32)	32	64	128	32	8	8	4	8	512	128	128	2
<i>E. faecalis</i> ATCC 29212	>128	>128	>128	>128	64	128	32	32	512	128	128	8
<i>E. faecium</i> ATCC 27270	>128	128	>128	128	32	64	8	16	512	128	128	16
<i>S. pneumoniae</i> ATCC 49619	>128	>128	>128	128	64	64	32	32	512	128	64	2
<i>E. coli</i> ATCC 25922	32	>128	>128	>128	128	512	128	32	512	128	128	0.5
<i>E. coli</i> CAN-ICU 61714 (GEN-R)	>128	>128	>128	>128	128	512	128	32	512	256	128	8
<i>E. coli</i> CAN-ICU 63074 (AMK 32)	>128	>128	>128	>128	128	512	32	32	512	128	128	8
<i>E. coli</i> CANWARD-2011 97615 (GEN-R, TOB-R, CIP-R) aac(3')iia	>128	>128	>128	>128	128	512	128	32	>512	128	128	128

<i>P. aeruginosa</i> ATCC 27853	128	>128	>128	>128	64	256	128	32	>512	512	256	1
<i>P. aeruginosa</i> CAN-ICU 62308 (GEN-R)	128	128	128	64	32	64	32	16	>512	512	256	16
<i>P. aeruginosa</i> CANWARD-2011 96846 (GEN-R, TOB-R)	>128	>128	>128	>128	64	256	128	32	512	512	256	128
<i>S. maltophilia</i> CAN-ICU 62584	>128	>128	>128	>128	>128	>512	128	128	512	128	>512	>512
<i>A. baumannii</i> CAN-ICU 63169	>128	>128	>128	>128	>128	512	512	64	>512	128	512	16
<i>K. pneumoniae</i> ATCC 13883	8	>128	>128	>128	>128	>512	256	64	512	128	256	≤0.25

MRSA: methicillin-resistant *Staphylococcus aureus*; MRSE: methicillin-resistant *Staphylococcus epidermidis*; CANWARD: Canadian ward surveillance study; CAN-ICU: Canadian intensive care unit surveillance study; CAZ: ceftazidime; GEN-R: gentamicin-resistant; AMK: amikacin; TOB-R: tobramycin-resistant; CIP-R: ciprofloxacin-resistant.

**Table 9.6.2.** Combination studies of TOB-EPIs (**1f**, **2**, and **3**) with doxycycline and tigecycline in *P. aeruginosa* PAO1

Anti- biotic	MIC <sub>an</sub> tibi- otic alone ( $\mu$ g/m L)	DJ	MI C <sub>ADJ</sub> alone ( $\mu$ g/mL)	F IC index	Absol- ute MIC ( $\mu$ g/m L)
Dox- y- cycline	8	<b>f</b>	64	13	0.5 <sup>a</sup>
Dox- y- cycline	8		32	13	0.125 <sup>a</sup>
Dox- y- cycline	16		8	19	0.25 <sup>b</sup>
Tige- cycline	4	<b>f</b>	64	14	0.5 <sup>a</sup>
Tige- cycline	4		32	25	0.5 <sup>a</sup>
Tige- cycline	4		16	19	0.25 <sup>a</sup>

<sup>a</sup> Absolute MIC of antibiotic in the presence of 8  $\mu$ g/mL of corresponding adjuvant; <sup>b</sup> Absolute MIC of antibiotic in the presence of a quarter MIC of corresponding adjuvant

**Table 9.6.3.** Combination studies of minocycline (MIN) with membrane-active agents in *P. aeruginosa* PAO1

A- nti- biotic	MIC <sub>an</sub> tibi- otic alone ( $\mu$ g/m L)	ADJ	MI C <sub>ADJ</sub> alone ( $\mu$ g/mL)	F IC index
M- IN	8	Benzethonium chloride	32	1.03

IN	M	8	Cetrimonium bromide	32	0. 75
IN	M	8	Colistin	1	0. 50

**Table 9.6.4.** MICs ( $\mu\text{g/mL}$ ) of clinical *P. aeruginosa* isolates against different antibiotic classes.

Stock no.	PTZ	A/C	AZT	FOX	CFZ	CTR	CPM	CAZ	IMI	MER	DOR	ETP	CIP	MXF	TOB	GEN	AMK	TGC	DOX	CST	SXT
100036	8	>32	8	>32	>128	32	4	8	8	4	4	>32	>16	>16	64	>32	32	>16	>32	2	>8
101885	16	>32	32	>32	>128	32	8	8	1	1	0.5	32	>16	>16	$\leq 0.5$	$\leq 0.5$	$\leq 1$	8	>32	1	>8
P259-96918	64	>32	16	>32	>128	>64	>64	>32	32	>32	>32	>32	>16	>16	>64	>32	>64	8	16	1	>8
P260-97103	128	>32	16	>32	>128	>64	16	32	32	16	16	>32	16	>16	32	>32	4	16	16	1	2
P262-101856	64	>32	32	>32	>128	64	32	16	32	32	8	>32	>16	>16	>64	>32	>64	>16	>32	1	>8
P264-104354	256	>32	64	>32	>128	>64	32	>32	32	>32	16	>32	>16	>16	64	>32	8	>16	>32	1	>8
91433	64	>32	ND	>32	>128	>64	16	>32	32	8	8	>32	2	16	8	32	>32	>16	32	4	1
101243	128	>32	ND	>32	>128	>64	64	>32	16	16	16	>32	1	8	$\geq 64$	>32	>64	8	4	1024	4

PTZ: piperacillin-tazobactam; A/C: amoxicillin-clavulanic acid; AZT: aztreonam; FOX: cefoxitin; CFZ: cefazolin; CTR: ceftriaxone; CPM: cefepime; CAZ: ceftazidime; IMI: imipenem; MER: meropenem; DOR: doripenem; ETP: ertapenem; CIP: ciprofloxacin; MXF: moxifloxacin; TOB: tobramycin; GEN: gentamicin; AMK: amikacin; TGC: tigecycline; DOX: doxycycline; CST: colistin; SXT: trimethoprim-sulfamethoxazole; ND: not determined.

**Table 9.6.5.** MICs ( $\mu\text{g/mL}$ ) of clinical *Klebsiella pneumoniae* and *Enterobacter cloacae* isolates against different antibiotic classes

Stock no. Organism	PTZ	A/C	AZT	FOX	CFZ	CPM	CAZ	CAZ-AVI	C/T	CTX	IMI	MER	ETP	CIP	MXF	TOB	GEN	AMK	TGC	DOX	CST	SXT
116381 <i>K. pneumoniae</i>	8	16	16	16	>128	16	8	0.5	1	>64	0.5	$\leq 0.03$	0.12	>16	>16	2	$\leq 0.5$	$\leq 1$	1	>32	0.5	>8
117029 <i>E. cloacae</i>	2	16	$\leq 0.12$	>32	>128	$\leq 0.25$	0.5	0.25	0.25	$\leq 0.25$	0.25	$\leq 0.03$	$\leq 0.03$	$\leq 0.06$	$\leq 0.06$	$\leq 0.5$	$\leq 0.5$	2	0.5	>32	0.25	>8

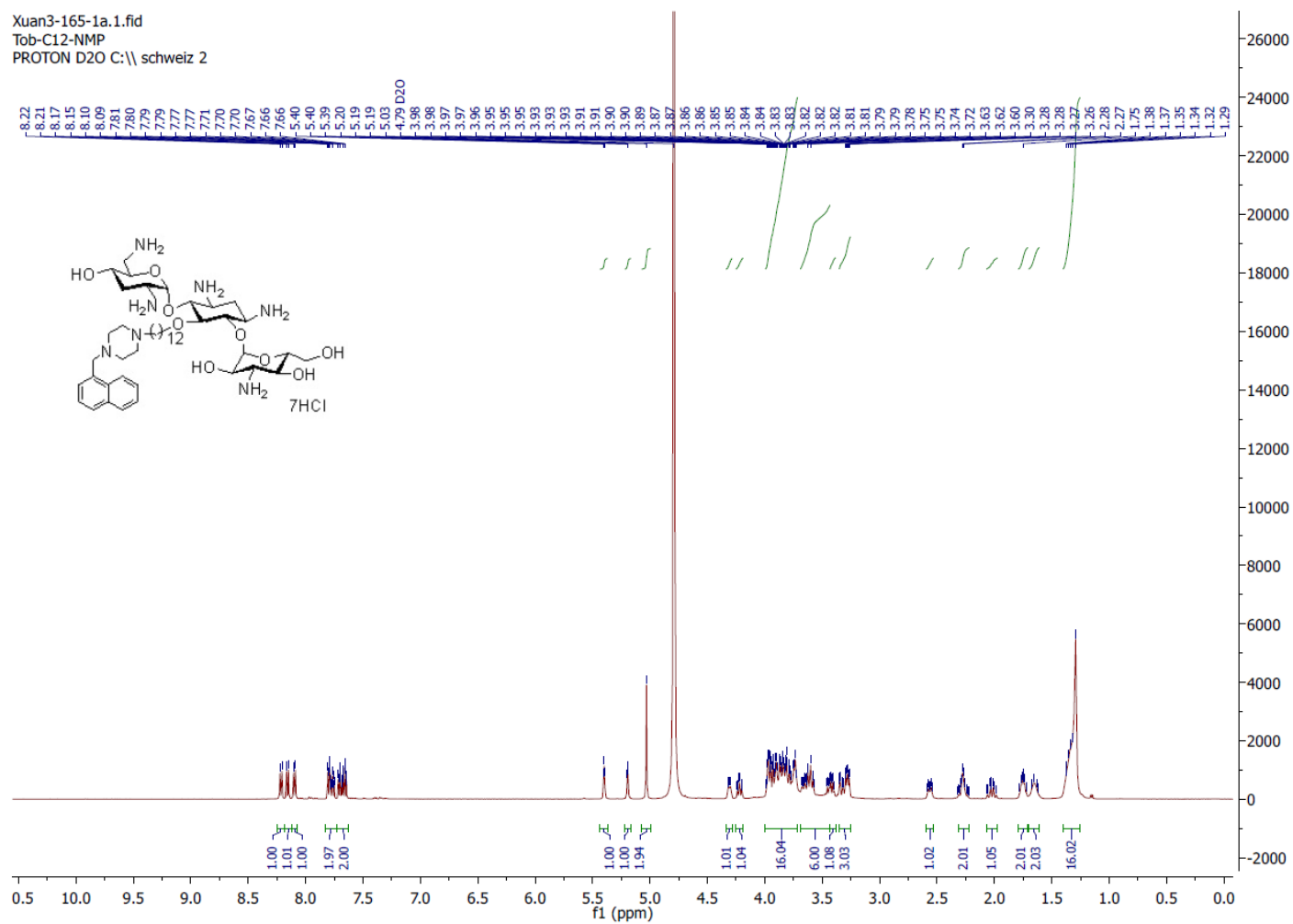
PTZ: piperacillin-tazobactam; A/C: amoxicillin-clavulanic acid; AZT: aztreonam; FOX: ceftaxime; CFZ: cefazolin; CPM: cefepime; CAZ: ceftazidime; CAZ-AVI: ceftazidime-avibactam; C/T: ceftolozane-tazobactam; CTX: ceftriaxone; IMI: imipenem; MER: meropenem; ETP: ertapenem; CIP: ciprofloxacin; MXF: moxifloxacin; TOB: tobramycin; GEN: gentamicin; AMK: amikacin; TGC: tigecycline; DOX: doxycycline; CST: colistin; SXT: trimethoprim-sulfamethoxazole; ND: not determined.

**Table 9.6.6.** MICs ( $\mu\text{g/mL}$ ) and FIC indices for conjugates **1f**, **2**, and **3**, or EPIs NMP, PAR, and DBP against *P. aeruginosa* PAO1 and efflux pump deficient strains PAO200 or PAO750

Compound	PAO1		PAO200		PAO750	
	MIC	FIC index (combination with MIN)	MIC	FIC index (combination with MIN)	MIC	FIC index (combination with MIN)
TOB-NMP ( <b>1f</b> )	64	0.19	64	0.38	8	0.53
NMP	512	1.02	>256	>2	>256	>0.5
TOB-PAR ( <b>2</b> )	32	0.19	32	0.27	16	0.38
PAR	512	1.02	128	2.00	16	0.50
TOB-DBP ( <b>3</b> )	16	0.09	16	0.75	4	0.75
DBP	256	0.13	128	0.31	32	0.38
MIN	8	N/A	1	N/A	0.5	N/A
RIF	16	N/A	8	N/A	8	N/A

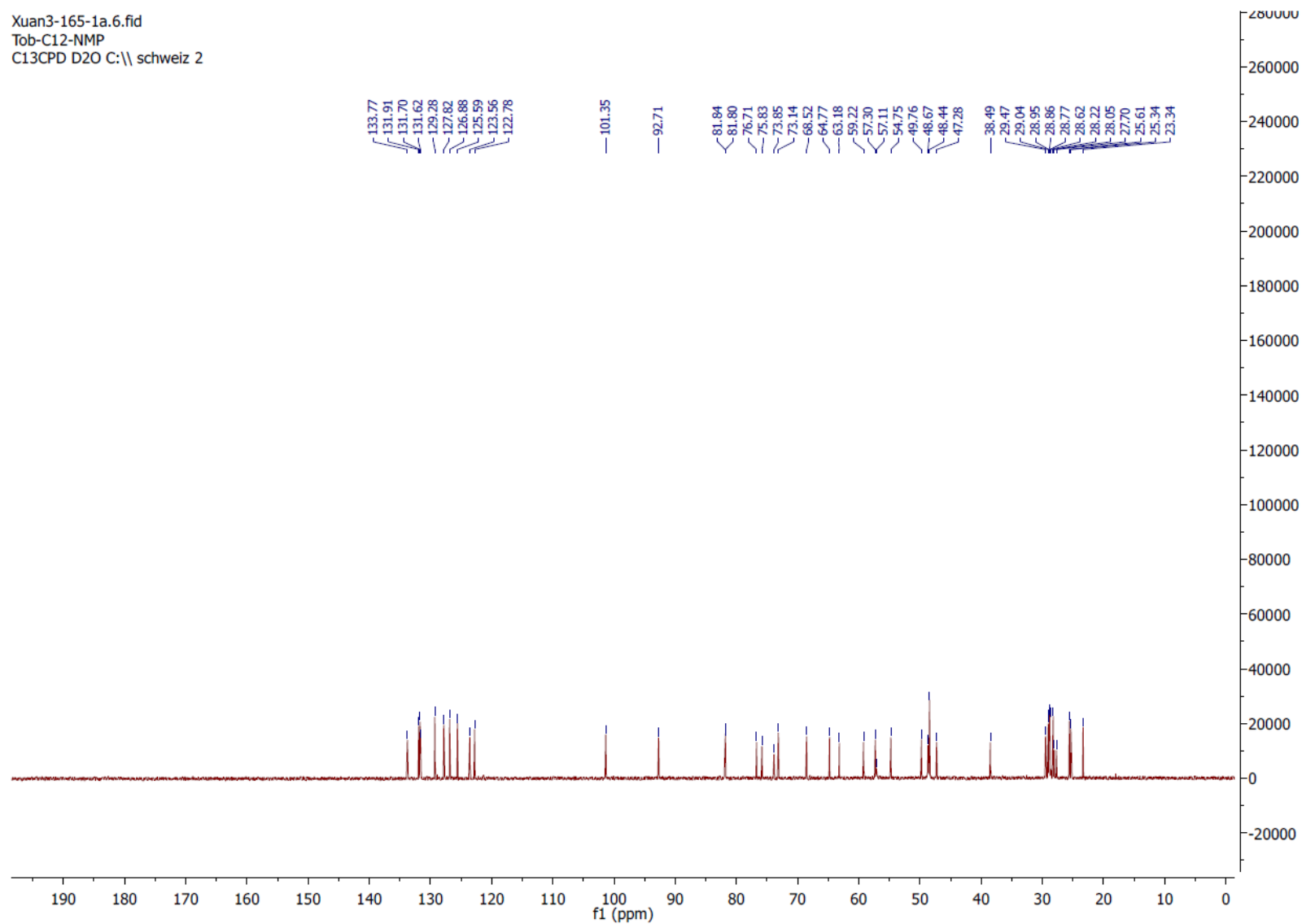
MIN: minocycline; RIF: rifampicin; *P. aeruginosa* PAO200 strain (with a MexAB-OprM pump deletion); *P. aeruginosa* strain (PAO750) that lacks five different clinically-relevant RND pumps (MexAB-OprM, MexCD-OprJ, MexEF-OprN, MexJK, and MexXY) and the outer membrane protein OpmH; N/A: not applicable.

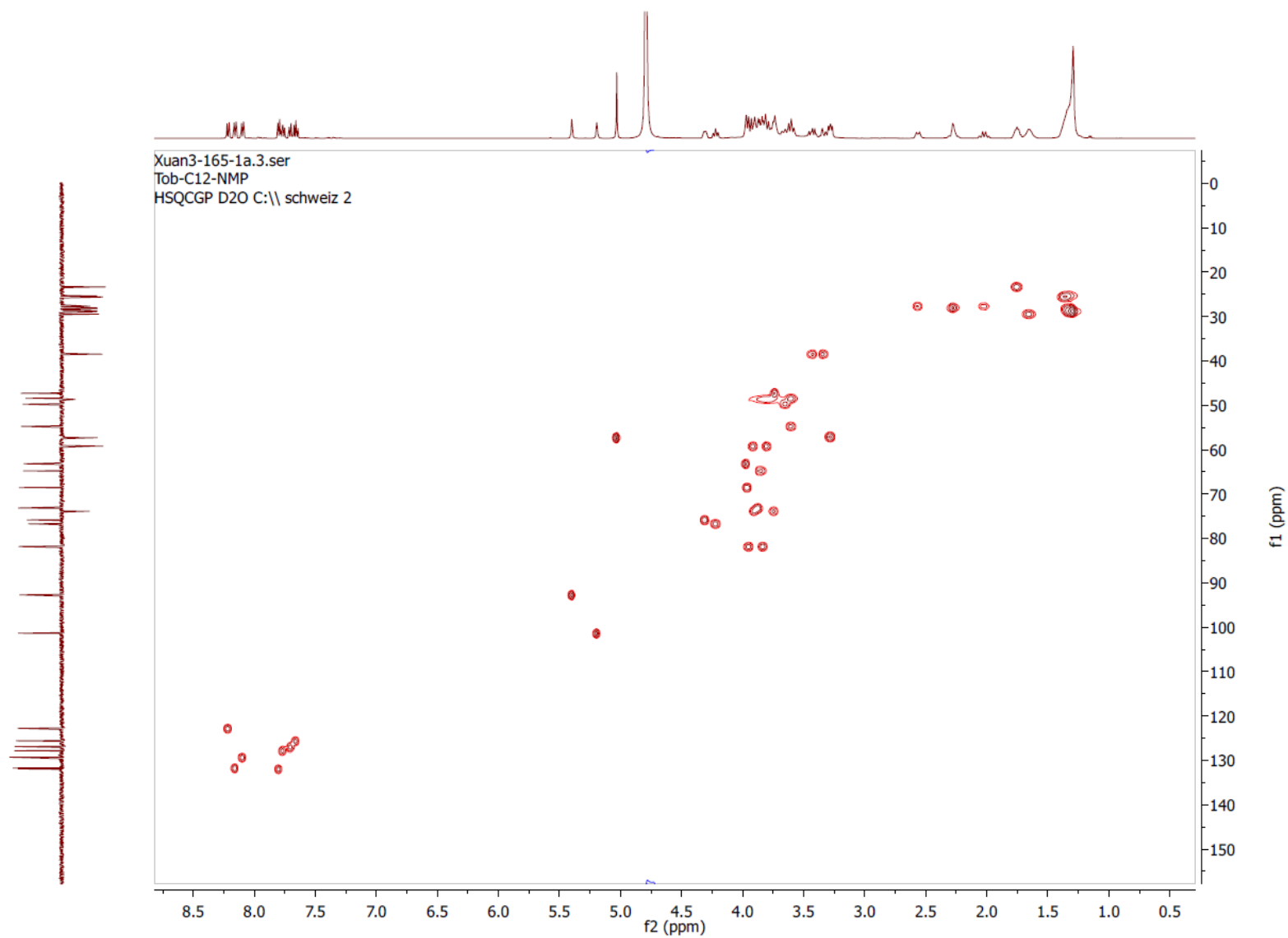
## 9.7 NMR SPECTRA

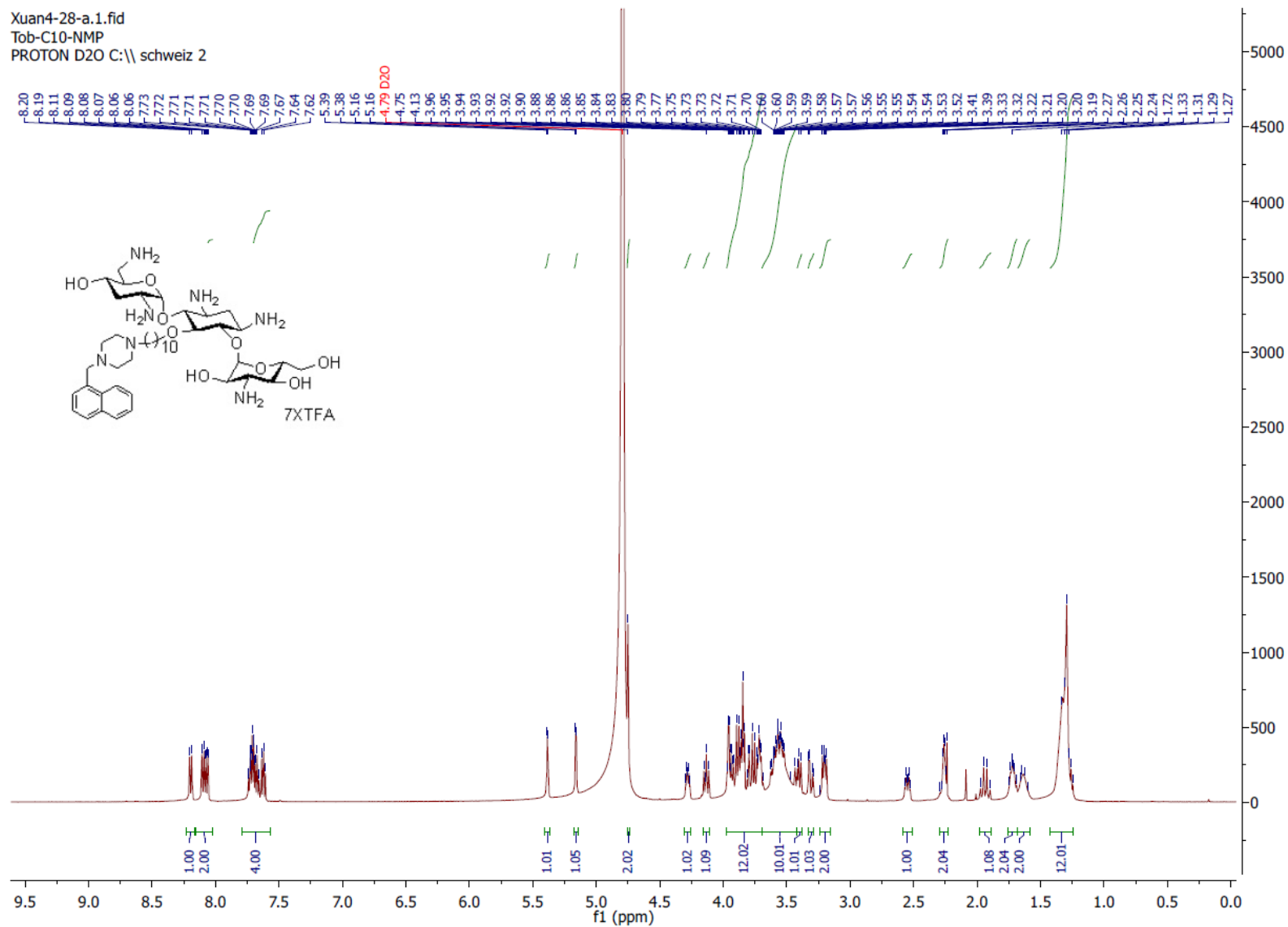
Appendix 1.  $^1\text{H}$  spectrum of compound 1f in  $\text{D}_2\text{O}$ 

Appendix 2.  $^{13}\text{C}$  spectrum of compound 1f in  $\text{D}_2\text{O}$ 

Xuan3-165-1a.6.fid  
Tob-C12-NMP  
C13CPD D2O C:\schweiz 2

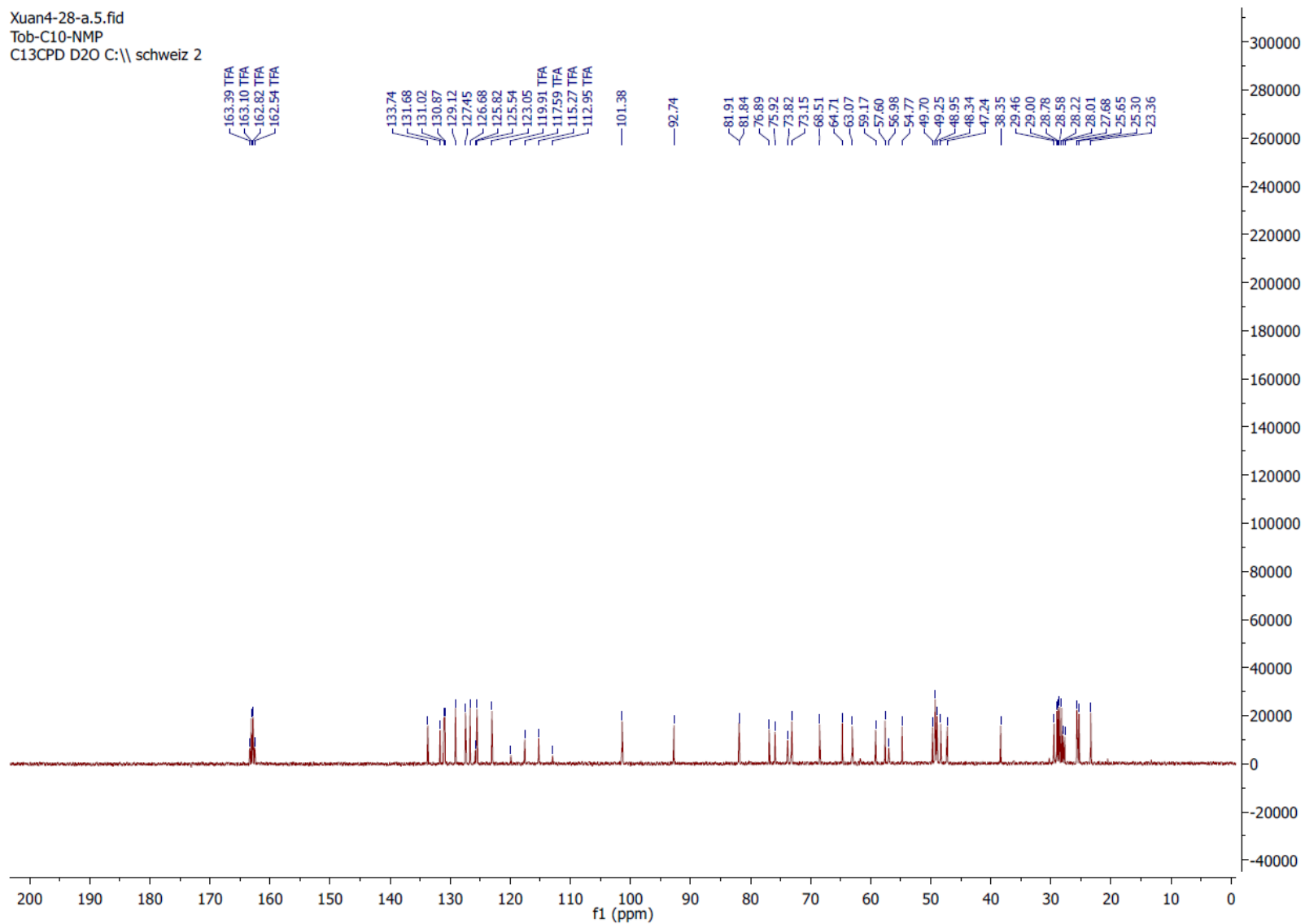


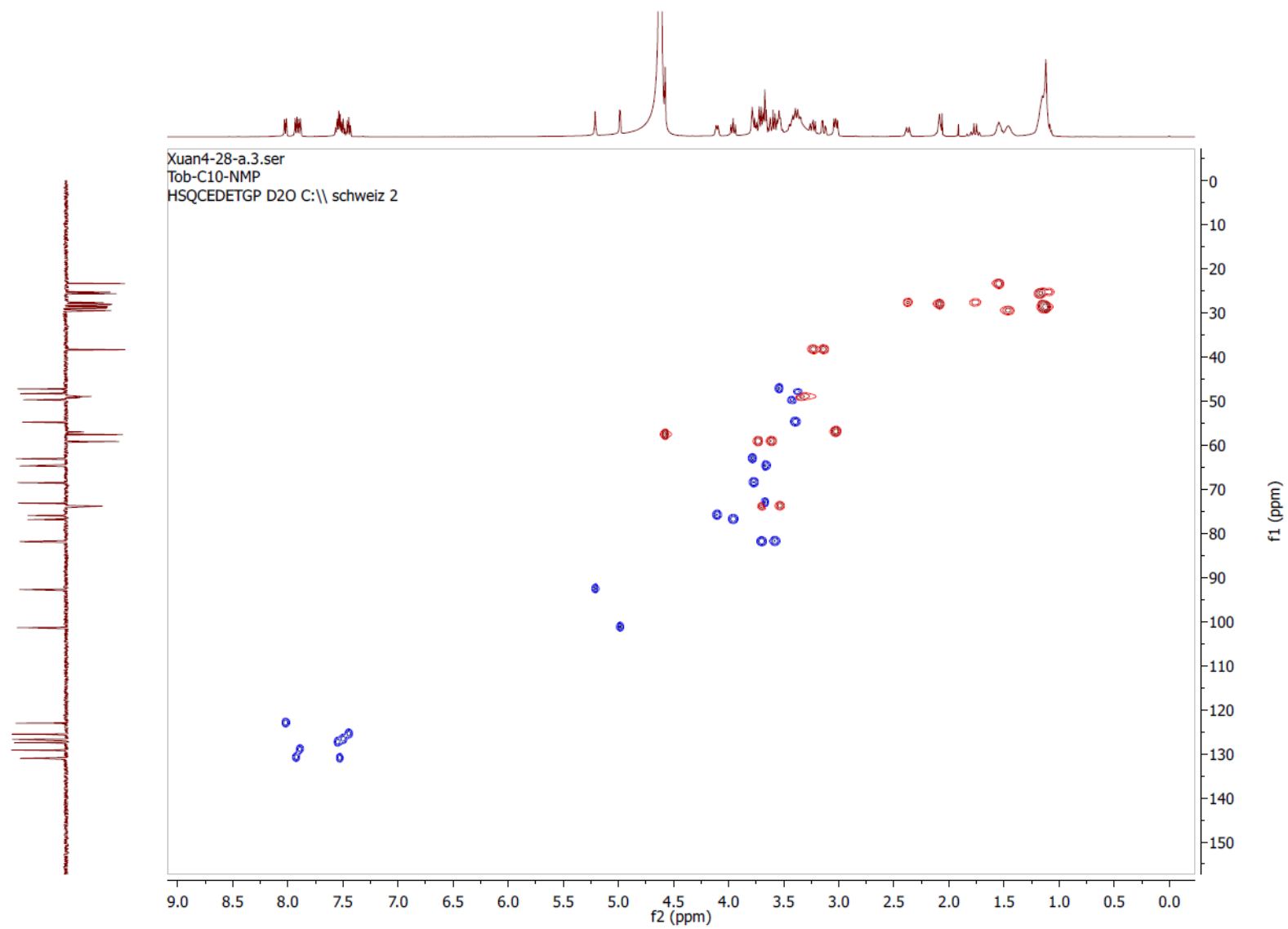
Appendix 3. HSQC spectrum of compound 1f in D<sub>2</sub>O

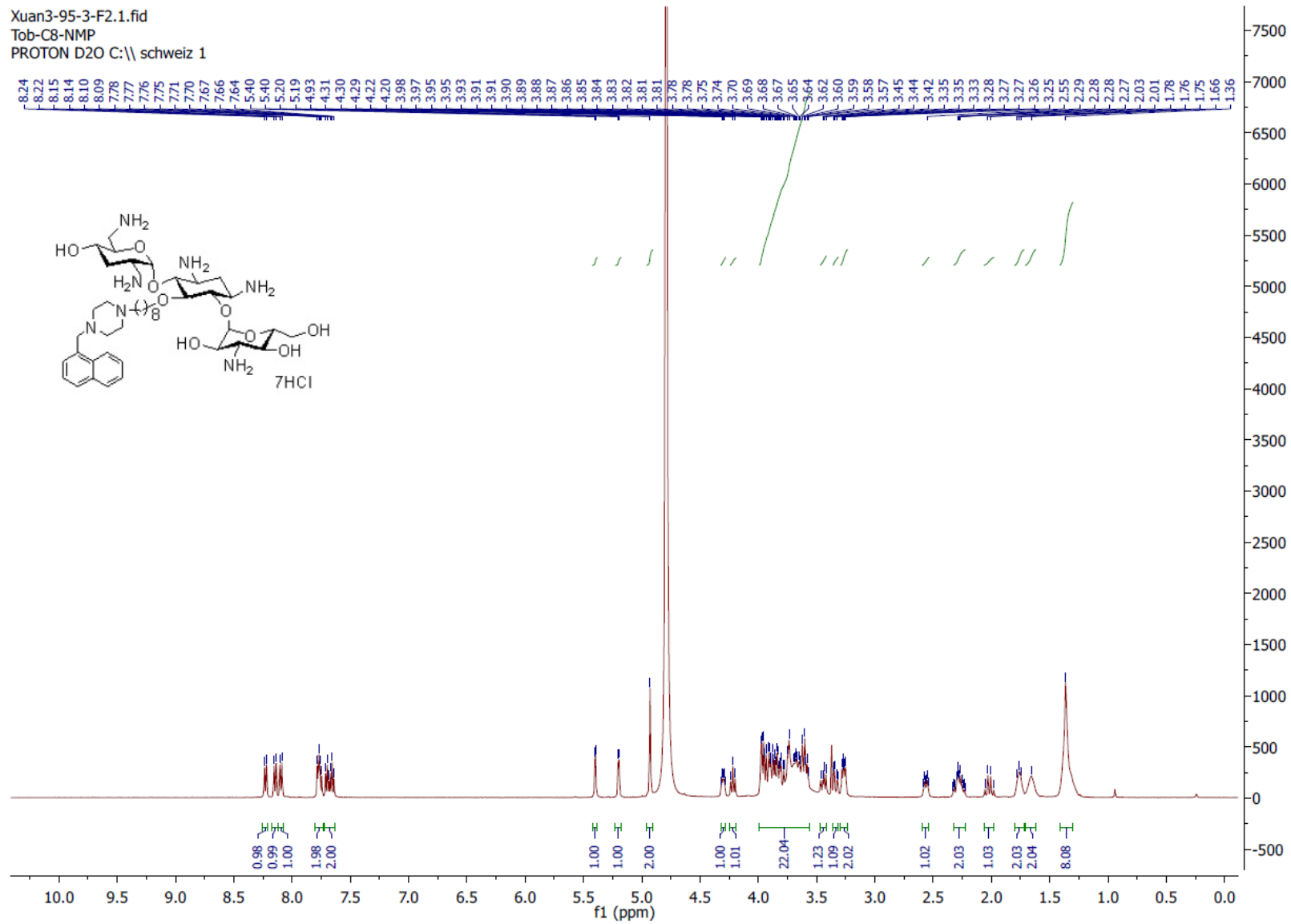
Appendix 4.  $^1\text{H}$  spectrum of compound 1e in  $\text{D}_2\text{O}$ 

Appendix 5.  $^{13}\text{C}$  spectrum of compound 1e in  $\text{D}_2\text{O}$ 

Xuan4-28-a.5.fid  
Tob-C10-NMP  
C13CPD D2O C:\\ schweiz 2

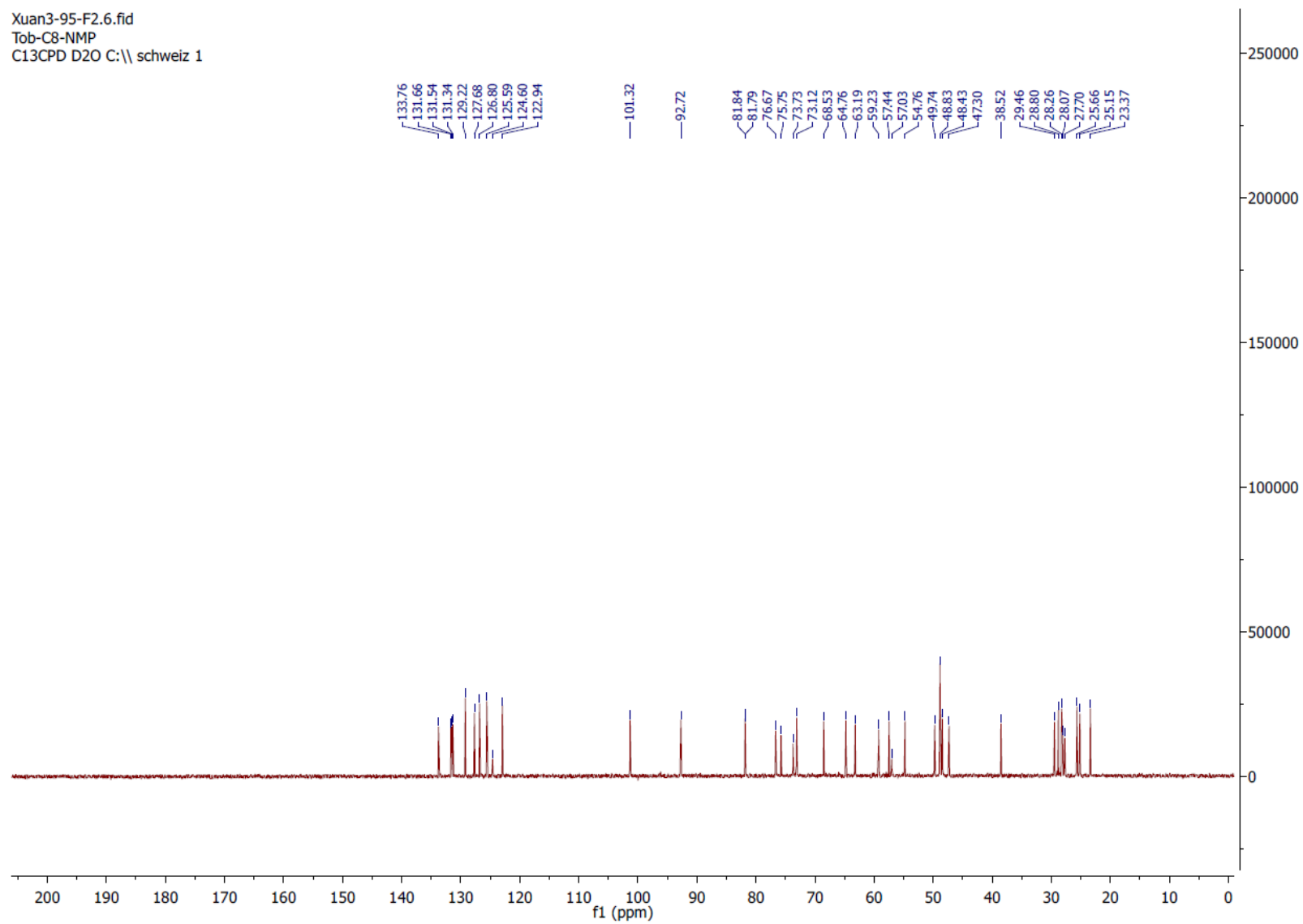


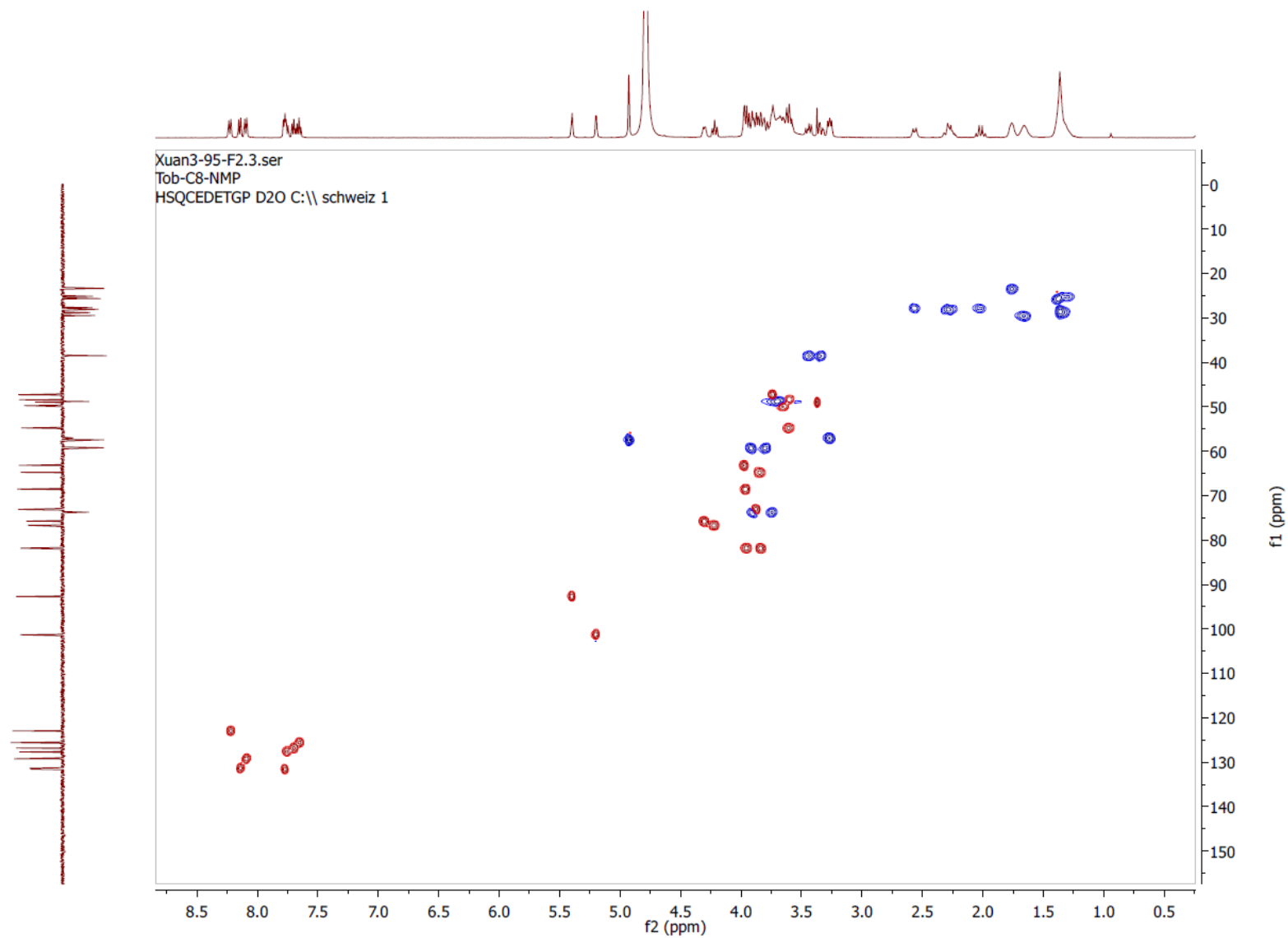
Appendix 6. HSQC spectrum of compound 1e in D<sub>2</sub>O

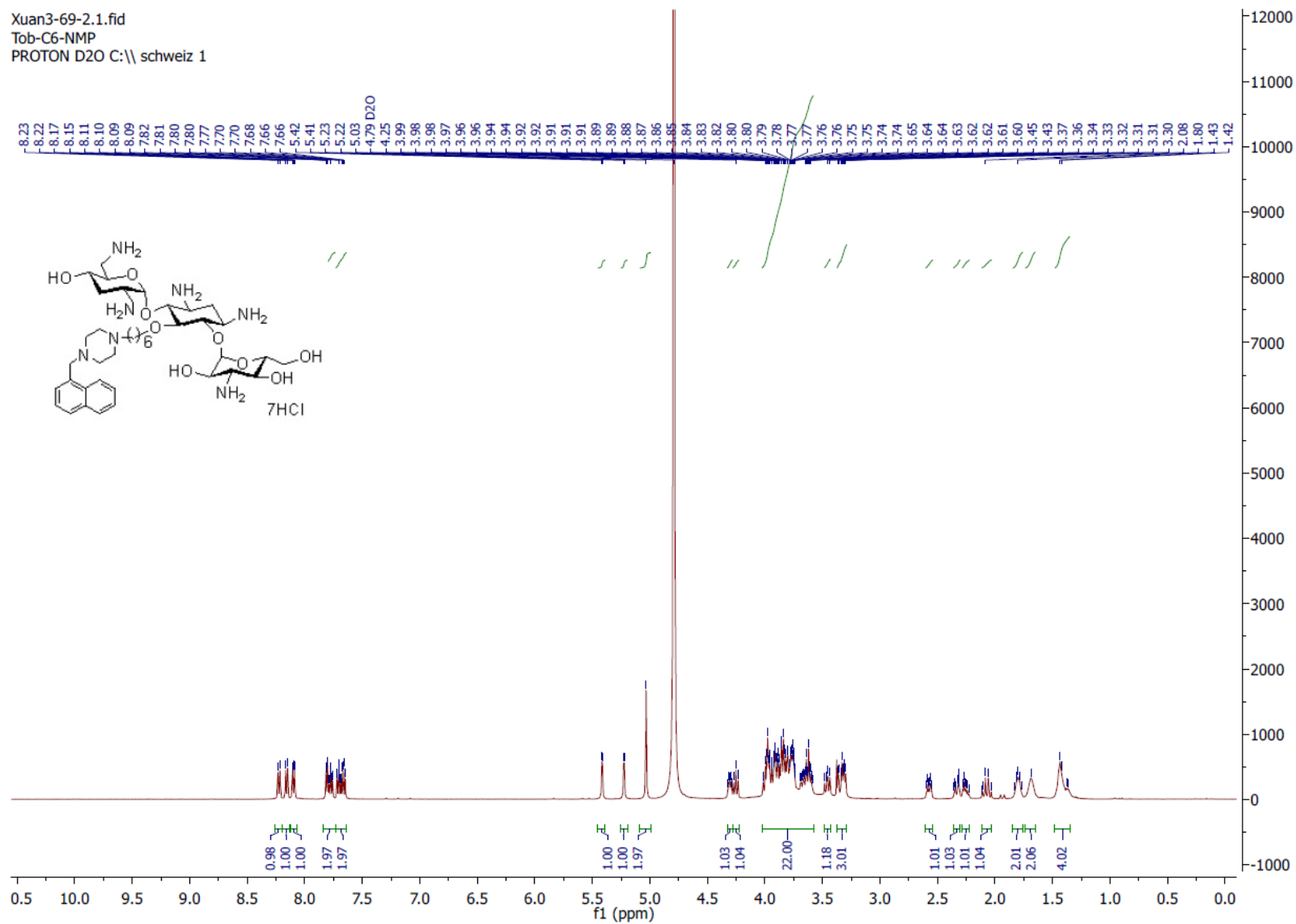
Appendix 7.  $^1\text{H}$  spectrum of compound 1d in  $\text{D}_2\text{O}$ 

Appendix 8.  $^{13}\text{C}$  spectrum of compound 1d in  $\text{D}_2\text{O}$ 

Xuan3-95-F2.6.fid  
Tob-C8-NMP  
C13CPD D2O C:\schweiz 1

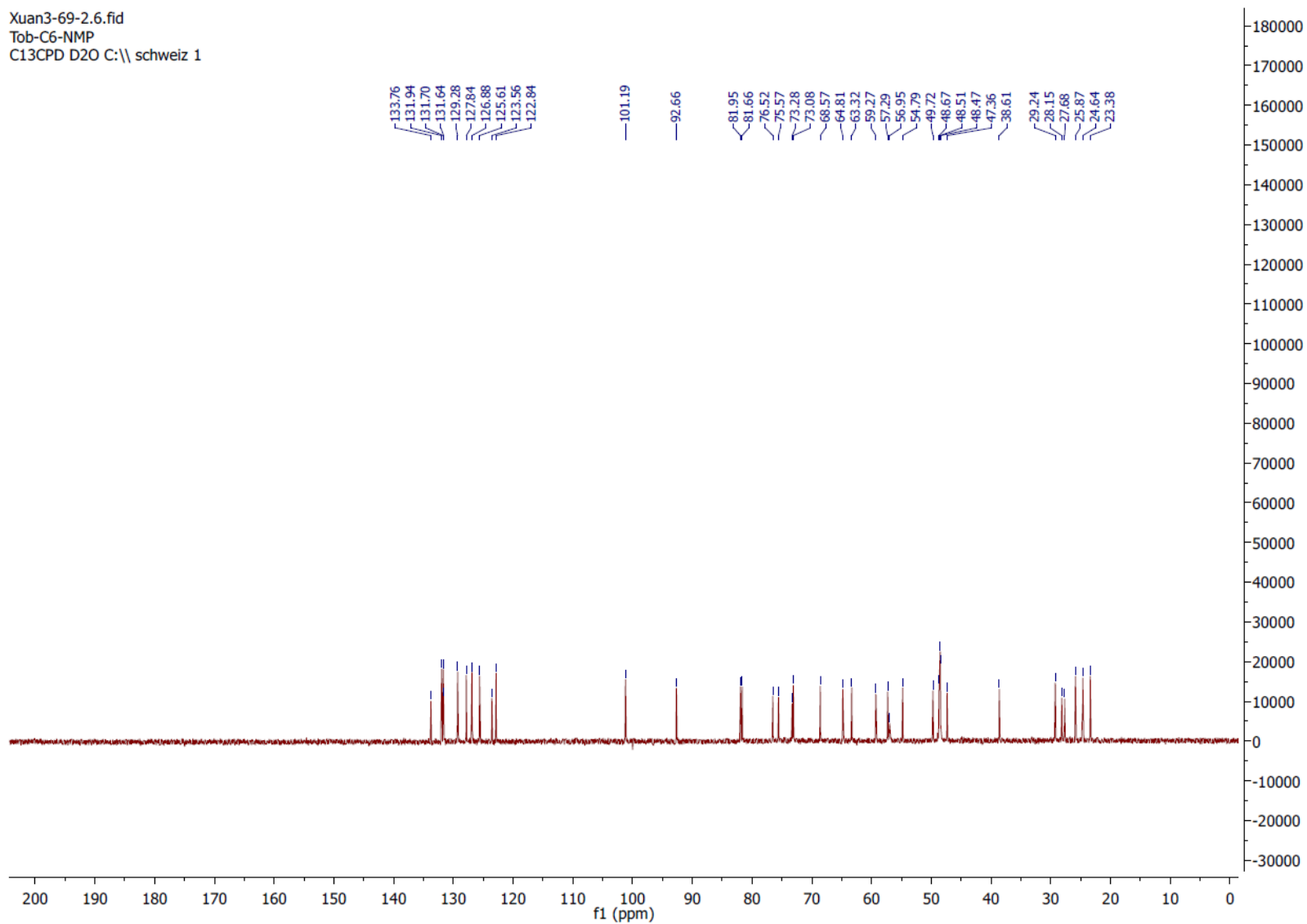


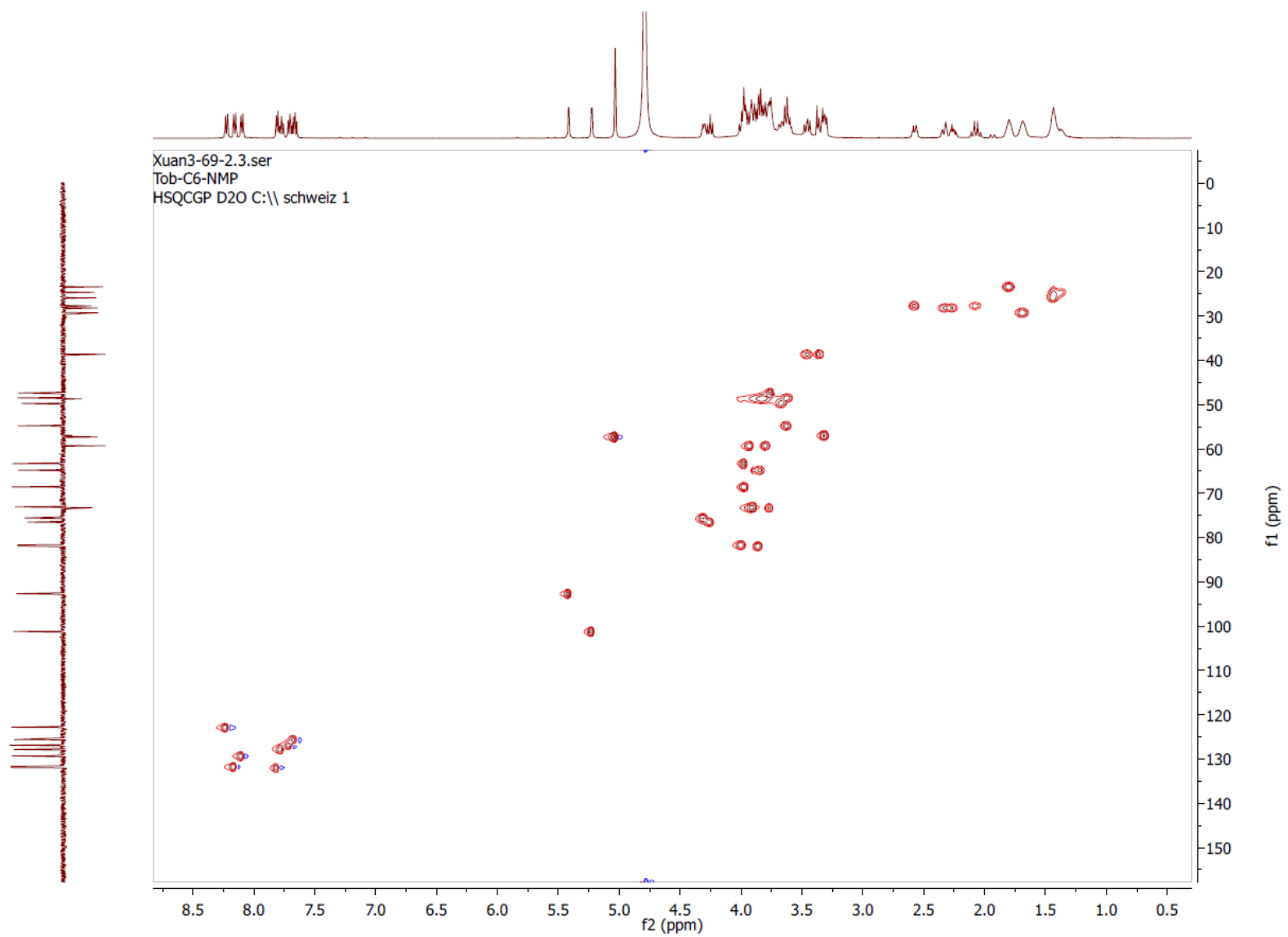
Appendix 9. HSQC spectrum of compound 1d in D<sub>2</sub>O

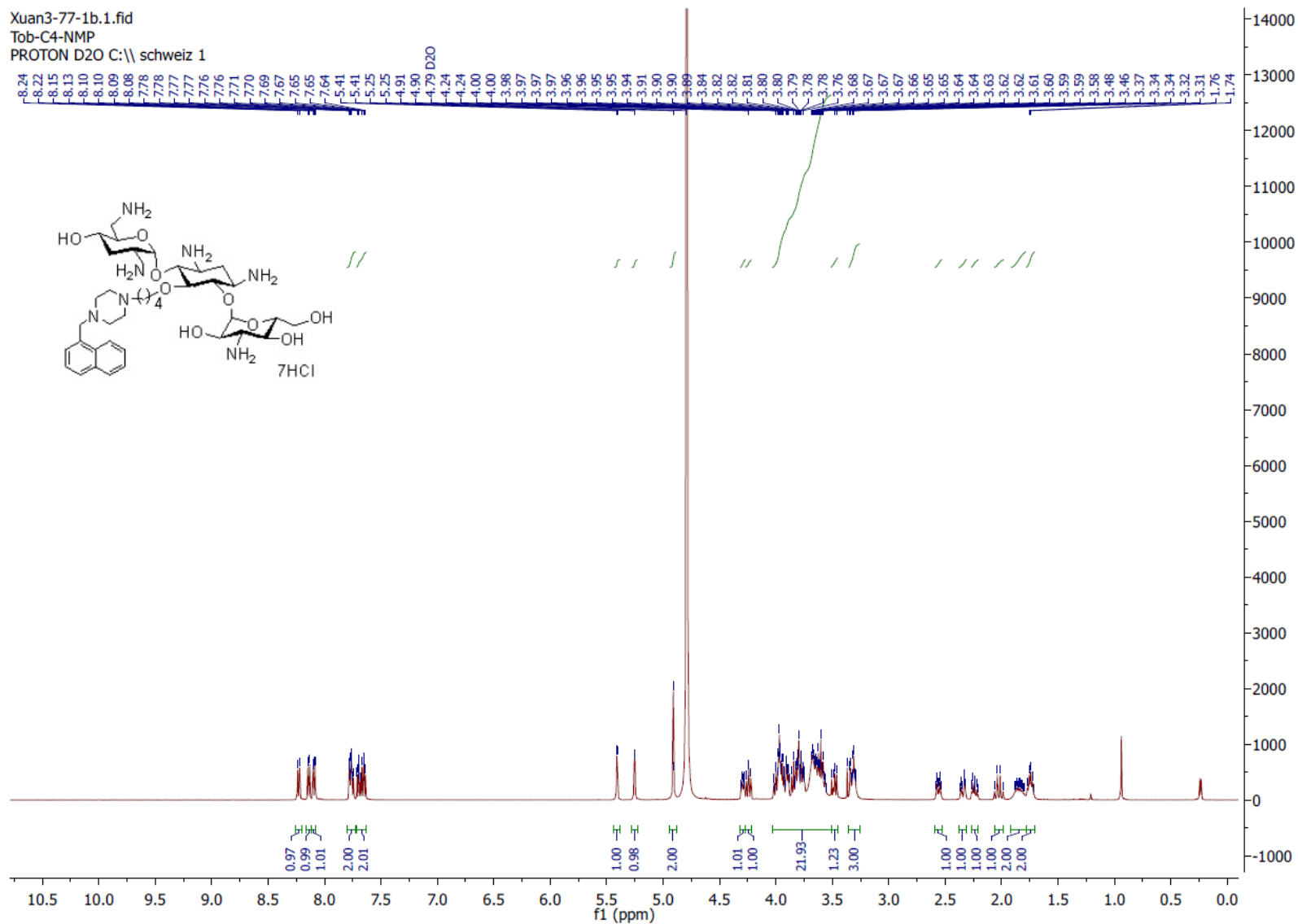
Appendix 10.  $^1\text{H}$  spectrum of compound 1c in  $\text{D}_2\text{O}$ 

Appendix 11.  $^{13}\text{C}$  spectrum of compound 1c in  $\text{D}_2\text{O}$ 

Xuan3-69-2.6.fid  
Tob-C6-NMP  
C13CPD D2O C:\\ schweiz 1

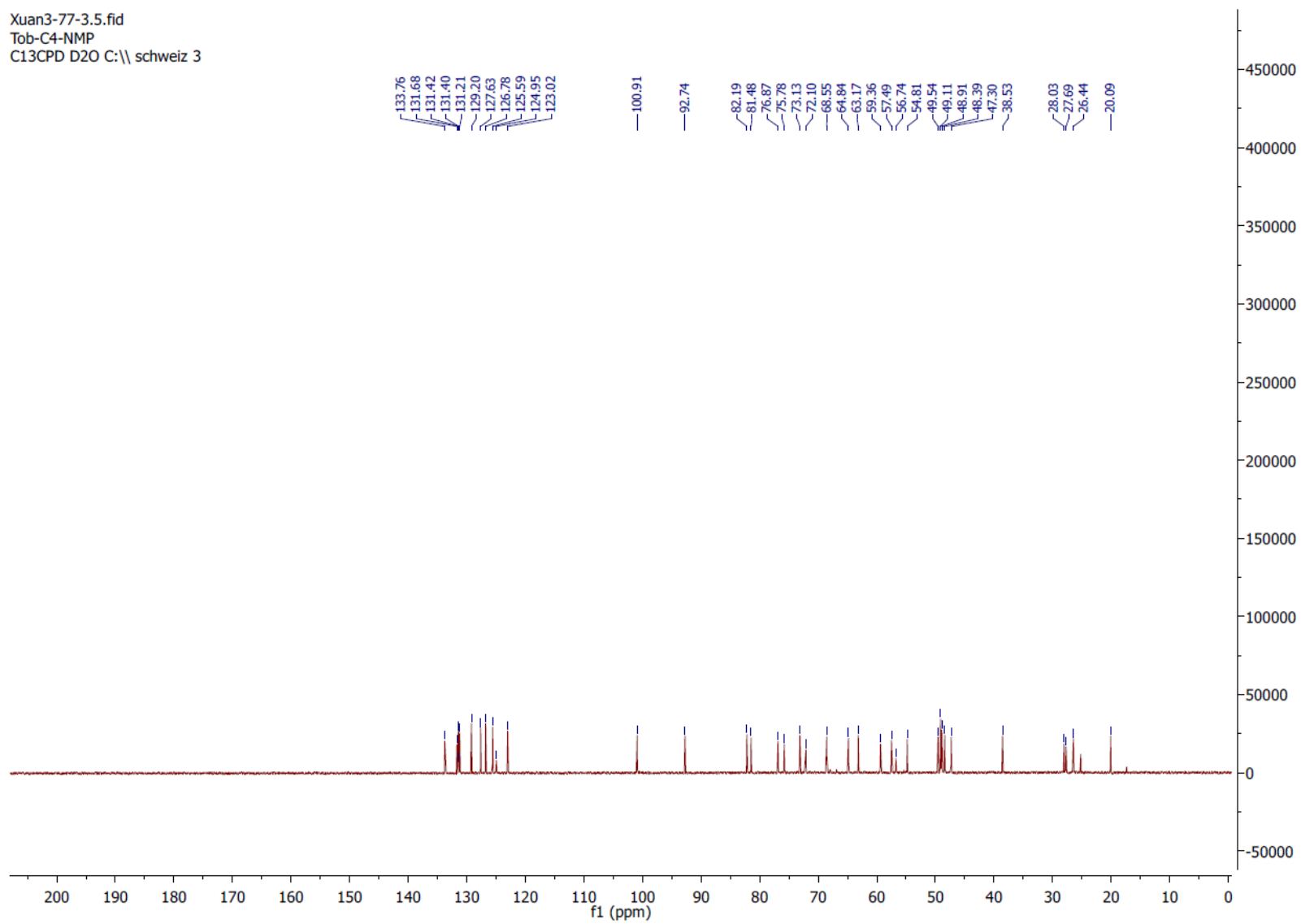


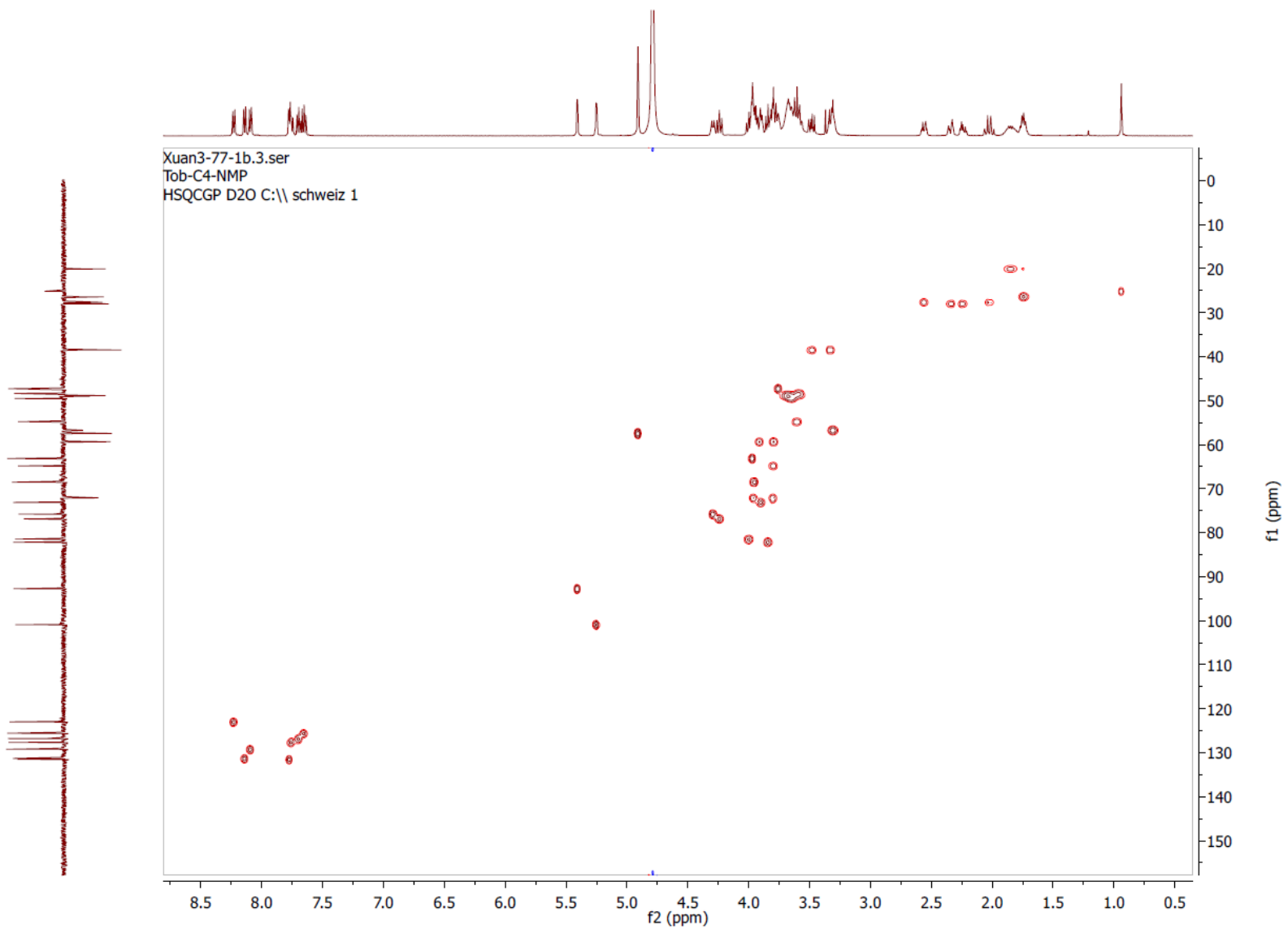
Appendix 12. HSQC spectrum of compound 1c in D<sub>2</sub>O

Appendix 13.  $^1\text{H}$  spectrum of compound 1b in  $\text{D}_2\text{O}$ 

Appendix 14.  $^{13}\text{C}$  spectrum of compound 1b in  $\text{D}_2\text{O}$ 

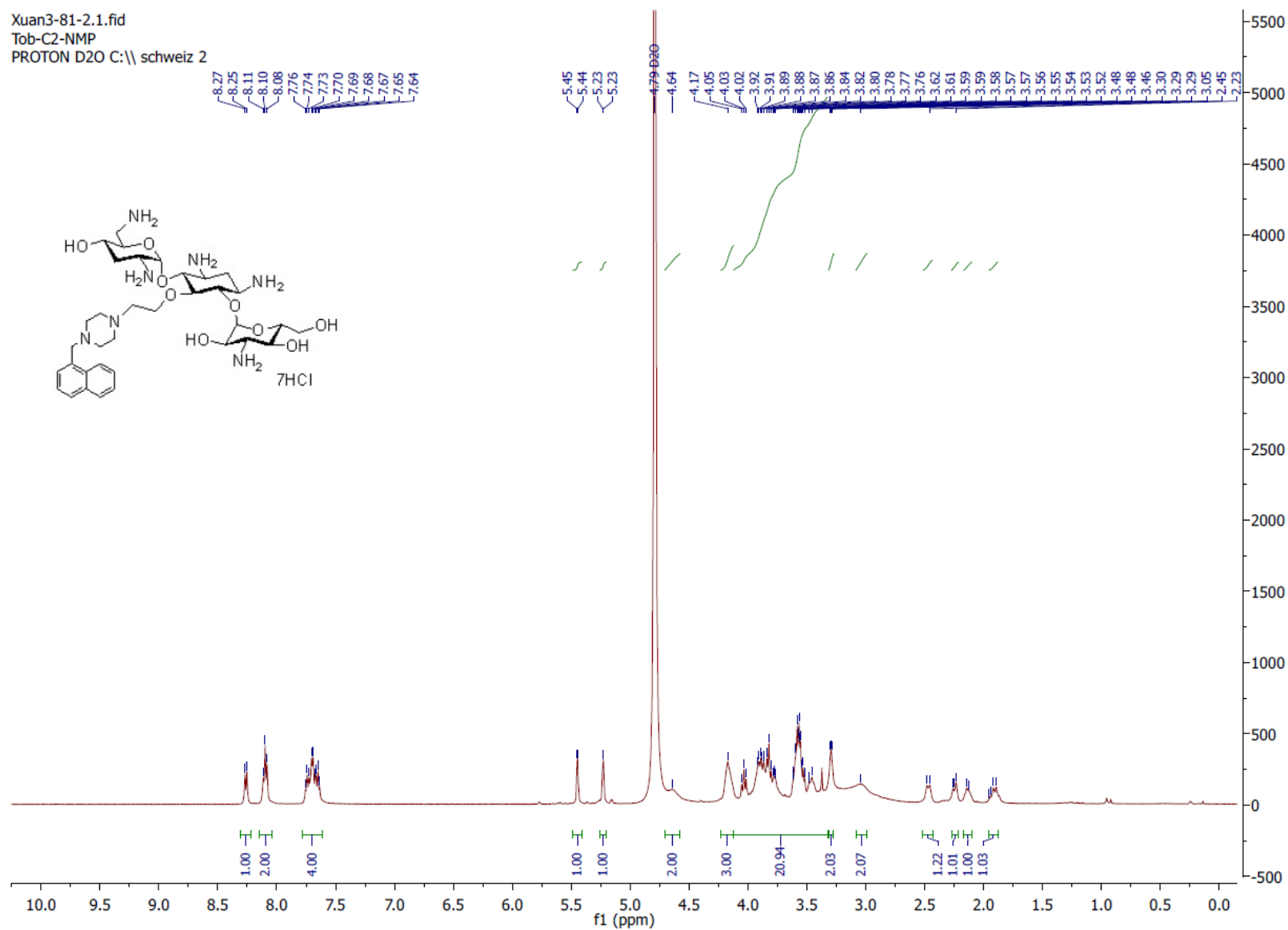
Xuan3-77-3.5.fid  
Tob-C4-NMP  
C13CPD D2O C:\\ schweiz 3



Appendix 15. HSQC spectrum of compound 1b in D<sub>2</sub>O

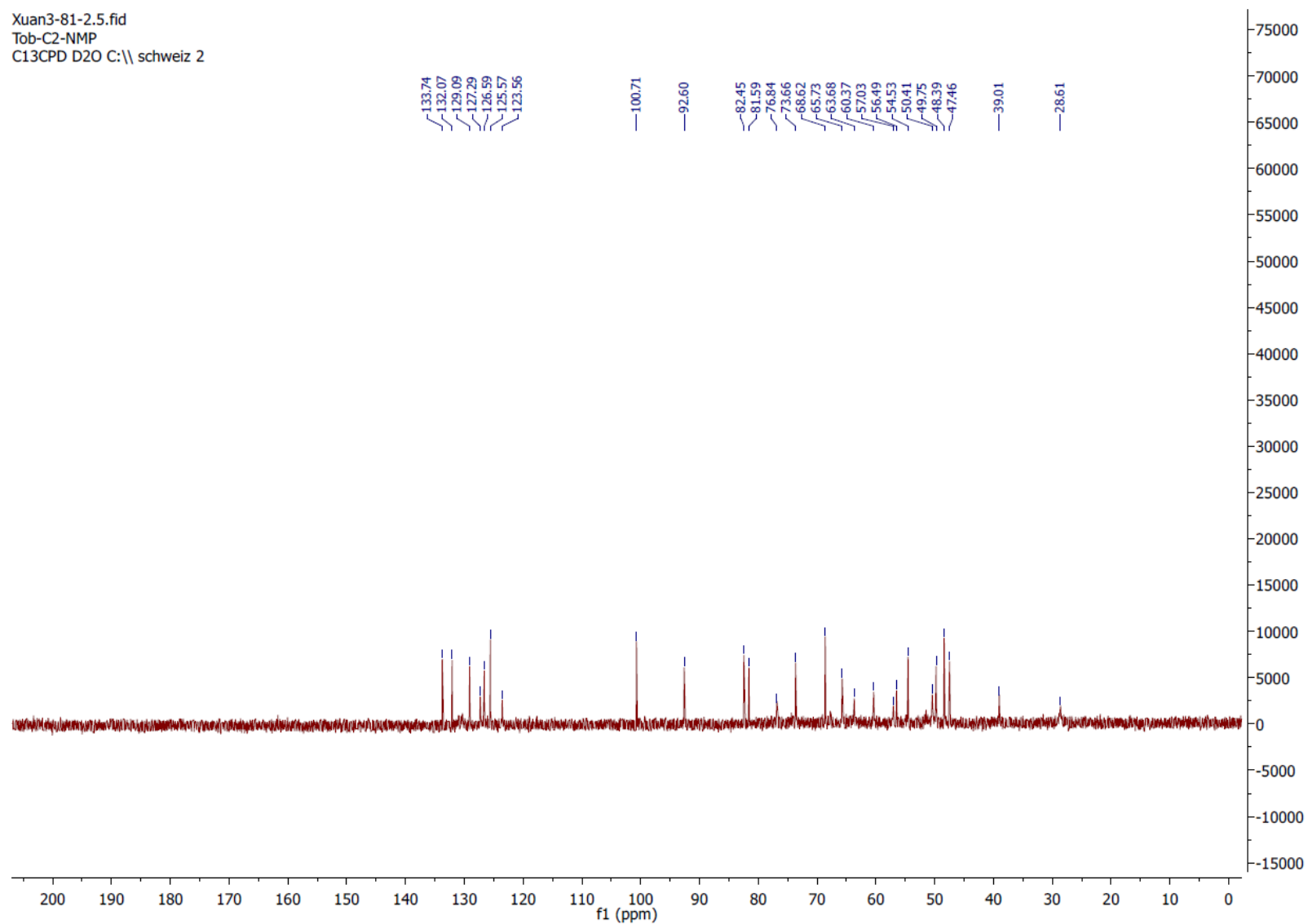
Appendix 16.  $^1\text{H}$  spectrum of compound 1a in  $\text{D}_2\text{O}$

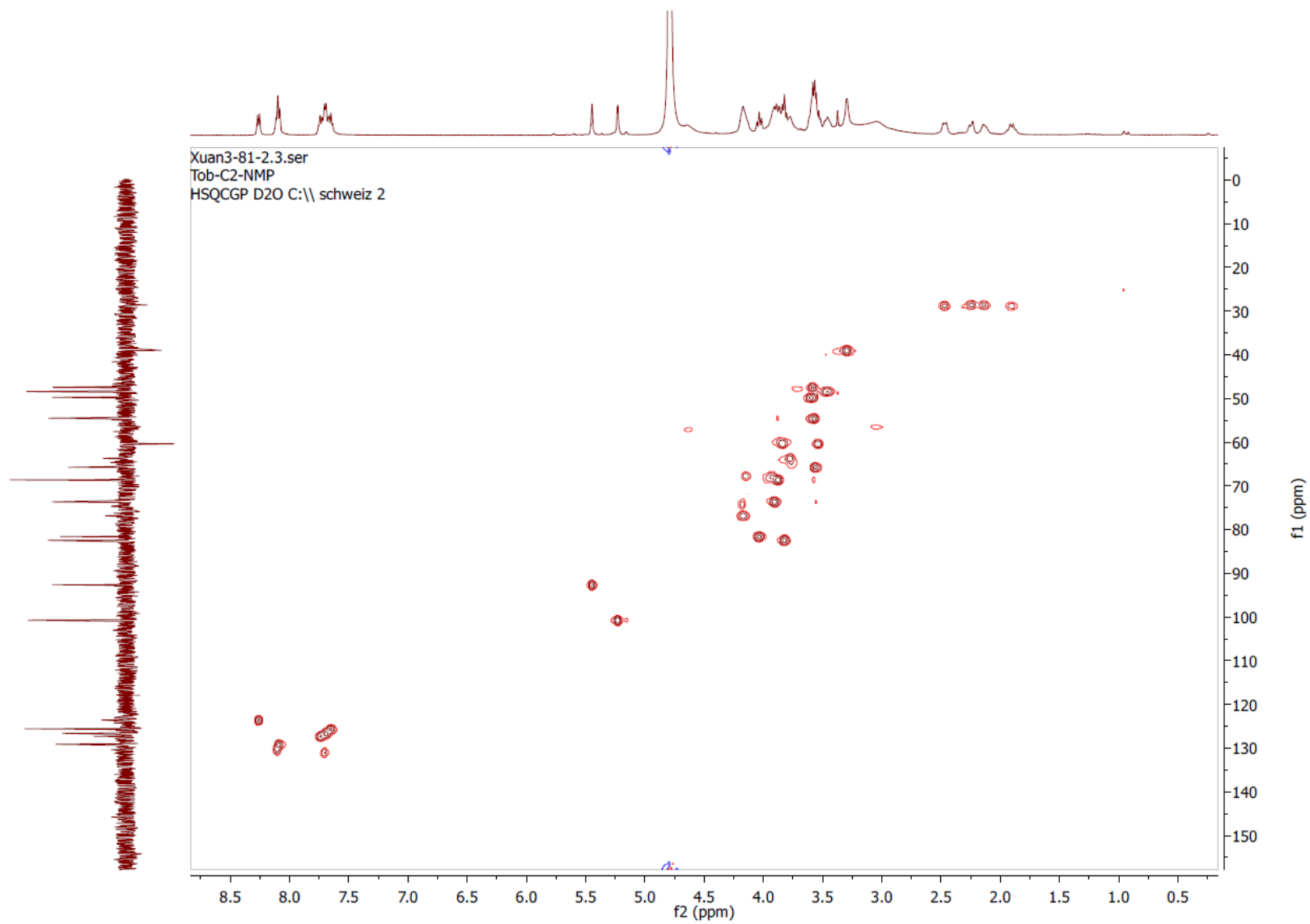
Xuan3-81-2.1.fid  
Tob-C2-NMP  
PROTON D2O C:\schweiz 2

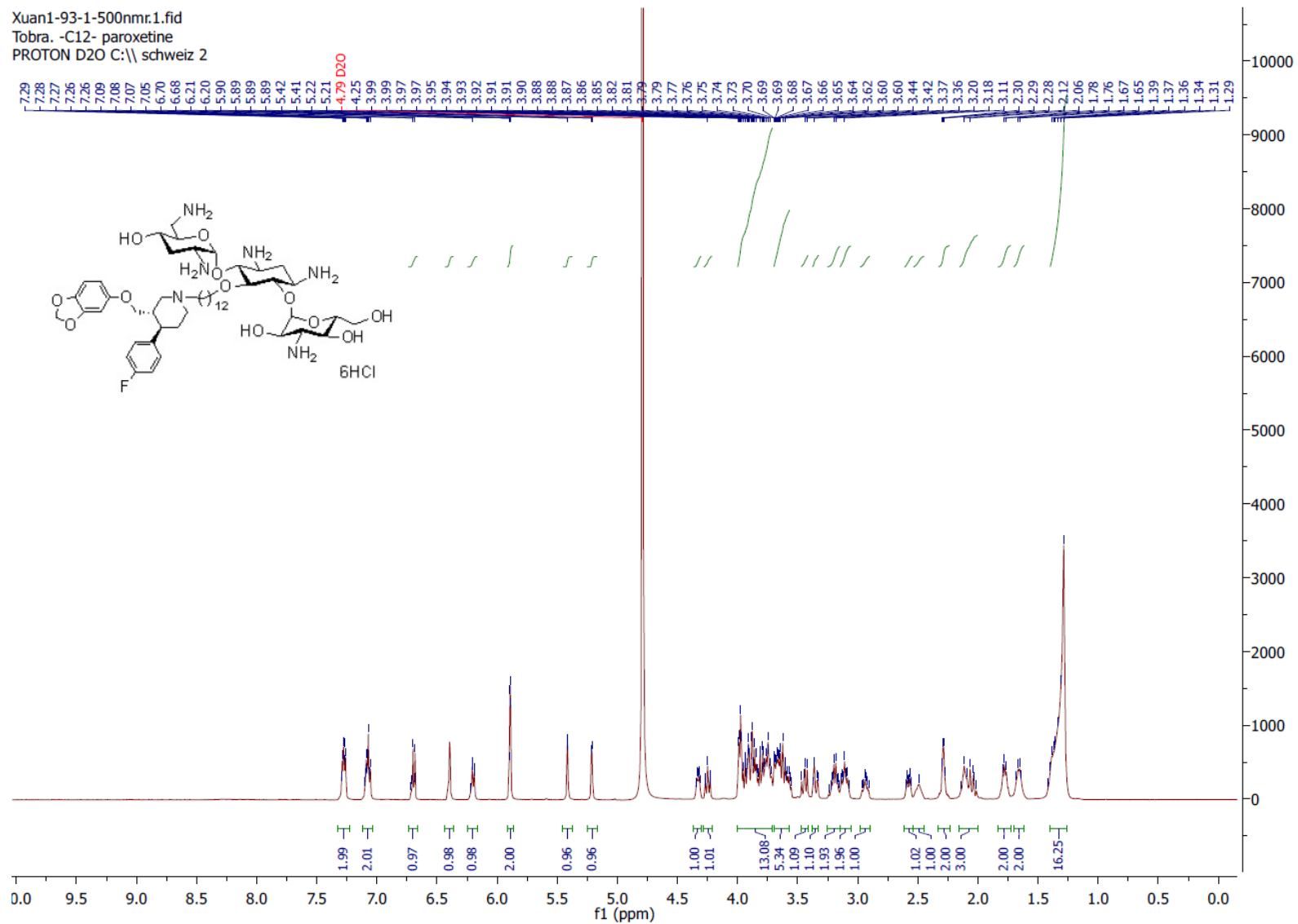


Appendix 17.  $^{13}\text{C}$  spectrum of compound 1a in  $\text{D}_2\text{O}$ 

Xuan3-81-2.5.fid  
Tob-C2-NMP  
C13CPD D2O C:\\ schweiz 2

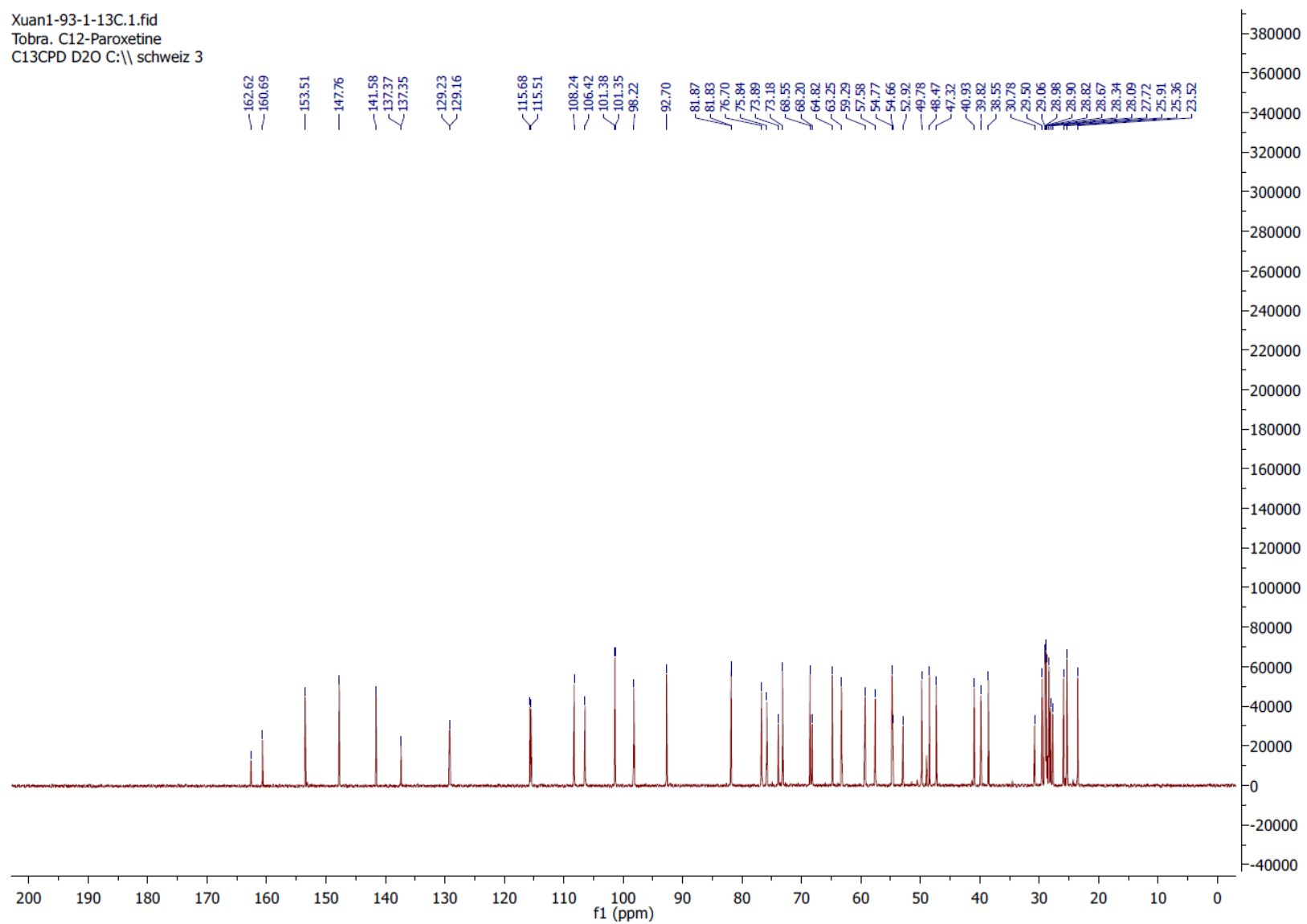


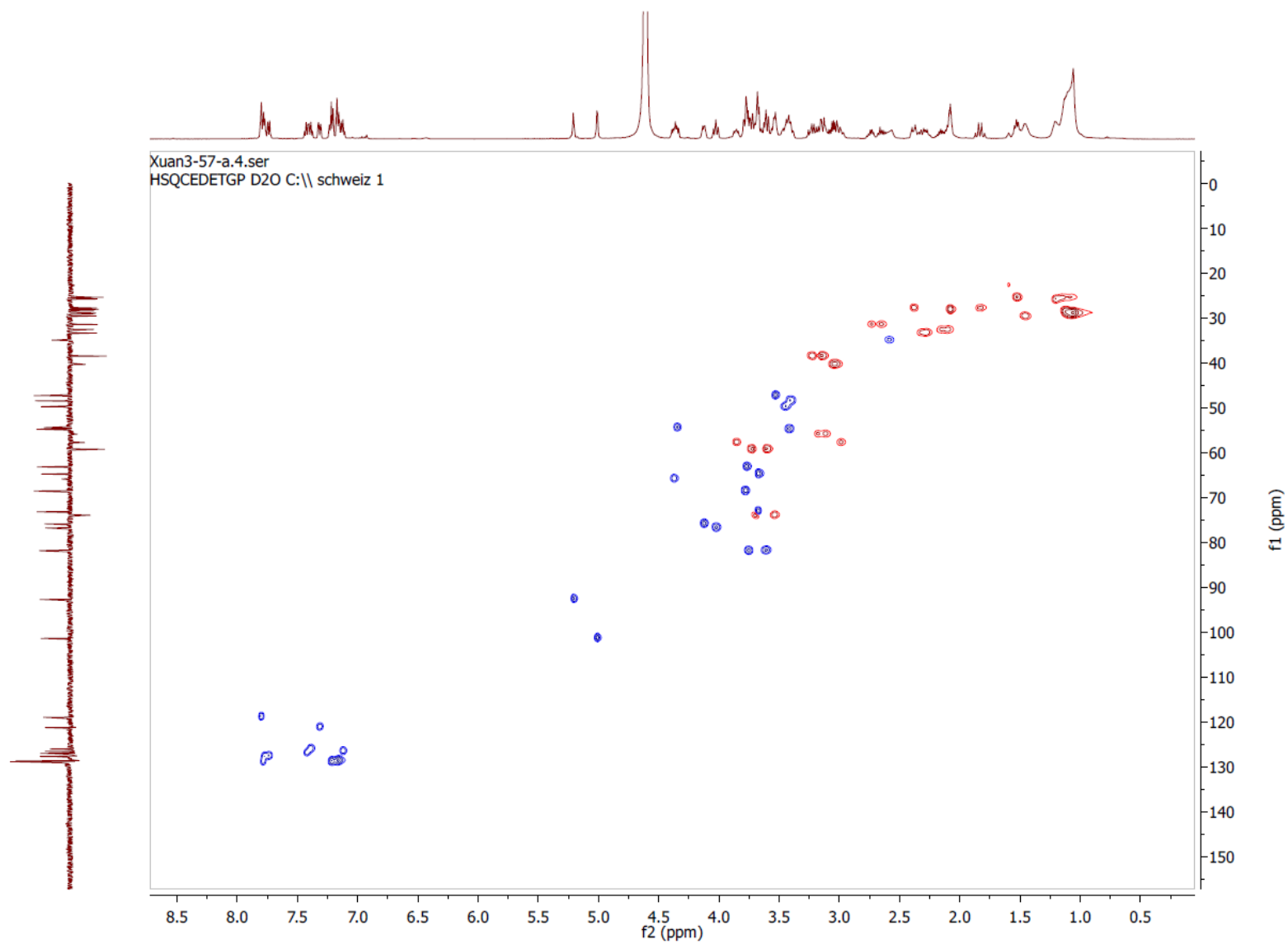
Appendix 18. HSQC spectrum of compound 1a in D<sub>2</sub>O

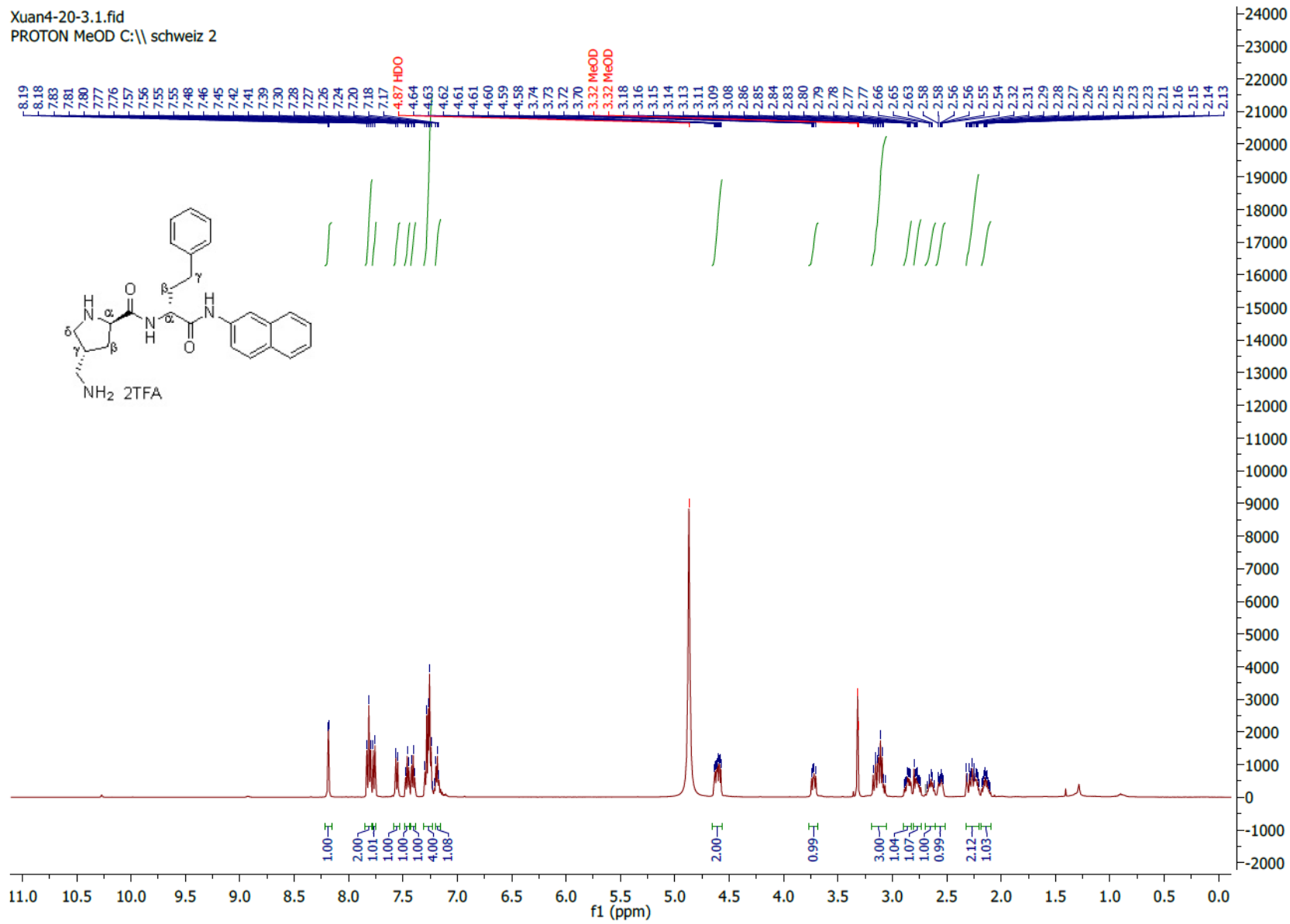
Appendix 19.  $^1\text{H}$  spectrum of compound 2 in  $\text{D}_2\text{O}$ 

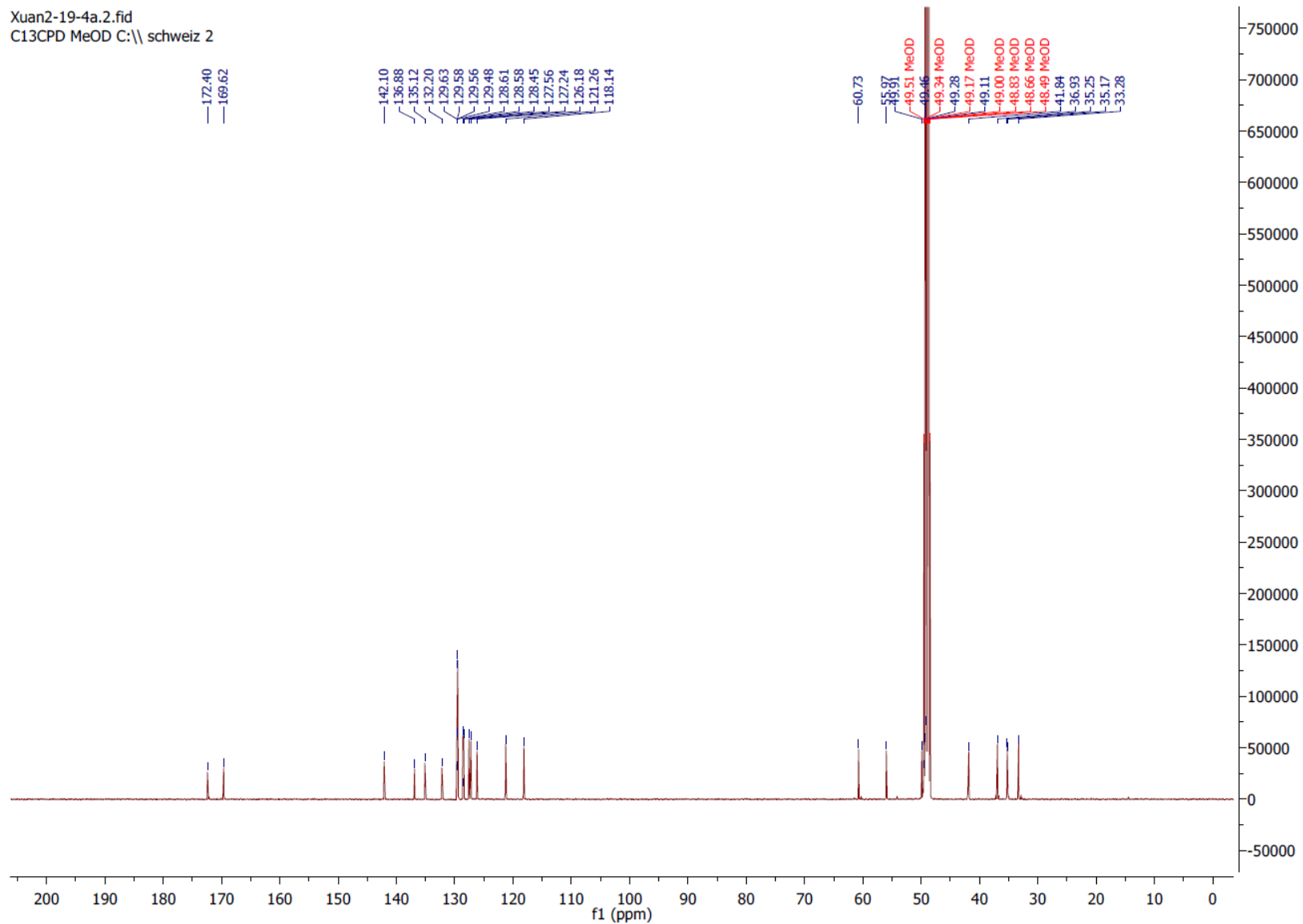
Appendix 20.  $^{13}\text{C}$  spectrum of compound 2 in  $\text{D}_2\text{O}$ 

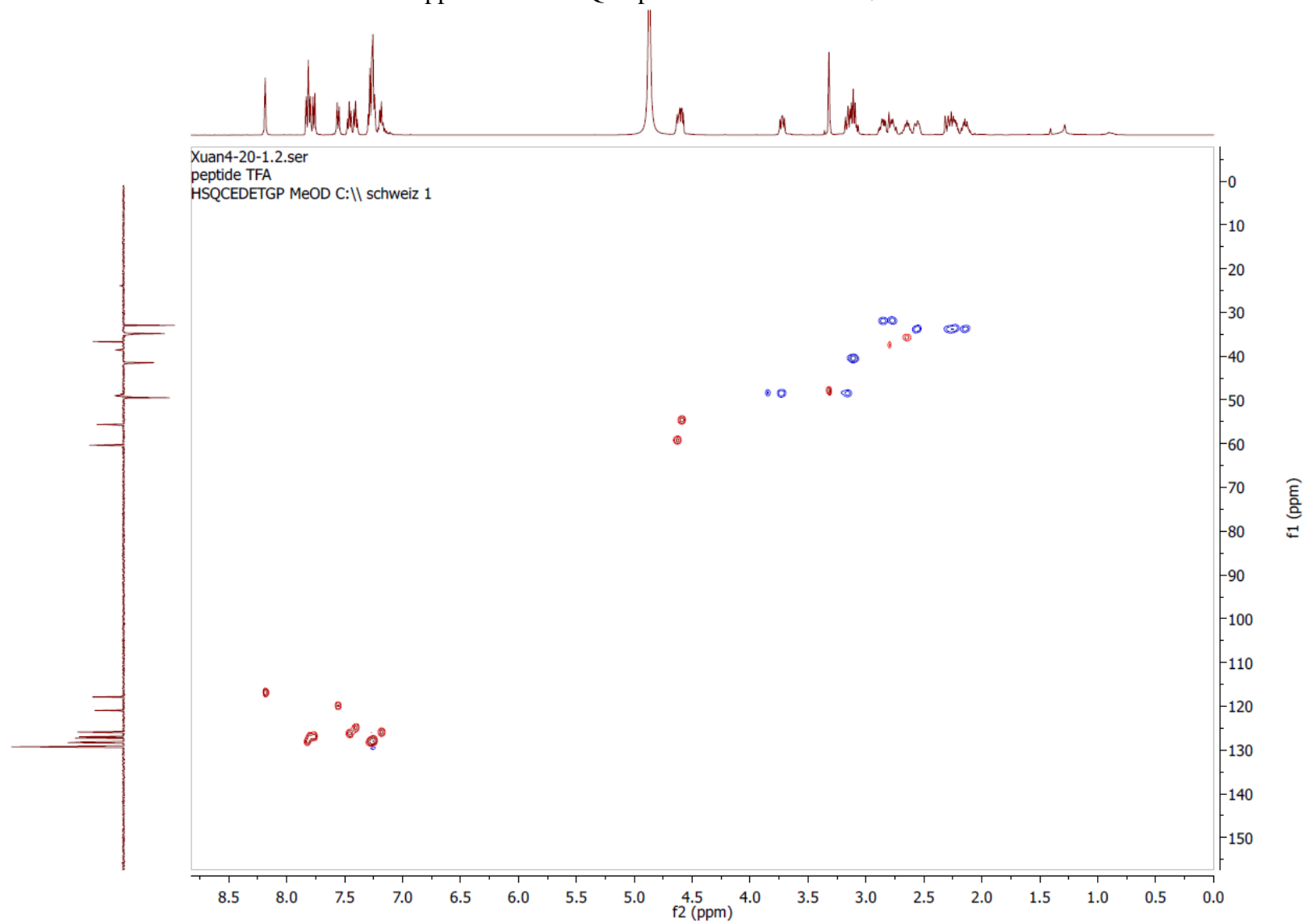
Xuan1-93-1-13C.1.fid  
Tobra. C12-Paroxetine  
C13CPD D2O C:\schweiz 3

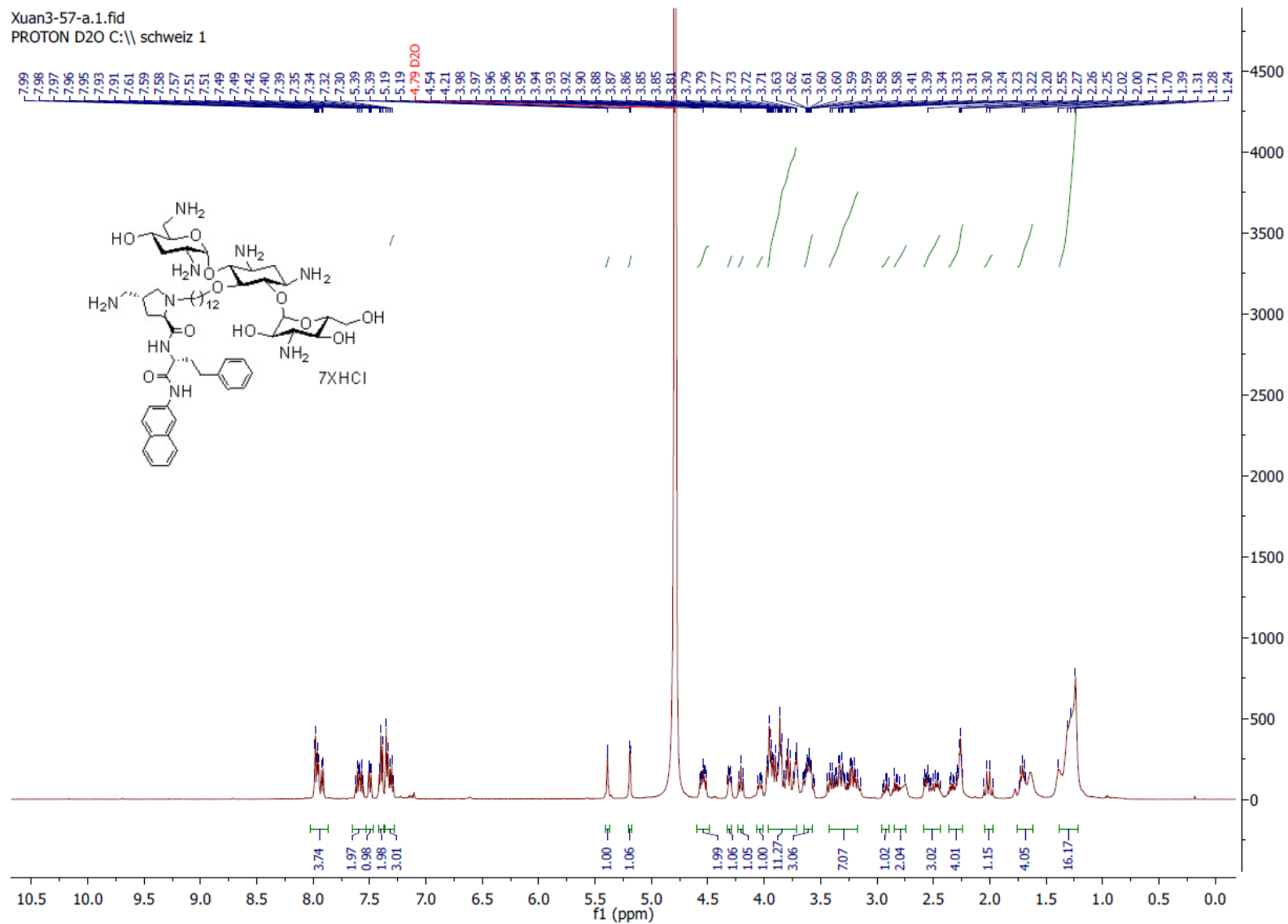


Appendix 21. HSQC spectrum of compound 2 in D<sub>2</sub>O

Appendix 22.  $^1\text{H}$  spectrum of DBP in  $\text{CD}_3\text{OD}$ 

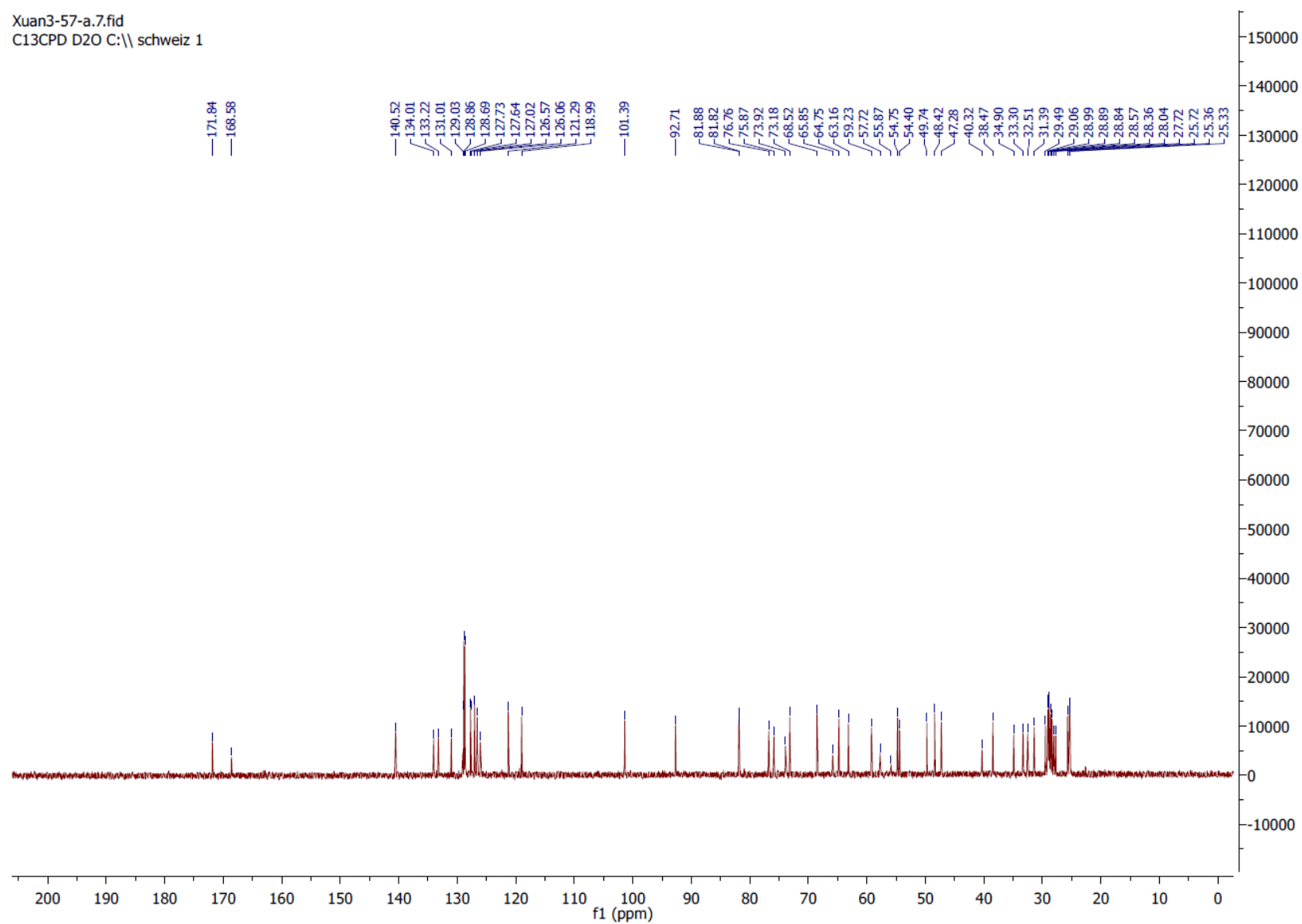
Appendix 23.  $^{13}\text{C}$  spectrum of DBP in  $\text{CD}_3\text{OD}$ 

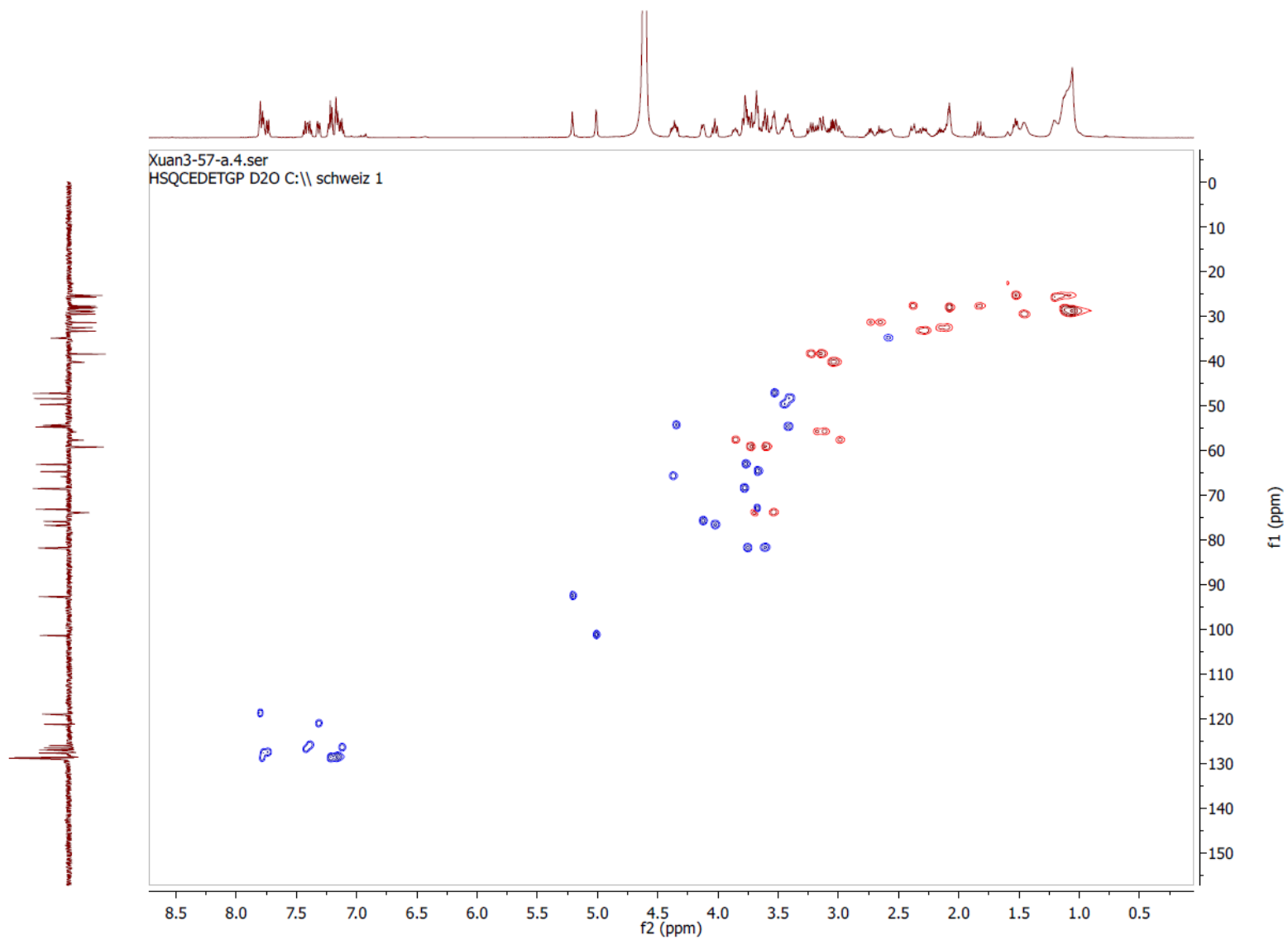
Appendix 24. HSQC spectrum of DBP in CD<sub>3</sub>OD

Appendix 25.  $^1\text{H}$  spectrum of compound 3 in  $\text{D}_2\text{O}$ 

Appendix 26.  $^{13}\text{C}$  spectrum of compound 3 in  $\text{D}_2\text{O}$ 

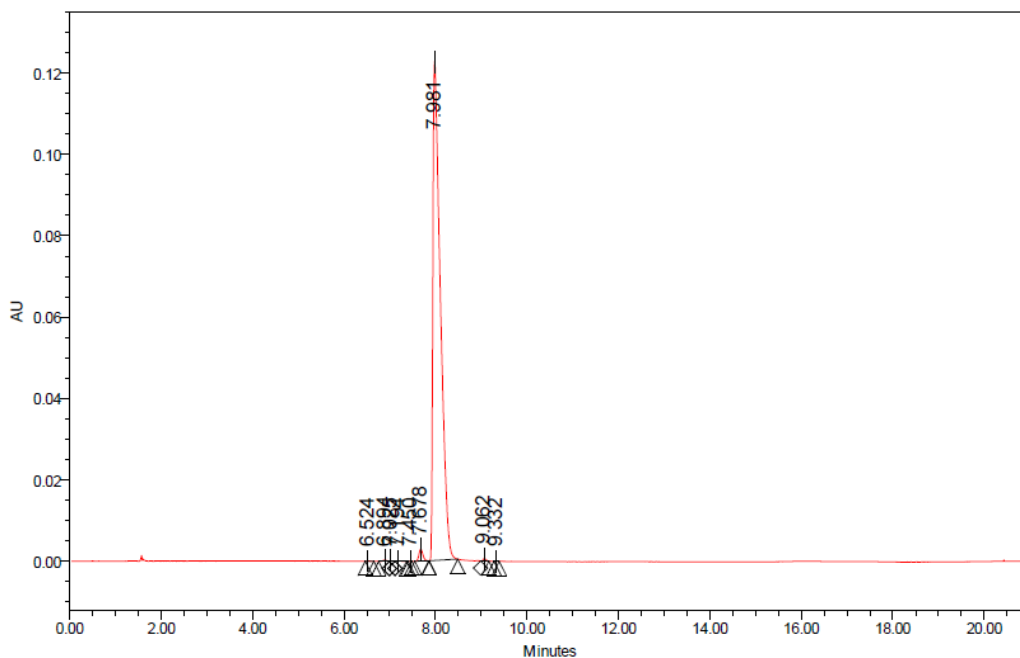
Xuan3-57-a.7.fid  
C13CPD D2O C:\\ schweiz 1



Appendix 27. HSQC spectrum of compound 3 in D<sub>2</sub>O

## 9.8 HPLC SPECTRA

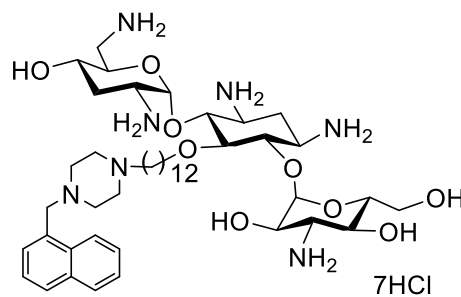
## Appendix 28. HPLC data of compound 1f



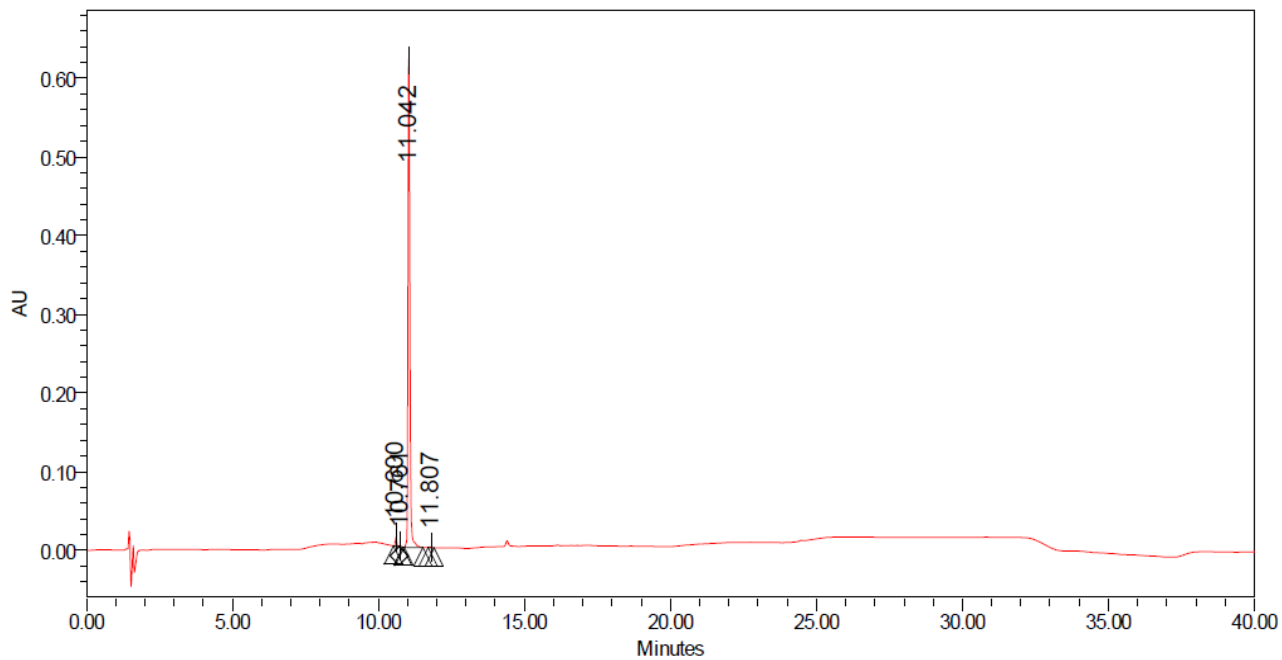
— Sample Name: Xuan1-89-1\_; Date Acquired: 09/06/2015 3:47:43 PM CDT

## Processed Channel: PDA 283.0 nm

	Processed Channel	Retention Time (min)	Area	% Area	Height
1	PDA 283.0 nm	6.524	336	0.02	72
2	PDA 283.0 nm	6.894	1890	0.13	320
3	PDA 283.0 nm	7.025	683	0.05	123
4	PDA 283.0 nm	7.194	762	0.05	107
5	PDA 283.0 nm	7.450	62	0.00	26
6	PDA 283.0 nm	7.678	17354	1.23	2925
7	PDA 283.0 nm	7.981	1389806	98.30	122666
8	PDA 283.0 nm	9.062	2749	0.19	610
9	PDA 283.0 nm	9.332	212	0.02	57



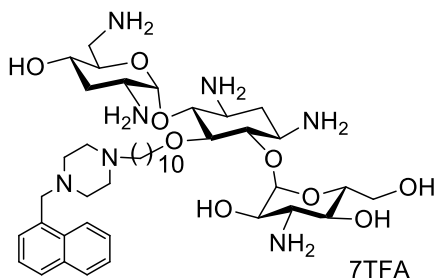
## Appendix 29. HPLC data of compound 1e



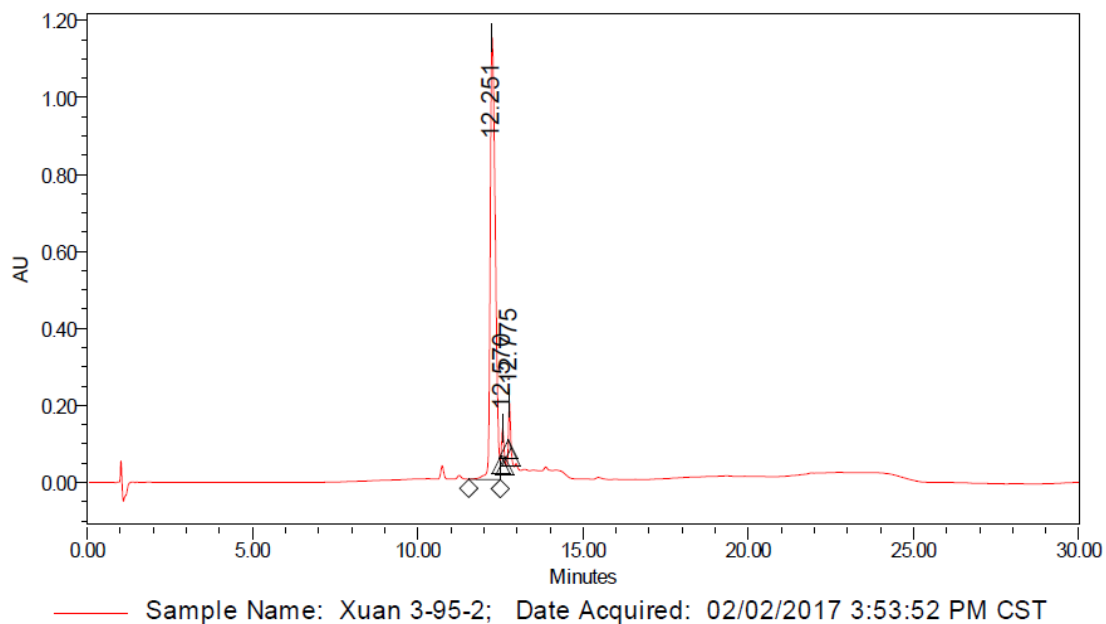
— Sample Name: Xuan 4-28-1; Date Acquired: 09/07/2015 7:10:57 PM CDT

**Processed Channel: PDA 223.0 nm**

	Processed Channel	Retention Time (min)	Area	% Area	Height
1	PDA 223.0 nm	10.600	39409	1.42	11276
2	PDA 223.0 nm	10.761	3129	0.11	881
3	PDA 223.0 nm	11.042	2724501	98.29	620175
4	PDA 223.0 nm	11.807	4875	0.18	852

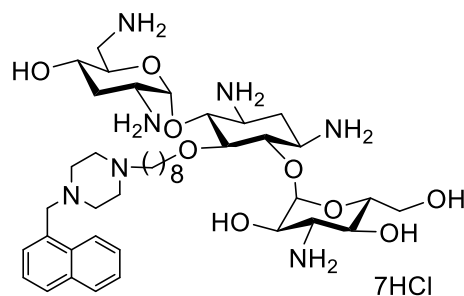


## Appendix 30. HPLC data of compound 1d

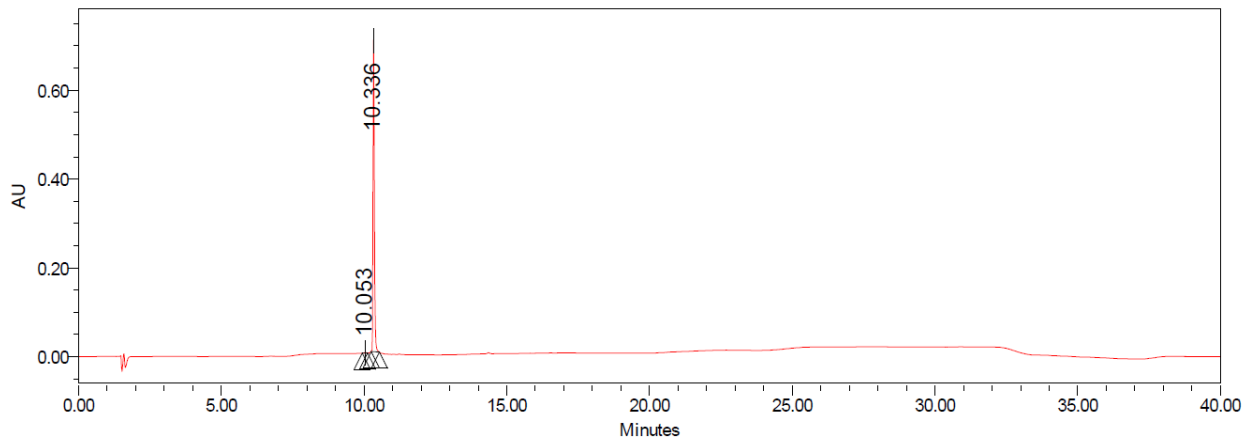


**Processed Channel: 2998 Ch1**  
**223nm@1.2nm**

	Processed Channel	Retention Time (min)	Area	% Area	Height
1	2998 Ch1 223nm@1.2nm	12.251	12344483	95.40	1147759
2	2998 Ch1 223nm@1.2nm	12.570	279629	2.16	72250
3	2998 Ch1 223nm@1.2nm	12.775	315897	2.44	104709

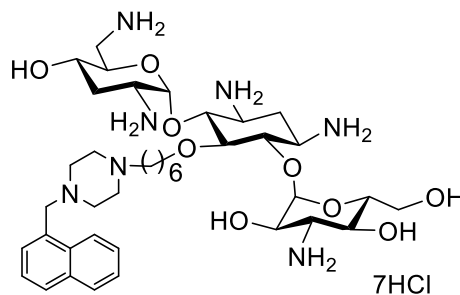


## Appendix 31. HPLC data of compound 1c

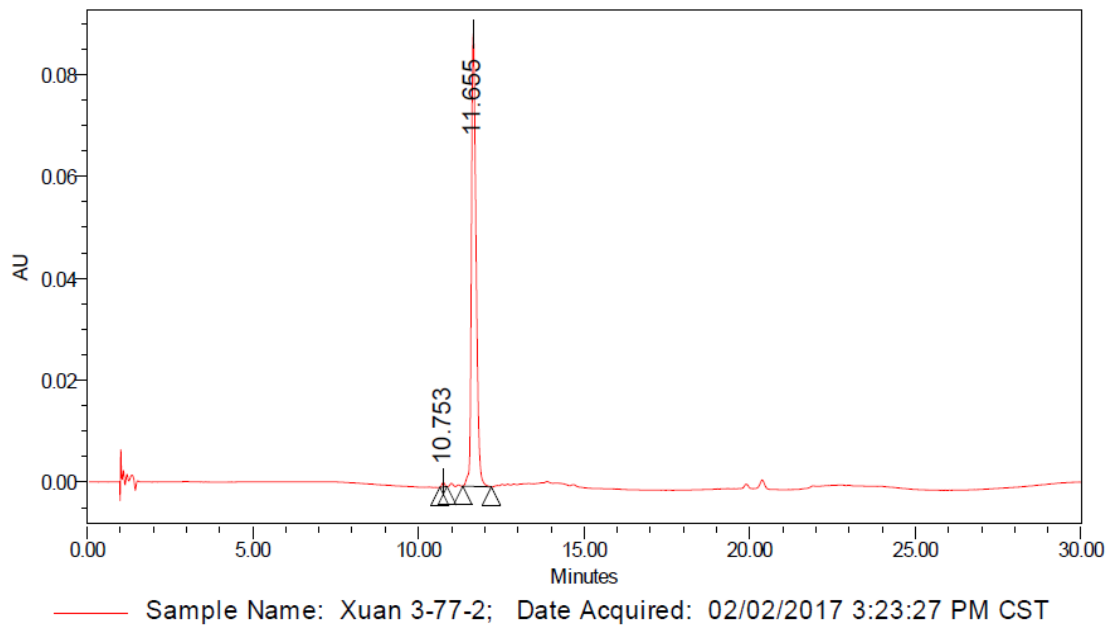


## Processed Channel: PDA 223.0 nm

Processed Channel	Retention Time (min)	Area	% Area	Height	
1	PDA 223.0 nm	10.053	5689	0.25	1031
2	PDA 223.0 nm	10.336	2240369	99.75	702405

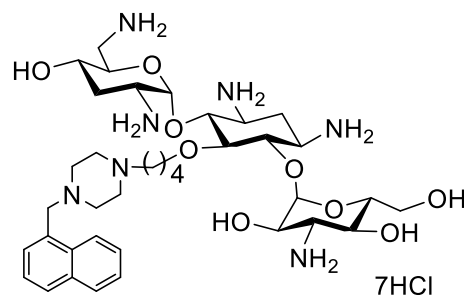


## Appendix 32. HPLC data of compound 1b

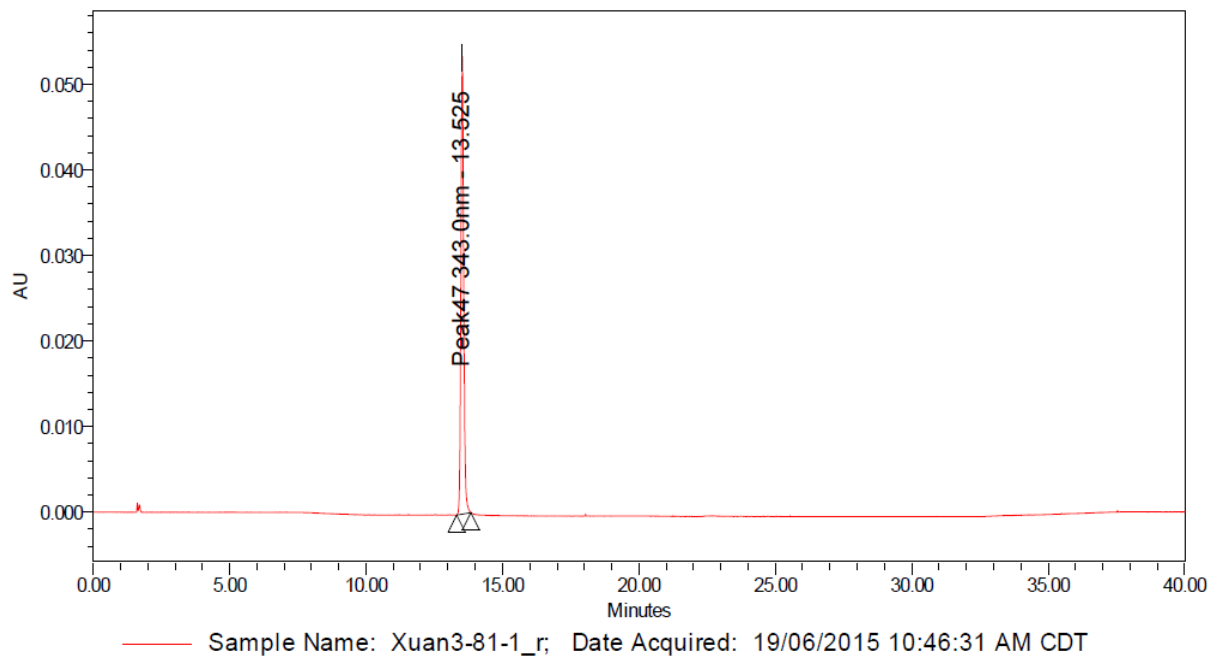


## Processed Channel: PDA 283.0 nm

	Processed Channel	Retention Time (min)	Area	% Area	Height
1	PDA 283.0 nm	10.753	5136	0.59	900
2	PDA 283.0 nm	11.655	866520	99.41	88771

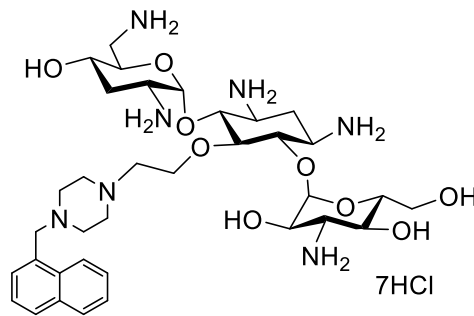


## Appendix 33. HPLC data of compound 1a

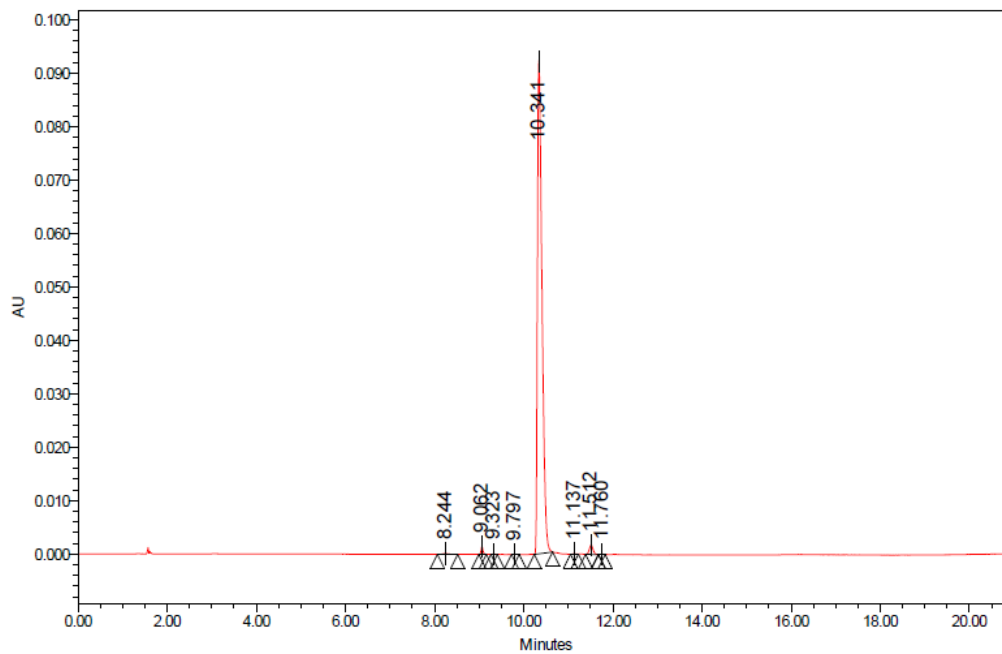


## Processed Channel: PDA 343.0 nm

	Peak Name	Processed Channel	Retention Time (min)	Area	% Area	Height
1	Peak47 343.0nm	PDA 343.0 nm	13.525	380425	100.00	53479



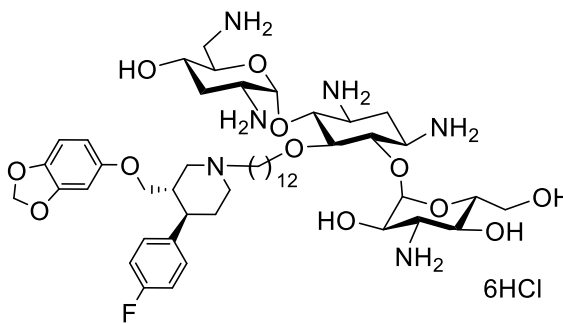
## Appendix 34. HPLC data of compound 2



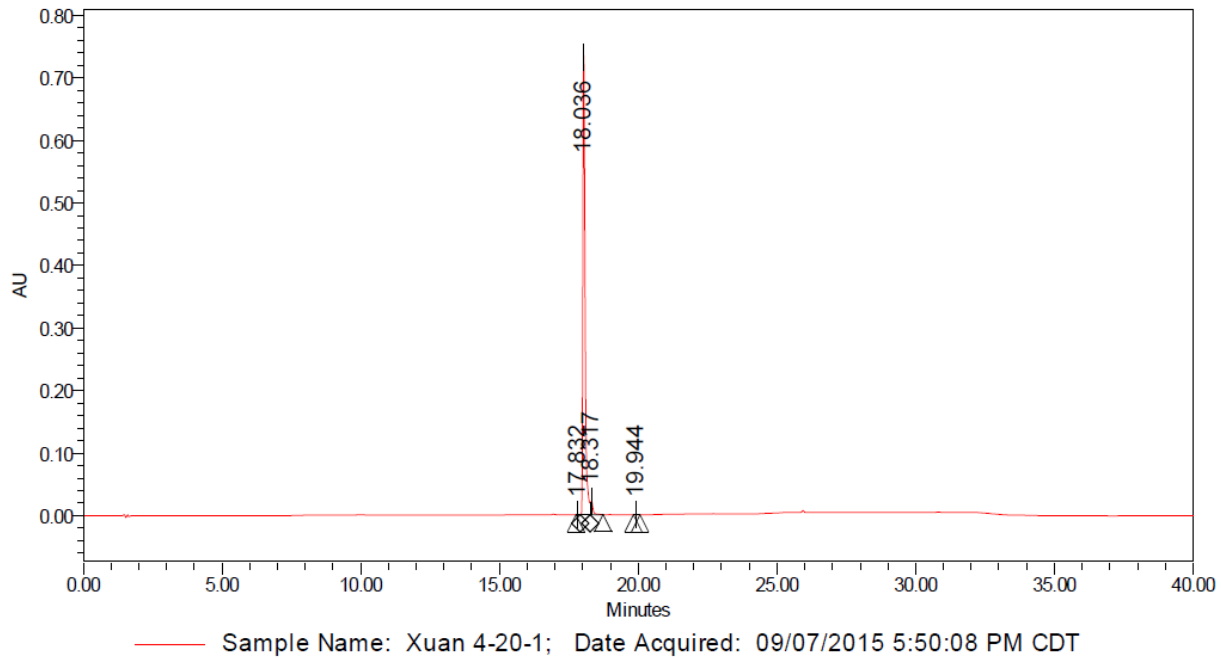
— Sample Name: Xuan1-93-1\_; Date Acquired: 09/06/2015 3:26:17 PM CDT

## Processed Channel: PDA 295.0 nm

	Processed Channel	Retention Time (min)	Area	% Area	Height
1	PDA 295.0 nm	8.244	1264	0.19	140
2	PDA 295.0 nm	9.062	4292	0.64	1503
3	PDA 295.0 nm	9.323	386	0.06	113
4	PDA 295.0 nm	9.797	525	0.08	93
5	PDA 295.0 nm	10.341	655493	97.39	92308
6	PDA 295.0 nm	11.137	436	0.06	90
7	PDA 295.0 nm	11.512	10280	1.53	1724
8	PDA 295.0 nm	11.760	417	0.06	102

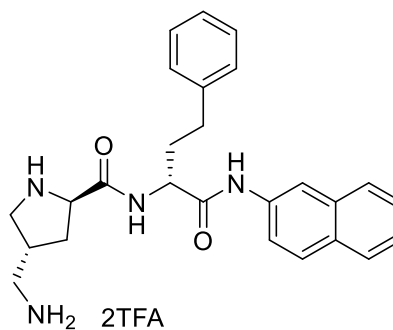


## Appendix 35. HPLC data of DBP

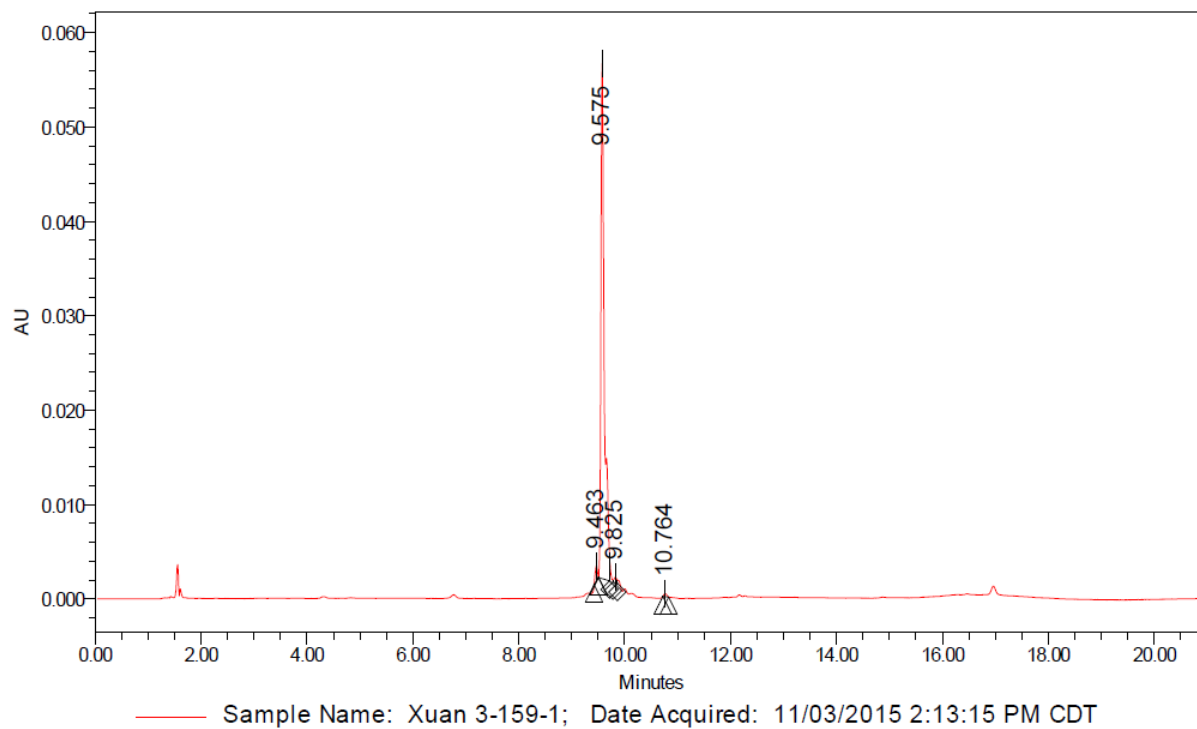


## Processed Channel: PDA 244.0 nm

	Processed Channel	Retention Time (min)	Area	% Area	Height
1	PDA 244.0 nm	17.832	964	0.02	235
2	PDA 244.0 nm	18.036	4083282	96.60	734426
3	PDA 244.0 nm	18.317	141132	3.34	21521
4	PDA 244.0 nm	19.944	1536	0.04	212

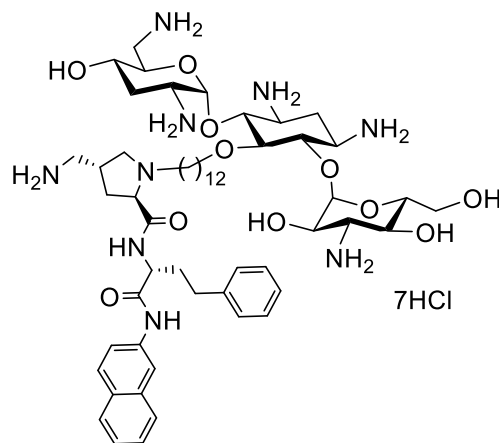


## Appendix 36. HPLC data of compound 3



## Processed Channel: PDA 271.0 nm

	Processed Channel	Retention Time (min)	Area	% Area	Height
1	PDA 271.0 nm	9.463	4610	1.84	1608
2	PDA 271.0 nm	9.575	242584	96.87	54570
3	PDA 271.0 nm	9.825	2070	0.83	578
4	PDA 271.0 nm	10.764	1146	0.46	322



## Chapter 10: Supporting Information for Chapter 5

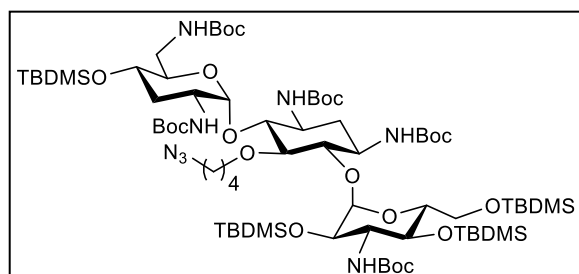
### 10.1 CHEMICAL SYNTHESSES

#### 10.1.1 Synthesis of Boc-Lys(Boc)-OH

Commercially available L-lysine (0.146 g, 1.0 mmol) dissolved in H<sub>2</sub>O (5.0 mL) was mixed with NaHCO<sub>3</sub> (0.252 g, 3.0 mmol). Boc<sub>2</sub>O (1.048 g, 4.8 mmol) in 10 mL of THF was subsequently added to the mixture at 0 °C and stirred at room temperature overnight. At the end, THF was evaporated and the mixture was washed with diethyl ether. The aqueous layer was acidified to pH = 6 with citric acid, followed by DCM extraction. The organic layer was washed with water and brine, then dried over anhydrous Na<sub>2</sub>SO<sub>4</sub>. The mixture was concentrated and purified by flash column chromatography (eluted with DCM/MeOH from 100:1 to 15:1, v/v) to afford the desired compound as a white solid (0.312 g, 90%). <sup>1</sup>H NMR (500 MHz, Methanol-*d*<sub>4</sub>)  $\delta$  4.08 – 4.01 (m, 1H,  $\alpha$ -CH), 3.03 (t, *J* = 6.8 Hz, 2H,  $\epsilon$ -CH<sub>2</sub>), 1.83 – 1.75 (m, 1H,  $\beta$ -CH<sup>1</sup>H<sup>2</sup>), 1.69 – 1.60 (m, 1H,  $\beta$ -CH<sup>1</sup>H<sup>2</sup>), 1.49 – 1.35 (m, 22H,  $\delta$ -CH<sub>2</sub>,  $\gamma$ -CH<sub>2</sub>, CCH<sub>3</sub>). <sup>13</sup>C NMR (126 MHz, Methanol-*d*<sub>4</sub>)  $\delta$  174.95 (NCOCH), 157.14, 156.70 (2 COOC), 79.01, 78.42, 53.50 ( $\alpha$ -CH), 39.60 ( $\epsilon$ -CH<sub>2</sub>), 31.12 ( $\beta$ -CH<sub>2</sub>), 29.12 ( $\delta$ -CH<sub>2</sub>), 27.39 - 27.17 (O-CCH<sub>3</sub>), 22.72 ( $\gamma$ -CH<sub>2</sub>); ESI-MS: *m/z* calc'd for C<sub>16</sub>H<sub>30</sub>N<sub>2</sub>O<sub>6</sub>Na: 369.2, found: 369.2 [M+Na]<sup>+</sup>.

## 10.1.2 Synthesis of 11a–c

### 10.1.2.1 Synthesis of 5-O-(4-azidobutyl)-1,3,2',6',3''-penta-N-(tert-butoxycarbonyl)-4',2'',4'',6''-tetra-OTBDMS-tobramycin (11a)

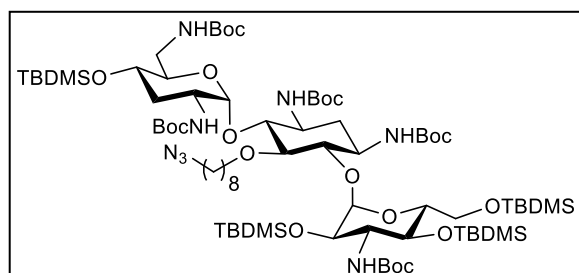


Yield: 98%.  $^1\text{H}$  NMR (500 MHz,

Chloroform-*d*)  $\delta$  5.22 – 5.10 (m, 2H, H-1', H-1''), 4.31 – 4.01 (m, 3H), 3.85 – 3.15 (m, 17H), 2.53 – 2.37 (m, 1H), 2.00 – 1.96 (m, 1H), 1.68 – 1.59 (m,

2H,  $\text{CH}_2$  of linker), 1.57 – 1.53 (m, 2H,  $\text{CH}_2$  of linker), 1.51 - 1.29 (m, 46H), 1.10 – 0.99 (m, 1H), 0.96 – 0.81 (m, 36H, Si- $\text{CCH}_3$ ), 0.19 – -0.01 (m, 24H, Si- $\text{CH}_3$ ).  $^{13}\text{C}$  NMR (126 MHz, Chloroform-*d*)  $\delta$  155.69, 155.47, 154.75, 154.60, 154.26 (5 COOC), 97.87 (anomeric CH-1''), 96.42 (anomeric CH-1'), 85.91, 79.96, 79.42, 79.27, 79.15, 78.73, 75.41, 72.65, 72.47, 71.57, 67.99, 67.10, 63.25, 57.14, 51.41, 50.51, 48.84, 48.30, 41.60, 35.95, 35.63, 28.61 - 28.38 (O-C $\text{CH}_3$ ), 27.59, 26.08 - 25.42 (Si-C $\text{CH}_3$ ), 18.46, 18.28, 18.07, 17.90 (4 Si-C $\text{CH}_3$ ), -3.48, -3.77, -4.23, -4.37, -4.70, -4.90, -5.11, -5.21 (8 Si- $\text{CH}_3$ ); ESI-MS:  $m/z$  calc'd for  $\text{C}_{71}\text{H}_{140}\text{N}_8\text{O}_{19}\text{Si}_4\text{Na}$ : 1545.2, found: 1544.9 [M+Na] $^+$ .

### 10.1.2.2 Synthesis of 5-O-(8-azido-octyl)-1,3,2',6',3''-penta-N-(tert-butoxycarbonyl)-4',2'',4'',6''-tetra-OTBDMS-tobramycin (11b)

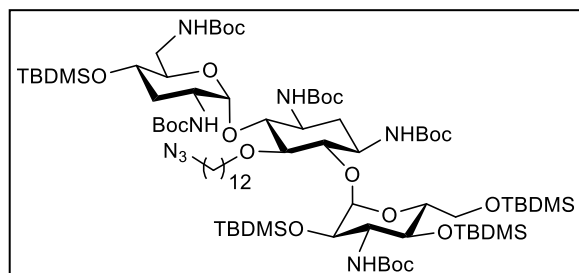


Yield: 97%.  $^1\text{H}$  NMR (500 MHz,

Chloroform-*d*)  $\delta$  5.24 – 5.10 (m, 2H, H-1', H-1''), 4.30 – 4.19 (m, 1H), 4.19 – 4.11 (m, 1H), 4.11 –

4.04 (m, 1H), 3.82 – 3.16 (m, 17H), 2.52 – 2.37 (m, 1H), 2.02 – 1.97 (m, 1H), 1.60 – 1.55 (m, 2H, CH<sub>2</sub> of linker), 1.53 – 1.39 (m, 46H), 1.38 – 1.20 (m, 10H), 1.08 – 0.99 (m, 1H), 0.97 – 0.82 (m, 36H, Si-CCH<sub>3</sub>), 0.18 – -0.02 (m, 24H, Si-CH<sub>3</sub>). <sup>13</sup>C NMR (126 MHz, Chloroform-*d*) δ 155.69, 155.47, 154.72, 154.59, 154.29 (5 COOC), 97.79 (anomeric CH-1''), 96.49 (anomeric CH-1'), 85.90, 79.95, 79.41, 79.27, 79.11, 78.78, 75.41, 72.67, 72.26, 71.59, 67.98, 67.08, 63.22, 57.14, 50.49, 48.83, 48.31, 41.64, 35.97, 35.61, 33.72, 29.47, 29.22, 28.60 - 28.41 (O-CCH<sub>3</sub>), 26.68, 26.09 - 25.76 (Si-CCH<sub>3</sub>), 18.46, 18.28, 18.07, 17.89 (4 Si-CCH<sub>3</sub>), -3.42, -3.76, -4.22, -4.91, -4.93, -5.06, -5.17, -5.20 (8 Si-CH<sub>3</sub>); ESI-MS: *m/z* calc'd for C<sub>75</sub>H<sub>148</sub>N<sub>8</sub>O<sub>19</sub>Si<sub>4</sub>Na: 1601.3, found: 1601.0 [M+Na]<sup>+</sup>.

**10.1.2.3 Synthesis of 5-O-(12-azidododecyl)-1,3,2',6',3''-penta-N-(tert-butoxycarbonyl)-4',2'',4'',6''-tetra-OTBDMS-tobramycin (11c)**



Yield: 94%. <sup>1</sup>H NMR (500 MHz,

Chloroform-*d*) δ 5.24 – 5.10 (m, 2H, H-1', H-1''), 4.31 – 4.21 (m, 1H), 4.19 – 4.11 (m, 1H), 4.11 – 4.02 (m, 1H), 3.81 – 3.14 (m, 17H), 2.51 – 2.40

(m, 1H), 2.03 – 1.96 (m, 1H), 1.61 – 1.55 (m, 2H, CH<sub>2</sub> of linker), 1.54-1.51 (m, 1H), 1.47 – 1.38 (m, 45H), 1.37 – 1.18 (m, 18H), 1.11 – 1.00 (m, 1H), 0.95 – 0.81 (m, 36H, Si-CCH<sub>3</sub>), 0.17 – 0.00 (m, 24H, Si-CH<sub>3</sub>). <sup>13</sup>C NMR (126 MHz, Chloroform-*d*) δ 155.70, 155.49, 154.71, 154.54, 154.21 (5 COOC), 97.81 (anomeric CH-1''), 96.51 (anomeric CH-1'), 85.70, 79.87, 79.34, 79.18, 79.02, 78.79, 75.27, 73.36, 72.65, 71.53, 68.00, 66.80, 63.08, 57.26, 51.45, 50.51, 48.94, 48.35, 41.64, 35.89, 35.62, 30.60, 29.99, 29.62, 29.52, 29.45, 29.15 - 28.37 (O-CCH<sub>3</sub>), 26.69, 26.14 - 25.76 (Si-CCH<sub>3</sub>), 18.46, 18.31, 18.07, 17.89 (4 Si-CCH<sub>3</sub>), -3.44, -3.82, -4.23, -4.91, -4.97, -5.10,

-5.21, -5.26 (8 Si-CH<sub>3</sub>); ESI-MS:  $m/z$  calc'd for C<sub>79</sub>H<sub>156</sub>N<sub>8</sub>O<sub>19</sub>Si<sub>4</sub>Na: 1657.4, found: 1658.1 [M+Na]<sup>+</sup>.

### 10.1.3 General Procedure for 5-*O*-(amino-alkylated)-1,3,2',6',3''-penta-*N*-(tert-butoxycarbonyl)-4',2'',4'',6''-tetra-OTBDMS-tobramycin (**12a–c**)

Compounds **11a–c** (1.0 mmol) dissolved in methanol (20 mL) was exposed to a hydrogen atmosphere with a catalytic amount of palladium hydroxide on carbon (0.014 g, 0.1 mmol). The mixture was stirred at room temperature for 3 h, followed by filtration through celite and concentration under vacuum to afford compounds **12a–c** as white solid (Yield: 85%–90%).

Compound **12a** (Yield 85%): ESI-MS:  $m/z$  calc'd for C<sub>71</sub>H<sub>143</sub>N<sub>6</sub>O<sub>19</sub>Si<sub>4</sub>: 1497.2, found: 1496.7

[M+H]<sup>+</sup>; Compound **12b** (Yield 90%): ESI-MS:  $m/z$  calc'd for C<sub>75</sub>H<sub>151</sub>N<sub>6</sub>O<sub>19</sub>Si<sub>4</sub>: 1553.3, found:

1553.7 [M+H]<sup>+</sup>. Compound **12c** (Yield 90%): ESI-MS:  $m/z$  calc'd for C<sub>79</sub>H<sub>159</sub>N<sub>6</sub>O<sub>19</sub>Si<sub>4</sub>: 1609.5, found: 1609.0 [M+H]<sup>+</sup>.

## 10.2 FIGURES

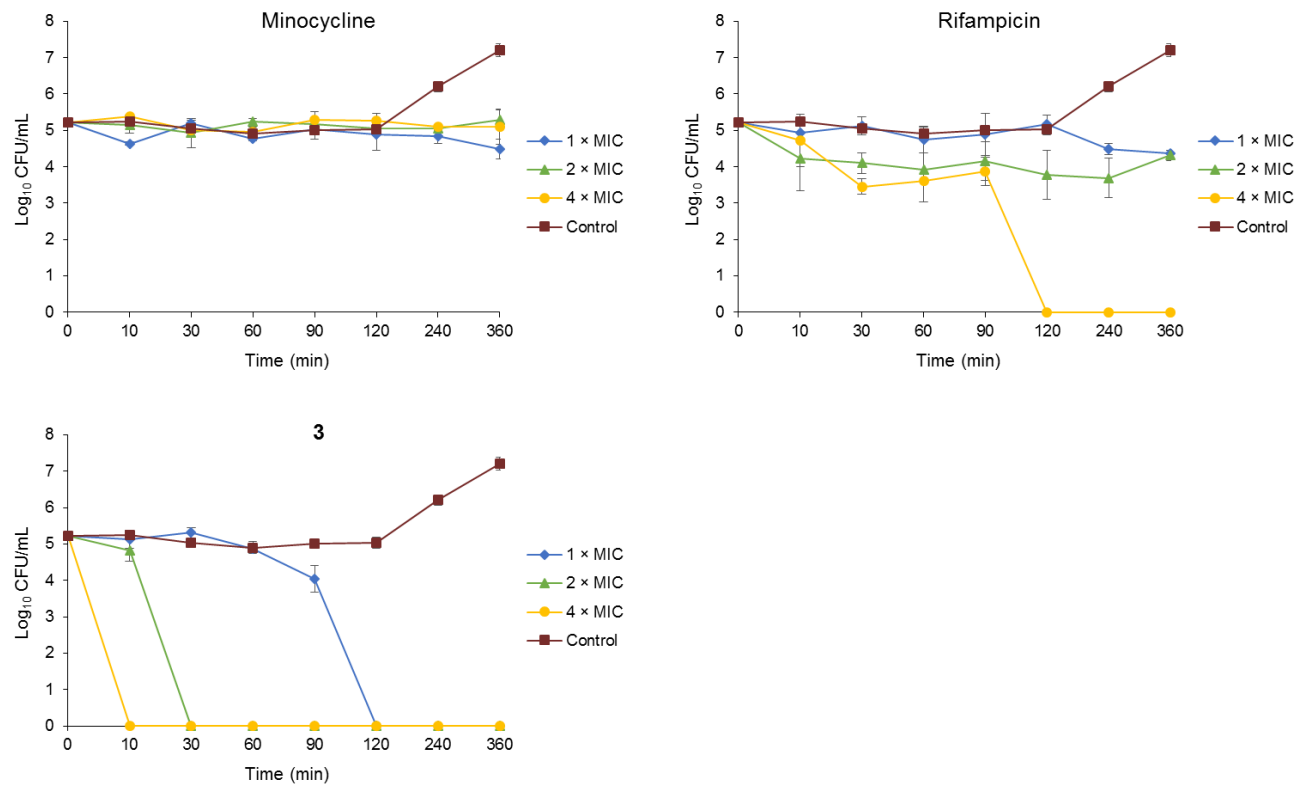


**Figure 10.2.1.** Time killing kinetics of minocycline, rifampicin, and **3** as monotherapy against *P. aeruginosa* PAO1 at 1 × MIC, 2 × MIC, and 4 × MIC, respectively.

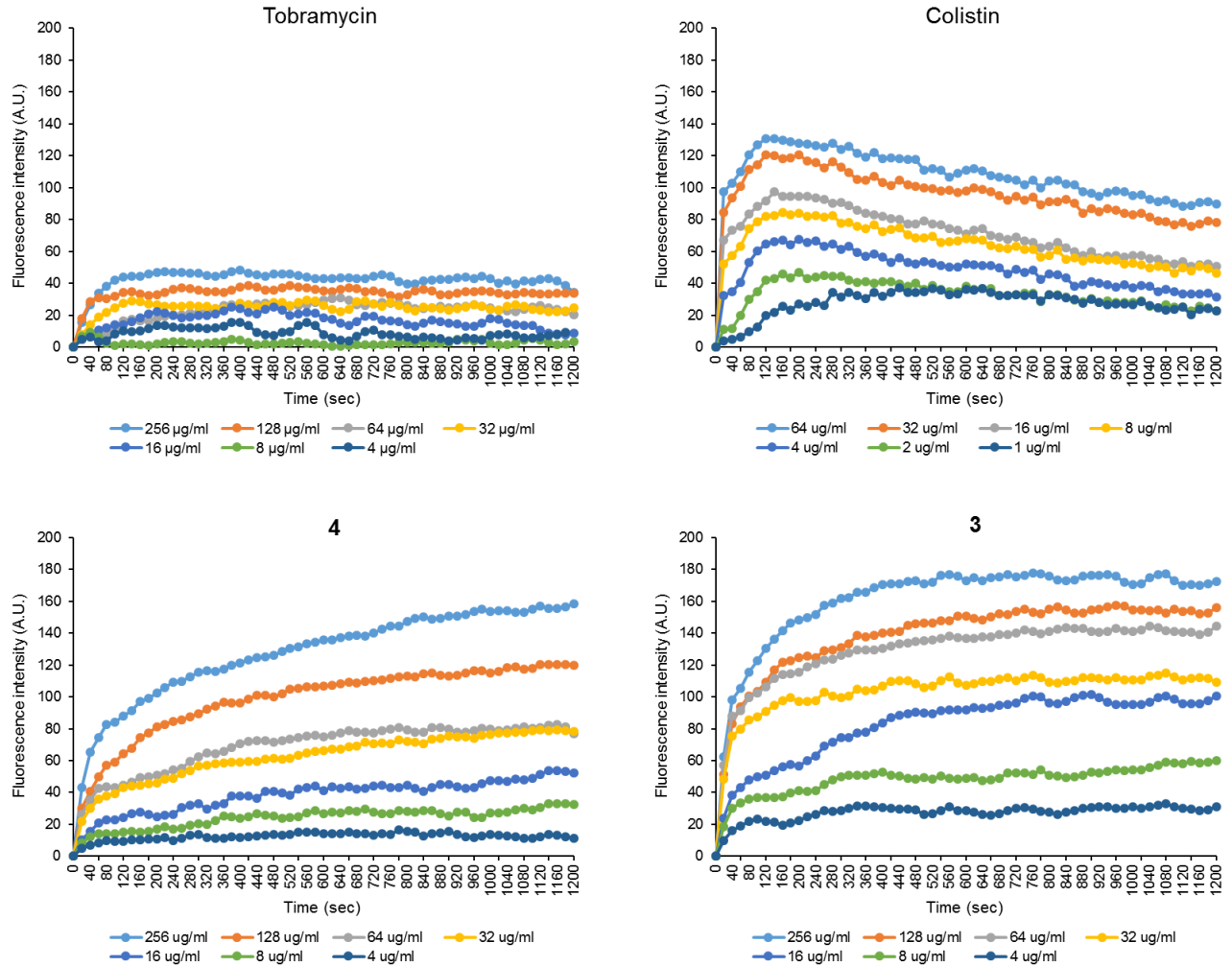


**Figure 10.2.2.** Cytoplasmic membrane depolarization of *P. aeruginosa* PAO1 when treated with tobramycin, colistin, **3**, and **4** was measured at differential concentrations using the membrane potential-sensitive dye DiSC<sub>3</sub>(5).

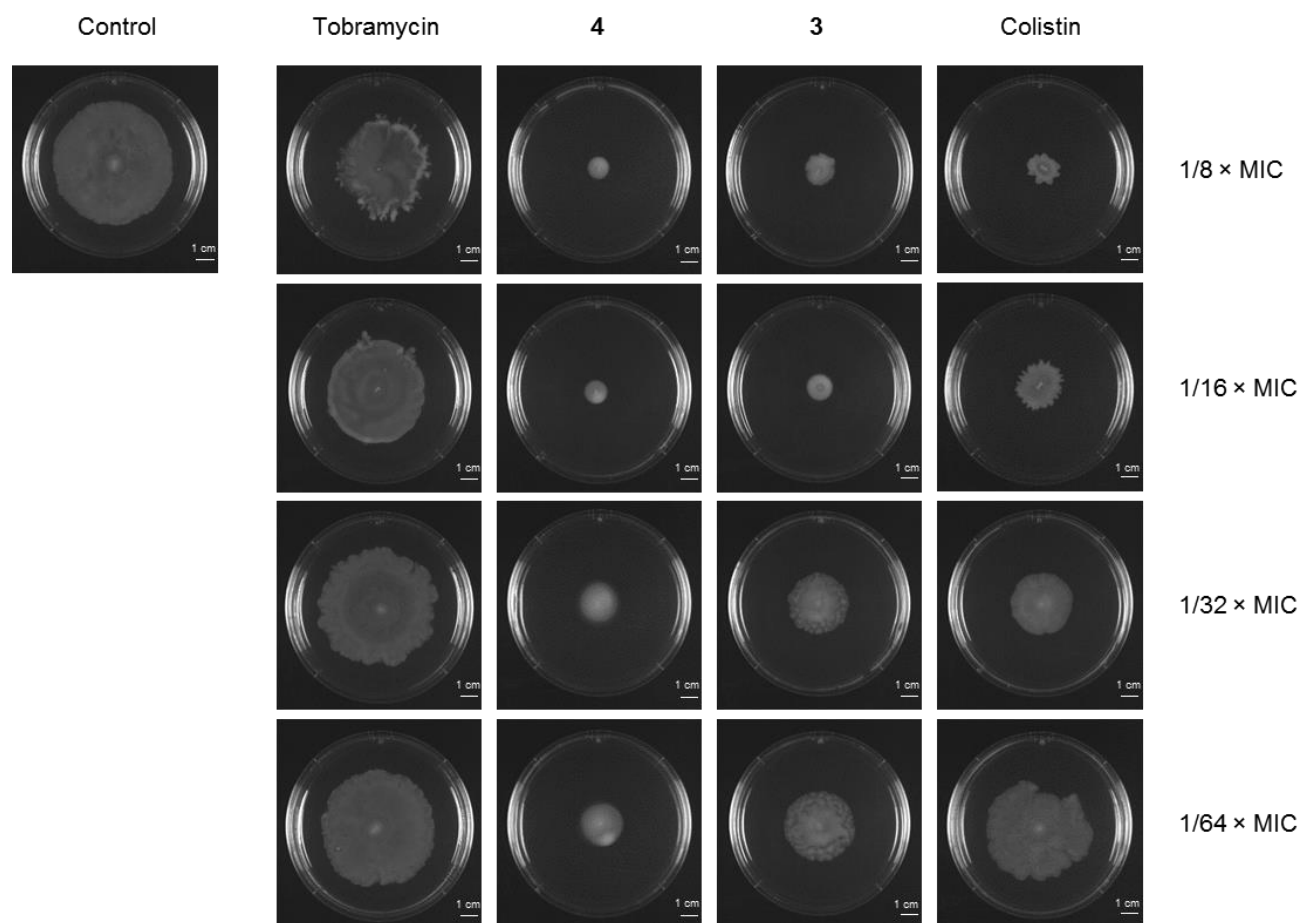


**Figure 10.2.3.** Swimming motility of *P. aeruginosa* PAO1 treated with tobramycin, colistin, compound **3**, or **4** at  $1/8 \times \text{MIC}$ ,  $1/16 \times \text{MIC}$ ,  $1/32 \times \text{MIC}$ , and  $1/64 \times \text{MIC}$ .

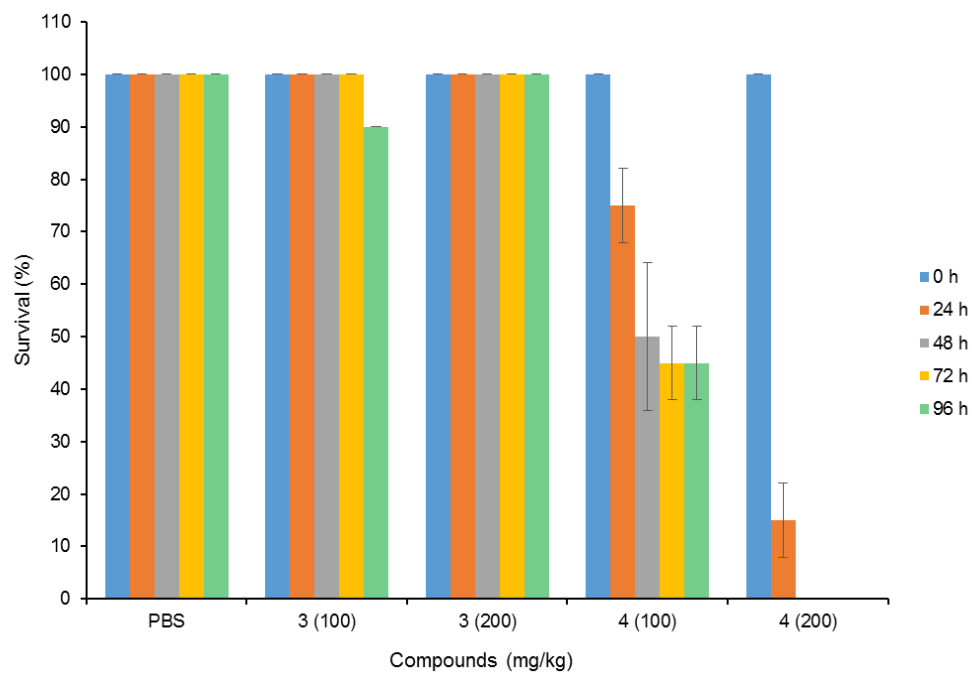


**Figure 10.2.4.** Tolerability of *Galleria mellonella* treated with compound **3** and **4** at 100 and 200 mg/kg. The numbers of surviving larvae were scored daily for 4 days.

## 10.3 TABLES

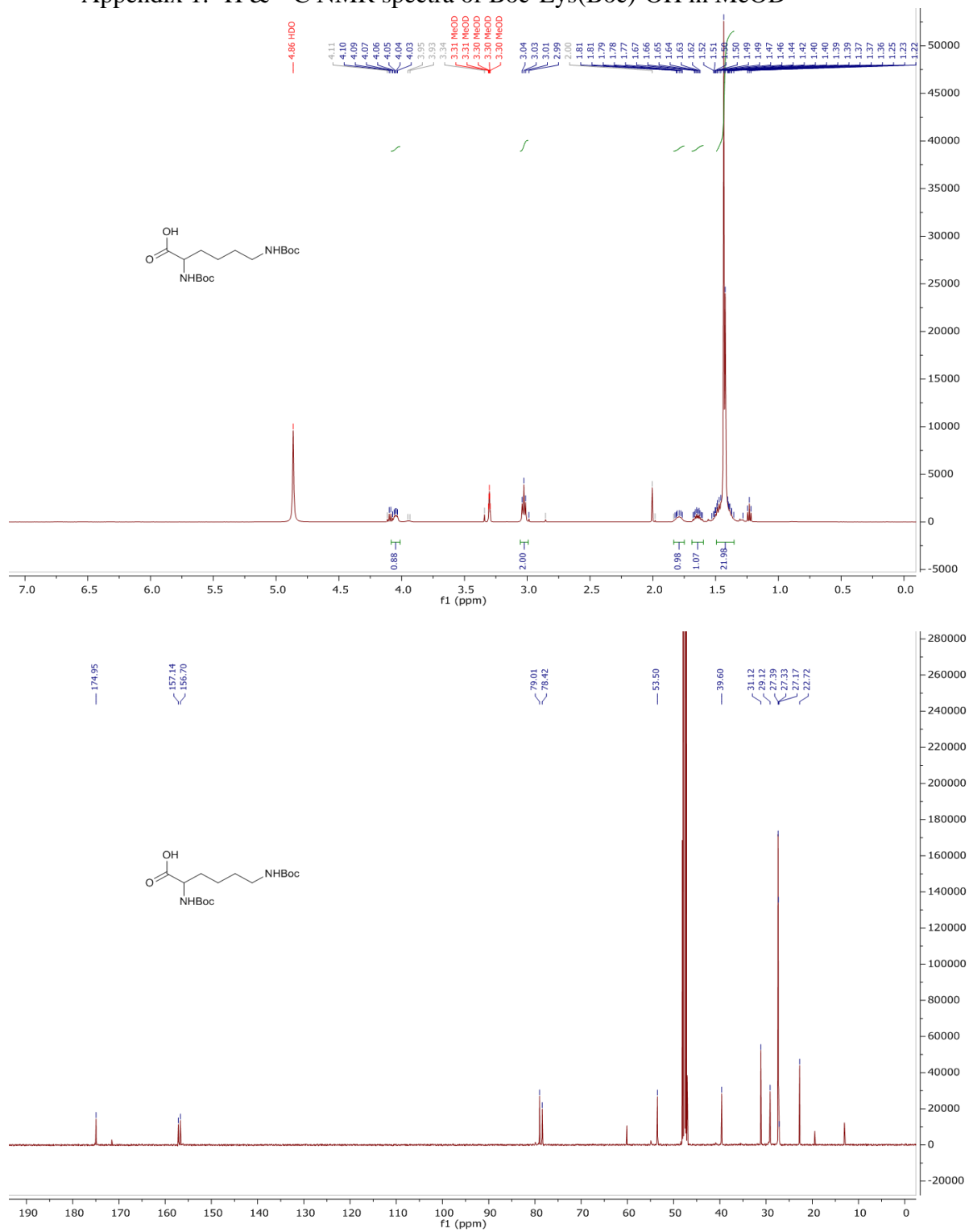
**Table 10.3.1.** Synergistic effects comparison of tobramycin, compound **4**, and hybrids **1–3** with minocycline or rifampicin against *P. aeruginosa* PAO1.

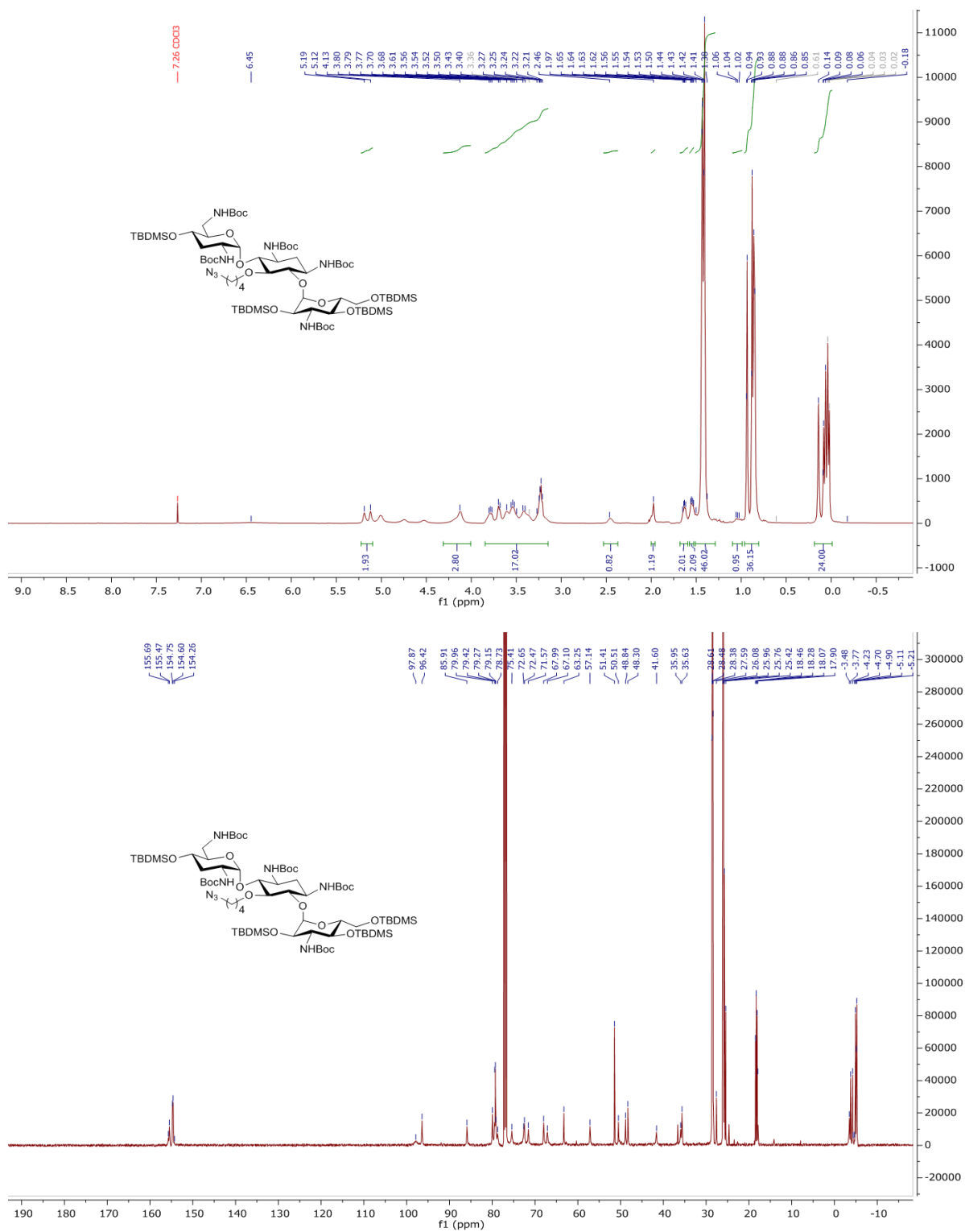
<i>P. aeruginosa</i> strain	Antibiotics	MIC <sub>alone</sub> (μg/mL)	Synergistic MIC (μg/mL)	FIC <sub>antibiotic</sub>	Adjuvant	MIC <sub>alone</sub> (μg/mL)	Synergistic MIC (μg/mL)	FIC <sub>hybrid</sub>	FIC index
PAO1	Minocycline	8	8	1	Tobramycin	0.25	0.016	0.064	1.064
PAO1	Minocycline	8	8	1	<b>4</b>	256	1	0.004	1.004
PAO1	Minocycline	8	4	0.5	<b>1</b>	>256	1	<0.004	0.5<x<0.504
PAO1	Minocycline	8	0.5	0.063	<b>2</b>	128	1	0.008	0.071
PAO1	Minocycline	8	0.5	0.063	<b>3</b>	32	1	0.031	0.094
PAO1	Rifampicin	16	8	0.5	Tobramycin	0.25	0.125	0.5	1
PAO1	Rifampicin	16	8	0.5	<b>4</b>	256	1	0.004	0.504
PAO1	Rifampicin	16	8	0.5	<b>1</b>	>256	1	<0.004	0.5<x<0.504
PAO1	Rifampicin	16	1	0.063	<b>2</b>	128	1	0.008	0.071
PAO1	Rifampicin	16	1	0.063	<b>3</b>	32	1	0.031	0.094

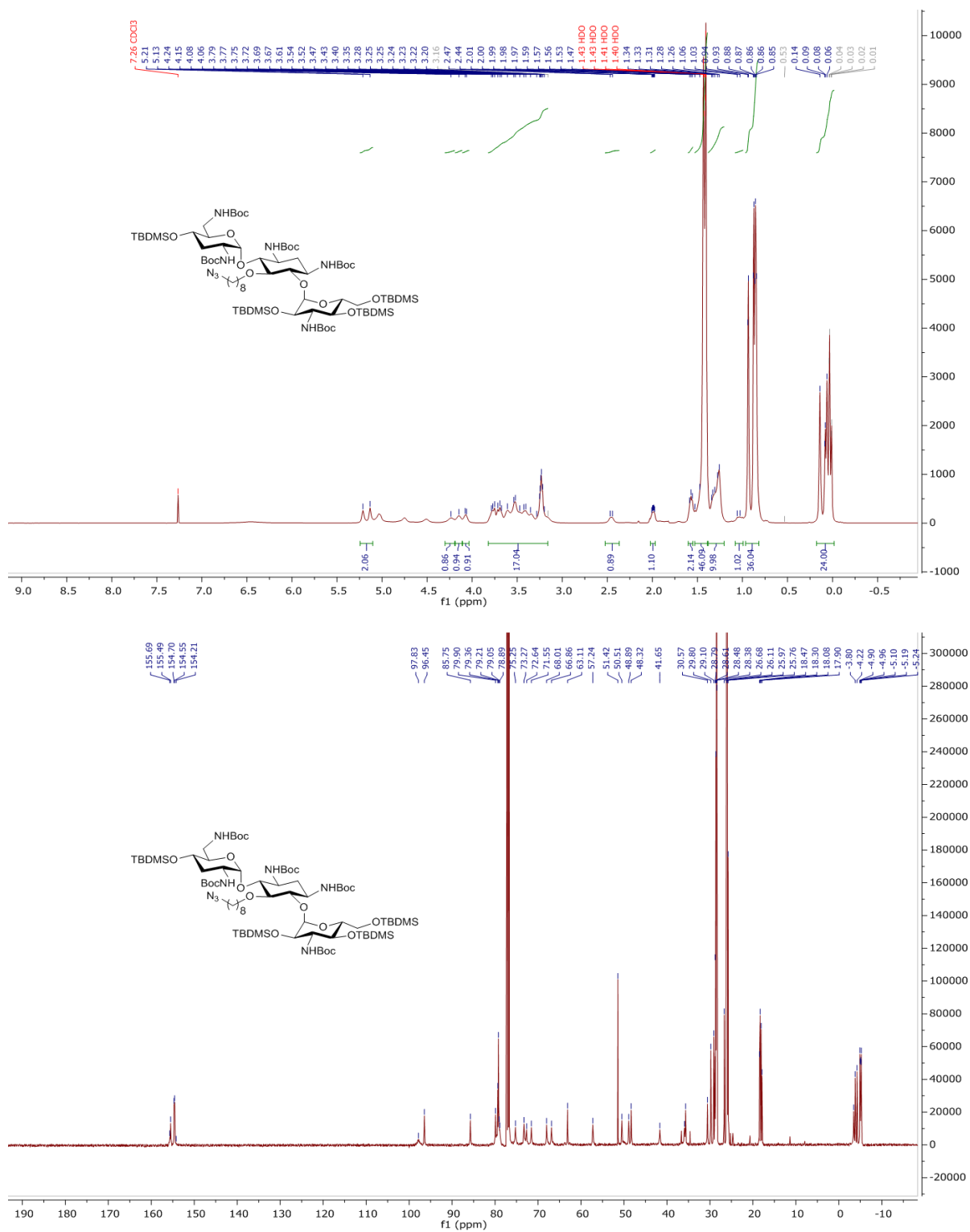
**Table 10.3.2.** Combination study of compound **3** with chloramphenicol, erythromycin, trimethoprim, or moxifloxacin against *P. aeruginosa* PAO1 or efflux pump deficient *P. aeruginosa* PAO200 and PAO750.

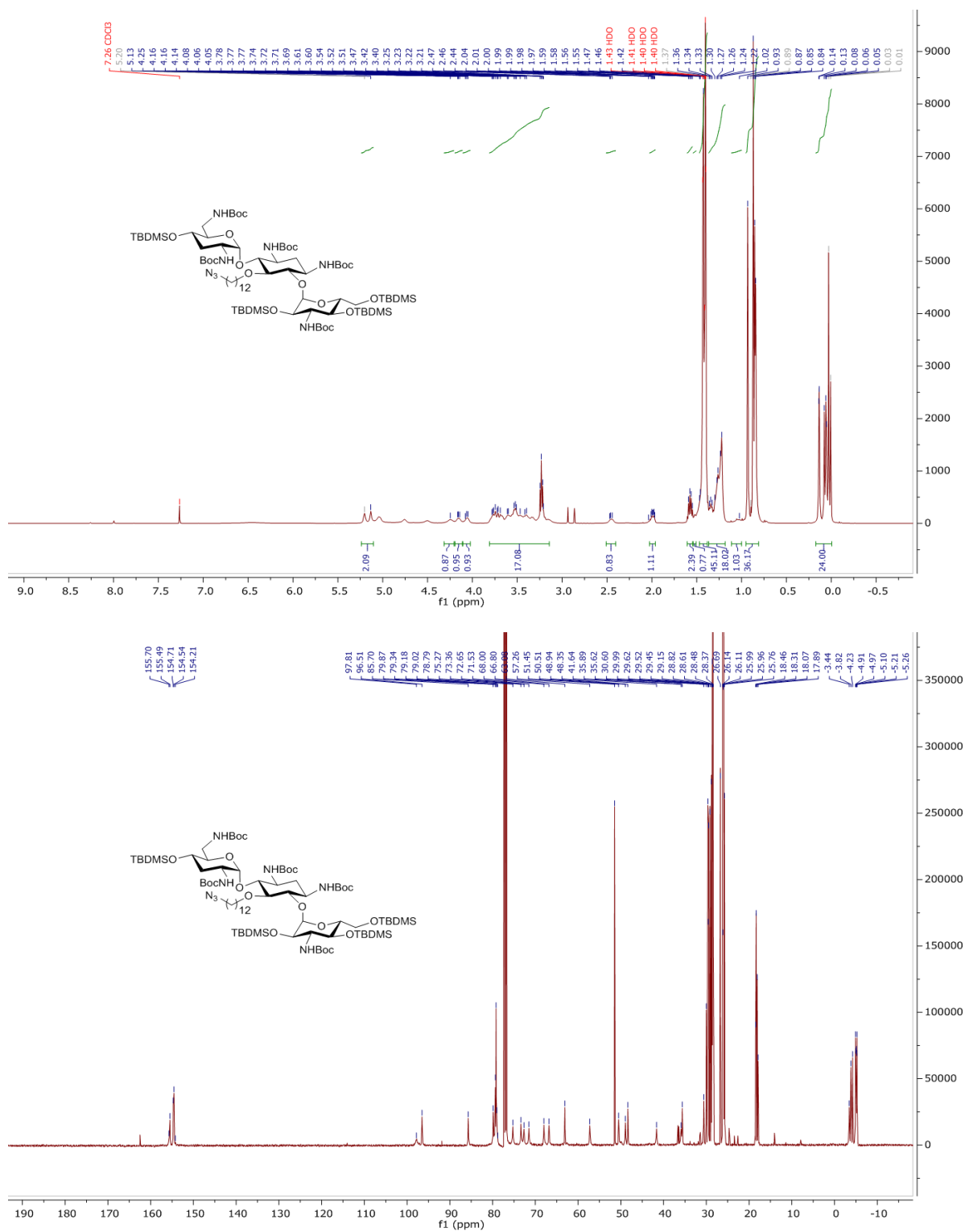
<i>P. aeruginosa</i> strain	Antibiotic (MIC $\mu\text{g/mL}$ )	Adjuvant (MIC $\mu\text{g/mL}$ )	FIC index
PAO1	Chloramphenicol (64)	<b>3</b> (32)	0.156
PAO1	Erythromycin (256)	<b>3</b> (32)	0.156
PAO1	Trimethoprim (256)	<b>3</b> (32)	0.126
PAO1	Moxifloxacin (1)	<b>3</b> (32)	0.313
PAO200	Chloramphenicol (2)	<b>3</b> (16)	0.25
PAO200	Erythromycin (32)	<b>3</b> (16)	0.281
PAO200	Trimethoprim (32)	<b>3</b> (16)	0.375
PAO200	Moxifloxacin (0.125)	<b>3</b> (16)	0.375
PAO750	Chloramphenicol (1)	<b>3</b> (8)	1.016
PAO750	Erythromycin (16)	<b>3</b> (8)	0.375
PAO750	Trimethoprim (4)	<b>3</b> (8)	0.563
PAO750	Moxifloxacin (0.016)	<b>3</b> (8)	0.5

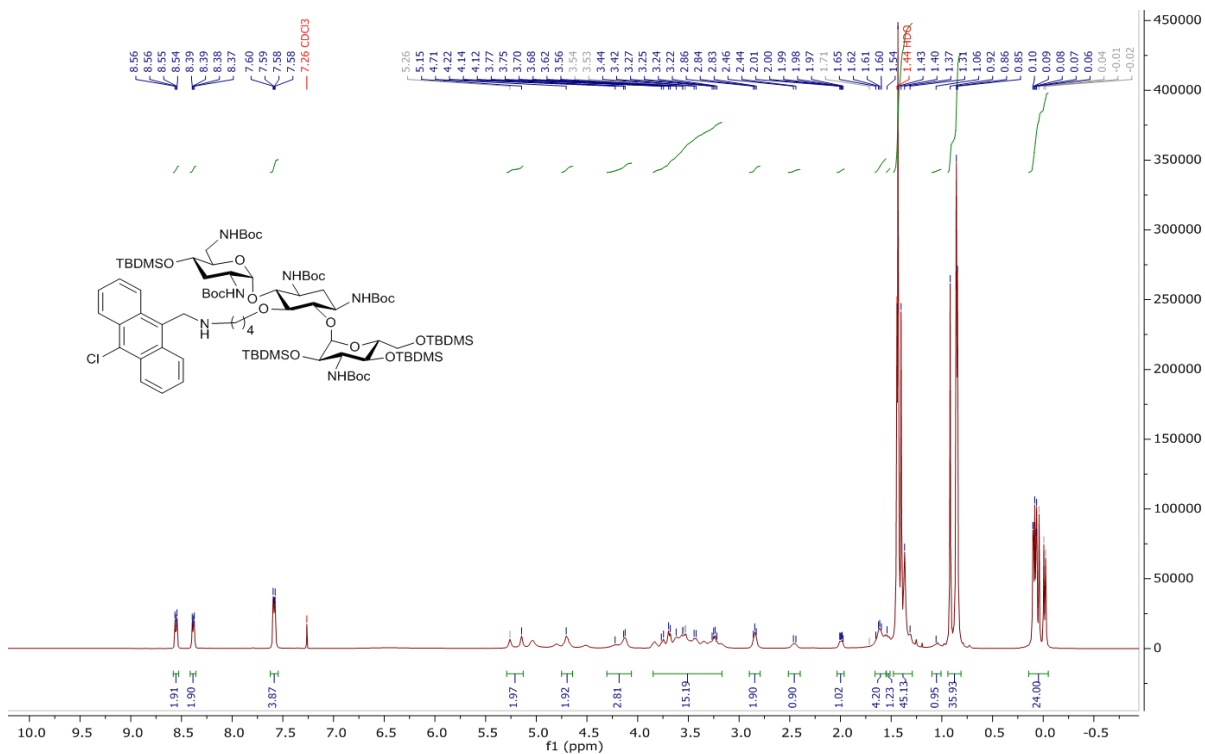
## 10.4 NMR SPECTRA

Appendix 1.  $^1\text{H}$  &  $^{13}\text{C}$  NMR spectra of Boc-Lys(Boc)-OH in MeOD

Appendix 2.  $^1\text{H}$  &  $^{13}\text{C}$  NMR spectra of compound **11a** in  $\text{CDCl}_3$ 

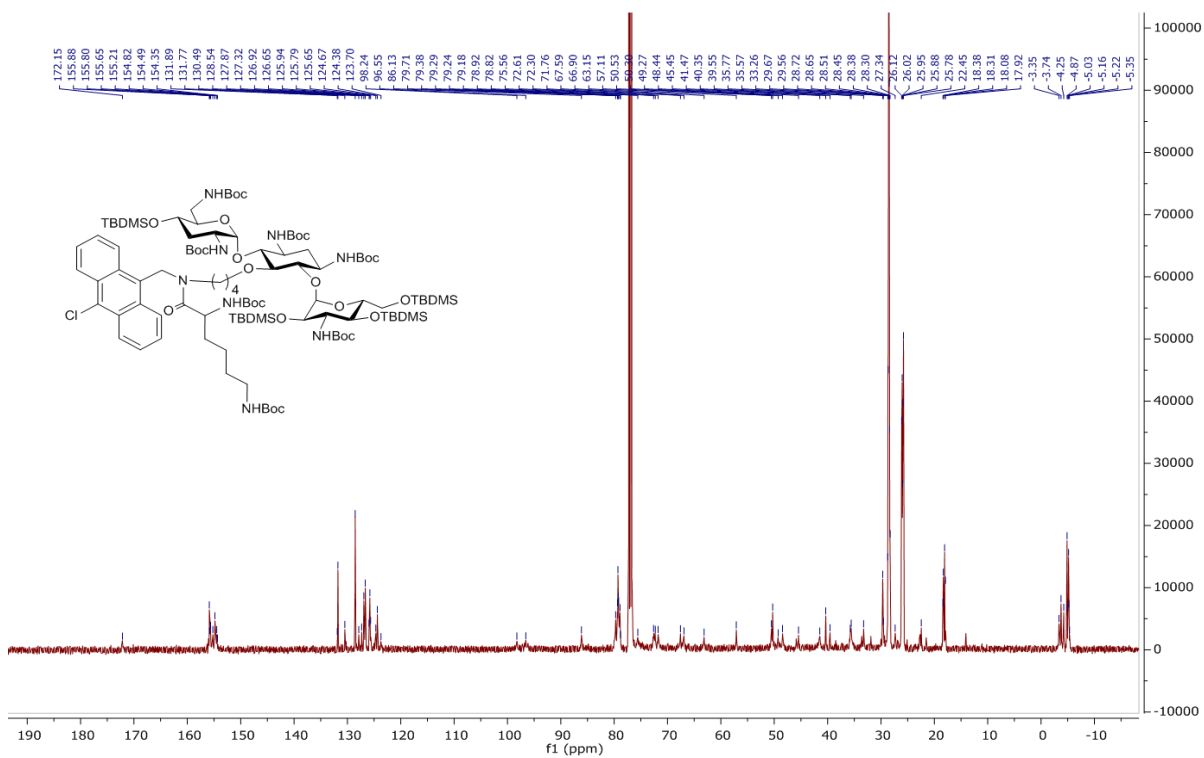
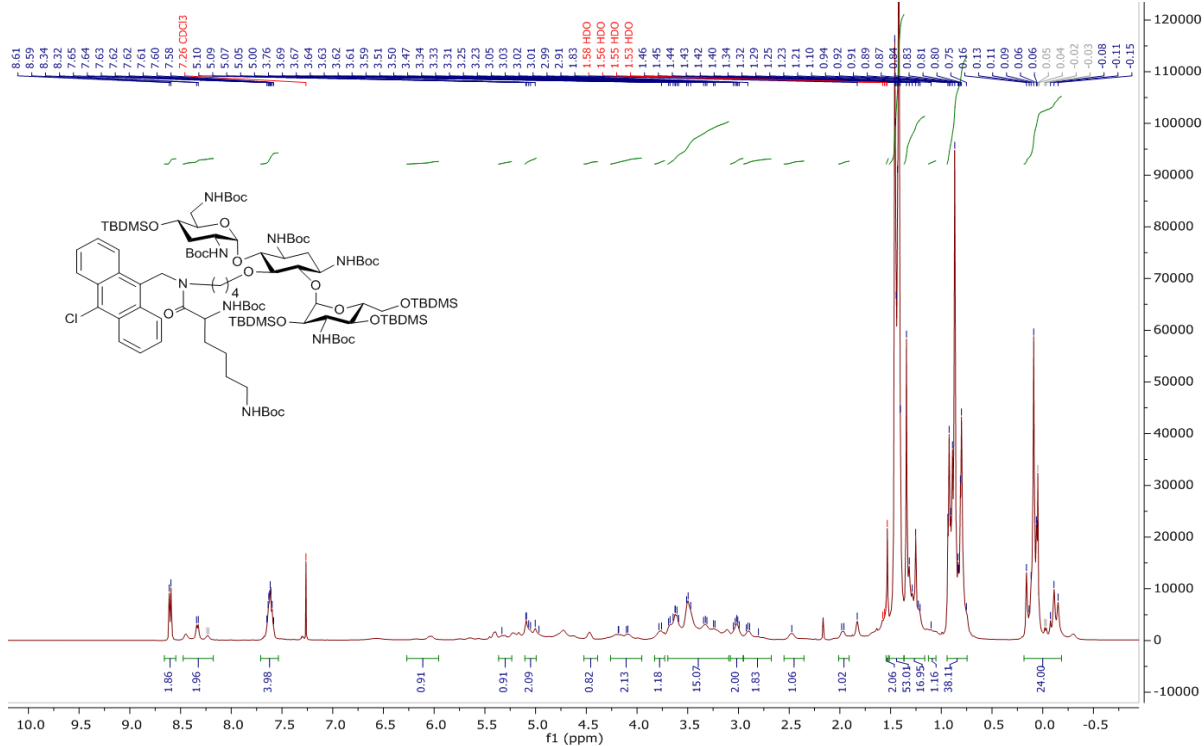
Appendix 3.  $^1\text{H}$  &  $^{13}\text{C}$  NMR spectra of compound **11b** in  $\text{CDCl}_3$ 

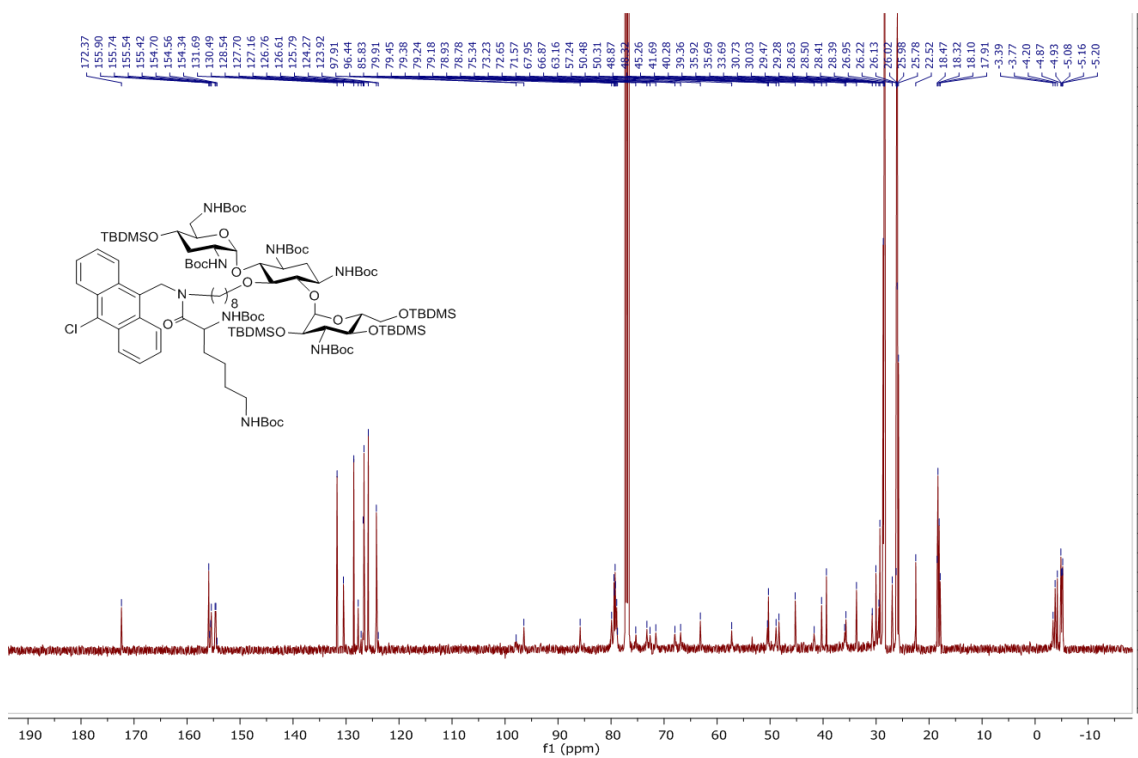
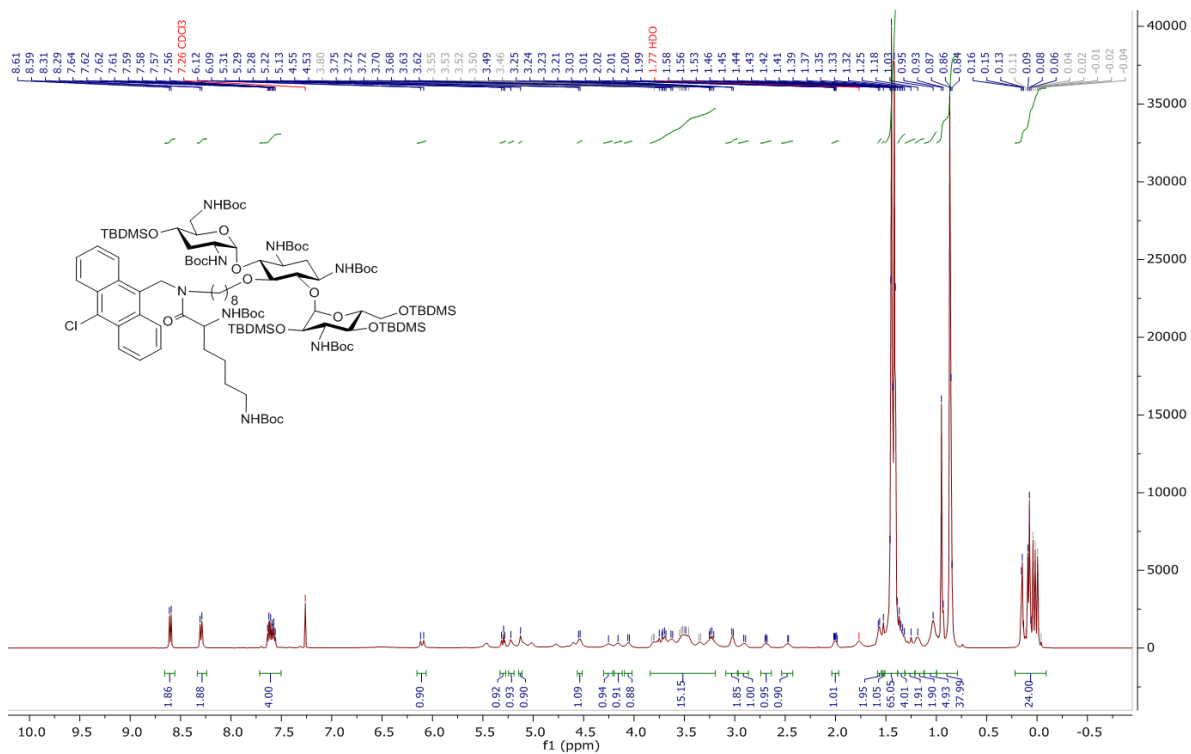
Appendix 4.  $^1\text{H}$  &  $^{13}\text{C}$  NMR spectra of compound **11c** in  $\text{CDCl}_3$ 

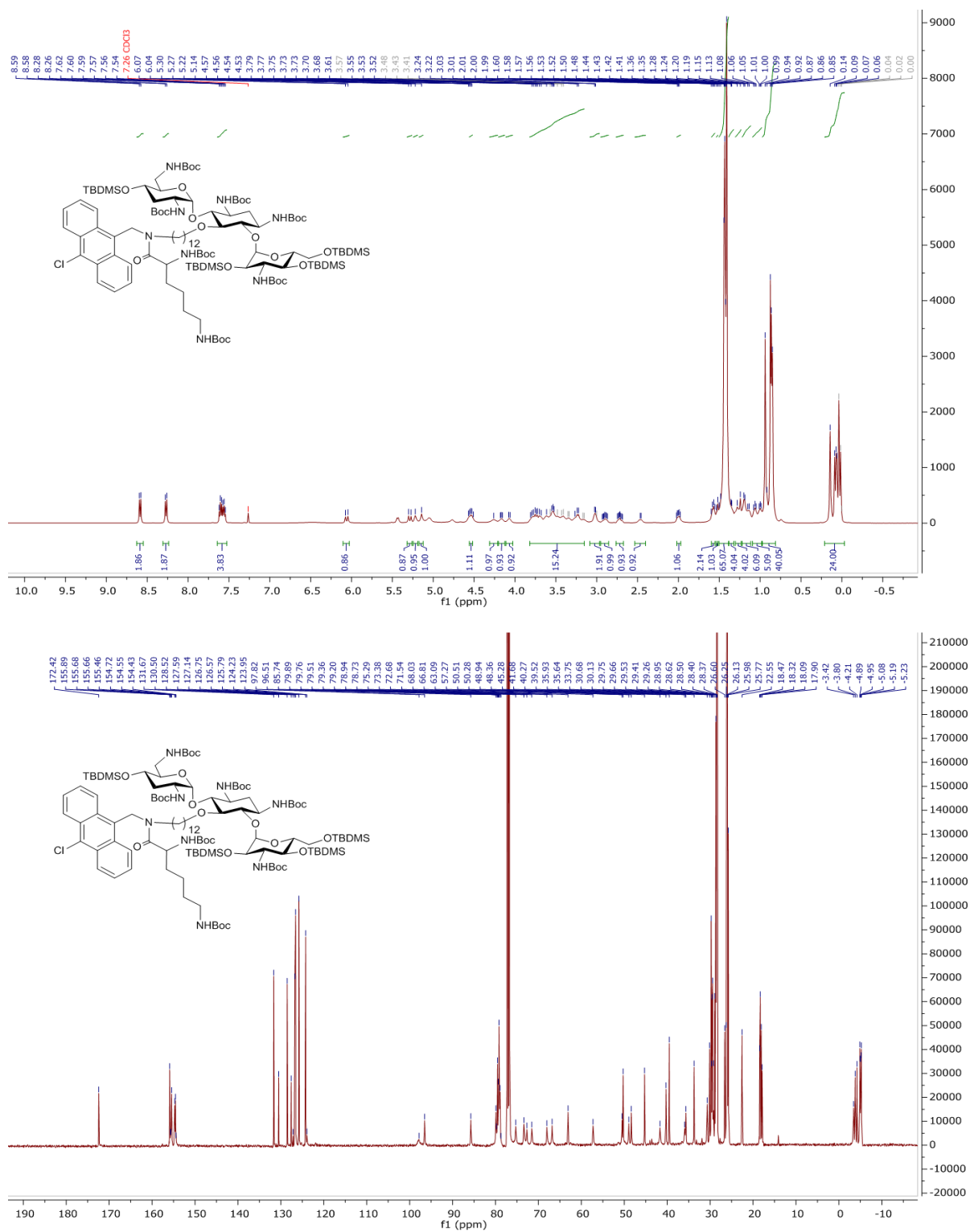
Appendix 5.  $^1\text{H}$  &  $^{13}\text{C}$  NMR spectra of compound **13a** in  $\text{CDCl}_3$ 

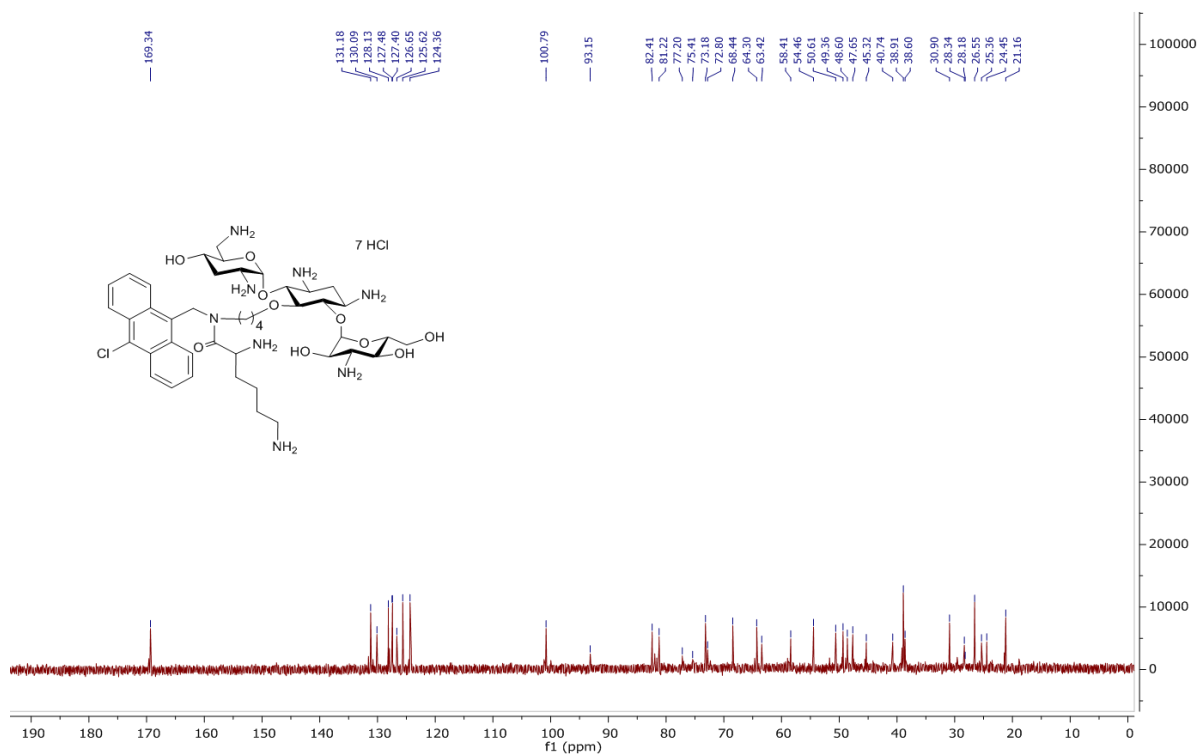
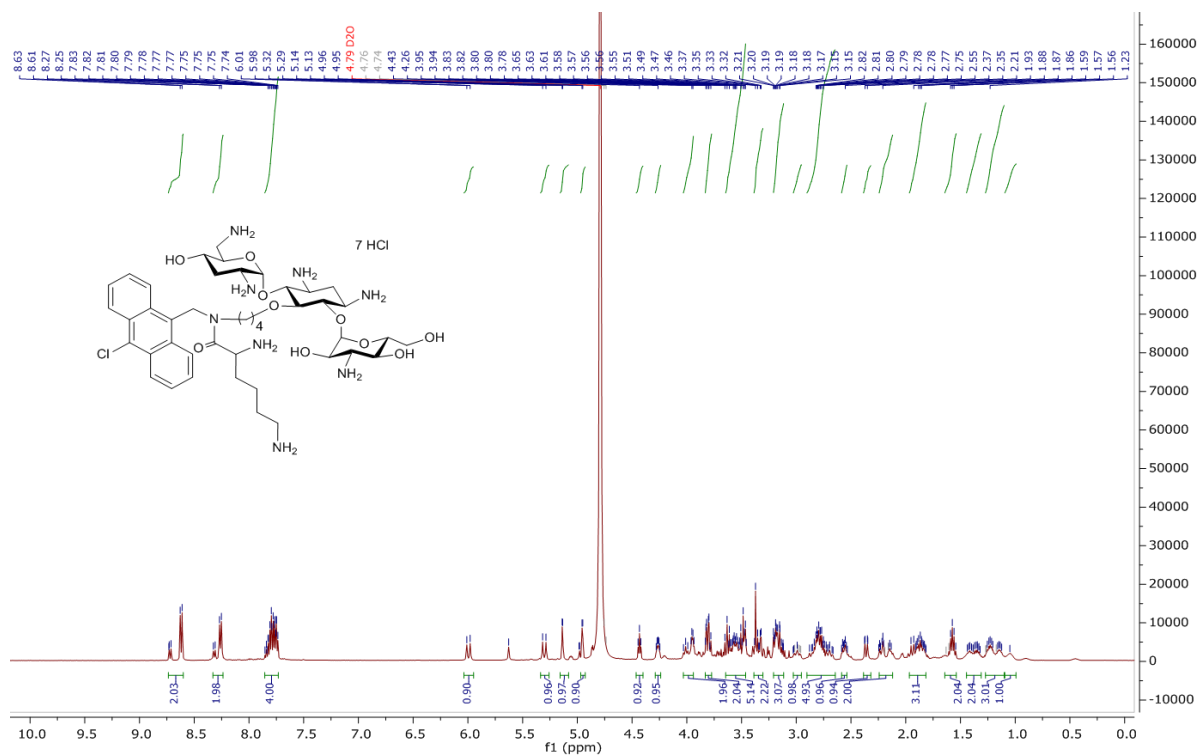


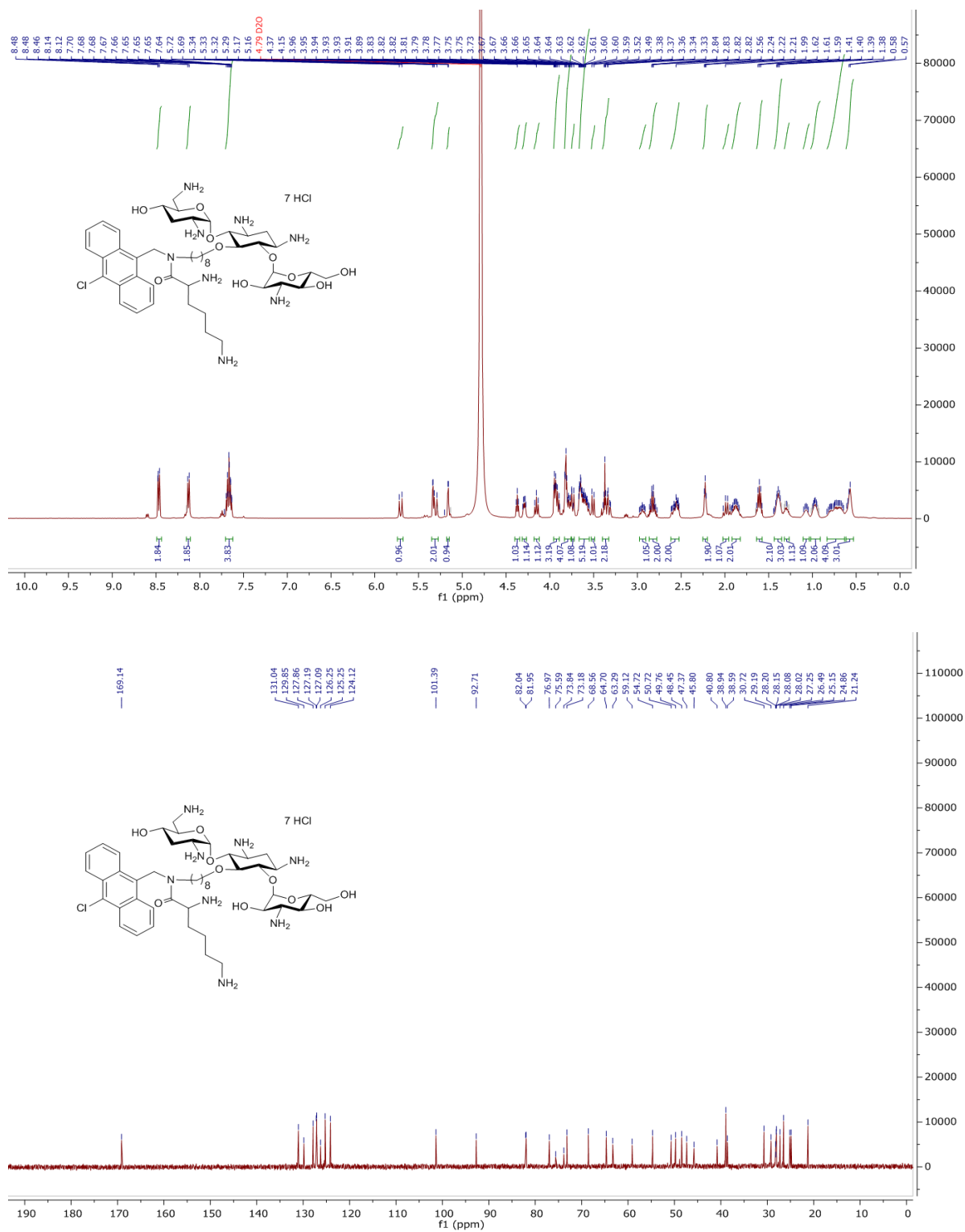


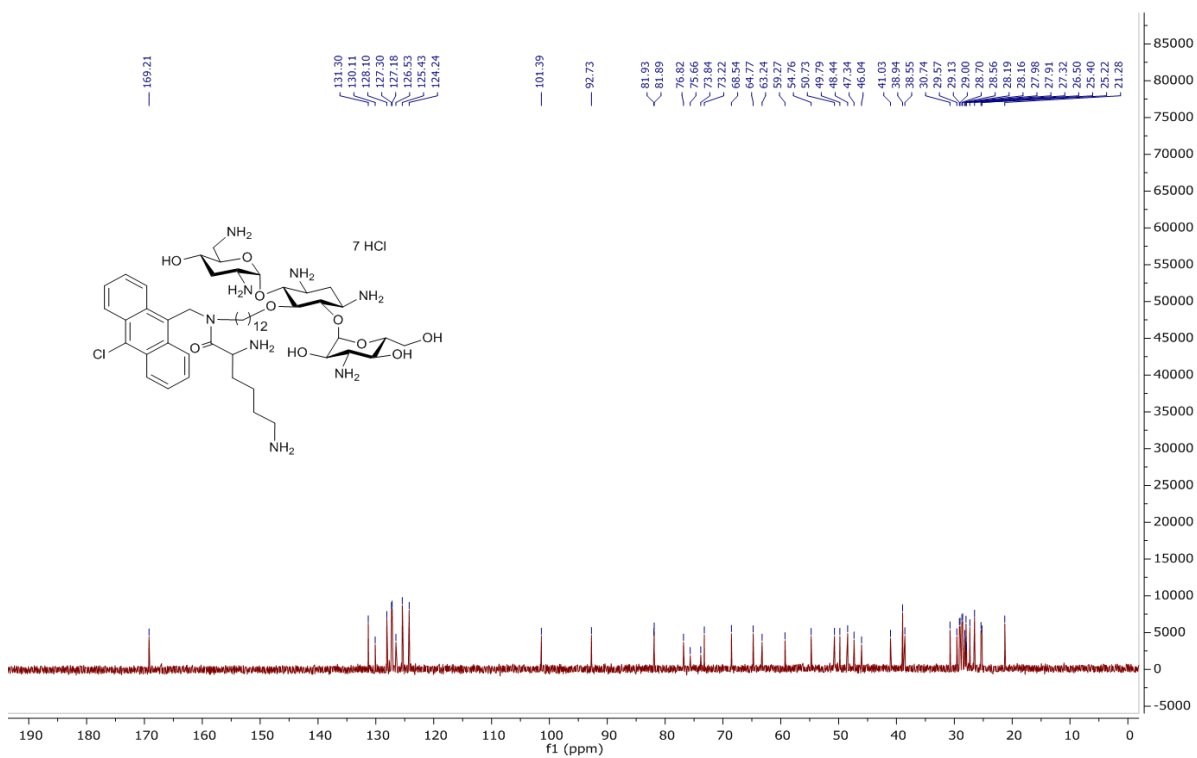
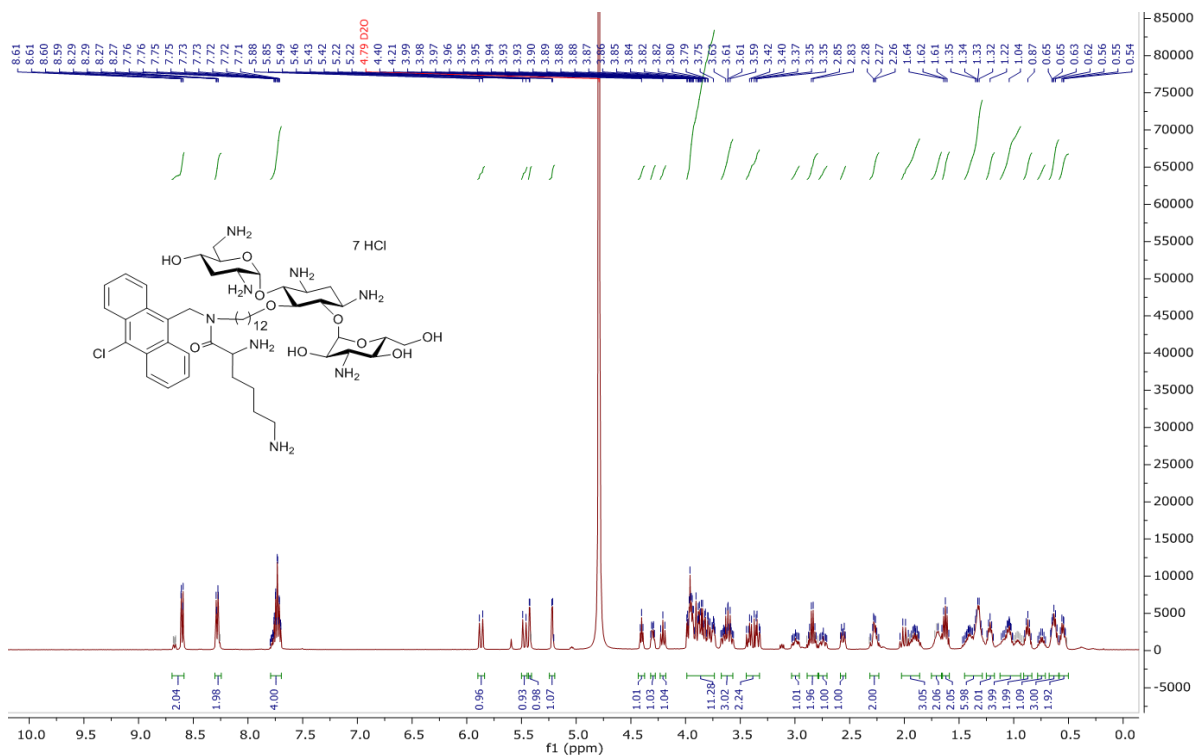
Appendix 8.  $^1\text{H}$  &  $^{13}\text{C}$  NMR spectra of compound **14a** in  $\text{CDCl}_3$ 

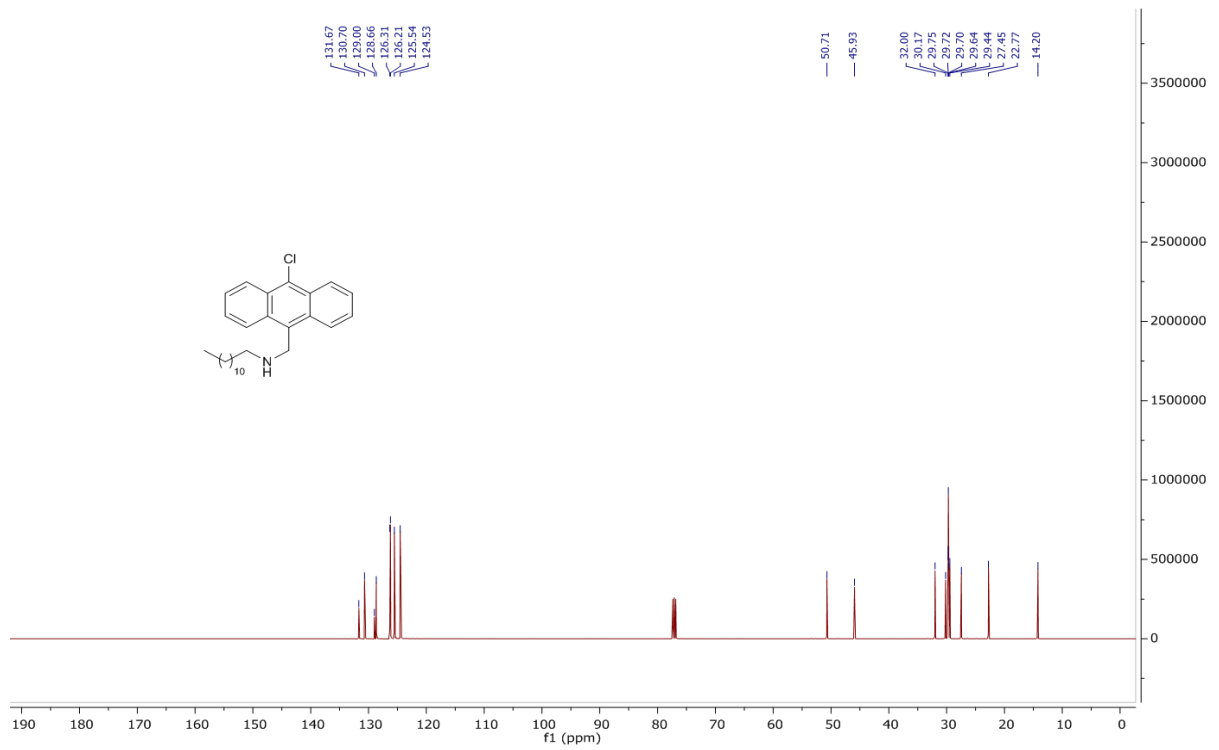
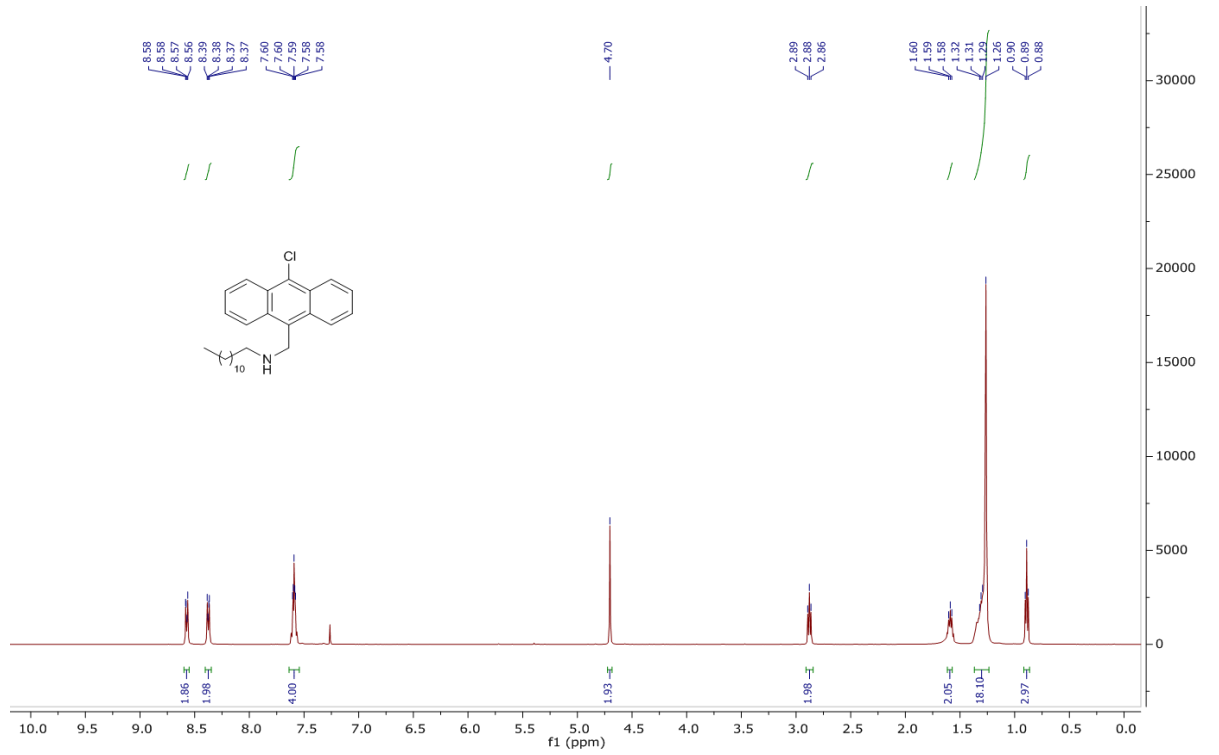
Appendix 9.  $^1\text{H}$  &  $^{13}\text{C}$  NMR spectra of compound **14b** in  $\text{CDCl}_3$ 

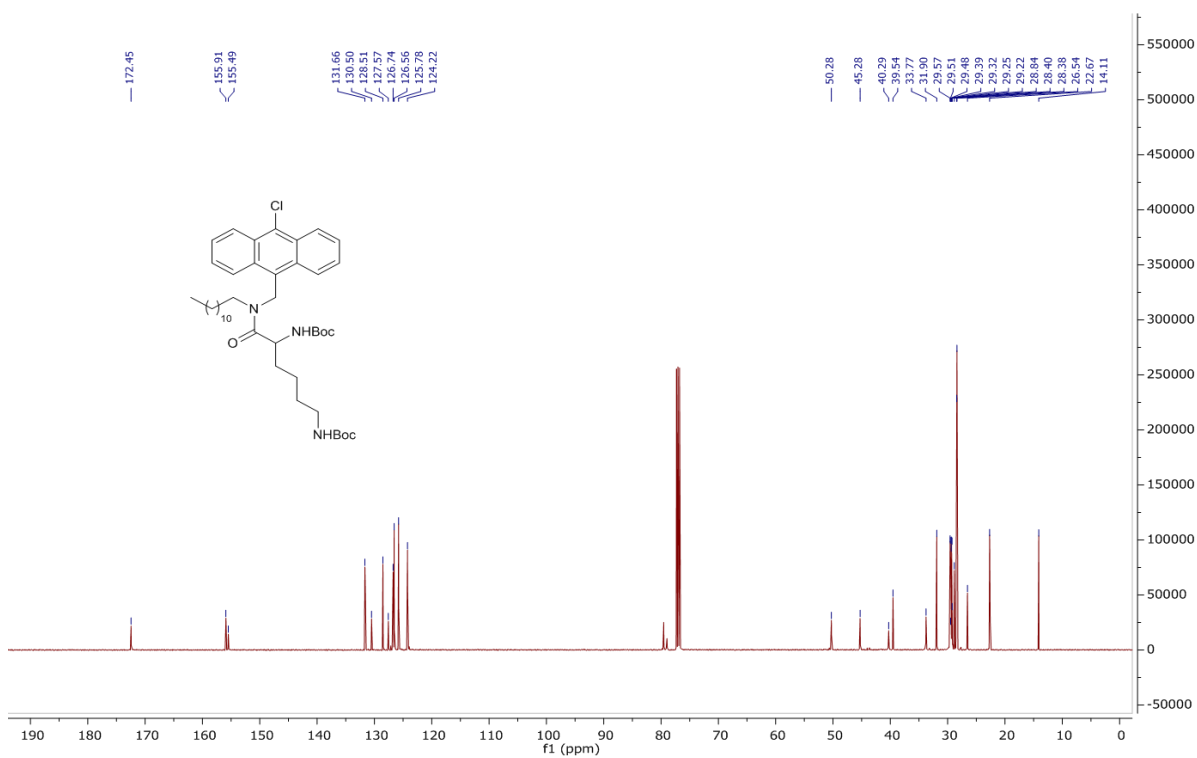
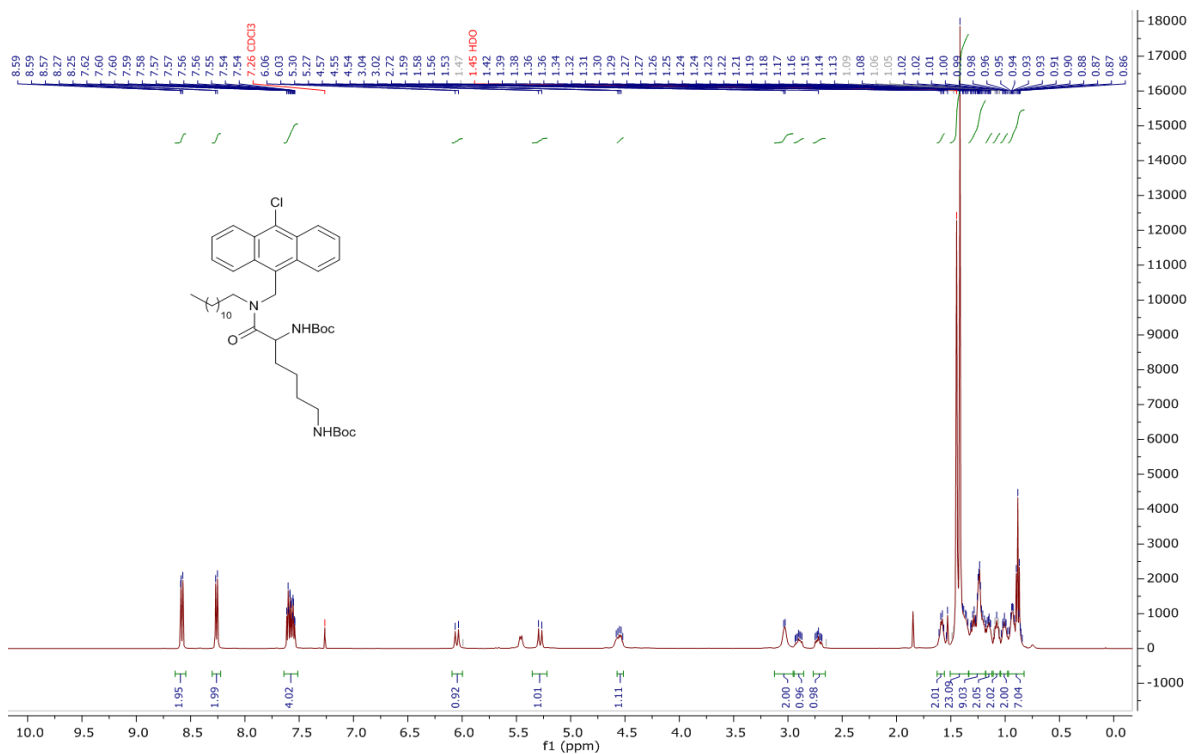
Appendix 10.  $^1\text{H}$  &  $^{13}\text{C}$  NMR spectra of compound **14c** in  $\text{CDCl}_3$ 

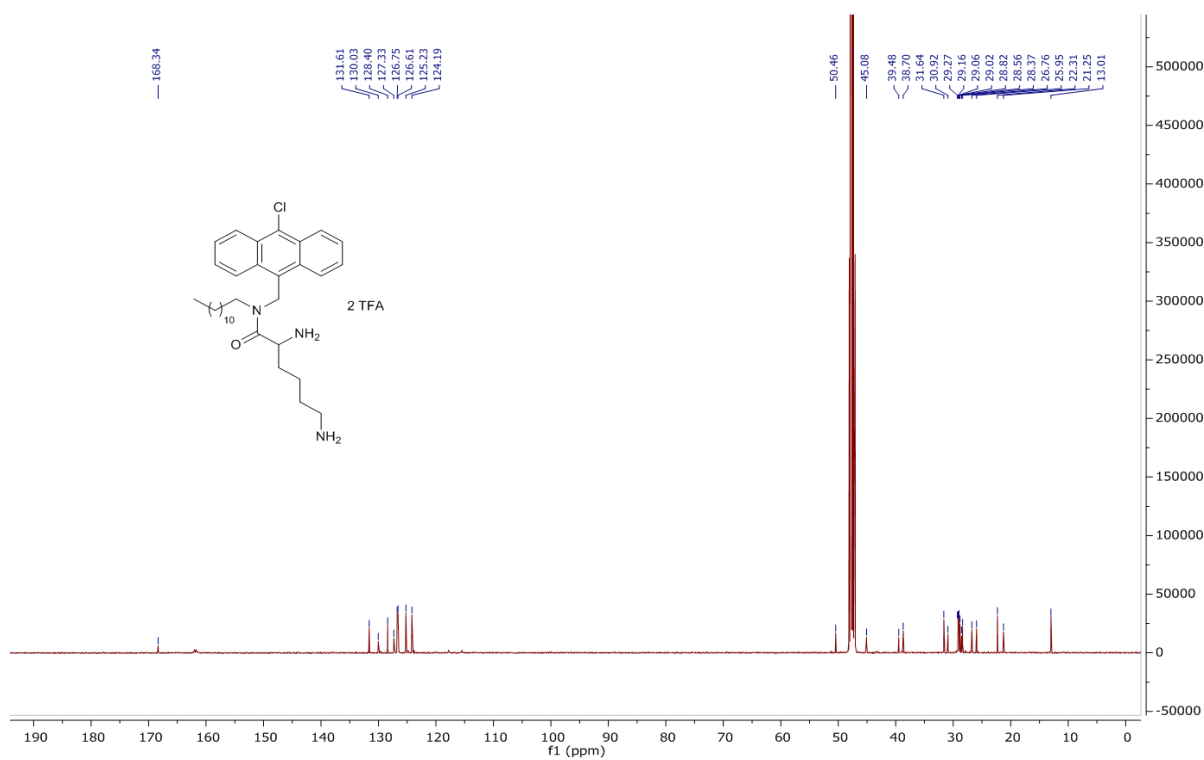
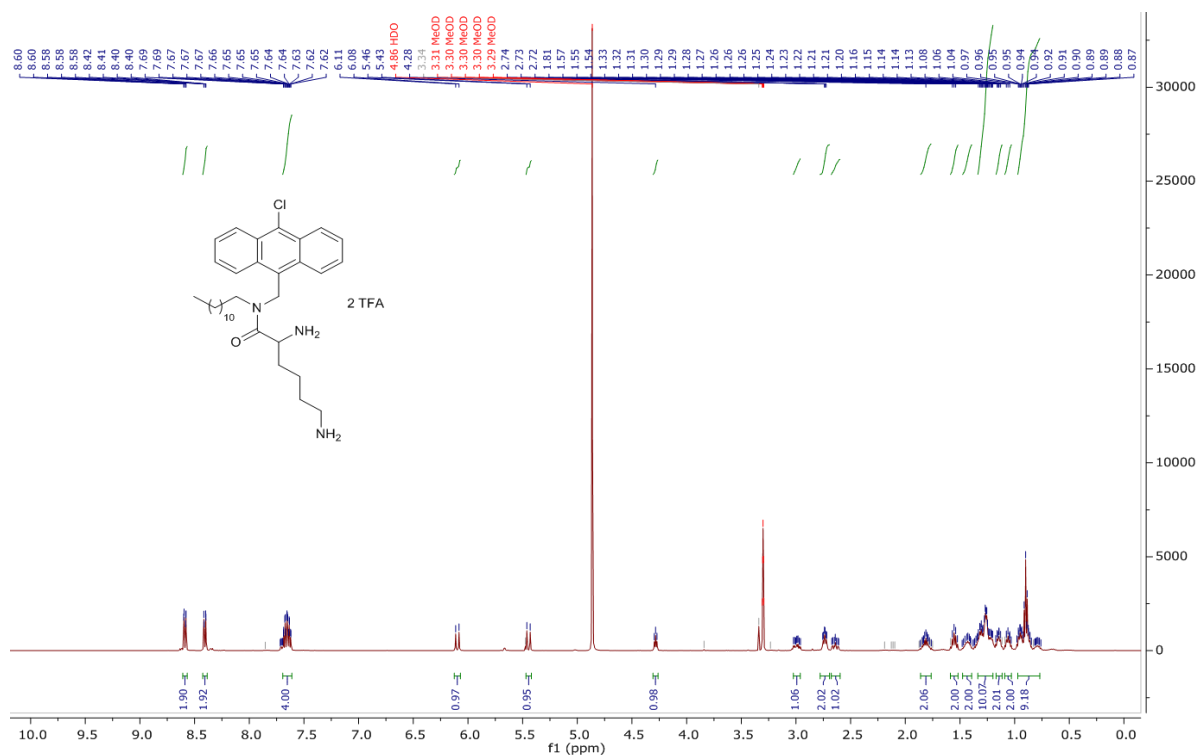
Appendix 11.  $^1\text{H}$  &  $^{13}\text{C}$  NMR spectra of compound **1** in  $\text{D}_2\text{O}$ 

Appendix 12.  $^1\text{H}$  &  $^{13}\text{C}$  NMR spectra of compound **2** in  $\text{D}_2\text{O}$ 

Appendix 13.  $^1\text{H}$  &  $^{13}\text{C}$  NMR spectra of compound **3** in  $\text{D}_2\text{O}$ 

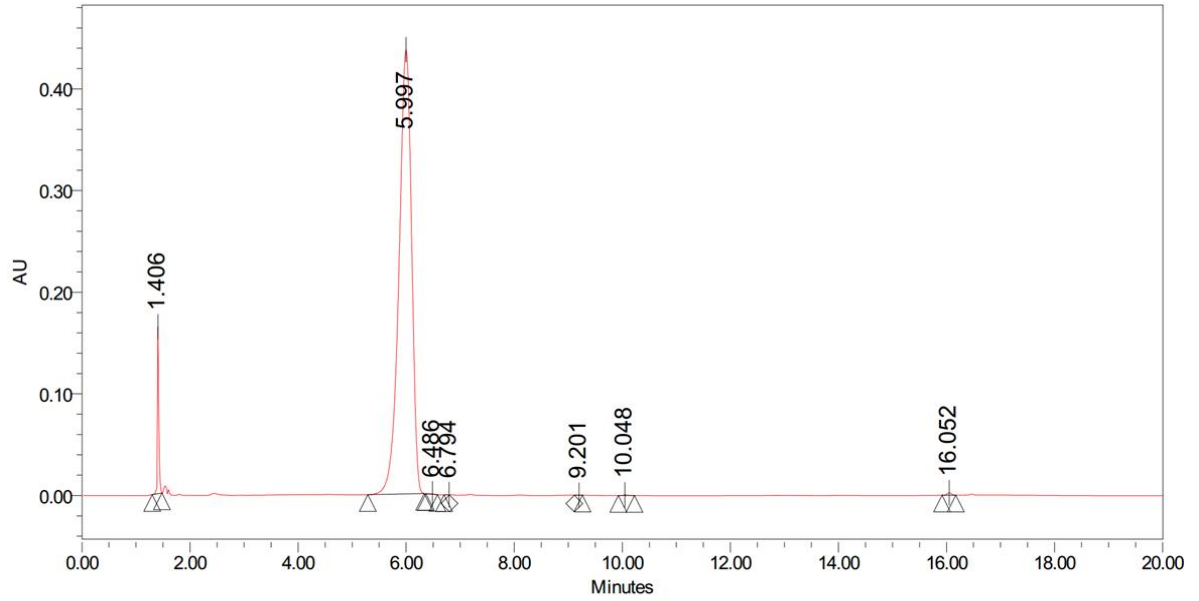
Appendix 14.  $^1\text{H}$  &  $^{13}\text{C}$  NMR spectra of compound **7** in  $\text{CDCl}_3$ 

Appendix 15.  $^1\text{H}$  &  $^{13}\text{C}$  NMR spectra of compound **8** in  $\text{CDCl}_3$ 

Appendix 16.  $^1\text{H}$  &  $^{13}\text{C}$  NMR spectra of compound **4** in  $\text{CDCl}_3$ 

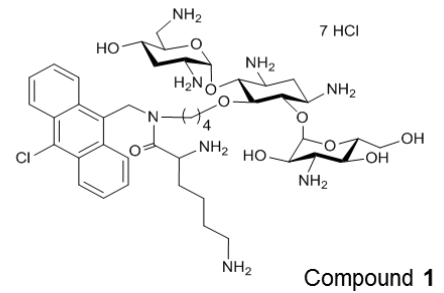
## 10.5 HPLC SPECTRA

## Appendix 17. HPLC spectra of compound 1



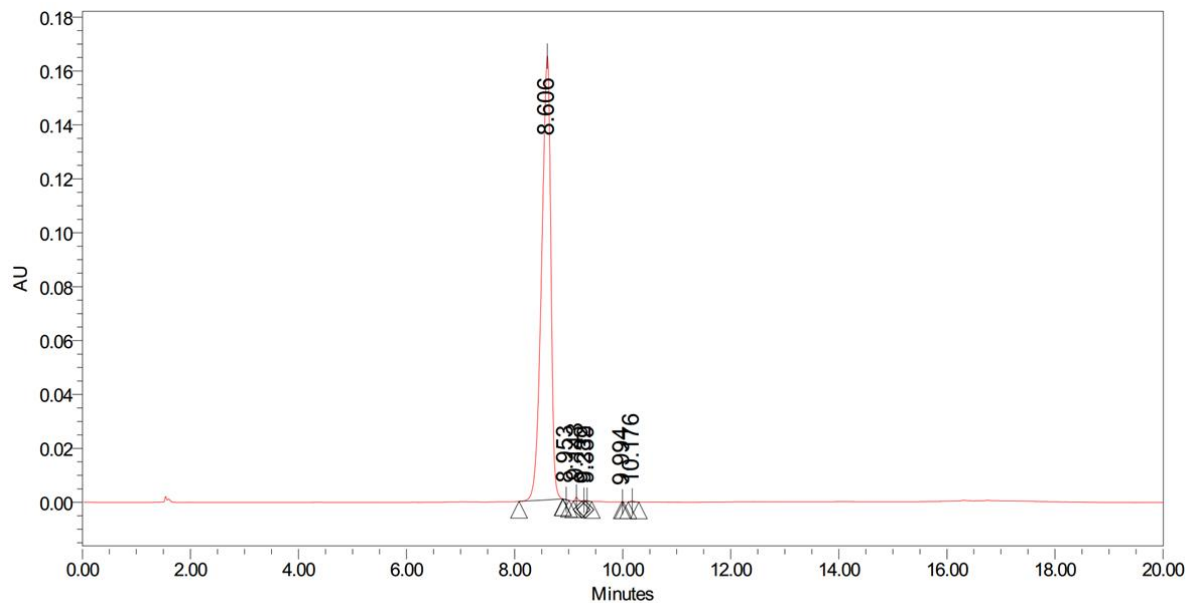
## Processed Channel: PDA 260.0 nm

	Processed Channel	Retention Time (min)	Area	% Area	Height
1	PDA 260.0 nm	1.406	289386	3.91	165087
2	PDA 260.0 nm	5.997	7090245	95.82	437026
3	PDA 260.0 nm	6.486	2211	0.03	371
4	PDA 260.0 nm	6.794	1075	0.01	319
5	PDA 260.0 nm	9.201	710	0.01	129
6	PDA 260.0 nm	10.048	4201	0.06	703
7	PDA 260.0 nm	16.052	11923	0.16	2372



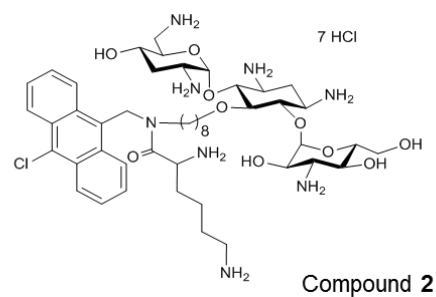
Compound 1

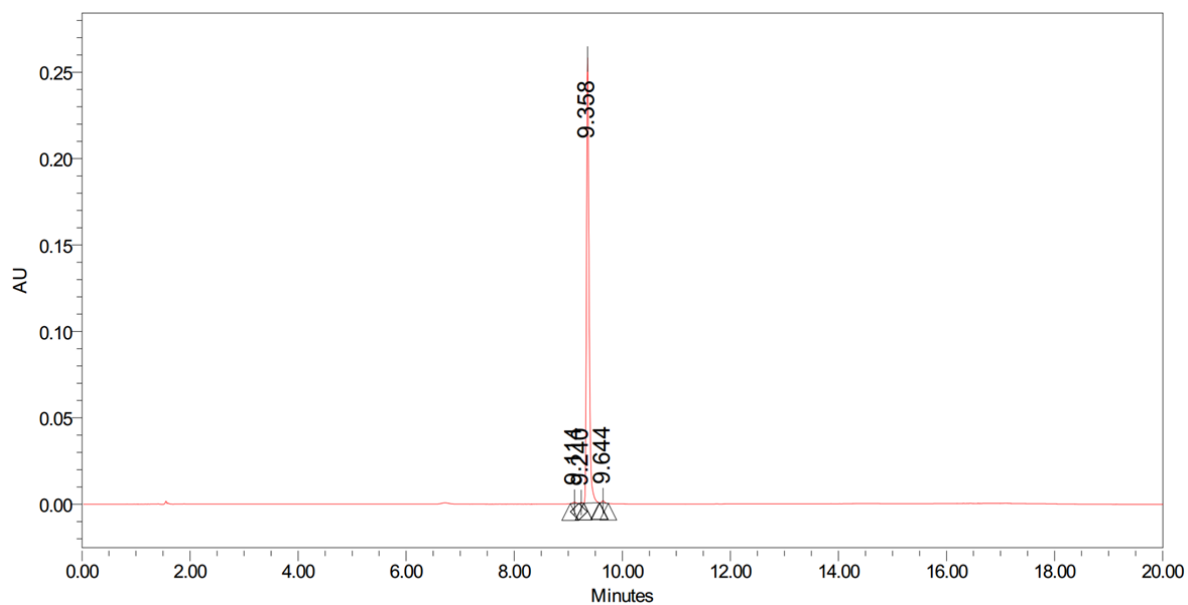
## Appendix 18. HPLC spectra of compound 2



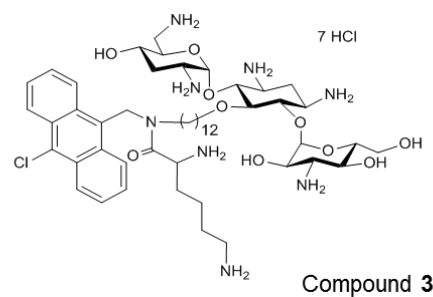
## Processed Channel: PDA 260.0 nm

	Processed Channel	Retention Time (min)	Area	% Area	Height
1	PDA 260.0 nm	8.606	1950731	99.50	164682
2	PDA 260.0 nm	8.953	494	0.03	153
3	PDA 260.0 nm	9.143	5066	0.26	1440
4	PDA 260.0 nm	9.282	1070	0.05	393
5	PDA 260.0 nm	9.339	1269	0.06	404
6	PDA 260.0 nm	9.994	18	0.00	23
7	PDA 260.0 nm	10.176	1835	0.09	392

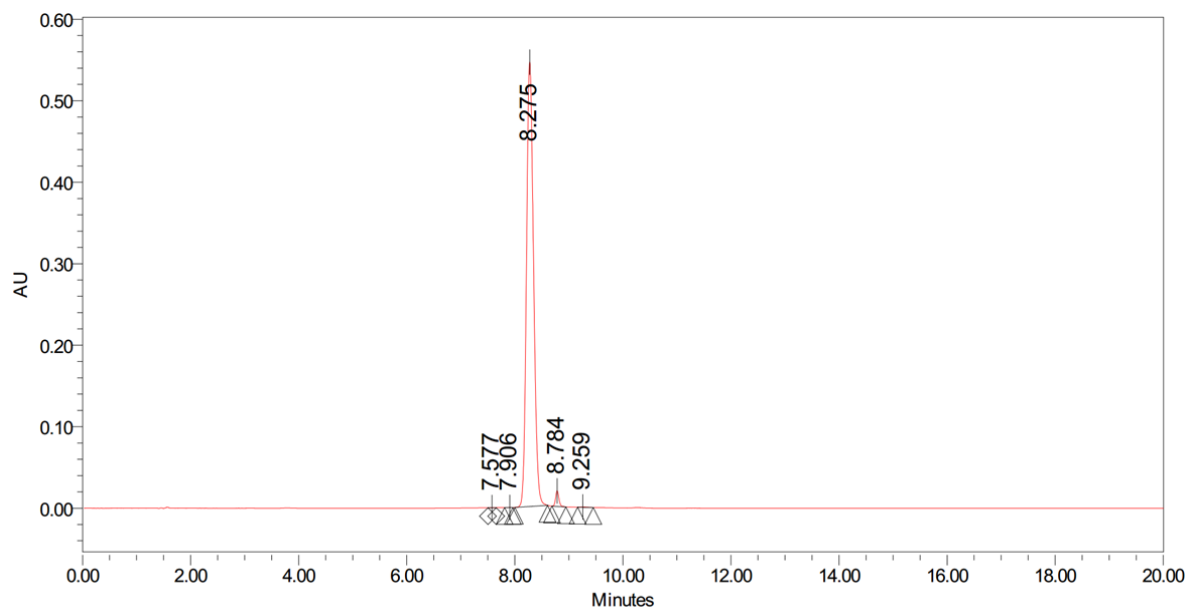


Appendix 19. HPLC spectra of compound **3****Processed Channel: PDA 260.0 nm**

	Processed Channel	Retention Time (min)	Area	% Area	Height
1	PDA 260.0 nm	9.114	3415	0.40	828
2	PDA 260.0 nm	9.240	1245	0.14	483
3	PDA 260.0 nm	9.358	851456	98.93	257802
4	PDA 260.0 nm	9.644	4541	0.53	1345

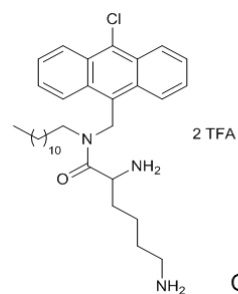


## Appendix 20. HPLC spectra of compound 4



## Processed Channel: PDA 260.0 nm

	Processed Channel	Retention Time (min)	Area	% Area	Height
1	PDA 260.0 nm	7.577	869	0.02	205
2	PDA 260.0 nm	7.906	647	0.01	193
3	PDA 260.0 nm	8.275	4925122	98.25	545545
4	PDA 260.0 nm	8.784	82137	1.64	19255
5	PDA 260.0 nm	9.259	3857	0.08	561



Compound 4

## Chapter 11: Supporting Information for Chapter 6

### 11.1 CHEMICAL SYNTHESSES

#### 11.1.1 Synthetic procedures and characterizations of moxifloxacin methyl ester and ciprofloxacin methyl ester

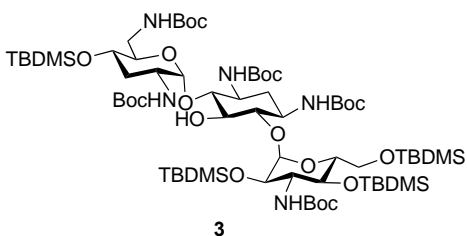
*General procedure of synthesis of moxifloxacin methyl ester and ciprofloxacin methyl ester.* To a stirred solution of moxifloxacin or ciprofloxacin (0.69 mmol) in methanol (30 mL) was added *p*-toluenesulfonic acid (215 mg, 1.13 mmol). The reaction mixture was refluxed for 24 h at 100 °C and then cooled it to room temperature. Methanol was removed via reduced pressure before saturated NaHCO<sub>3</sub> a.q. solution (100 mL) was added into the residue. The above solution was extracted with DCM (40 mL×3). The organic layer was dried over anhydrous sodium sulfate and evaporated under reduced pressure. The crude product was purified by flash chromatography (DCM:MeOH = 10:1 + 1% NH<sub>4</sub>OH to 5:1 + 1% NH<sub>4</sub>OH) to afford a pale yellow solid.

*Moxifloxacin methyl ester.* Yield: 260 mg (83%). <sup>1</sup>H NMR (500 MHz, Methanol-*d*<sub>4</sub>) δ 8.69 (s, 1H), 7.64 (d, *J* = 14.6 Hz, 1H), 4.14 – 4.06 (m, 1H), 4.01 – 3.90 (m, 2H), 3.86 (s, 3H), 3.64 (s, 3H), 3.62 – 3.56 (m, 1H), 3.49 – 3.43 (m, 2H), 3.07 – 3.00 (m, 1H), 2.75 – 2.67 (m, 1H), 2.43 – 2.34 (m, 1H), 1.89 – 1.82 (m, 2H), 1.81 – 1.70 (m, 1H), 1.62 – 1.53 (m, 1H), 1.29 – 1.21 (m, 1H), 1.15 – 1.04 (m, 2H), 0.97 – 0.87 (m, 1H). <sup>13</sup>C NMR (126 MHz, Methanol-*d*<sub>4</sub>, some carbons are doubling due to fluorine atom) δ 174.92, 174.90, 166.68, 154.64 (d, *J* = 248.9 Hz, C-F), 152.29, 142.18, 142.13, 138.06, 137.97, 135.20, 135.19, 121.67, 121.60, 109.73, 108.65,

108.46, 61.71, 58.39, 58.34, 57.22, 57.20, 53.95, 53.89, 52.02, 44.99, 41.15, 37.74, 37.73, 24.31, 22.74, 10.44, 9.37. MS (ESI)  $m/e$  calcd for  $C_{22}H_{27}FN_3O_4$   $[M+H]^+$ : 416.2, found: 416.7.

*Ciprofloxacin methyl ester*. Yield: 232 mg (72%).  $^1H$  NMR (300 MHz,  $CDCl_3$ )  $\delta$  8.32 (s, 1H), 7.68 (d,  $J = 13.4$  Hz, 1H), 7.14 (d,  $J = 7.1$  Hz, 1H), 3.74 (s, 3H, COO- $CH_3$ ), 3.37 (tt,  $J = 7.1$ , 4.0 Hz, 1H), 3.25 – 3.09 (m, 4H), 3.05 – 2.91 (m, 4H), 1.30 – 1.14 (m, 2H), 1.09 – 0.96 (m, 2H).  $^{13}C$  NMR (75 MHz,  $CDCl_3$ , some carbons are doubling due to fluorine atom)  $\delta$  173.14, 165.56, 154.87, 151.57, 148.20, 144.81, 144.67, 137.91, 122.33, 122.23, 112.64, 112.34, 109.16, 105.03, 104.99, 51.64, 50.36, 45.35, 34.70, 7.95. MS (ESI)  $m/e$  calcd for  $C_{18}H_{20}FN_3O_3$   $[M+H]^+$ : 346.1, found: 346.5.

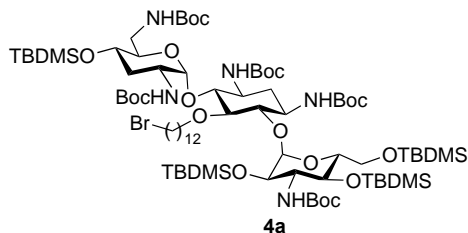
### 11.1.2 Synthetic procedures and characterizations of 3, 4a, 4b, 5, 6, 9



**1,3,2',6',3''-penta-N-(tert-butoxycarbonyl)-4',2'',4'',6''-tetra-O-TBDMS-tobramycin (3).** To a stirred solution of tobramycin (4.0 g, 8.6 mmol) in MeOH (80 mL) and  $H_2O$  (40 mL), triethylamine (27.2 mL, 188.3

mmol) and di-*tert*-butyl dicarbonate ( $(Boc)_2O$ ) (18.7 g, 85.6 mmol) were added at room temperature. The resultant reaction mixture was stirred at 55 °C overnight. It was then concentrated under reduced pressure to afford Boc-protected tobramycin as a white solid. Yield: 8.0 g (97%). To a stirred solution of this solid (8.0 g, 8.3 mmol) in anhydrous DMF (20 mL) under  $N_2$  gas, TBDMSCl (12.5 g, 83 mmol) and 1-methylimidazole (6.6 mL, 83 mmol) were added subsequently. The reaction mixture was stirred at room temperature for 4 days. Water (30 mL) was added into the mixture and extracted with ethyl acetate (30 mL $\times$ 3). The combined organic extracts were washed with saturated brine, dried over anhydrous sodium sulfate and

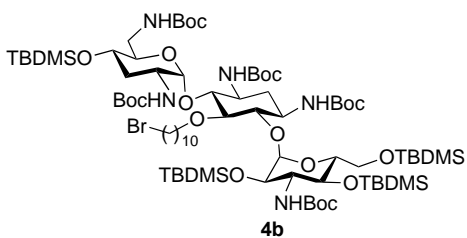
purified by flash chromatography (elution with a gradient of hexanes/ethyl acetate = from 20:1 to 3:1, v/v) to give **3** as a white solid. Yield: 10.6 g (90%).  $^1\text{H}$  NMR (500 MHz, chloroform-*d*)  $\delta$  5.04 – 4.81 (m, 2H, anomeric H), 3.95 – 3.79 (m, 3H), 3.79 – 2.98 (m, 13H), 2.78 – 2.66 (m, 1H), 2.03 – 1.94 (m, 1H), 1.70 – 1.32 (m, 47H), 0.96 – 0.79 (m, 36H), 0.17 – -0.02 (m, 24H).  $^{13}\text{C}$  NMR (126 MHz, chloroform-*d*)  $\delta$  156.27, 155.87, 155.56, 155.09, 154.61, 99.35 (anomeric C), 98.97 (anomeric C), 84.03, 81.83, 79.84, 79.49, 79.42, 78.92, 78.67, 76.05, 75.33, 72.90, 71.10, 68.72, 67.53, 63.19, 56.69, 51.06, 50.37, 49.62, 41.50, 34.75, 33.64, 28.57, 28.47, 28.43, 28.41, 26.12, 26.04, 25.96, 25.76, 18.47, 18.19, 18.11, 17.85, -3.53, -3.75, -4.17, -4.67, -4.87, -4.91, -4.99, -5.15. MS (ESI) *m/e* calcd for  $\text{C}_{67}\text{H}_{133}\text{N}_5\text{O}_{19}\text{Si}_4\text{Na}$   $[\text{M}+\text{Na}]^+$ : 1448.1, found: 1448.8.



**5-O-(12-bromododecyl)-1,3,2',6',3''-penta-N-(tert-butoxycarbonyl)-4',2'',4'',6''-tetra-O-TBDMS-tobramycin (4a).** Compound **3** (2.0 g, 1.4 mmol) was dissolved in anhydrous toluene (10 mL). 1,12-

Dibromododecane (1.39 g, 4.2 mmol) and a catalytic amount of tetrabutylammonium hydrogen sulfate (TBAHS) (48 mg, 0.14 mmol) were added into this solution subsequently, followed by KOH (237 mg, 4.2 mmol). This reaction mixture was stirred at room temperature under  $\text{N}_2$  gas overnight and then concentrated under reduced pressure. The residue was purified by flash chromatography (elution with a gradient of hexanes/ethyl acetate = from 10:1 to 4:1, v/v) to give the desired product as a white solid. Yield: 1.84 g (78%).  $^1\text{H}$  NMR (500 MHz, chloroform-*d*)  $\delta$  5.26 – 5.12 (m, 2H, anomeric H), 4.33 – 4.21 (m, 1H), 4.16 (d,  $J = 9.9$  Hz, 1H), 4.12 – 4.02 (m, 1H), 3.82 – 3.17 (m, 17H), 2.46 (d,  $J = 7.7$  Hz, 1H), 2.04 – 1.96 (m, 1H), 1.87 – 1.82 (m, 2H), 1.59 – 1.53 (m, 1H), 1.47 – 1.39 (m, 45H), 1.34 – 1.20 (m, 18H), 1.10 – 1.00 (m, 1H), 0.97 –

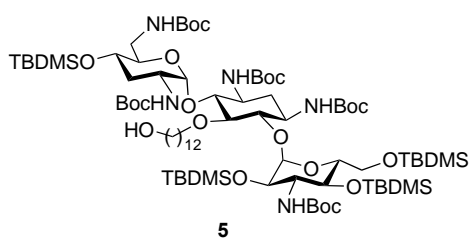
0.81 (m, 36H), 0.23 – -0.04 (m, 24H).  $^{13}\text{C}$  NMR (126 MHz, chloroform-*d*)  $\delta$  155.89, 155.67, 154.93, 154.88, 154.71, 97.94 (anomeric C), 96.68 (anomeric C), 85.87, 80.04, 79.99, 79.51, 79.35, 79.24, 75.45, 73.55, 72.85, 71.68, 68.16, 66.98, 63.49, 63.45, 63.25, 57.44, 50.67, 49.09, 48.52, 41.79, 36.79, 36.05, 35.79, 34.13, 33.97, 33.07, 33.01, 32.96, 30.77, 30.46, 30.17, 29.79, 29.70, 29.64, 29.58, 29.55, 29.53, 29.41, 29.30, 29.11, 28.94, 28.90, 28.87, 28.78, 28.66, 28.55, 28.34, 28.31, 28.29, 28.22, 26.31, 26.28, 26.16, 26.14, 25.93, 25.81, 24.83, 24.02, 23.57, 18.63, 18.48, 18.25, 18.06, -3.26, -3.65, -4.05, -4.73, -4.80, -4.93, -5.03, -5.08. MS (ESI) *m/e* calcd for  $\text{C}_{79}\text{H}_{156}\text{BrN}_5\text{O}_{19}\text{Si}_4\text{Na}$   $[\text{M}+\text{Na}]^+$ : 1695.4, found: 1695.5.



**5-O-(10-bromodocyl)-1,3,2',6',3''-penta-N-(tert-butoxycarbonyl)-4',2'',4'',6''-tetra-O-TBDMS-tobramycin (4b).** Compound **3** (713 mg, 0.5 mmol) was dissolved in anhydrous toluene (5 mL). 1,10-

Dibromodecane (450 mg, 1.5 mmol), a catalytic amount of tetrabutylammonium hydrogen sulfate (TBAHS) (0.05 mmol), and KOH (1.5 mmol) were added into this solution subsequently. This reaction mixture was stirred at room temperature under  $\text{N}_2$  gas overnight and then concentrated under reduced pressure. The residue was purified by flash chromatography (elution with a gradient of hexanes/ethyl acetate from 10:1 to 4:1) to give the desired product as a white solid. Yield: 666 mg (81%).  $^1\text{H}$  NMR (300 MHz, chloroform-*d*)  $\delta$  5.23 (d,  $J = 3.1$  Hz, 1H, anomeric H), 5.19 – 5.13 (m, 1H, anomeric H), 4.33 – 4.22 (m, 1H), 4.18 (d,  $J = 10.2$  Hz, 1H), 4.09 (d,  $J = 5.8$  Hz, 1H), 3.87 – 3.10 (m, 17H), 2.48 (d,  $J = 11.4$  Hz, 1H), 2.07 – 1.96 (m, 1H), 1.92 – 1.80 (m, 2H), 1.57 – 1.50 (m, 1H), 1.48 – 1.40 (m, 45H), 1.39 – 1.18 (m, 14H), 1.12 – 1.00 (m, 1H), 0.99 – 0.82 (m, 36H), 0.22 – -0.03 (m, 24H).  $^{13}\text{C}$  NMR (75 MHz, chloroform-*d*)  $\delta$

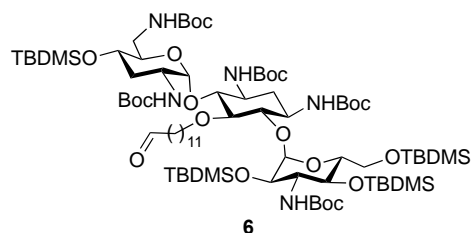
155.63, 155.55, 154.85, 154.77, 154.59, 97.87 (anomeric C), 96.54 (anomeric C), 85.78, 79.95, 79.63, 79.39, 79.24, 79.11, 77.45, 75.31, 73.37, 72.69, 71.56, 68.07, 66.88, 63.16, 63.13, 57.32, 50.57, 48.97, 48.38, 41.73, 36.66, 35.97, 35.90, 35.68, 33.99, 33.80, 32.88, 30.66, 30.43, 29.98, 29.72, 29.70, 29.65, 29.56, 29.47, 29.38, 28.80, 28.66, 28.53, 28.42, 28.20, 26.15, 26.02, 26.01, 25.80, 24.70, 23.45, 18.51, 18.35, 18.12, 17.93, -3.39, -3.77, -4.18, -4.86, -4.92, -5.06, -5.14, -5.20. MS (ESI)  $m/e$  calcd for  $C_{77}H_{152}BrN_5O_{19}Si_4Na$   $[M+Na]^+$ : 1667.3, found: 1667.4.



**5-O-(12-Hydroxydodecyl)-1,3,2',6',3''-penta-N-(tert-butoxycarbonyl)-4',2'',4'',6''-tetra-O-TBDMS-tobramycin (5).** DMF (45 mL) and H<sub>2</sub>O (3 mL) were added to a flask containing compound **4** (1.84 g, 1.1

mmol) and Cs<sub>2</sub>CO<sub>3</sub> (1.08 g, 3.3 mmol). The reaction mixture was heated to 75 °C and stirred for 12 h. Water (15 mL) was added and the resulting mixture was extracted with ethyl acetate (40 mL×3). The organic layer was washed with saturated brine and dried over anhydrous sodium sulfate. The solvent was removed *in vacuo* followed by purification using flash chromatography (elution with a gradient of hexanes/ethyl acetate = from 10:1 to 2:1, v/v) to give product **5** as a white solid. Yield: 1.19 g (67%). <sup>1</sup>H NMR (500 MHz, chloroform-*d*) δ 5.25 – 5.19 (m, 1H, anomeric H), 5.12 (m, 1H, anomeric H), 4.32 – 4.21 (m, 1H), 4.21 – 4.12 (m, 1H), 4.13 – 4.02 (m, 1H), 3.82 – 3.13 (m, 16H), 2.47 (d, *J* = 12.6 Hz, 1H), 2.06 – 1.95 (m, 1H), 1.62 – 1.52 (m, 3H), 1.52 – 1.38 (m, 48H), 1.38 – 1.17 (m, 17H), 0.98 – 1.13 (m, 1H), 1.00 – 0.78 (m, 36H), 0.21 – -0.02 (m, 24H). <sup>13</sup>C NMR (126 MHz, chloroform-*d*) δ 155.70, 155.52, 154.75, 154.70, 154.57, 97.85 (anomeric C), 96.52 (anomeric C), 85.73, 79.90, 79.22, 77.20, 75.29, 73.37, 72.65, 71.55, 68.01, 66.82, 63.11, 63.01, 57.27, 50.52, 48.95, 48.37, 41.67, 35.89, 35.63, 32.81, 30.61, 29.95,

29.57, 29.52, 29.38, 18.48, 18.32, 18.09, 17.91, -3.42, -3.80, -4.20, -4.89, -4.95, -5.09, -5.19, -5.24. MS (ESI)  $m/e$  calcd for  $C_{79}H_{157}N_5O_{20}Si_4Na$   $[M+Na]^+$ : 1632.5, found: 1632.5.

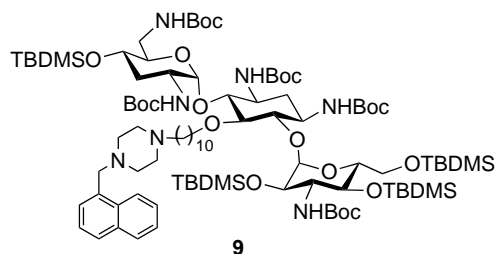


**5-O-(12-Dodecanal)-1,3,2',6',3''-penta-N-(tert-butoxycarbonyl)-4',2'',4'',6''-tetra-O-TBDMS-**

**tobramycin (6).** PCC (pyridinium chlorochromate, 477 mg, 2.2 mmol) and NaOAc (12 mg, 0.15 mmol) were added to

a stirred solution of compound **5** (1.19 g, 0.74 mmol) in dry DCM (25 mL). The reaction mixture was stirred at room temperature under  $N_2$  gas for 1 h. When a TLC analysis shows that the starting alcohol is consumed, the chromium species were removed by filtration through a pad of silica gel and washed with ethyl acetate. The collected organic phase was concentrated under reduced pressure to afford the crude which was then purified via flash chromatography (elution with a gradient of hexanes/ethyl acetate = 1:1 to 100% ethyl acetate, v/v) to give the desired aldehyde **6** as a white solid. Yield: 1.07 g (90%).  $^1H$  NMR (500 MHz, chloroform- $d$ )  $\delta$  9.74 (s, 1H, CHO), 5.24 – 5.15 (m, 1H, anomeric H), 5.16 – 5.10 (m, 1H, anomeric), 4.33 – 4.19 (m, 1H), 4.19 – 4.10 (m, 1H), 4.09 – 3.99 (m, 1H), 3.84 – 3.28 (m, 12H), 3.28 – 3.03 (m, 3H), 2.52 – 2.42 (m, 1H), 2.42 – 2.35 (m, 2H), 2.02 – 1.94 (m, 1H), 1.63 – 1.57 (m, 2H), 1.55 – 1.33 (m, 48H), 1.33 – 1.14 (m, 15H), 1.09 – 0.99 (m, 1H), 0.99 – 0.75 (m, 36H), 0.21 – -0.07 (m, 24H).  $^{13}C$  NMR (126 MHz, chloroform- $d$ )  $\delta$  202.8 (CHO), 155.67, 155.49, 154.70, 154.68, 154.53, 97.82 (anomeric C), 96.48 (anomeric C), 85.70, 79.85, 79.33, 79.17, 78.77, 75.25, 73.33, 72.64, 71.52, 67.99, 66.81, 63.08, 57.24, 50.50, 48.91, 48.34, 43.87, 41.64, 35.89, 35.61, 30.59, 29.97, 29.63, 29.58, 29.56, 29.39, 29.31, 29.15, 28.80 – 28.17, 26.28 – 25.50, 22.06, 18.45, 18.30, 18.07, 17.88,

-3.45, -3.82, -4.23, -4.92, -4.98, -5.11, -5.21, -5.27. MS (ESI)  $m/e$  calcd for  $C_{79}H_{155}N_5O_{20}Si_4Na$   $[M+Na]^+$ : 1630.5, found: 1630.9.



**5-O-((10-(4-(naphthalen-1-ylmethyl)piperazin-1-yl)docyl)-1,3,2',6',3''-penta-N-(tert-butoxycarbonyl)-4',2'',4'',6''-tetra-O-TBDMS-tobramycin (9).** 1-(1-

Naphthylmethyl)-piperazine (NMP) (68 mg, 0.3 mmol) and  $K_2CO_3$  (83 mg, 0.6 mmol) were subsequently added to stirred solutions of compound **4b** (329 mg, 0.2 mmol) in anhydrous DMF (5 mL) under  $N_2$  gas. The reaction mixture was heated to 75 °C and stirred for 8 h. The solvent was removed *in vacuo* followed by purification using a flash chromatography (elution with hexanes/ethyl acetate from 8:1 to 1:2) to afford the desired compounds **9** as a white solid. Yield: 179 mg (50%).  $^1H$  NMR (500 MHz, chloroform-*d*)  $\delta$  8.32 – 8.24 (m, 1H), 7.83 (dd,  $J = 7.7, 1.7$  Hz, 1H), 7.75 (d,  $J = 8.0$  Hz, 1H), 7.54 – 7.34 (m, 4H), 5.27 – 5.18 (m, 1H, anomeric H), 5.18 – 5.12 (m, 1H, anomeric H), 4.33 – 4.21 (m, 1H), 4.20 – 4.12 (m, 1H), 4.12 – 4.02 (m, 1H), 3.90 (s, 2H), 3.86 – 3.05 (m, 15H), 2.71 – 2.35 (m, 8H), 2.35 – 2.27 (m, 2H), 2.05 – 1.96 (m, 1H), 1.65 – 1.35 (m, 50H), 1.35 – 1.13 (m, 13H), 1.00 – 0.78 (m, 36H), 0.20 – -0.04 (m, 24H).  $^{13}C$  NMR (126 MHz, chloroform-*d*)  $\delta$  155.72, 155.58, 155.52, 154.73, 154.55, 134.14, 133.79, 132.55, 128.30, 127.79, 127.28, 125.62, 125.50, 125.07, 124.76, 97.83 (anomeric C), 96.52 (anomeric C), 85.71, 79.89, 79.36, 79.20, 75.27, 73.37, 72.67, 71.53, 68.00, 66.82, 63.09, 61.21, 61.07, 60.34, 58.84, 57.27, 53.32, 53.29, 52.97, 50.52, 48.95, 48.36, 43.76, 41.66, 36.69, 35.90, 35.63, 30.63, 30.03, 29.69, 29.64, 29.62, 28.63, 28.50, 28.48, 28.40, 27.70, 26.91, 26.19, 26.13, 26.01, 25.98, 25.92, 25.78, 24.73, 22.62, 21.01, 18.48, 18.32, 18.09, 17.91, -3.43, -3.80, -4.20, -4.88, -4.95, -5.08, -5.18, -5.24. MS (ESI)  $m/e$  calcd for  $C_{92}H_{170}N_7O_{19}Si_4$   $[M+H]^+$ : 1790.7, found: 1790.5.

## 11.2 HPLC ANALYSIS

### 11.2.1 HPLC Methodology

**Method:** Synergi 4  $\mu\text{m}$  Plolar-RP 80 Å LC column (50  $\times$  4.6 mm, Phenomenex); flow: 0.7 mL/min; buffer A: 0.1% TFA in water; buffer B: 0.1% TFA in acetonitrile; see Table 2.1.1 for gradient used; run time: 30 min; UV detection at 295 nm.

**Table 11.2.1.1.** HPLC methodology

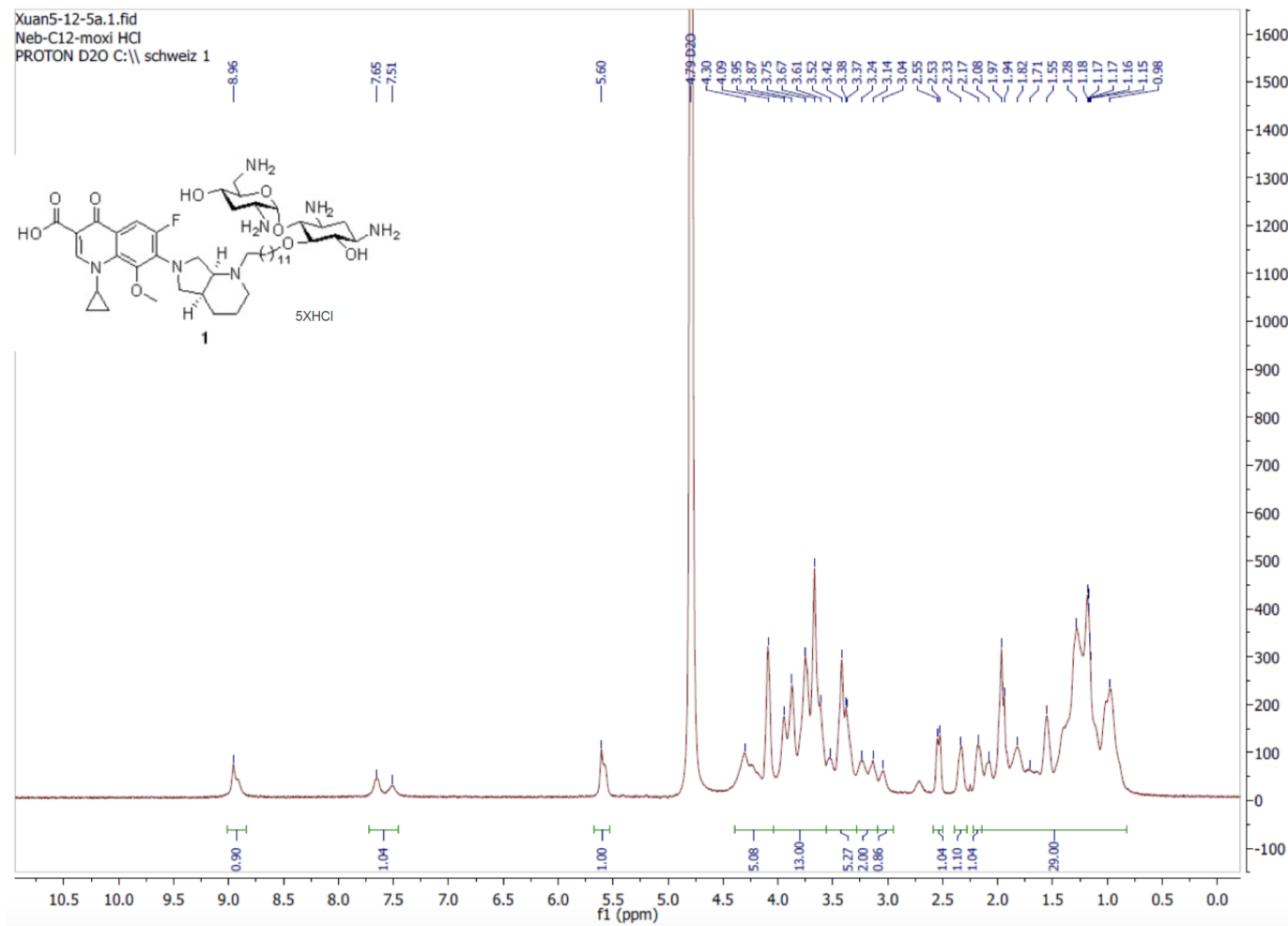
Time duration (min)	% Buffer A	% Buffer B
0.01	95	5
5	95	5
8	80	20
10	80	20
12	70	30
15	70	30
17	60	40
19	60	40
20	50	50
22	50	50
23	70	30
27	95	5
30	95	5

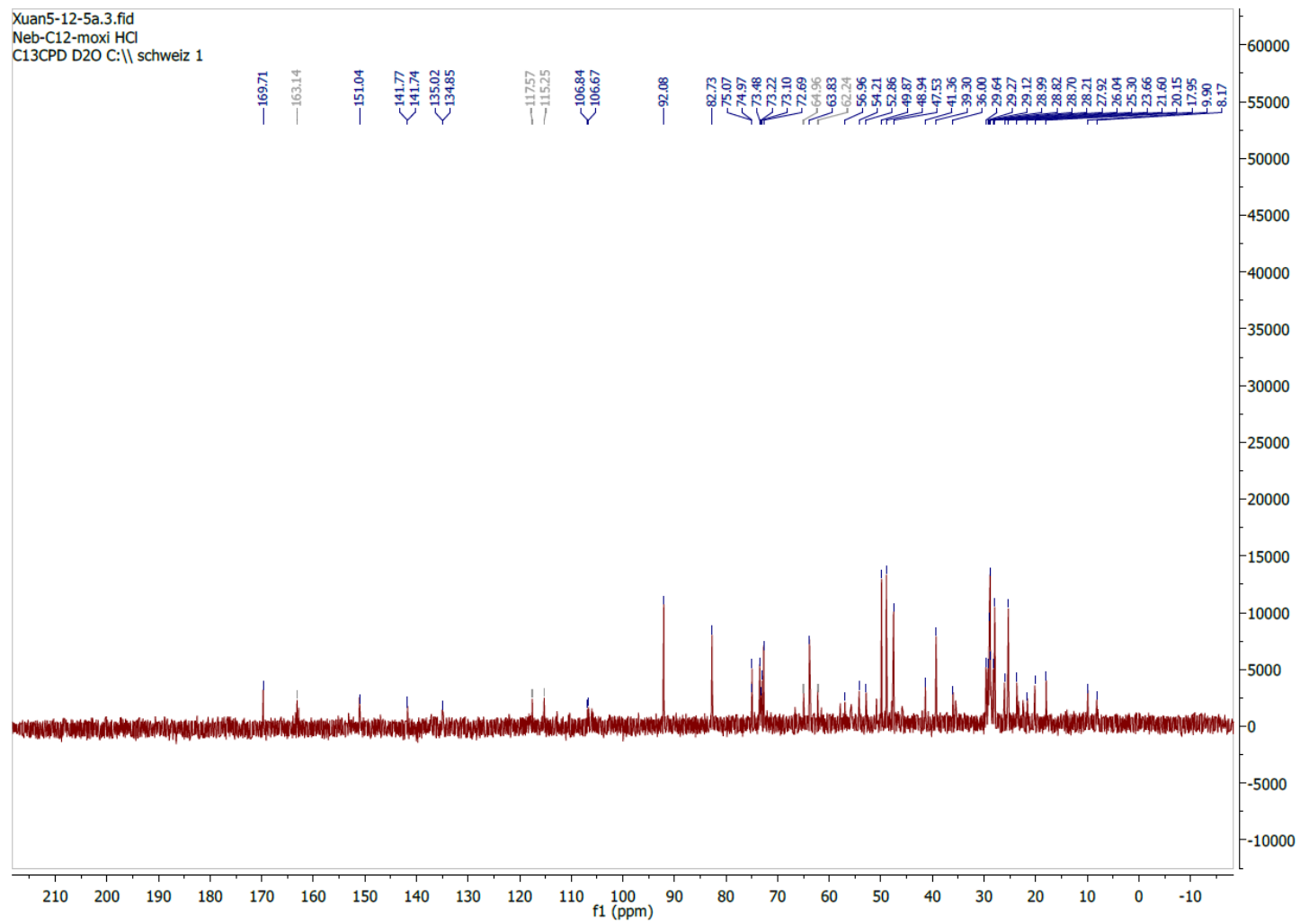
### 11.2.2 Purity determination of final compound using HPLC

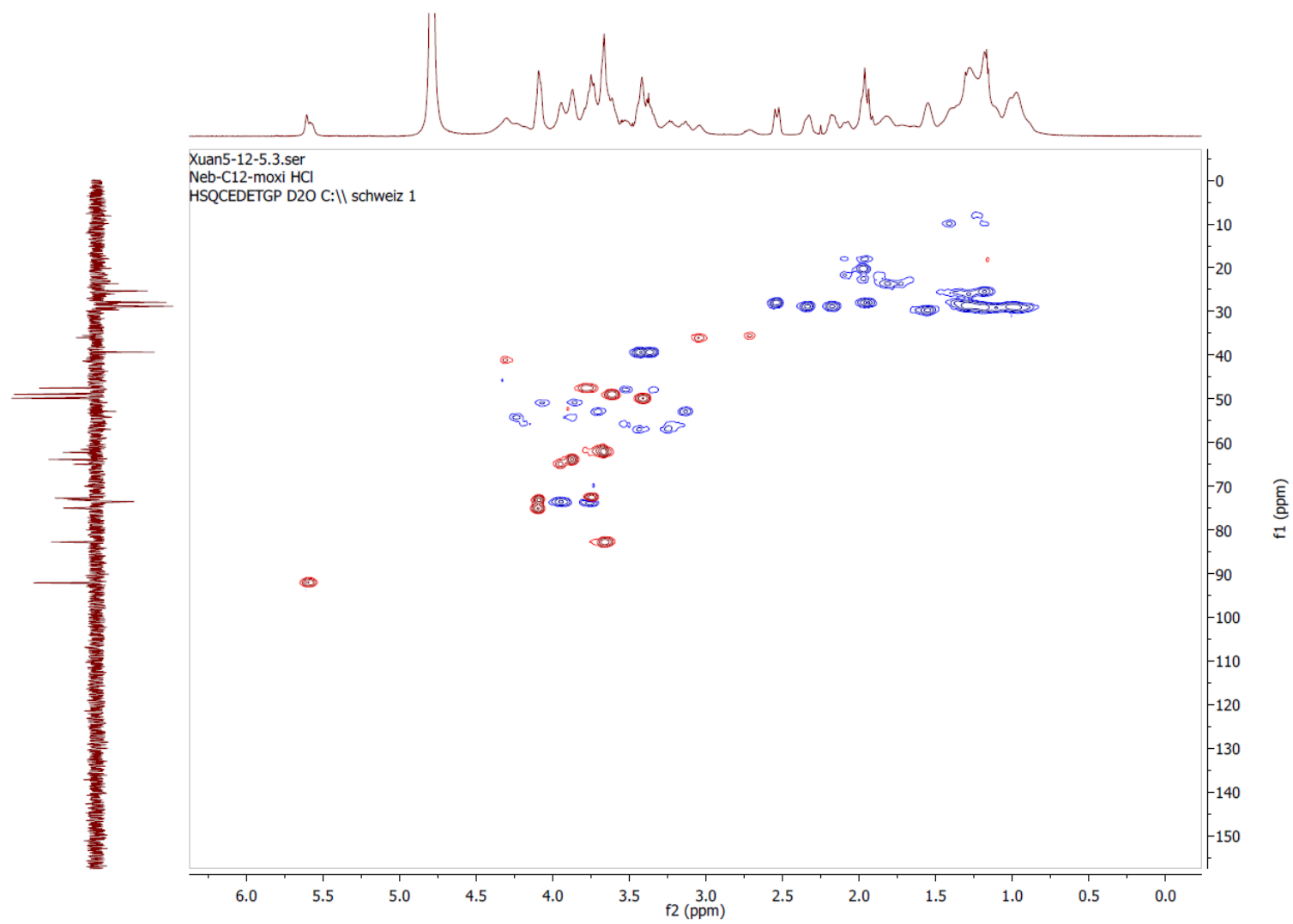
**Table 11.2.2.1.** Purity determination of final compounds

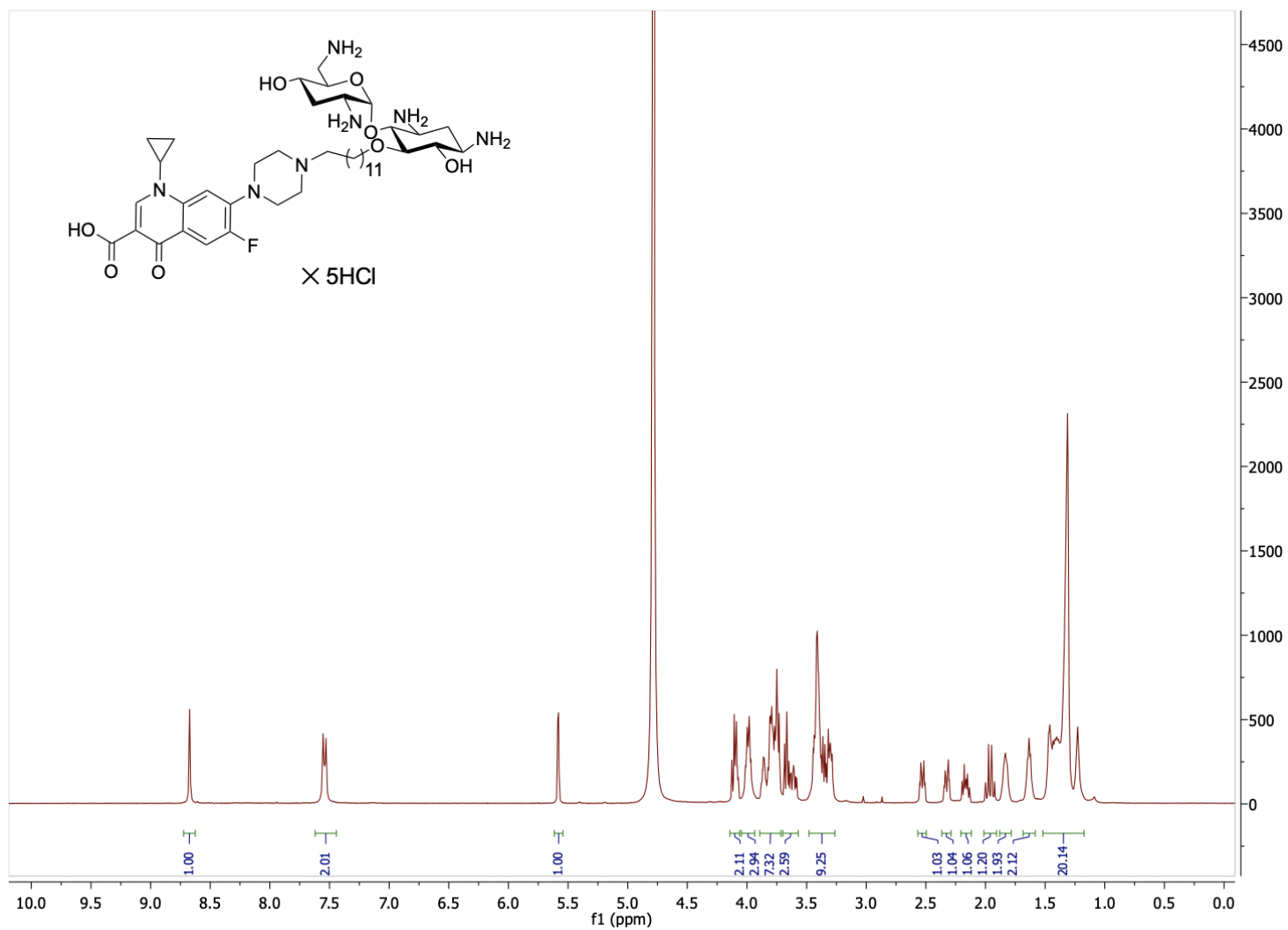
Compound	Retention Time (min)	% Purity
<b>1a</b>	14.585	95.02
<b>1b</b>	14.945	95.46
<b>2</b>	12.917	99.87

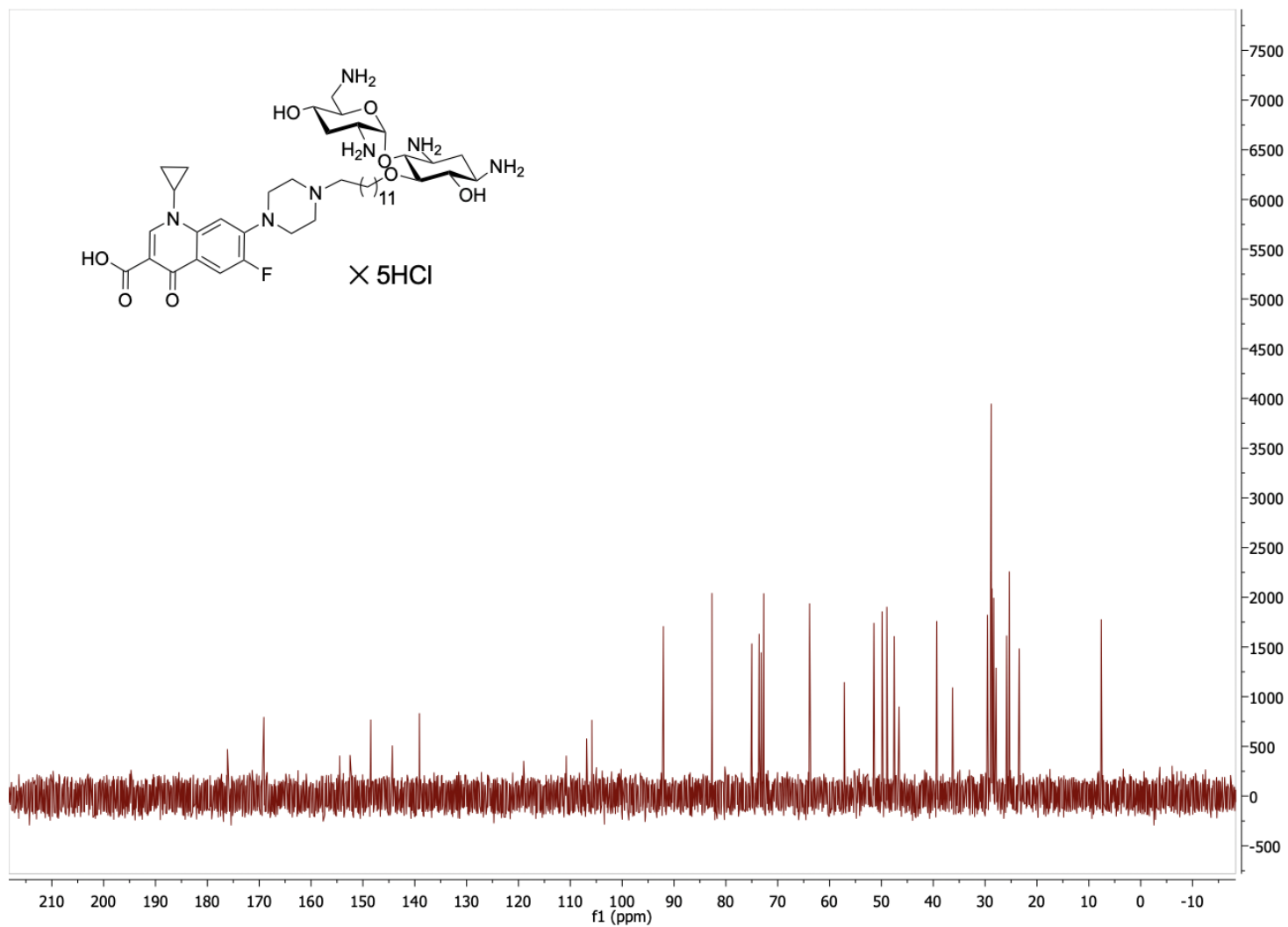
## 11.3 NMR SPECTRA

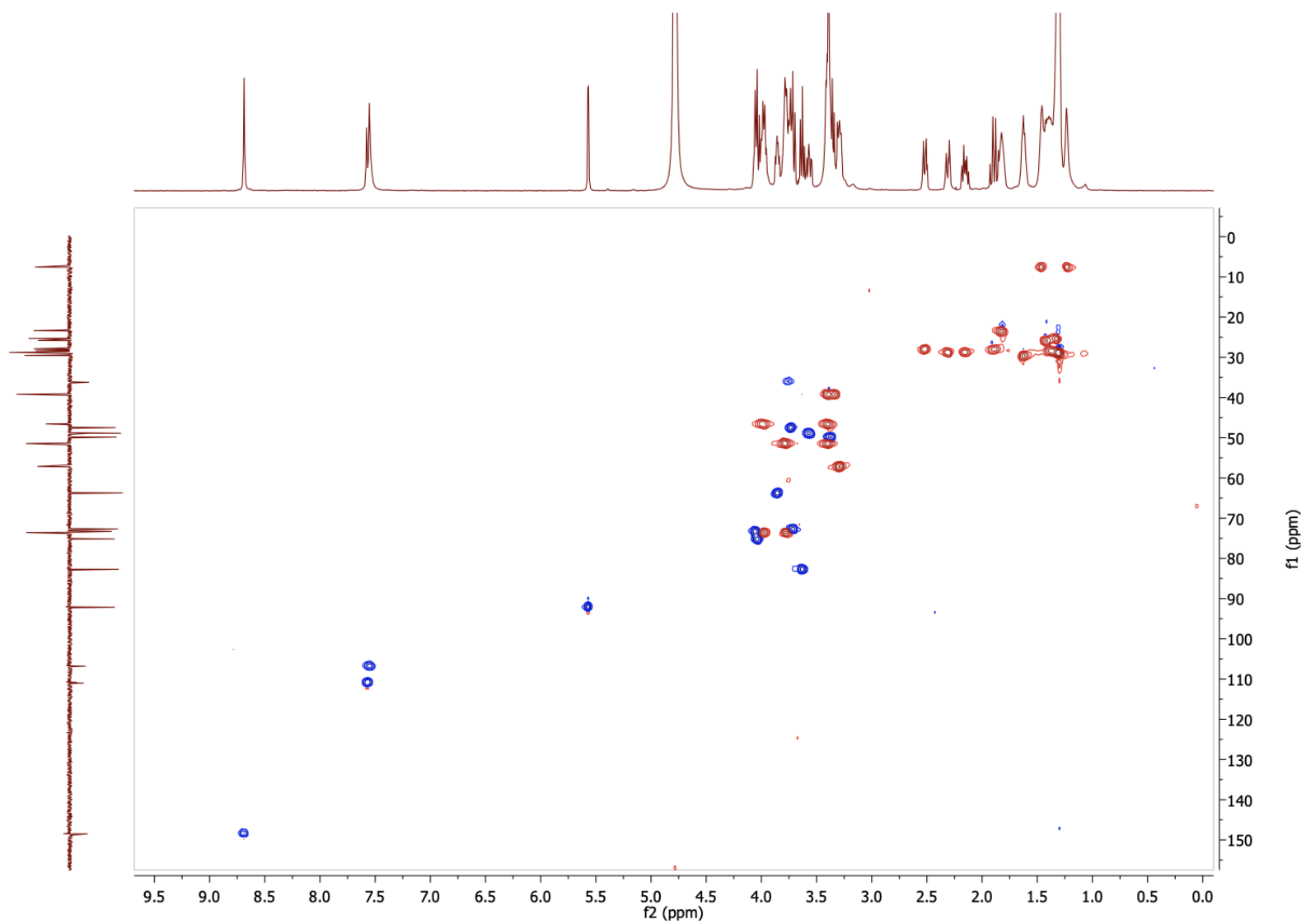
Appendix 1.  $^1\text{H}$  spectrum of NEB-MOX **1a** in  $\text{D}_2\text{O}$ 

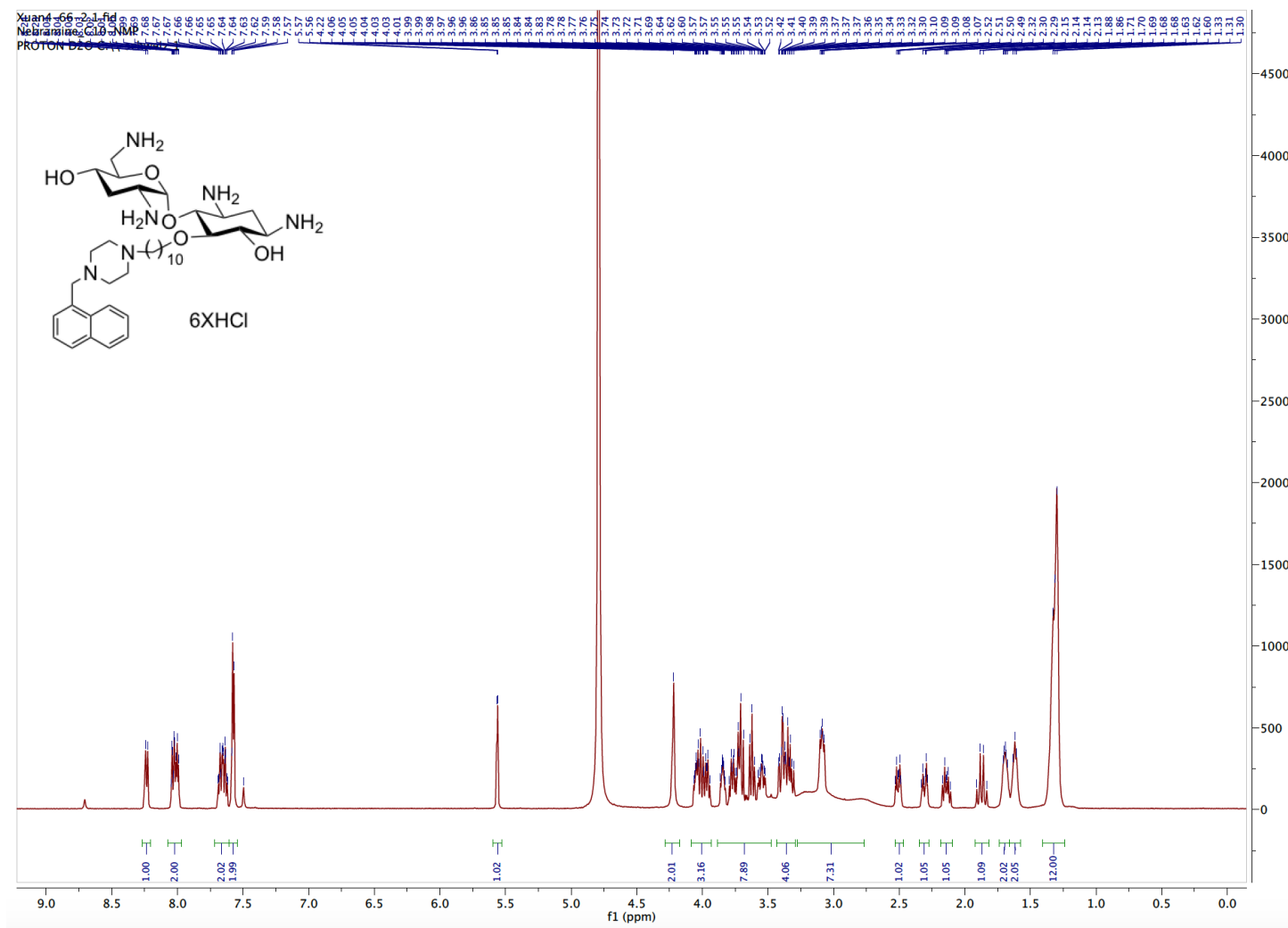
Appendix 2.  $^{13}\text{C}$  spectrum of NEB-MOX **1a** in  $\text{D}_2\text{O}$ 

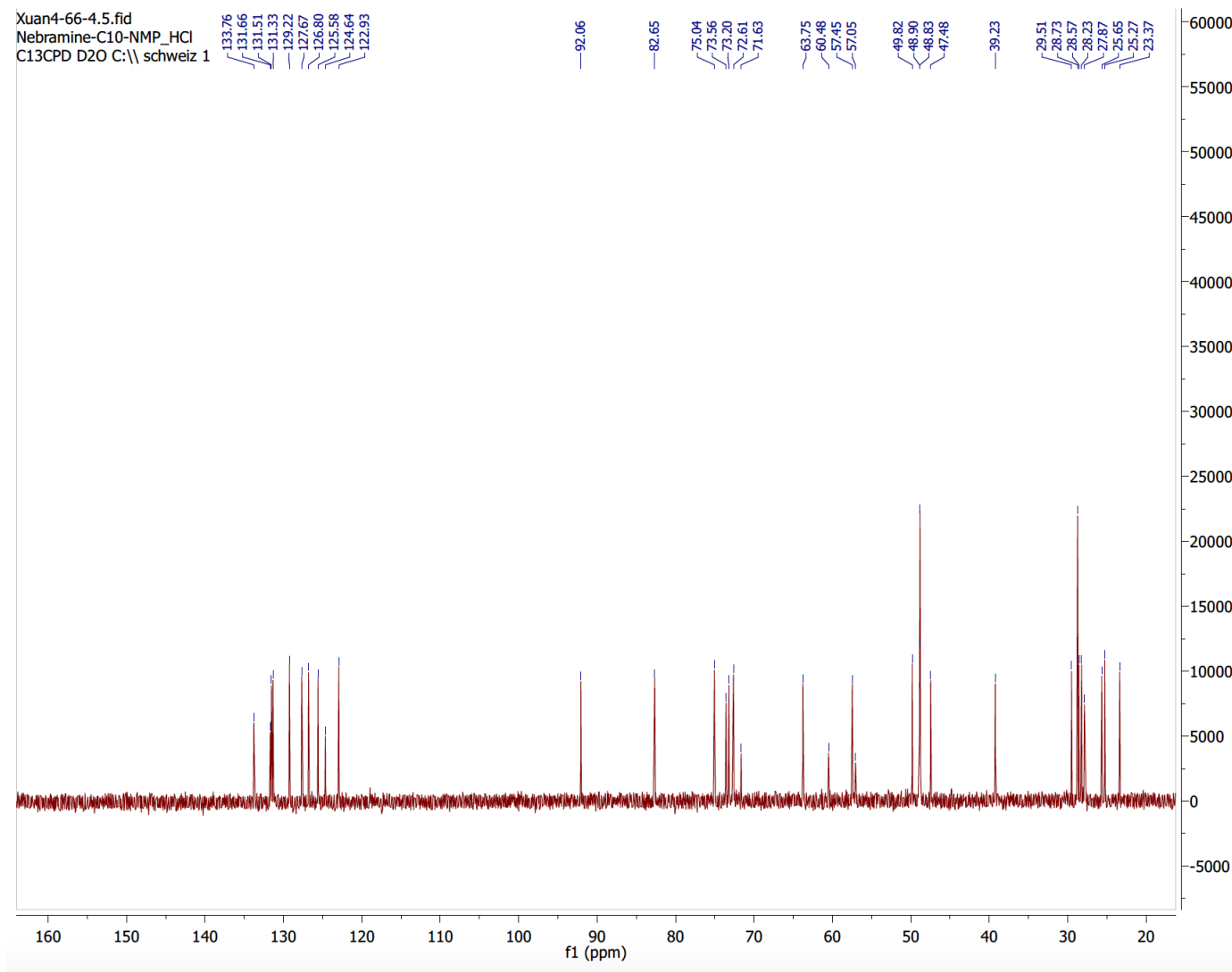
Appendix 3. HSQC spectrum of NEB-MOX **1a** in D<sub>2</sub>O

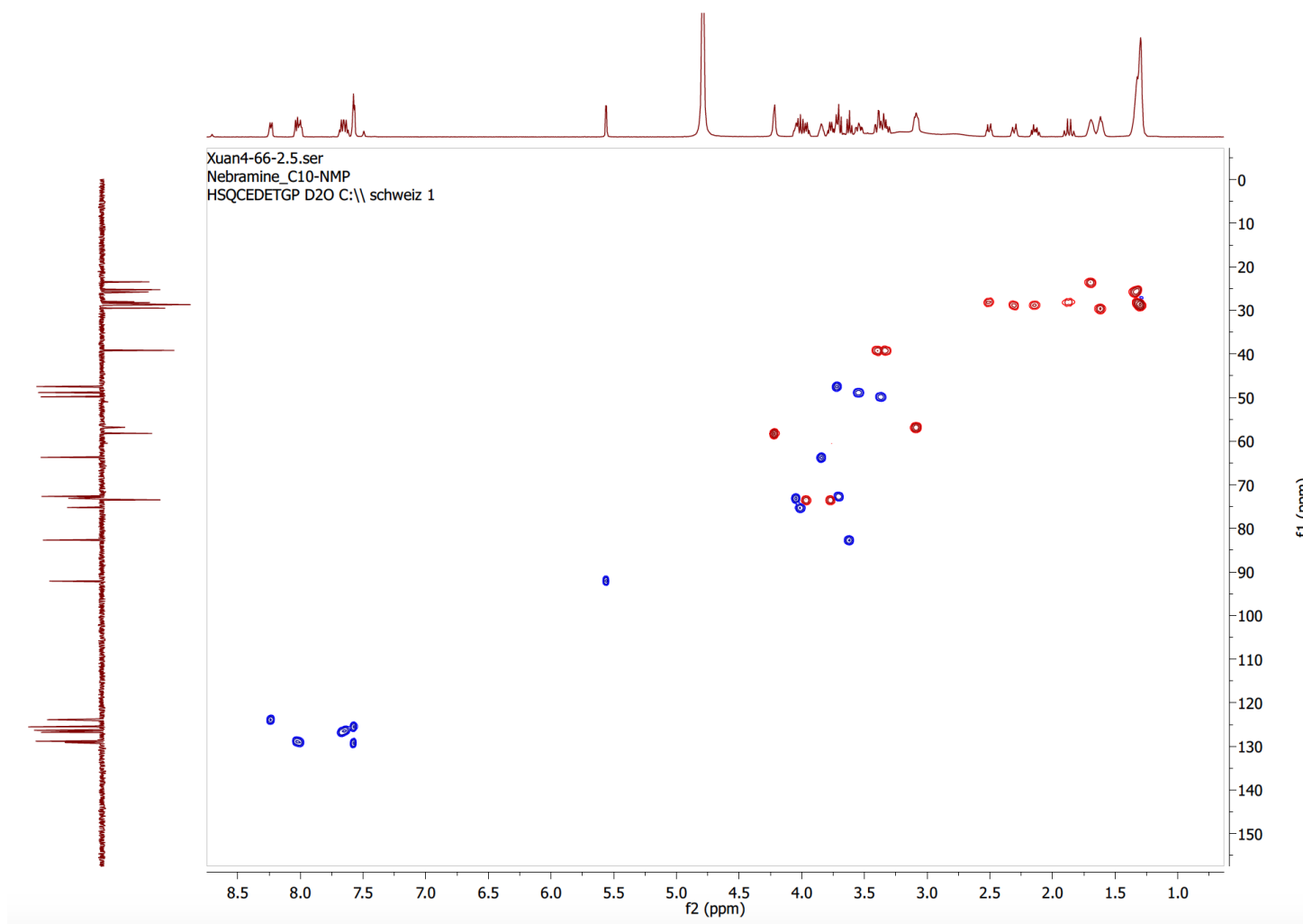
Appendix 4.  $^1\text{H}$  spectrum of NEB-CIP **1b** in  $\text{D}_2\text{O}$ 

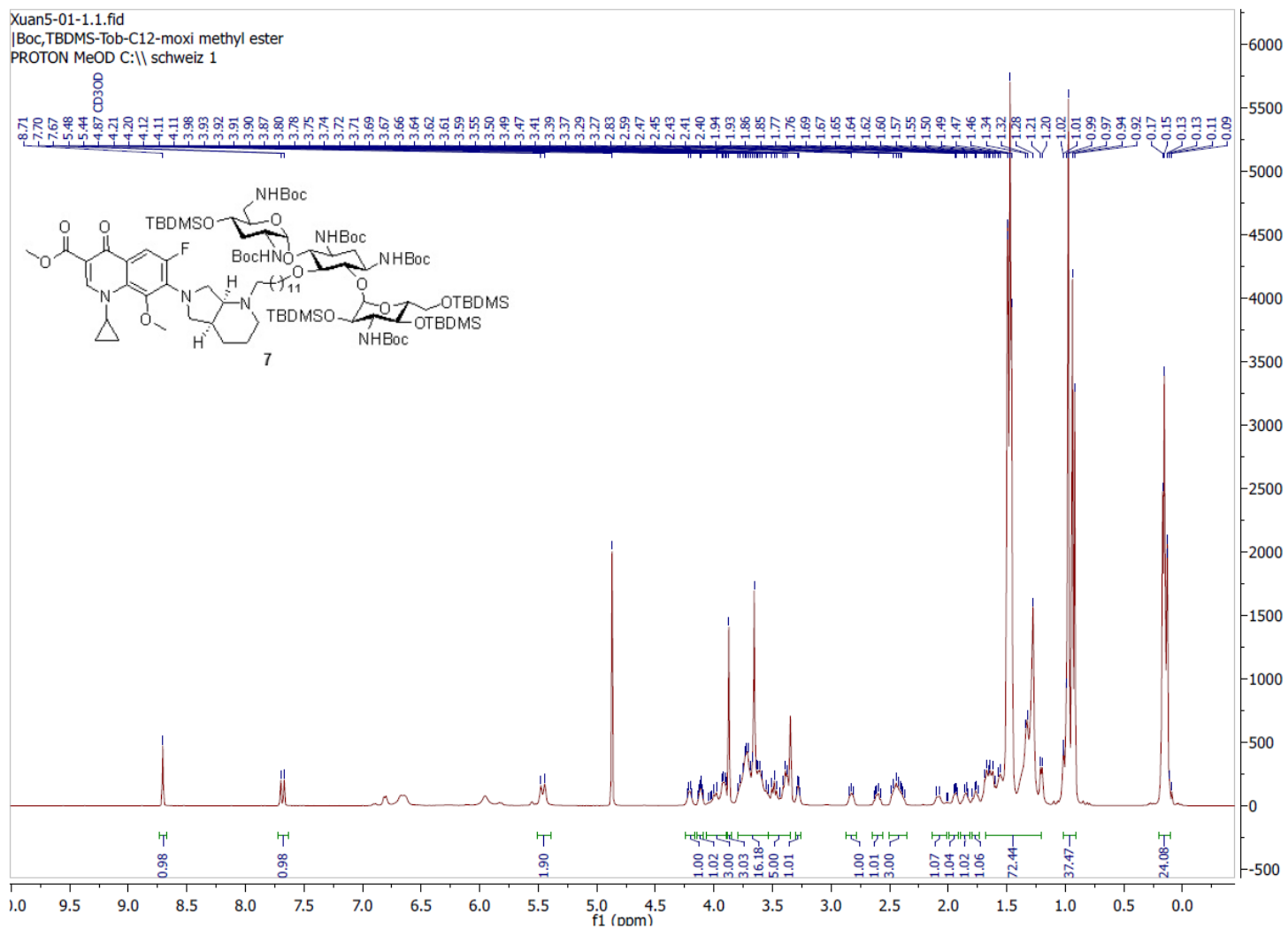
Appendix 5.  $^{13}\text{C}$  spectrum of NEB-CIP **1b** in  $\text{D}_2\text{O}$ 

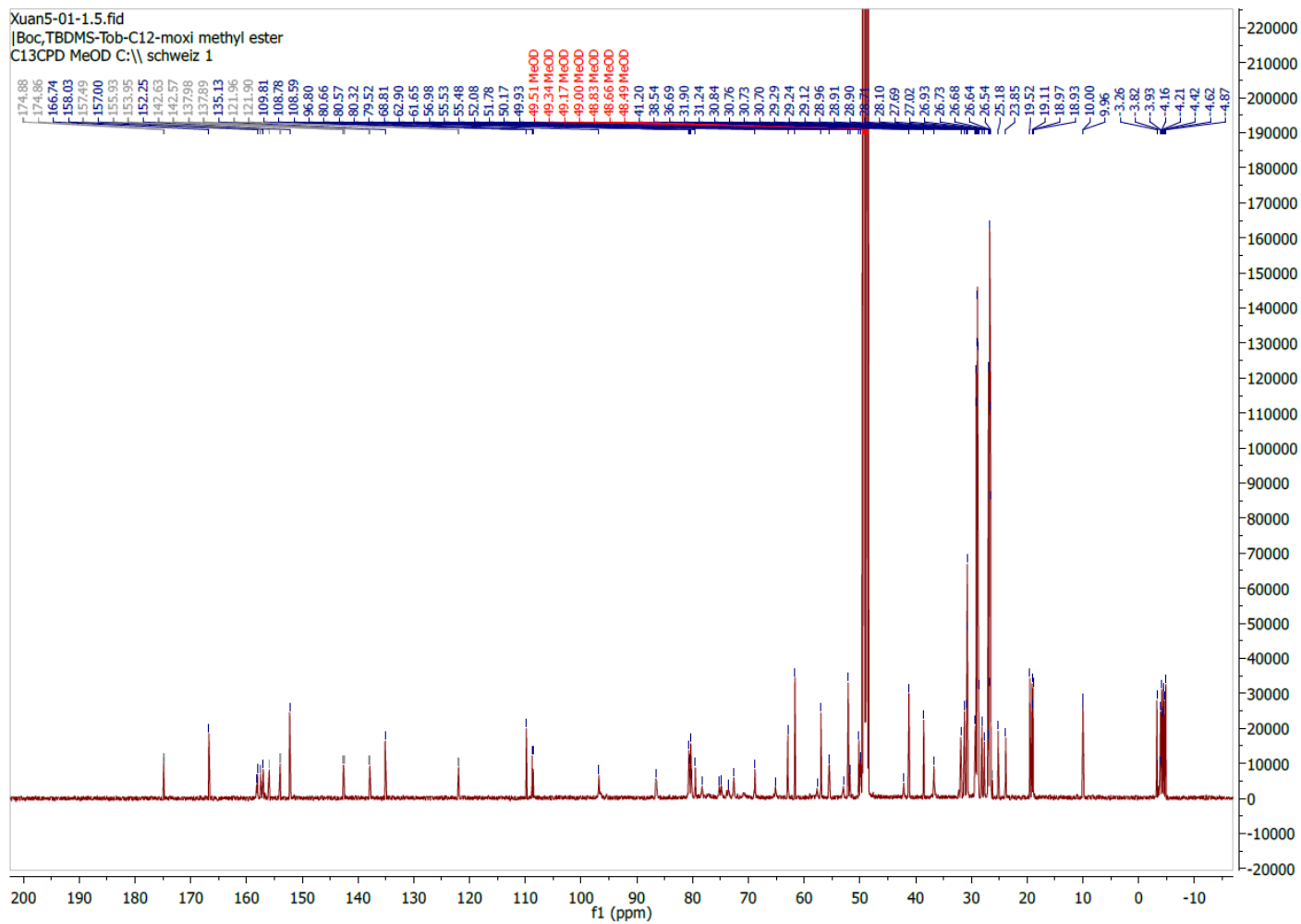
Appendix 6. HSQC spectrum of NEB-CIP **1b** in D<sub>2</sub>O

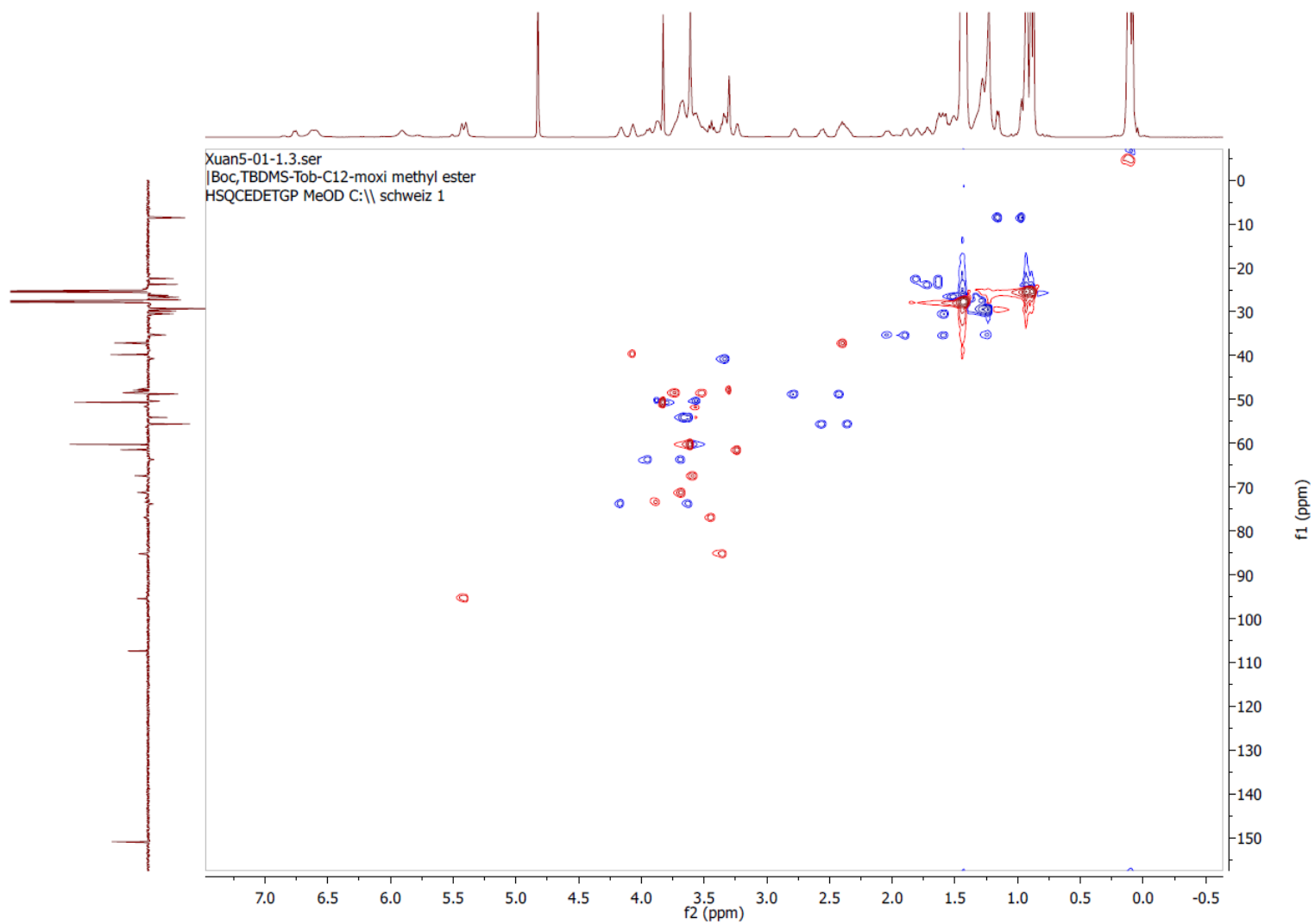
Appendix 7.  $^1\text{H}$  spectrum of NEB-NMP 2 in  $\text{D}_2\text{O}$ 

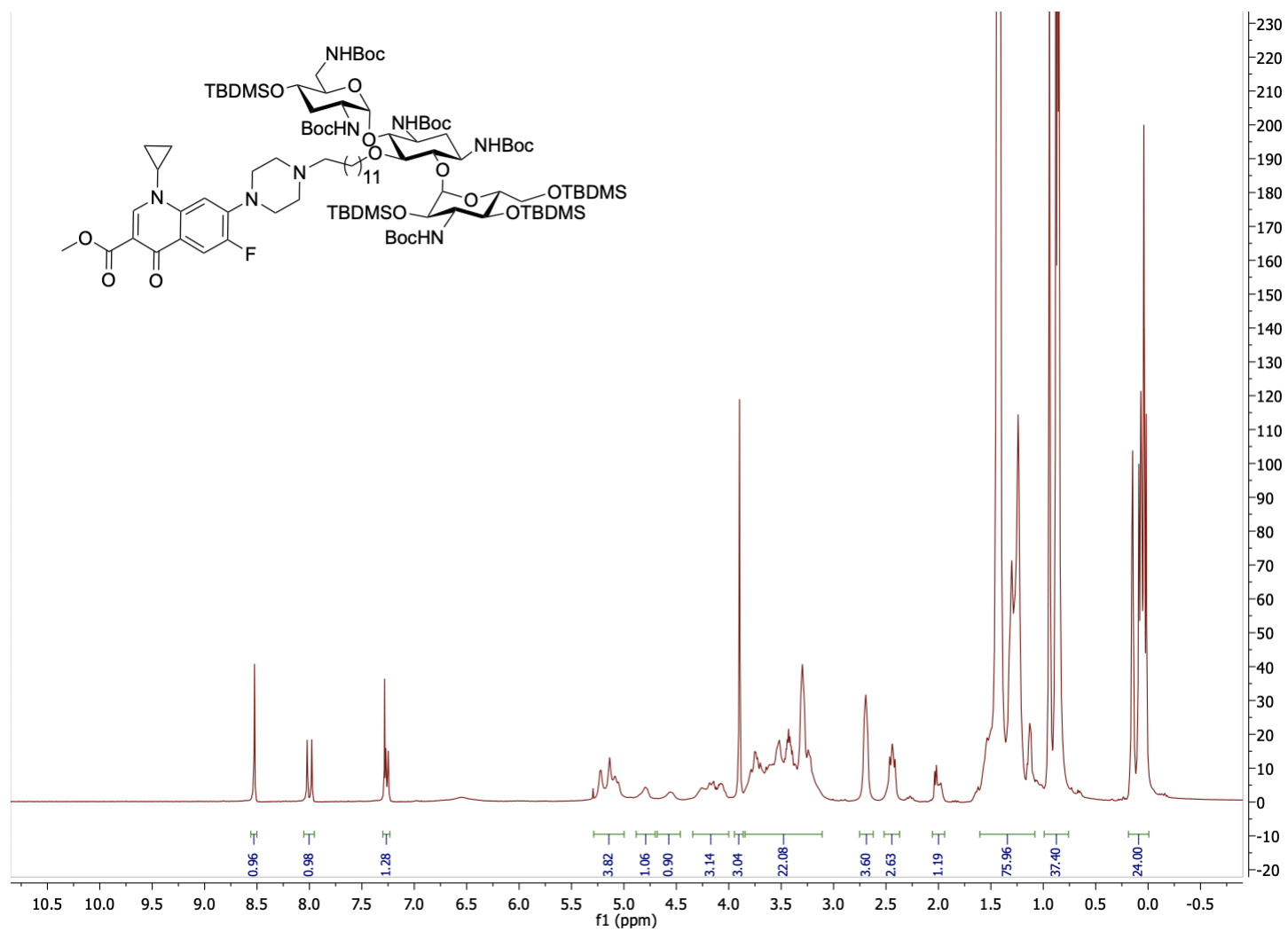
Appendix 8.  $^{13}\text{C}$  spectrum of NEB-NMP 2 in  $\text{D}_2\text{O}$ 

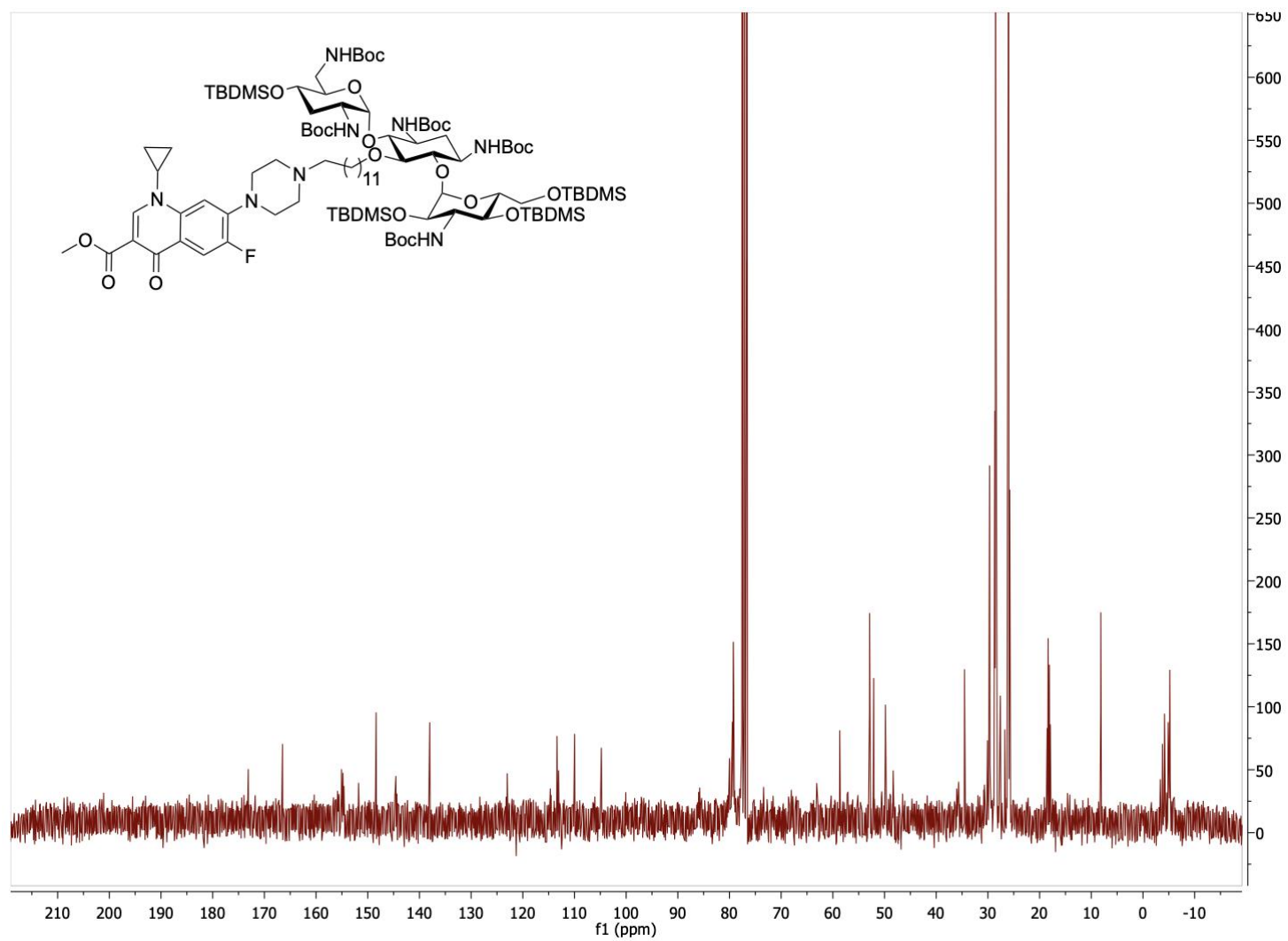
Appendix 9. HSQC spectrum of NEB-NMP 2 in D<sub>2</sub>O

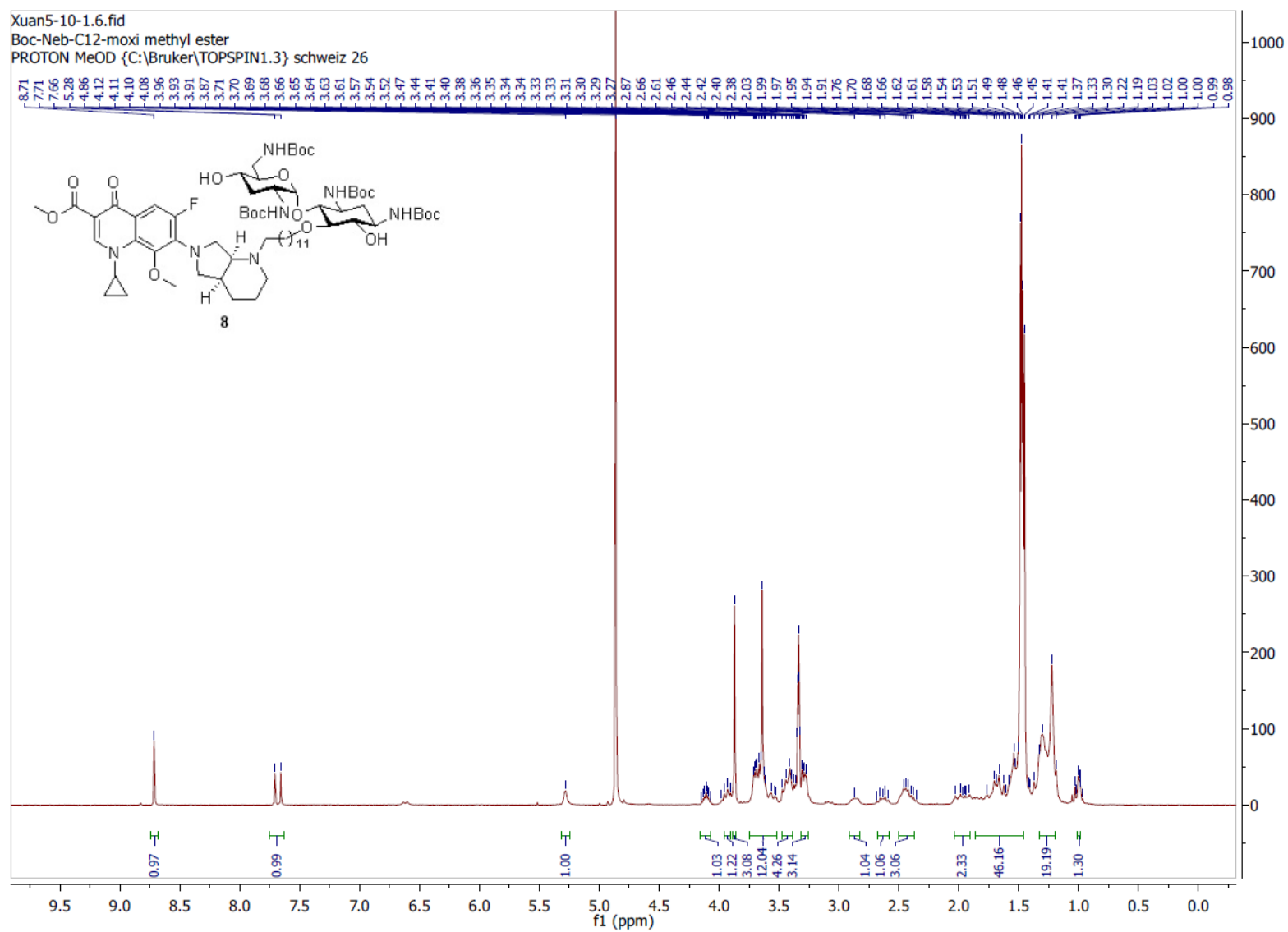
Appendix 10.  $^1\text{H}$  spectrum of compound **7a** in  $\text{CD}_3\text{OD}$ 

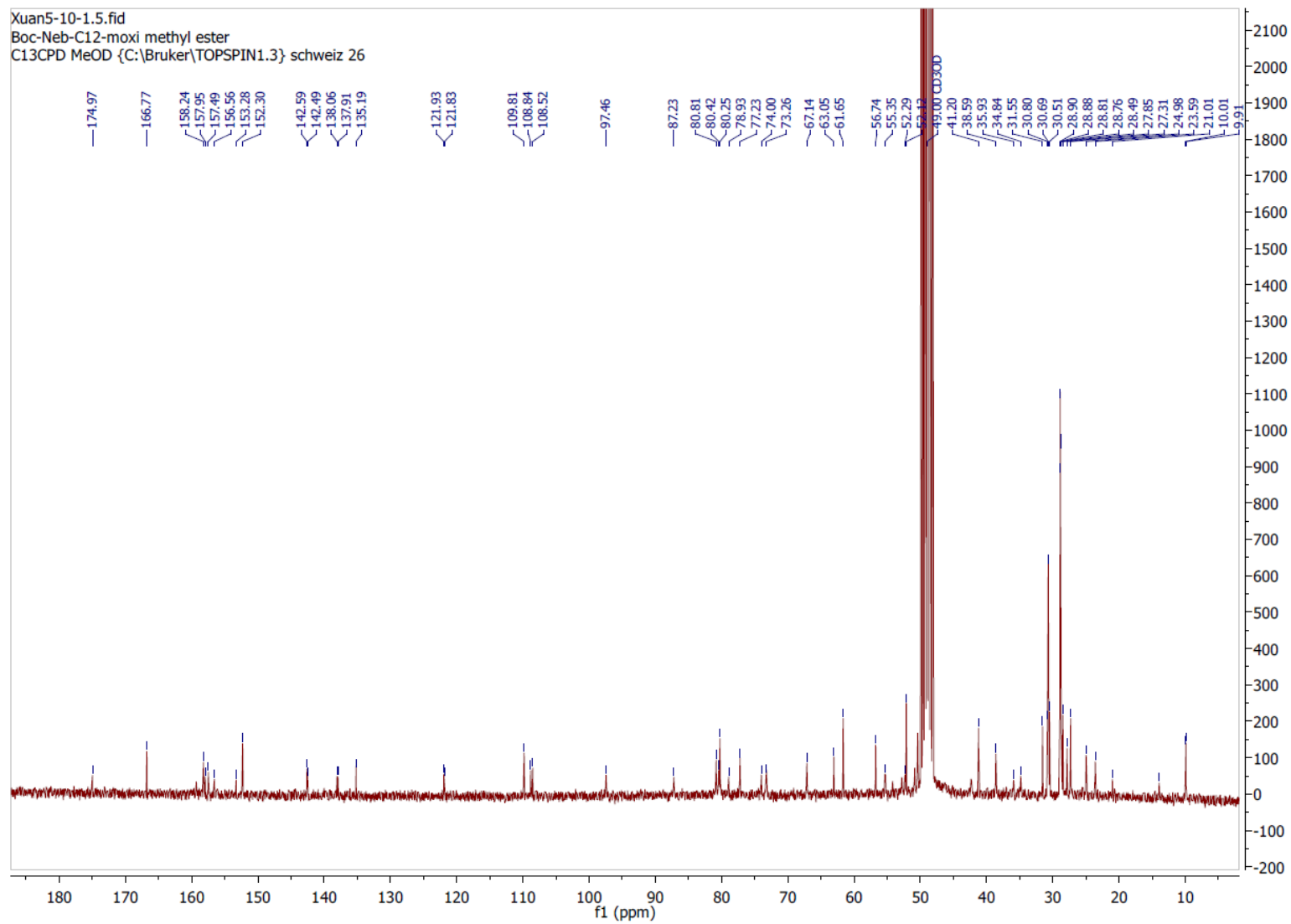
Appendix 11.  $^{13}\text{C}$  spectrum of compound **7a** in  $\text{CD}_3\text{OD}$ 

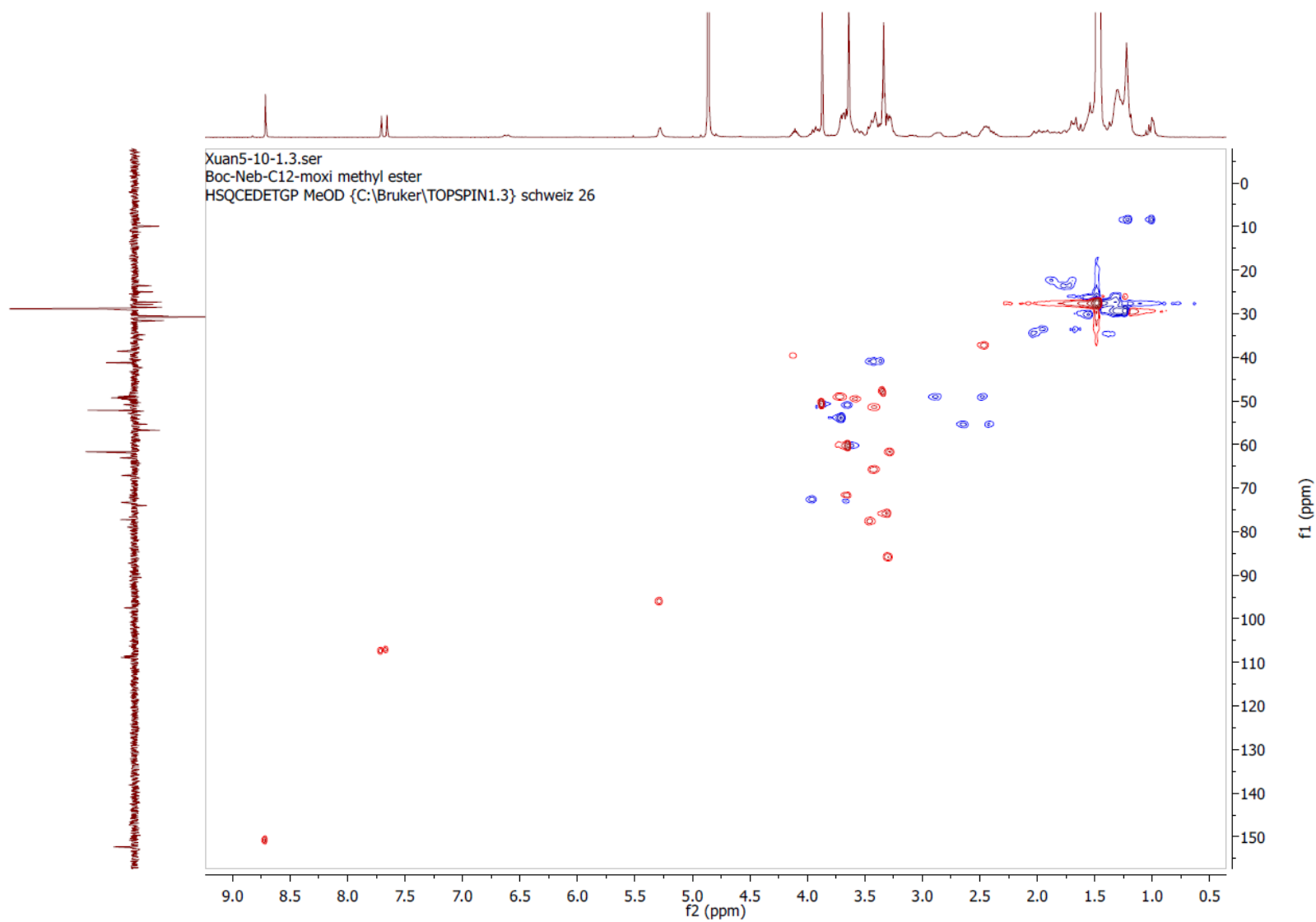
Appendix 12. HSQC spectrum of compound **7a** in CD<sub>3</sub>OD

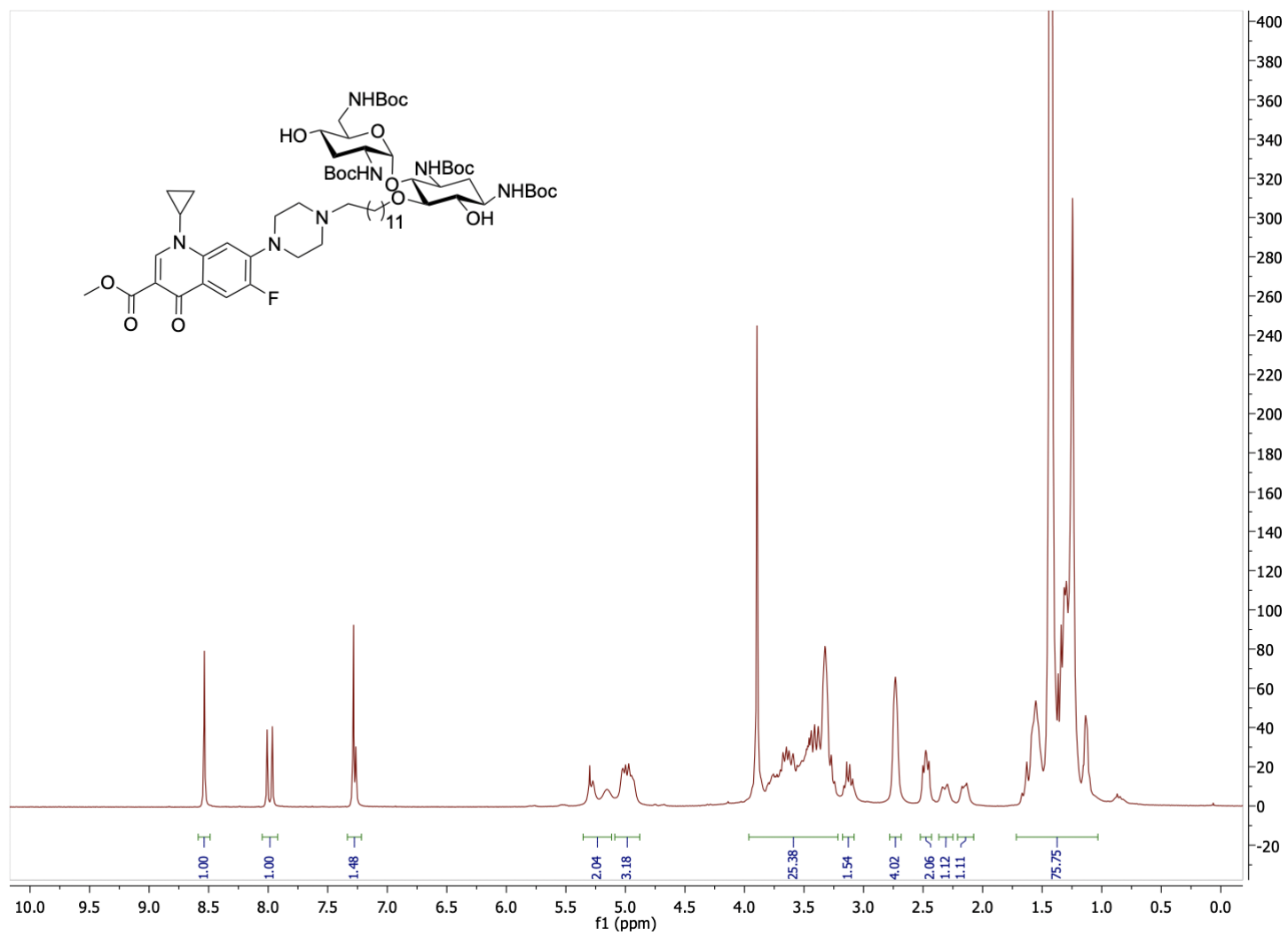
Appendix 13.  $^1\text{H}$  spectrum of compound **7b** in  $\text{CD}_3\text{OD}$ 

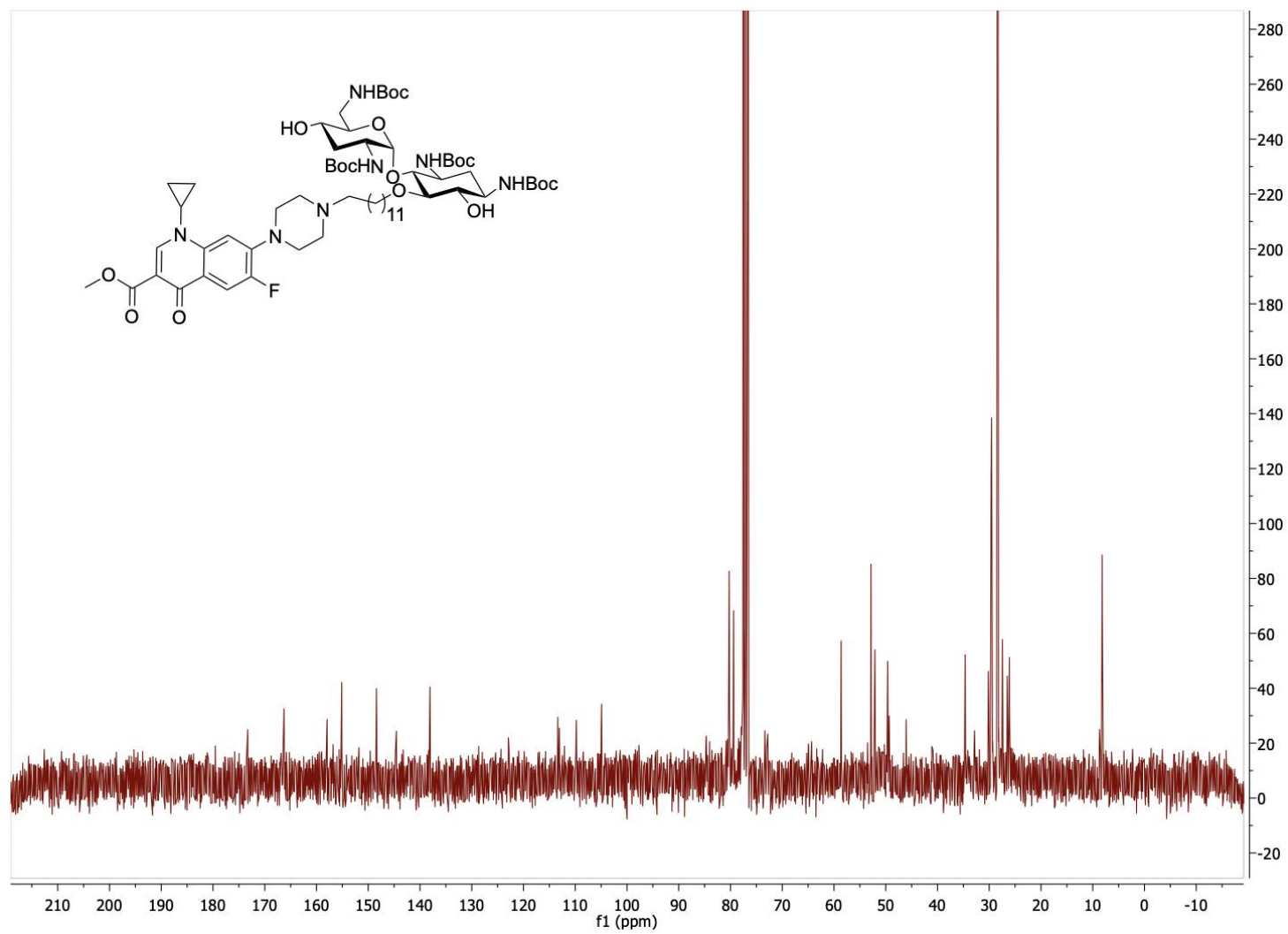
Appendix 14.  $^{13}\text{C}$  spectrum of compound **7b** in  $\text{CD}_3\text{OD}$ 

Appendix 15.  $^1\text{H}$  spectrum of compound **8a** in  $\text{CD}_3\text{OD}$ 

Appendix 16.  $^{13}\text{C}$  spectrum of compound **8a** in  $\text{CD}_3\text{OD}$ 

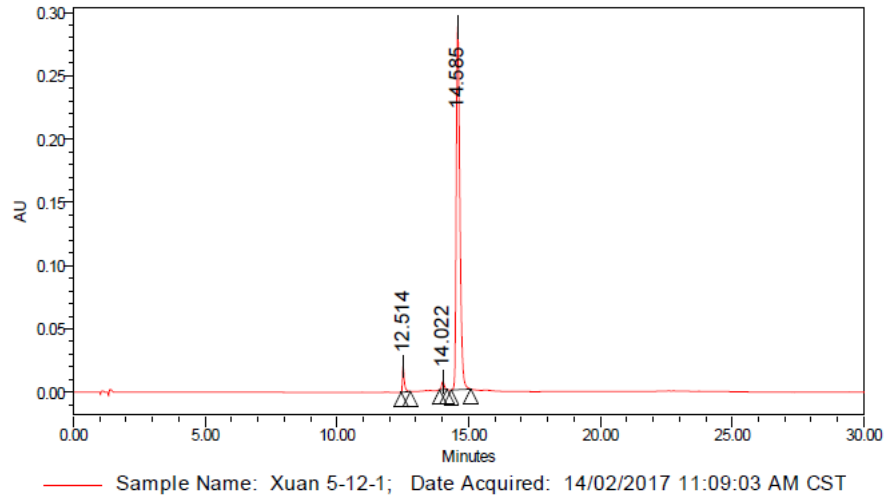
Appendix 17. HSQC spectrum of compound **8a** in CD<sub>3</sub>OD

Appendix 18.  $^1\text{H}$  spectrum of compound **8b** in  $\text{CDCl}_3$ 

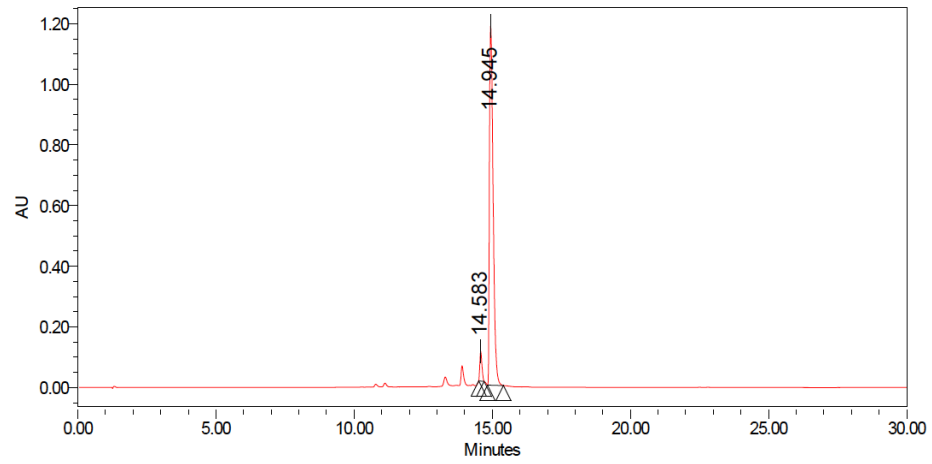
Appendix 19.  $^{13}\text{C}$  spectrum of compound **8b** in  $\text{CDCl}_3$ 

## 11.4 HPLC SPECTRA

## Appendix 20. HPLC data of NEB-MOX 1a

**Processed Channel: PDA 295.0 nm**

	Processed Channel	Retention Time (min)	Area	% Area	Height
1	PDA 295.0 nm	12.514	99498	3.47	20071
2	PDA 295.0 nm	14.022	43447	1.51	6384
3	PDA 295.0 nm	14.585	2727236	95.02	286740

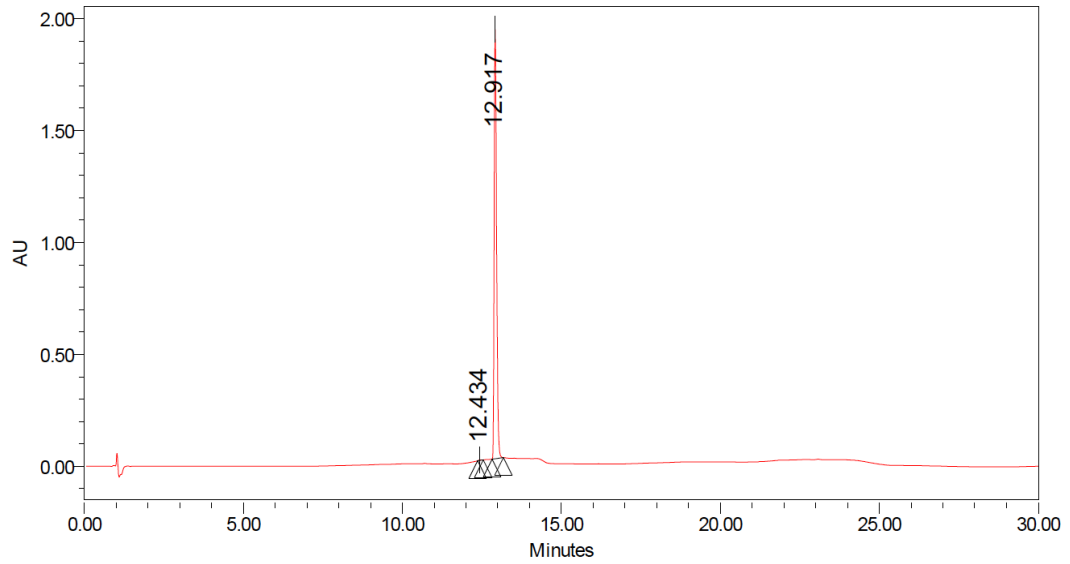
Appendix 21. HPLC data of NEB-CIP **1b**

Sample Name: DA-01-137 - 06-nov-18; Date Acquired: 06/11/2018 11:59:23 AM  
CST

**Processed Channel: PDA 278.5 nm**

	Processed Channel	Retention Time (min)	Area	% Area	Height
1	PDA 278.5 nm	14.583	520637	4.54	98645
2	PDA 278.5 nm	14.945	10941336	95.46	1185185

## Appendix 22. HPLC data of NEB-NMP 2



— Sample Name: Xuan 4-66-1; Date Acquired: 06/02/2017 12:39:12 PM CST

**Processed Channel: PDA 223.0 nm**

	Processed Channel	Retention Time (min)	Area	% Area	Height
1	PDA 223.0 nm	12.434	12897	0.13	2442
2	PDA 223.0 nm	12.917	10179693	99.87	1919005

## 11.5 TABLE

**Table 11.5.1** MICs ( $\mu\text{g/mL}$ ) of clinical *P. aeruginosa* isolates against different antibiotic classes

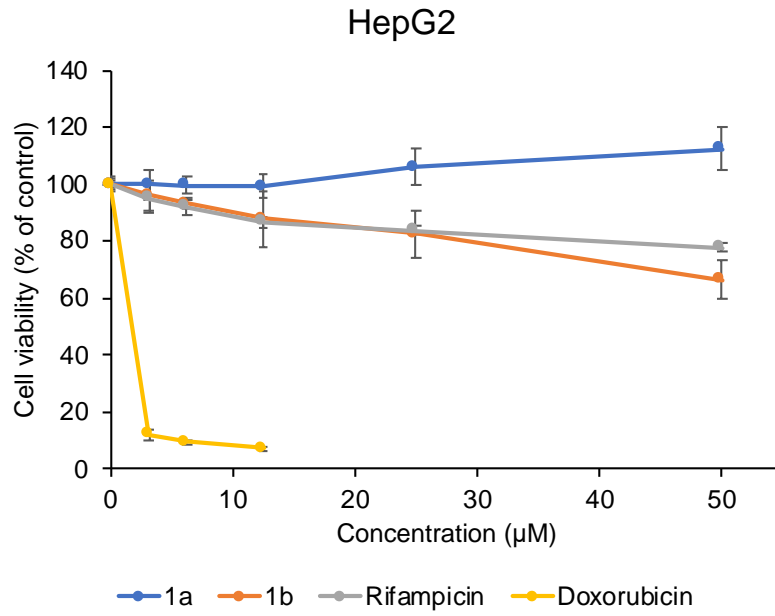
Stock no.	PTZ	A/C	AZT	FOX	CFZ	CTR	CPM	CAZ	IMI	MER	DOR	ETP	CIP	MXF	TOB	GEN	AMK	TGC	DOX	CST	SXT
100036	8	>32	8	>32	>128	32	4	8	8	4	4	>32	>16	>16	64	>32	32	>16	>32	2	>8
101885	16	>32	32	>32	>128	32	8	8	1	1	0.5	32	>16	>16	≤0.5	≤0.5	≤1	8	>32	1	>8
P259-96918	64	>32	16	>32	>128	>64	>64	>32	32	>32	>32	>32	>16	>16	>64	>32	>64	8	16	1	>8
P260-97103	128	>32	16	>32	>128	>64	16	32	32	16	16	>32	16	>16	32	>32	4	16	16	1	2
P262-101856	64	>32	32	>32	>128	64	32	16	32	32	8	>32	>16	>16	>64	>32	>64	>16	>32	1	>8
P264-104354	256	>32	64	>32	>128	>64	32	>32	32	>32	16	>32	>16	>16	64	>32	8	>16	>32	1	>8
91433	64	>32	ND	>32	>128	>64	16	>32	32	8	8	>32	2	16	8	32	>32	>16	32	4	1
101243	128	>32	ND	>32	>128	>64	64	>32	16	16	16	>32	1	8	≥64	>32	>64	8	4	1024	4

PTZ: piperacillin-tazobactam; A/C: amoxicillin-clavulanic acid; AZT: aztreonam; FOX: ceftiofloxacin; CFZ: cefazolin; CTR: ceftriaxone; CPM: cefepime; CAZ: ceftazidime; IMI: imipenem; MER: meropenem; DOR: doripenem; ETP: ertapenem; CIP: ciprofloxacin; MXF: moxifloxacin; TOB: tobramycin; GEN: gentamicin; AMK: amikacin; TGC: tigecycline; DOX: doxycycline; CST: colistin; SXT: trimethoprim-sulfamethoxazole; ND: not determined

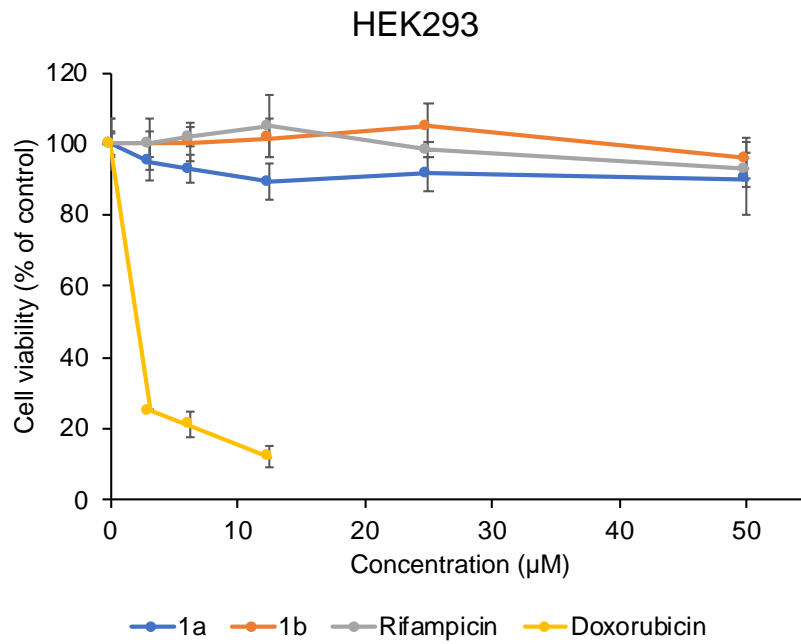
## 11.6. CYTOTOXICITY STUDIES

**Cytotoxicity Assay.** Human embryonic kidney cells (HEK293) and HepG2 cells were grown in Dulbecco's modified eagle's medium supplemented with 10% fetal bovine serum in a humidified 5% atmospheric incubator at 37 °C. Equal number of cells (100  $\mu$ L of media containing ~ 8000 cells) were dispersed into 96-well plates and wells with medium but no cells were used as blanks. After incubating for 24 h, 100  $\mu$ L of varying concentrations of test compounds (at twice the desired concentrations) were added to each well, including the blanks. The treated cells were then incubated further for 48 h, after which PrestoBlue reagent was added to each well. The plates were then incubated for an additional hour on a nutator mixer in a 5% CO<sub>2</sub> incubator. The fluorescence was read at 490 nm on a SpectraMax M2 plate reader (Molecular Devices Corp., Sunnyvale, CA, USA). The values of blank were subtracted from each value, and the viability values of the treated samples relative to the controls with vehicle were calculated. The values for the plots are the means  $\pm$  standard deviation.

(A)



(B)



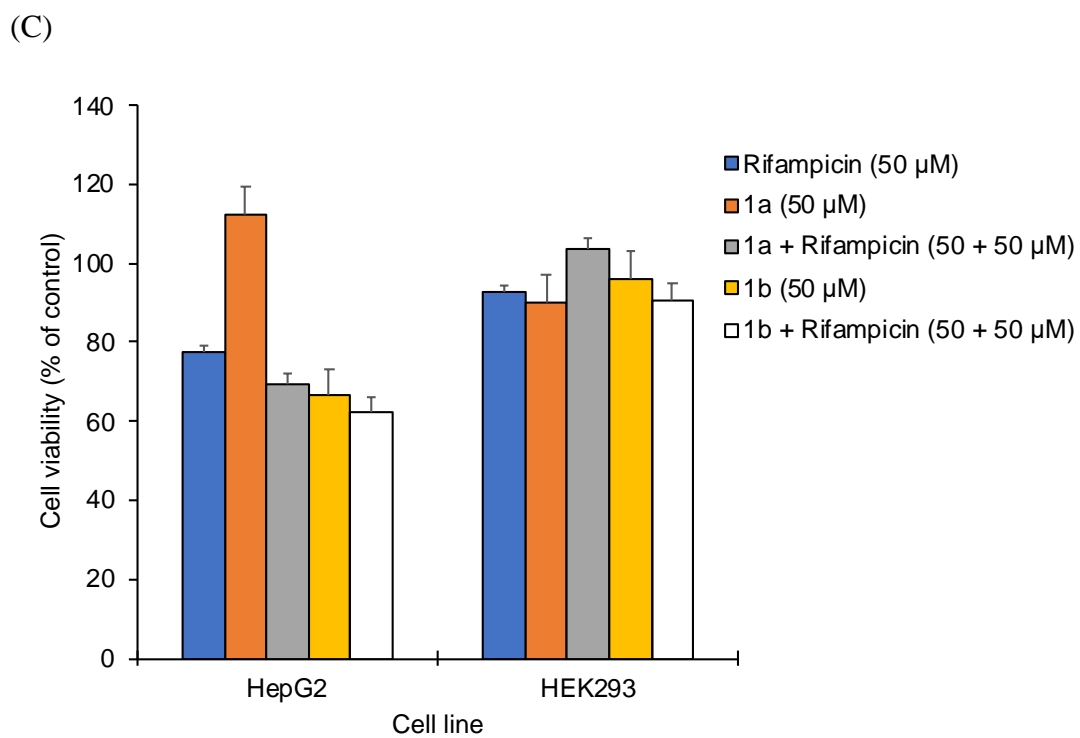
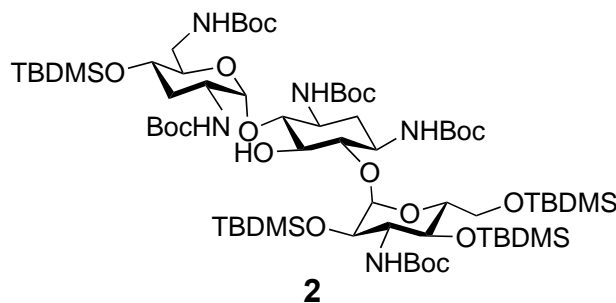


**Figure 11.6.1** Cytotoxicity studies of adjuvant **1a** or **1b** (alone) and in combination with rifampicin against HepG2 and HEK293 cell lines (A-C).

## Chapter 12: Supporting Information for Chapter 7

### 12.1 SYNTHESIS AND CHARACTERISATION OF TOBRAMYCIN DERIVATIVES



#### 12.1.1 Synthesis and characterization of 1,3,2',6',3''-penta-*N*-(tert-butoxycarbonyl)- 4',2'',4'',6''-tetra-*O*-TBDMS-tobramycin (**2**).

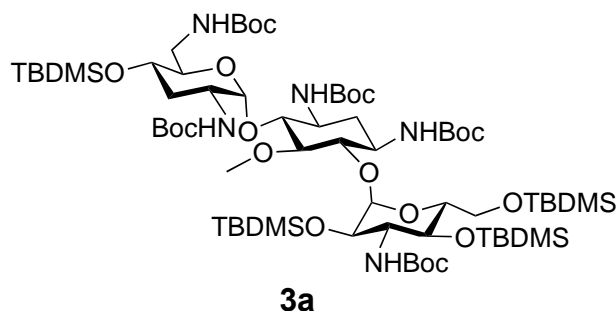
Boc-protected Tobramycin (6.0 g, 6.2

mmol) was dissolved in dry DMF (10.0 mL) and TBDMS-Cl (5.6 g, 37.2 mmol) was added, followed by methylimidazole (2.9 mL, 37.2 mmol). The reaction was stirred at room temperature for 24 h. The solution was then poured into water and extracted three times with dichloromethane, washed with brine and dried with sodium sulfate. This crude mixture was then purified through flash chromatography (4:1 Hex:EtOAc) to give the desired product as a white solid (8.1 g, 91%). <sup>1</sup>H NMR (500 MHz, CDCl<sub>3</sub>): δ 4.94 (s, 1H), 4.89 (s, 1H), 3.97 – 3.04 (m, 15H), 2.84 – 2.56 (m, 2H), 2.01 (s, 1H), 1.73 – 1.18 (m, 47 H), 0.96 – 0.67 (m, 36H), 0.23 – 0.13 (m, 24H); <sup>13</sup>C NMR (125 MHz, CDCl<sub>3</sub>): δ 156.2, 155.7, 155.2, 154.9, 154.9, 99.5, 98.5, 82.1, 80.0, 79.7, 79.6, 78.9, 76.1, 75.4, 73.0, 67.6, 63.3, 51.0, 51.0, 50.5, 49.7, 41.5, 34.8, 28.7 – 28.4 (CH<sub>3</sub>), 26.4 – 25.7 (CH<sub>3</sub>), 18.6, 18.3, 18.2, 18.0, -3.4, -3.7, -4.0, -4.1, -4.5, -4.6, -4.8, -4.9, -5.1; EIMS: *m/z* calc'd for C<sub>67</sub>H<sub>133</sub>N<sub>5</sub>O<sub>19</sub>Si<sub>4</sub>Na: 1448.1, found: 1448.3 [M+Na]<sup>+</sup>.

### 12.1.2 General procedure for *O*-5 alkylation

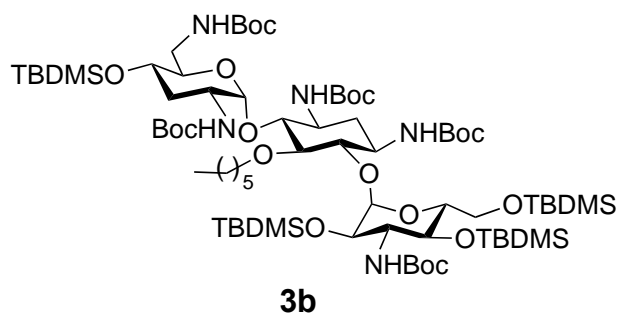
Compound **3** (1 mmol) dissolved in toluene (1.0 mL) was added KOH (3 mmol), an excess of 1,4-dibromoalkane (3 mmol) or alkyl iodide (3 mmol) and a catalytic amount of tetrabutyl ammonium hydrogen sulfate (0.1 mmol). This mixture was stirred at room temperature overnight and then water was added. The aqueous layer was extracted thrice with EtOAc and the organic layers combined washed with brine and dried over Na<sub>2</sub>SO<sub>4</sub>. The crude organic layer was purified via flash chromatography (eluted with hexane/EtOAc from 100/0 to 100/10) to give desired product as a solid.

### 12.1.3 Characterizations of compounds **3a–f**



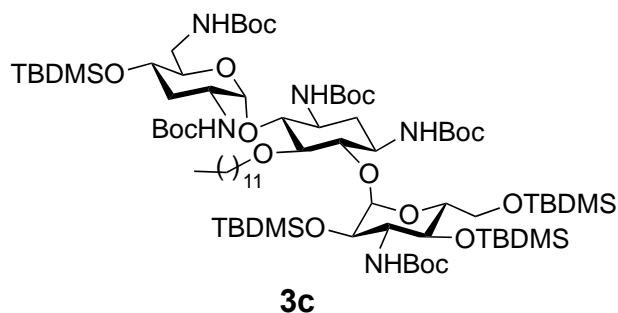
*5-O-methyl-1,3,2',6',3''-penta-N-(tert-butoxycarbonyl)-4',2'',4'',6''-tetra-O-TBDMS-tobramycin (3a)*. Yield: 75%. <sup>1</sup>H NMR (300 MHz, CDCl<sub>3</sub>): δ 5.15 (br d, *J* = 3.0 Hz, 1H, H-1'), 5.03 (br s, 1H), 3.96 – 3.04 (m, 18H), 2.89

– 2.56 (m, 2H), 2.02 (s, 1H), 1.73 – 1.22 (m, 47 H), 0.98– 0.72 (m, 36H), 0.23 – 0.12 (m, 24H); <sup>13</sup>C NMR (75 MHz, CDCl<sub>3</sub>) δ 156.2, 155.7, 155.2, 154.9, 100.0 (anomeric C), 99.6 (anomeric C), 86.4, 82.1, 80.0, 79.7, 79.6, 78.9, 76.1, 74.6, 73.0, 70.8, 66.0, 63.3, 51.0, 51.0, 50.5, 49.7, 40.9, 34.8, 28.7 – 28.4 (CCH<sub>3</sub>), 26.4 – 25.7 (CCH<sub>3</sub>), 18.6, 18.3, 18.2, 18.0, -3.4 – 5.1 (Si-CH<sub>3</sub>); EIMS: *m/z* calc'd for C<sub>68</sub>H<sub>135</sub>N<sub>5</sub>O<sub>19</sub>Si<sub>4</sub>Na: 1462.2, found: 1462.2. [M+Na]<sup>+</sup>.



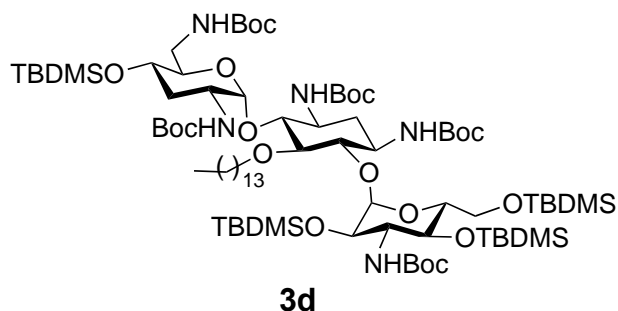
*5-O-hexyl-1,3,2',6',3''-penta-N-(tert-butoxycarbonyl)-4',2'',4'',6''-tetra-O-TBDMS-tobramycin (3b)*. Yield: 84%. <sup>1</sup>H NMR (300 MHz, CDCl<sub>3</sub>): δ 5.28 (br d, *J* = 3.0 Hz, 1H, H-1'), 5.20 (s, 1H), 4.25 – 3.97 (m, 2H), 3.88 –

3.07 (m, 16H), 2.50 – 1.58 (m, 1 H), 2.03 – 1.73 (m, 1H), 1.61 – 1.19 (m, 55H), 1.16 – 0.65 (m, 39H), 0.23 – 0.16 (m, 24H); <sup>13</sup>C NMR (75 MHz, CDCl<sub>3</sub>): δ 157.7, 155.7, 155.3, 154.3, 98.0 (anomeric C), 96.9 (anomeric C), 86.8, 80.9, 80.8, 80.6, 80.4, 79.7, 78.3, 75.2, 75.0, 73.7, 72.8, 71.1, 68.8, 65.3, 57.9, 55.2, 53.2, 50.2, 42.3, 36.9, 34.5, 34.4, 34.4, 34.3, 34.2, 33.9, 31.8, 29.5 – 28.9 (CCH<sub>3</sub>), 27.2 – 26.6 (CH<sub>3</sub>), 19.7, 19.2, 19.1, 14.1, -3.0 – 4.8 (Si-CH<sub>3</sub>); EIMS: *m/z* calc'd for C<sub>73</sub>H<sub>145</sub>N<sub>5</sub>O<sub>19</sub>Si<sub>4</sub>Na: 1532.3, found: 1532.5 [M+Na]<sup>+</sup>.



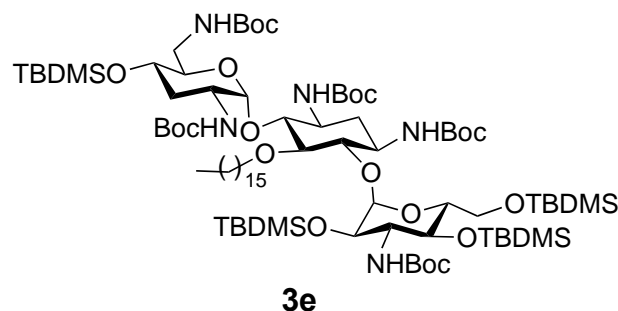
*5-O-(dodecyl)-1,3,2',6',3''-penta-N-(tert-butoxycarbonyl)-4',2'',4'',6''-tetra-O-TBDMS-tobramycin (3c)*. Yield: 83%. <sup>1</sup>H NMR (300 MHz, CDCl<sub>3</sub>): δ 5.29 (br d, *J* = 3.0 Hz, 1H, H-1'), 5.23 (br s, 1H, H-1''), 4.39 –

4.12 (m, 2H), 3.92 – 3.24 (m, 16H), 2.50 – 1.58 (m, 1 H), 2.13 – 2.06 (m, 1H), 1.43 – 1.23 (m, 67H), 0.93 – 0.85 (m, 39H), 0.14 – 0.01 (m, 24H); <sup>13</sup>C NMR (75 MHz, CDCl<sub>3</sub>): δ 155.7, 154.9, 154.7, 98.1 (anomeric C), 96.7 (anomeric C), 85.9, 80.1, 79.5, 79.3, 78.0, 75.6, 73.6, 71.7, 68.1, 67.0, 63.3, 57.5, 53.4, 50.7, 48.6, 41.9, 36.8, 35.8, 33.9, 32.1, 30.8 – 28.6 (CCH<sub>3</sub>), 26.3 – 21.6 (CCH<sub>3</sub>), 18.5 – 17.9 (CCH<sub>3</sub>), 14.3, -3.4 – 5.2 (Si-CH<sub>3</sub>); EIMS: *m/z* calc'd for C<sub>79</sub>H<sub>157</sub>N<sub>5</sub>O<sub>19</sub>Si<sub>4</sub>Na: 1616.4, found: 1616.5 [M+Na]<sup>+</sup>.



*5-O-(tetradecyl)-1,3,2',6',3''-penta-N-(tert-butoxycarbonyl)-4',2'',4'',6''-tetra-O-TBDMS-tobramycin (3d)*. Yield: 82%. <sup>1</sup>H NMR (300 MHz, CDCl<sub>3</sub>): δ 5.23 (br s, 1H, H-1'), 5.20 (br s, 1H, H-1''), 4.234–.14 (m, 1H),

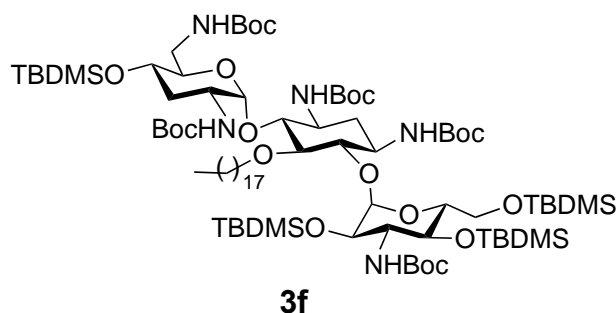
4.07 – 3.97 (m, 1H), 3.85 – 3.17 (m, 16H), 2.64 – 2.48 (m, 1 H), 2.13 – 2.06 (m, 1H), 1.53 – 1.29 (m, 71H), 1.03 – 0.91 (m, 39H), 0.14 – 0.01 (m, 24H); <sup>13</sup>C NMR (75 MHz, CDCl<sub>3</sub>): δ 156.0, 155.9, 155.1, 154.7, 97.3 (anomeric C), 97.2 (anomeric C), 85.9, 80.2, 79.9, 79.2, 78.2, 75.6, , 75.3, 73.3, 71.5, 68.2, 67.1, 66.8, 62.6, 62.1, 56.3, 53.0, 49.2, 48.5, 41.9, 35.6, 33.7, 31.9, 30.1 – 28.4 (CCH<sub>3</sub>), 26.2 – 22.6 (CCH<sub>3</sub>), 18.5 – 17.9 (CCH<sub>3</sub>), 14.1, -4.25.2 – (Si-CH<sub>3</sub>); EIMS: *m/z* calc'd for C<sub>81</sub>H<sub>161</sub>N<sub>5</sub>O<sub>19</sub>Si<sub>4</sub>Na: 1644.5, found: 1644.5 [M+Na]<sup>+</sup>.



*5-O-(hexadecyl)-1,3,2',6',3''-penta-N-(tert-butoxycarbonyl)-4',2'',4'',6''-tetra-O-TBDMS-tobramycin (3e)*. Yield: 84%. <sup>1</sup>H NMR (300 MHz, CDCl<sub>3</sub>): δ 5.22 (br d, *J* = 3.1 Hz, 1H, H-1'), 5.15 (br s, 1H, H-1''), 4.27 – 4.06

(m, 2H), 3.82 – 3.16 (m, 16H), 2.49 – 2.45 (m, 1 H), 2.03 – 1.97 (m, 1H), 1.45 – 1.24 (m, 75H), 0.95 – 0.86 (m, 39H), 0.15 – 0.02 (m, 24H); <sup>13</sup>C NMR (75 MHz, CDCl<sub>3</sub>): δ 155.7, 154.9, 154.8, 98.0 (anomeric C), 96.8 (anomeric C), 85.9, 80.1, 79.5, 79.4, 77.4, 75.6, 73.6, 71.7, 68.2, 67.0, 63.3, 57.5, 50.7, 49.2, 48.6, 42.0, 36.1, 35.8, 33.8, 33.0, 32.1, 30.8 – 28.6 (CCH<sub>3</sub>), 26.4 – 25.9

(CCH<sub>3</sub>), 22.8, 18.7 – 18.1 (CCH<sub>3</sub>), 14.3, 7.46, -3.4 – 5.2 (Si-CH<sub>3</sub>); EIMS: *m/z* calc'd for C<sub>83</sub>H<sub>165</sub>N<sub>5</sub>O<sub>19</sub>Si<sub>4</sub>Na: 1672.5, found: 1672.6 [M+Na]<sup>+</sup>.



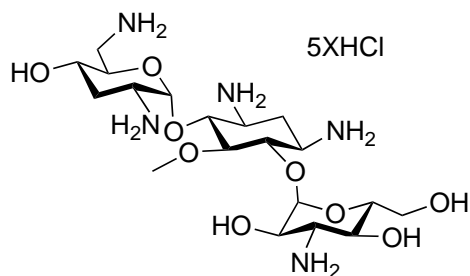
*5-O-(octadecyl)-1,3,2',6',3''-penta-N-(tert-butoxycarbonyl)-4',2'',4'',6''-tetra-O-TBDMStobramycin (3f)*. Yield: 78%. <sup>1</sup>H NMR (300 MHz, CDCl<sub>3</sub>): δ 5.14 (br d, *J* = 3.0 Hz, 1H, H-1'), 5.13 (br s, 1H, H-1''), 4.29 – 4.03

(m, 2H), 3.82-3.16 (m, 16H), 2.48 – 2.44 (m, 1 H), 2.03-1.96 (m, 1H), 1.44 – 1.24 (m, 79H), 0.94 – 0.85 (m, 39H), 0.14 – 0.01 (m, 24H); <sup>13</sup>C NMR (75 MHz, CDCl<sub>3</sub>): δ 155.7, 154.9, 154.7, 98.0 (anomeric C), 96.8 (anomeric C), 85.9, 80.1, 79.5, 79.4, 77.4, 75.5, 73.6, 73.0, 71.7, 68.2, 67.0, 63.3, 57.5, 50.7, 49.2, 48.6, 41.9, 36.1, 35.8, 33.8, 33.0, 32.1, 30.8 – 28.6 (CCH<sub>3</sub>), 26.4 – 25.8 (CCH<sub>3</sub>), 22.8, 18.7 – 18.1 (CCH<sub>3</sub>), 14.3, 7.46, -3.3 – 5.1 (Si-CH<sub>3</sub>); EIMS: *m/z* calc'd for C<sub>85</sub>H<sub>169</sub>N<sub>5</sub>O<sub>19</sub>Si<sub>4</sub>Na: 1700.6, found: 1700.6 [M+Na]<sup>+</sup>.

#### 12.1.4 General procedure for final deprotection

All BOC and TBDMS protected compounds were treated with 40% HCl in MeOH at room temperature for 1–5 h. Methanolic HCl was removed at reduced pressure. To the residue 2% methanol in ether was added and the solvent was decanted to get the solid tobramycin conjugate as salt. Further the crude of final compound has been purified with C-18 column chromatography (eluted with deionized water) to get analytically pure compound.

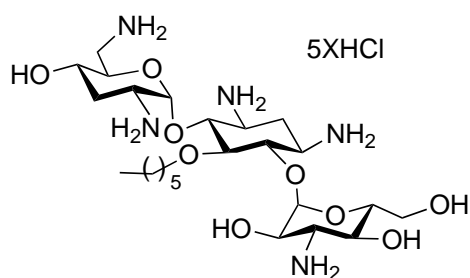
## 12.1.5 Characterizations of compounds 4a–f

**4a**

*5-O-methyltobramycin.5HCl (4a)*. Yield: 82%.  $^1\text{H}$

NMR (500 MHz,  $\text{CD}_3\text{OD}$ ):  $\delta$  5.57 (d,  $J = 2.6$  Hz, 1H, H-1'), 5.16 (d,  $J = 3.5$  Hz, 1H, H-1''), 4.42 (dd,  $J_1 = J_2 = 9.6$  Hz, 1H, H-4), 4.23 – 4.17 (m, 1H, H-5'), 4.05 (dd,  $J_1 = J_2 = 9.5$  Hz, 1H, H-6), 3.93 (dd,  $J = 10.7, 3.5$  Hz, 1H, H-2''), 3.88 –

3.81 (m, 4H, H-5'', H-6'', H-4', H-5), 3.77 – 3.65 (m, 5H, H-6'', H-4'', H-3, H-1, H-2'), 3.64 (s, 3H,  $\text{OCH}_3$ ), 3.53 (dd,  $J_1 = J_2 = 10.5$  Hz, 1H, H-3''), 3.35 – 3.32 (m, 1H, H-6'), 2.88–2.82 (m, 1H, H-6'), 2.63 – 2.53 (m, 1H, H-2), 2.33 – 2.11 (m, 3H, H-3', H-2);  $^{13}\text{C}$  (NMR, 125 MHz,  $\text{CD}_3\text{OD}$ ):  $\delta$  102.5 (anomeric C-1''), 93.8 (anomeric C-1'), 84.3, 82.3, 81.3, 76.1, 75.0, 74.6, 69.9, 69.8, 61.0, 60.0, 56.3, 51.3, 49.9, 40.3, 31.4, 29.7, 28.7; MALDI TOFMS  $m/z$  calc'd for  $\text{C}_{19}\text{H}_{39}\text{N}_5\text{O}_9\text{Na}$ : 504.2640, found: 504.2626  $[\text{M}+\text{Na}]^+$ .

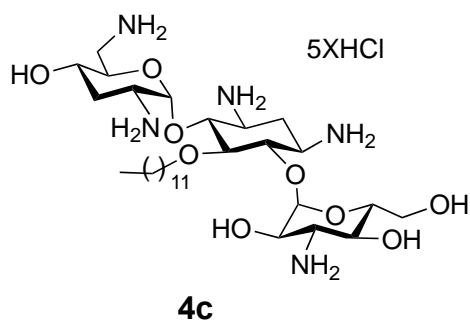
**4b**

*5-O-n-hexyltobramycin.5HCl (4b)* Yield: 84%.  $^1\text{H}$

NMR (500 MHz,  $\text{CD}_3\text{OD}$ ):  $\delta$  5.47 (d,  $J = 2.6$  Hz, 1H, H-1'), 5.17 (d,  $J = 3.4$  Hz, 1H, H-1''), 4.45 (dd,  $J_1 = J_2 = 9.5$  Hz, 1H, H-4), 4.26 – 4.23 (m, 1H, H-5'), 3.95 – 3.87 (m, 2H, H-6,  $\text{OCH}_2$ ), 3.83 – 3.75 (m, 5H, H-2'', H-5'', H-6'', H-4',

H-5) 3.72 – 3.56 (m, 5H, H-4'',  $\text{OCH}_2$ , H-3, H-1, H-2'), 3.52 (dd,  $J_1 = J_2 = 10.4$  Hz, 1H, H-3''), 3.33 – 3.31 (m, 1H, H-6'), 3.25 (dd,  $J = 13.3, 3.5$  Hz, 1H, H-6') 2.51– 2.46 (m, 1H, H-2), 2.30 – 2.18 (m, 3H, H-3', H-2), 1.67 (br s, 2H,  $\text{CH}_2$ ), 1.38 – 1.25 (m, 6H, 3 $\text{CH}_2$ ), 0.90 (t, 3H,  $J_1 = J_2 = 6.6$  Hz,  $\text{CH}_3$ );  $^{13}\text{C}$  (NMR, 125 MHz,  $\text{CD}_3\text{OD}$ ):  $\delta$  102.3 (anomeric C-1''), 93.9 (anomeric C-1'),

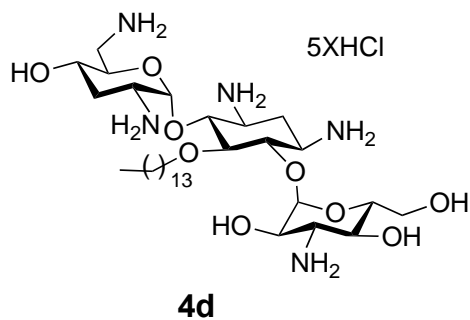
83.4, 82.7, 77.1, 76.4, 75.4, 74.0, 70.5, 67.0, 66.9, 65.6, 61.5, 56.4, 51.0, 40.5, 33.2, 31.1, 30.1, 29.0, 26.8, 26.5, 23.8, 14.5 ; MALDI TOFMS  $m/z$  calc'd for  $C_{24}H_{49}N_5O_9Na$ : 574.3422, found: 574.3432  $[M+Na]^+$ .



*5-O-dodecyltobramycin.5HCl (4c)*. Yield: 85%.  $^1H$

NMR (500 MHz,  $CD_3OD$ ):  $\delta$  5.46 (d,  $J = 2.6$  Hz, 1H, H-1'), 5.17 (br d,  $J = 3.5$  Hz, 1H, H-1''), 4.46 (dd,  $J_1 = J_2 = 9.5$  Hz, 1H, H-4), 4.26-4.23 (m, 1H, H-5'), 3.98 – 3.87 (m, 2H, H-6, OCH<sub>2</sub>), 3.83 – 3.75 (m, 6H, H-2'', H-5'', H-6''(2), H-4',

H-5) 3.73 – 3.57 (m, 5H, H-4'', OCH<sub>2</sub>, H-3, H-1, H-2'), 3.52 (dd,  $J_1 = J_2 = 10.4$  Hz, 1H, H-3''), 3.33 – 3.31 (m, 1H, H-6'), 3.25 (dd,  $J = 13.3, 3.5$  Hz, 1H, H-6') 2.51 – 2.45 (m, 1H, H-2), 2.30 – 2.18 (m, 3H, H-3', H-2), 1.67 (br s, 2H, CH<sub>2</sub>), 1.38-1.25 (m, 18H, 9CH<sub>2</sub>), 0.90 (t, 3H,  $J_1 = J_2 = 6.6$  Hz, CH<sub>3</sub>);  $^{13}C$  (NMR, 125 MHz,  $CD_3OD$ ):  $\delta$  102.3 (anomeric C-1''), 93.9 (anomeric C-1'), 83.4, 82.7, 77.1, 76.4, 75.4, 74.0, 70.5, 66.9, 65.6, 61.4, 56.4, 51.0, 50.0, 49.1, 40.5, 33.0, 31.3, 31.1, 31.0, 30.9, 30.8, 30.7, 30.5, 30.2, 29.0, 27.2, 23.8, 14.6; MALDI TOFMS  $m/z$  calc'd for  $C_{30}H_{61}N_5O_9Na$ : 658.4361, found: 658.4367  $[M+Na]^+$ .

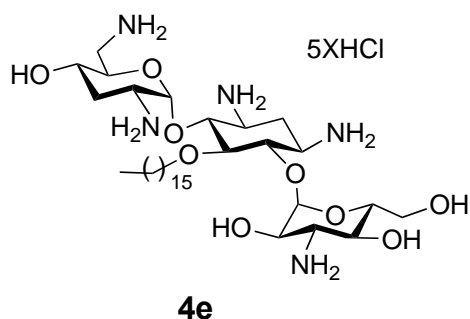


*5-O-tetradecyltobramycin.5HCl (4d)*. Yield:

81%.  $^1H$  NMR (500 MHz,  $CD_3OD$ ):  $\delta$  5.46 (d,  $J = 2.6$  Hz, 1H, H-1'), 5.17 (br d,  $J = 3.3$  Hz, 1H, H-1''), 4.44 (dd,  $J_1 = J_2 = 9.6$  Hz, 1H, H-4), 4.25 – 4.21 (m, 1H, H-5'), 3.95 – 3.88 (m, 2H, H-6, OCH<sub>2</sub>), 3.82 – 3.74 (m, 6H, H-2'', H-5'',

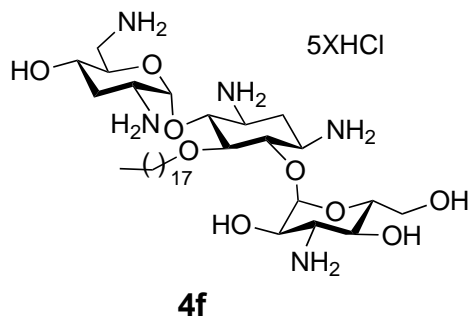
H-6'', H-4', H-5) 3.73 – 3.55 (m, 5H, H-4'', OCH<sub>2</sub>, H-3, H-1, H-2'), 3.52 (dd,  $J_1 = J_2 = 10.5$  Hz,

1H, H-3''), 3.33 – 3.31 (m, 1H, H-6'), 3.26 (dd,  $J = 13.6, 3.7$  Hz, 1H, H-6'), 2.50 – 2.46 (m, 1H, H-2), 2.29 – 2.18 (m, 3H, H-3', H-2), 1.67 (br s, 2H, CH<sub>2</sub>), 1.38 – 1.24 (m, 22H, 11CH<sub>2</sub>), 0.90 (t, 3H,  $J_1 = J_2 = 6.7$  Hz, CH<sub>3</sub>); <sup>13</sup>C (NMR, 125 MHz, CD<sub>3</sub>OD):  $\delta$  102.3 (anomeric C-1''), 93.9 (anomeric C-1'), 83.4, 82.8, 77.1, 76.4, 75.4, 74.0, 70.5, 66.9, 65.6, 61.3, 56.4, 51.0, 40.5, 33.0, 31.1, 31.0, 30.9, 30.8, 30.5, 30.2, 27.1, 23.7, 14.6; MALDI TOFMS  $m/z$  calc'd for C<sub>32</sub>H<sub>65</sub>N<sub>5</sub>O<sub>9</sub>Na: 686.4782, found: 686.4671 [M+Na]<sup>+</sup>.



*5-O-hexadecyltobramycin.5HCl (4e)*. Yield: 84%.

<sup>1</sup>H NMR (500 MHz, CD<sub>3</sub>OD):  $\delta$  5.46 (d,  $J = 2.6$  Hz, 1H, H-1'), 5.17 (br d,  $J = 3.3$  Hz, 1H, H-1''), 4.44 (dd,  $J_1 = J_2 = 9.5$  Hz, 1H, H-4), 4.23 – 4.20 (m, 1H, H-5'), 3.94 – 3.88 (m, 2H, H-6, OCH<sub>2</sub>), 3.82 – 3.74 (m, 6H, H-2'', H-5'', H-6'', H-4', H-5) 3.73 – 3.55 (m, 5H, H-4'', OCH<sub>2</sub>, H-3, H-1, H-2'), 3.51 (dd,  $J_1 = J_2 = 10.4$  Hz, 1H, H-3''), 3.33 – 3.31 (m, 1H, H-6'), 3.26 (dd,  $J = 13.5, 3.6$  Hz, 1H, H-6') 2.48 – 2.43 (m, 1H, H-2), 2.27 – 2.18 (m, 3H, H-3', H-2), 1.67 (br s, 2H, CH<sub>2</sub>), 1.38 – 1.23 (m, 26H, 13CH<sub>2</sub>), 0.90 (t, 3H,  $J_1 = J_2 = 6.7$  Hz, CH<sub>3</sub>); <sup>13</sup>C (NMR, 125 MHz, CD<sub>3</sub>OD):  $\delta$  102.3 (anomeric C-1''), 93.9 (anomeric C-1'), 83.4, 82.8, 77.1, 76.6, 75.4, 74.0, 70.5, 65.5, 65.6, 61.3, 56.3, 40.4, 33.0, 31.3, 31.1, 30.9, 30.8, 30.5, 27.2, 23.7, 14.4; MALDI TOFMS  $m/z$  calc'd for C<sub>34</sub>H<sub>69</sub>N<sub>5</sub>O<sub>9</sub>Na: 686.4675, found: 686.4671 [M+Na]<sup>+</sup>.



*5-O-octadecyltobramycin.5HCl (4f)*. Yield: 80%.

<sup>1</sup>H NMR (500 MHz, CD<sub>3</sub>OD):  $\delta$  5.46 (s, 1H, H-1'), 5.17

(br d,  $J = 3.3$  Hz, 1H, H-1''), 4.47 (dd,  $J_1 = J_2 = 9.1$  Hz, 1H, H-4), 4.25 – 4.22 (m, 1H, H-5'), 3.95 – 3.87 (m, 2H, H-6, OCH<sub>2</sub>), 3.83 – 3.75 (m, 6H, H-2'', H-5'', H-6'', H-4', H-5) 3.73 – 3.55 (m, 5H, H-4'', OCH<sub>2</sub>, H-3, H-1, H-2'), 3.53 (dd,  $J_1 = J_2 = 10.4$  Hz, 1H, H-3''), 3.33 – 3.31 (m, 1H, H-6'), 3.25 (dd,  $J = 13.1, 3.3$  Hz, 1H, H-6') 2.50 – 2.46 (m, 1H, H-2), 2.29 – 2.19 (m, 3H, H-3', H-2), 1.67 (brs, 2H, CH<sub>2</sub>), 1.35 – 1.25 (m, 30H, 15CH<sub>2</sub>), 0.90 (t, 3H,  $J_1 = J_2 = 6.7$  Hz, CH<sub>3</sub>); <sup>13</sup>C (NMR, 125 MHz, CD<sub>3</sub>OD):  $\delta$  102.3 (anomeric C-1''), 93.9 (anomeric C-1'), 83.4, 82.8, 77.1, 76.5, 75.4, 74.0, 70.5, 66.9, 65.5, 65.6, 61.4, 56.4, 51.1, 50.0, 40.5, 33.0, 31.3, 31.1, 30.9, 30.8, 30.7, 30.5, 30.2, 29.0, 27.2, 23.7, 14.4; MALDI TOFMS  $m/z$  calc'd for C<sub>36</sub>H<sub>73</sub>N<sub>5</sub>O<sub>9</sub>Na: 742.5408, found: 742.5308 [M+Na]<sup>+</sup>.

## 12.2 ELEMENTAL ANALYSIS

Table S1: Results of elemental analysis for compounds **4a–f**.

Compounds	Carbon (%)		Hydrogen (%)		Nitrogen (%)		Chlorine (%)	
	Theoretical	Found	Theoretical	Found	Theoretical	Found	Theoretical	Found
<b>4a</b>	34.38	34.54	6.68	6.8	10.55	10.54	26.7	27.02
<b>4b</b>	39.27	39.26	7.42	7.35	9.54	9.5	24.15	23.82
<b>4c</b>	44.04	44.35	8.13	8.45	8.56	8.69	21.67	21.88
<b>4d</b>	45.42	45.79	8.34	8.08	8.28	7.97	20.95	20.64
<b>4e</b>	46.71	46.49	8.53	8.28	8.01	8.31	20.28	20.45
<b>4f</b>	47.92	47.67	8.71	8.99	7.76	7.53	19.65	20.01

## 12.3 BIOLOGICAL ACTIVITY ASSAYS

### 12.3.1 Bacterial isolates

Study isolates were obtained as part of the Canadian National Intensive Care Unit (CAN-ICU) study<sup>1</sup> and CANWARD studies.<sup>2,3</sup> The CAN-ICU study included 19 medical centers from all regions of Canada with active ICUs. From September 2005 to June 2006, inclusive, each center collected a maximum of 300 consecutive isolates recovered from clinical specimens including from blood, urine, wound/tissue, and respiratory specimens (one pathogen per cultured site per patient) of ICU patients. The 4180 isolates obtained represented 2580 patients (or 1.62 isolates/patient). Participating study sites were requested to only obtain “clinically significant” specimens from patients with a presumed infectious disease. Isolates were shipped to the reference laboratory (Health Sciences Centre, Winnipeg, Canada) on Amies charcoal swabs, subcultured S10 onto appropriate media, and stocked in skim milk at -80°C until minimum inhibitory concentration (MIC) testing was carried out.

### 12.3.2 Antimicrobial susceptibilities

Following two subcultures from frozen stock, the *in vitro* activities of antimicrobials were determined by macrobroth dilution in accordance with the Clinical and Laboratory Standards Institute (CLSI) guidelines. The MICs of the antimicrobial agents for the isolates were determined using glass test tubes (2 mL/tube) containing doubling antimicrobial dilutions of cation adjusted Mueller-Hinton broth and inoculated to achieve a final concentration of approximately  $5 \times 10^5$  CFU/mL then incubated in ambient air for 24 h prior to reading.

Reference strains including *Staphylococcus aureus* ATCC 29213, methicillin-resistant *S. aureus* (MRSA) ATCC 33592, *Enterococcus faecalis* ATCC 29212, *Enterococcus faecium* ATCC 27270, *Streptococcus pneumoniae* ATCC 49619, *Escherichia coli* ATCC 25922, *Pseudomonas aeruginosa* ATCC 27853 and *Klebsiella pneumoniae* ATCC 13883 were acquired from the American Type Culture Collection (ATCC) and were used as a quality control strain. The clinical strains methicillin-resistant *Staphylococcus epidermidis* (MRSE cefazolin MIC >32 µg/mL) CAN-ICU 61589, gentamicin resistant *E. coli* CAN-ICU 61714, Amikacin-resistant (MIC = 32 µg/mL) *E. coli* CAN-ICU 63074, gentamicin resistant *P. aeruginosa* CAN-ICU 62584, *Stenotrophomonas maltophilia* CAN-ICU 62584 and *Acinetobacter baumannii* CAN-ICU 63169 were obtained from hospitals across Canada as a part of the Canadian National Intensive Care Unit (CAN-ICU) study. Methicillin-susceptible *S. epidermidis* (MSSE) CANWARD-2008 81388 was obtained from the 2008 Canadian Ward Surveillance (CANWARD) study while gentamicin-resistant tobramycin-resistant ciprofloxacin-resistant [aminoglycoside modifying enzyme aac(3)-IIa present] *E. coli* CANWARD- 2011 97615 and gentamicin-resistant tobramycin-resistant *P. aeruginosa* CANWARD-2011 96846 were obtained from the 2011 CANWARD study.

### 12.3.3 Cytotoxicity assessment

Human monocytic THP-1 (ATCC TIB-202) cells were cultured and maintained in RPMI-1640 medium (GIBCO) containing 2 mM L-glutamine, 1 mM sodium pyruvate and 10% (v/v) FBS, in a humidified incubator at 37 °C and 5% CO<sub>2</sub> as previously described.<sup>4</sup> The cells were differentiated into plastic adherent macrophage-like cells with phorbol 12-myristate 13-acetate (Sigma-Aldrich) and rested for an additional 24 h before stimulations as previously described.<sup>5</sup>

Macrophage-like THP-1 cells were stimulated with the amphiphilic tobramycin ether analogs (5 to 80  $\mu\text{M}$ ) for 24 h. Cellular cytotoxicity was evaluated by monitoring the release of lactate dehydrogenase and enzyme activity in the tissue culture (TC) supernatants employing a colorimetric detection kit (Roche Diagnostics) as per the manufacturer's instructions.

#### **12.3.4 ELISA for monitoring cytokine production**

Macrophage-like THP-1 cells (as described above) were stimulated with the selected tobramycin analogs (10  $\mu\text{M}$ ) for either 24 or 48 h. TC supernatants were centrifuged at  $1500 \times g$  for 5–7 min to obtain cell-free samples and aliquots were stored at  $-20^{\circ}\text{C}$ . Production of pro-inflammatory cytokines TNF- $\alpha$  and IL-1 $\beta$  were monitored in the TC supernatants by ELISA using specific antibody pairs from eBioscience, Inc., as per the manufacturer's instructions. Production of chemokines Gro- $\alpha$  and IL-8, and cytokine IL-1RA were monitored in the TC supernatants by ELISA employing human DuoSet (R&D Systems Inc.) as per the manufacturer's instructions. The concentration of the cytokines or chemokines in the TC supernatants was evaluated by establishing a standard curve with serial dilutions of the recombinant human cytokines or chemokines.

#### **12.3.5 Endotoxin stimulations**

To assess the effect of the tobramycin analogs on endotoxin-induced responses in macrophages, the plastic adherent macrophage-like THP-1 cells (as described above) were stimulated with 10 ng/mL bacterial lipopolysaccharide (LPS) for 24 h. The selected tobramycin analogs (10  $\mu\text{M}$ ) were added either simultaneously with LPS or added 30 min prior to LPS

stimulation as indicated.<sup>6</sup> In experiments to ascertain effect of the analogs on LPS-primed macrophages, the cells were stimulated with LPS for 30 min, the medium was removed and the cells were washed  $\times 2$ , followed by addition of new complete RPMI medium containing 10  $\mu\text{M}$  of the tobramycin analogs as indicated.<sup>7</sup> TC supernatants were collected after 24 h for monitoring the production of cytokines and chemokines as described above.

## 12.4 REFERENCES

- (1) Zhanel, G. G.; DeCorby, M.; Laing, N.; Weshnoweski, B.; Vashisht, R.; Tailor, F.; Nichol, K. A.; Wierzbowski, A.; Baudry, P. J.; Karlowisky, J. A.; Lagace-Wiens, P.; Walkty, A.; McCracken, M.; Mulvey, M. R.; Johnson, J.; Hoban, D. J. Antimicrobial-Resistant Pathogens in Intensive Care Units in Canada: Results of the Canadian National Intensive Care Unit (CAN-ICU) Study, 2005-2006. *Antimicrob. Agents Chemother.* **2008**, *52* (4), 1430–1437.
- (2) Zhanel, G. G.; Adam, H. J.; Baxter, M. R.; Fuller, J.; Nichol, K. A.; Denisuik, A. J.; Lagace-Wiens, P. R. S.; Walkty, A.; Karlowisky, J. A.; Schweizer, F.; Hoban, D. J. Antimicrobial Susceptibility of 22746 Pathogens from Canadian Hospitals: Results of the CANWARD 2007-11 Study. *J. Antimicrob. Chemother.* **2013**, *68 Suppl 1*, i7-22.
- (3) Zhanel, G. G.; DeCorby, M.; Adam, H.; Mulvey, M. R.; McCracken, M.; Lagace-Wiens, P.; Nichol, K. A.; Wierzbowski, A.; Baudry, P. J.; Tailor, F.; Karlowisky, J. A.; Walkty, A.; Schweizer, F.; Johnson, J.; Hoban, D. J. Prevalence of Antimicrobial-Resistant Pathogens in Canadian Hospitals: Results of the Canadian Ward Surveillance Study (CANWARD 2008). *Antimicrob. Agents Chemother.* **2010**, *54* (11), 4684–4693.

- (4) Choi, K. Y. G.; Napper, S.; Mookherjee, N. Human Cathelicidin LL-37 and Its Derivative IG-19 Regulate Interleukin-32-Induced Inflammation. *Immunology* **2014**, *143* (1), 68–80.
- (5) Mookherjee, N.; Brown, K. L.; Bowdish, D. M. E.; Doria, S.; Falsafi, R.; Hokamp, K.; Roche, F. M.; Mu, R.; Doho, G. H.; Pistolic, J.; Powers, J.-P.; Bryan, J.; Brinkman, F. S. L.; Hancock, R. E. W. Modulation of the TLR-Mediated Inflammatory Response by the Endogenous Human Host Defense Peptide LL-37. *J. Immunol.* **2006**, *176* (4), 2455–2464.
- (6) Mookherjee, N.; Wilson, H. L.; Doria, S.; Popowych, Y.; Falsafi, R.; Yu, J.; Li, Y.; Veatch, S.; Roche, F. M.; Brown, K. L.; Brinkman, F. S. L.; Hokamp, K.; Potter, A.; Babiuk, L. A.; Griebel, P. J.; Hancock, R. E. W. Bovine and Human Cathelicidin Cationic Host Defense Peptides Similarly Suppress Transcriptional Responses to Bacterial Lipopolysaccharide. *J. Leukoc. Biol.* **2006**, *80* (6), 1563–1574.
- (7) Chen, Q.; Jin, Y.; Zhang, K.; Li, H.; Chen, W.; Meng, G.; Fang, X. Alarmin HNP-1 Promotes Pyroptosis and IL-1 $\beta$  Release through Different Roles of NLRP3 Inflammasome via P2X7 in LPS-Primed Macrophages. *Innate Immun.* **2014**, *20* (3), 290–300.

## Chapter 13: Copyrighted Works for which Permission was Obtained

**Chapter 3:** A tobramycin vector enhances synergy and efficacy of efflux pump inhibitors against multidrug-resistant Gram-negative bacteria

Xuan Yang, Sudeep Goswami, Bala Kishan Gorityala, Ronald Domalaon, Yinfeng Lyu, Ayush Kumar, George G. Zhanel, Frank Schweizer.

Copyright © American Chemical Society, *Journal of Medicinal Chemistry*, 60 (9), 2017, 3913-3932. doi: 10.1021/acs.jmedchem.7b00156.

**Chapter 5:** Amphiphilic tobramycin-lysine conjugates sensitize multidrug resistant Gram-negative bacteria to rifampicin and minocycline

Yinfeng Lyu, Xuan Yang, Sudeep Goswami, Bala Kishan Gorityala, Temilolu Idowu, Ronald Domalaon, George G. Zhanel, Frank Schweizer.

Copyright © American Chemical Society, *Journal of Medicinal Chemistry*, 60 (9), 2017, 3684-3702. doi: 10.1021/acs.jmedchem.6b01742.

**Chapter 6:** Amphiphilic nebramine-based hybrids rescue legacy antibiotics from intrinsic resistance in multidrug-resistant Gram-negative bacilli

Xuan Yang, Derek Ammeter, Temilolu Idowu, Ronald Domalaon, Marc Brizuela, Oreofe Okunnu, Liting Bi, Yanelis Acebo Guerrero, George G. Zhanel, Ayush Kumar, Frank Schweizer.

Copyright © Elsevier, *European Journal of Medicinal Chemistry*, 175, 2019, 187–200. doi: 10.1016/j.ejmech.2019.05.003.

**Chapter 7:** Amphiphilic tobramycins with immunomodulatory properties

Goutam Guchhait, Antony Altieri, Balakishan Gorityala, Xuan Yang, Brandon Findlay, George G. Zhanel, Neeloffer Mookherjee, Frank Schweizer.

Copyright © WILEY-VCH Verlag GmbH & Co. KGaA, Weinheim, *Angewandte Chemie, International Edition*, 54 (21), 2015, 6278-6282. doi: 10.1002/anie.201500598.

## List of Publications and Patents Related to Thesis Work

### Publications:

- (1) Yang, X.; Ammeter, D.; Idowu, T.; Domalaon, R.; Brizuela, M.; Okunnu, O.; Bi, L.; Guerrero, Y. A.; Zhanel, G. G.; Kumar, A.; Schweizer, F. Amphiphilic Nebramine-Based Hybrids Rescue Legacy Antibiotics from Intrinsic Resistance in Multidrug-Resistant Gram-Negative Bacilli. *Eur. J. Med. Chem.* **2019**, *175*, 187–200.
- (2) Yang, X.; Domalaon, R.; Lyu, Y.; Zhanel, G.; Schweizer, F. Tobramycin-Linked Efflux Pump Inhibitor Conjugates Synergize Fluoroquinolones, Rifampicin and Fosfomycin against Multidrug-Resistant *Pseudomonas aeruginosa*. *J. Clin. Med.* **2018**, *7* (7), 158.
- (3) Yang, X.; Goswami, S.; Gorityala, B. K.; Domalaon, R.; Lyu, Y.; Kumar, A.; Zhanel, G. G.; Schweizer, F. A Tobramycin Vector Enhances Synergy and Efficacy of Efflux Pump Inhibitors against Multidrug-Resistant Gram-Negative Bacteria. *J. Med. Chem.* **2017**, *60* (9), 3913–3932.
- (4) Domalaon, R.; Yang, X.; Lyu, Y.; Zhanel, G. G.; Schweizer, F. Polymyxin B3 – Tobramycin Hybrids with *Pseudomonas aeruginosa* -Selective Antibacterial Activity and Strong Potentiation of Rifampicin, Minocycline, and Vancomycin. *ACS Infect. Dis.* **2017**, *3* (12), 941–954.
- (5) Lyu, Y.; Yang, X.; Goswami, S.; Gorityala, B. K.; Idowu, T.; Domalaon, R.; Zhanel, G. G.; Shan, A.; Schweizer, F. Amphiphilic Tobramycin–Lysine Conjugates Sensitize Multidrug Resistant Gram-Negative Bacteria to Rifampicin and Minocycline. *J. Med. Chem.* **2017**, *60* (9), 3684–3702.
- (6) Lyu, Y.; Domalaon, R.; Yang, X.; Schweizer, F. Amphiphilic Lysine Conjugated to

Tobramycin Synergizes Legacy Antibiotics against Wild-Type and Multidrug-Resistant *Pseudomonas Aeruginosa*. *Biopolymers* **2017**, e23091.

- (7) Guchhait, G.; Altieri, A.; Gorityala, B.; Yang, X.; Findlay, B.; Zhanel, G. G.; Mookherjee, N.; Schweizer, F. Amphiphilic Tobramycins with Immunomodulatory Properties. *Angew. Chem., Int. Ed. Engl.* **2015**, *54* (21), 6278–6282.
- (8) Domalaon, R.; Yang, X.; O’Neil, J.; Zhanel, G. G.; Mookherjee, N.; Schweizer, F. Structure-Activity Relationships in Ultrashort Cationic Lipopeptides: The Effects of Amino Acid Ring Constraint on Antibacterial Activity. *Amino Acids* **2014**, *46*, 2517–2530.

#### **Patents:**

- (1) Schweizer, F.; Gorityala, B. K.; Guchhait, G.; Yang, X.; Zhanel, G. G. Hybrid Antibiotics-Based Adjuvants Overcome Resistance in *Pseudomonas aeruginosa*. WO2017027968A1, February 23, **2017**.